ISSN
1678-4618

2024

ECLÉTICA
QUÍMICA

Volume 49

unesp
UNIVERSIDADE ESTADUAL PAULISTA
"JÚLIO DE MESQUITA FILHO"

Instituto de Química - UNESP
Araraquara

Summary

LETTER

REVIEW

ORIGINAL ARTICLES

Summary

ORIGINAL ARTICLES

ORIGINAL ARTICLES AND EDUCATION IN CHEMISTRY

REVIEWERS OF ARTICLES PUBLISHED IN 2024

Adam Wiryawan
Adelino Vieira de Godoy Netto
Ahmet Kilic
Alejandro Junior Aranda Aguirre
Alejandro Lopez Castillho
Alexandre Araujo de Souza
André Henrique Baraldi Dourado
Canan Koçak
Carlos Arterio Sorgi
Carlos Cezar da Silva
Claudia Alejandra Aguilar Ucan
Cristiane Regina Budziak Parabocz
Daniella Rodrigues
Darlisson de Alexandria Santos
David E. Q. Jimenez
Deiver Alessandro Teixeira
Edilson Ferreira
Elaine da Silva Ramos
Euclesio Simionatto
Habiddin Habiddin
Hayuni Retno Widarti
Hernán
José Tiago Claudino Barragan
Karen Tauceda
Leandro Zatta
Leticia Machado
Luis Llanes Pitarch
Luiz Alberta Beraldo de Moraes
Luiz Antonio Sodre Costa
Manuel Ignacio Azocar Guzman
Mariete Barbosa Moreira
Masrid Pikoli
Mauro Carlos Costa Ribeiro
Michael Ibok
Miriam de Resende
Mohamed El Fadili
Muntholib Muntholib
Ojah Emmanuel
Pedro Henrique Reis
Pedro Miranda Junior
R. Ahmad Zaky El Islami
Rafael Mafra
Ratna Dewi
Rivelino Martins Cavalcante
Rodrigo Della Noce
Salma Al-Kindi
Sofía Rezende
Tiago André Denck Colman
Vanderlei Aparecido de Lima
Vinicius Rangel Campos
Zakariya Yahya Algamal

The total number of reviewers of the articles published in 2024 was 50, of which only 3 were from UNESP.

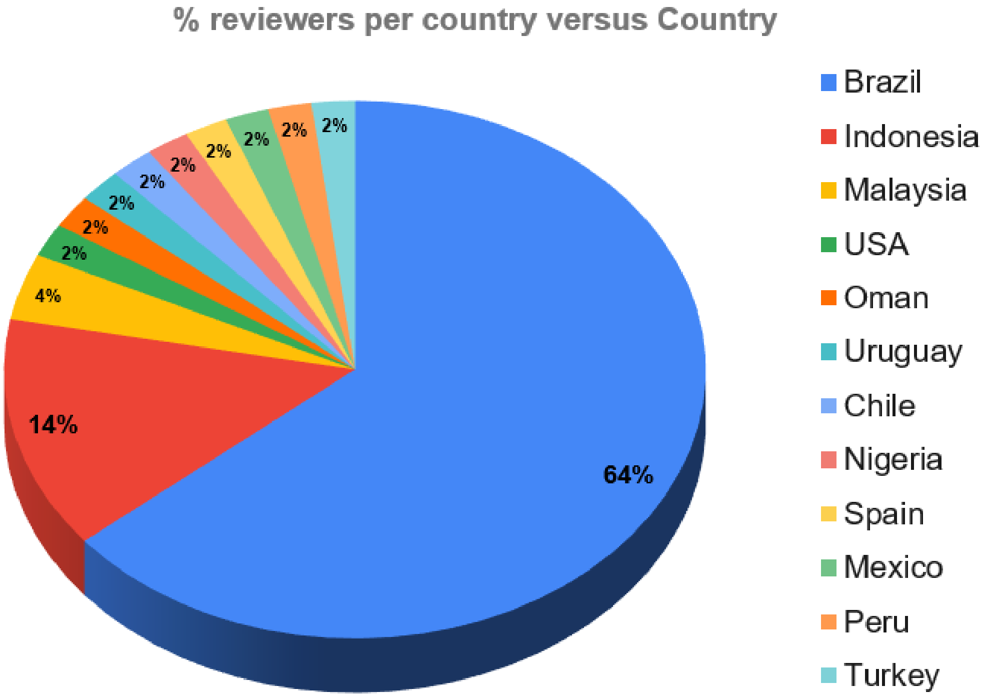

ECLÉTICA QUÍMICA

Eclet. Quim. 49 | e-1492, 2024

Original Article

https://doi.org/10.26850/1678-4618.eq.v49.2024.e1492

Predicting the biological activity of selected phytochemicals in *Alsophila spinulosa* leaves against 4-aminobutyrate-aminotransferase: A potential antiepilepsy agents

Oyebamiji Abel **Kolawole**[1+], Olujinmi Faith **Eniola**[1], Akintelu Sunday **Adewale**[2], Adetuyi **Babatunde**[3], Ogunlana **Olubanke**[4], Semire **Banjo**[5], Akintayo Emmanuel **Temitope**[1,6], Akintayo Cecilia **Olufunke**[1,7], Babalola Jonathan **Oyebamiji**[8], Olawoye Bolanle **Mary**[9], Aworinde Juliana **Oluwasayo**[10]

Abstract

The use of medicinal plants as an alternative mean of treating various diseases has drawn the attention of several researchers. The desire to find lasting solutions to epilepsy among humans increases every day. Thus, this work was aimed at investigating the potential capacity of the studied phytochemicals in *Alsophila spinulosa* against human 4-aminobutyrate-aminotransferase as well as to predict the nonbonding interactions involved in the studied complexes. In this work, ten compounds with biological activities were selected and studied using molecular docking method. The molecules selected obtained from *A. spinulosa* leaves were optimized and various descriptors that described the anti-4-aminobutyrate-aminotransferase features were obtained. More so, 2-(3,4-dihydroxyphenyl)-5,7-dihydroxy-3-(((2S,3R,4R,5R,6S)-3,4,5-trihydroxy-6-methyltetrahydro-2H-pyran-2-yl)oxy)-4H-chromen-4-one (compound 9) with highest binding affinity proved to have greater strength to inhibit 4-aminobutyrate-aminotransferase thereby downregulating epilepsy than other studied compounds and the reference drug (clobazam). The ADMET features of both compound 9 and clobazam were explored and reported.

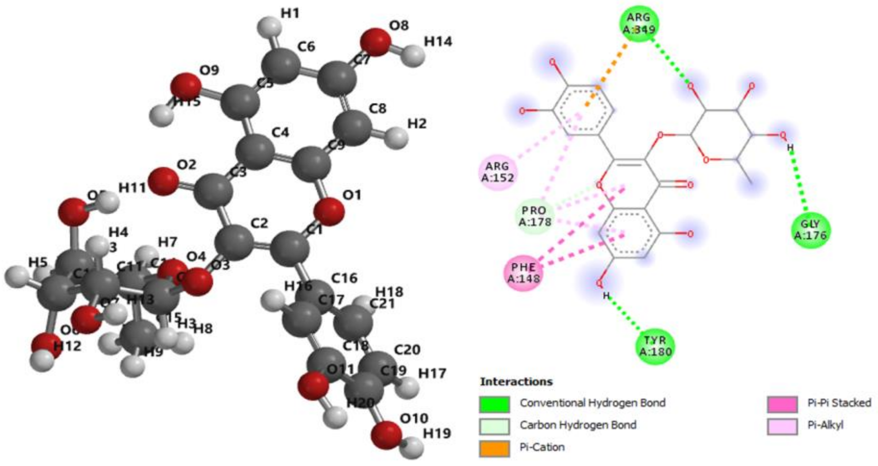

Article History

Received	May 06, 2023
Accepted	October 23, 2023
Published	January 03, 2024

Keywords

1. heterocycles;
2. binding sites;
3. ligands;
4. ADMET;
5. herbs.

Section Editor

Irlon Maciel Ferreira

Highlights

- The descriptors that enhance the inhibiting activity of the studied ligands were observed.
- The amino acid residues involved in the interaction were investigated.
- Pharmacokinetic analysis on the ligand with highest binding affinity was examined.

[1]Bowen University, Industrial Chemistry Programme, Iwo, Osun State, Nigeria. [2]Beijing Institute of Technology, School of Chemistry and Chemical Engineering, Beijing, China. [3]Precious Cornerstone University, Faculty of Pure and Applied Sciences, Ibadan, Nigeria. [4]Covenant University, Department of Biochemistry, Ota, Ogun State, Nigeria. [5]Ladoke Akintola University of Technology, Department of Pure and Applied Chemistry, Ogbomoso, Oyo State, Nigeria. [6]Ekiti State University, Department of Chemistry, Ado-Ekiti, Nigeria. [7]Federal University Oye-Ekiti, Department of Chemistry, Oye-Ekiti, Ekiti State, Nigeria. [8]University of Ibadan, Department of Chemistry, Ibadan, Oyo State, Nigeria. [9]Adeleke University, Department of Basic Sciences, Ede, Osun State, Nigeria. [10]University of Jos, Department of Medical Laboratory Science, Jos, Nigeria.
+Corresponding author: Oyebamiji Abel Kolawole, **Phone:** +234 08032493676, **Email address:** abeloyebamiji@gmail.com

1. Introduction

Traditional medicine has played a crucial role in boosting human health for years (Kebede *et al.*, 2021). Many ground-breaking successes in recent therapeutic science depend greatly on natural/local resources (Shriram *et al.*, 2018; Poulakou *et al.,* 2018). Over the years, many medicinal agents of synthetic and natural products have been used to combat diseases and infections (Pitout 2008). The World Health Organization reports that more than 60% of developing countries still use herbal drugs originating from medicinal plants as alternative medicine (Duraipandiyan *et al.*, 2006; Mishra *et al.*, 2013; Vaou *et al.*, 2021).

One of the most common neurological syndromes in the world is epilepsy, which remains in third position among the diseases that affect people with old age (Hirtz *et al.*, 2007; Werhahn 2009; Queeny *et al.*, 2018; Dunkel *et al.,* 2023). Its rate of increase has been observed to be high in infants and aged people (Hesdorffer *et al.*, 2011; Jeżowska-Jurczyk *et al.*, 2023). As stated by Gagliano *et al.* (2018), more than 45 million people have been reported to have epilepsy. Antiepileptic agents are one way of combating epilepsy; nevertheless, the activities of epilepsy in 80% of patients remain unrestrained. The tactics behind the treatment failure of epilepsy still seem to be unclear; however, the fight against epilepsy by scientists all over the world has been observed to be increasing (Kwan and Brodie, 2000; Bartolini *et al.*, 2023). According to Mukhopadhyay *et al.* (2012), epilepsy is a combination of many syndromes, each of which has various warning signs such as intermittent irregular electrical activity in the brain.

Gamma-aminobutyrate-aminotransferase played a significant role in the degradation of the inhibitory neurotransmitter. It has been the target of several antiepileptic drug-like compounds (Choi and Churchich, 1986). 4-Aminobutyrate-aminotransferase was observed to have the ability to transfer nitrogenous groups and catalyze the combination of 4-aminobutanoate and 2-oxoglutarate, resulting in succinate semialdehyde and L-glutamate (Shen *et al.*, 2023; Kim and Yoon, 2023; Zhang *et al.,* 2022; Gao *et al.,* 2022; Yasuhide *et al.,* 1999).

Alsophila spinulosa is a plant with much biological importance. According to Morton (1971), it is a fern that looks like a tree. It grows in humus soil and can be found in countries such as China, Japan, and India. In China, it is used to treat various ailments, including rheumatism, helminthic infections, cough, and gout (Abbas *et al.*, 2016). More so, in American continents, it is used in teas and as poultices for treating some ailments (Irene *et al.*, 2023).

It belongs to the Cyatheaceae family and is commonly called the flying spider-monkey tree fern (Chiang *et al.*, 1994; Lanza *et al.*, 2022). The trunk of *A. spinulosa* can grow taller than 5 m (Chinese DmgDictionay, 1985; Yan *et al.*, 2022). It is a fern and it possesses the potential ability to inhibit tumors (Kan, 1986).

Therefore, this work aims to evaluate the potential inhibitory properties of selected phytochemicals present in *A. spinulosa* against human 4-aminobutyrate-aminotransferase and investigate the potential nonbonding interaction involved in the studied complexes and their efficiency.

2. Methodology

2.1 Software and hardware

The optimization of the studied compounds was accomplished using density functional theory via Spartan ’14 software (Semire *et al.,* 2017). The binding affinity and nonbonding interactions between selected phytochemicals in *A. spinulosa* leaves and 4-aminobutyrate-aminotransferase were investigated via docking study using Pymol for treating enzyme, Discovery Studio software for viewing the interaction between the docked complexes, AutoDock tool for locating a binding site in the studied protein and AutoDock Vina software for docking calculation. The names and the two-dimensional structures of the selected phytochemicals are shown in **Table 1**.

Table 1. Studied phytochemicals obtained from *A. spinulosa.*

	Structures	IUPAC Names
1	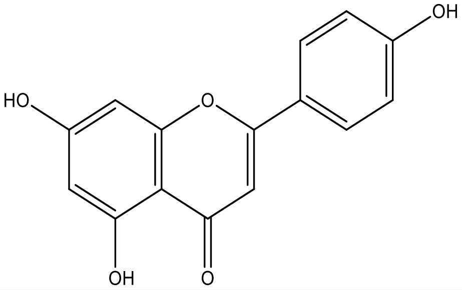	5,7-dihydroxy-2-(4-hydroxyphenyl)-4H-chromen-4-one
2	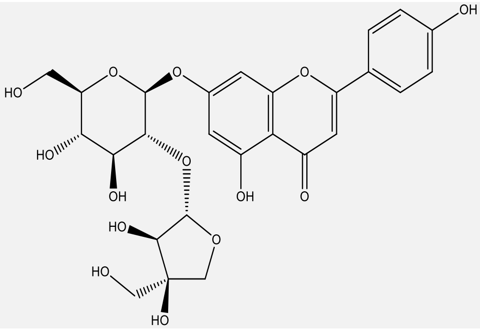	7-(((2S,3R,4S,5S,6R)-3-(((2S,3R,4R)-3,4-dihydroxy-4-(hydroxymethyl)tetrahydrofuran-2-yl)oxy)-4,5-dihydroxy-6-(hydroxymethyl)tetrahydro-2H-pyran-2-yl)oxy)-5-hydroxy-2-(4-hydroxyphenyl)-4H-chromen-4-one

3	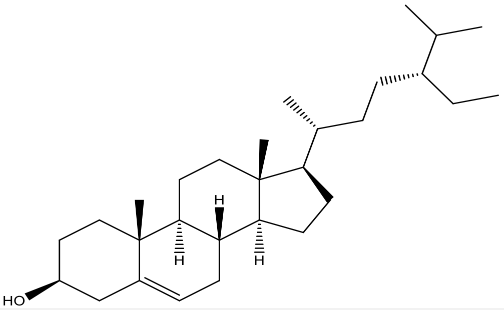	(3S,8S,9S,10R,13R,14S,17R)-17-((2R,5R)-5-ethyl-6-methylheptan-2-yl)-10,13-dimethyl-2,3,4,7,8,9,10,11,12,13,14,15,16,17-tetradecahydro-1H-cyclopenta[a]phenanthren-3-ol
4	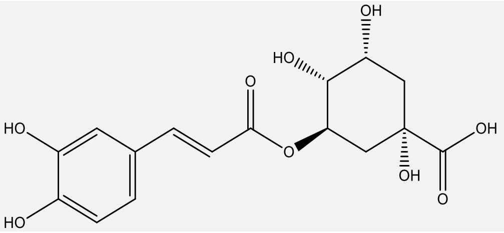	(1S,3R,4R,5R)-3-(((E)-3-(3,4-dihydroxyphenyl)acryloyl)oxy)-1,4,5-trihydroxycyclohexanecarboxylic acid
5	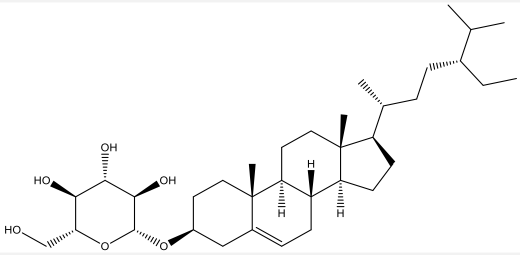	(2R,3R,4S,5S,6R)-2-(((3S,8S,9S,10R,13R,14S,17R)-17-((2R,5R)-5-ethyl-6-methylheptan-2-yl)-10,13-dimethyl-2,3,4,7,8,9,10,11,12,13,14,15,16,17-tetradecahydro-1H-cyclopenta[a]phenanthren-3-yl)oxy)-6-(hydroxymethyl)tetrahydro-2H-pyran-3,4,5-triol
6	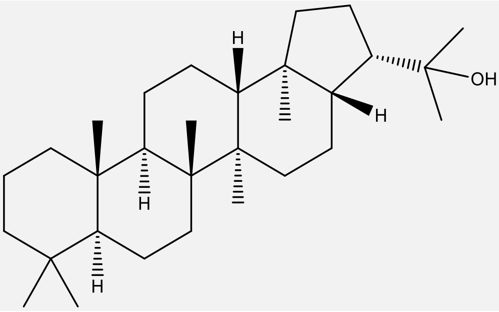	2-((3S,3aS,5aR,5bR,7aS,11aS,11bR,13aR,13bS)-5a,5b,8,8,11a,13b-hexamethylicosahydro-1H-cyclopenta[a]chrysen-3-yl)propan-2-ol
7	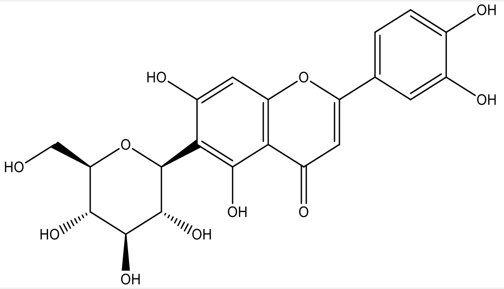	2-(3,4-dihydroxyphenyl)-5,7-dihydroxy-6-((2S,3R,4R,5S,6R)-3,4,5-trihydroxy-6-(hydroxymethyl)tetrahydro-2H-pyran-2-yl)-4H-chromen-4-one
8	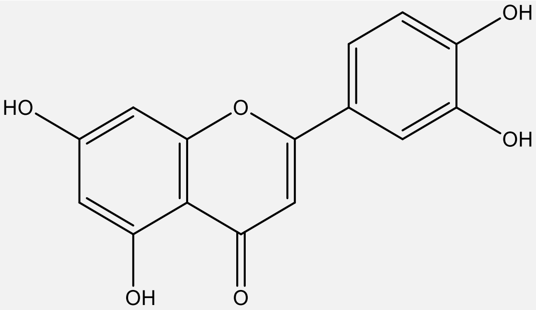	2-(3,4-dihydroxyphenyl)-5,7-dihydroxy-4H-chromen-4-one

9	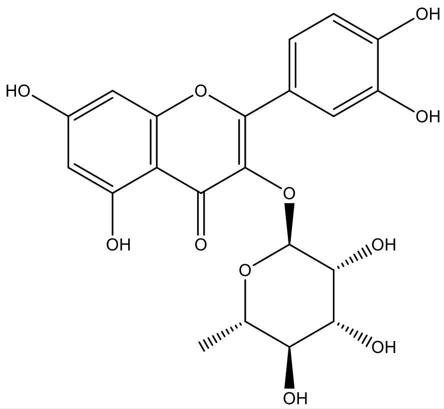	2-(3,4-dihydroxyphenyl)-5,7-dihydroxy-3-(((2S,3R,4R,5R,6S)-3,4,5-trihydroxy-6-methyltetrahydro-2H-pyran-2-yl)oxy)-4H-chromen-4-one
10	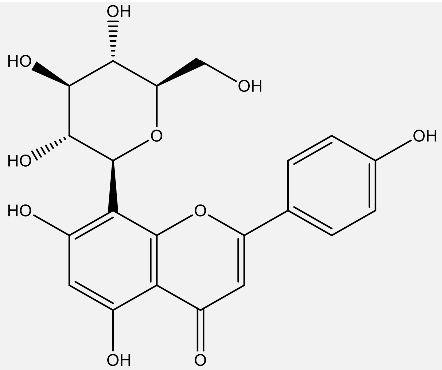	5,7-dihydroxy-2-(4-hydroxyphenyl)-8-((2S,3R,4R,5S,6R)-3,4,5-trihydroxy-6-(hydroxymethyl)tetrahydro-2H-pyran-2-yl)-4H-chromen-4-one

Source: Retrieved from Storici *et al.*, (2004).

2.2. Receptor (target)

The studied receptor (4-aminobutyrate-aminotransferase with protein data bank code: 1OHV) used in this work was repossessed from the recognized database (protein data bank) (Storici *et al.*, 2004).

2.3. Studied pharmacophore

Ten pharmacophores from *A. spinulosa* leaves were selected and prepared for a molecular docking study (Chen *et al.,* 2008). The selected compounds were chosen based on descriptions from literature (Vijayakumar *et al.*, 2018) and the compounds were obtained from a recognized database (https://pubchem.ncbi.nlm.nih.gov/).

2.4. Studied protein preparation

The studied receptor was retrieved from a protein data bank and a series of small molecules such as acetate ion (ACT), pyridoxal-5'-phosphate (PLP) and FE_2/S_2 (inorganic) cluster (FES) as well as water molecules were downloaded with it. The necessary factors for the downloaded receptor (resolution, R-value free, and R-value work) were observed to be 2.30, 0.221 and 0.118 Å, respectively. The studied receptor was treated using Pymol v 1.7.4 software and both small molecules such as ACT, PLP and FES as well as water molecules were removed and saved the clean 4-Aminobutyrate-Aminotransferase in .pdb format (El Fadili *et al.*, 2022a; Erazua *et al.*, 2023). The binding site in clean/treated 4-aminobutyrate-aminotransferase (PDB ID:1ohv) was predicted using AutoDockTools-1.5.6 (Waziri *et al.*, 2023; El Fadili *et al.*, 2022b). The calculation and analysis of site map of the studied receptor revealed the likely binding site and the figure for center (center_x = 5.638; center_y = 3.578 and center_z = 21.309) as well as the size of the site area (size_x = 62; size_y = 62 and size_z = 84) were reported accordingly. The docking calculation was executed using AutoDock Vina software to calculate binding affinity between the studied complexes.

2.5. ADMET investigation

This study was executed using ADMETsar 2.0 online software (Oyebamiji *et al.*, 2022). The ligands with higher binding affinity were investigated and absorption, distribution, metabolism, excretion, and toxicity (ADMET) factors such as physicochemical property, medicinal chemistry, absorption, distribution, metabolism, excretion, toxicity, environmental toxicity, tox21 pathway, and toxicophoric rule were considered.

3. Results and Discussion

3.1. Calculated descriptors

The descriptors obtained from optimization of the phytochemicals of *A. spinulosa* leaves revealed the activities of the studied medicinal plants. The descriptors obtained are reported in Table 2. According to Adeoye *et al.* (2022), the higher the highest occupied molecular orbital energy (E_{HOMO}), the better the tendency of the compound to release electrons to the nearby molecules. The unit for highest occupied molecular orbital energy was electron volt (eV) and as shown in Table 2, (1S,3R,4R,5R)-3-(((E)-3-(3,4-dihydroxyphenyl)acryloyl)oxy)-1,4,5-trihydroxycyclohexanecarboxylic acid (compound 4) possess the potential strength to react better than other studied compounds. Also, the lower the lowest unoccupied molecular orbital energy (E_{LUMO}), the greater the strength of molecules to receive electrons from the compound that can give it out; thus, 2-(3,4-dihydroxyphenyl)-5,7-dihydroxy-3-(((2S,3R,4R,5R,6S)-3,4,5-trihydroxy-6-methyltetrahydro-2H-pyran-2-yl)oxy)-4H-chromen-4-one (compound 9) showed potential strength to receive electron from nearby compounds thereby brings about better interactions.

Other calculated descriptors (band gap, dipole moment, molecular weight (≤ 500 amu) ovality, log P (≤5), polarizability, hydrogen bond donor (HBD) (≤5) and hydrogen bond acceptor (HBA) (≤10)) are reported in **Table 2**.

Table 2. The selected descriptors obtained from *A. spinulosa* leaves.

	E_{HOMO} (eV)	E_{LUMO} (eV)	EG (eV)	DM (Debye)	MW (amu)	AREA (Å²)	OVA	LOG P	POL (Å³)	HBD	HBA
1	−6.06	−1.60	4.46	4.39	270.24	266.07	1.38	−2.38	60.79	3	5
2	−6.06	−1.64	4.42	12.60	564.49	517.78	1.69	−5.68	81.15	8	14
3	−6.16	0.71	6.87	2.11	414.71	493.59	1.63	8.14	79.85	1	1
4	−5.74	−1.60	4.14	2.03	354.31	350.48	1.54	−2.42	66.53	6	7
5	−6.21	0.69	6.90	5.94	576.85	628.71	1.77	6.40	90.98	4	6
6	−6.79	1.77	8.56	1.76	428.74	460.39	1.51	8.49	79.90	1	1
7	−5.87	−1.68	4.19	4.35	448.38	400.84	1.55	−6.39	72.21	8	11
8	−5.85	−1.64	4.21	7.55	286.23	273.50	1.39	−3.46	61.40	3	6
9	−5.86	−1.74	4.12	11.36	448.38	404.80	1.55	−5.68	72.50	7	11
10	−6.10	−1.67	4.43	5.06	432.38	384.94	1.50	−5.31	71.61	7	10

EG: Energy gap; DM: Dipole moment; MW: Molecular Weight; OVA: Ovality; LOG P: Lipophilicity; POL: Polarozability; HBD: Hydrogen bond donor; HBA: Hydrogen Bond Acceptor.

3.2. Molecular docking investigation

The docking of selected phytochemicals in *A. spinulosa* leaves was executed in 4-aminobutyrate-aminotransferase. Ten phytochemicals were docked into the active site of the 4-aminobutyrate-aminotransferase with PDB ID 1ohv and binding affinity, residue involved in the interactions as well as types of nonbonding interaction involved in the docked complexes were observed. The report obtained for studied docked complexes were: compound **1** (–33.472 kJ mol^{-1}; Lys442, Asp441, Asp415, Arg404, Met186, Arg222; conventional hydrogen bond, carbon hydrogen bond, pi-cation, pi-anion, pi-alkyl); compound **2** (–35.564 kJ mol^{-1}; Cys169, Phe161, Arg156, Pro178, Arg152, Arg349, Tyr180; conventional hydrogen bond, pi-cation, pi-sulfur, pi-pi stacked, pi-alkyl); compound **3** (–34.7272 kJ mol^{-1}; Lys145, Pro178, Trp215, Met149, Phe144, Phe148, Phe213, Cys177, Gly176; carbon hydrogen bond, alkyl, pi-alkyl); compound **4** (–32.6352 kJ mol^{-1}; Phe148, Arg349, Tyr180, Pro178, Arg156, Arg152, Gly176; conventional hydrogen bond, unfavorable donor-donor, pi-pi stacked, pi-alkyl); compound **5** (–33.472 kJ mol^{-1}; Val231, Leu223, Leu227, Gly409, Ala381; conventional hydrogen bond, unfavorable acceptor-acceptor, alkyl) (**Figs. 1–9**).

Moreover, compound **6** (–35.1456 kJ mol^{-1}; Val88, Leu363, Tyr79, Gln71, Ile75, Val85, Leu84, Tyr49; conventional hydrogen bond, pi-alkyl, alkyl); compound **7** (–33.0536 kJ mol^{-1}; Glu270, Ile426, Gly440, Asn423, Arg430; conventional hydrogen bond, unfavorable donor-donor, alkyl); compound **8** (–33.0536 kJ mol^{-1}; Lys442, Ser443, Cys439, Asp415, Asp441, Arg404, Pro221, Phe220, Met186, Arg222; conventional hydrogen bond, carbon hydrogen bond, pi-cation, pi-anion, pi-alkyl); compound **9** (-35.9824 kJ mol^{-1}; Arg152, Pro178, Phe148, Tyr180, Gly176, Arg349; conventional hydrogen bond, carbon hydrogen bond, pi-cation, pi-pi stacked, pi-stacked); compound **10** (–33.0536 kJ mol^{-1}; Leu355, Ile131, Pro344, Gln129, Leu130, Arg343; conventional hydrogen bond, carbon hydrogen bond, unfavorable donor-donor, unfavorable acceptor-acceptor, pi-sigma, alkyl).

According to the report shown in **Table 3**, 2-(3,4-dihydroxyphenyl)-5,7-dihydroxy-3-(((2S,3R,4R,5R,6S)-3,4,5-trihydroxy-6-methyltetrahydro-2H-pyran-2-yl)oxy)-4H-chromen-4-one (compound **9**) proved to be superior based on the docking score of –35.9824 kJ mol^{-1} when compared to other studied compounds as well as the reference drug (clobazam). Oyeneyin *et al.* (2022) reported that lower binding affinity value of any molecule is an indication that such compound has a higher potential ability to inhibit than other studied compounds; thus, the selection of compound **9** as superior to other studied compound was considered appropriate. As shown in **Fig. 9**, series of nonbonding interactions were observed in the interaction between 2-(3,4-dihydroxyphenyl)-5,7-dihydroxy-3-(((2S,3R,4R,5R,6S)-3,4,5-trihydroxy-6-methyltetrahydro-2H-pyran-2-yl)oxy)-4H-chromen-4-one (compound **9**) and 4-aminobutyrate-aminotransferase; the nonbonding interaction involved wee conventional hydrogen bond, carbon hydrogen, pi-pi stacked and pi-alkyl. The conventional hydrogen bond was observed between Tyr180 and hydrogen (H14), Gly176 and hydrogen (H11) as well as Arg349 and oxygen (O7), which showed the specificity of compound **9** in the active site of 4-aminobutyrate-aminotransferase. Also, the hydrogen bond formed by compound **9** with the studied receptor was observed to enhance the exactness of calculated binding affinity (**Fig. 10**). Also, carbon hydrogen bond was observed between Pro178 and oxygen (O1); pi-cation interaction was observed between Arg349 and the aromatic ring attached to the parent compound; its presence between Arg349 and Pi-electron cloud in the aromatic compound was observed to enhance the lowest calculated binding affinity value when compared to the binding for other studied compounds as well as the binding score for the reference drug. The result also revealed the level of bioavailability, selectivity, steadiness, and lipophilicity of 2-(3,4-dihydroxyphenyl)-5,7-dihydroxy-3-(((2S,3R,4R,5R,6S)-3,4,5-trihydroxy-6-methyltetrahydro-2H-pyran-2-yl)oxy)-4H-chromen-4-one (compound **9**) to be more desirable when compares to that of the other studied compounds and clobazam (referenced drug).

The presence of pi-pi stacked (Phe148 and the electron cloud of the aromatic ring of the parent compound) and pi-alkyl (Pro178 and Arg152 attracted to the electron cloud of the aromatic ring of the studied compound) interactions also augmented the accomplishment of lowest binding score by compound **9** when compared to other studied compounds (**Fig. 11**).

Yan *et al.* (2022) investigated the activity of *A. spinulosa* leaves as potential anti-Alzheimer disease agents. It was observed that the polyphenols isolated from *A. spinulosa* leaves were excellent antioxidant agents and a potential ingredient for the alleviation of Alzheimer disease. Therefore, their report agreed well with the work carried out in this study as antiepilepsy agents. Also, the activity of *Alsophila* spp. against Gram positive and negative bacteria using the Kirby–Bauer disc diffusion method was investigated by Longtine and Tejedor (2017). It was observed that ethanolic extract of *Alsophila* spp. proved to be more active again Gram positive than Gram negative bacteria. The activity of these plants as anti-Gram positive bacteria goes in line with the *A. spinulosa* as antiepilepsy.

Table 3. Calculated binding score.

	Binding Affinity (kJ mol⁻¹)	Residues involved in the interactions	Types of Nonbonding interaction involved
1	−33.472	Lys442, Asp441, Asp415, Arg404, Met186, Arg222	Conventional hydrogen bond, carbon hydrogen bond, pi-cation, pi-anion, pi-alkyl
2	−35.564	Cys169, Phe161, Arg156, Pro178, Arg152, Arg349, Tyr180,	Conventional hydrogen bond, pi-cation, pi-sulfur, pi-pi stacked, pi-alkyl
3	−34.7272	Lys145, Pro178, Trp215, Met149, Phe144, Phe148, Phe213, Cys177, Gly176	Carbon hydrogen bond, alkyl, pi-alkyl
4	−32.6352	Phe148, Arg349, Tyr180, Pro178, Arg156, Arg152, Gly176	Conventional hydrogen bond, unfavorable donor-donor, pi-pi stacked, pi-alkyl
5	−33.472	Val231, Leu223, Leu227, Gly409, Ala381	Conventional hydrogen bond, unfavorable acceptor-acceptor, alkyl
6	−35.1456	Val88, Leu363, Tyr79, Gln71, Ile75, Val85, Leu84, Tyr49	Conventional hydrogen bond, pi-alkyl, alkyl
7	−33.0536	Glu270, Ile426, Gly440, Asn423, Arg430	Conventional hydrogen bond, unfavorable donor-donor, alkyl
8	−33.0536	Lys442, Ser443, Cys439, Asp415, Asp441, Arg404, Pro221, Phe220, Met186, Arg222	Conventional hydrogen bond, carbon hydrogen bond, pi-cation, pi-anion, pi-alkyl
9	−35.9824	Arg152, Pro178, Phe148, Tyr180, Gly176, Arg349	Conventional hydrogen bond, carbon hydrogen bond, pi-cation, pi-pi stacked, pi-stacked
10	−33.0536	Leu355, Ile131, Pro344, Gln129, Leu130, Arg343	Conventional hydrogen bond, carbon hydrogen bond, unfavorable donor-donor, unfavorable acceptor-acceptor, pi-sigma, alkyl
Clobazam	−31.7984	-	-

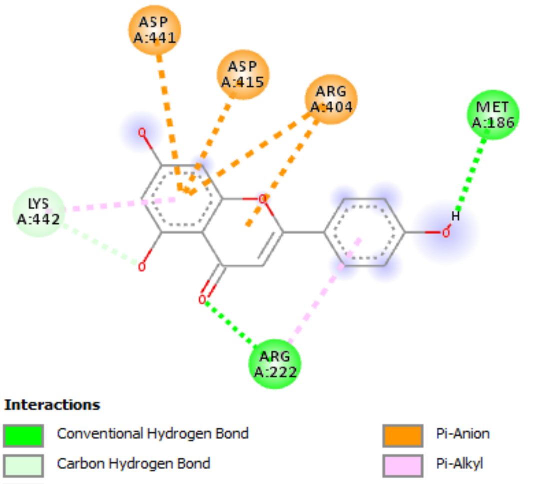

Figure 1. 2D structures of interaction between compound **1** and 4-aminobutyrate-aminotransferase (PDB ID: 1ohv).

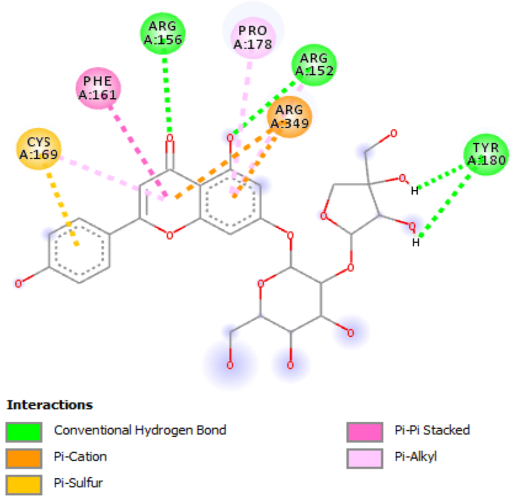

Figure 2. 2D structures of interaction between compound **2** and 4-aminobutyrate-aminotransferase (PDB ID: 1ohv).

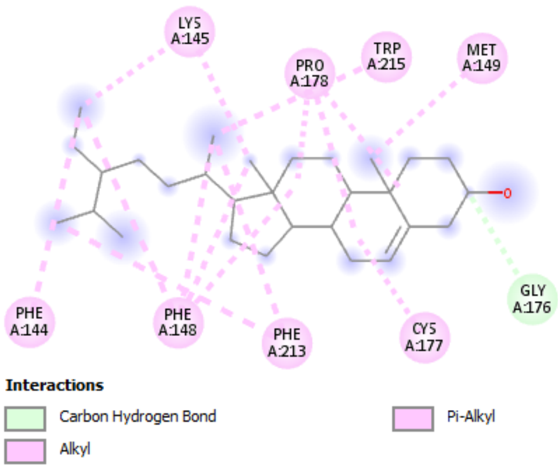

Figure 3. 2D structures of interaction between compound **3** and 4-aminobutyrate-aminotransferase (PDB ID: 1ohv).

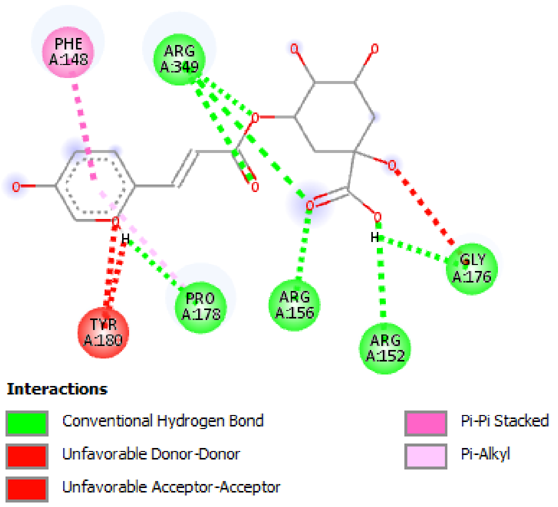

Figure 4. 2D structures of interaction between compound **4** and 4-aminobutyrate-aminotransferase (PDB ID: 1ohv).

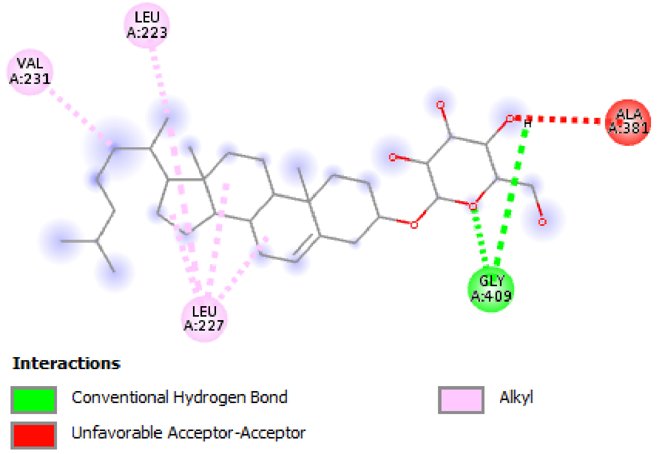

Figure 5. 2D structures of interaction between compound **5** and 4-aminobutyrate-aminotransferase (PDB ID: 1ohv).

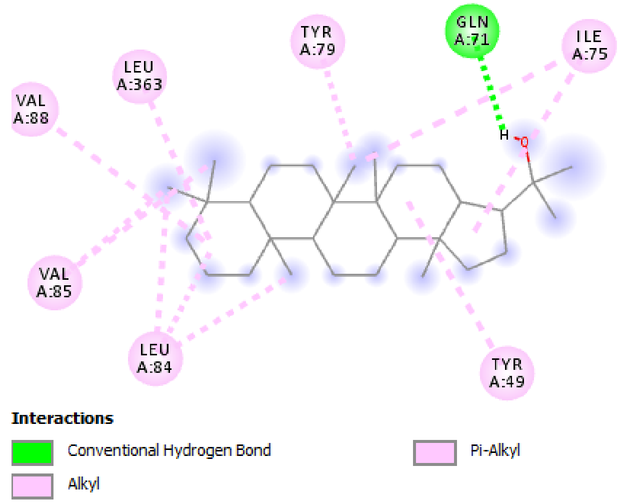

Figure 6. 2D structures of interaction between compound **6** and 4-aminobutyrate-aminotransferase (PDB ID: 1ohv).

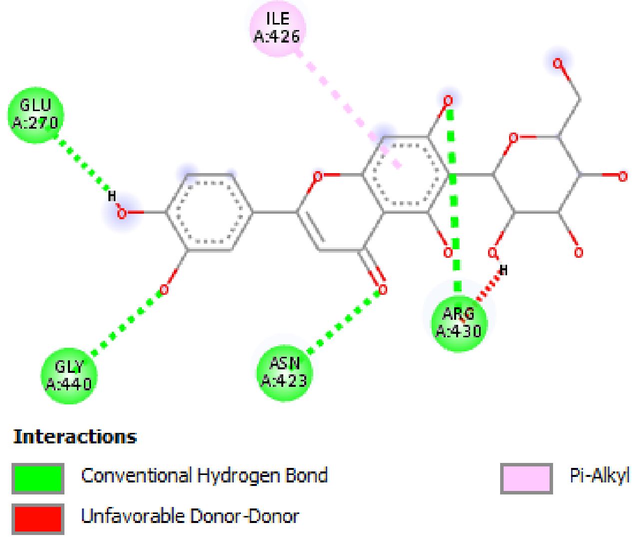

Figure 7. 2D structures of interaction between compound **7** and 4-aminobutyrate-aminotransferase (PDB ID: 1ohv).

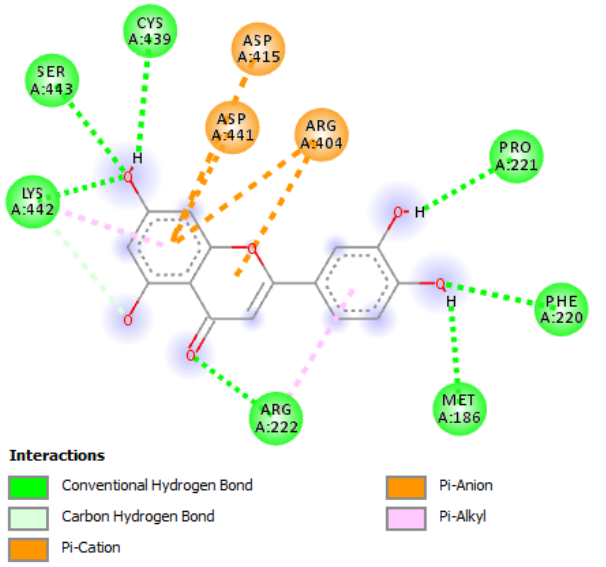

Figure 8. 2D structures of interaction between compound **8** and 4-aminobutyrate-aminotransferase (PDB ID: 1ohv).

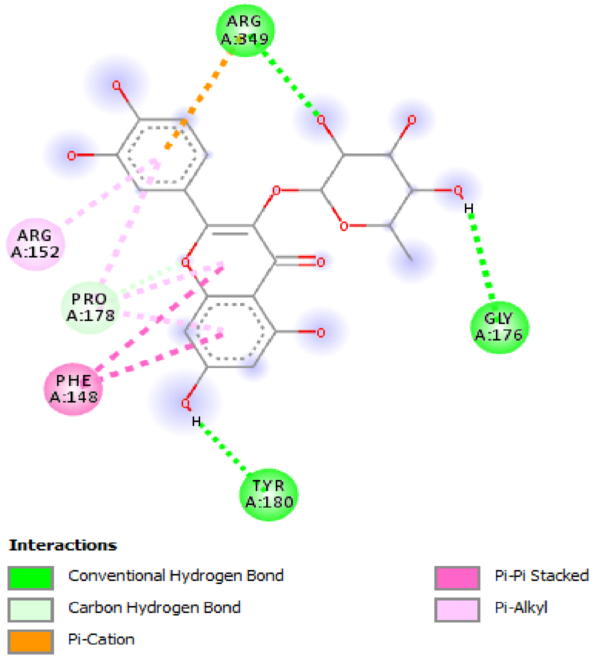

Figure 9. 2D structures of interaction between compound **9** and 4-aminobutyrate-aminotransferase (PDB ID: 1ohv)

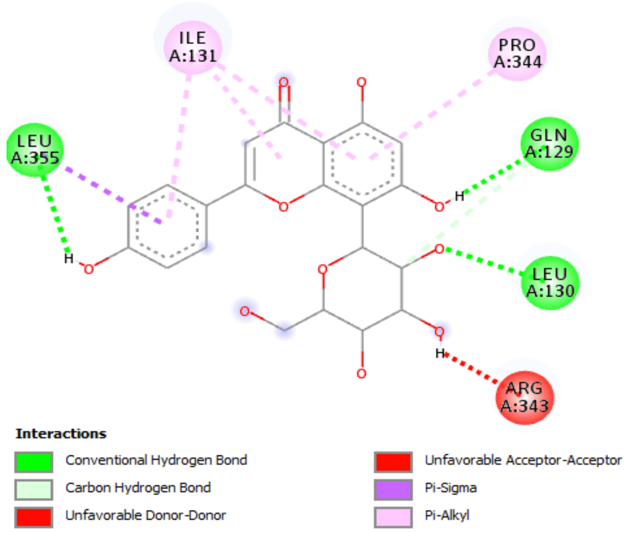

Figure 10. 2D structures of interaction between compound **10** and 4-aminobutyrate-aminotransferase (PDB ID: 1ohv).

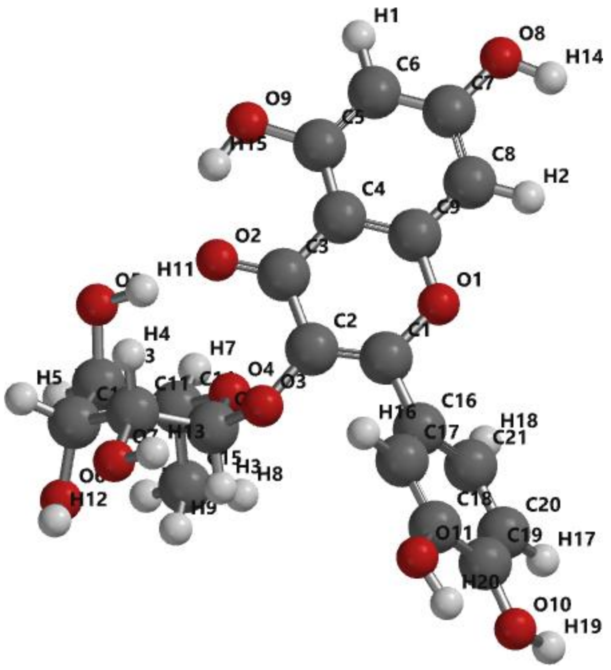

Figure 11. 3D structure of 2-(3,4-dihydroxyphenyl)-5,7-dihydroxy-3-(((2S,3R,4R,5R,6S)-3,4,5-trihydroxy-6-methyltetrahydro-2H-pyran-2-yl)oxy)-4H-chromen-4-one (compound **9**).

3.3. Pharmacokinetic analysis

The calculated ADMET features were obtained using ADMETsar (Cheng *et al.*, 2012). The ADMET properties compound with the lowest binding score (compound **9**) and the reference drug (clobazam) were investigated and the result for each compound are shown in **Tables 4** and **5**. The ADMET properties obtained for compound **9** were in a close range to the properties obtained for the reference drug. This indicates that 2-(3,4-dihydroxyphenyl)-5,7-dihydroxy-3-(((2S,3R,4R,5R,6S)-3,4,5-trihydroxy-6-methyltetrahydro-2H-pyran-2-yl)oxy)-4H-chromen-4-one (compound **9**) possess a greater attribute of a drug to inhibit 4-aminobutyrate-aminotransferase thereby downregulate epilepsy.

Table 4. Pharmacokinetic prediction for compound **9**.

ADMET Predicted Profile --- Classification		
Model	**Result**	**Probability**
Absorption		
Blood-brain barrier	BBB-	0.7568
Human intestinal absorption	HIA+	0.9051
Caco-2 permeability	Caco2-	0.7493
P-glycoprotein substrate	Substrate	0.6415
P-glycoprotein inhibitor	Noninhibitor	0.8740
	Noninhibitor	0.7784
Renal organic cation transporter	Noninhibitor	0.9396
Distribution		
Subcellular localization	Mitochondria	0.7163
Metabolism		
CYP450 2C9 substrate	Nonsubstrate	0.7557
CYP450 2D6 substrate	Nonsubstrate	0.9171
CYP450 3A4 substrate	Nonsubstrate	0.6312
CYP450 1A2 inhibitor	Noninhibitor	0.5306
CYP450 2C9 inhibitor	Noninhibitor	0.8538
CYP450 2D6 inhibitor	Noninhibitor	0.9547
CYP450 2C19 inhibitor	Noninhibitor	0.8339
CYP450 3A4 inhibitor	Noninhibitor	0.7109
CYP inhibitory promiscuity	Low CYP inhibitory promiscuity	0.5648
Human ether-a-go-go-related gene inhibition	Weak inhibitor	0.9846
	Noninhibitor	0.8181
AMES toxicity	Non-AMES toxic	0.9319
Carcinogens	Noncarcinogens	0.9461
Fish toxicity	High FHMT	0.9657
Tetrahymena pyriformis toxicity	High TPT	0.9945

Honey bee toxicity	High HBT	0.6560
Biodegradation	Not biodegradable	0.9073
Acute oral toxicity	III	0.5184
Carcinogenicity (three-class)	Nonrequired	0.6170
ADMET Predicted Profile --- Regression		
Model	**Value**	**Unit**
Absorption		
Aqueous solubility	−3.4974	LogS
Caco-2 permeability	−0.3114	LogPapp, cm s^{-1}
Rat acute toxicity	2.5458	LD50, mol kg^{-1}
Fish toxicity	0.6766	pLC50, mg L^{-1}
Tetrahymena pyriformis toxicity	0.8401	pIGC50, ug L^{-1}

Table 5. Pharmacokinetic prediction for Clobazam.

ADMET Predicted Profile --- Classification		
Model	**Result**	**Probability**
Absorption		
Blood-brain barrier	BBB+	0.9904
Human intestinal absorption	HIA+	0.9900
Caco-2 permeability	Caco2+	0.7487
P-glycoprotein substrate	Nonsubstrate	0.5733
P-glycoprotein inhibitor	Noninhibitor	0.5462
	Noninhibitor	0.9204
Renal organic cation transporter	Noninhibitor	0.7373
Distribution		
Subcellular localization	Mitochondria	0.4586
Metabolism		
CYP450 2C9 substrate	Nonsubstrate	0.7058
CYP450 2D6 substrate	Nonsubstrate	0.8607
CYP450 3A4 substrate	Substrate	0.6871
CYP450 1A2 inhibitor	Noninhibitor	0.6829
CYP450 2C9 inhibitor	Noninhibitor	0.5296
CYP450 2D6 inhibitor	Noninhibitor	0.8908
CYP450 2C19 inhibitor	Noninhibitor	0.5791
CYP450 3A4 inhibitor	Inhibitor	0.7008
CYP inhibitory promiscuity	Low CYP inhibitory promiscuity	0.5308
Excretion		
Toxicity		
Human ether-a-go-go-related gene inhibition	Weak inhibitor	0.9896
	Noninhibitor	0.8651
AMES toxicity	Non-AMES toxic	0.9132
Carcinogens	Noncarcinogens	0.7846
Fish toxicity	High FHMT	0.9713
Tetrahymena pyriformis toxicity	High TPT	0.9399
Honey bee toxicity	Low HBT	0.9163
Biodegradation	Not biodegradable	1.0000
Acute oral toxicity	IV	0.6201
Carcinogenicity (three-class)	Nonrequired	0.5725
ADMET Predicted Profile --- Regression		
Absorption		
Aqueous solubility	−4.5627	LogS
Caco-2 permeability	1.8526	LogPapp, cm s^{-1}
Rat acute toxicity	1.7313	LD50, mol kg^{-1}
Fish toxicity	1.0749	pLC50, mg L^{-1}
Tetrahymena pyriformis toxicity	0.8911	pIGC50, ug L^{-1}

4. Conclusions

Ten molecular compounds obtained from *A. spinulosa* leaves were investigated using *in silico* approach. The assessment of the potential inhibitory properties of selected phytochemicals present in *A. spinulosa* against human 4-aminobutyrate-aminotransferase and exploration of the potential nonbonding interaction involved in the studied complexes and their efficiency were accomplished in this work. The descriptors obtained from the optimized phytochemicals revealed that the studied medicinal plant have potential antiepileptic capacity. Moreover, the selected phytochemicals and the studied 4-aminobutyrate-aminotransferase (PDB ID: 1ohv), which were subjected to docking study, resulted into series of binding scores to expose the inhibiting capability of each compound. Compound 9 (2-(3,4-dihydroxyphenyl)-5,7-dihydroxy-3-(((2S,3R,4R,5R,6S)-3,4,5-

trihydroxy-6-methyltetrahydro-2H-pyran-2-yl)oxy)-4H-chromen-4-one) proved to possess highest binding strength to inhibit 4-aminobutyrate-aminotransferase than other selected phytochemicals in *A. spinulosa* leaves and the reference drug thereby down-regulating epilepsy. The pharmacokinetic features calculated for compound **9** and clobazam (reference drug) revealed that compound **9** (2-(3,4-dihydroxyphenyl)-5,7-dihydroxy-3-(((2S,3R,4R,5R,6S)-3,4,5-trihydroxy-6-methyltetrahydro-2H-pyran-2-yl)oxy)-4H-chromen-4-one) have superior characteristic to inhibit 4-aminobutyrate-aminotransferase than other selected studied phytochemicals obtained from *A. spinulosa* leaves, thereby hindering the operation of epilepsy in human. These findings may open door for the design and development of library of efficient 2-(3,4-dihydroxyphenyl)-5,7-dihydroxy-3-(((2S,3R,4R,5R,6S)-3,4,5-trihydroxy-6-methyltetrahydro-2H-pyran-2-yl)oxy)-4H-chromen-4-one-based drug-like compounds as potential antiepileptic agent.

Authors' contributions

Conceptualization: Oyebamiji, A. K.; **Data curation**: Olujinmi, F. E.; **Formal Analysis**: Akintelu, S. A.; **Funding acquisition**: Not applicable; **Investigation**: Adetuyi, B. O.; Ogunlana, O. O.; **Methodology**: Semire, B.; **Project administration**: Oyebamiji, A. K.; **Resources**: Babalola, J. O.; **Software**: Semire, B.; **Supervision**: O'Reilly, R. K.; **Validation**: Olawoye, B. M.; Aworinde, J. O.; **Visualization**: Oyebamiji, A. K.; **Writing – original draft**: Oyebamiji, A. K.; Semire, B.; **Writing – review & editing**: Oyebamiji, A. K.

Data availability statement

All data sets were generated or analyzed in the current study.

Funding

Not applicable.

Acknowledgments

We are grateful to the computational chemistry research laboratory, Industrial Chemistry Programme, BOWEN University, Nigeria for the computational resources and Mrs E.T. Oyebamiji and Miss Priscilla F. Oyebamiji for their assistance in the course of this work.

References

Abbas, M.; Saeed, F.; Anjum, F. M.; Afzaal, M.; Tufail, T.; Bashir, M. S.; Ishtiaq, A.; Hussain, S.; Suleria, H. A. R. Natural polyphenols: An overview. *Int J Food Prop.* **2016**, *20*, 1689–1699. https://doi.org/10.1080/10942912.2016.1220393

Adeoye, M. D.; Oyebamiji, A. K.; Ashiru, M. A.; Adigun, R. A.; Olalere, O. H.; Semire, B. Biological evaluation of selected metronidazole derivatives as anti-nitroreductase via *in silico* approach. *Eclét Quím.* **2022**, *47* (4), 27–36. https://doi.org/10.26850/1678-4618eqj.v47.4.2022.p27-36

Bartolini, E.; Ferrari, A. R.; Fiori, S.; Della Vecchia, S. Glycaemic imbalances in seizures and epilepsy of paediatric age: A literature review. *J Clin Med.* **2023**, *12*, 2580. https://doi.org/10.3390/jcm12072580

Chen, F.-Z.; Xiang, Q.-X.; Li, S.-H. Chemical constituents in the leaves of *Alsophila spinulosa*. *Xibei Zhiwu Xuebao.* **2008**, *28* (6), 1246–1249.

Cheng, F.; Li, W.; Zhou, Y.; Shen, J.; Wu, Z.; Liu, G.; Lee, P. W.; Tang, Y. AdmetSAR: a comprehensive source and free tool for evaluating chemical ADMET properties. *J Chem Inf Model.* **2012**, *52* (11), 3099–3105. https://doi.org/10.1021/ci300367a

Chiang, H.-C.; Ying-Jui, L.; Fung-Jou, L. Xanthine oxidase inhibitors from the leaves of *Alsophila spinulosa* (HOOK) TRYON. *J Enzyme Inhihitron*. **1994**, *8* (1), 61–71. https://doi.org/10.3109/14756369409040777

Chinese DmgDictionay, New Edition, (1985), Vol. 2, p. 1409, Fig. 2721. Sin Wen Hong Publications Inc., Taipei, Taiwan.

Choi, S.-Y.; Churchich, J. E. Biosynthesis of 4-aminobutyrate aminotransferase. *Eur J Biochem.* **1986**, *161*, 289–294. https://doi.org/10.1111/j.1432-1033.1986.tb10445.x

Dunkel, H.; Strzelczyk, A.; Schubert-Bast, S.; Kieslich, M. Facial emotion recognition in patients with juvenile myoclonic epilepsy. *J Clin Med.* **2023**, *12*, 4101. https://doi.org/10.3390/jcm12124101

Duraipandiyan, V.; Ayyanar, M.; Ignacimuthu, S. Antimicrobial activity of some ethnomedicinal plants used by Paliyar Tribe from Tamil Nadu, India. *BMC Complement. Altern Med.* **2006**, *6*. https://doi.org/10.1186/1472-6882-6-35

El fadili, M.; Er-Rajy, M.; Kara, M.; Assouguem, A.; Belhassan, A.; Alotaibi, A.; Mrabti, N.N.; Fidan, H.; Ullah, R.; Ercisli, S.; Zarougui, S.; Elhallaoui, M. QSAR, ADMET *in silico* pharmacokinetics, molecular docking and molecular dynamics studies of novel bicyclo (aryl methyl) benzamides as potent GlyT1 inhibitors for the treatment of schizophrenia. *Pharmaceuticals*. **2022a**, *15*, 670. https://doi.org/10.3390/ph15060670

El Fadili, M.; Er-Rajy, M.; Imtara, H.; Kara, M.; Zarougui, S.; Altwaijry, N.; Al Kamaly, O.; Al Sfouk, A.; Elhallaoui, M. 3D-QSAR, ADME-tox *In Silico* Prediction and molecular docking studies for modeling the analgesic activity against neuropathic pain of novel NR2B-selective NMDA receptor antagonists. *Processes*. **2022b**, *10*, 1462. https://doi.org/10.3390/pr10081462

Erazua, E. A.; Oyebamiji, A. K.; Akintelu, S. A.; Adewole, P. D.; Adelakun, A.; Adeleke, B. B. Quantitative Structure-Activity relationship, Molecular docking and ADMET screening of tetrahydroquinoline derivatives as anti-small cell lung cancer agents. *Eclét Quím.* **2023**, *48* (1), 55–71. https://doi.org/10.26850/1678-4618eqj.v48.1.2023.p55-71

Gaglianoa, L.; Elie Bou, A.; Dang, K. N.; Sandy, R.; Mohamad, S. Bilateral preictal signature of phase-amplitude coupling in canine epilepsy. *Epilepsy Res.* **2018**, *139*, 123–128. https://doi.org/10.1016/j.eplepsyres.2017.11.009

Gao, X.; Jia, X.; Xu, M.; Xiang, J.; Lei, J.; Li, Y.; Lu, Y.; Zuo, S. Regulation of gamma-aminobutyric acid transaminase expression and its clinical significance in hepatocellular carcinoma. *Front Oncol.* **2022**, *12*, 879810. https://doi.org/10.3389/fonc.2022.879810

Hesdorffer, D. C.; Logroscino, G.; Benn, E. K.; Katri, N.; Cascino, G.; Hauser, W. A. Estimating risk for developing epilepsy: A population-based study in Rochester, Minnesota. *Neurology.* **2011**, *76*, 23–27. https://doi.org/10.1212/WNL.0b013e318204a36a

Hirtz, D.; Thurman, D. J.; Gwinn-Hardy, K.; Mohamed, M.; Chaudhuri, A. R.; Zalutsky R. How common are the 'common' neurologic disorders? *Neurology.* **2007**, *68*, 326–337. https://doi.org/10.1212/01.wnl.0000252807.38124.a3

Irene, C.-H.; Juan, R.-R.; Luis, G. B.-B.; Lilia, M.-L. Tree ferns (Cyatheaceae) as a source of phenolic compounds – A review. *J Herb Med.* **2022**, *35*, 100587. https://doi.org/10.1016/j.hermed.2022.100587

Jeżowska-Jurczyk, K.; Jurczyk, P.; Budrewicz, S.; Pokryszko-Dragan, A. Evaluation of event-related potentials in assessing cognitive functions of adult patients with epilepsy of unknown etiology. *J Clin Med.* **2023**, *12*, 2500. https://doi.org/10.3390/jcm12072500

Kan, W. S. *Pharmaceutical botany*. National Research Institute of Chinese Medicine, 1986.

Kebede, T.; Gadisa, E.; Tufa A. Antimicrobial activities evaluation and phytochemical screening of some selected medicinal plants: A possible alternative in the treatment of multidrug-resistant microbes. *PLoS ONE.* **2021**, *16* (3), e0249253. https://doi.org/10.1371/journal.pone.0249253

Kim, K.; Yoon, H. Gamma-aminobutyric acid signaling in damage response, metabolism, and disease. *Int J Mol Sci.* **2023**, *24*, 4584. https://doi.org/10.3390/ijms24054584

Kwan, P.; Brodie, M. J. Early identification of refractory epilepsy. *N Engl J Med*. **2000**, *342*, 314–319. https://doi.org/10.1056/NEJM200002033420503

Lanza, K.; Gohlke, J.; Wang, S.; Sheffield, P. E.; Wilhelmi, O. Predicting the potential suitable habitats of *Alsophila spinulosa* and their changes. *Int J Biometeorol.* **2022**, *66* (8), 1575–1588. https://doi.org/10.1007/s00484-022-02302-5

Longtine, C.; Tejedor A. Antimicrobial activity of ethanolic and aqueous extracts of medicinally used tree ferns *Alsophila cuspidata* and *Cyathea microdonta*. *Acta Bot Malacit.* **2017**, *42* 119–123. https://doi.org/10.24310/abm.v42i1.2885

Mishra, A.; Sharma A.; Kumar, S.; Saxena, A.; Pandey, A. *Bauhinia variegata* leaf extracts exhibit considerable antibacterial, antioxidant, and anticancer activities. *BioMed Res Int.* **2013**, 2013, 1–10. https://doi.org/10.1155/2013/915436

Morton, C. V. Society the classification of the Cyatheaceae by R. M. Tryon. *Am Fern J.* **1971**, *61*, 142–143. https://doi.org/10.2307/1546647

Mukhopadhyay, H. K.; Kandar, C. C.; Das, S. K.; Ghosh, L.; Gupta, B. K. Epilepsy and its management: A review. *Journal of PharmaSciTech.* **2012**, *1*(2), 20-26.

Oyebamiji, A. K.; Akintayo, E. T.; Semire, B.; Odelade, K. A.; Adetuyi, B. O.; Amin, H.; Batiha, G. E. *Insilico* investigation on isatin(1H-indole-2,3-dione) derivatives as potential anti-tumor necrosis factor-alpha. *Trop J Nat Prod Res*. **2022**, *6* (11), 1870–1875.

Oyeneyin, O. E.; Iwegbulam, C. G.; Ipinloju, N.; Olajide, B. F.; Oyebamiji, A. K. Prediction of the antiproliferative effects of some benzimidazolechalcone derivatives against MCF-7 breast cancer cell lines: QSAR and molecular docking studies. *Org. Commun.* **2022**, *15* (3), 273–287. https://doi.org/10.25135/acg.oc.132.2203.2374

Pitout, J. D. D. Multiresistant Enterobacteriaceae: New threat of an old problem. *Expert Rev Anti Infect Ther.* **2008**, *6* (5), 657–669. https://doi.org/10.1586/14787210.6.5.657

Poulakou, G.; Lagou, S.; Karageorgopoulos, D. E.; Dimopoulos, G. New treatments of multidrug-resistant Gram-negative ventilator-associated pneumonia. *Ann Transl Med.* **2018**, *6* (20), 423–423. https://doi.org/10.21037/atm.2018.10.29

Queeny, I. P.; Daniel, C. M.; Jenny, C.; Robin, B. H.; David, M. L. An update on the prevalence and incidence of epilepsy among older adults. *Epilepsy Res.* **2018**, *139*, 107–112. https://doi.org/10.1016/j.eplepsyres.2017.11.022

Semire, B.; Oyebamiji, A. K.; Odunola O. Tailoring of Energy Levels in (2Z)-2-cyano-2-[2-[(E)-2-[2-[(E)-2-(p-tolyl)vinyl]thieno[3,2-b]thiophen-5-yl]vinyl]pyran-4-ylidene]acetic acid Derivatives via Conjugate Bridge and Fluorination of Acceptor units for Effective D-π-A Dye-Sensitized Solar Cells: DFT-TDDFT Approach. *Res Chem Intermed.* **2017**, *43*, 1863–1879. https://doi.org/10.1007/s11164-016-2735-0

Shen, S.; Butrin, A.; Beaupre, B. A.; Ferreira, G. M.; Doubleday, P. F.; Grass, D. H.; Zhu, W.; Kelleher, N. L.; Moran, G. R.; Liu, D.; Silverman, R. B. Structural and mechanistic basis for the inactivation of human ornithine aminotransferase by (3*S*,4*S*)-3-amino-4-fluorocyclopentenecarboxylic acid. *Molecules*. **2023**, *28* (3), 1133. https://doi.org/10.3390/molecules28031133

Shriram, V.; Khare, T.; Bhagwat, R.; Shukla, R.; Kumar, V. Inhibiting bacterial drug efflux pumps via phytotherapeutics to combat threatening antimicrobial resistance. *Front Microbiol*. **2018**, *9*, 1–18. https://doi.org/10.3389/fmicb.2018.00001

Storici, P.; Biase, D.; Bossa, F.; Bruno, S.; Mozzarelli, A.; Peneff, C.; Silverman, R. B.; Schirmer, T. Structures of y-aminobutyric acid (GABA) aminotransferase, a pyridoxal 5'-phosphate, and [2Fe-2S] cluster-containing enzyme, complexed with y-ethynyl-GABA and with the antiepilepsy drug vigabatrin. *J Biol Chem* **2004**, *279* (1), 363–373. https://doi.org/10.1074/jbc.M305884200

Vaou, N.; Stavropoulou, E.; Voidarou, C.; Tsigalou, C.; Bezirtzoglou, E. Towards advances in medicinal plant antimicrobial activity: A review study on challenges and future perspectives. *Microorganisms* **2021**, *9*, 2041. https://doi.org/10.3390/microorganisms9102041

Vijayakumar, S.; Kasthuri, G.; Prabhu, S.; Manogar, P.; Parameswari, N. Screening and identification of novel inhibitors against human 4-aminobutyrate-aminotransferase: A computational approach. *Egypt J Basic Appl Sci.* **2018**, *5*, 210–219. https://doi.org/10.1016/j.ejbas.2018.05.008

Waziri, I.; Kelani, M. T.; Oyedeji-Amusa, M. O.; Oyebamiji, A. K.; Coetzee, L.-C. C.; Adeyinka, A. S.; Muller, A. J. Synthesis and computational investigation of N,N-dimethyl-4-[(Z)-(phenylimino)methyl] aniline derivatives: Biological and quantitative structural activity relationship studies. *J Mol Struct.* **2023**, *1276*, 134756. https://doi.org/10.1016/j.molstruc.2022.134756

Werhahn, K. J. Epilepsy in the elderly. *Dtsch Arztebl Int.* **2009**, *106*, 135–142. https://doi.org/10.3238/arztebl.2009.0135

Yan, N.; Zhang, H.; Zhang, Z.; Zhou, L.; Chen, T.; Feng, S.; Ding, C.; Yuan, M. The extraction, antioxidant and against b-amyloid induced toxicity of polyphenols from *Alsophila spinulosa* leaves. *Arabian J Chem.* **2022**, *15*, 103707. https://doi.org/10.1016/j.arabjc.2022.103707

Yasuhide, K.; Shigeko, F. S.; Koichi, M.; Tomoko, O.; Keiji, S.; Nanaya, T. The mature size of rat 4-aminobutyrate aminotransferase is different in liver and brain. *Eur J Biochem.* **1999**, *264*, 218–222. https://doi.org/10.1046/j.1432-1327.1999.00612.x

Zhang, M.; Zhong, H.; Cao, T.; Huang, Y.; Ji, X.; Fan, G. C.; Peng, T. Gamma-aminobutyrate transaminase protects against lipid overload-triggered cardiac injury in mice. *Int J Mol Sci*. **2022**, *23* (4), 2182. https://doi.org/10.3390/ijms23042182

Eclet. Quim. 49 | e-1512, 2024

Original Article

https://doi.org/10.26850/1678-4618.eq.v49.2024.e1512

Phytochemical screening, antiproliferative evaluation, and molecular docking studies of *Acacia nilotica* fruit from Nigeria

William Ojoniko **Anthony**[1], Ejike Onwudiegwu **Okpala**[1], Obiyenwa Kehinde **Gabriel**[1], Godfrey Okechukwu **Eneogwe**[1], Semire **Banjo**[1,2+]

Abstract

Acacia nilotica, (*Fabaceae*), is valued for its medicinal properties. We examine the antiproliferative properties of the aqueous fruit extract of *A. nilotica*. Aqueous extract from *Acacia* has been associated with potential anticancer effects in fruits and vegetables through screening, antiproliferative, and molecular docking evaluation. Phytochemical screening reveals the presence of alkaloids, saponins, tannins, flavonoids, steroids, and carbohydrates. The extracts showed significant antiproliferative effects at eight concentrations (8–50 mg mL^{-1}) examined in comparison to the standard (methotrexate). When compared to *Sorghum bicolor* seed radicles treated with methotrexate at 48, 72, and 96 h, 50 mg mL^{-1} extract significantly inhibited the generation of seed radicals, with potent inhibitions of 87.06, 83.48, and 81.45%. Analysis of molecular docking results showed that [(2*R*,3*S*)-2-(3,4-dihydroxyphenyl)-3,5-dihydroxy-3,4-dihydro-2*H*-chromen-7-yl]3,4,5-trihydroxybenzoate (D21), (5*R*,9*R*,10*R*,13*S*,14*S*,17*S*)-17-[(2*S*,4*R*)-4-[(2*S*)-3,3-dimethyloxiran-2-yl]-4-hydroxybutan-2-yl]-4,4,10,13,14-pentamethyl-1,2,5,6,9,11,12,15,16,17-decahydrocyclopenta[a]phenanthren-3-one (D28) and [(2*R*,3*S*)-2-(3,4-dihydroxyphenyl)-3,7-dihydroxy-3,4-dihydro-2*H*-chromen-5-yl] 3,4,5-trihydroxybenzoate (D29) have strong tendency to inhibit dihydrofolate reductase (1VDR), capase-9 (6J15) and *Mycobacterium tuberculosis* (Mtb) (6J17) better than methotrexate and azacitidine, known antiproliferative drugs. These findings support the use of *A. nilotica* in traditional medicine for the treatment of tuberculosis and cancer.

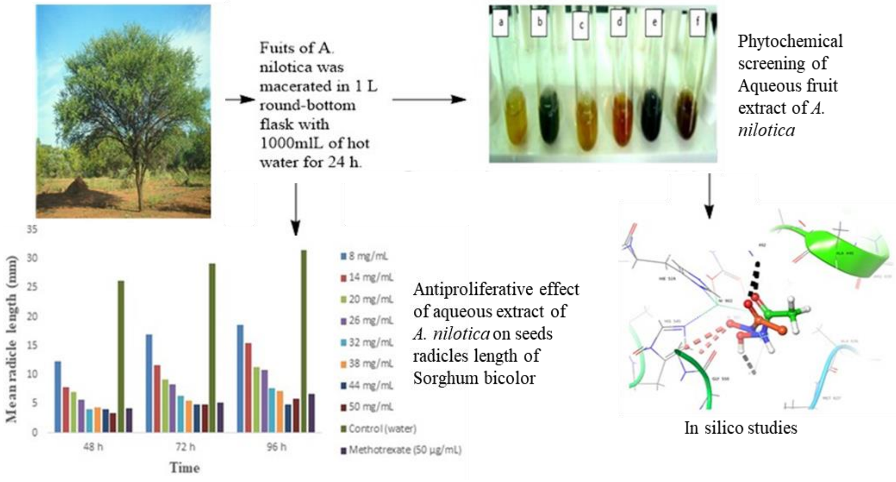

Article History

Received August 13, 2023
Accepted November 07, 2023
Published January 18, 2024

Keywords

1. *Acacia nilotica*;
2. *Fabaceae* family;
3. *Sorghum bicolor* seed radicles;
4. inhibitory effects;
5. in-silico studies.

Section Editor

Assis Vicente Benedetti

Highlights

- Aqueous extract of *Acacia nilotica* fruit was obtained.
- Phytochemical screening of aqueous fruit extract of *A. nilotica.*
- Evaluation of antiproliferative properties of the aqueous fruit extract.
- Molecular docking studies of phytochemicals identified in leaves and fruits.

[1]Federal University Lokoja, Faculty of Science, Kogi State, Nigeria. [2]Ladoke Akintola University of Technology, Department of Pure and Applied Chemistry, Ogbomosho, Nigeria. **+Corresponding author:** Banjo Semire, **Phone:** +234 8038269809, **Email address:** bsemire@lautech.edu.ng

1. Introduction

Cancer stands as one of the most terrifying diseases of the twenty-first century, emerging as a leading cause of mortality. It is a challenging inherited disorder that poses a serious public health risk, with factors such as exposure to chemicals, poor dietary habits, genetic mutations, and environmental influences contributing to its onset. Due to its high mortality rate, cancer has become a huge global public health concern (Sung *et al.,* 2021). However, recent predictions also suggested that the number of cancer-related deaths could rise to roughly 16 million by 2040 (Gopal and Sharpless, 2021), making it urgently necessary to develop the ideal anticancer treatments that would effectively treat this condition (Mukherji *et al.,* 2021). Sixty per cent of the currently used anticancer drugs were reportedly developed from medicinal plants (Enegide *et al.,* 2014; Li-Weber, 2009).

The natural diversity of medicinal plants and their diverse phytochemicals have greatly benefited the use of medicinal plants as biomodifiers. They have been successfully used as precursors in the discovery and development of novel drugs (Butler, 2008; Muschietti *et al.,* 2013). One benefit of using medicinal plants is their synergistic nature, which is superior to using individual medications to treat diseases (Yuan *et al.,* 2016). Some of the successful medications that were made from natural products include artemisinin and its analogues, which are frequently used as antimalarials, acetyldigoxin from *Digitalis lanata*, which is used as a cardiotonic, aescin from *Aesculus hippocastanum*, which is used as an anti-inflammatory, lapachol as an anticancer, and antitumor from *Tabebuia* species (Kumari *et al.,* 2019; Taylor, 2000).

The Leguminosae family includes the *Acacia nilotica* tree, which may reach heights of 15 to 18 m and a diameter of 2 to 3 m. Bagaruwa is a frequent name for it among Hausa people from northern Nigeria. In Western and Northern Nigeria, the plant is known to be used medicinally. Young delicate pods of the plant are consumed as vegetables; roasted seeds are used as a seasoning or fermented to produce alcoholic beverages; and boiling bark is used to produce a beverage that has a coffee-like flavor (Tanko *et al.,* 2014). For skin conditions, diarrhea, dysentery, cough, diabetes, eczema, wound healing, and burning feeling, as well as an astringent, demulcent, and antiasthmatic, the bark, root, gum, leaves, fruit, and flowers have all been used. Teeth are washed with delicate twigs (Roozbeh and Darvish, 2016). In Nigeria's northern region, leaves are used to cure typhoid disease. Although there are many methods to prepare it, boiling it in water and letting it cool before eating is a common method. Before consuming the herbal mixture, the patient may breathe in the steam as an alternate form of treatment (Sarkiyayi and Abdul Rasheed, 2013). Therefore, the goal of our research is to evaluate and screen the phytochemicals in *A. nilotica* fruit's aqueous extract for potential antiproliferative activity, which has historically been utilized in Nigeria to treat cancer and other ailments.

Furthermore, the main bioactive chemicals of the *A. nilotica* that had been isolated and reported (Eldeen *et al.,* 2010; Kumari *et al.,* 2020; Mohmmed and Babiker, 2019; Singh *et al.,* 2010) were downloaded from the online library, PubChem (www.https://pubchem.ncbi.nlm.nih.gov/) and screened using molecular docking method against dihydrofolate reductase (**DHFR**), X-linked inhibitor of apoptosis protein (**XIAP**) and *Mycobacterium tuberculosis* (Mtb) type VII secretion system (**T7SS**). Dihydrofolate reductase (**DHFR**, **ID: 1VDR**) is a vital enzyme in the catalysis of the NADPH-linked reduction of 7,8-dihydrofolate and subsequent production of thymidylate. DHFR and thymidylate synthase are target enzymes in cancer chemotherapy (Pieper *et al.,*1998). It has been reported that DHFR is inhibited by antineoplastic and immunosuppressive agents, such as methotrexate by the nonproliferation of malignant cells, it also serves as an antirheumatic agent (Askari and Krajinovic, 2010). Another critical form of cancer is leukemia, which affects blood-forming tissues such as the bone marrow and the lymphatic system. The causes of leukemia are X-linked inhibitor of apoptosis protein (**XIAP**, **ID: 6J15**), an apoptotic regulator protein that binds to the effector caspases-3 and -7 through its BIR2 domain, and initial caspase-9 through its BIR2 and BIR3 (Cossu *et al.,* 2009). Azacitidine is one of the medicines that work well as XIAP antagonists. The human tuberculosis pathogen Mtb infects around 33% of the global population and causes at least one million deaths annually (WHO, 2018). For the treatment of tuberculosis, several medications are available that target the type VII secretion system (**T7SS**, **ID: 6J17**). These medications, like isoniazid, must be used for an extended period (Mi *et al.,* 2022). Due to the rise of multidrug-resistant Mtb strains, these medications can be costly, have major side effects, and lose their effectiveness (Salvatore and Zhang, 2017; Wang *et al.,* 2020).

2. Material and methods

2.1 Plant

2.1.1. Collection and identification

Biological Science Department of Federal University Lokoja, Kogi State, Nigeria.

2.1.2. Plant preparation and extraction

Fifty grams (50 g) of the air-dried and pulverized fruits of *A. nilotica* were macerated in a 1 L round-bottom flask with 1,000 mL of water for 24 h. The resultant mixture was filtered. Using a rotating evaporator under reduced pressure, the clear filter was concentrated to dryness at 60–80 °C to obtain *A. nilotica* fruit aqueous extract.

2.2. Preliminary phytochemical screening

A powder sample of *A. nilotica* fruit was subjected to phytochemical screening using the methods outlined by (Yusuf *et al.,* 2014) to detect chemical components.

2.2.1. Identification of steroids and triterpenes

A test tube containing 3 g of the powdered sample and 10 mL of 50% ethanol was filled with the mixture. The tube was then submerged in a water bath and heated for 3 min. After that, it was filtered and allowed to cool to ambient temperature. After the filtrate had been dried out in an evaporating dish, 5 mL of petroleum ether was added, and the mixture was swirled for 5 min before the petroleum ether portion was decanted and disposed of. After adding 10 mL of chloroform and stirring it for around 5 min, the mixture was put into a test tube. Next, 0.5 mg of anhydrous sodium sulphate was added, gently agitated, and filtered. The filtrate was then separated into two test tubes and utilized for the subsequent experiments.

Lieberman–Burchard's reaction: An equivalent volume of acetic anhydride was added to test tube I and gently stirred. Subsequently, 1 mL of concentrated H_2SO_4 was poured into the tube's side. Sterols and triterpenes are indicated by the formation of a brownish-red ring at the point of contact between the two liquids and a greenish color in the separation layer.

Salwoski's Test: In test tube II, a lower layer was created by adding two to three drops of concentrated sulfuric acid. A steroidal ring was present when the interphase was reddish-brown.

2.2.2. Identification of alkaloids

Two grams of powdered leaves and 20 mL of 5% sulfuric acid in 50% ethanol were cooked together in a water bath. After cooling, the mixture was filtered. There was a reserved amount. A second part of the filtrate was added to a 100 mL separating funnel, and two drops of strong ammonia solution were added to the solution to turn it alkaline. To let the layer separate, an equal volume of chloroform was added and gently shaken. The lower layer of chloroform was drained into an additional separating funnel. The layer of ammonia was set aside. Two volumes of diluted sulfuric acid, each containing 5 mL, were used to remove the chloroform layer. Next, the different extracts were put to the following test:

Mayer's Test: 1 mL of Mayer's reagent was applied drop by drop to the filtrate in test tube I. Alkaloids were presented when a cream-colored or greenish-colored precipitate formed.

Dragendorff's Test: 1 mL of Dragendorff's reagent was applied, drop by drop, to the filtrate in test tube II. A reddish-brown precipitate's formation suggests the presence of alkaloids.

Wagner's Test: 1 mL of Wagner's reagent was applied, drop by drop, to the filtrate in tube III. A reddish-brown precipitate's formation suggests the presence of alkaloids.

2.2.3. Identification of tannins

Ten milliliters of 50% alcohol were used to extract 2 g of fruit sample. The mixture was then filtered, and the resulting filtrate was split into three sections for the subsequent tests.

Ferric chloride test: Three drops of a diluted $FeCl_3$ solution were applied to test tube I; the presence of tannins is indicated by the formation of a blue or greenish-black color that turns olive green when more ferric chloride is added.

Bromine water test: The second part of the filtrate received three drops of bromine water added to it. Condensed tannins are indicated by a buff-colored precipitate, whereas hydrolysable tannins produce none.

Lead subacetate test: In the third section, three drops of lead subacetate solution were added. The presence of tannins is shown by the formation of a colored precipitate.

2.2.4. Identification of anthraquinones

Borntrager's test (for free anthracene derivatives): 5 min were spent shaking the 0.5 g of the powdered fruit of *A. nilotica* in a test tube with 5 mL of chloroform added. After the mixture was filtered, an equivalent volume of 10% ammonia solution was shaken with the filtrate. When the aqueous layer is agitated, the presence of free anthraquinone is indicated by a pink, red, or violet color.

Modified Borntrager's test (for combined anthracene derivatives): 5 mL of 10% hydrochloric acid was heated with 1 g of the powdered fruit for 3 min. After cooling and filtering the heated solution in a test tube, 5 mL of benzene was carefully removed from it. After pipetting off the top layer of benzene, the test tube containing half of its volume of 10% ammonium hydroxide solution was gently shaken. The ammonia layer's color changes from rose pink to cherry red when anthraquinone is present.

2.2.5. Identification of saponins

Frothing test: A test tube containing 0.5 g of powdered fruit was filled with 10 mL of distilled water, and the mixture was forcefully shaken for 30 s. After that, it was left to stand for 30 min and examined. The presence of saponins is indicated by the formation of honeycomb foam.

Hemolysis test: 1 g of the fruit sample was extracted using distilled water, and 2 mL of an aqueous NaCl solution was added to a test tube along with 2 mL of the filtrate. Next, three drops of animal blood were added to the tube using a syringe, and the tube was gently mixed by inverting it (no shaking) and left to stand for 15 min. The red blood cells' tendency to settle indicates the presence of saponins.

2.2.6. Identification of flavonoids

Two grams of the fruit sample that had been powdered were fully detained using acetone. After letting the acetone evaporate in a water bath, the residue was removed using warm water. Following a hot filtering of the combination, the filtrate was allowed to cool before being utilized in the subsequent test:

Shinoda's Test: 3 mL of the aqueous solution was mixed with a small amount of magnesium chips, and two drops of diluted hydrochloric acid and heated. A pink or red color indicates the presence of flavonoids.

Sodium Hydroxide Test: 2 mL of a 10% NaOH solution was added to test tube II; the yellow solution shows the presence of flavonoids, which turn colorless when diluted hydrochloric acid is added.

$FeCl_3$ Test: After adding three drops of $FeCl_3$ solution to test tube III, a phenolic nucleus is indicated by the development of a greenish-black color.

2.2.7. The Molisch's test for carbohydrates

The fruit sample was extracted with 10 mL of ethanol. To extract the fruit extract, the mixture was filtered via filter paper. A dry test tube containing approximately 2 mL of the fruit sample was filled with 2-3 drops of concentrated tetraoxosulphate (VI) acid and 3 drops of 1% α-naphthol in 80% ethanol. The combination was then stirred vigorously to create an upper phase. The presence of carbohydrates is indicated by the development of a purple or brown color.

2.3. Experimental materials (*Sorghum bicolor*)

Sorghum bicolor, the experimental plant, was purchased from Lokoja's new market in Kogi State. It was put in a water-filled container to undergo a viability screening. The submerged seeds were dried for use and cleaned with alcohol while the floating seeds were thrown away (Ayinde and Agbakwuru, 2010). Commercial methotrexate was acquired from the Lokoja, Kogi State, Nigeria pharmacy.

2.3.1. Determination of growth inhibitory effects of *A. nilotica* fruit aqueous extract on *S. bicolor* seed radical length

Acacia nilotica (4,000 mg) was dissolved in 40 mL of distilled water to obtain a 100 mg mL^{-1} stock solution. Various concentrations (8, 14, 20, 26, 32, 38, 44, and 50 mg mL^{-1}) of *A. nilotica* aqueous extract were prepared and methotrexate 0.167 mg mL^{-1} was used as the positive control. Petri dishes were layered with cotton wool and filter paper (Whatman No. 1). Twenty seeds of *S. bicolor* were placed in each of the Petri dishes. The negative control samples were seeds treated with 15 mL of distilled water containing no extracts. The tested seeds were treated with 15 mL of different prepared concentrations of *A. nilotica* and methotrexate in different Petri dishes, incubated in a dark room, and observed for growth after 24 h. The mean lengths (mm) of radicles emerging from the seeds were measured after 48, 72 and 92 h respectively. The experiment was done in triplicates. The percentage inhibition was calculated as **Eq. 1**:

$$\%\text{inb}=\frac{\text{mean radicle length negative control} - \text{mean radicle length treated}}{\text{mean radicle length negative control}} \times 100 \qquad (1)$$

where percentage growth = 100 – % inhibition (Ayinde *et al.,* 2011; Chinedu *et al.,*2014).

2.3.2. Statistical analysis

The data obtained were expressed as mean ± standard error mean. A two-way analysis of variance was used to test for significance. $P < 0.001$ was considered significant. Graph pad prism (version 6) was used for the analysis.

3. Procedures for molecular docking study

The biochemicals downloaded from PubChem (https://pubchem.ncbi.nlm.nih.gov/) as shown in **Table 1** were optimized (using Density Functional Theory (DFT-B3LYP/6-31G(d,p)) method and docked with the receptors using AutoDock Vina integrated in PyRx software (Horaira *et al.,* 2023; Krishnan *et al.,* 2022; Kirubhanand *et al.,* 2023; Shil *et al.,* 2023).

The receptor proteins (dihydrofolate reductase, (**DHFR**, **ID: 1VDR**); X-linked inhibitor of apoptosis protein (**XIAP**, **ID: 6J15**), and the type VII secretion system (**T7SS**, **ID: 6J17**)) were downloaded from protein data bank website (https://www.rcsb.org/) and were cleaned up with Edupymol version 1.7.4.4 and BIOVIA Discovery Studio 2019 as reported (Adegbola *et al.,* 2021; Adepoju *et al.,* 2022; Oyebamiji *et al.,* 2023). The BIOVIA Discovery Studio 2019 was used to view the 2-D structure of the receptor complexed with co-ligand to determine the active gorge of each receptor, and a grid box was set around the active site. The center and size of the grid box are (x = 16.3147, y = -0.4604, z = 27.9177) and (x = 28.1977, y = 25.0013, z = 25.0231) for 1VDR receptor; (x = 62.4438, y = 14.1519, z = 32.9565) and (x = 33.5779, y = 32.4740, z = 38.0195) for 6J15 receptor; and (x = 17.4933, y = 0.213, z = 14.43267) and x = 37.1836, y = 35.6242, z = 40.9731) for 6J17 receptor, respectively.

Table 1. Bioactive phytochemicals from *A. nilotica* leaf and fruit plant.

Code	3D Structure with IUPAC name	Code	3D Structure with IUPAC name
D1	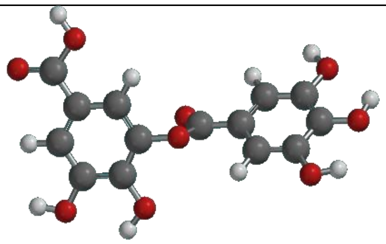 3,4-dihydroxy-5-(3,4,5-trihydroxybenzoyl) oxybenzoic acid	D2	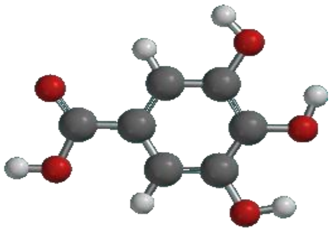 3,4,5-trihydroxybenzoic acid
D3	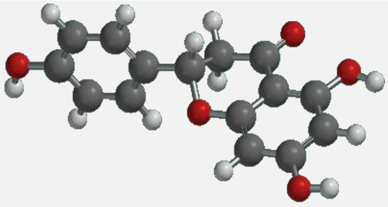 5,7-dihydroxy-2-(4-hydroxyphenyl)-2,3-dihydrochromen-4-one	D4	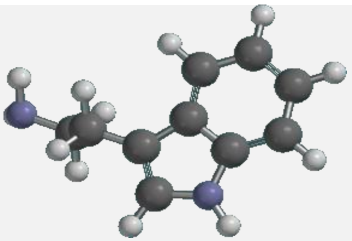 2-(1H-indol-3-yl)ethanamine
D5	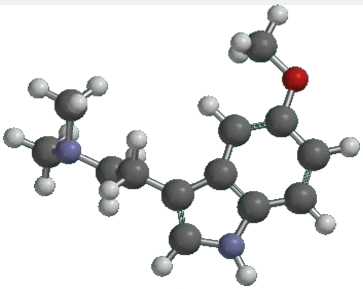 2-(5-methoxy-1H-indol-3-yl)-N,N-dimethylethanamine	D6	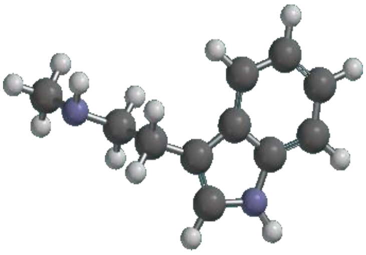 2-(1H-indol-3-yl)-N-ethylethanamine

D7	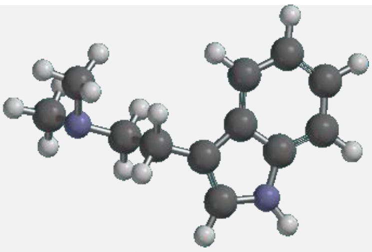 2-(1H-indol-3-yl)-N,N-dimethylethanamine	**D8**	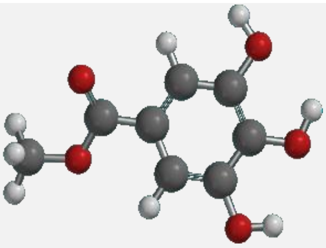 Methyl 3,4,5-trihydroxybenzoate
D9	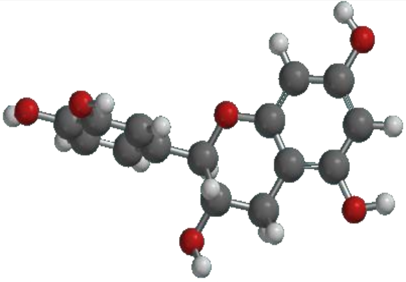 (2*R*,3*S*)-2-(3,4-dihydroxyphenyl)-3,4-dihydro-2*H*-chromene-3,5,7-triol	**D10**	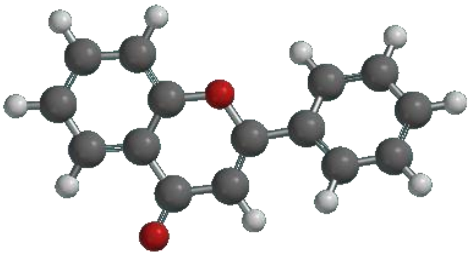 2-phenylchromen-4-one
D11	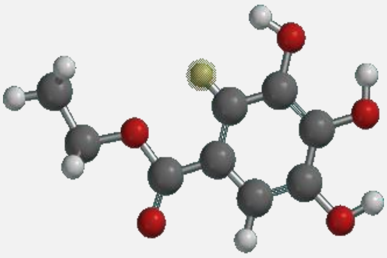 ethyl 3,4,5-trihydroxybenzoate	**D12**	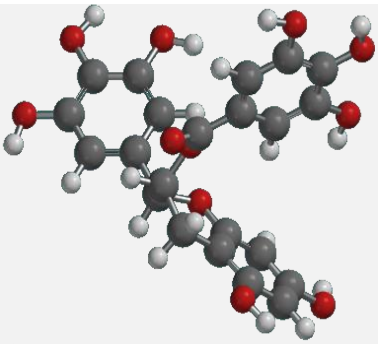 [(2*R*,3*R*)-5,7-dihydroxy-2-(3,4,5-trihydroxyphenyl)-3,4-dihydro-2*H*-chromen-3-yl] 3,4,5-trihydroxybenzoate
D13	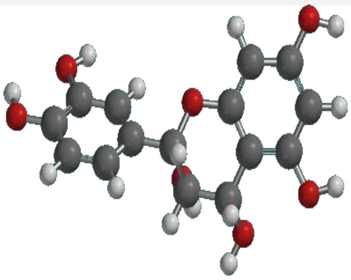 2-(3,4-dihydroxyphenyl)-3,4-dihydro-2*H*-chromene-3,4,5,7-tetrol	**D14**	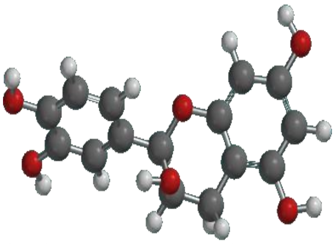 (2*R*,3*R*)-2-(3,4-dihydroxyphenyl)-3,4-dihydro-2*H*-chromene-3,5,7-triol
D15	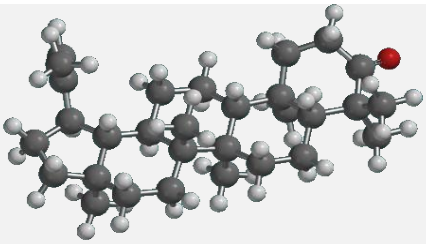 (1*R*,3*aR*,5*aR*,5*bR*,7*aR*,11*aR*,11*bR*,13*aR*,13*bR*)-3*a*,5*a*,5*b*,8,8,11*a*-hexamethyl-1-prop-1-en-2-yl-2,3,4,5,6,7,7*a*,10,11,11*b*,12,13,13*a*,13*b*-tetradecahydro-1*H*-cyclopenta[a]chrysen-9-one	**D16**	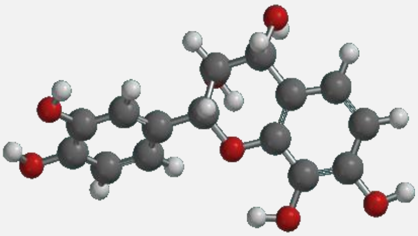 [(2*S*,3*R*,4*S*,5*S*,6*R*)-3,4,5-trihydroxy-6-(hydroxymethyl)oxan-2-yl] 3,4,5-trihydroxybenzoate
D17	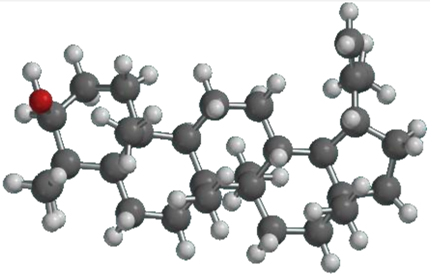	**D18**	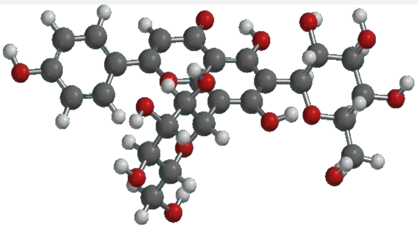 (2*R*,3*R*,4*R*)-2-(3,4-dihydroxyphenyl)-3,4-dihydro-2*H*-chromene-3,4,7,8-tetrol

	2*R*,3*S*,4*R*)-2-(3,4-dihydroxyphenyl)-3,4-dihydro-2*H*-chromene-3,4,7-triol		
D19	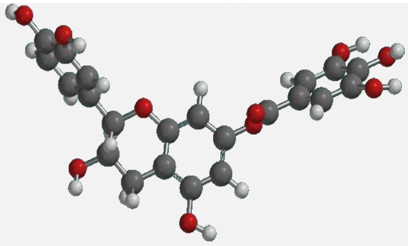 (1*R*,3a*R*,5a*R*,5b*R*,7a*R*,9*S*,11a*R*,11b*R*,13a*R*,13b*R*)-3*a*,5*a*,5*b*,8,8,11*a*-hexamethyl-1-prop-1-en-2-yl-1,2,3,4,5,6,7,7*a*,9,10,11,11*b*,12,13,13*a*,13*b*-hexadecahydrocyclopenta[a]chrysen-9-ol	**D20**	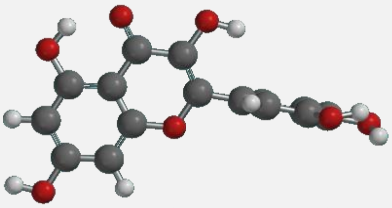 5,7-dihydroxy-2-(4-hydroxyphenyl)-6,8-bis[(2*S*,3*R*,4*R*,5*S*,6*R*)-3,4,5-trihydroxy-6-(hydroxymethyl)oxan-2-yl]chromen-4-one
D21	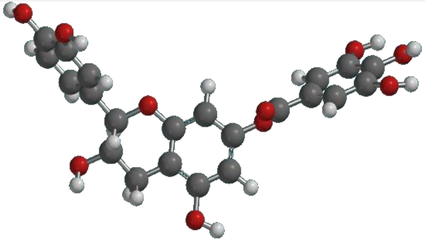 [(2*R*,3*S*)-2-(3,4-dihydroxyphenyl)-3,5-dihydroxy-3,4-dihydro-2*H*-chromen-7-yl] 3,4,5-trihydroxybenzoate	**D22**	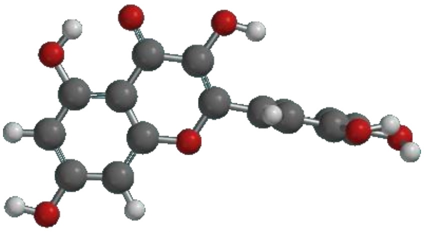 2-(3,4-dihydroxyphenyl)-3,5,7-trihydroxychromen-4-one
D23	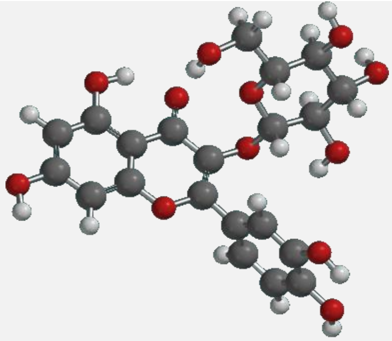 2-(3,4-dihydroxyphenyl)-5,7-dihydroxy-3-[(2*S*,3*R*,4*S*,5*S*,6*R*)-3,4,5-trihydroxy-6-(hydroxymethyl)oxan-2-yl]oxychromen-4-one	**D24**	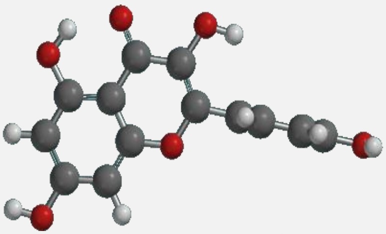 3,5,7-trihydroxy-2-(4-hydroxyphenyl)chromen-4-one
D25	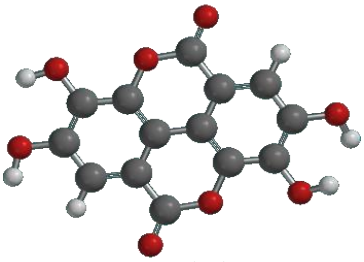 6,7,13,14-tetrahydroxy-2,9-dioxatetracyclo[6.6.2.0^{4,16}.0^{11,15}]hexadeca-1(15),4,6,8(16),11,13-hexaene-3,10-dione	**D26**	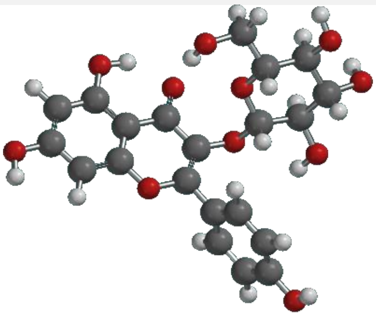 5,7-dihydroxy-2-(4-hydroxyphenyl)-3-[(2*S*,3*R*,4*S*,5*S*,6*R*)-3,4,5-trihydroxy-6-(hydroxymethyl)oxan-2-yl]oxychromen-4-one
D27	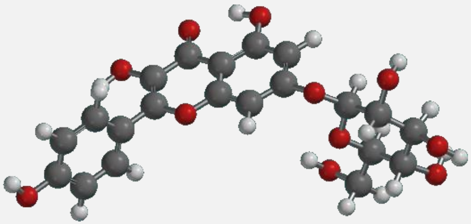 3,5-dihydroxy-2-(4-hydroxyphenyl)-7-[(2*S*,3*R*,4*S*,5*S*,6*R*)-3,4,5-trihydroxy-6-(hydroxymethyl)oxan-2-yl]oxychromen-4-one	**D28**	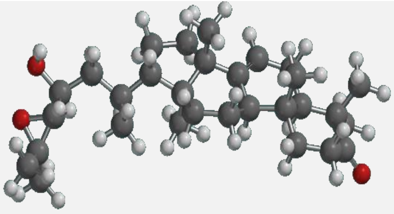 (5*R*,9*R*,10*R*,13*S*,14*S*,17*S*)-17-[(2*S*,4*R*)-4-[(2*S*)-3,3-dimethyloxiran-2-yl]-4-hydroxybutan-2-yl]-4,4,10,13,14-pentamethyl-1,2,5,6,9,11,12,15,16,17-decahydrocyclopenta[a]phenanthren-3-one

D29

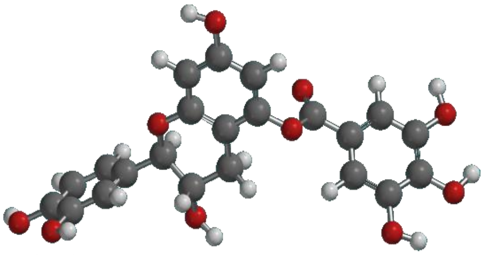

[(2*R*,3*S*)-2-(3,4-dihydroxyphenyl)-3,7-dihydroxy-3,4-dihydro-2*H*-chromen-5-yl] 3,4,5-trihydroxybenzoate

D30

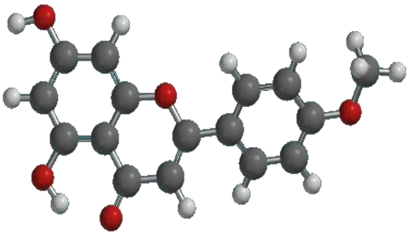

5,7-dihydroxy-2-(4-methoxyphenyl)chromen-4-one

4. Results and discussion

4.1. Phytochemical screening

Five grams of the dried aqueous extract of *A. nilotica* fruit was obtained from a sample of 50 g of powdered *A. nilotica* fruits by water infusion. The yield is 10% (w/w%). **Table 2** displays the findings of the phytochemical analysis of the fruit aqueous extract of *A. nilotica.*

Table 2. Preliminary Phytochemical screening of aqueous fruit extract of *A. nilotica.*

S/No.	Test	Water
1	Carbohydrates	+
2	Flavonoids	+
3	Saponins	+++
4	Tannins	+
5	Anthraquinones	-
6	Alkaloids	+
7	Terpenoids	+
8	Steroids	+

Note: + ve indicates presence, whereas; - ve indicates the absence.

According to the results of the phytochemical analysis, *A. nilotica* fruit contains tannins, alkaloids, saponins, flavonoids, terpenes, steroids, and carbohydrates. Due to the compelling experimental data supporting their capacity to alter how the body responds to allergens, viruses, and cancer-causing substances, flavonoids have also been referred to as *natural biological response modifiers.* According to Bello *et al.* (2011), most identified alkaloids and flavonoids exhibit antiallergic, anti-inflammatory, antibacterial, and anticancer properties. Tannins have antibacterial, antiviral, and antitumor properties, while saponins have antioxidant, anticancer, and anti-inflammatory properties (Kunle and Egbarevba, 2009).

4.2 Inhibitory effects of A. nilotica fruit on the growth of S. bicolor seed radicle

Table 3 and **Fig. 1** show the mean radicle length of *S. bicolor* seeds from treated and untreated *A. nilotica* fruit at 48, 72, and 92 h after incubation. As well as the negative control and the positive control, **Table 4** shows the percentage growth inhibition and percentage growth at 48, 72, and 92 h for seeds treated with various doses (8–50 mg mL^{-1}) of aqueous fruit extract of *A. nilotica* fruit.

This study reveals that *A. nilotica* fruit has good growth-inhibitory effects on *S. bicolor* seed radicals as compared to the negative control seeds. In the lack of nutrients (the negative control), the *S. bicolor* seed sprouts quickly, mimicking the development of cancer cells in people. Like seeds treated with methotrexate (the reference standard), the length of the radicles of seeds exposed to various concentrations of the extract dramatically shrank. *Acacia nilotica* fruit antiproliferative actions are concentration-dependent because the maximum percentage of inhibitions was seen at 50 mg mL^{-1} after 48, 72, and 96 h of incubation, respectively (**Table 4**). Thiagarajan *et al.* (2020) revealed *A. nilotica* leaf extract's antiproliferative properties against the human cancer cell line KB. *A. nilotica* fruit species have reportedly been shown to possess analgesic, antiplasmodial, antimicrobial, antihyperglycemic, and antimicrobial activities (Abd-Ulgadir and El-Kamali, 2017; Raji *et al.,* 2002;). According to Ogbadoyi *et al.* (2011), the methanol extract of *A. nilotica* pods has antihypertensive properties, while the aqueous extract of the seeds has spasmogenic and vasoconstrictor properties.

Table 3. Antiproliferative effect of aqueous extract of *A. nilotica* fruit on seeds radicle length of *S. bicolor.*

S No.	Concentration (mg ml^{-1})	Percentage inhibition			Percentage growth		
		48 h	72 h	96 h	48 h	72 h	96 h
1	H_2O (negative control)	0	0	0	100	100	100
2	MTX (positive control)	83.92	82.19	78.76	16.08	17.80	21.24
3	8	52.99	42.05	41.03	47.01	57.95	58.97
4	14	69.74	59.86	50.86	30.26	40.14	49.14
5	20	73.45	68.59	64.09	26.55	31.41	35.90
6	26	78.02	71.16	65.68	21.98	28.84	34.32
7	32	84.20	78.17	75.51	15.79	21.83	24.49
8	38	84.77	80.91	76.94	15.23	19.09	23.06
9	44	85.14	82.98	80.05	14.86	17.02	19.95
10	50	87.06	83.48	81.45	12.94	16.52	18.55

Note: MTX = methotrexate.

Table 4. Mean radical length growth of *S. bicolor* seeds treated with aqueous extract of *A. nilotica* fruit and reference standards.

S No.	Concentration (mg ml^{-1})	Mean radical length (mm)		
		48 h	72 h	96 h
1	Water (-ve control)	26 ± 2	29 ± 2	31 ± 2
2	Methotrexate (+ve control)	4.2 ± 0.2	5.2 ± 0.4	6.7 ± 0.8
3	8	12.4 ± 0. 9	17 ± 1	19 ± 1
4	14	8.0 ± 0.4	11.7 ± 0.7	16 ± 1
5	20	7.0 ± 0.6	9.2 ± 0.7	11.3 ± 0.8
6	26	5.8 ± 0.4	8.4 ± 0. 7	10.8 ± 0.6
7	32	4.2 ± 0.4	6.4 ± 0.8	8 ± 1
8	38	4.0 ± 0.5	5.6 ± 0.8	7 ± 1
9	44	3.8 ± 0.3	5.0 ± 0.5	6.3 ± 0.9
10	50	3.4 ± 0.5	4.8 ± 0.7	6 ± 1

Note: Values measured as mean ±standard deviation.

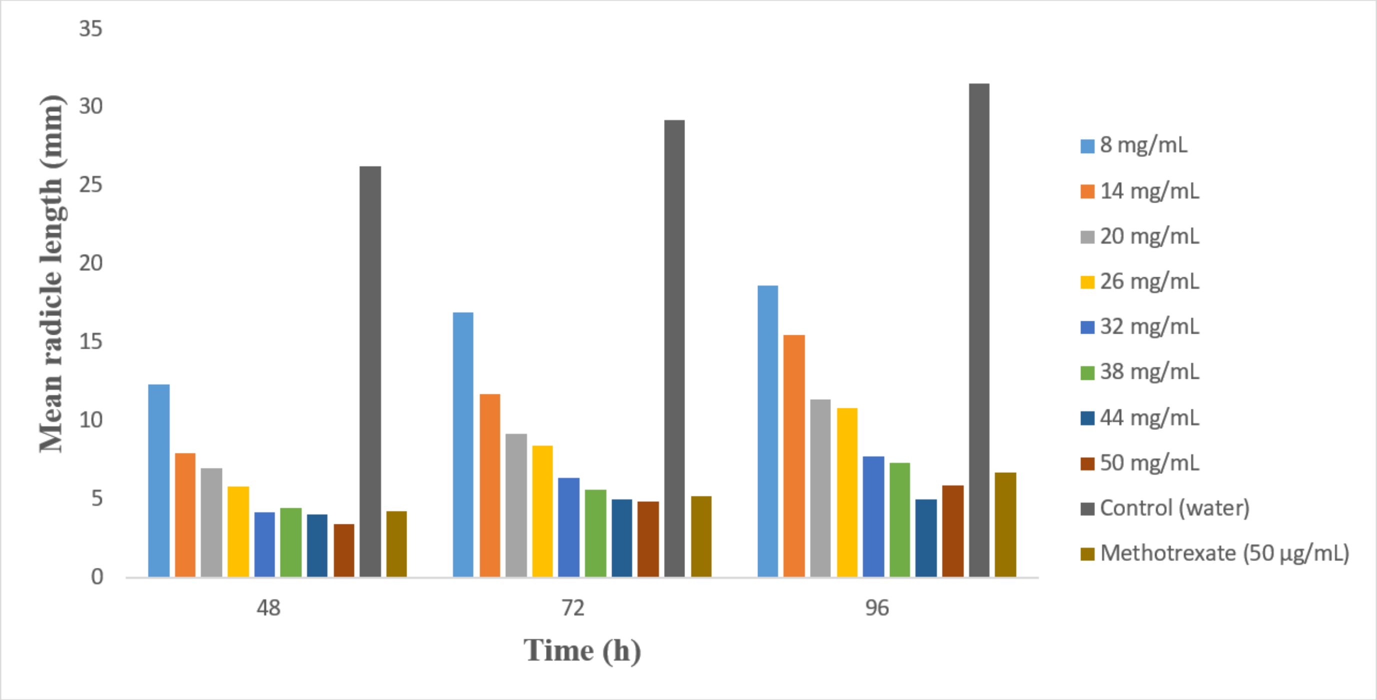

Figure 1. The growth inhibitory effects of the aqueous extract of *A. nilotica* fruit on *S. bicolor* seeds radical length and reference standards.

4.3 Molecular docking analysis

The binding affinities calculated from docking simulation of the bioactive compounds or phytochemicals in the leaf and fruit of the *A. nilotica* plant with the cell proliferating enzymes are presented in **Table 5**. The phytochemicals are docked against dihydrofolate reductase (**DHFR**) for the proliferation of cancer cells (**ID: 1VDR**), X-linked inhibitor of apoptosis protein (**XIAP**) that initials another enzyme called capase-9 for accelerating spreading of cancer (**ID: 6J15**) and enzyme type VII secretion system (**T7SS**) that aids the multiplications of Mtb in human body (**ID: 6J17**), and the interacting modes (hydrogen bonding, hydrophobic and Van der Waal interactions) of the phytochemicals with promising affinities are displayed in **Figs. 2–4**.

Molecular docking results of dihydrofolate reductase (DHFR; 1VDR) docked with the phytochemicals from *A. nilotica* showed that most of the ligands have higher binding affinities than methotrexate, a chemotherapeutic drug for cancer patients. The calculated binding affinities for the most outstanding compounds are **D12** (–36.0 kJ mol^{-1}), **D15** (–39.7 kJ mol^{-1}), **D21** (–38.5 kJ mol^{-1}), **D19** (–38.9 kJ mol^{-1}), **D27** (–35.6 kJ mol^{-1}), **D28** (–37.7 kJ mol^{-1}) and **D29** (39.7 kJ mol^{-1}) compare to methotrexate with binding affinity of –35.1 kJ mol^{-1} (**Tables 1 and 5**), indicating that these compounds can inhibit dihydrofolate reductase better than methotrexate. The drug-likeness of a compound increases with decreasing binding affinity, thus, increasing the ability of the compound to inhibit well (Oyewole *et al.*, 2020; Omotayo *et al.*, 2022). In **1VDR**–ligand complex, **D12** is hydrogen bonded with Tyr 108, also interacted through π–π stacking and π–alkyl with Tyr 33 and Ile 15, respectively; **D15** is interacted with Ala 103 through hydrogen bond, whereas **D19** formed hydrogen with Gly 19; **D21** is hydrogen bonded to Gly 19, Gly 20, Thr 48, Val 6 and Ala 8; π–alkyl with Leu 21, Tyr 33 and Ala 8; **D27** formed two hydrogen bonds with Gly 19 and Ala 8; **D28** interacted via hydrogen bond with Asp 29 and Lys 30 while **D29** is hydrogen bonded to Tyr 108 and Ile 26 (**Fig. 2**).

Similarly, results from docking of **XIAP (ID: 6J15)** with the ligands showed that six phytochemicals have higher inhibitory activities than azacitidine (Table 5) vis-à-vis **D12** (–31.8 kJ mol^{-1}), **D15** (–31.4 kJ mol^{-1}), **D21** (–33.9kJ mol^{-1}), **D27** (–32. 2 kJ mol^{-1}), **D28** (31.8 kJ mol^{-1}) and

D29 (–33.9 kJ mol^{-1}). Thus, these phytochemicals can be better drug candidates than azacitidine (–23.8 kJ mol^{-1}) for the treatment of leukemia. The **6J15**-ligand complex revealed that **D15**, **D21**, **D27** and **D28** were involved in nonbonding interactions with 6J15. However, **D12** formed a hydrogen bond with Trp 99 and Val 48, while **D29** interacted through a hydrogen bond with Gly 97 (**Fig. 3**).

Furthermore, for Mtb (**ID: 6J17**), the docking results presented in Table 5 revealed that **D9** (–32.6 kJ mol^{-1}), **D21** (–33.1 kJ mol^{-1}), **D22** (–32.6 kJ mol^{-1}), **D26** (–32.2 kJ mol^{-1}), **D27** (–33.5 kJ mol^{-1}) and **D29** (–38.1 kJ mol^{-1}) displayed outstanding binding affinities against Mtb than isoniazid (–22.2 kJ mol^{-1}), a chemotherapeutic drug for the treatment of tuberculosis. In **6J17**–ligand complex showed that **D9** has four hydrogen bonds, **D21** and **D29** have five hydrogen bonds, **D22** has one hydrogen bond and **D27** has six hydrogen bonds with amino acid residues in the active site of the **6J17**.

Therefore, both experimental and *in silico* results supported the use of *A. nilotica* for the treatment of cancer and related diseases including tuberculosis, and that hydrogen bonding, hydrophobic and Van der Waal interactions (**Figs. 2–4**) play crucial roles in inhibitory activities of these phytochemicals.

Table 5. Binding affinities of active phytochemicals with **DHFR (ID: 1VDR)**, **XIAP (ID: 6J15)**, and **T7SS (ID: 6J17)**.

S/N	Ligand	PDB ID: 1VDR		PDB ID: 6J15		PDB ID: 6J17	
		Binding affinity (kJ mol^{-1})	Inhibitory constant (Ki, μmol/L)	Binding affinity (kJ mol^{-1})	Inhibitory constant (Ki, μmol/L)	Binding affinity (kJ mol^{-1})	Inhibitory constant (Ki, μmol/L)
1	D1	−32.6	1.90	−29.3	7.35	−30.1	5.24
2	D2	−23.4	78.14	−20.9	215.24	−23.8	66.00
3	D3	−33.9	1.15	−28.5	10.30	−32.2	2.25
4	D4	−23.8	66.00	−23.8	66.00	−23.4	78.14
5	D5	−26.4	23.96	−21.8	153.55	−22.6	109.54
6	D6	−25.5	33.59	−23.4	78.14	−24.3	55.74
7	D7	−24.3	55.74	−22.2	129.69	−22.2	129.69
8	D8	−22.6	109.54	−20.9	215.24	−25.1	39.77
9	D9	−32.6	1.90	−28.9	8.70	−32.6	1.90
10	D10	−33.9	1.15	−30.1	5.24	−31.0	3.74
11	D11	−23.0	92.52	−21.3	181.80	−23.8	60.00
12	D12	−36.0	0.49	−31.8	2.67	−32.2	2.25
13	D13	−33.1	1.61	−26.8	20.24	−30.1	5.24
14	D13	−32.6	1.90	−28.5	10.30	−31.4	3.16
15	D15	−39.7	0.11	−31.4	3.16	−31.8	2.67
16	D16	−30.1	5.24	−26.8	20.24	−29.3	7.35
17	D17	−32.2	2.25	−29.7	6.21	−31.4	3.16
18	D18	−33.1	1.61	−28.9	8.70	−31.4	3.16
19	D19	−38.9	0.15	−31.0	3.74	−31.0	3.74
20	D20	−33.5	1.34	−31.0	3.74	−31.0	3.74
21	D21	−38.5	0.18	−33.9	1.15	−33.1	1.61
22	D22	−33.1	1.61	−28.0	12.19	−32.6	1.90
23	D23	−33.9	1.15	−27.6	14.44	−30.5	4.43
24	D24	−32.6	1.90	−27.2	17.09	−31.4	3.16
25	D25	−33.5	1.36	−28.0	12.19	−31.8	2.67
26	D26	−34.3	0.97	−30.1	5.24	−32.2	2.25
27	D27	−35.6	0.58	−32.2	2.25	−33.5	1.36
28	D28	−37.7	0.25	−31.8	2.67	−30.5	4.43
29	D29	−39.7	0.11	−33.9	1.15	−38.1	0.21
30	D30	−31.0	3.74	−28.0	12.19	−31.0	3.74
Methotrexate		−35.1	0.69				
Azacitidine				−23.8	47.08		
Isoniazid						−22.2	129.69

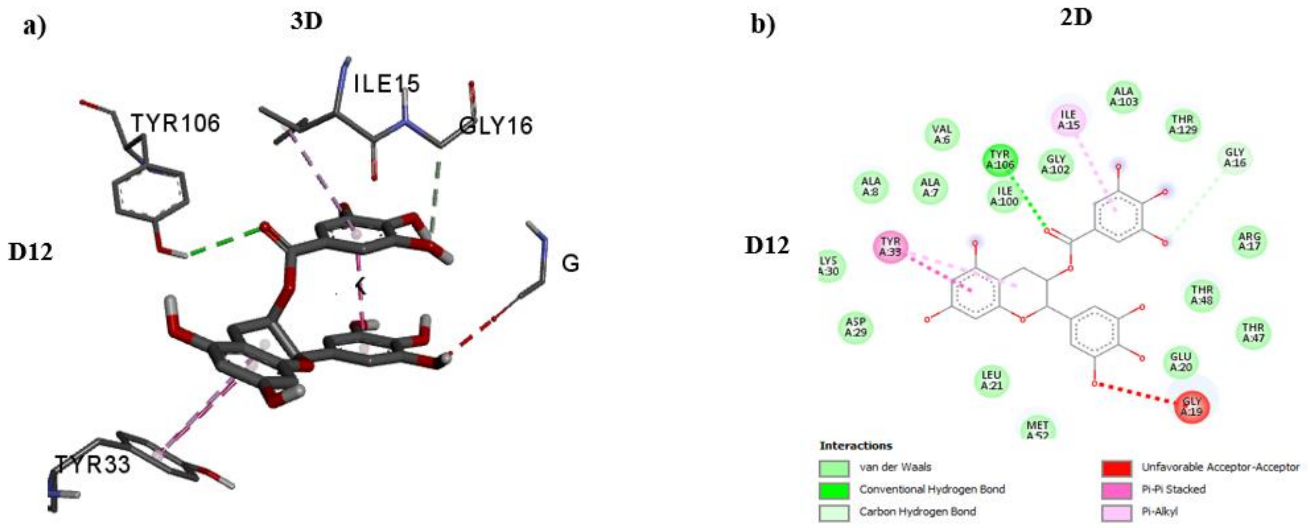

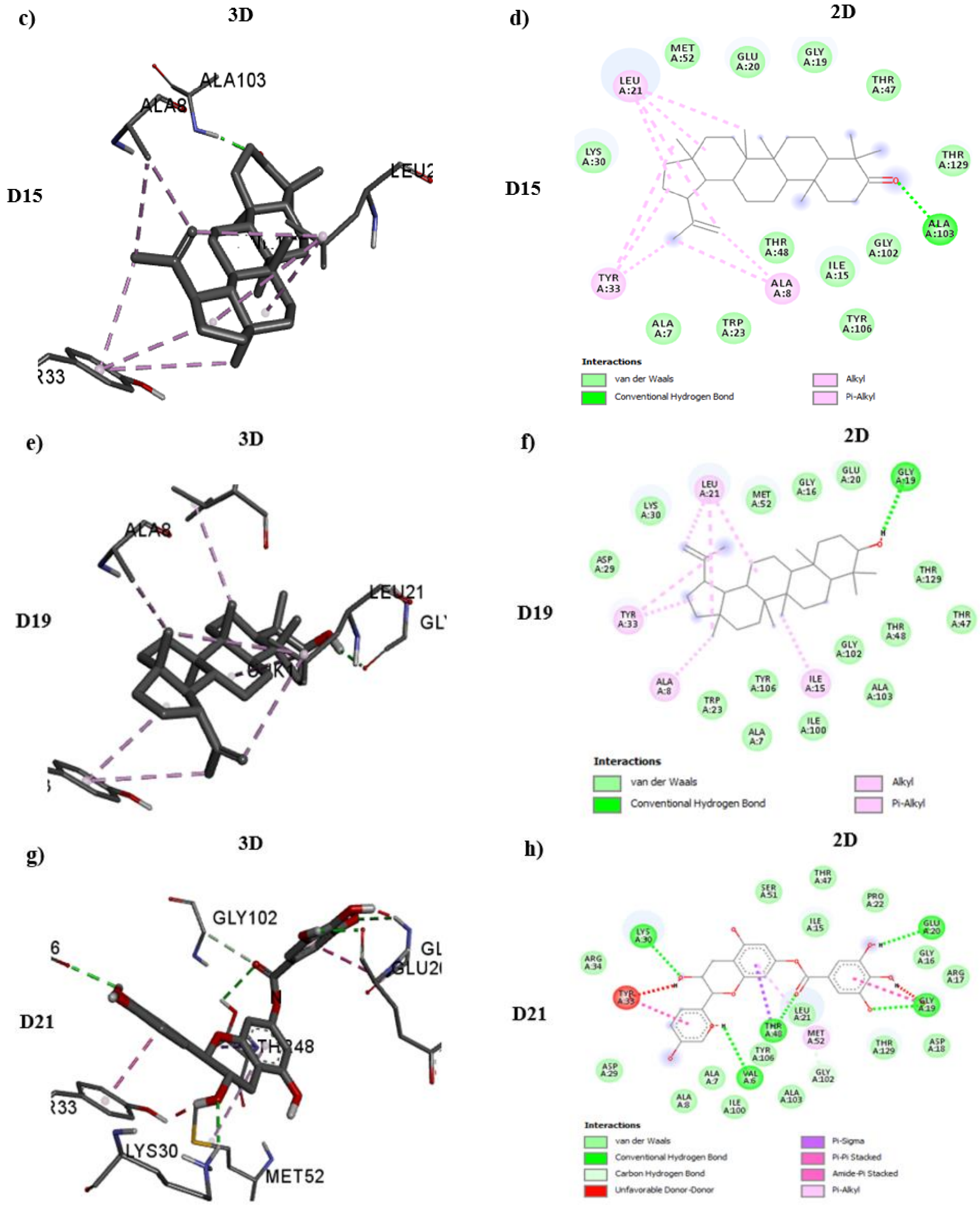
c)
3D
D15
ALA103
ALA8
LEU2
R33
d)
2D
D15
MET A:52
GLU A:20
GLY A:19
LEU A:21
THR A:47
LYS A:30
THR A:129
ALA A:103
THR A:48
GLY A:102
ILE A:15
TYR A:33
ALA A:8
ALA A:7
TRP A:23
TYR A:106
Interactions
van der Waals
Conventional Hydrogen Bond
Alkyl
Pi-Alkyl
e)
3D
D19
ALA8
LEU21
GLY
f)
2D
D19
LEU A:21
GLU A:20
GLY A:19
GLY A:16
MET A:52
LYS A:30
ASP A:29
THR A:129
TYR A:33
THR A:47
THR A:48
GLY A:102
ALA A:8
TYR A:106
ILE A:15
ALA A:103
TRP A:23
ALA A:7
ILE A:100
Interactions
van der Waals
Conventional Hydrogen Bond
Alkyl
Pi-Alkyl
g)
3D
D21
GLY102
6
GL
GLU20
THR48
R33
LYS30
MET52
h)
2D
D21
THR A:47
SER A:51
PRO A:22
ILE A:15
LYS A:30
GLU A:20
ARG A:34
GLY A:16
ARG A:17
TYR A:33
GLY A:19
LEU A:21
THR A:48
MET A:52
THR A:129
ASP A:18
TYR A:106
ASP A:29
ALA A:7
VAL A:6
GLY A:102
ALA A:8
ILE A:100
ALA A:103
Interactions
van der Waals
Conventional Hydrogen Bond
Carbon Hydrogen Bond
Unfavorable Donor-Donor
Pi-Sigma
Pi-Pi Stacked
Amide-Pi Stacked
Pi-Alkyl

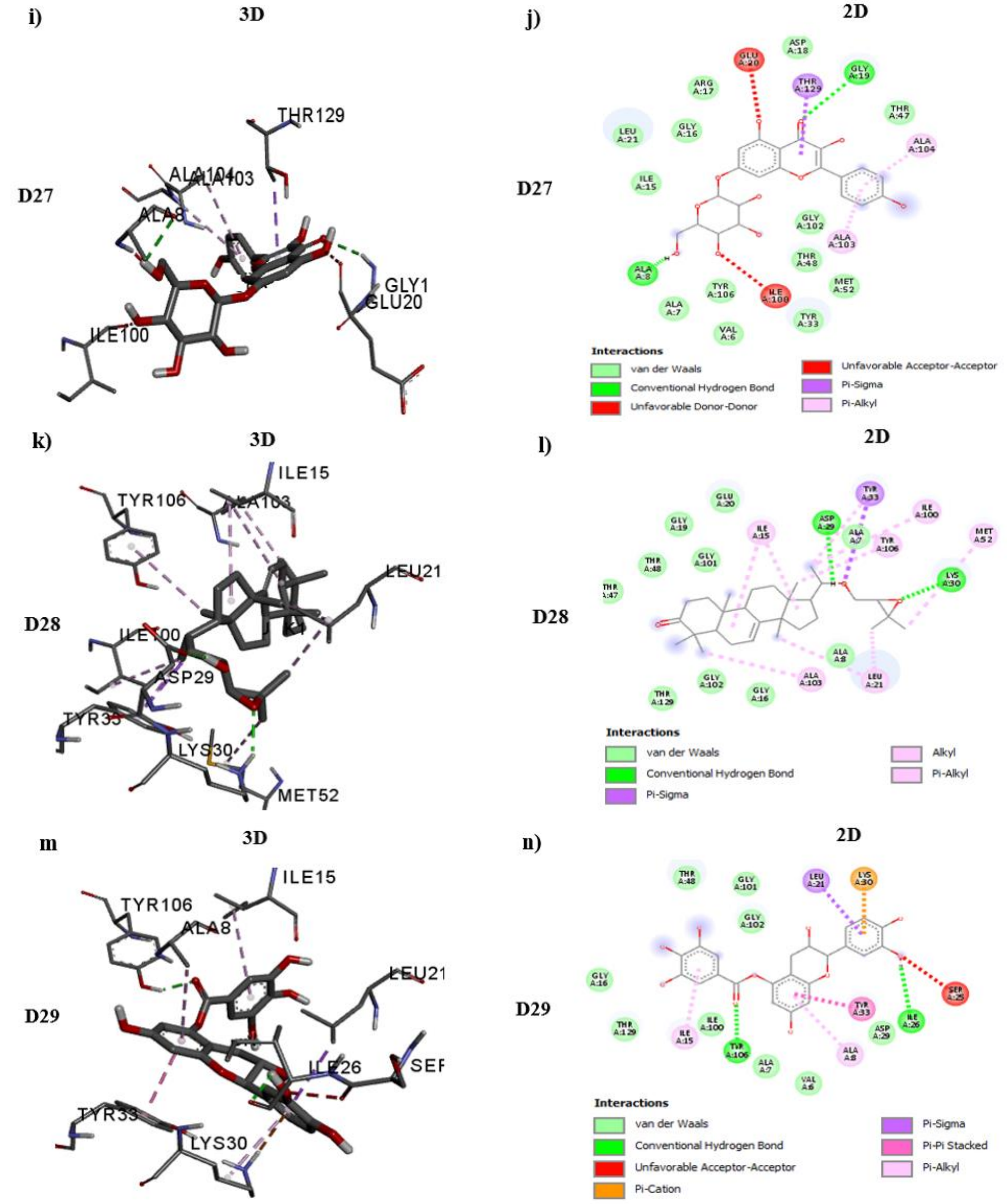

Figure 2. Docking ligand-receptor complexes of selected ligands with the highest binding affinity (PDB ID: 1VDR).

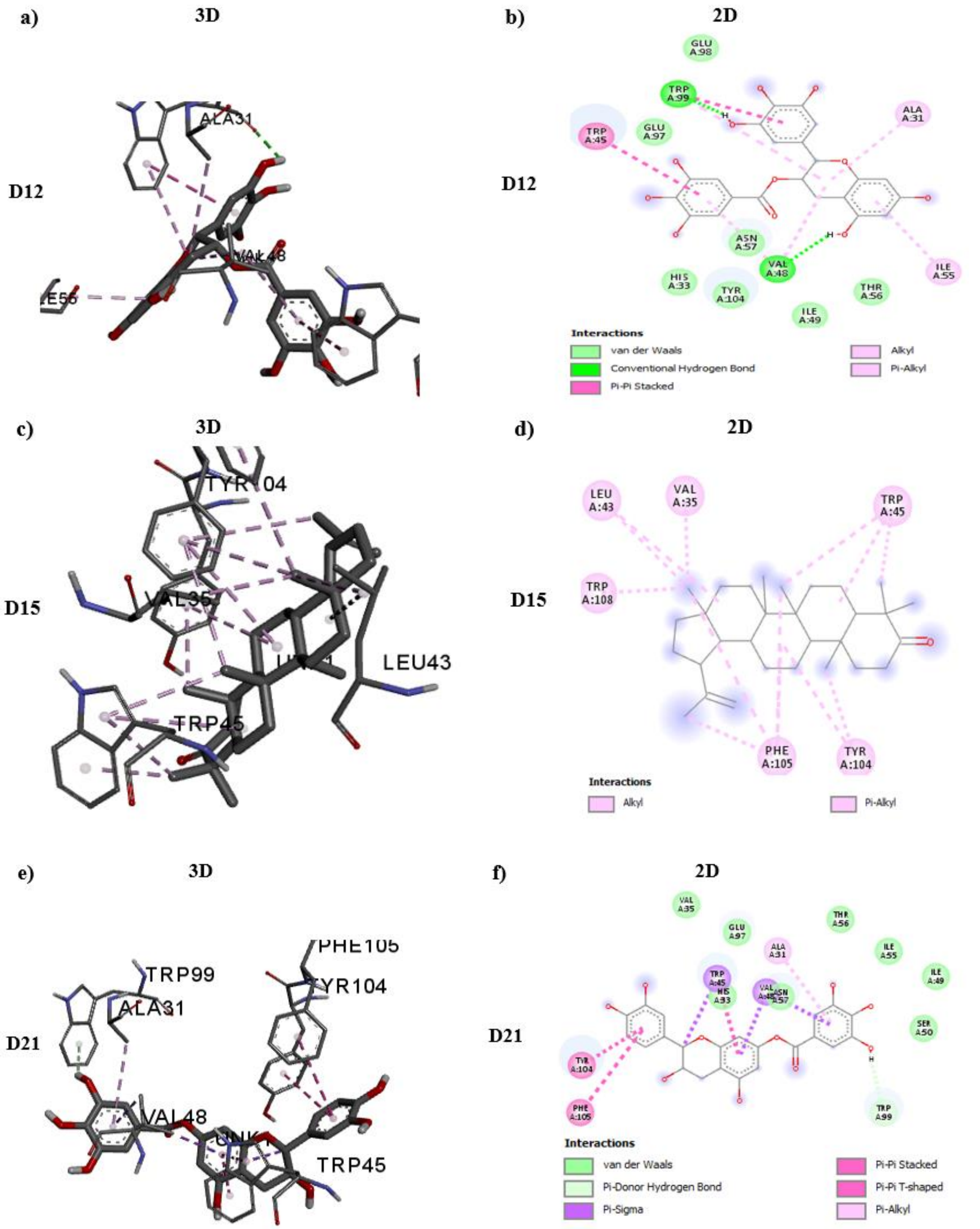
a)
3D
D12
ALA31
VAL48
E56
b)
2D
D12
GLU A:98
TRP A:99
TRP A:45
GLU A:97
ALA A:31
ASN A:57
VAL A:48
HIS A:33
TYR A:104
THR A:56
ILE A:49
ILE A:55
Interactions
van der Waals
Conventional Hydrogen Bond
Pi-Pi Stacked
Alkyl
Pi-Alkyl
c)
3D
D15
TYR104
VAL35
LEU43
TRP45
d)
2D
D15
LEU A:43
VAL A:35
TRP A:45
TRP A:108
PHE A:105
TYR A:104
Interactions
Alkyl
Pi-Alkyl
e)
3D
D21
TRP99
ALA31
PHE105
TYR104
VAL48
TRP45
f)
2D
D21
VAL A:35
GLU A:97
THR A:56
ALA A:31
ILE A:55
TRP A:45
HIS A:33
VAL A:48
ASN A:57
ILE A:49
SER A:50
TYR A:104
PHE A:105
TRP A:99
Interactions
van der Waals
Pi-Donor Hydrogen Bond
Pi-Sigma
Pi-Pi Stacked
Pi-Pi T-shaped
Pi-Alkyl

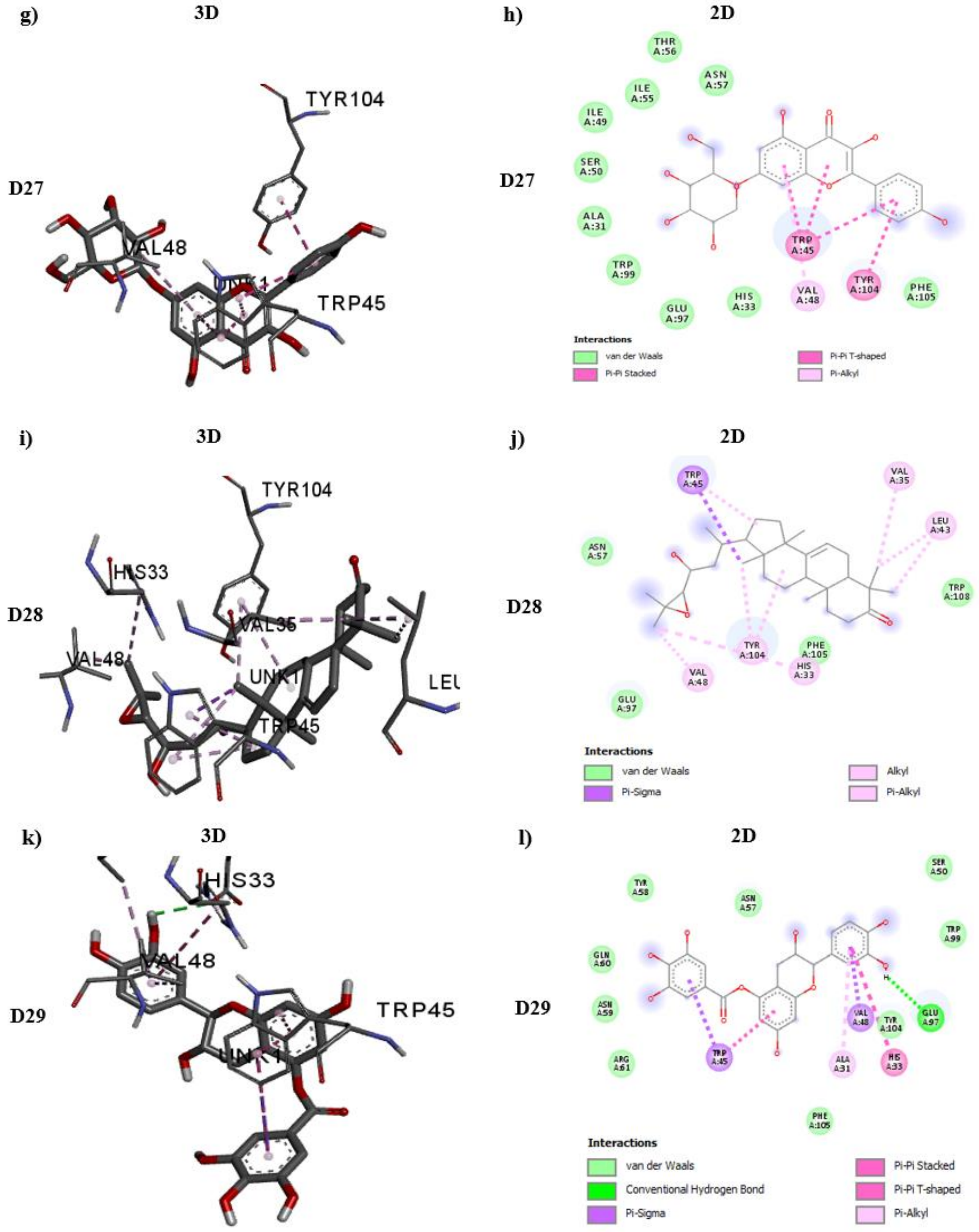

Figure 3. Ligand-receptor complexes of THE selected ligands with the highest binding affinity (PDB ID: 6J15).

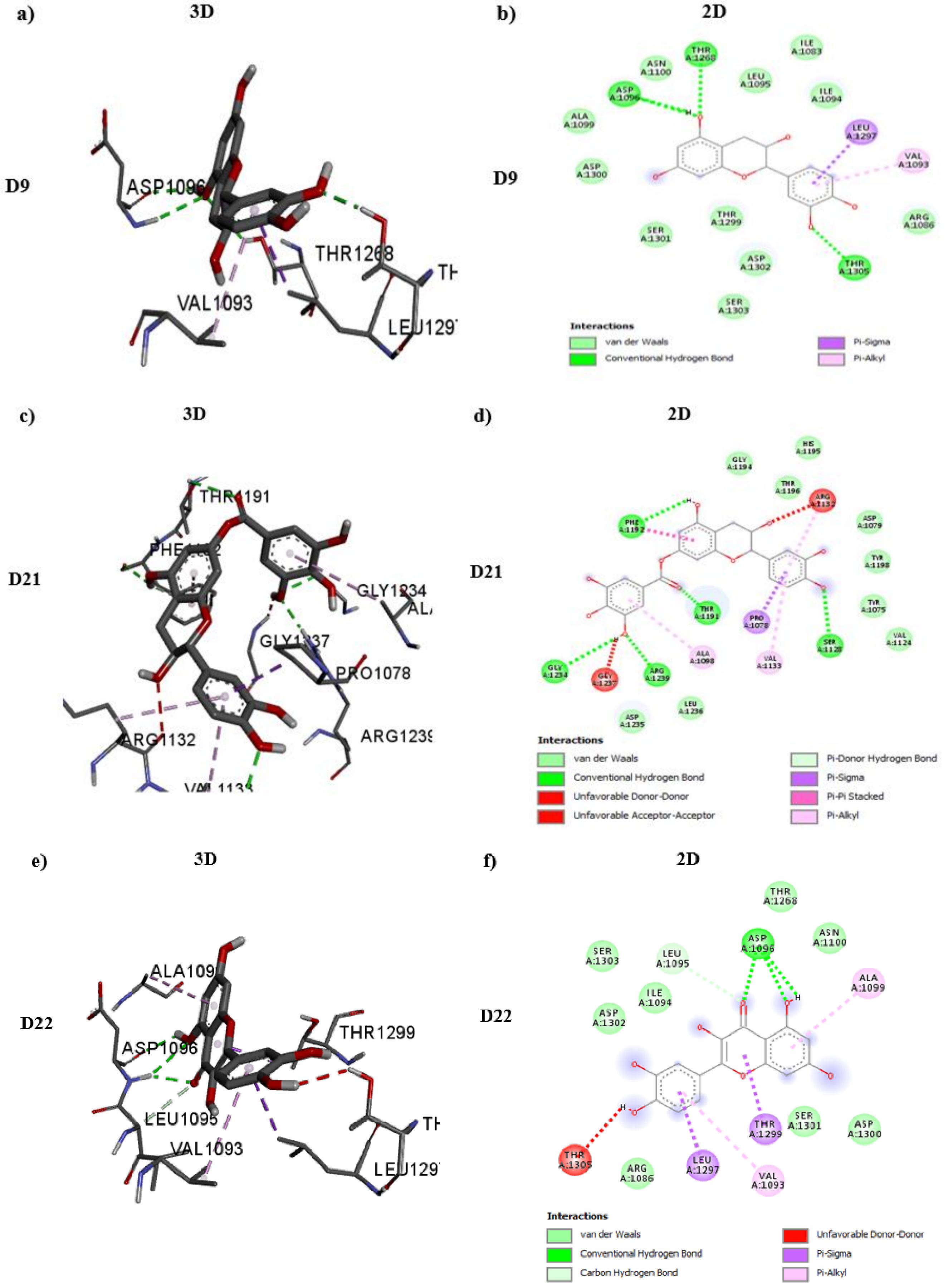
a)
3D
D9
ASP1096
THR1268
VAL1093
LEU1297
b)
2D
D9
THR A:1268
ASN A:1100
ILE A:1083
ASP A:1096
LEU A:1095
ILE A:1094
ALA A:1099
LEU A:1297
VAL A:1093
ASP A:1300
ARG A:1086
THR A:1299
SER A:1301
ASP A:1302
THR A:1305
SER A:1303
Interactions
van der Waals
Conventional Hydrogen Bond
Pi-Sigma
Pi-Alkyl
c)
3D
D21
THR1191
PHE1192
GLY1234
GLY1237
PRO1078
ARG1132
ARG1239
d)
2D
D21
HIS A:1195
GLY A:1194
THR A:1196
ARG A:1132
ASP A:1079
PHE A:1192
TYR A:1198
TYR A:1075
THR A:1191
PRO A:1078
SER A:1128
VAL A:1124
ALA A:1098
VAL A:1133
GLY A:1234
GLY A:1237
ARG A:1239
LEU A:1236
ASP A:1235
Interactions
van der Waals
Conventional Hydrogen Bond
Unfavorable Donor-Donor
Unfavorable Acceptor-Acceptor
Pi-Donor Hydrogen Bond
Pi-Sigma
Pi-Pi Stacked
Pi-Alkyl
e)
3D
D22
ALA1099
ASP1096
THR1299
LEU1095
VAL1093
f)
2D
D22
THR A:1268
ASP A:1096
ASN A:1100
SER A:1303
LEU A:1095
ALA A:1099
ILE A:1094
ASP A:1302
THR A:1299
SER A:1301
ASP A:1300
THR A:1305
ARG A:1086
LEU A:1297
VAL A:1093
Interactions
van der Waals
Conventional Hydrogen Bond
Carbon Hydrogen Bond
Unfavorable Donor-Donor
Pi-Sigma
Pi-Alkyl

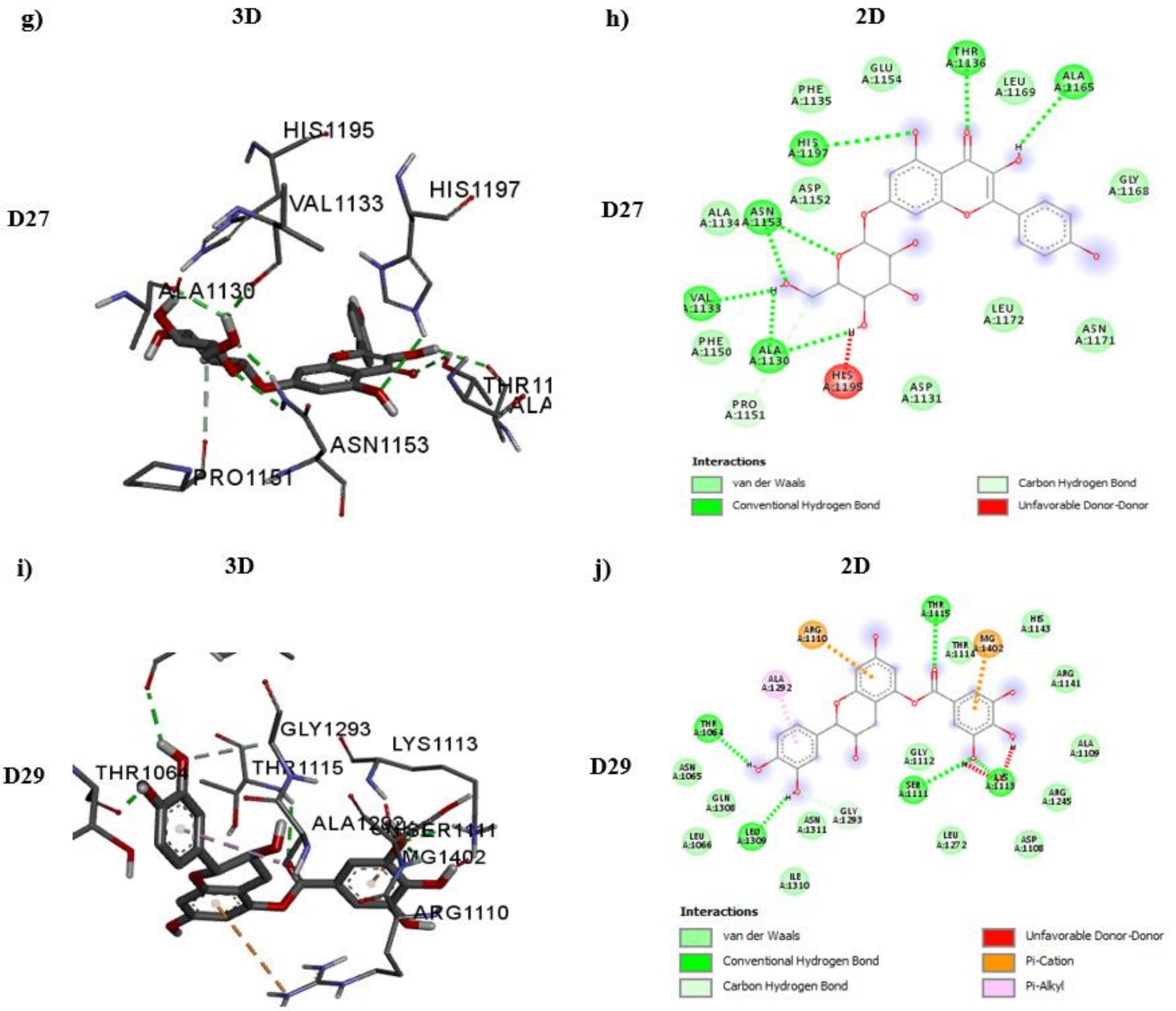

Figure 4. Ligand-receptor complexes of selected ligands with the highest binding affinity (PDB ID: 6J17).

4. Conclusions

The phytochemical screening on the *A. nilotica* fruit aqueous extract was carried out using standard procedures to identify chemical constituents and saponins are observed to be present in abundance in the aqueous extract. The aqueous extract showed maximum antiproliferative activity at 50 mg mL^{-1} on seed radicles of *S. bicolor.* Molecular docking results revealed that D21, D28 and D29 displayed stronger binding affinities against 1VDR, 6J15 and 6J17 receptors than the standard drugs used in the work. Although the compound D29 ([(2R,3S)-2-(3,4-dihydroxyphenyl)-3,7-dihydroxy-3,4-dihydro-2H-chromen-5-yl] 3,4,5-trihydroxybenzoate) has highest binding affinity, these compounds might play essential roles in the antiproliferation activity of *A. nilotica*. Thus, the docking results supported the antiproliferative activity of *A. nilotica*, which may rationalize the use of *A. nilotica* as a traditional medicine for the treatment of cancer and other related diseases.

Authors' contributions

Conceptualization: William, O. A.; Semire, B.; **Data curation:** William, O. A.; Semire, B.; Ejike, O. O.; **Formal Analysis:** William, O. A.; Semire, B.; Godfrey, O. E.; **Funding acquisition:** Not applicable; **Investigation:** William, O. A.; Semire, B.; **Methodology:** William, O. A.; Semire, B.; **Project administration:** Semire, B.; Obiyenwa, K. G.; **Resources:** William, O. A.; Semire, B.; Ejike, O. O.; **Software:** William, O. A.; Semire, B.; Ejike, O. O.; **Supervision:** Semire, B.; Ejike, O. O.; Obiyenwa, K. G.; **Validation:** Godfrey, O. E.; Semire, B.; Obiyenwa, K. G.; **Visualization:** William, O. A.; Semire, B.; **Writing – original draft:** William, O. A.; Semire, B.; **Writing – review & editing:** William, O. A.; Semire, B.; Ejike, O. O.; Obiyenwa, K. G.; Godfrey, O. E.

Data availability statement

All data sets were generated or analyzed in the current study.

Funding

Not applicable.

Acknowledgments

The authors are grateful to the Departments of Chemistry, Federal University Lokoja Nigeria for providing the laboratory space and facilities used in this research work.

References

Abd-Ulgadir, K.; El-Kamali, H. Antimicrobial activity of *Acacia nilotica* ssp. *nilotica* against some causative agents of urogenital infections. *Annu Res Rev Biol.* **2017**, *19* (5), 1–14. https://doi.org/10.9734/ARRB/2017/36026

Adegbola, A. E.; Fadahunsi, O. S.; Alausa, A.; Abijo, A. Z.; Balogun, T. A.; Aderibigbe, T. S.; Semire, B.; Adegbola, P. I. Computational prediction of nimbanal as potential antagonist of respiratory syndrome coronavirus. *Informatics in Medicine Unlocked*. **2021**, *24*, 100617. https://doi.org/10.1016/j.imu.2021.100617

Adepoju, A. J.; Latona, D. F.; Olafare, O. G.; Oyebamiji, A. K.; Abdul-Hammed, M.; Semire, B. Molecular docking and pharmacokinetics studies of *Curcuma longa* (curcumin) potency against Ebola virus. *"Ovidius" Univ Ann Chem.* **2022**, *33* (1), 23–35. https://doi.org/10.2478/auoc-2022-0004

Askari, B. S.; Krajinovic, M. Dihydrofolate reductase gene variations in susceptibility to disease and treatment outcomes. *Curr Genomics.* **2010**, *11*, 578–583. https://doi.org/10.2174/138920210793360925

Ayinde, B. A.; Agbakwuru, U. Cytotoxic and growth inhibitory effects of the methanol extract *Struchium sparganophora* Ktze (Asteraceae) leaves. *Pharmacogn Mag.* **2010**, *6* (24), 293–297. https://doi.org/10.4103/0973-1296.71795

Ayinde, B. A.; Omogbai, E. K.; Ikpefan, E. O. Comparative cytotoxic and antiproliferative effects of *Persea americana* mill (Lauraceae) leaf, stem, and root barks. *Niger J Pharm Sci.* **2011**, *10*, 16–26.

Bello, I. A.; Ndukwe, G. I.; Audu, O.T. Chemical analysis and biological activity of a precipitate from *Pavetta crassipes. J Med Plant Res.* **2011**, *8* (6), 285–287. https://doi.org/10.5897/JMPR10.088

Butler, M. S. Natural products to drugs: Natural product-derived compounds in clinical trials. *Nat Prod Rep.* **2008**, *25*, 475–516. https://doi.org/10.1039/b514294f

Chinedu, E.; Arome, D.; Ameh, S. F.; Ameh, G. E. Evaluation of the antiproliferative and cytostatic effect of *Citrus sinensis* (orange) fruit juice. *Int J App Basic Med Res.* **2014**, *4* (Suppl. 1), S20–S22. https://doi.org/10.4103/2229-516X.140711

Cossu, F.; Milani, M.; Mastrangelo, E.; Vachette, P.; Servida, F.; Lecis, D.; Canevari, G.; Delia, D.; Drago, C.; Rizzo, V.; Manzoni, L.; Seneci, P.; Scolastico, C.; Bolognesi, M. Structural basis for bivalent smac-mimetics recognition in the IAP protein family. *J Mol Biol.* **2009**, *392*, 630–644. https://doi.org/10.1016/j.jmb.2009.04.033

Eldeen, I. M. S.; Van Heerden, F. R.; Van Staden, J. *In vitro* biological activities of niloticane, a new bioactive cassane diterpene from the bark of *Acacia nilotica* subsp. *kraussiana*. *J Ethnopharmacol*. **2010**, *128* (3), 555–560. https://doi.org/10.1016/j.jep.2010.01.057

Enegide, C.; Arome, D.; Dabum, L. J. Preliminary assessment of the antiproliferative potential of *Ananas comosus* (pineapple) fruit juice. *J HerbMed Pharmacol.* **2014**, *5* (2), 50–53. https://doi.org/10.1016/S1995-7645(14)60257-1

Gopal, S.; Sharpless, N. E. Cancer as a global health priority. *JAMA.* **2021**, *326* (9), 809–810. https://doi.org/10.1001/jama.2021.12778

Horaira, M. A.; Islam, M. A.; Kibria, M. K.; Alam, M. J.; Kabir, S. R.; Mollah, M. N. H. Bioinformatics screening of colorectal-cancer causing molecular signatures through gene expression profiles to discover therapeutic targets and candidate agents. *BMC Med. Genomics.* **2023** *16* (1), 64. https://doi.org/10.1186/s12920-023-01488-w

Kirubhanand, C.; Merciline, L. J.; Anitha, S.; Sangeetha, R.; Nachammai, K. T.; Langeswaran, K.; Gowtham, K. S. Targeting potential receptor molecules in non-small cell lung cancer (NSCLC) using *in silico* approaches Front. *Mol Biosci.* **2023**, *10*, 1124563. https://doi.org/10.3389/fmolb.2023.1124563

Krishnan, M.; Babu, S.; Thomas, S. A.; Surulivel, J. S.; Ayyanar, K.; Molecular docking analysis of VEGF with compounds from tomato. *Bioinformation*. **2022**, *18* (5), 478–481. https://doi.org/10.6026/97320630018478

Kumari, A.; Karnatak, M.; Singh, D.; Shankar, R.; Jat, J. L.; Sharma, S.; Yadav, D.; Shrivastava, R.; Verma, V. P. Current scenario of artemisinin and its analogues for antimalarial activity. *Eur J Med Chem.* **2019**, *163*, 804–829. https://doi.org/10.1016/j.ejmech.2018.12.007

Kumari, R.; Mishra, R. C.; Sheoran, R.; Yadav, E. J. Fractionation of antimicrobial compounds from *Acacia nilotica* twig extract against oral pathogens. *Biointerface Res Appl Chem.* **2020**, *10* (6), 7097–7105. https://doi.org/10.33263/BRIAC106.70977105

Kunle, O. F.; Egbarevba, H. O. Preliminary studies on *Vernonia ambigua*. Phytochemical and antimicrobial screening of the whole plant. *Ethnobot Leaflets.* **2009**, *13*, 216–221.

Li-Weber, M. New therapeutic aspects of flavones: The anticancer properties of *Scutellaria* and its main active constituents wogonin, baicalein and baicalin. *Cancer Treat Rev.* **2009**, *35*, 57–68. https://doi.org/10.1016/j.ctrv.2008.09.005

Mi, J.; Gong, W.; Wu, X. Advances in key drug target identification and new drug development for tuberculosis. *BioMed Res Int.* **2022**, *2022*, 5099312. https://doi.org/10.1155/2022/5099312

Mohmmed, R. A.; Babiker, E. E. Bioactive compounds, antioxidant activity, minerals composition and antimicrobial activity of *Acacia nilotica* fruit flesh and seeds. *Res J Med Plants.* **2019**, *13* (1), 18–25. https://doi.org/10.3923/rjmp.2019.18.25

Mukherji, D.; Murillo, R. H.; Van Hemelrijck, M.; Vanderpuye, V.; Shamieh, O.; Torode, J.; Pramesh, C. S.; Yusuf, A.; Booth, C. M.; Aggarwal, A.; Sullivan, R. Global cancer research in the post-pandemic world. *Lancet Oncol.* **2021**, *22* (12), 1652–1654. https://doi.org/10.1016/s1470-2045(21)00602-1

Muschietti, L.; Vila, R.; Cechinel Filho, V.; Setzer, W. Tropical protozoan diseases: Natural product drug discovery and development. *Evid Based Complement Altern Med.* **2013**, *2013*, 404250. https://doi.org/10.1155/2013/404250

Ogbadoyi, E. O.; Garba, M. H.; Kabiru, A. Y.; Mann, A.; Okogun, J. I. Therapeuticevaluations of *Acacia nilotica* (Linn) stem bark extract in experimental Africa trypanosomiasis. *Int J Appl Res Nat Prod.* **2011**, *4* (2), 11–18.

Omotayo, I. A.; John, A. A.; Gbenga, O. O.; Misbaudeen, A.-H., Felix, L. D., Kolawole, O. A.; Banjo, S. *In-silico* assessment via molecular docking and ADMET profile of Botanical drugs (bergamottin and casticin) against trial drugs for Lassa virus. *Int J Pharm Sci Res.* **2022**, *13* (9), 3494–3518. https://doi.org/10.13040/IJPSR.0975-8232.13(9).3494-18

Oyebamiji, A. K.; Akintelu, S. A.; Akande, I. O.; Aworinde, H. O.; Adepegba, O. A.; Akintayo, E. T.; Akintayo, C. O.; Semire, B.; Babalola,

J. O. Dataset on biochemical inhibiting activities of selected phytochemicals in *Azadirachta indica* L. as potential NS2B–NS3 proteases inhibitors. *Data in Brief.* **2023**, *48*, 109162. https://doi.org/10.1016/j.dib.2023.109162

Oyewole, R. O.; Oyebamiji, A. K.; Semire, B. Theoretical calculations of molecular descriptors for anticancer activities of 1,2,3-triazole-pyrimidine derivatives against gastric cancer cell (MGC-803): DFT, QSAR and docking approaches. *Heliyon.* **2020**, *6* (5), e03926. https://doi.org/10.1016/j.heliyon.2020.e03926

Pieper, U.; Kapadia, G.; Mevarech, M.; Herzberg, O. Structural features of halophilicity derived from the crystal structure of dihydrofolate reductase from the Dead Sea halophilic archaeon, *Haloferax volcanii*. *Structure.* **1998**, *6* (1), 75–88. https://doi.org/10.1016/S0969-2126(98)00009-4

Raji, M. A.; Adekeye, J. O.; Kwaga, J. K. P.; Bale, J. O. O. Antimicrobial effects of *Acacia nilotica* and *Vitex doniana* on the thermophilic campylobacter species. *African J Sci Technol*. **2002**, *3* (2), 9–13. https://doi.org/10.4314/ajst.v3i2.15262

Roozbeh, N.; Darvish, L. *Acacia nilotica*: new plant for help in pelvic organ prolapse. *J Menopausal Med* **2016**, *22* (3), 129. https://doi.org/10.6118/jmm.2016.22.3.129

Salvatore, P. P.; Zhang, Y. Tuberculosis molecular basis of pathogenesis. *Reference Module in Biomedical Sciences*. 2017. https://doi.org/10.1016/B978-0-12-801238-3.95697-6

Sarkiyayi, S.; Abdul Rasheed, K. Properties of *Acacia nilotica* leaf extract: A preliminary investigation on anti-typhoid. *Int J Curr Biochem Res.* **2013**, *1* (2), 9–14.

Shil, A.; Akter, A.; Sultana, A.; Halder, S.K.; Himel, M.K.; Targeting Shikimate Kinase Pathway of Acinetobacter baumannii: A Structure-Based Computational Approach to Identify Antibacterial Compounds. J. Tropical Med. **2023**, https://doi.org/10.1155/2023/6360187

Singh, R.; Singh, B.; Singh, S.; Kumar, N.; Kumar, S.; Arora, S. Umbelliferone–an antioxidant isolated from *Acacia nilotica* (L.) Willd. Ex. Del. *Food Chem.* **2010**, *120*, 825–830. https://doi.org/10.1016/j.foodchem.2009.11.022

Sung, H.; Ferlay, J.; Siegel, R. L.; Laversanne, M.; Soerjomataram, I.; Jemal, A.; Bray, F. Global Cancer Statistics 2020: GLOBOCAN estimates of incidence and mortality worldwide for 36 cancers in 185 countries. *CA Cancer J Clin.* **2021**, *71* (3), 209–249. https://doi.org/10.3322/caac.21660

Tanko, Y.; Abdulazeez, A.; Muhammad, A.; Jimoh, A.; Mohammed, K. H.; Mohammed, A. Effect of methanol crude leaves extract and aqueous fraction of *Acacia nilotica* on lipid profile and liver enzymes on alloxan-induced diabetic wistar rats. *J. Exp Biol.* **2014**, *2* (3), 36–40. https://doi.org/10.1242/jeb.105148

Taylor, L. *Plant-based drugs and medicines.* Square One Publishers, 2000.

Thiagarajan, K.; Mohan, S.; Roy, T. K. Chandrasekaran R. Antiproliferative effect of *Acacia nilotica* (L.) leaf extract rich in ethyl gallate against human carcinoma cell line KB. *Indian J Pharmacol.* **2020**, *52* (6), 488–494. https://doi.org/10.4103/ijp.IJP_223_17

Wang, S.; Zhou, K.; Yang, X.; Zhang, B.; Zhao, Z.; Xiao, Y.; Yang, X.; Yang, H.; Guddat, L. W.; Li, J.; Rao, Z. Structural insights into substrate recognition by the type VII secretion system. *Protein Cell.* **2020**, *11* (2), 124–137. https://doi.org/10.1007/s13238-019-00671-z

[WHO] World Health Statistics. *World Health Statistics 2018*: Monitoring health for the SDGs, sustainable development goals. WHO, 2018. https://apps.who.int/iris/handle/10665/272596 (accessed 2023-10-02).

Yuan, H.; Ma, Q.; Ye, L.; Piao, G. The traditional medicine and modern medicine from natural products. *Molecules* **2016**, *21* (5), 559. https://doi.org/10.3390/molecules21050559

Yusuf, A. Z.; Zakir, A.; Shemau, Z.; Abdullahi, M.; Halima, S. A. Phytochemical analysis of the methanol leaves extract of *Paullinia pinnata* Linn. *J Pharmacognosy Phytother.* **2014**, *6* (2), 10–16. https://doi.org/10.5897/JPP2013.0299

ECLÉTICA QUÍMICA

Eclet. Quim. 49 | e-1535, 2024

Original Article

https://doi.org/10.26850/1678-4618.eq.v49.2024.e1535

In memoriam of Cecilia Laluce (1940 - 2023)

Antonio Carlos **Massabni**[1,2+], Maria Célia **Bertolini**[2]

Article History

Received December 31, 2023
Accepted January 15, 2024
Published February 02, 2024

Section Editor

Assis Vicente Benedetti

In 2019 Professor Cecilia Laluce, then serving as an emeritus professor since 2010, joined the Institute of Chemistry of Araraquara (IQAr) for the last time. The COVID-19 pandemic prevented face-to-face encounters at the university until 2021. We met again sometime later, when Cecilia was already diagnosed with colon cancer followed by a stroke, both of which left her with numerous sequels. Native from Birigui (SP), Cecilia passed away on May 23 at the age of 83 in Araçatuba (SP), to where was transferred at the end of 2022 and remained for a few months until her passing, closely accompanied by a few relatives.

Laluce was part of the first IQAr's graduating chemistry class with both bachelor and teacher degrees from the former Chemistry Department in the Faculty of Science and Letters of Araraquara (FCLAr), in 1964 and 1965 respectively, standing out as one of the top students. As a third-year undergraduate student, Cecilia was already collaborating in the Biochemistry Laboratory, assisting the practical classes under the supervision of the Biochemistry Professor Rubens Molinari. In 1965, Laluce started her teaching career, as an assistant professor, and in 1973, she completed her PhD in the same institution. In 1976, the creation of UNESP led to an academic and administrative reorganization of the university, resulting in the establishment of IQAr in 1977, where Cecilia became a professor in the Biochemistry Department. She was a pioneer in the research area of Applied Microbiology.

Laluce dedicated almost her entire life to the Institute of Chemistry both as a teacher and researcher; the Institute of Chemistry was her second home. As a result of her outstanding work capacity and ease in establishing scientific interactions, she established many collaborations throughout her academic career, in Brazil and other countries. She was the first woman from IQAr to carry out a Postdoctoral Internship abroad, first at the Faculty of Medicine in Buenos Aires, Argentina, in 1980, and later at the University of Colorado, USA, from 1981 to 1982. Always in pursuit of knowledge and scientific improvement, she participated in numerous national and international conferences, presented lectures, and received several awards and honorable mentions. She was the first woman to become a Full Professor at IQAr. At a time when research in the field of Technology was still embrionary at UNESP, Cecilia coordinated, in the 1980s, a project sponsored by the Banco do Brasil Foundation, in collaboration with some department colleagues, aimed at developing improved yeast strains for the alcoholic fermentation process. At that time, the National Ethanol Program (Proálcool) was created, and the project under her coordination significantly impacted the academic community. From then on, her research activities were concentrated on projects related to Applied Microbiology including a partnership with the Biotechnology Center of Fleischmann & Royal. She became a reference researcher in alcoholic fermentation, and the results of her work were recognized by the scientific community.

The entire Institute of Chemistry body in Araraquara immensely appreciates her scientific legacy and dedication to the development of science and technology in Brazil.

[1]University of Araraquara, Araraquara, Brazil. [2]São Paulo State University, Institute of Chemistry, Araraquara, Brazil. **+Corresponding author:** Antonio Carlos Massabni, **Phone:** +55 16 3301-9630, **Email address:** amassabni@uol.com.br

Eclet. Quim. 49 | e-1491, 2024

Original Article

https://doi.org/10.26850/1678-4618.eq.v49.2024.e1491

Complex compound of trinitrotriamminecobalt(III): in theoretical studies

Deni Ainur **Rokhim**[1,2+], Muhammad Roy **Asrori**[1], Husni Wahyu **Wijaya**[1]

Abstract

$[Co(NH_3)_3(NO_2)_3]$ is an octahedral complex compound that can have several isomers. The complex compound has magnetic properties. Its stability has been explained. It can be easily synthesized and is known as a bioinorganic synthesis reagent, oxidant compound and base hydrolysis.

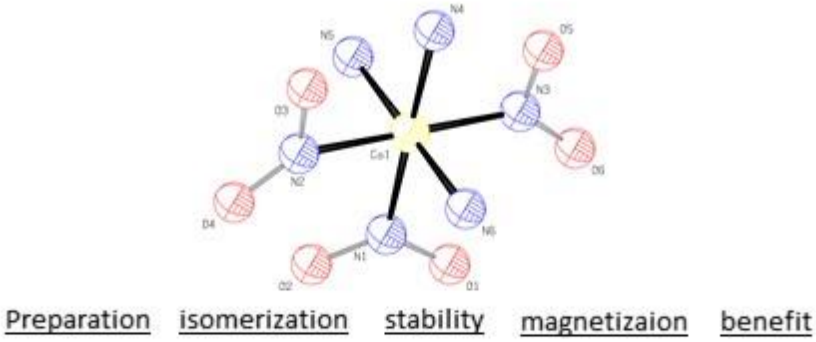

Article History

Received May 17, 2023
Accepted November 20, 2023
Published February 16, 2024

Keywords

1. complex compound;
2. cobalt complex;
3. trinitrotriamminecobalt(III).

Section Editor

Manuel Ignacio Azocar Guzmán

Highlights

- Trinitroamminecobalt(III) with its isomerization and magnetization theoretically.
- The stability of the complex compound is discussed theoretically.
- The complex compound has beneficial properties.

[1]State University of Malang, Faculty of Mathematics and Natural Sciences, Malang, Indonesia. [2]Chemistry and PKWU, SMAN 3 Sidoarjo, Malang, Indonesia.
+Corresponding author: Deni Ainur Rokhim, **Phone:** +6283857257301, **Email address:** deniainurrokhim@gmail.com

1. Introduction

The recent development of complex compounds is increasingly changing along with its usefulness in everyday life. The applications of complex compounds, especially as catalysts (Alhafez *et al.*, 2022), continue to be developed. Complex compounds of d-block elements have an advantage over other compounds because they have empty d orbitals. This d orbital generally plays a role in the catalytic process (Feng *et al.*, 2022). In addition, potential applications in many areas include metal purification, photography, medicine, and colouring agents (Habiddin and Hartanto, 2023).

Complex compounds in the laboratory are synthesized by reacting a base ligand with a metal by donor-acceptor of the electron pair. Based on the number of electrons donated by the ligand, the ligands can be classified into monodentate, bidentate, and polydentate ligands (Effendy, 2013; Verma *et al.*, 2022). A monodentate ligand donates only one pair of electrons to the metal. A bidentate ligand donates its two pairs of electrons to a metal, and many electrons can be donated to a metal by a polydentate ligand. These polydentate ligands can also form chelate structures (Eivazihollagh *et al.*, 2019).

These metals are inert and stable in forming complex compounds with various ligands. One metal that has these properties is cobalt. These metals were used by Werner (Ernst *et al.*, 2011), the father of coordination chemistry who studied complex compounds (Deblitz *et al.*, 2014), the first to produce Werner's coordination theory, which lasted long enough and is still being introduced in the early days of studying coordination chemistry (Constable and Housecroft, 2013; Nguyen *et al.*, 2014).

One of the complex compounds with a cobalt central atom is trinitrotriamminecobalt(III) compound which has the chemical formula of $[Co(NH_3)_3(NO_2)_3]$ as shown in **Fig. 1** (Bąk *et al.*, 2013; Laing *et al.*, 1971). The trinitrotriamminecobalt(III) compound has a central atomic number 6 with an octahedral compound structure (**Fig. 1**). The objective of this work is to introduce $[Co(NH_3)_3(NO_2)_3]$ in theoretical studies and relate the potential application.

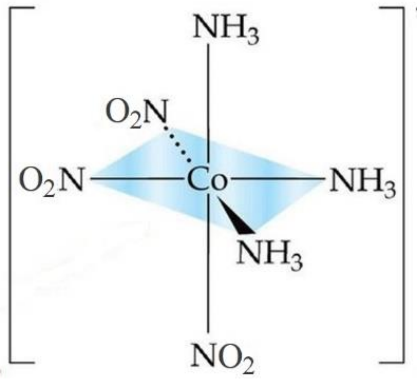

Figure 1. Molecular structure of $[Co(NH_3)_3(NO_2)_3]$.

2. Experimental

2.1. Reagents and solutions

The reagents and solutions used included cobalt carbonate ($CoCO_3$), glacial acetic acid, distilled water, cold solution mixture (10.6 g of sodium nitrate in 50 mL of ammonia), ice, and activated charcoal.

2.2. Synthesis of trinitrotriamminecobalt(III) compound

The trinitrotriamminecobalt(III) compound can be synthesized on a laboratory scale. The compound was synthesized by dissolving 5 g of $CoCO_3$ in 7 mL of a hot solution of glacial acetic acid and 14 mL of H_2O. After that, the solution was put in a cold solution mixture (10.6 g of sodium nitrate in 50 mL of ammonia) in an Erlenmeyer flask. The resulting mixture was cooled on ice and dripped with 28 mL of 30% water slowly for 5 – 20 min. Activated charcoal (0.5 g) was then added. In the next step, the mixture was heated for 30 min in a bath. In the last stage, the mixture was filtered, and the product compounds formed were on filter paper.

3. Results and discussion

3.1. Isomerization of trinitrotriamminecobalt(III) compound

The trinitrotriamminecobalt(III) compound has several different atomic arrangements known as isomerization (Bąk *et al.*, 2013). The compound shows structural isomerism and spatial isomerism. The structural isomerism of the compound is linkage isomerism. The linkage isomerism occurs in the compound containing ambidentate ligands such as NO_2^-. The NO_2^- ligand can bind to the central atom via an N or O atom. In $[Co(NH_3)_3(NO_2)_3]$, the nitrite ion, NO_2^-, binds to the central atom via an N atom and a nitro complex is formed, whereas in $[Co(NH_3)_3(ONO)_3]$, nitrite ion binds to the central atom via the O atom and a nitrite complex is formed. The different types of donor atoms attached to the central atom in the two complex compounds produce different colours. The two-coloured compounds are because the central atom, Co^{3+}, has 3d orbitals that are not completely filled with electrons. The two compounds are linked isomer pairs (Effendy, 2013). The following is the structure of a linked isomer compound pair (**Fig. 2**).

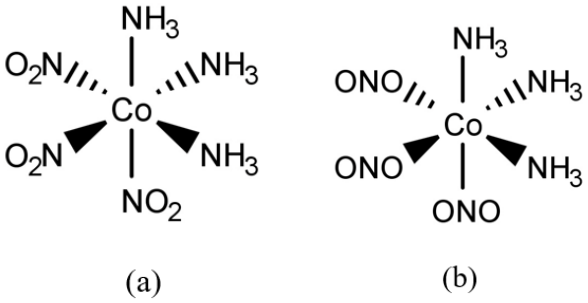

Figure 2. **(a)** trinitrotriamminecobalt(III) and **(b)** trinitritotriamminecobalt(III).

Spatial isomerization of the trinitrotriamminecobalt(III) compound is facial-meridional isomerism (fac-mer isomerism) (Bernal *et al.*, 1996; Nuber *et al.*, 1979; Palmer and Hill, 1993; Tanito *et al.*, 1952). This isomerism only occurs in octahedral complex molecules that have the same 3 ligands and the same 3 other ligands. The structures of the facial (fac-) and meridional (mer-) isomers of the trinitrotriamminecobalt(III) compound are given in Figs. 3 and 4.

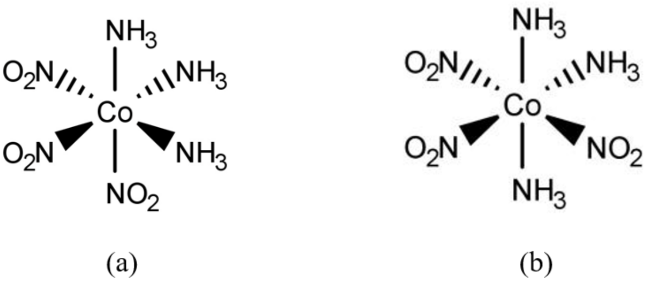

Figure 3. **(a)** *fac*-trinitrotriamminecobalt(III) and **(b)** *mer*-trinitrotriamminecobalt(III).

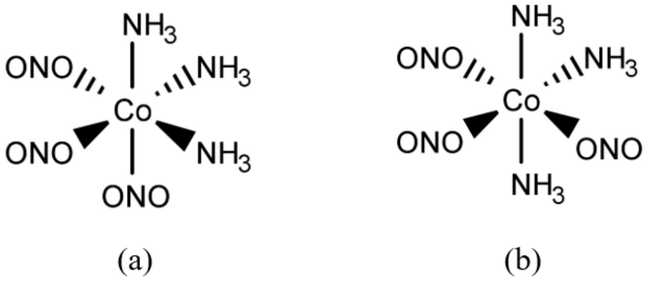

Figure 4. **(a)** *fac*-triaminetrinitrito-O-cobalt(III) and **(b)** *mer*-triaminetrinitrito-O-cobalt(III).

In the same fac- isomer the three ligands are located on an equilateral triangle which is one of the octahedral faces, whereas in the mer- isomer the three ligands are in an isosceles triangle.

3.2. Magnetism of trinitrotriamminecobalt(III) Compounds

Based on the energetic principle, the energy level of $[Co(NH_3)_3(NO_2)_3]$ is lowest when the repulsion between the three NH_3 ligands and three NO_2^- ligands is minimal. This happens when the position is as far as possible, namely at the octahedral corners (Kilic *et al.*, 2015), so that the complex has an octahedral structure (Alhafez *et al.*, 2022; Kilic *et al.*, 2017). Besides that, $[Co(NH_3)_3(NO_2)_3]$ is diamagnetic in that its magnetism is equivalent to the pairing of all the electrons present. This property indicates that the formation of the compound occurs electron excitation. Therefore, the formation of this compound involves d^2sp^3 hybridization. The following is an explanation with the electron configuration shown in **Fig. 5**.

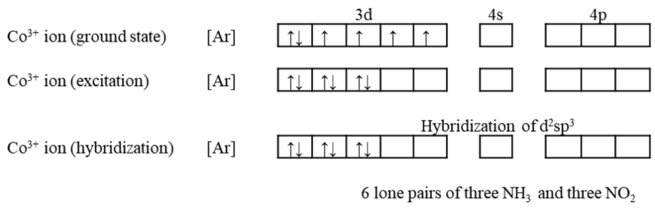

Figure 5. Electron configuration of Co^{3+} ion in $[Co(NH_3)_3(NO_2)_3]$.

Meanwhile, based on the crystal field theory, the complex compound of $[Co(NH_3)_3(NO_2)_3]$ is also diamagnetic. The compound is octahedral in shape and has a central atom (Kılıç *et al.*, 2017), namely Co^{3+} with an electron configuration in the ground state of Co^{3+} = [Ar] $3d^6$. The ligand attached to the central Co^{3+} atom is a strong field, so it is energetically more advantageous if the six electrons occupy the t_2g orbital, paired with the electrons already in the orbital so that a configuration is obtained as shown in **Fig. 6**.

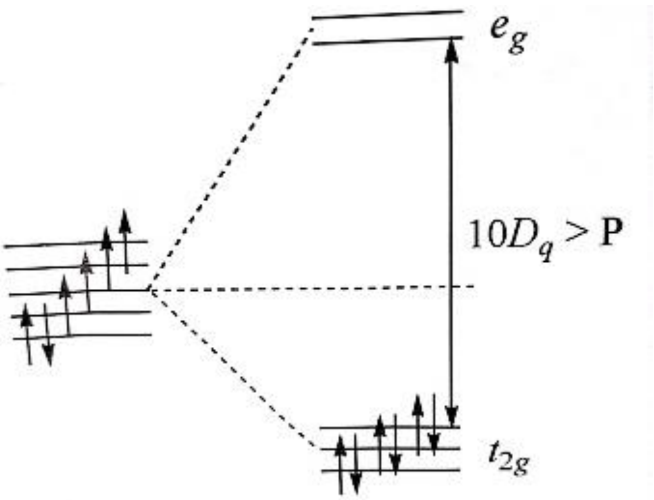

Figure 6. Electron configuration of strong field octahedral complex compound of $[Co(NH_3)_3(NO_2)_3]$ with d^6 central atom.

According to molecular orbital theory, the complex compound of $[Co(NH_3)_3(NO_2)_3]$ is also diamagnetic. The compound is octahedral in shape and has a central atom (Kılıç *et al.*, 2017), namely Co^{3+} with an electron configuration in the ground state of Co^{3+} = [Ar] $3d^6$. The number of electrons in the 3d orbital of the central atom and the electrons donated by three NH_3 ligands and three NO_2^- ligands is 18 electrons. The 18 electrons are filled in the molecular orbitals of the octahedral complex compound as shown in **Fig. 7**.

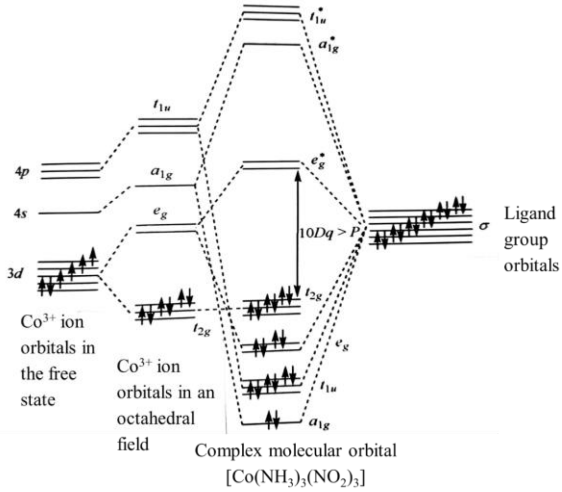

Figure 7. Molecular orbital diagram of $[Co(NH_3)_3(NO_2)_3]$.

The way of filling the 18 electrons in the molecular orbitals of the complex is as follows. First, fill the six pairs of electrons in the a_1g, t_1u, and e.g. orbitals. Second, filling the remaining six electrons in the t_2g orbital in pairs because $[Co(NH_3)_3(NO_2)_3]$ is a complex with a strong field, the value is 10 Dq > P. Its diamagnetic properties are indicated by the pairing of all the electrons present in the molecular orbitals of the compound.

3.3. Stability and colour of $[Co(NH_3)_3(NO_2)_3]$

The stability of $[Co(NH_3)_3(NO_2)_3]$ is based on the central atom with a certain oxidation number. The oxidation number of the central atom of $[Co(NH_3)_3(NO_2)_3]$ is +3, where in the Co^{3+} complex with d^6 configuration, the e.g. orbitals are not filled with electrons so that the complex formed will be stable. This could happen due to the influence of strong ligands.

The colour that appears in a complex depends on the strength of the crystal field. The greater the strength of the crystal field of a complex, the transition will require radiation with smaller wavelengths, and the absorbed colour shifts from red to purple with the complementary results seen by the eye shifting from dark colours (green-blue) to more vibrant colours, namely pale (lemon yellow). Because the strength of the crystal field depends on the strength of the existing ligands, for complex compounds with the same central atom the colour of the complex tends to get paler with increasing ligand strength. If we compare the colour of $[Co(NH_3)_3(NO_2)_3]$ which is pale yellow and the colour of $[Co(H_2O)_6]^{3+}$ which is blue. This colour change is due to the influence of the ligand where the NH_3 and NO_2^- ligands are stronger than the H_2O ligands so that $[Co(NH_3)_3(NO_2)_3]$ has a paler colour.

3.4. Benefits of $[Co(NH_3)_3(NO_2)_3]$

$[Co(NH_3)_3(NO_2)_3]$ has several benefits, including as a reagent in the synthesis of bioinorganic complex compounds and as an oxidant compound ferredoxin in parsley extract (Adzamli *et al.*, 1982) or therapeutic potential as reduction-activated complexes, or can be applied in imaging by MRI (Renfrew *et al.*, 2018). In addition, $[Co(NH_3)_3(NO_2)_3]$ can also react as base hydrolysis (Singh and Shanker, 1989).

4. Conclusions

$[Co(NH_3)_3(NO_2)_3]$ can be explored in the future about the potency as medicinal agent such as therapy and imaging instruments. The chemical characteristics of the complex show the unique compound as diamagnetic compound, and stable. Deep understanding of the complex may encourage us to apply it in many fields.

Authors' contributions

Conceptualization: Rokhim, D. A.; **Data curation:** Rokhim, D. A.; **Formal Analysis:** Rokhim, D. A.; **Funding acquisition:** Not applicable; **Investigation:** Rokhim, D. A.; **Methodology:** Rokhim, D. A.; **Project administration:** Rokhim, D. A.; **Resources:** Rokhim, D. A.; **Software:** Not applicable; **Supervision:** Wijaya, H. W.; **Validation:** Wijaya, H. W.; **Visualization:** Asrori, M. R.; **Writing – original draft:** Rokhim, D. A.; **Writing – review & editing:** Asrori, M. R.

Data availability statement

All data sets were generated or analyzed in the current study.

Funding

Not applicable.

Acknowledgments

Thanks to Department of Chemistry, Faculty of Mathematics and Natural Sciences, Universitas Negeri Malang for supporting this study.

References

Abd-Ulgadir, K.; El-Kamali, H. Antimicrobial activity of *Acacia nilotica* ssp. *nilotica* against some causative agents of urogenital infections. *Annu Res Rev Biol.* **2017**, *19* (5), 1–14. https://doi.org/10.9734/ARRB/2017/36026

Adzamli, I. K.; Kim, H. O.; Sykes, A. G. Neutral complexes as oxidants for the reduced form of parsley (*Petroselinum crispum)* [2Fe--2S] ferredoxin. Evidence for partial blocking by redox-inactive Cr(III) complexes. *Biochem. J.* **1982**, *203* (3), 669–673. https://doi.org/10.1042/bj2030669

Alhafez, A.; Aytar, E.; Kilic, A. Enhancing catalytic strategy for cyclic carbonates synthesized from CO2 and epoxides by using cobaloxime-based double complex salts as catalysts. *J. CO_2 Util.* **2022**, *63* (8), 102129. https://doi.org/10.1016/j.jcou.2022.102129

Bernal, I.; Cetrullo, J.; Somoza, F.; Ricci, J. S.; Lewis, R.; Massoud, S. S. The phenomenon of conglomerate crystallization. Part 42: The crystallization mode and conformational and configurational behavior of mer-trinitro cobalt triamines: mer-$[Co(NH_3)_3(NO_2)_3]$ (I) and mer-$[Co(dpt)(NO_2)_3]$ (II). *J. Coord. Chem.* **1996**, *38* (1–2), 41–53. https://doi.org/10.1080/00958979608022689

Constable, E. C.; Housecroft, C. E. Coordination chemistry: the scientific legacy of Alfred Werner. *Chem. Soc. Rev.* **2013**, *42* (4), 1429–1439. https://doi.org/10.1039/c2cs35428d

Deblitz, R.; Hrib, C. G.; Blaurock, S.; Jones, P. G.; Plenikowski, G.; Edelmann, F. T. Explosive Werner-type cobalt(III) complexes. *Inorg. Chem. Front.* **2014**, *1* (8), 621–640. https://doi.org/10.1039/C4QI00094C

Effendy. *Perspektif Baru Kimia Koordinasi*; Indonesian Academic Publishing, 2013.

Eivazihollagh, A.; Svanedal, I.; Edlund, H.; Norgren, M. On chelating surfactants: Molecular perspectives and application prospects. *J. Mol. Liq.* **2019**, *278*, 688–705. https://doi.org/10.1016/j.molliq.2019.01.076

Ernst, K.-H.; Wild, F. R. W. P.; Blacque, O.; Berke, H. Alfred Werners coordination chemistry: New insights from old samples. *Angew. Chemie Int. Ed.* **2011**, *50* (46), 10780–10787. https://doi.org/10.1002/anie.201104477

Feng, Y.; Yang, H.; Wang, X.; Hu, C.; Jing, H.; Cheng, J. Role of transition metals in catalyst designs for oxygen evolution reaction: A comprehensive review. *Int. J. Hydrogen Energy.* **2022**, *47* (41), 17946–17970. https://doi.org/10.1016/j.ijhydene.2022.03.270

Habiddin, H.; Hartanto, D. Synthesis, characterization and application of complex compounds: Review of studies among Indonesian scholars. AIP Conf. Proc. 2023, 2569, 70001. https://doi.org/10.1063/5.0112075

Kılıç, A.; Durgun, M.; Erdoğan, A. The Novel bis-dioxime-based and boronic acid-capped groups containing Fe(II) and Co(II) complexes: Synthesis, characterization and spectroscopy. *J. Turkish Chem. Soc. Sect. A Chem.* **2017**, *4*, 11–22. https://doi.org/10.18596/jotcsa.318141

Kilic, A.; Fırat, H.; Aytar, E.; Durgun, M.; Baytak, A. K.; Aslanoglu, M.; Ulusoy, M. Dicobaloxime/organodicobaloximes bridged by different axial groups: synthesis, characterization, spectroscopy, and catalysis. *Chem. Pap.* **2017**, *71*, 1705–1720. https://doi.org/10.1007/s11696-017-0165-0

Kilic, A.; Keles, A.; Aytar, E.; Durgun, M.; Ulusoy, M. Synthesis of the multinuclear cobaloxime complexes via click chemistry as catalysts for the formation of cyclic carbonates from carbon dioxide and epoxides. *J. Chem. Sci.* **2015**, *127*, 1665–1674. https://doi.org/10.1007/s12039-015-0932-9

Laing, M.; Baines, S.; Sommerville, P. Crystal structure of trinitrotriamminecobalt(III). *Redetermination. Inorg. Chem.* **1971**, *10* (5), 1057–1061. https://doi.org/10.1021/ic50099a040

Nguyen, D. T.; Cavazos, R. J.; Harris, A. N.; Petros, R. A. Werner complexes viewed anew: Utilizing cobalt coordination chemistry for ‘traceless’ stimuli-responsive bioconjugation involving therapeutic nanoparticles, protein PEGylation, and drug-(bio)polymer conjugates. *Comments Inorg. Chem.* **2014**, *34* (3–4), 59–77. https://doi.org/10.1080/02603594.2014.940103

Nuber, B.; Siebert, H.; Weidenhammer, K.; Weiss, J.; Ziegler, M. L. The crystal structure of fac-triamminetrinitrocobalt(III), fac-$[Co(NH_3)_3(NO_2)_3$. *Acta Crystallogr. Sect. B* **1979**, *B35*, 1020–1023. https://doi.org/10.1107/S0567740879005483

Palmer, B. J.; Hill, R. H. Solid state photochemistry of fac-$Co(NH_3)_3(NO_2)_3$ and mer-$Co(NH_3)_3(N_3)_3$ as thin films on Si(111) surfaces. *J. Photochem. Photobiol. A Chem.* **1993**, *72*, 243–249. https://doi.org/10.1016/1010-6030(93)80020-A

Renfrew, A. K.; O’Neill, E. S.; Hambley, T. W.; New, E. J. Harnessing the properties of cobalt coordination complexes for biological application. *Coord. Chem. Rev.* **2018**, *375*, 221–233. https://doi.org/10.1016/j.ccr.2017.11.027

Singh, S.; Shanker, R. Base Hydrolysis of $[Co(NO_2)_3(NH_3)_3]_0$. *Inorg. Chem.* **1989**, *28* (14), 2695–2696. https://doi.org/10.1021/ic00313a001

Tanito, Y.; Saito, Y.; Kuroya, H. The crystal structure of trinitrotriammine-cobalt (III), $[Co(NH_3)_3(NO_2)_3]$. *Bull. Chem. Soc. Jpn*. **1952**, *25* (3), 188–191. https://doi.org/10.1246/bcsj.25.188

Bąk, J. M.; Effendy; Grabowsky, S.; Lindoy, L. F.; Price, J. R.; Skelton, B. W.; White, A. H. True and quasi-isomorphism in tetrakis(acetonitrile)coinage metal(I) salts. *Cryst. Eng. Comm*. **2013**, *15*, 1125–1138. https://doi.org/10.1039/c2ce26824h

Verma, C.; Quraishi, M. A.; Rhee, K. Y. Natural ligands: Promising ecofriendly alternatives for corrosion protection and plethora of many prospects. *Process Saf. Environ. Prot.* **2022**, *162*, 253–290. https://doi.org/10.1016/j.psep.2022.04.014

ECLÉTICA QUÍMICA

Eclet. Quim. **49** | e-1484, 2024

Original Article

https://doi.org/10.26850/1678-4618.eq.v49.2024.e1484

Determination of amoxicillin: A penicillin antibiotic in pharmaceutical dosage samples by spectrophotometric method

Chand **Pasha**[1+]

Abstract

New coupling agents such as 2,4-toluene diamine or sulphanilamide for the determination of amoxicillin spectrophotometrically are described. These methods are straightforward based on the reaction of amoxicillin with diazotized products of 2,4-toluene diamine or sulphanilamide to produce coloured azo dyes with maximum absorption at 462 or 468 nm. Amoxicillin responds linearly from 1.2–24.8 or 1.8–32.0 µg mL^{-1} when coupled with diazotized 2,4-toluene diamine or sulphanilamide. The molar absorptivity and Sandell's sensitivity of amoxicillin with 2,4-toluene diamine or amoxicillin with sulphanilamide azo dyes were 3.307×10^4 or 2.632×10^4 L mol^{-1} cm^{-1} and 1.105×10^{-2} or 1.388×10^{-2} µg cm^{-2}, respectively. The regression equation, correlation coefficient (R^2), detection limit and quantitation limit of amoxicillin with 2,4-toluene diamine or amoxicillin with sulphanilamide were evaluated. The percentage recoveries ranged from 97.00 to 100.50 with a relative standard deviation value was ± 0.98 to ± 1.85%. The method does not need temperature control or solvent extraction and has been applied successfully to determine amoxicillin in pharmaceutical preparation (tablets).

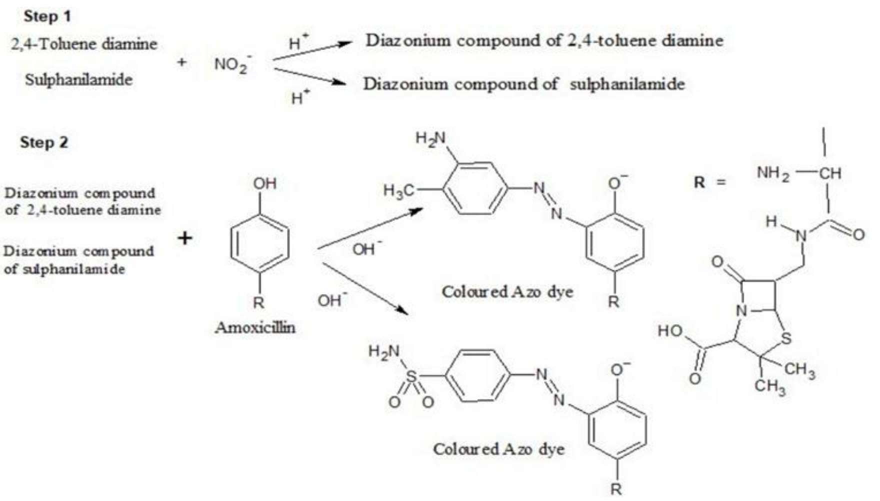

Article History

Received March 07, 2023
Accepted November 20, 2023
Published March 29, 2024

Keywords

1. spectrophotometry;
2. diazotization;
3. amoxicillin;
4. 2,4-toluene diamine;
5. sulphanilamide.

Section Editor

Paulo Clairmont Feitosa Lima Gomes

Highlights

- The 2,4-toluene diamine and sulphanilamide were used for amoxicillin determination.
- The coupling agents with amoxicillin showed high molar absorptivity and sensitivity.
- The method is very simple, sensitive, accurate, and has a high dye stability.
- The method applied to the analysis of amoxicillin in pharmaceutical samples.

[1]Royal Commission Yanbu Colleges and Institutes, Yanbu Industrial College, Yanbu, Kingdom of Saudi Arabia. **+Corresponding author:** Chand Pasha, **Phone:** +966531810596, **Email address:** drcpasha@gmail.com

1. Introduction

Amoxicillin is a β-lactam penicillin antibiotic with the chemical formula $C_6H_{19}N_3O_5S$, that is active against both gram-positive and gram-negative bacteria (Wilson *et al.*, 2004). It is used to treat a variety of bacterial infections caused by susceptible microorganisms, including skin, yeast, urinary tract and middle ear infections, strep throat, and pneumonia. Some of the side effects include nausea and rash, and those who are allergic to penicillin should avoid using it. However, those with kidney issues can use it without risk, and it is safe to use during pregnancy and breastfeeding (Amoxicillin, 2015). According to the most recent report from the European Centre for Disease Prevention and Control (ECDC, 2020), the average consumption of antimicrobial drugs for systemic use in the European Union in 2019 was 18.0 defined as daily doses per 1,000 inhabitants per day. After consumption, antibiotics are excreted as metabolites and unaltered compounds (Boix *et al.*, 2016) together with the high consumption of these compounds, it is not surprising that they reach the aquatic environment through wastewater discharges (Dinh *et al.*, 2011). Thus, the investigation of antibiotic residues in water has become an important topic in environmental science, including the analytical determination at trace levels (ng L^{-1} or μg L^{-1}) (Fonseca *et al.*, 2020; Hernández *et al.*, 2015; Rossmann *et al.*, 2014). The chemical structure of amoxicillin is shown in **Fig. 1**.

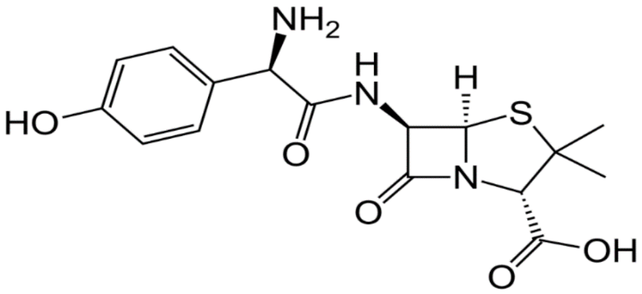

Figure 1. Chemical structure of amoxicillin.

Amoxicillin works by preventing the synthesis of bacterial cell walls (Wilson *et al.*, 2004), and it belongs to the penicillin class of antibiotics, which are broad-spectrum, semisynthetic, acid-stable, orally absorbed antibiotics that inhibit bacterial cell wall synthesis (Blumberg and Strominger, 1974).

According to a review of the literature, there are several methods for determining amoxicillin in pharmaceutical samples, including voltammetry (Fouladgar *et al.*, 2011; Uslu and Biryol, 1999; Santos *et al.*, 2008), fluorimetry (Muñoz de la Peña *et al.*, 2002), colourimetry (Elshafie *et al.*, 1996; Rao and Mohan, 1982), liquid chromatography (Aliev and Babazade, 2011; Fabregat-Safont *et al.*, 2021; Foroutan *et al.*, 2007; Hailekiros *et al.*, 2022; Wen *et al.*, 2008), chemiluminescence (Li *et al.*, 2003; Sun *et al.*, 2005), capillary electrophoresis (Oliva *et al.*, 2011), atomic absorption spectrometry (Mahmoud *et al.*, 2008), UV spectroscopy (Ergin and Yasa, 2022) and spectrophotometry (Ahmed *et al.*, 2004; Al-Abachi *et al.*, 2005; Asan and Seddiq, 2022; Al-Uzri, 2012; Jalal *et al.*, 2023; Othman and Al-Saffar, 2015; Quanmin and Zhanjun, 2006; Singh and Maheshwari, 2010; Ünal *et al.*, 2008). However, some of the methods (Ahmed *et al.*, 2004; Al-Abachi *et al.*, 2005; Foroutan *et al.*, 2007; Fouladgar *et al.*, 2011; Li *et al.*, 2003; Mahmoud *et al.*, 2008; Muñoz de la Peña *et al.*, 2002; Oliva *et al.*, 2011; Quanmin and Zhanjun, 2006; Sun *et al.*, 2005) presented for determining amoxicillin in pharmaceutical dosage were associated with major flaws such as tedious extraction methods, time consumption, lack of sensitivity, heating issues, and cooling effects.

The diazotization reaction of 2,4-toluene diamine or sulphanilamide with sodium nitrite in an acid medium yields diazonium compounds, which are then coupled with amoxicillin in an alkaline medium to yield yellow water-soluble azo dyes. The proposed methods are free of the drawbacks mentioned above and they are risk-free, simple, selective, and precise used for the determination of amoxicillin—a penicillin antibiotic—in pharmaceutical dosage samples by spectrophotometric method.

2. Experimental

2.1. Equipment

A JASCO V-730 spectrophotometer (Serial No. A 023561798) and pH meter (Eutech Instruments pH 510 Serial o. 1398504) were used for spectrometric analysis.

2.2. Chemicals and reagents

Amoxicillin stock solution (1,000 μg mL^{-1}), (Gift sample from Karnataka antibiotics and Pharmaceuticals Limited, Bangalore, India): A 0.104 g of amoxicillin was weighed accurately and dissolved in 5–10 mL of ethanol, shaken thoroughly then the solution is transferred to a 100 mL calibrated flask and filled to the proper level with double-distilled water. By dilution, the working solution was prepared as needed.

A 0.1 mol L^{-1} sodium nitrite solution, 0.5 mol L^{-1} hydrochloric acid solution, 1% of 2,4-toluene diamine or sulphanilamide solutions each and 0.5 mol L^{-1} sodium hydroxide solution were used.

Amoxicillin tablets of different trademarks used:

Vemox 50 (500 mg): Vega Pharma, Panoptic Exim Private Limited, Nagpur, Maharashtra.
Amoxicillin trihydrate (500 mg): Sandmartin Pharmaceuticals Private Limited, New Delhi, India.
EMOX 250 (250 mg): Emkam Pharma private Limited, Meerut, India.
Cipmox-250 (250 mg): Cipla Limited, Mumbai, India.
Amoxirum forte injection (300 mg): 200 mg amoxicillin present with sodium (molecular weight 340.4 mg): Karnataka antibiotics and pharmaceuticals Limited, Bangalore, India.

Amoxicillin tablets solution (1,000 μg mL^{-1})

Amoxicillin tablets/capsules of various brands were obtained from a homegrown dispensary and finely powdered. A precisely weighed quantity of powder (~ 0.25 g) was dissolved in 5–10 mL ethanol, then 80–100 mL distilled water was added, shaken well, filtered into a 250 mL calibrated flask, then the volume was completed to the mark with distilled water and the preparation of amoxicillin solution was continued as described above.

2.3. Procedure for the determination of amoxicillin

In a sequence of 10 mL calibrated flasks, an aliquot of the sample solution containing a known quantity of amoxicillin (μg mL^{-1}) was added. It was then mixed well for 2 min with the addition of 1 mL of a 0.1 mol L^{-1} solution of sodium nitrite and 0.5 mL of a 0.5 mol L^{-1} solution of hydrochloric acid before being set aside to allow the diazotization reaction to finish. After that, the mixture was thoroughly mixed after being diluted to 10 mL with double-distilled water and added volumes of 1 mL of 1% 2,4-toluene diamine or sulphanilamide and 1.0 mL of 0.5 mol L^{-1} sodium hydroxide solutions. After 5 min the formed coloured azo dyes absorbance was measured at 462 or 468 nm in comparison to the blank reagent.

3. Results and discussion

In the presence of a base, amoxicillin is coupled with the diazonium salt of 2,4-toluene diamine or sulphanilamide to produce a coloured azo dye. The absorption spectra of the azo dye produced by reacting amoxicillin with diazotized 2,4-toluene diamine or sulphanilamide (**Fig. 2**) had an absorption maximum at 462 nm or 468 nm, respectively.

The plot of absorbance versus concentration of amoxicillin coupled with diazotized 2,4-toluene diamine or sulphanilamide (**Fig. 3**) demonstrates that the dyes obey Beer's law in the range of 1.2–24.8 μg mL^{-1} of amoxicillin with 2,4-toluene diamine or 1.8–32.0 μg mL^{-1} of amoxicillin with sulphanilamide. Absorption spectra of the azo dye resulted from the reaction of amoxicillin with diazotized sulphanilamide against a reagent blank (2) and a blank reagent against distilled water (3).

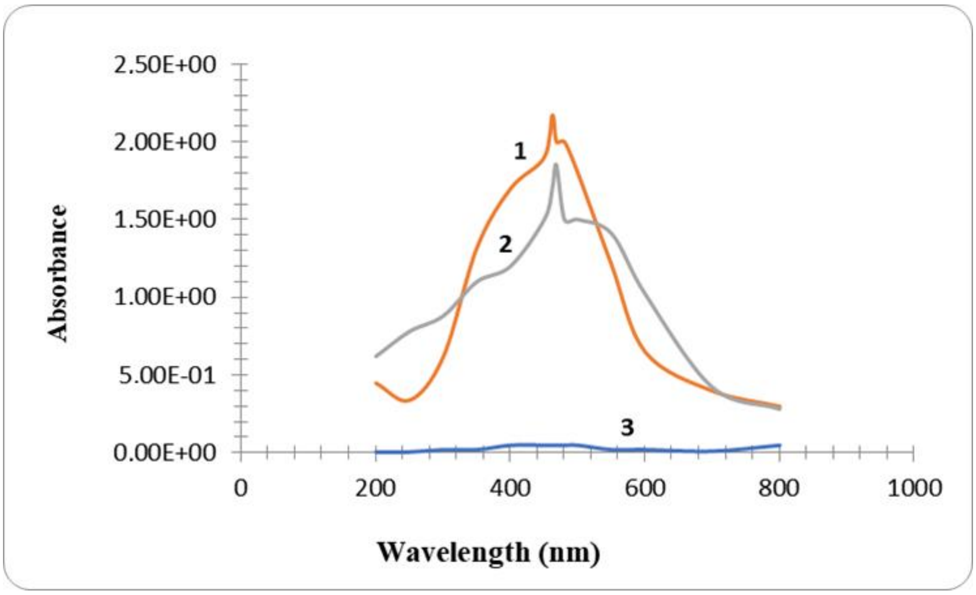

Figure 2. Absorption spectra of the azo dye produced by the reaction of amoxicillin with diazotized 2,4-toluene diamine (1) and sulphanilamide (2) against a blank reagent. The blank reagent spectrum is number (3).

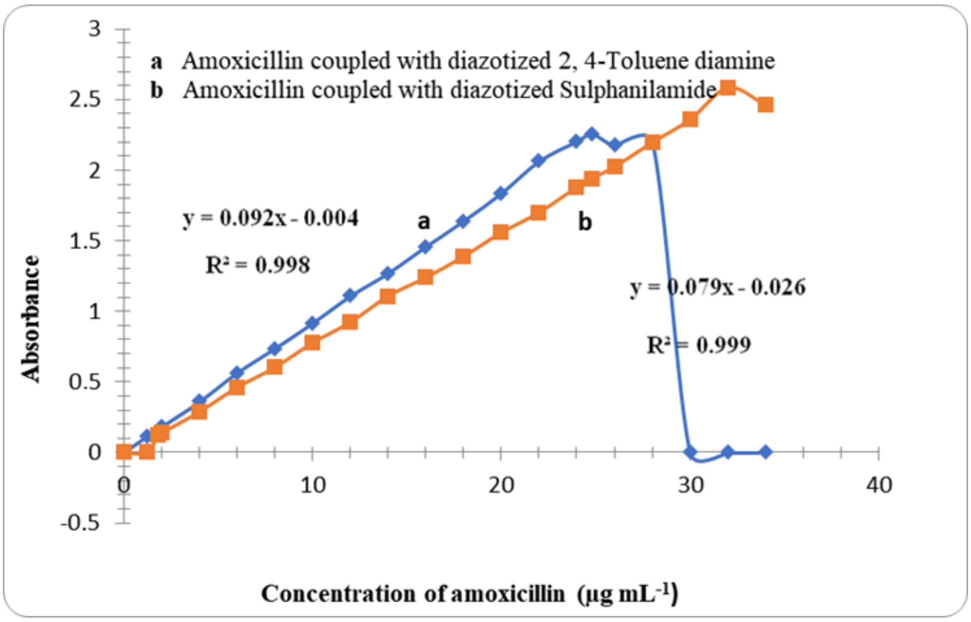

Figure 3. Adherence to Beer's law using amoxicillin coupled with diazotized 2,4-toluene diamine or sulphanilamide.

The reactions for steps 1 and 2 are shown in **Fig. 4**.

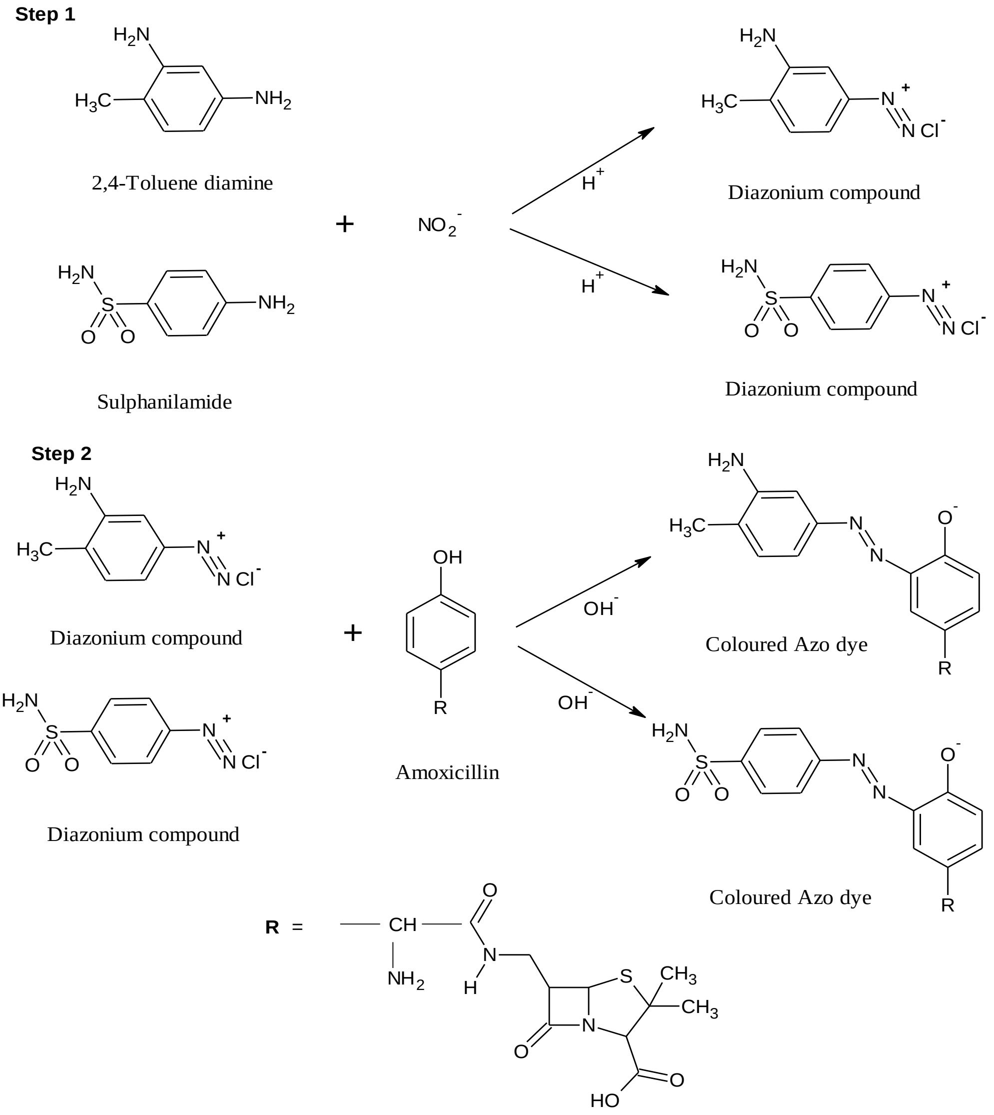

Figure 4. Diazonium salt of 2,4-toluene diamine or sulphanilamide is coupled with amoxicillin to produce coloured azo dyes.

3.1. Effect of temperature, acid and base concentration

The effect of temperature on diazotization reactions, room temperature (25 ± 5 °C) is advised because the loss in colour stability and intensity was seen at low and high temperatures.

The effect of acid on the diazotization reaction of amoxicillin (2 µg mL^{-1}) was examined by adding different acid solutions (0.5 mol L^{-1}), such as HCl, H_2SO_4, CH_3COOH and HNO_3. It was discovered that when amoxicillin was coupled with a diazotized 2,4-toluene diamine or sulphanilamide, CH_3COOH produced low absorbance with low colour stability while HCl produced high absorbance with highest colour stability. Therefore, for the amoxicillin diazotization reaction, 0.5 mL of 0.5 mol L^{-1} HCl was preferred (**Table 1**).

Table 1. Effect of acid concentration.

0.5 mol L^{-1} acid concentration	Absorbance (A) / mL of acid used					
	2,4-toluene diamine			Sulphanilamide		
	0.25 mL	0.5 mL	0.75 mL	0.25 mL	0.5 mL	0.75 mL
Hydrochloric acid	0.280	0.362	0.348	0.302	0.344	0.340
Sulfuric acid	0.256	0.292	0.306	0.288	0.276	0.287
Acetic acid	0.222	0.246	0.212	0.228	0.244	0.286
Nitric acid	0.248	0.284	0.293	0.232	0.248	0.262

The effect of the base on the diazotization reaction of amoxicillin (2 µg mL^{-1}) was examined by adding different base (0.5 mol L^{-1}) solutions such as NaOH, KOH, NH_4OH and Na_2CO_3. It was discovered that when amoxicillin was coupled with diazotized 2,4-toluene diamine or sulphanilamide, Na_2CO_3 produced low absorbance and NaOH produced high absorbance with highest colour stability. Therefore, for the amoxicillin diazotization reaction 1.0 mL of 0.5 mol L^{-1} NaOH solutions was preferred (Table 2).

3.2. Effect of coupling reagents and nitrite concentration

In the current method, 2,4-toluene diamine or sulphanilamide is used as a coupling agent by adding 0.50 to 2.0 mL of 1% 2,4-toluene diamine or sulphanilamide to a series of nitrite solutions. In an ultimate volume of 10 mL, it was discovered that 1 mL of 2,4-toluene diamine or sulphanilamide (1%) solution produced the brightest and firmest colour (Table 3).

Using the current method with 2 µg mL^{-1} of amoxicillin and adding 1 mL of 0.025-0.150 mol L^{-1} solutions of the nitrite in hydrochloric acid (0.5 mol L^{-1}) to a series of nitrite solutions, the colour reaches its peak intensity when using 1 mL of 0.1 mol L^{-1} sodium nitrite solution. Higher concentrations failed to further increase the absorbance while lower concentrations gave poor results (Table 4).

3.3. Effect of interference

The determination of amoxicillin in the presence of various excipients such as lactose (800 µg mL^{-1}), fructose (1,000 µg mL^{-1}), glucose (1,200 µg mL^{-1}), urea (300 µg mL^{-1}) and starch (600 µg mL^{-1}) did not interfere with the determination of the excipients.

Table 2. Effect of Base concentration.

0.5 mol L^{-1} acid concentration used	Absorbance (A) / mL of Base used					
	2,4-toluene diamine			Sulphanilamide		
	0.5 mL	1.0 mL	1.5 mL	0.5 mL	1.0 mL	1.5 mL
Sodium hydroxide	0.260	0.282	0.266	0.284	0.244	0.264
Potassium hydroxide	0.236	0.262	0.242	0.264	0.224	0.257
Ammonium hydroxide	0.214	0.254	0.204	0.242	0.208	0.246
Sodium carbonate	0.138	0.222	0.188	0.202	0.196	0.220

Table 3. Effect of 2,4-toluene diamine or sulphanilamide solution on absorbance.

1% 2,4-toluene diamine or sulphanilamide solution used (mL)	Absorbance (A) for 2,4-toluene diamine	Absorbance (A) for sulphanilamide
0.50	0.284	0.264
1.00	0.316	0.328
1.50	0.302	0.312
2.00	0.296	0.294

Table 4. Effect of sodium nitrite.

1 mL of $NaNO_2$ solution (mol L^{-1})	Absorbance (A)	
	2,4-toluene diamine	sulphanilamide
0.025	0.164	0.182
0.050	0.188	0.194
0.075	0.192	0.226
0.100	0.288	0.264
0.125	0.248	0.246
0.150	0.240	0.232

3.4. Analytical data

Plotting absorbance versus concentration of amoxicillin resulted in a straight line on the graph. Beer's law is obeyed between the concentrations of 1.2–24.8 µg mL^{-1} of amoxicillin with 2,4-toluene diamine or between the concentrations of 1.8–32.0 µg mL^{-1} with sulphanilamide. The molar absorptivity of the coloured azo dye of amoxicillin coupled with the diazonium salt of 2,4-toluene diamine or sulphanilamide was found to be 3.307 × 10^{4} L mol^{-1} cm^{-1} or 2.632 × 10^{4} L mol^{-1} cm^{-1}, and the Sandell's sensitivity of coloured system with a nitrite-2,4-toluene diamine or nitrite-sulphanilamide were found to be 1.105 × 10^{-2} µg cm^{-2} or 1.388 × 10^{-2} µg cm^{-2} with maximum absorption at 462 or 468 nm (Fig. 2 and 3).

The regression equation and correlation coefficient (R^2) of amoxicillin with 2,4-toluene diamine or amoxicillin with sulphanilamide were $y = 0.092x - 0.004$, or $y = 0.079x - 0.026$ and R^2 of 0.998 or 0.999 and have high dye stability (more than 10 h). The detection limit ($D_L = 3.3\sigma/S$) and quantitation limit ($Q_L = 10\sigma/S$) of amoxicillin coupled with diazotized 2,4-toluene diamine or sulphanilamide were found to be 0.351 µg mL^{-1} or 0.420 µg mL^{-1} and 1.065 µg mL^{-1} or 1.274 µg mL^{-1} (where σ = Standard Deviation, [n = 5] and S = slope of the curve). The better optical characteristics and statistical data were obtained under optimum conditions (Table 5).

Table 5. Determination of amoxicillin in various pharmaceutical samples.

Pharmaceutical Samples	Sample taken (µg mL^{-1})	Using 2,4-toluene diamine		Using sulphanilamide	
		Sample found[a] (µg mL^{-1}) ± %RSD	Rec. (%)	Sample found[a 1] (µg mL^{-1}) ± %RSD	Rec. (%)
Vemox 500 (500 mg/tab)	04.00	3.92 ± 1.43	98.00	3.96 ± 1.62	99.00
	08.00	7.91 ± 1.24	98.87	7.92 ± 1.46	99.00
	12.00	11.94 ± 1.32	99.50	11.90 ± 1.46	99.16
	16.00	15.90 ± 1.20	99.34	15.84 ± 1.28	99.00
	20.00	19.92 ± 1.26	99.60	19.90 ± 1.42	99.50
Amoxicillin Trihydrate (500 mg/tab)	04.00	3.94 ± 1.48	98.50	4.02 ± 1.22	100.5
	08.00	7.90 ± 1.24	98.70	7.98 ± 1.46	99.75
	12.00	11.88 ± 1.44	99.00	11.92 ± 1.32	99.33
	16.00	15.86 ± 1.26	99.12	15.90 ± 1.36	99.37
	20.00	19.92 ± 1.35	99.6	19.82 ± 1.45	99.10
EMOX 250 (250 mg/tab)	04.00	3.90 ± 1.23	97.50	3.94 ± 1.28	98.50
	08.00	7.92 ± 1.44	99.00	7.88 ± 1.32	98.50
	12.00	11.88 ± 1.66	99.00	11.90 ± 1.45	99.17
	16.00	15.92 ± 0.98	99.50	15.88 ± 1.42	99.25
	20.00	19.86 ± 1.46	99.30	19.80 ± 1.26	99.00
Cipmox-250 (250 mg/tab)	04.00	4.00 ± 1.54	100.0	3.94 ± 1.44	98.50
	08.00	7.90 ± 1.22	98.75	7.96 ± 1.28	99.50
	12.00	11.94 ± 1.49	99.50	11.88 ± 1.54	99.00
	16.00	15.94 ± 1.27	99.62	15.86 ± 1.64	99.12
	20.00	19.90 ± 1.33	99.50	19.82 ± 1.24	99.10
Amoxirum forte injection (300 mg/tab)	04.00	3.92 ± 1.42	98.00	3.88 ± 1.26	97.00
	08.00	7.91 ± 1.22	98.87	7.92 ± 1.34	99.00
	12.00	11.94 ± 1.26	99.50	11.84 ± 1.52	98.67
	16.00	15.86 ± 1.34	99.12	15.84 ± 1.26	99.00
	20.00	19.80 ± 1.65	99.00	19.78 ± 1.85	98.90

a. Mean (n=5) ± %RSD {relative standard deviation}.

3.5. Applications

Amoxicillin can be found in a variety of pharmaceutical samples using the provided method, which is straightforward and easy to use. The findings of the recommended methodology closely correspond to the acknowledged content. For all five samples, the percentage recoveries ranged, with a 95% level of confidence, from 97.00 to 100.50 and the relative standard deviation value was ±0.98–±1.85%. The appearance of pharmaceutical samples containing additional ingredients had no negative effects. The outcomes are contrasted with the endorsed spectrophotometric method (Al-Uzri, 2012; Othman and Al-Saffar, 2015). These attest to the fact that the proposed method and the recommended method are not significantly different. To evaluate precision and accuracy, replicate analyses were performed on five different samples that contained amoxicillin at various concentrations (Table 5).

4. Conclusions

New coupling agents such as 2,4-toluene diamine or sulphanilamide, used for the spectrophotometric determination of amoxicillin, are reasonably priced and selective. Compared to some of the reported methods, the procedure is very simple, fast, sensitive, accurate, and has a high dye stability (more than 10 h).

The method need not involve time-consuming separation or solvent extraction procedures and the high accuracy and precision of the proposed methods are highlighted by their low percentage relative standard deviation and percentage recovery values. The proposed methods produce precise, repeatable results that are free from excipient interference and was applied to the analysis of amoxicillin in pharmaceutical samples.

Data availability statement

All data sets were generated or analyzed in the current study.

Funding

Not applicable.

Acknowledgments

The author would like to thank YELI Management and HOD, General Studies for their moral guidance.

References

Ahmed, A. S.; Rahman, N.; Islam, F. Spectrophotometric determination of ampicillin, amoxicillin, carbenicillin using folin ciocalteu phenol reagent. *Anal. Chem.* **2004**, *59*, 119–123. https://doi.org/10.1023/B:JANC.0000014736.59554.5c

Al-Abachi, M. Q.; Haddi, H.; Al-Abachi, A. M. Spectrophotometric determination of amoxicillin by reaction with N,N-dimethyl-p-phenylenediamine and potassium hexacyanoferrate(III). *Anal. Chim. Acta.* **2005**, *554* (1–2), 184–189. https://doi.org/10.1016/j.aca.2005.08.030

Aliev, A. M.; Babazade, G. M. Comparative study of quantitative determination of amoxicillin in capsules by mercurimetry and liquid chromatography. *Pharm. Chem. J.*, **2011**, *45*, 257–260. https://doi.org/10.1007/s11094-011-0610-2

Al-Uzri, W. A. Spectrophotometric determination of amoxicillin in pharmaceutical preparations through diazotization and coupling reaction. *Iraqi Journal of Science*. **2012**, *53* (4), 713–722.

Amoxicillin. The American Society of Health-System Pharmacists. Archived from the original on 5 September 2015. Retrieved, 1 August 2015.

Asan, A.; Seddiq, N. A simple spectrophotometric determination of amoxicillin in Drug samples. *J. Turk. Chem. Soc.* **2022**, *9* (2), 423–432. https://doi.org/10.18596/jotcsa.978686

Blumberg, P. M.; Strominger, J. L. Interaction of penicillin with the bacterial cell: penicillin–binding proteins and penicillin–sensitive enzymes. *Bacterial Rev.* **1974**, *38* (3) 291–335. https://doi.org/10.1128/br.38.3.291-335.1974

Boix, C.; Ibáñez, M.; Bagnati, R.; Zuccato, E.; Sancho, J. V.; Hernández, F.; Castiglioni, S. High-resolution mass spectrometry to investigate omeprazole and venlafaxine metabolites in wastewater. *J. Hazard. Mater.* **2016**, *302*, 332–340. https://doi.org/10.1016/j.jhazmat.2015.09.059

Dinh, Q. T.; Alliot, F.; Moreau-Guigona, E.; Eurina, J.; Chevreuil, M.; Labadie, P. Measurement of trace levels of antibiotics in river water using online enrichment and triple-quadrupole. *Talanta.* **2011**, *85* (3), 1238–1245. https://doi.org/10.1016/j.talanta.2011.05.013

Elshafie, F. S.; Gad-Kariem, E. A.; Al-Rashood, K. A.; Al-Khamees, H. A.; El-Obeid, H. A. Colourimetric method for the determination of ampicillin and amoxicillin. *Anal. Lett.* **1996**, *29* (3), 381–393. https://doi.org/10.1080/00032719608000405

Ergin, M. F.; Yasa, H. Determination of amoxicillin trihydrate impurities 4-hydroxyphenylglycine (4-HPG) and 6-Aminopenicylanic acid (6-APA) by means of ultraviolet spectroscopy. *Methods Appl Fluoresc*, **2022**, *10* (3), 25–32. https://doi.org/10.1088/2050-6120/ac7037

Fabregat-Safont, D.; Elena, P.; Lubertus, B.; Ionut, M.; Félix, H. Rapid and sensitive analytical method for the determination of amoxicillin and related compounds in water meeting the requirements of the European union watch list David. *J. Chromatogr. B.* **2021**, *1658*, 462605. https://doi.org/10.1016/j.chroma.2021.462605

Fonseca, E.; Hernández, F.; Ibáñez, M.; Rico, A.; Pitarch, E.; Bijlsma, L. Occurrence and ecological risks of pharmaceuticals in a Mediterranean river in Eastern Spain. *Environ. Int.* **2020**, *144*, 106004. https://doi.org/10.1016/j.envint.2020.106004

Foroutan, S. M.; Zarghi, A.; Shafaati, A.; Khoddam, A.; Movahed, H. Simultaneous determination of amoxicillin and clavulanic acid in human plasma by isocratic reversed-phase HPLC using UV detection. *J. Pharm. and Biomed. Anal.* **2007**, *45* (3), 531–534. https://doi.org/10.1016/j.jpba.2007.06.019

Fouladgar, M.; Hadjmohammadi, M. R.; Khalilzadeh, M. A.; Biparva, P.; Teymoori, N.; Beitollah, H. Voltammetric determination of amoxicillin at the electrochemical sensor ferrocene dicarboxylic acid multi-wall carbon nanotubes paste electrode. *Int. J. Electrochem. Sci.* **2011**, *6* (5), 1355–1366. https://doi.org/10.1016/S1452-3981(23)15079-6

Hailekiros, G.; Getu, K.; Tadele, E.; Tesfamichael, G. A validated new RP-HPLC method for simultaneous determination of amoxicillin, ampicillin and cloxacillin in pharmaceutical formulations. *Acta Chromatographica*. **2022**, *35* (2), 193–203. https://doi.org/10.1556/1326.2022.01043

Hernández, F.; Ibáñez, V.; Portolés, T.; Cervera, M. I.; Sancho, J. V.; López, F. J. Advancing towards universal screening for organic pollutants in waters. *J. Hazard. Mater.* **2015**, *282*, 86–95. https://doi.org/10.1016/j.jhazmat.2014.08.006

Jalal, M. T. Spectrophotometric determination of amoxicillin trihydrate in pharmaceutical preparation. *HIV Nursing*. **2023**, *23* (2), 140–147. https://doi.org/10.31838/hiv23.02.24

Li, Y.; Tang, Y.; Yao, H.; Fu, J. Determination of ampicillin and amoxicillin by flow injection chemiluminescence method based on their enhancing effects on the luminal-periodate reaction. *Luminescence*. **2003**, *18* (6), 313–317. https://doi.org/10.1002/bio.741

Mahmoud, I. M.; Rafat, N. M.; Monzer, A.; Naser, E. S.; Rafik, H. S.; Akila, S. A. An indirect atomic absorption spectrometric determination of ciprofloxacin, amoxicillin and diclofenac sodium in pharmaceutical formulations. *J. Serb. Chem. Soc.* **2008**, *73* (5), 569–576. https://doi.org/10.2298/JSC0805569I

Muñoz de la Peña, A.; Acedo-Valenzuela, M. I.; Espinosa-Mansilla, A.; Sánchez Maqueda, R. Stopped-flow fluorimetric determination of amoxycillin and clavulanic acid by partial least-squares multivariate calibration. *Talanta*. **2002**, *56* (4), 635–642. https://doi.org/10.1016/S0039-9140(01)00612-9

Oliva, D. C.; Velez, K. T.; Vazquez, A. L. R. Simultaneous determination of bromhexine and amoxicillin in pharmaceutical formulations by capillary electrophoresis. *J. Mex. Chem. Soc*. **2011**, *55* (2), 79–83.

Othman, N. S.; Al-Saffar, R. S. Spectrophotometric determination of amoxicillin in pharmaceutical preparations. *Intern. J. Enhanced Res. Sci. Tech. Eng*. **2015**, *4* (6) 167–173. https://doi.org/10.13140/RG.2.2.22557.05604

Quanmin, L.; Zhanjun, Y. Study of spectrophotometric determination of amoxicillin using sodium 1,2-naphthoquinone-4-sulfonate as the chemical derivative chromogenic reagent. *Anal. Lett*. **2006**, *39* (4), 763–775. https://doi.org/10.1080/00032710600611525

Rao, G. R.; Mohan, K. R. Colorimetric method for estimation of amoxicillin and the dosage form. *Ind. Drugs.* **1982**, *19*, 326-337.

Rossmann, J.; Schubert, S.; Gurke, R.; Oertel, R.; Kirch, W. Simultaneous determination of most prescribed antibiotics in multiple urban wastewaters by SPE-LC–MS/MS. *J. Chromatogr. B.* **2014**, *969*, 162–170. https://doi.org/10.1016/j.jchromb.2014.08.008

Santos, D. P.; Bergamini, M. F.; Zanoni M. V. B. Voltammetric sensor for amoxicillin determination in human urine using Polyglutamic acid/glutaraldehyde film. *Sensors and Actuators B: Chemical*. **2008**, *133* (2), 398–403. https://doi.org/10.1016/j.snb.2008.02.045

Singh, D. K.; Maheshwari, G. Spectrophotometric determination of penicillins in pure and pharmaceutical formulations using folin-ciocalteu reagent. *Drug test. and Anal*. **2010**, *2* (10), 503–506. https://doi.org/10.1002/dta.157

European Centre for Disease Prevention and Control (ECDC). Antimicrobial consumption in the EU/EEA – Annual Epidemiological Report 2019. ECDC, 2020. https://www.ecdc.europa.eu/sites/default/files/documents/Antimicrobial-consumption-in-the-EU-Annual-Epidemiological-Report-2019.pdf (accessed 2023-10-20).

Sun, Y.; Tang, Y.; Yao, H.; Li, Y. Flow injection chemiluminescence analysis of some penicillins by their sensitizing effect on the potassium permanganate-glyoxal reaction. *Anal. Sci*. **2005**, *21*, 457–460. https://doi.org/10.2116/analsci.21.457

Ünal, K.; Palabiyik, I. M.; Karacan, E.; Onur, F. Spectrophotometric determination of amoxicillin in pharmaceutical formulations. *Turk. J. Pharm. Sci*. **2008**, *5* (1), 1–16.

Uslu, B.; Biryol, I. Voltammetric determination of amoxicillin using a poly (N-vinyl imidazole) modified carbon paste electrode. *J Pharm. Biomed. Anal.* **1999**, *20* (3), 591–598. https://doi.org/10.1016/S0731-7085(99)00059-X

Wen, A.; Hang, T.; Chen, S.; Wang, Z.; Ding, L.; Tiam, Y.; Zhang, M.; Xu, X. Simultaneous determination of amoxicillin and ambroxol in human plasma by LC-MS/MS: Validation and application to pharmacokinetic study. *J. Pharm. and Biomed. Anal*. **2008**, *48* (3), 829–834. https://doi.org/10.1016/j.jpba.2008.05.032

Wilson, O. C.; Ole, G.; Delgado, N. J. Textbook of organic medicinal and pharmaceutical chemistry; Lippincott Williams and Wilkins, 2004.

ECLÉTICA QUÍMICA

Eclet. Quim. 49 | e-1485, 2024

Original Article

https://doi.org/10.26850/1678-4618.eq.v49.2024.e1485

Influence of chitosan's purification methodology on the formation of layer-by-layer films

Ana Cristina Facundo de Brito **Pontes**[1+], Luciana Araújo **Nascimento**[1], Daniel de Lima **Pontes**[1], Ótom Anselmo de **Oliveira**[1], Francisco Ordelei da Silva **Nascimento**[1], Francimar Lopes da **Silva Júnior**[1]

Abstract

Concern for the environment for the development of new biodegradable materials has been constant in scientific circles. With this in mind, this work proposes a study on the formation of self-assembled thin films using chitosan (Qt), a biodegradable material. This polyelectrolyte has several purification methodologies, but we did not identify any studies on the effect of these methodologies on film formation. Thus, after the purification process and characterization of the three forms of chitosan purification, films were produced using the layer-by-layer (LBL) technique. The growth of the films was monitored using the UV-vis technique. Spectroscopy in the Infrared region showed positions in the main bands present in chitosan and sodium nitroprusside (NP) in the formed films. Two semi-reversible processes were found for the QtN/NP and QtAc/NP films, related to the reduction of iron oxide present in the NP. The effect of pH (4.0, 7.0 and 10) on the electrochemical processes indicated that the charge transfer occurs more efficiently at pH 7.0.

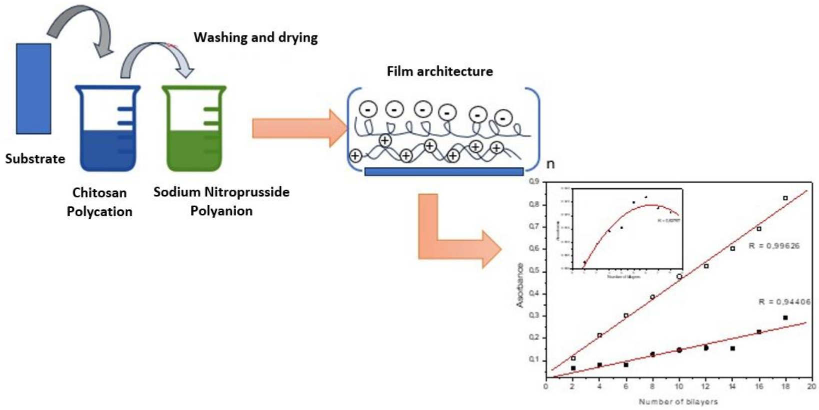

Article History

- Received March 23, 2023
- Accepted November 24, 2023
- Published April 22, 2024

Keywords

1. biodegradable;
2. self-assembled;
3. sodium nitroprusside.

Section Editor

Patricia Hatsue Suegama
Marcos Carlos de Mattos

Highlights

- The effect of chitosan purification methodology.
- Monitoring the formation of self-assembled films by UV-Vis.
- Electrochemical tests indicate different interaction mechanisms between species.

[1] Federal University of Rio Grande do Norte, Institute of Chemistry, Natal, Brazil. **+Corresponding author:** Ana Cristina Facundo de Brito Pontes, **Phone:** +5584987166346, **Email address:** ana.cristina.pontes@ufrn.br

1. Introduction

The layer-by-layer (LBL) deposition represents an interesting alternative for the development of films for several applications such as medicine and bio-applications (Ariga *et al.*, 2012; Nesic *et al.*, 2016; Xia *et al.*, 2019) to improve corrosion resistance (Gao *et al.*, 2019) and electrochemical sensing and biosensing (Pannell *et al.*, 2018; Si *et al.*, 2019).

LBL method (Crespilho *et al.*, 2006a), has been the main choice for the manufacture of nanostructured films, as they have several advantages, such as low cost, various materials can be used, the film is made under mild conditions and thus, multilayer structures can be constructed to obtain the desired number of bilayers, since apparently there are no limitations on the amount of layers that can be deposited (Cheung *et al.*, 1992; Oliveira Junior *et al.*, 2001). The most common interaction is provided by the electrostatic attraction, the alternative adsorption of opposites charged. Due to their low toxicity, biodegradability, and natural availability (Umoren and Eduok, 2016) polysaccharides can be rather good candidates.

Chitosan in an acidic environment presents positive charges due to the protonation of the amino groups (NH_3^+), a substrate with a high density of negative sites immersed in this solution will behave as a suitable support for the attraction and subsequent formation of a homogeneous film. Layer-by-layer films with chitosan have been studied as active surfaces with antimicrobial and antioxidant potential (Li and Peng, 2015; Luo *et al.*, 2012).

Chitosan is the most well-known natural biopolymer and has a wide range of applications, such as in the health area (Delolo *et al.*, 2014; Lins *et al.*, 2014; Silva *et al.*, 2006; Ungureanu *et al.*, 2015), environment (Marques Neto *et al.*, 2013) and technology (Souza *et al.*, 2015; Vinhola *et al.*, 2012).

The properties of chitosan, such as degree of purity, solubility, viscosity, degree of deacetylation (GD), molecular weight and others, are influenced by the methodology used to obtain it, as well as by the purification techniques to which they are subjected (Arrascue *et al.*, 2003; Battisti and Campana-Filho, 2008; Crini and Badot, 2008; Santos *et al.*, 2003; Gonsalves *et al.*, 2011; Kumar, 2000; Laranjeira and Fávere, 2009; Roberts, 1992; Silva *et al.*, 2006).

There are several methodologies used for the purification of chitosan, however, these procedures involve the steps of dissolving in an aqueous medium of controlled ionic strength, filtration, precipitation by the addition of non-solvent, washing and drying. This type of purification defines in advance the type of counter ion that will be present in the purified sample. Steps such as dialysis and lyophilization can be added to the procedures (Signini and Campana Filho, 2001).

As in the layer-by-layer technique, the production of films is based on the electrostatic interaction between molecules containing ionic groups and having chitosan as the amino group (NH_3^+), it is necessary to use another compound with opposite charge. Thinking about the production of films that may have applications as biosensors, NP was used, with molecular formula $Na_2[Fe(CN)_5(NO)]$. It has been used for more than 50 years as a vasodilator in cases of emergency in hypertension attacks, blood pressure control in surgeries and the treatment of chronic hypertension as it provides a quick response without the need for overuse (César *et al.*, 2001; Freitas *et al.*, 2012; Sass *et al.*, 2007; Stocche *et al.*, 2003). There are also reports of the use of NP in the determination of sulfur compounds in fresh and saline waters (Sonne and Dasgupta, 1991), as well as in the determination of phenols in aqueous two-phase systems (Rodrigues *et al.*, 2010).

The literature reports several types of film formation studies with chitosan, however, they all use it with modifications, whether in the form of Schiff bases or through crosslinking reactions (Amanulla *et al.*, 2017; Lu *et al.*, 2022; Suginta *et al.*, 2013). Therefore, this article makes a study on the effect of chitosan purification on the formation of self-assembled films obtained through electrostatic interaction.

2. Experimental

2.1. Chitosan purification

Chitosan of commercial origin (POLYMAR) was purified in three different ways, to obtain a pure and homogeneous material. The methodologies used in the purifications were proposed by Signini and Campana Filho (2001) with modifications and are described below:

a. **Neutral chitosan ($Qt_{Neutral}$):** It is solubilized in acetic acid, precipitated in ammonium hydroxide, filtration, dried, and stored in a dry environment.
b. **Chitosan acetate ($Qt_{Acetate}$):** It is solubilized in acetic acid, precipitated in ethanol, dried, and stored in a dry environment.
c. **Chitosan hydrochloride ($Qt_{Hydrochloride}$):** Solubilized in hydrochloric acid, sodium chloride added, precipitated in ethanol, filtered, dried, and stored in a dry environment.

2.2. Chitosan characterization

The infrared spectra of chitosan purified in different forms were obtained in the form of a KBr tablet, using a Shimadzu spectrophotometer, model FTIR-8400S, series IRAFFINITY-1, software IRSOLUTION, version 1.60, with scan number equal to 30 and resolution 4.

The determination of the degree of deacetylation of the purified chitosan (% GD) was made by conductivity measurement (Raymond *et al.*, 1993), and the viscometrical molar mass was obtained through capillary viscosimetry (Signini and Campana Filho, 1998; 2001). The values of the Huggins constant (K) and α used were 76.0 x 10^{-5} and 0.76 (Canella and Garcia, 2001).

The moisture percentage of chitosan samples was determined by thermogravimetric analysis using a thermogravimetric analyzer unit and simultaneously calorimeter, TA Instruments model SDTQ600 manufacturer. The samples were analyzed in an alumina crucible at a rate of 2.5 °C min^{-1}, heated from 25 °C to 900 °C under a nitrogen atmosphere, with a flow rate of 50 mL min^{-1}.

2.3. Sodium nitroprusside (NP)

The $Na_2[Fe(CN)_5(NO)]$ used was obtained from PROQUÍMIOS and no purification was necessary. For the preparation of the films, a solution of 23 g L^{-1} in methanol was prepared.

2.4. Layer-by-layer (LBL) fabrication

The LBL films were deposited on quartz and ITO glass substrates by alternating immersion into cationic chitosan and anionic NP solutions for 5 min. Chitosan solution (Qt) 5 g L^{-1} in 1% acetic acid and a solution of sodium nitroprusside (NP) 23 g L^{-1} in methanol. After each dive, the slide was washed with distilled water and dried under nitrogen flow. The films were prepared with $(Qt/NP)_n$, with "n" being the number of layers with n = 2, 4, 18 and 20 layers.

2.5. Characterization of LBL films

The growth monitoring of the films was performed using the UV-Vis absorbance spectroscopy technique (Agilent, model 8453) on a quartz plate, the same material used in the IR technique for LBL films using the Shimadzu spectrophotometer, model FTIR-8400S, series IRAFFINITY-1, software IRSOLUTION, version 1.60, with scan number equal to 30 and resolution 4.

The electrochemical experiments were performed using an AUTOLAB AUT 85282 system. The film $(Qt/NP)_{20}$ was deposited on ITO (glass covered with a thin indium-doped tin oxide layer) glass substrates used as a working electrode. The reference electrode was an Ag|AgCl/KCl saturated electrode and the counter electrode was a Pt plate The electrochemical cell used in the cyclic voltammetry measurements had a total volume of 50 mL with a cap with a plug for 3 electrodes and before the measurement, argon gas was bubbled into the solution. The experiments were conducted in a 0.1 mol L^{-1} KCl at 25 °C.

3. Results and discussion

The purification process of chitosan in neutral, acetate and hydrochloride forms yielded 82.5%, 64.1% and 85.6%, respectively. These yield values are due to loss due to handling and, mainly, to the presence of insoluble materials and aggregates present in chitosan that were eliminated during the filtration steps. The presence of insoluble materials in commercial products is reported in the literature (Ottøy *et al.*, 1996).

The purification process makes more polar groups available, which increases the ability to interact with other compounds (Signini and Campana Filho, 2001). The differences in purification methodologies resulted in different chitosan molecules in terms of visual aspect and solubility. All the purified samples were soluble in diluted acetic acid solution, the samples purified in the form of acetate and hydrochloride were partially soluble in water.

The number of amino groups present in the chitosan polymer chain is an important parameter and is related to electrostatic interactions for the formation of self-assembled films. Its order of magnitude can be determined through the degree of deacetylation (% GD). One of the simplest and most used techniques for this determination is conductometric titration. The data obtained for the different chitosan samples are shown in **Table 1**. The lower % GD of the $Qt_{Hydrochloride}$ sample can be explained by the change in inter- and intra-chain relationships, caused by using a strong acid in its purification.

The moisture content for the purified chitosan samples in the different forms obtained values lower than that observed in the literature (Signini and Campana Filho, 2001) (23.8 ±0.4) % for the same purification methodology. The difference may be related to the drying step, in the case of literature it was carried out at 25 °C, which does not remove the water present, whereas, in our work, the drying process was used with slight heating.

Viscosimetry is one of the most used processes for determining the molar mass of polymers, as it is a simple technique without requiring equipment with high costs. For the three purified chitosan holders, a good correlation index was obtained between the experimental measures with R > 0.99. As can be seen in **Table 1**, the application used in the purification of chitosan directly affects the viscosity of the polysaccharide and its molar mass, indicating differences in its properties.

Table 1. Chitosan properties in its different forms of purification.

Sample	% GD	η (mL g^{-1})	Mv(g mol^{-1})	Mv (g mol^{-1})*	Moisture content (%)
$Qt_{Neutral}$	68 ± 2	273.72	4.79 x 10^4	16.7 x 10^4	12.16
$Qt_{Neutral}$	69 ± 5	136.18	1.14 x 10^4	17.2 x 10^4	13.49
$Qt_{Hydrochloride}$	61 ± 4	44.72	4.54 x 10^3	16.1 x 10^4	16.84

Source: Elaborated by the authors using data from Signini and Campana Filho (2001).

The main characteristic bands of the infrared absorption spectrum of samples of chitosan in their different purified forms are shown in **Table 2**. The OH axial stretch band, between 3467 to 3502 cm^{-1}, appears to overlap the band N-H stretch. All bands identified are very similar to those described in the literature (Battisti and Campana-Filho, 2008; Vinhola *et al.*, 2012) and show that the same functional groups are present in all analyzed samples. The band in the 2926 to 2030 cm^{-1} region is attributed to the C-H stretching of the CH_2 groups of pyranoses. It is also possible to observe a peak from 1321 cm^{-1} to 1381 cm^{-1} characteristic of the angular deformation of CH_2 and CH_3.

Table 2. Main assignments of the infrared bands for the purified chitosan samples.

Sample	Infrared band assignments (cm^{-1})							
	$\nu_{C=O}$ (amide I)	δ_{N-H} (amide II)	δ_{C-N} (amide III)	δ_{CH}	ν_{COC} β-(1-4)	δ_{CO}	ν_{OH}	ν_{C-H}
$Qt_{Neutral}$	1664	1556	1381	1423	1156	1078	3467	2878
$Qt_{Acetate}$	1658	1566	1321	1415	1157	1074	3471	2879
$Qt_{hydrochloride}$	1643	1525	1381	1323	1155	1082	3502	2885
Signini and Campana Filho (2001)	1655	1600	1423	-	1153	1031	3450	2904

Note: δ = deformation; ν = Stretch.
Source: Elaborated by the authors using data from Signini and Campana Filho (2001).

The thermal analysis study for the chitosan samples in their different forms of purification showed two mass losses. The first event is related to the loss of moisture in the material, while the second event is related to the breaking of the polymer bonds, these occurred at 273.8, 260.3 °C and 185.6 °C for Qt_{neural}, $Qt_{Acetate}$ and $Qt_{hydrochloride}$, respectively.

3.2. Characterization of Sodium Nitroprusside (NP)

The infrared spectrum for sodium nitroprusside showed bands at 2161, 2158 e 2144 cm^{-1} related to the stretching vibrations of the cyanide ligand, another characteristic band of this complex is the NO stretch identified at 1942 cm^{-1}. In the region of the infrared spectrum below 700 cm^{-1}, it is possible to identify the signals attributed to the metal, so in 495 and 423 cm^{-1} bands related to the Fe-C≡N bond and Fe-C in 466 cm^{-1}. The very intense band at 661cm^{-1} is attributed to linear deformation Fe-N→O, all these bands follow what has been reported in the literature for complex (Palliani *et al.*, 1971).

The electronic spectrum of NP at 23 g L^{-1} (0.106 mol L^{-1}) in methanol is shown in **Fig. 1**, where initially only two bands are observed, the first at 208 nm related to the $d_{xy} \rightarrow \pi^*CN$ transition and the second at 270 nm attributed to d_{xz}, $d_{yz} \rightarrow d_z{}^2$. It was necessary to prepare higher concentrations to identify the band related to the $d_{xy} \rightarrow \pi^*NO$, transition, identified at 540 nm as can be seen in **Fig. 1a**. The 270 nm band was used to monitor the growth of the films since it is possible to monitor them at low concentrations (Palliani *et al.*, 1971; Swinehart, 1967).

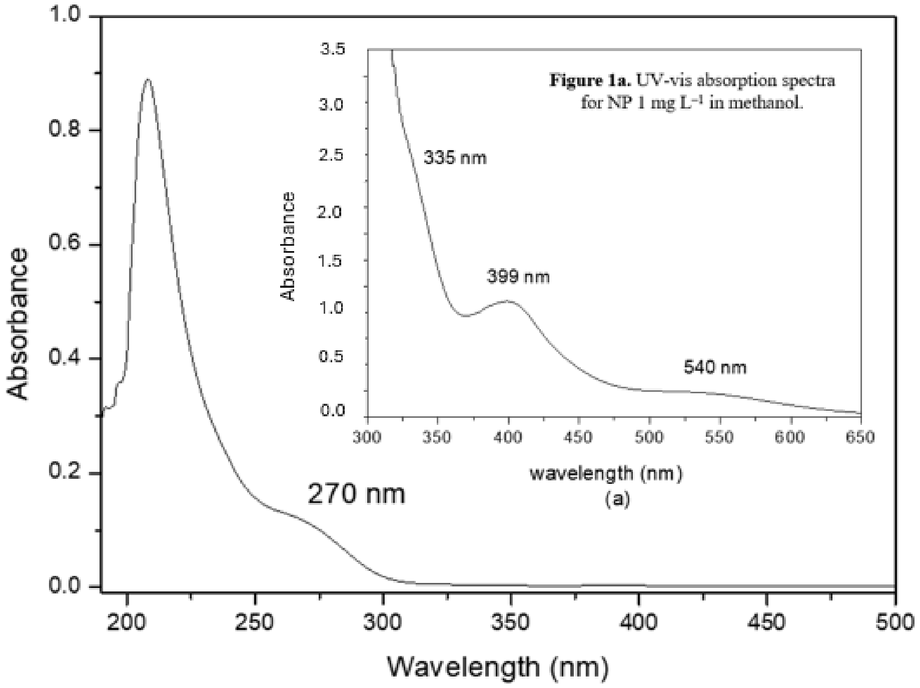

Figure 1. UV-vis absorption spectra for NP 0.03 mg L^{-1} and **(1a)** for NP 0.2 mg L^{-1} in methanol.

3.3. Characterization of LBL films

The deposition of materials in the LBL film formation process was investigated by monitoring its increase in absorbance after the preparation of each bilayer. This procedure makes it possible to assess whether the materials are deposited in quantities like each formed bilayer.

For all Qt/NP films, prepared with the three purification methodologies, have UV-vis absorption around 270 nm, this band is related to the electronic transition of NP (d_{xz}, $d_{yz} \rightarrow d_z{}^2$). The deposition of materials in the process of forming self-assembled films was investigated using its absorbance technique after the preparation of each bilayer, as shown in **Fig. 2** for $Qt_{Neutral}$/NP.

The thickness of the films can be controlled by the number of bilayers deposited and the polymer used. If linear growth is observed, it indicates that the same amount of material is adsorbed in each deposition step (Eiras *et al.*, 2007). **Figure 3** shows the relationship between absorbance and the number of layers formed for the three Qt purification methodologies. There is a linear growth for the three formed films, however with different slopes. The films obtained with Qt in neutral form and acetate obtained better correlation and slope indexes, according to Eiras *et al.* (2007), greater slopes in these graphs are related to greater affinities between the compounds that form a layer. Thus, we can conclude that among the three methodologies used in the purification, $Qt_{Acetate}$ showed a greater affinity with NP for the formation of self-assembled films and $Qt_{Hydrochloride}$ is the one with less affinity.

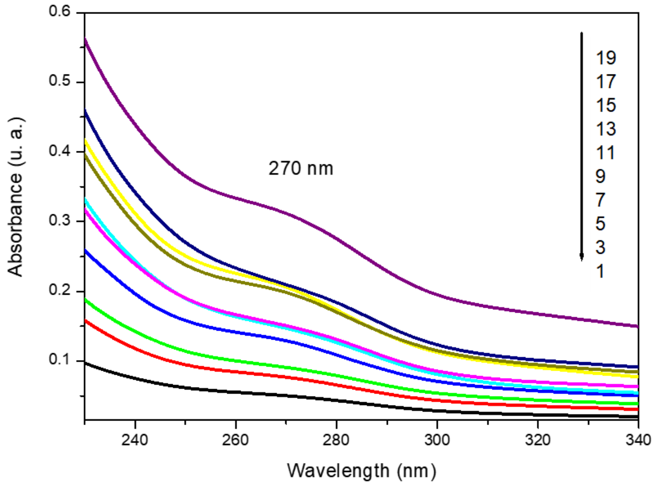

Figure 2. The electronic absorption spectrum in the UV-vis region of the films self-assembled with an increasing number of layers ($Qt_{Neutral}$/NP) prepared from a solution of Qt 5 g L^{-1} and NP 23 g L^{-1}.

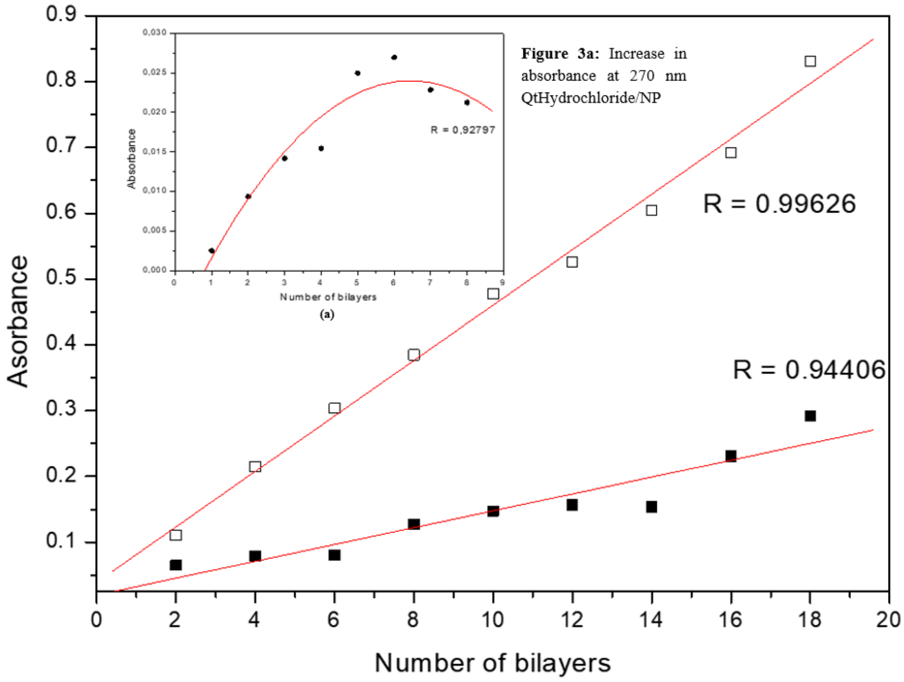

Figure 3. Increase in absorbance at 270 nm as a function of the number of bilayers of self-assembled films to $Qt_{Neutral}$/NP (■), $Qt_{Acetate}$/NP (□) and **(3a)** QtHydrochloride/NP (●) prepared from a solution of Qt 5 g L^{-1} and NP 23 g L^{-1}.

The more similar the amounts adsorbed in each adsorption step, the higher the value of the correlation index (R) (**Table 3**) because the closer the points are to the line. Thus, it can be observed that the film formed from $Qt_{Acetate}$ has a linear behavior of deposition of materials on the solid substrate with the number of layers, that is, the same amount of material is deposited in each step (Eiras *et al.*, 2007), for films containing $Qt_{Neutral}$ it presented an exponential behavior. Picart *et al.* (2002) demonstrated that growth can occur linearly or exponentially due to the ability of at least one of the polyelectrolytes to diffuse in and out of the film. This author monitored the growth of films using Poly-L-lysine and identified that it was present in the outermost layer of the film. Regarding the film obtained with $Qt_{Hydrochloride}$, an irregular behavior of deposition of the material in the film is noticed.

The observed data clearly indicate that the methodology used in the purification of chitosan directly influences the formation of films with the complex. According to Signini and Campana Filho (2001), the chitosan purified in the form of hydrochloride has charges that will alter the inter and intricate interactions, modifying its arrangement, these changes seem to disadvantage the formation of the chitosan film, as it presents a random growth probably caused by the inadequate electrostatic interactions between chitosan and the complex.

Table 3. Slope data and correlation indexes of the films of neutral chitosan, acetate, and hydrochloride with NP.

Purified form of Qt	Inclination	Correlation Index
$Qt_{Neutral}$	0.01280	0944.06
$Qt_{Acetate}$	0.04034	0.99737
$Qt_{Hydrochloride}$	0.00293	0.85615

The Spectroscopy technique in the Infrared region was also used to evidence the species present in the films, **Table 4** shows the main attributions for the Qt/NP film with 20 bilayers. In general, the spectra showed displacements, probably caused by the interaction between Qt and NP.

The N-H (1566 cm^{-1}) stretch characteristic of chitosan suffered displacements in the films of $Qt_{Neutral}$ (1556 cm^{-1}) and $Qt_{Acetate}$ (1556 cm^{-1}), respectively. The stretch attributed to NO present in the film was displaced to 1931 cm^{-1}, the Fe-C≡N deformation also showed a small displacement (**Table 4**). The characteristic band of the C-H stretching undergoes small shifts compared to the spectrum of purified chitosan, which was expected as it is an indication of a modification in its neighborhood.

The results of spectroscopy and UV-vis suggest that both chitosan and NP are being deposited in layers for the formation of the films and that this interleaving is directly related to the type of purification that the chitosan has undergone.

Table 4. Band assignments observed in the IR spectrum for chitosan films with NP.

Assignment	Film $Qt_{Neutral}$/NP	Film $Qt_{Acetate}$/NP	Film $Qt_{Hydrochloride}$/NP
ν_{OH}	3394	3398	3480
$\nu_{C\text{-}H}$	2924	2928	2840
$\nu_{\text{-}C\equiv N}$	2141	2140	2152
$\nu_{COC\ \beta\text{-}(1\text{-}4)}$ or δ_{CO}	1122	1070	1156
δFe-C≡N	482	482	500
$\nu_{NO}{}^{+}$	1931	1931	1940
δFe-N→O	471	488	490

The study on the thermal stability of chitosan in different forms of purification and Qt/NP films was carried out, except for the $Qt_{Hydrochloride}$/NP film, considering that the results obtained by UV-vis spectroscopy, since it did not show good interaction between chitosan and NP.

Figure 4 shows thermogravimetry (TG) and derivative thermogravimetry (DTG)for films Qt/NP, the moisture content in the films was 13.94% for $Qt_{Neutral}$ and 16.92% for $Qt_{Acetate}$. A second event is observed in the films at 174 and 182 °C for $Qt_{Neutral}$ and $Qt_{Acetate}$, respectively. Osiri *et al.* (2015) report that there is a loss of mass in coordination compounds containing cyanide and nitrosyl as a binder at temperatures close to 190 °C, thus we can infer that the mass losses previously mentioned are related to the decomposition of NP present in the films, coupled with the fact of these losses of mass are not seen in the purified chitosan.

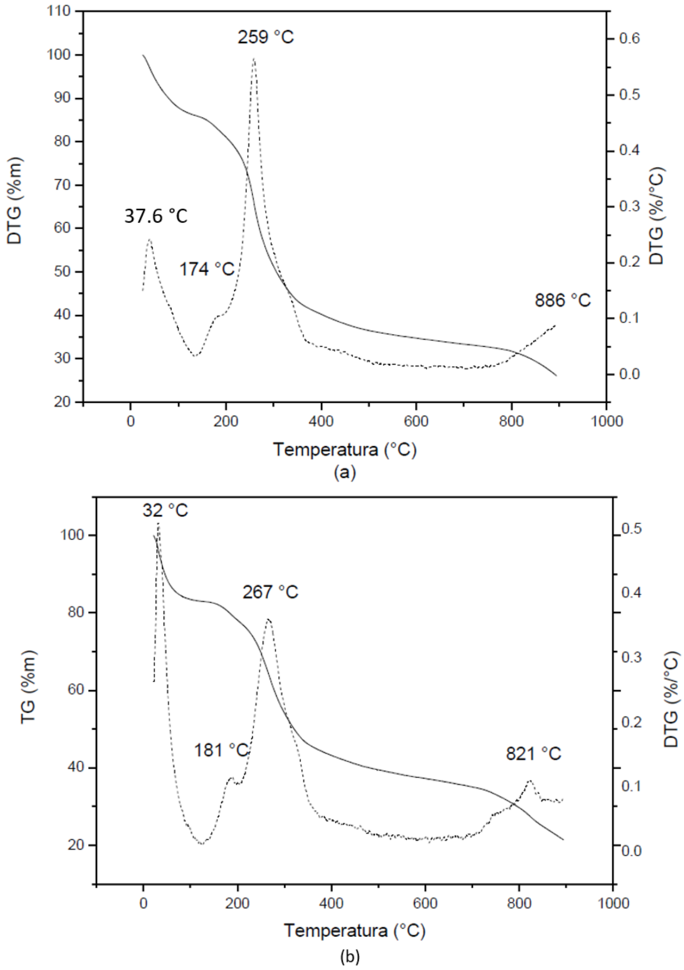

Figure 4. TG (solid) and DTG (dot) curves of **(a)** Qt$_{\text{Neutral}}$/NP e **(b)** Qt$_{\text{Acetate}}$/NP analyzed in an alumina crucible at a rate of 2.5 °C min^{-1}, heated from 25 to 900 °C under a nitrogen atmosphere, with a flow rate of 50 mL min^{-1}.

A third event is observed at temperatures above 250 °C which is related to the breakdown of glycosidic bonds, followed by the decomposition of the acetylated and deacetylated units (Martínez-Camacho *et al.*, 2010; Martins *et al.*, 2012; Nesic *et al.*, 2016). It was observed that in general the addition of the complex for the formation of self-assembled films decreased the thermal stability of chitosan. It is also possible to identify an event occurring at a temperature of 866 and 820 °C for Qt$_{\text{Neutral}}$ and Qt$_{\text{Acetate}}$, respectively, this event is related to NP degradation. A comparison of the decomposition temperatures for the different samples is shown in Table 5.

Table 5. Results of thermogravimetric analysis.

	1st mass loss (°C)	2nd mass loss (°C)	3rd mass loss (°C)	4th mass loss (°C)
Qt$_{\text{Neutral}}$	35.0	-	273.8	-
Qt$_{\text{Neutral}}$/NP	37.6	174	259.0	886.0
Qt$_{\text{Acetate}}$	35.4	-	260.3	-
Qt$_{\text{Acetate}}$/NP	32.0	181	267.0	821.0

Thus, it is possible to identify that the methodology used in the purification of chitosan plays an important role in the formation of LBL films with NP.

3.4. Cyclic voltammetry of LBL films

The cyclic voltammetry study in LBL films (20 layers) of chitosan purified in the form of acetate and neutral with the complete ones deposited on the ITO surface was analyzed in saline medium (KCl 0.1 mol L^{-1}). To evaluate the influence of the chitosan form of purification on the electrochemical response, a study was made of the current variation as a function of the applied potential. The Qt$_{\text{Hydrochloride}}$ sample was not characterized by the cyclic voltammetry technique, since it did not present good results in the deposition for forming the films.

The analysis of voltammograms showed that as the scanning speed increases, there is an increase in the value of the anodic and cathodic peak currents. It was observed that at 50 mV s^{-1} the electrochemical spectrum had higher resolution and the potentials could be determined with greater accuracy, that is, it presented a fast response, without loss of precision in detecting the anodic peak potentials (E$_{\text{pa}}$) and cathodic (E$_{\text{pc}}$), as well as anodic (i$_{\text{pa}}$) and cathodic (i$_{\text{pc}}$) peak currents. **Figure 5** shows the voltammetric profiles for the films of Qt$_{\text{Neutral}}$/NP and Qt$_{\text{Acetate}}$/NP, presenting 2 peaks, one of oxidation and one of reduction related to the redox process (Fe(III)/Fe(II) of the metal present in the complex. For the Qt$_{\text{Neutral}}$/NP film the anodic and cathodic peak values were 0.59 and 0.44 V, respectively, whereas for Qt$_{\text{Acetate}}$/NP we obtained the values of 0.62 and 0.45 V. Generally, small displacements are observed, for the film formed with the neutral chitosan, a displacement of 0.04 V was observed for the anodic peak when compared to the values obtained for the NP film (oxidation at 0.63 V and reduction at 0.50 V). It is possible to observe a small shift in the anodic peak towards more positive potentials and a shift in the cathodic peak towards more negative potentials; this behavior is characteristic of quasi-reversible processes. Another important aspect is the stability of these electrodes after carrying out several measurements. After electrochemical measurements, the electrolyte solution was analyzed using the UV-vis technique and no band was observed, confirming that there is no migration of the components to the electrolyte and indicating that the films are stable.

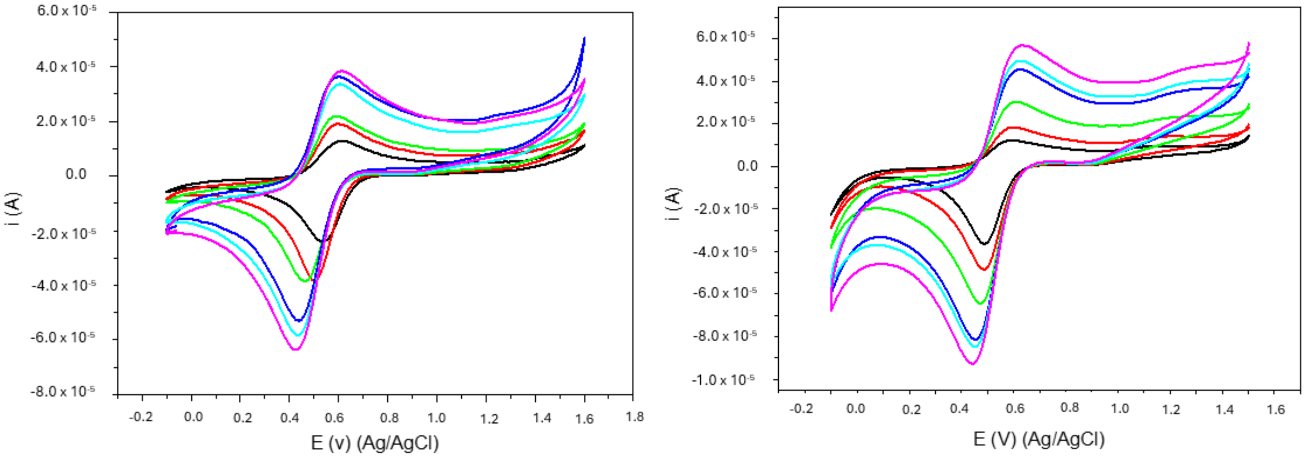

(a) (b)

Figure 5. Cyclic voltammograms for 20-bilayer **(a)** $Qt_{Neutral/NP}$ and **(b)** $Qt_{Acetate/NP}$ on ITO with multiple scans rates: (—) 5 mV s^{-1}; (—) 10 mV s^{-1}; (—) 25 mV s^{-1}; (—) 50 mV s^{-1}; (—) 75 mV s^{-1}; (—) 100 mV s^{-1}. Electrolyte: KCl 0.1 mol L^{-1}.

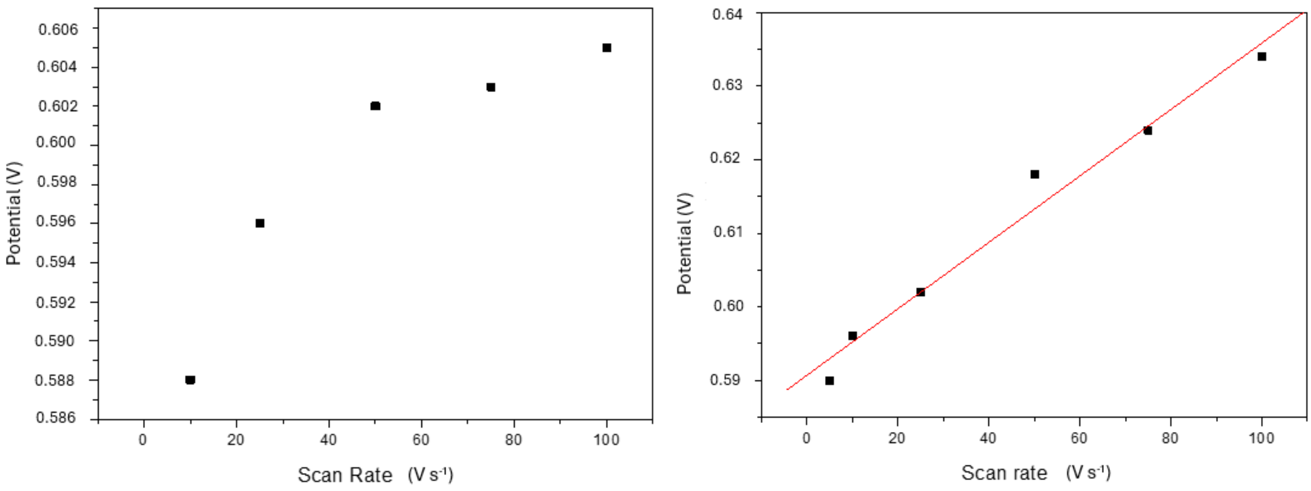

(a) (b)

Figure 6. Monitoring the oxidation peak potential with the scan rate for 20-bilayer **(a)** $Qt_{Neutral}$/NP and **(b)** $Qt_{Acetate}$/NP on ITO in KCl 0.1 mol L^{-1} at 50 mV s^{-1}.

The anodic peak potential increases linearly with the scan rate for the $Qt_{Acetate}$/NP film, as can be seen in **Fig. 6b**, with a correlation index of 0.98807 and for $Qt_{Neutral}$/NP (**Fig. 6a**) different behavior is observed. Study of chitosan/FeTsPc and chitosan/NiTsPc films (Crespilho *et al.*, 2006b) an increase in anodic potential was observed with the scan rate, even according to the author, this behavior is evidence of a load transport mechanism, like the results obtained for the $Qt_{Acetate}$/NP film. For the films formed by $Qt_{Neutral}$/NP, the diffusion process occurs, since there is no linear behavior with the scan rate.

Also, according to Crespilho *et al.* (2006b), for LBL films formed by chitosan/FeTsPc and chitosan/NiTsPc molecules, the type of mechanism that occurs is electron hopping, since the interaction between species is the ionic interaction between the groups amino of chitosan and the phthalocyanic sulfonic groups present in the complexes. This same type of interaction is proposed for films containing $Qt_{Acetate}$/NP, between the chitosan amino group and the $[Fe(CN)_5NO]^{-2}$ of the complex.

The value of ΔEp as a function of the scan rate is shown in **Fig. 7**, in which it is possible to observe that only the $Qt_{Neutral}$/NP film can be considered as a semi-reversible process since the potential values increased with the increase of scan rate. The graphic (**Fig. 7**) makes clear that the methodology used in the purification of chitosan directly influences the interaction and formation of thin films.

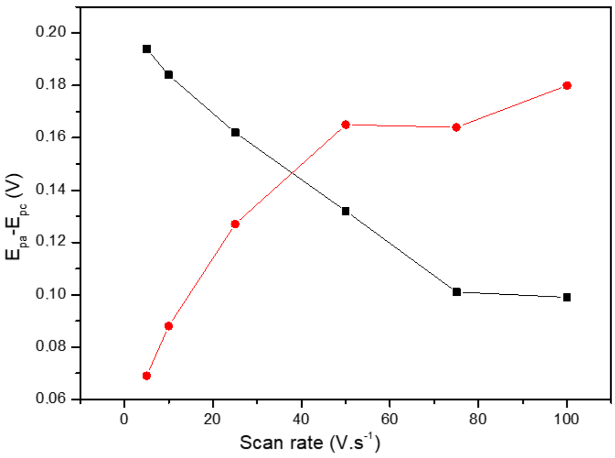

Figure 7. Relationship of potential variation (ΔEp) versus scan rate for $Qt_{Neutral}$/NP (■) e $Qt_{Acetate}$/NP (●).

The study of the effect of pH (4.0; 7.0 and 10) on the electrochemical behavior of the $\text{Qt}_{\text{Neutral}}$/NP and $\text{Qt}_{\text{Acetate}}$/NP films was carried out and the results are shown in **Fig. 8**. It is possible to observe that at pH 4, the obtained films did not present a good electrochemical response, making it difficult to identify the anodic process. At pH 10 divergence is observed in the electrochemical behavior for the films purified in different ways, for the $\text{Qt}_{\text{Neutral}}$/NP film it is not possible to identify the anodic process, different behavior for the $\text{Qt}_{\text{Acetate}}$/NP film, in which a displacement of the cathodic peaks is observed and anodic for 0.73 V and 0.19 V, respectively. These results indicate that the charge transfer process occurs more efficiently at pH equal to 7.0 for the different forms of purification.

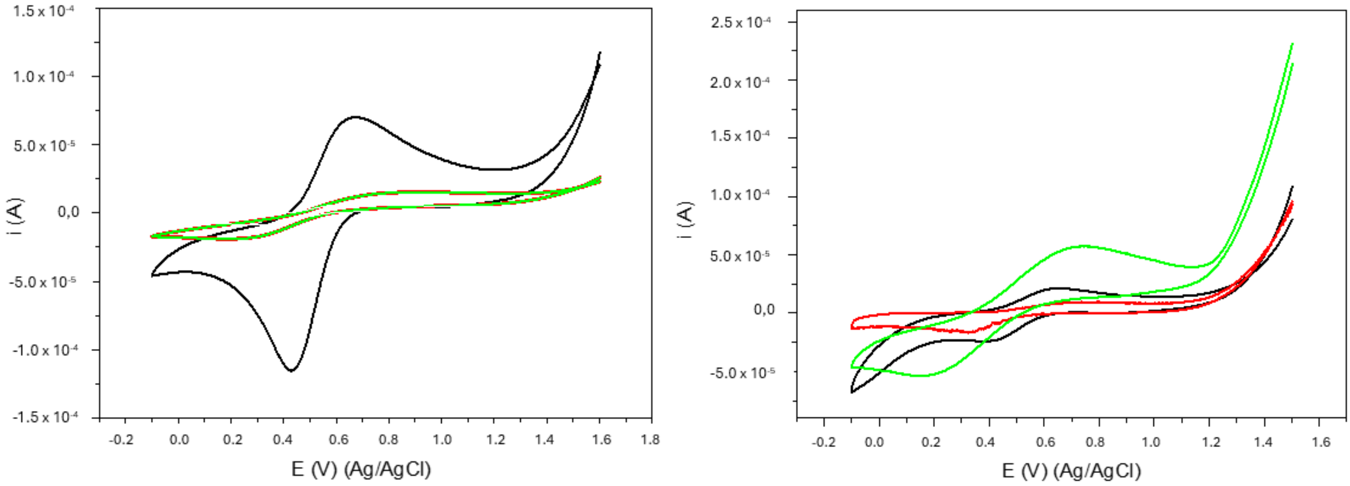

(a) **(b)**

Figure 8. Cyclic voltammograms obtained for **(a)** $\text{Qt}_{\text{Neutral}}$/NP **(b)** $\text{Qt}_{\text{Acetate}}$/NP in pH (—) 4.0; (—) 7.0 e (—) 10 with scan rate de 50 mV s^{-1}.

To identify if there was any change in the self-assembled films' thermal stability after the electrochemical study, thermal analysis tests were performed. It was possible to observe that the thermal stability (**Table 6**) of the films did not undergo any significant change, which may indicate the films are stable after being polarized i.e., after using in the form of electrodes.

Table 6. Data thermal analysis after voltammetry.

	1st mass loss (°C)	2nd mass loss (°C)	3rd mass loss (°C)	4rd mass loss (°C)
$\text{Qt}_{\text{Neutral}}$/NP	40.0	179	257.8	887.9
$\text{Qt}_{\text{Acetate}}$/NP	31.7	183.1	263.1	820.0

4. Conclusions

The methodology used in the purification of chitosan produced materials with different characteristics such as molar mass, viscosity, humidity, and degree of deacetylation. These characteristics seem to directly interfere with the deposition of layers for the formation of LBL films, as evidenced by UV-vis techniques, in which the chitosan purification methodology in the form of hydrochloride was the one that showed deposition of the material in the film completely random and, therefore, it was not used for the characterization of the electrochemical profile. The $\text{Qt}_{\text{tneutra}}$/NP film, presented an exponential growth, indicating that one of the polyelectrolytes can diffuse between the layers of the film, as far as the growth of the $\text{Qt}_{\text{Acetate}}$/NP film was linear. Differences regarding the thermal stability of the films were also identified, in which the film formed by $\text{Qt}_{\text{tneutra}}$/NP was the one that presented a greater reduction in the decomposition temperature, of approximately 15 °C when compared to purified chitosan. Through this technique it was also possible to identify the loss of mass related to the NP, confirming once again its presence in the film, as also observed by the spectroscopy technique in the infrared region.

The electrochemistry tests showed that the $\text{Qt}_{\text{Neutral}}$/NP and $\text{Qt}_{\text{Acetate}}$/NP films when used as working electrodes are stable and that there is no migration of their components to the electrolyte. Studies of thermal analysis of the films after electrochemical tests showed changes in relation to its decomposition temperatures. There was a shift towards more positive potentials of the anodic peak when compared to NP under the same conditions for $\text{Qt}_{\text{Neutral}}$/NP, whereas with respect to the cathodic peak the difference of 0.05 V was the same observed for the two films. There are distinct interactions and behaviors between the two films corroborating the UV-vis results. The $\text{Qt}_{\text{Neutral}}$/NP film presents a semi-reversible process while the other is reversible, indicating differences in the charge transfer process between the two films. For the $\text{Qt}_{\text{Acetate}}$/NP film the charge transport occurs, while for the $\text{Qt}_{\text{Neutral}}$/NP film the diffusion process occurs. In addition, pH equal to 7 proved to be ideal for electrochemical measurements.

Authors' contributions

Conceptualization: Pontes, A. C. F. B.; **Data curation:** Nascimento, L. A.; Silva Júnior, F. L.; **Formal Analysis:** Nascimento, L. A.; Silva Júnior, F. L.; Pontes, A. C. F. B.; **Funding acquisition:** Pontes, A. C. F. B.; Pontes, D. L.; Oliveira, O. A.; Nascimento, F. O. S.; **Investigation:** Nascimento, L. A.; Silva Júnior, F. L.; Pontes, A. C. F. B.; **Methodology:** Nascimento, L. A.; Pontes, A. C. F. B.; **Project administration:** Nascimento, L. A.; Silva Júnior, F. L.; Pontes, A. C. F. B.; Pontes, D. L.; Oliveira, O. A.; **Resources:** Pontes, A. C. F. B.; Pontes, D. L.; Oliveira, O. A.; Nascimento, F. O. S.; **Software:** Not applicable; **Supervision:** Pontes, A. C. F. B.; **Validation:** Not applicable; **Visualization:** Pontes, A. C. F. B.; **Writing – original draft:** Pontes, A. C. F. B.; Silva Júnior, F. L.; Pontes, D. L.; Oliveira, O. A.; Nascimento, F. O. S.; **Writing – review & editing:** Pontes, A. C. F. B.

Data availability statement

All data sets were generated or analyzed in the current study.

Funding

Not applicable.

Acknowledgments

The Analytical Center of the Chemistry Institute of UFRN for the use of the equipment used in this work.

References

Amanulla, B.; Palanisamy, S.; Chen, S.-M.; Chiu, T.-W.; Velusamy, V.; Hall, J. M.; Chen, T.-W.; Ramaraj, S. K. Selective Colorimetric Detection of Nitrite in Water using Chitosan Stabilized Gold Nanoparticles Decorated Reduced Graphene oxide. *Sci. Rep.* **2017**, *7* (9) 1–9. https://doi.org/10.1038/s41598-017-14584-6

Ariga, K.; Ji, Q.; McShane, M. J.; Lvov, Y. M.; Vinu, A.; Hill, J. P. Inorganic nanoarchitectonics for biological applications. *Chem. Mater.* **2012**, *24* (5), 728–737. https://doi.org/10.1021/cm202281m

Arrascue, M. L.; Garcia, H. M.; Horna, O.; Guibal, E. Gold sorption on chitosan derivatives. *Hydrometallurgy*. **2003**, *71* (1–2), 191–200. https://doi.org/10.1016/S0304-386X(03)00156-7

Battisti, M. V.; Campana-Filho, S. P. Obtenção e caracterização de α-quitina e quitosanas de cascas de Macrobrachium rosembergii. *Quim. Nova.* **2008**, *31* (8), 2014–2019. https://doi.org/10.1590/S0100-40422008000800019

Canella, K. M. N. D. C.; Garcia, R. B. Caracterização de quitosana por cromatografia de permeação em gel -Influência do metodo de preparacao e do solvente. *Quim. Nova.* **2001**, *24* (1), 13–17. https://doi.org/10.1590/S0100-40422001000100004

César, D. S.; Miyoshi, E.; Halpern, H.; Auler, J. Fenoldopam: Novo antihipertensivo parenteral; alternativa ao nitroprussiato. *Rev. Bras. Anestesiol*. **2001**, *51* (6), 528–536. https://doi.org/10.1590/s0034-70942001000600008

Cheung, J. H.; Punkka, E.; Rikukawa, M.; Rosner, R. B.; Royappa, A. T.; Rubner, M. F. New developments in the Langmuir-Blodgett manipulation of electroactive polymers. *Thin Solid Films.* **1992**, *210–211* (Part 1), 246–249. https://doi.org/10.1016/0040-6090(92)90224-Y

Crespilho, F. N.; Zucolotto, V.; Siqueira, J. R.; Carvalho, A. J. F.; Nart, F. C.; Oliveira Junior, O. N. Using electrochemical data to obtain energy diagrams for layer-by-layer films from metallic phthalocyanines. *Int. J. Electrochem. Sci.* **2006a**, *1* (4), 151–159. https://doi.org/10.1016/S1452-3981(23)17145-8

Crespilho, F. N.; Zucolotto, V.; Oliveira Junior, O. N.; Nart, F. C. Electrochemistry of layer-by-layer films: A review. *Int. J. Electrochem. Sci.* **2006b**, *1* (5), 194–214. https://doi.org/10.1016/S1452-3981(23)17150-1

Crini, G.; Badot, P. M. Application of chitosan, a natural aminopolysaccharide, for dye removal from aqueous solutions by adsorption processes using batch studies: A review of recent literature. *Prog. Polym. Sci.* **2008**, *33* (4), 399–447. https://doi.org/10.1016/j.progpolymsci.2007.11.001

Delolo, F. G.; Rodrigues, C.; Silva, M. M.; Dinelli, L. R.; Delling, F. N.; Zukerman-Schpector, J.; Batista, A. A. A new electrochemical sensor containing a film of chitosan-supported ruthenium: Detection and quantification of sildenafil citrate and acetaminophen. *J. Braz. Chem. Soc.* **2014**, *25* (3), 550–559. https://doi.org/10.5935/0103-5053.20140031

Eiras, C.; Passos, I. N. G.; Brito, A. C. F.; Santos Júnior, J. R.; Zucolotto, V.; Oliveira Junior, O. N.; Kitagawa, I. L.; Constantino, C. J. L.; Cunha, H. N. Nanocompósitos eletroativos de poli-o-metoxianilina e polissacarídeos naturais. *Quim. Nova.* **2007**, *30* (5), 1158–1162. https://doi.org/10.1590/S0100-40422007000500020

Freitas, A. F.; Bacal, F.; Oliveira, J. L.; Fiorelli, A. I.; Santos, R. H.; Moreira, L. F. P.; Silva, C. P.; Mangini, S.; Tsutsui, J. M.; Bocchi, E. A. Sildenafil vs. Sodium before nitroprusside for the pulmonary hypertension reversibility test before cardiac transplantation. *Arq. Bras. Cardiol.* **2012**, *99* (3), 848–856. https://doi.org/10.1590/S0066-782X2012005000076

Gao, F.; Hu, Y.; Gong, Z.; Liu, T.; Gong, T.; Liu, S.; Zhang, C.; Quan, L.; Kaveendran, B.; Pan, C. Fabrication of chitosan/heparinized graphene oxide multilayer coating to improve corrosion resistance and biocompatibility of magnesium alloys. *Mater. Sci. Eng. C.* **2019**, *104*, 109947. https://doi.org/10.1016/j.msec.2019.109947

Gonsalves, A. A.; Araújo, C. R. M.; Soares, N. A.; Goulart M. O. F.; Abreu, F. C. Diferentes estratégias para a reticulação de quitosana. *Quim. Nova.* **2011**, *34* (7), 1215–1223. https://doi.org/10.1590/S0100-40422011000700021

Kumar, M. N. V. R. A review of chitin and chitosan applications. *React. Funct. Polym.* **2000**, *46* (1), 1–27. https://doi.org/10.1016/S1381-5148(00)00038-9

Laranjeira, M. C. M.; Fávere, V. T. Quitosana: biopolímero funcional com potencial industrial biomédico. *Quim. Nova.* **2009**, *32* (3), 672–678. https://doi.org/10.1590/S0100-40422009000300011

Li, H.; Peng, L. Antimicrobial and antioxidant surface modification of cellulose fibers using layer-by-layer deposition of chitosan and lignosulfonates. *Carbohydr. Polym.* **2015**, *124*, 35–42. https://doi.org/10.1016/j.carbpol.2015.01.071

Lins, L. C.; Bazzo, G. C.; Barreto, P. L. M.; Pires, A. T. N. Composite PHB/Chitosan microparticles obtained by spray drying: Effect of chitosan concentration and crosslinking agents on drug relesase. *J. Braz. Chem. Soc.* **2014**, *25* (8), 1462–1471. https://doi.org/10.5935/0103-5053.20140129

Lu, X.; Chen, Z.; Yu, Q.; Zhu, W.; Li, S.; Han, L.; Yuan, J.; Li, S.; Wu, Y.; Lv, Z.; Chen, B.; You, H. Electrochemical Properties of Chitosan-Modified PbO2 as Positive Electrode for Lead–Acid Batteries. *Energy Technol.* **2022**, *10* (12), 2200910. https://doi.org/10.1002/ente.202200910

Luo, H.; Shen, Q.; Ye, F.; Cheng, Y. F.; Mezgebe, M.; Qin, R. J. Structure and properties of layer-by-layer self-assembled chitosan/lignosulfonate multilayer film. *Mater. Sci. Eng. C.* **2012**, *32* (7), 2001–2006. https://doi.org/10.1016/j.msec.2012.05.023

Marques Neto, J. O.; Bellato, C. R.; Milagres, J. L.; Pessoa, K. D.; Alvarenga, E. S. Preparation and evaluation of chitosan beads immobilized with iron(III) for the removal of As(III) and As(V) from water. *J. Braz. Chem. Soc.* **2013**, *24* (1), 121–132. https://doi.org/10.1590/S0103-50532013000100017

Martínez-Camacho, A. P.; Cortez-Rocha, M. O.; Ezquerra-Brauer, J. M.; Graciano-Verdugo, A. Z.; Rodriguez-Félix, F.; Castillo-Ortega, M. M.; Yépiz-Gómez, M. S.; Plascencia-Jatomea, M. Chitosan composite films: Thermal, structural, mechanical and antifungal properties. *Carbohydr. Polym.* **2010**, *82* (2), 305–315. https://doi.org/10.1016/j.carbpol.2010.04.069

Martins, J. T.; Cerqueira, M. A.; Vicente, A. A. Influence of α-tocopherol on physicochemical properties of chitosan-based filmes. *Food Hydrocoll.* **2012**, *27* (1), 220–227. https://doi.org/https://doi.org/10.1016/j.foodhyd.2011.06.011

Nesic, A. R.; Onjia, A.; Ostojic, S. B.; Micic, D. M.; Velickovic, S. J.; Antonovic, D. G. Novel biosensor films based on chitosan. *Mater. Lett.* **2016**, *167*, 47–49. https://doi.org/10.1016/j.matlet.2015.12.124

Oliveira Junior, O. N.; Raposo, M.; Dhanabalan, A. *Handbook of Surface and Interfaces of Materials*; Academic Press, 2001.

Osiri, H.; Cano, A.; Reguera, L.; Lemus-Santana, A. A.; Regueira, E. Mercury (I) nitroprusside: A 2D structure supported on homometallic interactions, *J. Solid State Chem.* **2015**, *221*, 79–84. https://doi.org/10.1016/j.jssc.2014.09.021

Ottøy, M. H.; Vårum, K. M.; Christensen, B. E.; Anthonsen, M. W.; Smidsrød, O. Preparative and analytical size-exclusion chromatography of chitosans. *Carbohydr. Polym*. **1996**, *31* (4), 253–261. https://doi.org/10.1016/S0144-8617(96)00096-3

Palliani, G.; Poletti, A.; Santucci, A. Vibrational spectrum of sodium nitroprusside. Normal coordinateanalysis for the $Fe(CN)_5NO^{2-}$ ion. *J. Mol. Struct.* **1971**, *8* (1–2), 63–74. https://doi.org/10.1016/0022-2860(71)80043-1

Pannell, M. J.; Doll, E. E.; Labban, N.; Wayu, M. B.; Pollock, J. A.; Leopold, M. C. Versatile sarcosine and creatinine biosensing schemes utilizing layer-by-layer construction of carbon nanotube-chitosan composite films. *J. Electroanal. Chem.* **2018**, *814*, 20–30. https://doi.org/10.1016/j.jelechem.2018.02.023

Picart, C.; Mutterer, J.; Richert, L.; Luo, Y.; Prestwich, G. D.; Schaaf, P.; Voegel, J. C.; Lavelle, P. Molecular basis for the explanation of the exponential growth of polyelectrolyte multilayers. *Proc Natl Acad Sci U S A*. **2002**, *20*, 1–99. https://doi.org/10.1073/pnas.202486099.

Raymond, L.; Morin, F. G.; Marchessault, R. H. Degree of deacetylation of chitosan using conductometric titration and solid-state NMR. *Carbohydr. Res.* **1993**, *246* (1), 331–336. https://doi.org/10.1016/0008-6215(93)84044-7

Roberts, G. A. F. *Chitin Chemistry*; Macmillan Publishers Limite, 1992. https://doi.org/https://doi.org/10.1007/978-1-349-11545-7

Rodrigues, G. D.; Silva, L. H. M.; Silva, M. C. H. Alternativas verdes para o preparo de amostra e determinação de poluentes fenólicos em água. Green alternatives for sample preparation and determination of phenolic pollutants in water. *Quim Nova.* **2010**, *33* (6), 1370–1378. https://doi.org/10.1590/S0100-40422010000600027

Santos, D. S.; Bassi, A.; Rodrigues, J. J.; Misoguti, L.; Oliveira, O. N.; Mendonça, C. R. Light-induced storage in layer-by-layer films of chitosan and an azo dye. *Biomacromolecules*. **2003**, *4* (6), 1502–1505. https://doi.org/10.1021/bm025754f

Sass, N.; Itamoto, C. H.; Silva, M. P.; Torloni, M. R.; Atallah, Á. N. Does sodium nitroprusside kill babies? A systematic review. *Sao Paulo Med. J.* **2007**, *125* (2), 108–111. https://doi.org/10.1590/S1516-31802007000200008

Si, Y.; Park, J. W.; Jung, S.; Hwang, G. S.; Park, Y. E.; Lee, J. E.; Lee, H. J. Voltammetric layer-by-layer biosensor featuring purine nucleoside phosphorylase and chitosan for inosine in human serum solutions. *Sens. Actuators B Chem.* **2019**, *298*, 126840. https://doi.org/10.1016/j.snb.2019.126840

Signini, R.; Campana Filho, S. P. Características e propriedades de quitosanas purificadas nas formas neutra, acetato e cloridrato. *Polímeros*. **2001**, *11* (2), 58–64. https://doi.org/10.1590/s0104-14282001000200007

Signini, R.; Campana Filho, S. P. Purificação e caracterização de quitosana comercial. *Polímeros*. **1998**, *8* (4), 63–68. https://doi.org/10.1590/s0104-14281998000400009

Silva, H. S. R. C.; Kátia, S. C. R.; Ferreira, E. I. Chitosan: hydrossoluble derivatives, pharmaceutical applications and recent advances. *Quim Nova.* **2006**, *29* (4), 776–785. https://doi.org/10.1590/S0100-40422006000400026

Sonne, K.; Dasgupta, P. K. Simultaneous Photometric Flow Injection Determination of Sulfide, Polysulfide, Sulfite, Thiosulfate, and Sulfate. *Anal. Chem.* **1991**, *63* (5), 427–432. https://doi.org/10.1021/ac00005a008

Souza, N. L. G. D.; Salles, T. F.; Brandão, H. M.; Edwards, H. G. M.; Oliveira, L. F. C. Synthesis, vibrational spectroscopic and thermal properties of oxocarbon cross-linked Chitosan. *J. Braz. Chem. Soc.* **2015**, *26* (6), 1247–1256. https://doi.org/10.5935/0103-5053.20150090

Stocche, R. M.; Garcia, L. V.; Reis, M. P.; Miranda, O. Clonidina por via venosa na técnica de hipotensão arterial induzida para timpanoplastias. *Rev. Bras. Anestesiol*. **2003**, *53* (4), 457–466. https://doi.org/10.1590/s0034-70942003000400005

Suginta, W.; Khunkaewla, P.; Schulte, A. Electrochemical biosensor applications of polysaccharides chitin and chitosan. *Chem. Rev.* **2013**, *113* (7), 5458–5479. https://doi.org/10.1021/cr300325r

Swinehart, J. H. The nitroprusside 1. *Coord. Chem. Rev.* **1967**, *2* (4), 385–401. https://doi.org/10.1016/S0010-8545(00)80220-9

Umoren, S. A.; Eduok, U. M. Application of carbohydrate polymers as corrosion inhibitors for metal substrates in different media: A review. *Carbohydr. Polym.* **2016**, *140*, 314–341. https://doi.org/10.1016/j.carbpol.2015.12.038

Ungureanu, C.; Ioniţă, D.; Berteanu, E.; Tcacenco, L.; Zuav, A.; Demetrescu, I. Improving natural biopolymeric membranes based on chitosan and collagen for biomedical applications introducing silver. *J. Braz. Chem. Soc.* **2015**, *26* (3), 458–465. https://doi.org/10.5935/0103-5053.20150298

Vinhola, L.; Facci, T.; Dias, L. G.; Azevedo, D. C.; Borissevitch, G.; Huguenin, F. Self-assembled films from chitosan and poly(vinyl sulfonic acid) on Nafion® for direct methanol fuel cell. *J. Braz. Chem. Soc.* **2012**, *23* (3), 531–537. https://doi.org/10.1590/S0103-50532012000300021

Xia, L.; Long, Y.; Li, D.; Huang, L.; Wang, Y.; Dai, F.; Tao, F.; Cheng, Y.; Deng, H. LBL deposition of chitosan and silk fibroin on nanofibers for improving physical and biological performance of patches. *Int. J. Biol. Macromol.* **2019**, *130*, 348–356. https://doi.org/10.1016/j.ijbiomac.2019.02.147

Eclet. Quim. 49 | e-1498, 2024

Original Article

https://doi.org/10.26850/1678-4618.eq.v49.2024.e1498

Foundations and applications of the orbital theory in chemistry: A philosophical perspective

Ricardo **Vivas-Reyes**[1+], Daniela **Navarro**[1], Luis Eduardo **Cortes**[1]

Abstract

The concept of atomic and molecular orbitals has been a fundamental pillar in modern chemistry, shedding light on the structures and reactivity of chemical compounds. This article examines the evolution and significance of orbital theory, its applications in chemistry, and the ongoing debate about the existence of orbitals from both physics and chemistry perspectives. Philosophical aspects related to the ontology of orbitals are explored, emphasizing the complex interplay between mathematical abstractions and tangible reality. The multifaceted nature of orbitals, their role in quantum mechanics, and their implications for understanding the quantum realm are discussed. While the debate surrounding the ontological status of orbitals remains ongoing, it highlights the profound nature of inquiries into the fundamental essence of reality. This exploration underscores the significance of continuous research and discourse in advancing our understanding of these fundamental constituents of the quantum world.

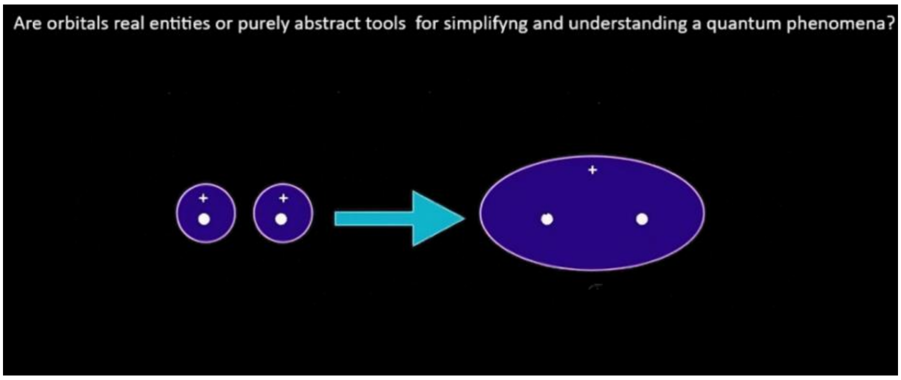

Article History

Received June 13, 2023
Accepted January 15, 2024
Published April 28, 2024

Keywords

1. molecular theory;
2. philosophy of chemistry;
3. orbitals;
4. ontology;
5. ontic.

Section Editor

Natanael de Carvalho Costa
Celly Mieko Shinohara Izumi

Highlights

- Concepts of atomic and molecular orbitals are foundational in modern chemistry.
- The orbital theory evolution and significance are crucial to understanding chemistry.
- The intricate mathematical abstraction and tangible reality balance are explored.
- The orbitals' multifaceted nature and significance in quantum mechanics are discussed.
- The existence of orbitals in physics and chemists' perspectives is addressed.

[1]University of Cartagena, Faculty of Exact and Natural Sciences, Cartagena, Colombia. **+Corresponding author:** Ricardo Vivas-Reyes, **Phone:** +573127269962, **Email address:** rvivasr@unicartagena.edu.co

1. Introduction

Indisputably, the introduction of a theory aimed at elucidating atomic and molecular orbitals has sparked a profound revolution in modern chemistry. This groundbreaking concept has granted us a deeper understanding of the intricate structures and reactivity patterns inherent to atoms and chemical compounds (Levine, 2017; Pauling, 1931; Smith and March, 2006). In the current chemistry landscape, the distribution of electrons within these orbitals governs the physical and chemical attributes of compounds, including their geometric arrangements, polarity, and bond energies. Scientific inquiry, particularly in the disciplines of quantum chemistry and physics, regards orbitals as a subject of perpetual discourse, offering varied perspectives that fuel ongoing debates (Bader, 1990; Ogilvie, 1990; McWeeny, 2002; Shaik and Hiberty, 2008). These mathematical representations play a fundamental role in facilitating our understanding of the microcosmic architecture and dynamic behavior of matter.

For example, Pauling (1931) introduced the Valence Bond Theory, which brought forth the innovative concept of orbital hybridization to elucidate the geometries of molecules and the intricacies of chemical bonding. Subsequently, in the 1950s, the Crystal Field Theory provided insights into the phenomena of coloration and magnetic properties within transition compounds (Levine, 2017; Smith and March, 2006). It becomes unmistakable that the theory of atomic and molecular orbitals is a cornerstone of modern chemistry, bestowing upon us the ability to unravel the structural intricacies and reactivity patterns of chemical compounds at the microscopic scale.

Orbitals may be succinctly defined as localized regions surrounding an atom or molecule, within which the likelihood of containing one or more electrons is notably high (Bader, 1990; Ogilvie, 1990; Pauling, 1931; Levine, 2017; McWeeny, 2002; Shaik and Hiberty, 2008; Smith and March, 2006). Within the realm of quantum chemistry, an orbital is a mathematical and spatial representation of the likelihood of encountering one or more electrons in the vicinity of an atomic nucleus or an assembly of nuclei within a molecule. These structures are derived from the equations of quantum mechanics and delineate not only the electrons' location but also their energy and angular momentum.

In simpler terms, an orbital takes the form of a three-dimensional nebula enveloping an atomic nucleus or a cluster of nuclei, demarcating the realm where the presence of an electron is astoundingly probable. Each orbital possesses a unique configuration and orientation, orchestrating the symphony of electron distribution in the spatial expanse around the nucleus. Orbitals are categorized into types such as s and p orbitals, each with distinctive shapes and used to describe the spatial distribution of electrons across varying energy levels and sublevels of an atom.

It is imperative to understand that orbitals do not represent precise trajectories or orbital pathways for electrons, as envisioned in the older Bohr atomic model. Instead, they depict territories where the likelihood of encountering an electron is elevated, and pinpointing the exact location of an electron within an orbital is a conundrum due to the probabilistic nature of quantum mechanics. Orbitals form the bedrock of comprehending the electronic architecture of atoms and molecules in contemporary chemistry.

In recent years, chemistry has witnessed significant progress, thanks to the emergence of Electron Density Theory, known as Density Functional Theory (DFT) (Parr and Yang, 1989; Sordo, 2014). DFT has become an indispensable tool for chemists, enabling the simulation and analysis of intricate molecular systems at the subatomic level. This theory pivots on the distribution of electron density within a molecular environment, granting the power to predict reactivity patterns and the architectural traits of chemical compounds. DFT harmoniously complements the concept of orbitals, which chronicles the spatial likelihood of finding electrons within atoms and molecules. In essence, DFT elevates the foundational concepts of orbitals and electron distribution to new heights. Through DFT, scientists gain a profound understanding of electron density, enabling predictions of not only the electrons' locations but also their behavior within molecular landscapes. This revelation bears significant weight in unraveling the intricacies of chemical reactions, molecular bonds, and the electronic characteristics of diverse substances. Together, orbitals and DFT have revolutionized the way chemists apprehend and manipulate matter at the atomic and molecular level. Their alliance empowers us to forge groundbreaking materials, forecast reaction mechanisms, and optimize chemical processes with unparalleled precision. This marriage of theoretical and computational instruments has opened new vistas in the exploration of the microscopic world of chemistry, infusing excitement into this dynamic and promising field, rich with potential for further discoveries and innovations.

On a broader scale, the prevailing definition of orbital posits that these entities fundamentally arise from solutions to Schrödinger's equation for the hydrogen atom, resulting in a set of wave functions. This definition enjoys a unanimous consensus within the scientific community and stands as a testament to its remarkable precision. Notably, Schrödinger referred to these functions, particularly when they exist independently of time, as amplitude rather than wave functions (Schrödinger, 1926).

At its core, it is imperative to understand that orbitals are fundamentally mathematical abstractions closely intertwined with the realm of quantum chemistry. These abstract constructs lack direct, observable attributes, establishing a foundational concept that every chemist must firmly grasp. However, this concept delves deep into philosophical realms, prompting a fundamental question: do orbitals represent genuine, objective entities, existing independently of our powers of observation and mathematical modeling, or are they purely abstract tools utilized to simplify and fathom quantum phenomena? This inquiry navigates the intricate intersection of metaphysics and quantum theory, emphasizing the enduring philosophical enigma woven into the fabric of orbitals.

Furthermore, the significance of orbitals transcends mere philosophical contemplation. In the domain of chemistry, the theory of molecular orbitals assumes a vital role, elucidating the stability and reactivity of organic and inorganic compounds. It also provides insights into the intricacies of regioselectivity and stereoselectivity in chemical reactions (Atkins, 2010; Kaskel, 2016; Smith and March, 2006). This holistic comprehension, rooted in the theory of orbitals, empowers chemists to unlock the mysteries of chemical compound structures and reactivity. It serves as the foundation for the design and synthesis of innovative materials, enriched with enhanced properties. Notably, it underpins the creation of molecular catalysts, enabling selective and efficient chemical reactions, all based on a profound understanding of electronic structure and its intricate interaction with chemical reactivity. This narrative underscores how orbitals move beyond philosophical musings to become indispensable tools shaping the world of chemistry (Armarego, 2003; Fujiwara, 2009; Vivas-Reyes, 2008).

Since the introduction of orbital theory, it has evolved and refined, giving rise to various tools and concepts that have transformed chemistry as a discipline. This evolution is evident in the textbooks in the field of chemistry, emphasizing the utilization of orbitals and the theories that underpin them (Atkins, 2010;

Levine, 2017; Kaskel, 2016; Smith and March, 2006). Undoubtedly, these recent advances in electron density theory and the simulation of complex molecular systems have opened new possibilities for the design and synthesis of materials with specific properties and for understanding fundamental chemical processes (Burke, 2012; Frisch et sl., 2016; Popelier, 2000).

However, despite the apparent usefulness of the orbital concept in chemistry, it remains a subject of controversy. Its applications sometimes vary, leading to differing interpretations. Some view orbitals as purely mathematical constructs arising from the solution of the Schrödinger equation. From this standpoint, orbitals are not seen as tangible entities in the physical world; instead, they serve as abstract tools for explaining the properties of atoms and molecules in different contexts. This contrast will be thoroughly examined in this text (Boys, 1950; Scerri, 2000a; Scerri, 2006).

2. Fundamentals of orbital theory

This section explores the foundational principles of atomic and molecular orbitals, elucidating their origins and intricate relationship with the electronic structure of atoms and molecules. Orbital theory constitutes a cornerstone in the realm of chemistry, facilitating a precise comprehension of the structures and properties of atoms and molecules (Bader, 1990; McQuarrie, 2008). Each orbital is defined by a set of quantum numbers that convey information about its energy, shape, and spatial orientation. Orbitals are categorized into sublevels s, p, d, and f based on their energy levels and shapes, and each sublevel corresponds to different values of quantum numbers, determining the maximum number of electrons that a particular orbital can accommodate (Levine, 2017; Shaik and Hiberty, 2008).

Molecular Orbitals emerge through the amalgamation of atomic orbitals stemming from the constituent atoms of a molecule. Electrons within molecular orbitals interact with one another, giving rise to molecular properties like structure, polarity, and chemical reactivity (Szabo, 1996).

The theory of orbitals originated from quantum mechanics, a fundamental theory of physics that describes the behavior of subatomic particles such as electrons. Quantum mechanics allows for the calculation of electron properties in orbitals, such as their energy and position, and predicts how these properties affect the structure and properties of atoms and molecules. The electronic structure of atoms and molecules is closely related to orbitals. Atoms with a complete electron configuration in their outermost orbitals are more stable and less reactive than atoms with unpaired electrons in their outermost orbitals. Similarly, the electronic structure of molecules determines their physical and chemical properties. Quantum mechanics is the fundamental theory that enables the calculation of electron properties in orbitals and predicts how these properties affect the structure and properties of atoms and molecules. Furthermore, orbital theory is essential in fields such as organic chemistry, inorganic chemistry, biochemistry, and materials chemistry, as it allows us to understand the properties and reactivities of molecules in these fields (Bader, 1990; Ogilvie, 1990; McQuarrie, 2008; Szabo, 1996).

Orbital theory has played an essential role in our understanding of the electronic structure of atoms and molecules. However, a contentious debate lingers regarding the existence and significance of orbitals in the domains of physics and chemistry, sparking ongoing discussions within the scientific community (Bensaude-Vincent, 2008; Labarca, 2010; Scerri, 2000a; Scerri, 2004). From some scientific perspectives, orbitals are seen as purely mathematical constructs, emerging as solutions to the Schrödinger equation, and not possessing a concrete presence in the physical world. They are abstract tools used to describe the properties of atoms and molecules. In the eyes of physicists, orbitals serve as valuable mathematical abstractions for unravelling electronic structures but should not be considered as actual physical entities (Perdew, 2001).

In stark contrast, chemists argue that orbitals are more than mere mathematical constructs. To them, orbitals are tangible entities with a real presence, and they view orbitals as indispensable tools for comprehending chemistry from a quantum perspective. Chemists see orbitals as actual components that enable the understanding of molecular structure and chemical properties (M. Morrison, 2006; Lombardi, 2005).

The divergence of opinion among some scientists has sparked extensive debates within the scientific community. Philosophers of chemistry, such as Scerri, suggest that the dispute regarding orbitals highlights a deeper contention between the realms of physics and chemistry regarding the role of mathematics in representing physical reality. According to Scerri, chemistry maintains its distinct identity, separate from physics, and this distinctiveness becomes evident in its approach to comprehending chemical phenomena in the context of molecular structure, reactivity, and physical characteristics (Scerri, 2004; Scerri, 2006; Van Brakel, 1999).

In the pursuit of a deeper understanding of modern chemistry, orbital theory has been recognized as an essential tool. By elucidating the electronic structure of atoms and molecules, this theory allows us to discern the chemical properties inherent to them. Quantum chemistry and the orbital approximation are being examined for their alignment with either a realistic or anti-realistic viewpoint concerning theoretical terms (Scerri, 2000a). This ongoing debate underscores the intricacy of the relationship between the abstract realm of mathematics and the tangible world of chemical reality (Bruice, 2017; Klein, 2017; R. Morrison, 1987; Vivas-Reyes, 2009).

The evolution of the Pauli Principle provides a concrete example of the ongoing debate regarding orbitals. Initially, this principle dictated that no two electrons within an atom or molecule could possess identical sets of four quantum numbers. However, this principle transformed when it was generalized to assert that the wave function for a system of fermions becomes anti-symmetric upon the interchange of any two electrons. Consequently, the traditional interpretation of the Pauli Principle, which assigned four quantum numbers to individual electrons, became obsolete. As Scerri affirms, this transformation led to the emergence of the concept known as the ‘orbital fallacy.’ In essence, it is no longer valid to claim the physical existence of atomic orbitals in systems with multiple electrons, except for one-electron systems. Many-electron orbitals are now regarded as ontologically redundant (Scerri, 2000b).

Despite the philosophical questions surrounding the existence of orbitals, their use remains fundamental in the practice of chemistry at all levels. The tension between the foundational status of orbitals and their continued utility in chemistry poses a philosophical dilemma that recent studies have begun to address. Quantum chemistry and the orbital approximation are being examined for their alignment with either a realistic or anti-realistic viewpoint concerning theoretical terms (Scerri, 2000b). This ongoing debate underscores the intricacy of the relationship between the abstract realm of mathematics and the tangible world of chemical reality.

3. Ontology of Orbitals

The debate surrounding the existence of atomic and molecular orbitals within the realm of the philosophy of chemistry is an intellectually captivating topic that delves deep into fundamental questions about the very nature of reality. Philosophers find themselves divided on whether orbitals represent actual ontological entities or are simply valuable mathematical tools employed to describe the behavior of electrons (Mulder, 2011, Perdew, 2001; Scerri, 2001).

To grasp the depth of this issue, it is crucial to differentiate between ontology, which concerns itself with the nature of reality in its essence, and ontics, which deals with the specific objects and entities within that reality. In the context of atomic orbitals, the debate primarily revolves around ontics, aiming to ascertain whether orbitals possess a genuine existence. Some proponents argue fervently that they do indeed exist as integral components of atomic structure, while others view them as mathematical constructs, akin to numbers or equations, contingent on our human representation (van Brakel,1999, van Brakel, 2000; Esfeld, 2013; Ladyman et al., 2007).

This ongoing philosophical discourse primarily centers on the challenge of directly observing orbitals through empirical experiments. While they may lack a tangible physical existence, their utility lies in elucidating the intricate behavior of electrons. What can be empirically observed is the electron density distribution, a tangible representation of the likelihood of encountering electrons in specific regions of space. This empirical observation forms the foundational basis for the descriptions and explanations of orbitals (Esfeld, 2013; van Brakel, 2000).

This philosophical discourse underscores the intricate and multifaceted nature of the topic, carrying profound implications not only for theoretical physics but also for practical applications in the field of chemistry. The question of whether orbitals exist as tangible physical entities or remain as valuable abstractions persists as a dynamic and ongoing philosophical debate that has yet to find a definitive resolution. However, irrespective of this debate, orbitals continue to play an irreplaceable and pivotal role in chemistry, serving as indispensable tools in both theoretical and practical contexts. This expanded version further explores the philosophical aspects of the debate regarding the existence of atomic and molecular orbitals.

4. Development and challenges in the interpretation of orbitals in chemistry

Unifying the profound role of orbitals in understanding complex systems is essential. Additionally, it is crucial to emphasize the concept of "perspective" when rationalizing these systems through phenomenological models, as chemistry and physics converge in adopting first-principles-based approaches, as evident in the prominence of orbital theory in modern textbooks on organic and inorganic chemistry.

Throughout this text, we have consistently emphasized that orbitals are foundational concepts, serving as essential instruments for describing and manipulating the structures, properties, and processes of actual molecules, crystals, and a variety of other systems. The characterization of orbitals is influenced by the intrinsic nature of molecules and the specific aspects that researchers aim to highlight through experimental investigations and theoretical analyses. (Schwarz, 2006)

Moreover, it is worth noting that many interpretations related to the concept of orbitals often arise due to a "lack of familiarity with the concept" rather than implying philosophical problems or adherence to a specific philosophy of thought. Many scientists may employ this concept without delving into its meaning in detail. Linus Pauling, a pioneer in these matters, provides a notable example by interpreting linear combinations of atomic orbitals (LCAO) while considering the most significant coefficients of the wave function. This approach led to the development of a coherent, understandable, and applicable model for the common chemist of the time, which constituted a significant success. The widespread use of hybridization persists and is successfully applied today, as evidenced in the case of the tetra valence of carbon, which was successfully explained using concepts from Valence Bond Theory (Chen, 2023; Lamoureux and Ogilvie, 2021).

In general terms, chemistry has approached the concept of orbitals qualitatively. Through this perspective, models have been developed to facilitate the understanding and modelling of chemical reactions and other concepts. Some concepts such as electronegativity and their correlated properties have been successfully integrated into a quantum framework. Similarly, non-linear reactions, which often pose challenges for mathematical interpretation outside the linear region, allow for a reasonable appreciation from a qualitative point of view. In the context of discussions about orbitals, the chemical perspective is associated qualitatively with the most significant LCAO coefficient, as evident in resonance studies described by the straightforward Hückel theory (Pauling, 1931).

Paradoxically, obtaining quantum results with extremely precise chemical resolution poses an intriguing challenge in interpreting the individual terms used in the Linear Combination of Atomic Orbitals (LCAO) approach. This approach involves a comprehensive qualitative description combined with a rigorous mathematical solution obtained through a specific methodology. However, one of the most notable challenges is the generation of multiple dissociated descriptions, particularly in complex chemical systems. When applying this approach, several different models or explanations that seem valid for specific aspects of these systems can be obtained. Each of these descriptions sheds light on certain specific aspects, but collectively, they fail to consolidate into a coherent and comprehensive theory. This fragmentation is evident in the procedures applied in organic chemistry, where rules are established for specific homologous molecules based on the highest LCAO coefficients, although these rules accumulate numerous exceptions. The central issue lies in determining the point of reasonableness in these fragmented descriptions (Chen, 2023; Lamoureux and Ogilvie, 2021; Schwarz, 2006).

Undoubtedly, chemistry is a highly complex discipline, and chemical thinking has proven capable of anticipating results described by equally complex theories. Therefore, the chemical perspective must remain in constant evolution. These points represent areas that the author could consider developing in greater depth.

5. Conclusions

The theory of atomic and molecular orbitals holds a central place in modern chemistry, bearing paramount significance. These electron distributions, essential in shaping the physical and chemical characteristics of compounds, including geometry, polarity, and bond energy, are pivotal from chemists' perspectives. The introduction of Density Functional Theory (DFT) has significantly advanced the simulation and in-depth analysis of complex molecular systems at the atomic level.

Moreover, the indispensable role of orbitals in chemistry is beyond dispute. Molecular orbital theory elucidates the stability and reactivity of organic compounds, as well as the regioselectivity and stereoselectivity of chemical reactions. The profound contributions of orbital theory have not only revolutionized the field of chemistry but have also played a key role in innovating and synthesizing novel materials with enhanced properties.

The ongoing debate surrounding the existence of orbitals underscores a profound schism in the perspectives of physicists and chemists concerning the role of mathematics in elucidating the physical world. Physicists regard orbitals as valuable mathematical abstractions, whereas chemists deem them as fundamental instruments for comprehending molecular structure and properties. Despite this enduring disparity, orbital theory remains an indispensable cornerstone of modern chemistry, exerting its influence across diverse domains within the field. In the eloquent words of Hückel, "Today, we possess a map, and that map is quantum mechanics."

From a more quantitative and mathematical perspective, some scientists argue that orbitals offer a valuable representation of a quantum system's wave function. From this perspective, orbitals provide a precise mathematical exposition of the probability distribution for electron localization across diverse spatial regions. In this framework, orbitals emerge as an indispensable mathematical reality, essential for accurately predicting subatomic particle behavior.

The discourse on the ontological existence of atomic and molecular orbitals remains a complex and captivating issue within the philosophy of chemistry. Some argue for their real ontological existence, while others view them as valuable mathematical constructs. This debate ultimately depends on our broader understanding of the nature of reality. It stands as a compelling and ongoing matter that touches upon fundamental aspects of our comprehension of reality. Despite the lack of a definitive resolution, it is imperative to persist in exploration and discourse to advance our understanding of the fundamental nature of reality.

The exploration of orbitals has revealed a profound aspect of quantum mechanics in the realm of atomic and molecular structure. Through various coordinate transformations within the Schrödinger equation, orbitals of varying shapes can be derived, each characterized by distinct quantum numbers. Practical applications have been instrumental in enhancing our comprehension of these orbitals, with the primary aim of obtaining "good quantum numbers" for predictive accuracy.

Furthermore, the duality of obtaining orbitals through both position and momentum descriptions exemplifies the multifaceted nature of these fundamental entities. The position description, intimately linked to spatial location, represents a well-established approach. Nevertheless, the potential for a more profound grasp of the momentum description, connected to concepts of velocity and change, holds promise for enriching our understanding of quantum systems.

The quest for a comprehensive understanding of orbitals, encompassing their existence and mathematical foundations, remains a dynamic and intellectually stimulating field of study that transcends the boundaries of both physics and chemistry. This enduring debate surrounding the ontological status of orbitals highlights the profound nature of our inquiries into the fundamental essence of reality. While a definitive resolution is lacking, the ongoing discourse underscores the significance of unwavering exploration and dialogue in advancing our grasp of the fundamental constituents of the quantum realm.

The examination of the ontological existence of atomic and molecular orbitals presents a complex issue within the realm of philosophical chemistry. Diverse perspectives emerge, with some advocating for their genuine existence, while others regard them as valuable mathematical constructs. This continuous debate is firmly rooted in our broader comprehension of reality and remains a compelling and vital subject in our pursuit of understanding.

The exploration of orbitals remains a dynamic and intellectually stimulating area of research that transcends the boundaries of physics and chemistry. The ongoing debate regarding their ontological status serves as a testament to the depth of our inquiries into the fundamental nature of reality. While a definitive resolution remains elusive, ongoing exploration and discourse are indispensable in advancing our comprehension of the foundational components of the quantum world.

Authors' contributions

Conceptualization: Vivas-Reyes, R.; Cortes, L. E.; **Data curation:** Navarro, D.; **Formal Analysis:** Vivas-Reyes, R.; Navarro, D.; Cortes, L. E.; **Funding acquisition:** Not applicable; **Investigation:** Not applicable; **Methodology:** Vivas-Reyes, R.; Navarro, D.; Cortes, L. E.; **Project administration:** Not applicable; **Resources:** Not applicable; **Software:** Not applicable; **Supervision:** Vivas-Reyes, R.; **Validation:** Vivas-Reyes, R.; Navarro, D.; Cortes, L. E.; **Visualization:** Not applicable; **Writing – original draft:** Vivas-Reyes, R.; **Writing – review & editing:** Vivas-Reyes, R.; Navarro, D.; Cortes, L. E.B.

Data availability statement

Data sharing is not applicable.

Funding

Not applicable.

Acknowledgments

To the University of Cartagena, thank you for your constant support. The authors also thank a referee for interesting and useful comments.

References

Armarego, W. L. F.; Chai, C. L. L. *Purification of laboratory chemicals*; Butterworth-Heinemann, 2003.

Atkins, P. W.; Paula, J. *Química física*; Oxford University Press, 2010.

Bader, R. F. W. *Atoms in molecules: a quantum theory*; Oxford University Press, 1990.

Bensaude-Vincent, B.; Simon, J. *Chemistry:* The Impure Science; Imperial College Press, 2008.

Boys, S. F. Electronic Wave Functions. I. A General Method of Calculation for the Stationary States of Any Molecular System. *Proceedings of the Royal Society of London Series A*. **1950**, *200* (1064), 542–554. https://doi.org/10.1098/rspa.1950.0036

Bruice, P. Y. *Organic chemistry*; Pearson, 2017.

Burke, K. Perspective on density functional theory. *J. Chem. Phys.* **2012**, *136* (15), 150901. https://doi.org/10.1063/1.4704546

Chen, P.; Fan, D.; Selloni, A.; Carter, E. A.; Arnold, C. B.; Zhang, Y.; Gross, A. S.; Chelikowsky, J. R.; Yao, N. Observation of electron orbital signatures of single atoms within metal-phthalocyanines using atomic force microscopy. *Nat. Commun.* **2023**, *14*, 1460. https://doi.org/10.1038/s41467-023-37023-9

Esfeld, M.; Lazarovici, D.; Hubert, M.; Dürr, D. The ontology of Bohmian mechanics. *Brit. J. Phil. Sci.* **2013**, *65* (4), 773–796. https://doi.org/10.1093/bjps/axt019

Frisch, M. J.; Trucks, G. W.; Schlegel, H. B.; Scuseria, G. E.; Robb, M. A.; Cheeseman, J. R.; Scalmani, G.; Barone, V.; Petersson, G. A.; Nakatsuji, H.; Li, X.; Caricato, M.; Marenich, A. V.; Bloino, J.; Janesko, B. G.; Gomperts, R.; Mennucci, B.; Hratchian, H. P.; Ortiz, J. V.; Izmaylov, A. F.; Sonnenberg, J. L.; Williams-Young, D.; Ding, F.; Lipparini, F.; Egidi, F.; Goings, J.; Peng, B.; Petrone, A.; Henderson, T.; Ranasinghe, D.; Zakrzewski, V. G.; Gao, J.; Rega, N.; Zheng, G.; Liang, W.; Hada, M.; Ehara, M.; Toyota, K.; Fukuda, R.; Hasegawa, J.; Ishida, M.; Nakajima, T.; Honda, Y.; Kitao, O.; Nakai, H.; Vreven, T.; Throssell, K.; Montgomery, J. A., Jr.; Peralta, J. E.; Ogliaro, F.; Bearpark, M. J.; Heyd, J. J.; Brothers, E. N.; Kudin, K. N.; Staroverov, V. N.; Keith, T. A.; Kobayashi, R.; Normand, J.; Raghavachari, K.; Rendell, A. P.; Burant, J. C.; Iyengar, S. S.; Tomasi, J.; Cossi, M.; Millam, J. M.; Klene, M.; Adamo, C.; Cammi, R.; Ochterski, J. W.; Martin, R. L.; Morokuma, K.; Farkas, O.; Foresman, J. B.; Fox, D. J. Gaussian, Inc., Wallingford CT, 2016.

Fujiwara, T. *Catalysis in asymmetric synthesis*; Wiley, 2009.

Kaskel, S. *The Chemistry of Metal-Organic Frameworks*; John Wiley & Sons, 2016.

Klein, D. R. *Organic chemistry*; Wiley, 2017.

Labarca, M.; Lombardi, O. 'Why orbitals do not exist?' *Found. Chem.* **2010**, *12*, 149–157. https://doi.org/10.1007/s10698-010-9086-5

Ladyman, J.; Ross, D. The World in the Wave Function: A Metaphysics for Quantum Chemistry. *In*: Ladyman, J.; Ross, D.; Spurrett, D.; Collier, J. (Ed.). *Everything Must Go*; Oxford University Press, **2007**. p. 355–376.

Lamoureux, G.; Ogilvie, J. F. Orbitals in general chemistry, part II: mathematical realities. *Quím. Nova*. **2021**, *44* (3), 348–354. https://doi.org/10.21577/0100-4042.20170664

Levine, I. N. *Quantum Chemistry*; Pearson, 2017.

Lombardi, O.; Labarca, M. The ontological autonomy of the chemical world: a response to Needham. *Found. Chem*. **2006**, *8* (1), 81–92. https://doi.org/10.1007/s10698-005-9004-4

McQuarrie, D. A. *Quantum Chemistry*; International Thomson Editores, 2008.

McWeeny, R. *Coulson's valence*; Oxford University Press, 2002.

Morrison, M. Emergence, Reduction, and Theoretical Principles: Rethinking Fundamentalism. *Philos. Sci*. **2006**, *73* (5), 730–741. https://doi.org/10.1086/518746

Morrison, R. T.; Boyd, R. N. *Química organica*; Prentice-Hall, 1987.

Mulder, P. Are Orbitals Observable? *Hyle*. **2011**, *17* (1), 24–35.

Ogilvie. J. F. The nature of the chemical bond—1990: There are no such things as orbitals! *Chem. Educ.* **1990**, 67 (4), 280–289. https://doi.org/10.1021/ed067p280

Parr, R. G.; Yang, W. *Density-Functional Theory of Atoms and Molecules*; Oxford University Press, 1989.

Pauling, L. The nature of the chemical bond. Application of results obtained from the quantum mechanics and from a theory of paramagnetic susceptibility to the structure of molecules. *J. Am. Chem. Soc.* **1931**, *53* (4), 1367–1400. https://doi.org/10.1021/ja01355a027

Perdew, J. P.; Schmidt, K. Jacob's ladder of density functional approximations for the exchange-correlation energy. *AIP Conf. Proc*. **2001**, *577* (1), 1–20. https://doi.org/10.1063/1.1390175

Popelier, P. L. A. *Atoms in molecules*: an introduction; Pearson College Div, 2000.

Scerri, E. R. The failure of reduction and how to resist disunity of the sciences in the context of chemical education. *Science & Education*. **2000a**, *9* (5), 405–425. https://doi.org/10.1023/A:1008719726538

Scerri, E. R. Have orbitals really been observed? *J. Chem. Educ.* **2000b**, *77* (11), 1492–1494. https://doi.org/10.1021/ed077p1492

Scerri, E. R. Just how ab initio is ab initio quantum chemistry? *Found. Chem*. **2004**, *6* (1), 93–116. https://doi.org/10.1023/B:FOCH.0000020998.31689.16

Scerri, E. R. *The Periodic Table: Its Story and Its Significance*; Oxford University Press, **2006**.

Scerri, E. R. The Recently Claimed Observation of Atomic Orbitals and Some Related Philosophical Issues. *Philos. Sci*. **2001**, *68* (S3), S76–S88. https://doi.org/10.1086/392899

Schrodinger, E. Quantisierung als Eigenwertproblem. *Annalen der Physik*. **1926**, *384*, 361-376. https://doi.org/10.1002/andp.19263840404

Schwarz, W. H. E. Measuring orbitals: provocation or reality? *Angew. Chemi.* **2006**, *45* (10), 1508–1517. https://doi.org/10.1002/anie.200501333

Shaik, S.; Hiberty, P. C. *A chemist's guide to valence bond theory*; John Wiley & Sons, 2008.

Smith, M. B.; March, J. *March's Advanced Organic Chemistry*: Reactions, Mechanisms, and Structure; John Wiley & Sons, 2006. https://doi.org/10.1002/0470084960

Sordo, T. L.; García-Fernández, E. *Teoría del funcional de la densidad*: una introducción práctica; John Wiley & Sons, 2014.

Szabo, A.; Ostlund, N. S. *Modern quantum chemistry*: Introduction to advanced electronic structure theory; Dover Publications, 1996.

Van Brakel, J. On the neglect of the philosophy of chemistry *Found. Chem.* **1999**, *1*, 111–174. https://doi.org/10.1023/a:1009936404830

Van Brakel, J. *Philosophy of Chemistry*: Between the Manifest and the Scientific Image; Leuven University Press, 2000.

Vivas-Reyes, R. Filosofía de la Química: un área ampliamente olvidada. *Rev. Acad. Colomb. Cienc.* **2009**, *33* (126), 165–174. https://doi.org/10.18257/raccefyn.33(126).2009.1817

Vivas-Reyes, R.; Aria, A. Evaluation of group electronegativities and hardness (softness) of group 14 elements and containing functional groups through density functional theory and correlation with NMR spectra data. *Eclét. Quím*. **2008**, *33* (3), 69–76. https://doi.org/10.1590/S0100-46702008000300010

ECLÉTICA QUÍMICA

Eclet. Quim. 49 | e-1505, 2024

Original Article

https://doi.org/10.26850/1678-4618.eq.v49.2024.e1505

Estimation of nitrogen dioxide levels on streets from Fortaleza Brazil using passive sampling and multivariate analysis

Francisco Wagner de Sousa[1+], Maxwell Lima Maia[2], Wendy Fernandes Lavigne Quintanilha[3], Demostenis Ramos Cassiano[3], Bruno Vieira Bertoncini[3], Ronaldo Ferreira Nascimento[2], Cleidiane Silva Oliveira[1], Jefferson Pereira Ribeiro[2]

Abstract

The increase in the fleet of motor vehicles circulating in urban centers is one of the main generators of gaseous pollutants harmful to human health and the environment. Pollutants can be economically and effectively monitored through passive sampling. This study aims to estimate NO_2 levels on roads of Fortaleza city /CE using the passive sampling method. 12 campaigns covered the rainy (March-June) and the dry (July-November) seasons in 2019. The seasonal averages of NO_2 in the rainy season were higher than the dry one, and Almirante Rubim Street showed the greatest difference in the averages: 26.6 µg m^{-3} in the rainy and 19.3 µg m^{-3} in the dry season. The principal component analysis applied to the averages of NO_2 concentration in the rainy and dry seasons, vehicle traffic and Height of the road/width ratio indicated that components 1, 2 and 3 explain 94.4% of the studied cases. Passive sampling proved to be efficient, contributing to the production of unpublished data about NO_2 levels in streets of Fortaleza/Ceará/Brazil from mobile sources.

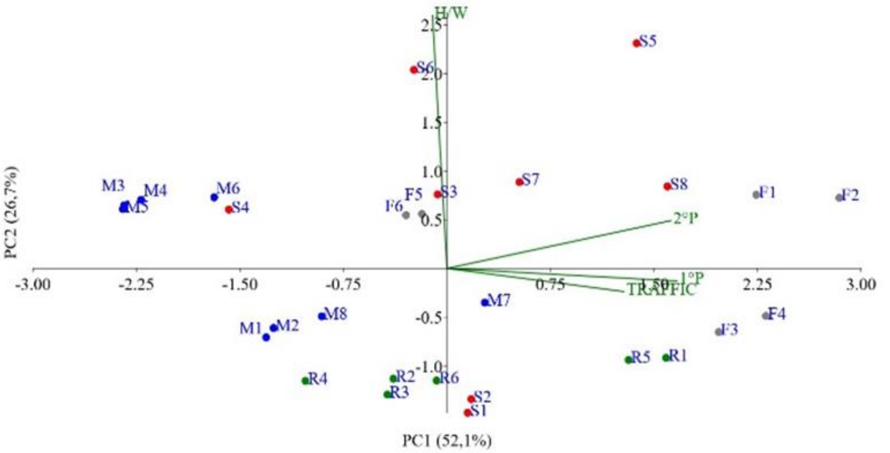

The PCA was used to group the sampling points that present similar behavior about the average NO_2 variables in the rainy and dry seasons, H/W ratio and vehicle traffic, through a two-dimensional graph.

Article History

Received	August 02, 2023
Accepted	January 15, 2024
Published	May 19, 2024

Keywords

1. passive sampling;
2. nitrogen dioxide;
3. seasonality;
4. principal component analysis.

Section Editor

Natanael de Carvalho Costa
Paulo Clairmont Feitosa Lima Gomes

Highlights

- Passive sampling was efficient in indicating NO2 levels from mobile sources.
- Meteorological data and the H/W ratio of roads influence the NO2 levels.
- The PCA is a powerful and suitable statistical tool for interpreting NO2 levels.

[1]Federal Institute of Ceará, Caucaia, Brazil. [2]Federal University of Ceará, Department of Analytical Chemistry and Physical Chemistry, Fortaleza, Brazil. [3]Federal University of Ceará, Department of Transportation Engineering, Fortaleza, Brazil.

+Corresponding author: Francisco Wagner de Sousa, **Phone:** +5585999025637, **Email address:** fr.wagner@ifce.edu.br

1. Introduction

Economic development in a region favors, among other factors, population growth, urbanization of green areas and the installation of diverse industries. This situation also contributes to the considerable increase in the emission of harmful compounds that in significant quantities reduce the air quality of the region and thus significantly affect the dynamics of the ecosystem and the health of the population (Baird and Cann, 2011; Ding *et al.*, 2022; Guo *et al.*, 2019; Lenzi and Favero, 2014; Zanetti and Melli, 1992). Nitrogen dioxide (NO_2) is one of these compounds and its main sources in urban areas are largely from industry and vehicle emissions from the burning of fossil fuels (Aránguez *et al.*, 1999; Biswal *et al.*, 2020; Januševičius and Grubliauskas, 2019; Lenzi and Favero, 2014; Richmond-Bryant *et al.*, 2017). At low altitude atmospheres, NO_2 is part of the photochemical smog that causes oxidation of any material it meets and at high altitudes, it causes the depletion of the ozone layer (Lenzi and Favero, 2014). Plants, by absorbing NO_2 through their leaf stomata, can oxidize this pollutant to nitrate through photochemical reactions, favoring the internal spaces of the leaf to become acidic, thus damaging them (Freedman, 1995; Rao *et al.*, 2014).

In the human population, NO_2 can cause eye irritation and when inhaled it favors inflammation of lung tissue, emphysema, and installation of respiratory infections, caused by changes in local immunity (Ghozilaki *et al.*, 2016; Negrisoli and Nascimento, 2013; Russo *et al.*, 2014), in addition to increase the susceptibility to bronchoconstrictor agents and respiratory infections caused by bacteria, especially in children (Shiraiwa *et al.*, 2012; Ugucione *et al.*, 2002) and positively increase the number of hospitalizations and mortality (Arbex *et al.*, 2012; Duan *et al.*, 2019; Hatzopoulou *et al.*, 2013; Martins *et al.*, 2002; Nascimento *et al.*, 2006; Pestana *et al.*, 2017). Between 2009 and 2018, about 115 thousand hospital admissions of people residing in Fortaleza were carried out because of asthma, bronchitis, influenza, and pneumonia. Of this total, more than 50% of cases are due to pneumonia. The number of deaths due to these diseases in the period from 2009 to 2017 was 29,292, with 89.5% being people aged 50 years or older (Datasus, 2019).

Emissions of atmospheric pollutants produced by vehicular sources are difficult to control, thus leading much research to studies that verify the reduction of car emissions using catalytic converters (Halim *et al.*, 2018; Mehta and Dey, 2020). In Fortaleza, until December 2018, about 1.1 million vehicles were registered, with more than 50% of this fleet being private cars and more than 13% being diesel vehicles (IBGE, 2019). To evaluate the number of atmospheric pollutants, as well as NO_2, several types of sampling were developed that can be classified according to the analysis methodology, among which passive sampling equipment stands out (Harner *et al.*, 2013; Miranda *et al.*, 2017) due to its low cost, easy handling and understanding, without any automatic systems, it does not require electricity, has easy labor logistics and can absorb pollutants of a gaseous nature or polluted vapors from the atmosphere through the process of diffusion and permeation by concentration difference (Cruz and Campos, 2008; Hauser *et al.*, 2015; Lacava *et al.*, 2002; Lisboa and Kawano, 2010; Masey *et al.*, 2017; Piceli and Lisboa, 2018; Souza *et al.*, 2017).

Considering these facts, in the city of Fortaleza there is no annual monitoring of the levels of all legislated inorganic compounds (SO_2, Total Suspended Particulates, CO, O_3, PM 2.5, PM 10 and even NO_2) on high-traffic roads. The absence of monitoring work on NO_2 and other parameters is due to the lack of financial incentives, the lack of qualified and trained human resources and the high costs of materials and equipment needed. This lack of information emerges as a very serious problem, which makes it difficult for health inspection and surveillance agencies to establish a mechanism for preventing and controlling atmospheric pollution.

Faced with this problem, the present study aims to estimate NO_2 levels using the passive sampling method in commercial streets in Fortaleza/CE.

2. Experimental

2.1. Study area

The city of Fortaleza has 2,473,614 inhabitants and a total area of 313.8 km^2 (**Fig. 1**). The city has an Aw' climate on the Koppen-Geiger scale, with an average annual temperature of 26.5 °C, an average wind speed of 12.7 km h^{-1} and an average annual rainfall of 1600 mm, with the highest occurrences between February and May featuring the city's rainy season (IBGE, 2019; M. Moura *et al.*, 2008; M. Moura, 2015).

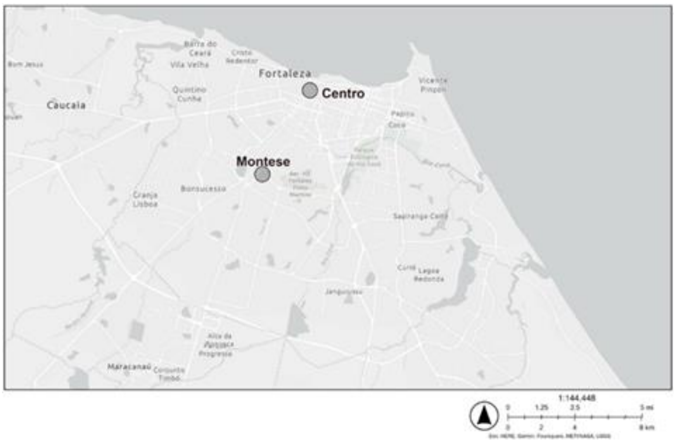

Figure 1. Map of the city of Fortaleza with the location of Montese and Centro.

Almirante Rubim (Street R) and Antônio Fiúza (Street F) streets, both in the Montese neighborhood and General Sampaio (Street S) and 24 de Maio (street M) Streets, both in the Centro neighborhood, were selected because they have two lanes and one-way traffic. Each road was divided into sectors and each sector has two sampling points, one on each side of the road. The chosen nomenclature and the georeferenced location of the sampling points were given as shown in **Table 1**.

Points F3 and F4 are close to the corner of Street Antônio Fiúza and Street 15 de Novembro, the access road to Fortaleza airport. Points M7, and M8, from 24 de Maio and points S7 and S8, from General Sampaio, then fixed on the corner with Street Castro e Silva. In this block is located the bus terminal of Praça da Estação. On all 4 lanes, the odd-numbered points are located on the posts on the right side of the street and the even points are on the posts on the left side, as illustrated in **Fig. 2**.

Table 1. Nomenclature and georeferenced location of sampling points.

Street	Point	Latitude	Longitude	Street	Point	Latitude	Longitude
Street F	F1	3°46'07.7"S	38°33'06.3"W	**Street M**	M3	3°43'44.1"S	38°31'57.7"W
	F2	3°46'07.7"S	38°33'06.0"W		M4	3°43'44.1"S	38°31'57.4"W
	F3	3°46'12.3"S	38°33'08.2"W		M5	3°43'26.8"S	38°31'52.2"W
	F4	3°46'12.7"S	38°33'07.8"W		M6	3°43'26.3"S	38°31'51.6"W
	F5	3°46'17.8"S	38°33'10.0"W		M7	3°43'22.3"S	38°31'50.6"W
	F6	3°46'17.8"S	38°33'09.8"W		M8	3°43'22.3"S	38°31'50.3"W
Street R	R1	3°46'22.5"S	38°33'26.3"W	**Street S**	S1	3°43'57.5"S	38°31'56.7"W
	R2	3°46'22.5"S	38°33'26.8"W		S2	3°43'57.2"S	38°31'57.1"W
	R3	3°46'19.1"S	38°33'25.1"W		S3	3°43'47.1"S	38°31'53.6"W
	R4	3°46'18.4"S	38°33'25.4"W		S4	3°43'46.3"S	38°31'53.9"W
	R5	3°46'13.0"S	38°33'22.9"W		S5	3°43'29.4"S	38°31'48.6"W
	R6	3°46'12.7"S	38°33'23.3"W		S6	3°43'29.4"S	38°31'48.8"W
Street M	M1	3°43'56.4"S	38°32'01.7"W		S7	3°43'23.6"S	38°31'46.6"W
	M2	3°43'56.4"S	38°32'01.4"W		S8	3°43'23.4"S	38°31'47.1"W

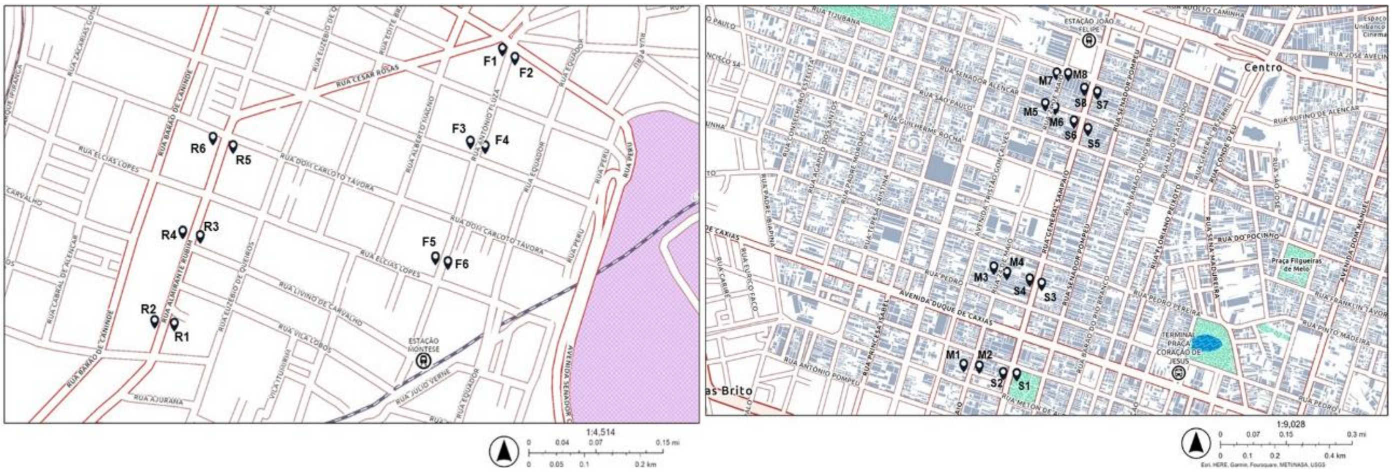

Figure 2. Schematic of the location of sampling points – (from left to right) – Str. F, Str. R, Str. M and Str. S.

2.2. Sampling period

The sampling period was carried out from March 10, 2019, to December 10, 2019, with a total of 12 campaigns (Table 2) comprising the rainy season, from March to May and the dry season, from June to November.

Table 2. Rainy and dry period of passive sampling of NO_2 filters.

Campaign	Period	Season
1º	10/03 – 31/03	Rainy
2º	31/03 – 21/04	Rainy
3°	21/04 – 05/05	Rainy
4°	05/05 – 26/05	Rainy
5°	26/05 – 16/06	Rainy
6°	16/06 – 07/07	Dry
7°	07/07 – 28/07	Dry
8°	28/07 – 18/08	Dry
9°	18/08 – 08/09	Dry
10°	08/09 – 29/09	Dry
11°	29/09 – 20/10	Dry
12º	20/10 – 10/11	Dry

Each campaign has a period of 21 days, except for the 3rd campaign which took place in 14 days due to strategic reasons. The change of samplers from one campaign to another took place on Sundays, due to the low flow of vehicles on the roads and consequently little emission of pollutants and for the safety of the sampling team. Overall, 360 filters were produced, with 30 filters per campaign (28 for sampling points and 2 for blanks).

2.3. Nitrogen dioxide methodology

Among the various methodologies for sampling NO_2, the methodology used in this work was based on the works of Saltzman (1954) where an absorber solution (0.5 M KI (Campinas, Brazil, Dinâmica) + 0.2 M KOH (Campinas, Brazil, Dinâmica) in Methanol (Suzano, Brazil, Neon)) was prepared, used to be added directly (impregnated) in cellulose filters to capture and adsorb NO_2 molecules present in the environment. Then, a reagent solution (0.5% w/v Sulfanilamide (Suzano, Brazil, Neon), 0.005% w/v N–1-Naphthyl-ethylenediamine (St. Louis, USA, Sigma-Aldrich) and 1% v/v Phosphoric Acid (St. Louis, USA, Sigma-Aldrich)) was used on the filters after the sampling period to the extraction of NO_2 present in the filters and converting it into nitrite ion $[NO_2]^-$. A stock solution (0.0203 g of Sodium Nitrite P.A in 1 L of water) was prepared to construct the UV-VIS (Barueri, Brazil, Shimadzu) calibration curve, where the levels of NO_2 present in the filters were determined (Dita and Dias, 2016; Lodge, 1988; Saltzman, 1954; Shaw, 1967).

2.4. Street morphology and traffic

Urban morphology can be considered one of the factors that contribute to the dispersion of a pollutant, along with the wind direction and speed on a road. The calculation of the morphology of a road is obtained through the ratio between the height of the road (H) and width (W) - distance between buildings (Aguiar *et al.*, 2017; Bender and Dziedzic, 2014; Muniz-Gäal *et al.*, 2018;

Nakata-Osaki *et al*., 2016). The values of H and W were manually measured from the distance between the buildings and for the height of the road, consider that each building floor is 3 m high.

To quantify the number of vehicles that travel on the Streets where the sampling took place, a count of vehicles that pass-through a given reference point in the first 15 min of each hour was performed.

2.5. Principal component analysis (PCA)

The PCA was used to group the sampling points that present similar behavior about the average NO_2 variables in the rainy and dry seasons, H/W ratio and vehicle traffic, through a two-dimensional graph (Azevedo and Anzanello, 2015; Ghosh and Dubey, 2013; Honda *et al*., 2010; Moori *et al*., 2002; Stricker *et al*., 2013; Xu *et al*., 2015). To perform the calculation of these algorithms, PCA, the free software PAST (Hammer *et al*., 2001), version 3.26b for Windows was used, in which it is possible to analyze scientific data, with functions for data manipulation, plotting, univariate and multivariate statistics. Before applying the data obtained in the software, they were pre-treated by self-scaling to minimize the influence of the dominant variable (Ferreira, 2015; Hongyu *et al*., 2016; Karamizadeh *et al*., 2013; Lyra *et al*., 2010; Maia *et al*., 2019).

3. Results and discussion

The results of the 360 NO_2 samples analyzed in this study over 12 collection campaigns on the studied streets are shown in **Table 3**. The street with the lowest overall mean concentration was on 24 de Maio (Street M) with 19.2 μg m^{-3} with a variation between 1.6 and 33.6 μg m^{-3}. Antônio Fiúza (Street F) presented the highest average concentration with 25.3 μg m^{-3} with a variation between 1.5 and 55.7 μg m^{-3}. The other streets showed average concentrations of 22.4 μg m^{-3} in Almirante Rubim (Street R), 24.3 μg m^{-3} and General Sampaio (Street S).

Table 3. Average concentration of NO_2 during the 12 campaigns.

Campaign	Street					
	Street F			Street R		
	$\overline{x}$	Conc. Min-Max	sd	$\overline{x}$	Conc. Min-Max	sd
1º	23.8	6.5−38.9	13.0	23.5	15.4−31.5	5.9
2º	32.7	21.3−44.3	9.2	24.7	18.8−31.5	5.2
3°	22.9	13.4−29.4	7.0	34.0	20.3−45.2	11.1
4°	26.5	17.0−35.7	8.5	27.9	23.1−34.3	4.3
5°	26.5	17.6−35.1	6.7	22.5	15.6−30.2	5.5
6°	25.0	19.2−32.0	5.3	23.4	17.4−32.7	6.1
7°	29.5	16.2−47.7	13.4	20.1	15.6−24.4	3.6
8°	24.4	18.6−27.5	4.3	23.2	17.8−30.7	5.3
9°	23.3	20.1−26.6	2.8	20.2	13.8−25.9	5.8
10°	30.0	19.4−55.7	17.2	16.1	10.7−21.9	4.8
11°	24.6	21.4−28.6	3.3	16.6	10.9−22.7	4.6
12º	21.3	6.5−38.9	13.0	16.1	13.5−20.6	2.8

Note: $\overline{x}$ is average; **sd** is standard derivation; **conc. min-max** is the minimum and maximum concentration.

The low average concentrations of NO_2 presented by M Street, as well as the higher average concentrations of NO_2 presented by F Street, may be related to the flow of vehicles, since M Street presented an average daily traffic of 5,402 vehicles, the lowest among the routes, while Street F had 12,406 daily vehicles, indicating that the levels of NO_2 present in the streets may come from vehicular sources and secondary chemical reactions from the reaction of NO with O_3 (Carslaw *et al*., 2016; Lenzi and Favero, 2014).

None of the analyzed samples showed values above the current standards established by National Council for the Environment No. 491/2018 (CONAMA, 2018) which is 260 μg m^{-3} h^{-1} and by international bodies such as the World Health Organization (WHO, 2005) and the Environmental European Agency (EEA, 2018) that set a maximum limit of 200 μg m^{-3} per hour and the Environmental Protection Agency (EPA, 2018) that established a maximum limit of 188 μg m^{-3} per hour.

The concentration of NO_2 levels using passive sampling varies from one street to another according to the studied sites' local characteristics. Hien *et al*., 2014, found a maximum concentration of 84 μg m^{-3} in the city of Hanoi, Vietnam, using passive sampling with an estimated annual variation between 45.2 and 79.7 μg m^{-3} for high-flow lanes and between 18, 7 to 41.2 μg m^{-3} for streets with access to industries. Grundström and Pleijel, 2014, analyzed NO_2 with passive samplers arranged inside and outside treetops located in regions close to the highway in the city of Gothenburg, Sweden, obtaining results ranging from 12.9 to 47.1 μg m^{-3}. Bari *et al*., 2015, monitored NO_2 in Alberta province of Canada, between 2006 and 2010, obtaining data ranging from 0.4 to 34.0 μg m^{-3}, with a total average of 3.9 μg m^{-3}. Bozkurt *et al*., 2018, obtained mean concentrations of NO_2 between 18.3 and 33.8 μg m^{-3}, in the city of Düzce, Turkey. In Brazil, Campos *et al*. (2010) found mean values ranging from 3.6 to 12 μg m^{-3} in Salvador city, BA and from 6.7 to 11.0 μg m^{-3} in residential areas of the city of Curitiba/PR.

3.1. Analysis by sampling point

Figure 3a shows NO_2 concentrations in μg m^{-3} at all sampling points located on Antônio Fiúza (Street F) during the 12 campaigns. In it, we observed that F5 and F6 were the points that presented the lowest concentrations both in the rainy and dry seasons and this may be related to the low circulation of vehicles, especially heavy vehicles such as buses and trucks, in addition to factors that may have corroborated a deviation that occurred during a city hall work on this road on the sampling days (Nakata-Osaki *et al*., 2013). The averages for F5 and F6 in the rainy season were, respectively, 18.4 and 17.9 μg m^{-3} and in the dry season, the averages were 20.0 and 19.6 μg m^{-3}, respectively, according to presented in **Table 1**.

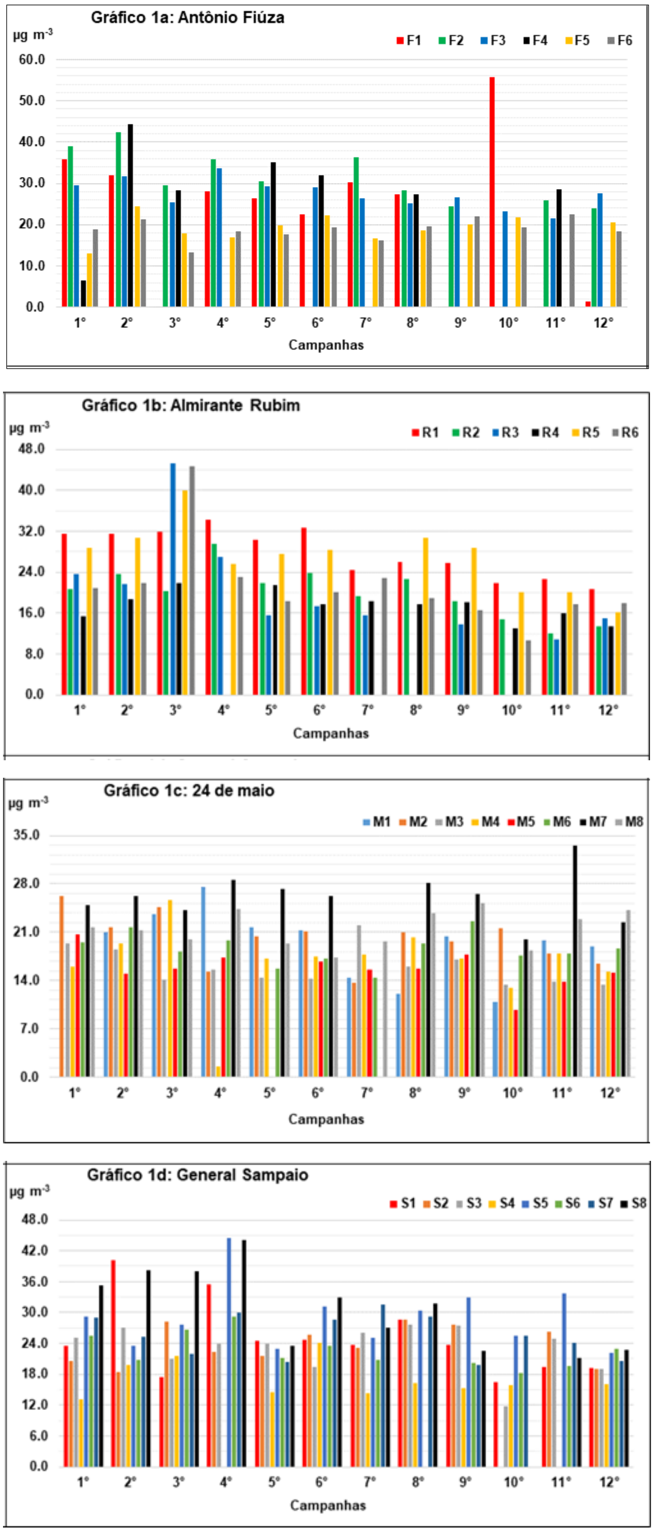

Figure 3. **(a)** NO_2 levels obtained at the points located at Antônio Fiúza; **(b)** at Almirante Rubim; **(c)** at 24 de Maio; **(d)** at General Sampaio.

Figure 3b shows the NO_2 concentrations in µg m^{-3} at all sampling points at Almirante Rubim (Street R) during the 12 campaigns. We can observe that R1 and R5 are the points that present the highest concentrations of this road, in most of the samples, except in campaign 3. This fact can be explained by the location of these points being close to the crossing of streets. Although R1 and R5 presented values above the others, they did not register levels above 40 µg m^{-3}. On the other hand, R3 and R6, in the 3rd campaign, when they reached the highest levels recorded in this street, being 45.2 and 44.8 µg m^{-3}, respectively. During this campaign, the sampling lasted 14 days, different from the rest of the campaigns, and presented an average temperature of 22.9 °C, the lowest recorded during the study, and the highest average daily amount of rain recorded, reaching 17.9 mm. Such factors may have contributed to the reduction in the flow of vehicles and, consequently, there was a higher concentration of NO_2 at these points of the road. It also shows the absence of samples R3 in the 8th and 10th campaigns; R4 in the 4th campaign; and R5 in the 10th campaign. Such samples were lost during the sampling period.

Figure 3c shows the NO_2 concentrations in µg m^{-3} at all sampling points on the 24th of May (Via M) during the 12 campaigns. In this one, we observed that all points had concentrations below 28.0 µg m^{-3}, except M7 in campaigns 4, 8 and 12. We also observed that all, except the 4th campaign of M4, had concentrations above 7.0 µg m^{-3}. Point M7 stands out among the other points for presenting the highest concentration in most campaigns and this can be explained by the fact that this point is located close to the bus terminal and a crossroads, contributing to the higher concentration of NO_2 in this region of the street (Carslaw *et al.*, 2016).

Figure 3d shows NO_2 concentrations in µg m^{-3}, at all sampling points, in General Sampaio Street (Street S) during the 12 campaigns. In it, we observed that the points, except for S1, S5 and S8 in the rainy season, do not reach concentrations above 30 µg m^{-3}, with S1 and S5 being located near bus stops and S8 being located at road crossings and close to a bus terminal. From the 7th campaign onwards, there was a drop in NO_2 levels in S8, as works began at that moment in the station square, reducing vehicle traffic on the road.

3.2. Influence of meteorological data and H/W ratio of roads

According to the data obtained from Instituto Nacional de Meteorologia (INMET, 2019) meteorological stations, the average temperature of the 12 campaigns was 26.72 °C, except in excess, a single campaign had an average of 22.9°C with winds blowing mostly from the southeast and east directions. Such meteorological parameters did not suffer sudden variations during the sampling campaigns (22.9–27.8 °C). However, humidity (%), wind speed (km h^{-1}) and precipitation (mm) in each campaign had notable variations and these values are shown in **Table 4**, together with the general average of NO_2 in µg m^{-3}, per campaign, in each studied route. As can be seen, the average humidity and precipitation gradually decreased over the sampling period, while the average wind speed increased, characterizing the rainy and dry periods in Fortaleza city. It is important to emphasize that the individual assessment of these parameters should not be related to the concentration since it can lead to misinterpretations.

Table 4. Mean values of humidity in (%), wind speed in (km h^{-1}), temperature (°C), precipitation (mm) and average at streets during the 12 campaigns.

Variable	Rainy Season						Dry Season							
	1°	2°	3°	4°	5°	$\overline{x}$	6°	7°	8°	9°	10°	11°	12°	$\overline{x}$
Moisture (%)	90.0	86.9	85.8	82.3	76.3	84.3	74.1	71.8	68.2	66.0	66.7	66.6	65.8	68.5
Wind Speed (km h^{-1})	4.4	4.6	5.9	6.5	7.4	5.8	8.0	9.2	10.7	11.8	12.2	12.0	11.1	10.6
Temperature (°C)	26.4	26.8	22.9	27.1	26.9	26.0	26.6	26.6	26.7	27.1	27.3	27.4	27.8	27.1
Precipitation (mm)	13.8	10.7	17.9	10.1	9.6	12.4	6.2	2.7	0.9	0.5	0.5	0.4	0.0	1.9
$\overline{x}$ of NO_2 St. F ($\mu g\ m^{-3}$)	23.8	32.7	22.9	26.5	26.5	26.6	25.0	29.5	24.4	23.3	30.0	24.6	21.3	25.5
$\overline{x}$ of NO_2 St. R ($\mu g\ m^{-3}$)	23.5	24.7	34.0	27.9	22.5	26.5	23.4	20.1	23.2	20.2	16.1	16.6	16.1	19.3
$\overline{x}$ of NO_2 St. M ($\mu g\ m^{-3}$)	21.2	20,6	20.8	18.8	19.4	20.0	18.9	16.8	19.5	20.8	15.5	19.7	18.1	18.5
$\overline{x}$ of NO_2 St. S ($\mu g\ m^{-3}$)	25.2	24.7	25.3	30.9	21.5	25.3	26.2	24.0	27.5	23.7	18.9	24.2	20.2	23.6

Note: **$\overline{x}$ of NO_2 St. F** is NO_2 average on Antônio Fiúza Street; **$\overline{x}$ of NO_2 St. R** is NO_2 average on Almirante Rubim Street; **$\overline{x}$ of NO_2 St. M** is NO_2 average on 24 de Maio Street; **$\overline{x}$ of NO_2 St. S** is NO_2 average on General Sampaio Street.

The results showed that, for the rainy season, the NO_2 levels are slightly higher than in the dry season. However, the R Street showed a greater difference from 26.5 $\mu g\ m^{-3}$ to 19.3 $\mu g\ m^{-3}$. This small reduction of NO_2 for the dry season to the levels obtained in the rainy season may be consistent with a reduction in the speed of cars, high traffic jams and a decrease in secondary reactions (Arbex *et al.*, 2012; Moura *et al.*, 2015). Other parameters that may have influenced this reduction were meteorological conditions.

For this, a Pearson correlation matrix was elaborated to verify the influence of Relative Humidity (RH), Wind Speed (WS), Precipitation (PP) and Temperature (T) with the levels of NO_2 obtained in each route (**Table 5**). In it, we found that the correlation of RH and PP with NO_2 concentration was positive in all streets, especially the R Street. However, WS showed negative correlation with NO_2 levels, especially for the R Street. Concerning T, the correlation was negative in the streets, except for the F Street. From what was shown by the matrix, except for the F Street, the increase in the values of UR and PP together with the reduction of WS and T, favors a slight increase in NO_2 concentrations, especially in the R Street.

Table 5. Pearson's correlation matrix between Relative Humidity (RH), Wind Speed (WS), Precipitation (PP) and Temperature (T) with the average concentrations of NO_2 of the studied streets.

	RH	WS	PP	T	NO_2 Str F	NO_2 Str R	NO_2 Str M	NO_2 Str S
RH	1							
WS	−0.976	1						
PP	0.941	−0.917	1					
T	−0.519	0.461	−0.707	1				
NO_2 St. F	0.193	−0.206	0.030	0.169	1			
NO_2 St. R	0.753	−0.741	0.855	−0.807	−0.063	1		
NO_2 St. M	0.526	−0.504	0.533	−0.372	−0.370	0.522	1	
NO_2 St. S	0.437	−0.445	0.371	−0.228	−0.077	0.635	0.418	1

Note: **NO_2 St. F** is average concentrations of NO_2 on Antônio Fiúza Street; **NO_2 St. R** is average concentrations of NO_2 on Almirante Rubim Street; **NO_2 St. M** is average concentrations of NO_2 on 24 de Maio Street; **$\overline{x}$ of NO_2 St. S** is average concentrations of NO_2 on General Sampaio Street.

The literature reports that low relative humidity and wind speed favor the increase of NO_2 levels while the occurrence of precipitation and the increase of wind speed can favor the reduction of NO_2 levels (Drumm *et al.*, 2013; Kamińska, 2019; Monte *et al.*, 2016). The increase in temperature near the surface, especially during the summer, can increase the kinetics of gases and consequently improve vertical mixing, contributing to the reduction of NO_2 concentrations in the lower atmosphere (Gasmi *et al.*, 2017). In addition to meteorological conditions, the secondary chemical reactions of NO_2 with photochemical oxidants that occur in the atmospheric lower layers and the morphology of the pathway normally influence NO_2 concentrations (Gasmi *et al.*, 2017; Han *et al.*, 2011).

Compared with the results obtained in the literature, a study performed in Dhahran City, Saudi Arabia showed that NO_2 concentration is strongly affected by traffic emission and photochemistry. Ambient air temperature and wind speed had negative correlation coefficients with NO_2 concentrations while relative air humidity had a positive correlation coefficient (Gasmi *et al.*, 2017). In Mato Grosso do Sul, Brazil, a study found negative correlations between relative humidity and wind speed with NO_2 concentration and a positive correlation between temperature and NO_2 concentration (Souza and Santos, 2018).

Regarding the morphology of the street, the mean values of the H/W ratio for the F, R, M and S Streets were 0.45, 0.23, 0.50 and 0.55, respectively. According to the simplified classification of different urban forms, the H/W ratio with values between 0.2 and 0.6 and with an area occupied by buildings of 70 to 90% are highly developed streets, with low or medium urban density, with large low-rise buildings (Oke *et al.*, 2004). This description confirms the studied streets, as there are shopping centers, restaurants, and parking lots. The results also show that even with the winds blowing perpendicularly to the direction of the street, there were no discrepancies in concentration on one side of the street that was contrary to what was cited in the literature. It is important to report that the influence of meteorological parameters and morphology on NO_2 levels requires a more detailed study, using meteorological stations at the sampling site.

3.3. Principal component analysis

The Principal Component Analysis of the 4-way sampling points related the average NO_2 concentration with the average estimate of vehicle traffic and the H/W ratio according to **Fig. 4**.

The variance of the 4 principal components (CP) analyzed CP1, CP2, CP3 and CP4 are 52.1, 25.6, 16.7 and 5.6%, respectively. These results show that two main components (CP1 and CP2) explain 77.7% of the cases studied. The CP1, represented by the X axis, indicates that the points in the positive direction of this axis have great influence on the variables Average of NO_2 in the rainy (1°P) and dry (2°P) periods, since both have Loading (weight) of 0.63 and 0.61, respectively, while the Loadings for altimetry and traffic are –0.04 and 0.48, respectively. CP2, represented by the Y axis, indicates that its positive axis has a great influence of the altimetry variable, with a Loading of 0.98.

In **Fig. 4**, the blue points belong to M Street, the red points belong to S Street, the grey are points of F Street and the green are those of R Street. Note that all points of the M Street, except M7, were on the negative axis of the principal component 1, indicating that they presented values of NO_2 below the general average in both periods, which were 24.3 µg m^{-3}, 21.5 µg m^{-3}, for 1°P and 2°P, respectively. It is also worth noting that all points on the R Street are on the negative axis of the principal component 2, indicating that the H/W ratio was below the general average that was 0.4. Most of the points on F Street, except for points F5 and F6, were on the positive axis of the main component 2, indicating that these points presented NO_2 levels in both periods and vehicle traffic above the general average. The S Street points did not show clusters in a specific region of the graph.

Applying PCA with PC1 and PC3, we obtain **Fig. 5**. In this graph, the percentage of the total variance (%) of the data of the two principal components (PC) is explained by 68.8% of the cases, PC1 being represented on the X axis and PC3 on the Y axis. Due to the high loading presented by the Traffic variable in PC3, which was 0.87, the points were grouped according to the average number of vehicles that travel on the street per day, with a general average of 8,535 vehicles. As a result, we can observe that, although the total variance of this graph is smaller than the previous one, all samples were separated by streets, with the F Street having the highest values and the M Street having the lowest traffic values. We also observed in this graph that the points F1, F2, F3, F4, R1, R5, S5, S8 and M7 are in the positive region of the average NO_2 variables in the rainy and dry periods, that is, they presented the highest values for these variables.

Applying PCA with PC2 and PC3, we obtain **Fig. 6**, in which the percentage of total variance of the data is explained by 42.3% of the cases, PC2 being represented by the Y axis and PC3 by the X axis. The highest Loading in CP2 was the H/W ratio and in CP3 was the vehicle traffic variable. From this graph, we can see that the points of lane F are all located on the positive axis of CP3, indicating that they presented a greater flow of vehicles among the studied streets, confirming what was described in **Fig. 6**, about CP2, F3 and F4 are on the negative axis, indicating the low H/W ratio. However, the other points of this street are on the positive axis of CP2.

The points of the R Street are grouped on the negative axis of CP2, indicating the low H/W ratio, as mentioned in **Fig. 4**. The points of the M Street are all located on the negative axis of CP3, indicating the lowest flow of vehicles among the lanes studied, as also shown by **Fig. 6**. Both in **Fig. 5** and **6**, the points belonging to the S Street are more dispersed among the streets, indicating that the points of this street do not present a similarity between the samples.

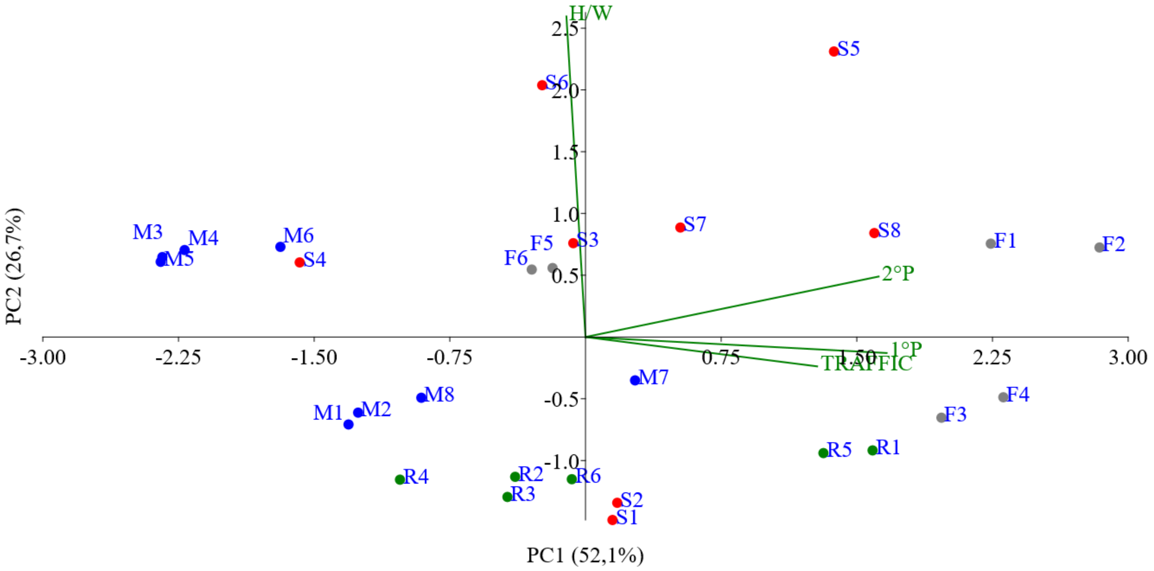

Figure 4. PCA with principal components 1 and 2 of the sampling points using the variables' general average of NO_2 in the rainy and dry seasons, altimetry (H/W) and vehicle traffic.

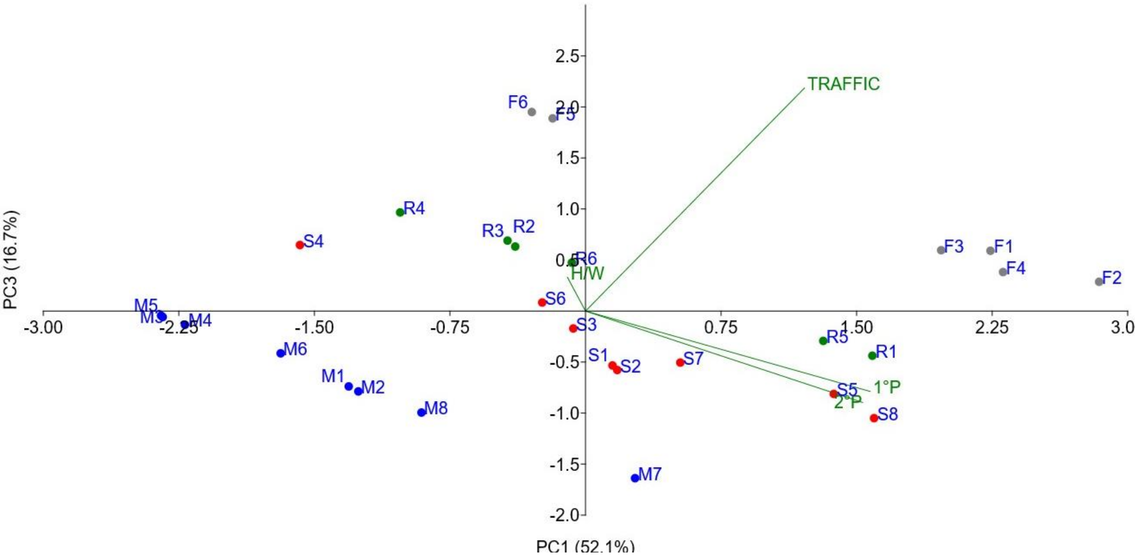

Figure 5. PCA with principal components 1 and 3 of the sampling points using the variables' general average of NO_2 in the rainy and dry seasons, altimetry (H/W) and vehicle traffic.

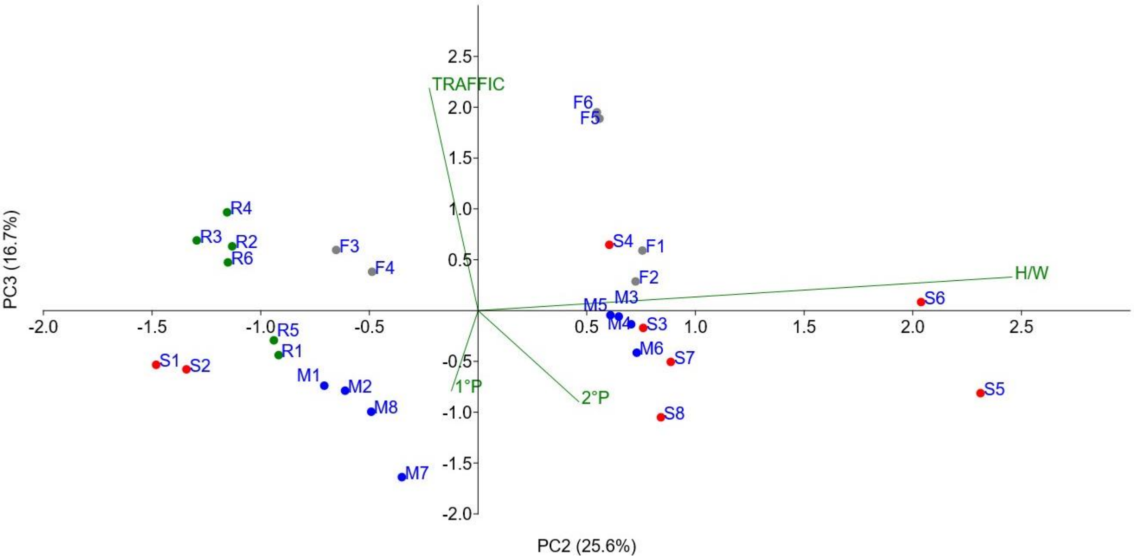

Figure 6. PCA with principal components 1 and 2 of the sampling points using the variables general average of NO_2 in the rainy and dry seasons, altimetry (H/W) and vehicle traffic.

4. Conclusions

Although difficult to compare, the results obtained showed that this pollutant did not exceed the limits established by current Brazilian legislation (CONAMA, 2018 – Resolution 491) and by international legislation (EEA, 2018; EPA, 2018; WHO, 2005) with levels like those previously mentioned in the literature using a methodology equivalent. This dataset also provided this work with a specific analysis of the pollutant behavior studied along a road using principal component analysis, in which it is possible to observe that NO_2 levels are dependent on the street profile, such as terrain and vehicle traffic. In front of the PCA graph, it was easy to visualize points that, although located in different ways, presented similar behavior of the analyzed variables. It is important to emphasize that the results observed throughout this research should be seen as indicative and not conclusive since a broader follow-up is necessary for the care to be elaborated.

Authors' contributions

Conceptualization: Sousa, F. W.; Bertoncini, B. V.; Nascimento, R. F.; Ribeiro, J. P.; **Data curation:** Maia, M. L.; Oliveira, C. S.; R. F.; Ribeiro, J. P.; **Formal Analysis:** Maia, M. L.; Oliveira, C. S.; Quintanilha, W. F. L.; Cassiano, D. R.; **Funding acquisition:** Not applicable; **Investigation:** Maia, M. L.; Sousa, F. W.; Quintanilha, W. F. L.; Cassiano, D. R.; Ribeiro, J. P.; Bertoncini, B. V.; Oliveira, C. S.; **Methodology:** Maia, M. L.; Sousa, F. W.; Quintanilha, W. F. L.; Nascimento, R. F.; Ribeiro, J. P.; Bertoncini, B. V.; Oliveira, C. S.; Cassiano, D. R.; **Project administration:** Sousa, F. W.; **Resources:** Sousa, F. W.; Maia, M. L.; **Software:** Quintanilha, W. F. L.; Cassiano, D. R.; **Supervision:** Sousa, F. W.; Bertoncini, B. V.; **Validation:** Maia, M. L.; Sousa, F. W.; Quintanilha, W. F. L.; **Visualization:** Sousa, F. W.; Maia, M. L.; **Writing – original draft**: Maia, M. L.; Sousa, F. W.; Bertoncini, B. V.; Nascimento, R. F.; Ribeiro, J. P.; **Writing – review & editing:** Maia, M. L.; Sousa, F. W.; Bertoncini, B. V.; Nascimento, R. F.; Ribeiro, J. P.

Data availability statement

All data sets were generated or analyzed in the current study.

Funding

Not applicable.

Acknowledgments

Not applicable.

References

Aguiar, L. F. M. C.; Silva, M. V. C.; Gandu, A. W.; Rocha, C. A.; Cavalcante, R. M. Caracterização de Cânions Urbanos e seus Efeitos Climáticos em Área com Intenso Processo de Verticalização na Cidade de Fortaleza, Ceará. *Revista Brasileira de Geografia Física*. **2017**, *10* (4), 1046–1058. https://doi.org/10.26848/rbgf.v10.4.p1046-1058

Aránguez, E.; Ordóñes, J. M.; Serrano, J.; Aragonés, N.; Fernández-Partier, R.; Gandarillas, A.; Galán, I. Contaminantes Atmosféricos y su Vigilancia. *Revista Española de Salud Pública*. **1999**, *73* (2), 123–132. https://doi.org/10.1590/S1135-57271999000200003

Arbex, M. A.; Santos, U. P.; Martins, L. C., Saldiva, P. H. N.; Pereira, L. A. A.; Braga, A. L. F. Air pollution and the respiratory system. *Jornal Brasileiro de Pneumologia*. **2012**, *38* (5), 643–655. https://doi.org/10.1590/S1806-37132012000500015

Azevedo, B. B.; Anzanello, M. J. Agrupamento de trabalhadores com perfis semelhantes de aprendizado apoiado em Análise de Componentes Principais. *Gestão & Produção*. **2015**, *22* (1), 35–52. https://doi.org/10.1590/0104-530X1094

Baird, C.; Cann, M. *Química Ambiental*; Bookman, 2011.

Bari, A.; Curran, R. L. T.; Kindzierski, W. B. Field performance evaluation of Maxxam passive samplers for regional monitoring of ambient SO_2, NO_2 and O_3 concentrations in Alberta, Canada. *Atmospheric Environment*. **2015**, *114*, 39–47. https://doi.org/10.1016/j.atmosenv.2015.05.031

Bender, A. P.; Dziedzic, M. Dispersão de poluentes nos eixos estruturais em Curitiba (PR), Brasil. *Engenharia Sanitária e Ambiental*. **2014**, *19* (spe), 31–42. https://doi.org/10.1590/S1413-41522014019010000364

Biswal, A.; Singh, T.; Singh, V.; Ravindra, K.; Mor, S. COVID–19 lockdown and its impact on tropospheric NO_2 concentrations over India using satellite-based data. *Helion*. **2020**, *6* (9), E04764. https://doi.org/10.1016/j.heliyon.2020.e04764

Bozkurt, Z.; Üzmez, Ö. Ö.; Döğeroğlu, T.; Artun, G.; Gaga, E. O. Atmospheric concentrations of SO_2, NO_2, ozone and VOCs in Düzce, Turkey using passive air samplers: Sources, spatial and seasonal variations and health risk estimation. *Atmospheric Pollution Research*. **2018**, *9* (6), 1146–1156. https://doi.org/10.1016/j.apr.2018.05.001

Campos, V.; Passos, L.; Godoi, R. H. M.; Godoi, A. F. L.; Tavares, T. M. Development and validation of passive samplers for atmospheric monitoring of SO_2, NO_2, O_3 and H_2S in tropical áreas. *Microchemical Journal*. **2010**, *96* (1), 132–138. https://doi.org/10.1016/j.microc.2010.02.015

Carslaw, D. C.; Murrells, T. P.; Anderssonc, J.; Keenanc, M. Have vehicle emissions of primary NO_2 peaked? *Faraday Discussions*. **2016**, *189*, 439–454. https://doi.org/10.1039/C5FD00162E

Conselho Nacional do Meio Ambiente (CONAMA). Resolução nº 491, de 19 de novembro de 2018. *Dispõe sobre padrões de qualidade do ar*; Ministério do Meio Ambiente, 2018. https://www.in.gov.br/web/guest/materia/-/asset_publisher/Kujrw0TZC2Mb/content/id/51058895/do1-2018-11-21-resolucao-n-491-de-19-de-novembro-de-2018-51058603 (accessed 2018-12-08).

Cruz, L. P. S.; Campos, V. Métodos de amostragem e análise para compostos reduzidos de enxofre atmosférico. *Química Nova*. **2008**, *31* (5), 1180–1189. https://doi.org/10.1590/S0100-40422008000500047

Datasus. Ministério da Saúde. Sistema de Informações sobre Internações Causadas por Doenças no Sistema Respiratório; Datasus, 2019. http://tabnet.datasus.gov.br/cgi/tabcgi.exe?sih/cnv/niuf.def (accessed 2019-11-17).

Ding, J.; Ronald van der A.; Mijling, B.; Laat, J.; Eskes, H.; Boersma, K. F. NO_x emissions in India derived from OMI satellite observations. *Atmospheric Environment: X*. **2022**, *14*, 100174. https://doi.org/10.1016/j.aeaoa.2022.100174

Dita, P. A.; Dias. J. W. C. *Método do Arsenito de Sódio para a Determinação de Dióxido de Nitrogênio na Atmosfera*; Energética, 2016.

Drumm, F. C.; Gerhardt, A. E.; Fernandes, G. D.; Chagas, P.; Sucolotti, M. S.; Kemerich, P. D. C. Air Pollution from the Burning of Fuels Derived from Petroleum in Motor Vehicles. *Revista Eletronica em Gestão, Educação e Tecnologia Ambiental*. **2013**, *18* (1), 66–78. https://doi.org/10.5902/2236117010537

Duan, Y.; Liao, Y.; Li, H.; Yan, S.; Zhao, Z.; Yu, S.; Fu, Y.; Wang, Z.; Yin, P.; Cheng, J.; Jiang, H. Effect of changes in season and temperature on cardiovascular mortality associated with nitrogen dioxide air pollution in Shenzhen, China. *Science of the Total Environment*. **2019**, *697*, 134051. https://doi.org/10.1016/j.scitotenv.2019.134051

European Environment Agency (EEA). *The European Union (EU) has developed an extensive body of legislation which establishes standards and objectives for a number of pollutants in air*; EEA, 2018 (Last updated on 2023-11-23). https://www.eea.europa.eu/themes/air/air-quality-concentrations/air-quality-standards (accessed 2018-04-07).

United States Environmental Protection Agency (EPA). *NAAQS Table*; EPA, 2018 (Last updated on 2024-02-07). https://www.epa.gov/criteria-air-pollutants/naaqs-table (accessed 2018-04-07).

Ferreira, M. M. C. *Quimiometria:* Conceitos. Métodos e Aplicações; Editora Unicamp, 2015. https://doi.org/10.7476/9788526814714

Freedman, B. The Ecological Effects of Pollution, Disturbance and Other Stresses. In *Environmental Ecology*; Academic Press, 1995.

Gasmi, K.; Aljalal, A.; Al-Basheer, W.; Abdulahi, M. Analysis of NO_x, NO and NO_2 ambient levels in Dhahran, Saudi Arabia. *Urban Climate*. **2017**, *21*, 232–242. https://doi.org/10.1016/j.uclim.2017.07.002

Ghosh, S.; Dubey, S. K. Comparative Analysis of K-Means and Fuzzy CMeans Algorithms. *International Journal of Advanced Computer Science and Applications*. **2013**, *4* (4), 35–39. https://doi.org/10.14569/IJACSA.2013.040406

Ghozilaki, M. G.; Heibati, B.; Naddafi, K.; Kloog, I.; Conti, G. O.; Polosa, R.; Ferrante, M. Evaluation of Chronic Obstructive Pulmonary Disease (COPD) attributed to atmospheric O_3, NO_2, and SO_2 using Air Q Model

(2011–2012 year). *Environmental Research*. **2016**, *144* (A), 99–105. https://doi.org/10.1016/j.envres.2015.10.030

Grundström, M.; Pleijel, H. Limited effect of urban tree vegetation on NO_2 and O_3 concentrations near a traffic Route. *Environmental Pollution*. **2014**, *189*, 73–76. https://doi.org/10.1016/j.envpol.2014.02.026

Guo, P.; Miao, H.; Chen, Y.; Fu, Y.; Zhao, Q.; Li, B. Maternal exposure to gaseous ambient air pollutants increases the risk of preterm birth in the Pearl River Delta, China 2014–2017. *Science of The Total Environment*. **2019**, *671*, 959–970. https://doi.org/10.1016/j.scitotenv.2019.03.375

Halim, N. D. A.; Latif, M. T.; Ahamad, F; Dominick, D.; Chung, J. X.; Juneng, L.; Khan, F. The long-term assessment of air quality on an island in Malaysia. *Helion*, **2018**, *4* (12), e01054. https://doi.org/10.1016/j.heliyon.2018.e01054

Hammer, Ø.; Harper, D. A. T.; Ryan, P. D. PAST: Paleontological statistics software package for education and data analysis. *Palaeontologia Electronica*. **2001**, *4* (1), 9.

Han, S.; Bian, H.; Feng, Y.; Liu, A.; Li, X.; Zeng, F.; Zhang, X. Analysis of the Relationship between O_3, NO and NO_2 in Tianjin, China. *Aerosol and Air Quality Research.* **2011**, *11* (2), 128–139. https://doi.org/10.4209/aaqr.2010.07.0055

Harner, T.; Su, K.; Genualdi, S.; Karpowicz, J.; Ahrens, L.; Mihele, C.; Schuster, J.; Charland, J. P.; Narayan, J. Calibration and application of PUF disk passive air samplers for tracking polycyclic aromatic compounds (PACs). *Atmospheric Environment*. **2013**, *75*, 123–128. https://doi.org/10.1016/j.atmosenv.2013.04.012.

Hatzopoulou, M.; Weichenthal, S.; Dugum, H.; Pickett, G.; Miranda-Moreno, L.; Kulka, R.; Andersen, R.; Goldberg, M. The impact of traffic volume, composition, and road geometry on personal air pollution exposures among cyclists in Montreal, Canada. *Journal of Exposure Science and Environmental Epidemiology*. **2013**, *23*, 46–51. https://doi.org/10.1038/jes.2012.85

Hauser, C. D.; Buckey, A.; Porter, J. Passive samplers and community science in regional air quality measurement, education and communication. *Environmental Pollution*. **2015**, *203*, 243–249. https://doi.org/10.1016/j.envpol.2014.12.028

Hien, P. D.; Hangartner, M.; Fabian, S.; Tan, P. M. Concentrations of NO_2, SO_2, and benzene across Hanoi measured by passive diffusion samplers. *Atmospheric Environment*. **2014**, *88*, 66–73. https://doi.org/10.1016/j.atmosenv.2014.01.036

Honda, K.; Notsu, A.; Ichihashi, H. Fuzzy PCA-Guided Robust k-Means Clustering. *IEEE Transactions on Fuzzy Systems*. **2010**, *18* (1), 67–79. https://doi.org/10.1109/TFUZZ.2009.2036603

Hongyu, K.; Sandanielo, V. L. M.; Oliveira Junior, G. J. Análise de Componentes Principais: Resumo Teórico, Aplicação e Interpretação. *Engineering and Science*. **2016**, *5* (1), 83–90. https://doi.org/10.18607/ES201653398

Instituto Nacional de Meteorologia (INMET). Banco de dados meteorológicos (BDMEP); INMET, 2019. https://bdmep.inmet.gov.br/ (accessed 2019-11-07).

Instituto Brasileiro de Geografia e Estatistica (IBGE). Frota de Veículos; IBGE, 2019. https://cidades.ibge.gov.br/brasil/ce/fortaleza/pesquisa/22/28120 (accessed 2019-11-03).

Januševičius, T.; Grubliauskas, R. The effect of speed bumps and humps on the concentrations of CO, NO and NO_2 in ambient air. *Air Quality, Atmosphere & Health*. **2019**, *12*, 635–642. https://doi.org/10.1007/s11869-019-00683-y

Kamińska, J. A. A random forest partition model for predicting NO2 concentrations from traffic flow and meteorological conditions. *Science of the Total Environment*. **2019**, *651* (1), 475–483. https://doi.org/10.1016/j.scitotenv.2018.09.196

Karamizadeh, S.; Abdullah, S. M.; Manaf, A. A.; Zamani, M.; Hooman, A. An Overview of Principal Component Analysis. *Journal of Signal and Information Processing*. **2013**, *4* (3B), 173–175. https://doi.org/10.4236/jsip.2013.43B031

Lacava, C. I. V.; Alvares Junior, O. M.; Fernandes, P. S. *Emissões Atmosféricas*; SENAI, 2002.

Lenzi, E.; Favero, L. O. B. *Introdução à Química da Atmosfera*: Ciência. Vida e Sobrevivência; LTC, 2014.

Lisboa, H.; Kawano, M. *Monitoramento de poluentes atmosféricos*. Controle da Poluição Atmosférica; ENS-UFSC, 2010.

Lodge, J. P. *Methods of Air Sampling and Analysis*; Lewis Publishers, 1988.

Lyra, W. S.; Silva, E. C.; Araújo, M. C. U.; Fragoso, W. D. Classificação Periódica: Um Exemplo Didático Para Ensinar Análise de Componentes Principais. *Química Nova*. **2010**. *33* (7), 1594–1597. https://doi.org/10.1590/S0100-40422010000700030

Maia, K. P.; Silva, G. A.; Libânio, M. Aplicação de análise multivariada no estudo da frequência de amostragem e do número de estações de monitoramento de qualidade da água. *Engenharia Sanitária e Ambiental*. **2019**, *24* (5), 1013–1025. https://doi.org/10.1590/S1413-41522019175743

Martins, L. C.; Latorre, M. R. D. O.; Cardoso, M. R. A.; Gonçanves, F. L. T.; Saldiva, P. H. N.; Braga, A. L. F. Poluição atmosférica e atendimentos por pneumonia e gripe em São Paulo, Brasil. *Revista de Saúde Pública*. **2002**, *36* (1), 88–94. https://doi.org/10.1590/S0034-89102002000100014

Masey, N.; Gillespie, J.; Heal, M. R.; Hamilton, S.; Beverland. I. J. Influence of wind-speed on short-duration NO_2 measurements using Palmes and Ogawa passive diffusion samplers. *Atmospheric Environment*. **2017**, *160*, 70–76. https://doi.org/10.1016/j.atmosenv.2017.04.008

Mehta, N. S.; Dey, S. Automobile pollution control using catalysis. *Resources, Environment and Sustainability*. **2020**, *2*, 100006. https://doi.org/10.1016/j.resenv.2020.100006

Miranda, D. C.; Ferreira, G. C.; Barbosa, L. D.; Pereira, N. L. A.; Ribeiro, T. C.; Maloncy, M. L.; Batista, M. S. Análise dos Poluentes Atmosféricos NO_2 E O_3 Via Amostradores Passivos de Baixo Custo. *E-Xacta*. **2017**, *10* (1), 29–35. https://doi.org/10.18674/exacta.v10i1.1960

Monte, E. Z.; Albuquerque, T. T. A.; Reisen, V. A. Impactos das Variáveis Meteorológicas na Qualidade do Ar da Região da Grande Vitória, Espírito Santo, Brasil. *Revista Brasileira de Meteorologia*. **2016**, *31* (4 suppl 1), 546–554. https://doi.org/10.1590/0102-7786312314b20150100

Moori, R. G.; Marcondes, R. C.; Ávila, R. T. A Análise de Agrupamentos como Instrumento de Apoio à Melhoria da Qualidade dos Serviços aos Clientes. *Revista de Administração Contemporânea*. **2002**, *6* (1), 63–84. https://doi.org/10.1590/S1415-65552002000100005

Moura, I. S. M.; Santos, D. F.; Pinheiro, F. G. M.; Oliveira, C. J. Characterization of Dry and Wet Periods of Fortaleza City (CE). *Ciência e Natura*. **2015**, *37*, 3–7. https://doi.org/10.5902/2179460X16206

Moura, M. O.; Zanella, M. E.; Sales, M. C. L. Ilhas Térmicas na Cidade de Fortaleza/CE.; *Boletim Goiano de Geografia*. **2008**, *28* (2), 33–44. https://doi.org/10.5216/bgg.v28i2.5718

Moura, M. O. Anomalias das temperaturas extremas do ar em Fortaleza, Ceará, Brasil. *Revista Brasileira de Geografia Física*. **2015**, *8* (6), 1588–1600. https://doi.org/10.5935/1984-2295.20150089

Muniz-Gäal, L. P.; Pezzuto, C. C.; Carvalho, M. F. H.; Mota, L. T. M. Parâmetros urbanísticos e o conforto térmico de cânions urbanos: o exemplo de Campinas, SP. *Ambiente Construído*. **2018**, *18* (2), 177–196. https://doi.org/10.1590/s1678-86212018000200249

Nakata-Osaki, C. M.; Souza, L. C. L.; Rodrigues, D. S. Impacto da geometria do cânion urbano na intensidade de ilha de calor noturna: análise através de um modelo simplificado adaptado a um SIG. *Ambiente Construído*. **2016**, *16* (3), 73–87. https://doi.org/10.1590/s1678-86212016000300093

Nascimento, L. F. C.; Braga, A. L. F.; Modolo, M. C. C. Effects of air pollution on children's health in a city in Southeastern Brazil. *Revista de Saúde pública*. **2006**, *40* (1), 77–82. https://doi.org/10.1590/S0034-89102006000100013

Negrisoli, J.; Nascimento, L. F. C. Atmospheric pollutants and hospital admissions due to pneumonia in children. *Revista Paulista de Pediatria*. **2013**, *31* (4), 501–506. https://doi.org/10.1590/S0103-05822013000400013

Oke, T. R.; *Initial Guidance to Obtain Representative Meteorological Observations at Urban Sites*; World Meteorological Organization, 2004.

Pestana, P. R. S.; Braga, A. L. F.; Ramos, E. M. C.; Oliveira, A. F.; Osadnik, C. R.; Ferreira, A. D.; Ramos, D. Effects of air pollution caused by sugarcane burning in Western São Paulo on the cardiovascular system. *Revista de Saúde Pública*. **2017**, *51*, 13. https://doi.org/10.1590/s1518-8787.2017051006495

Piceli, P. C.; Lisboa, H. M. Quantificação de benzeno, tolueno, etilbenzeno e xilenos no ar de ambientes internos. *Engenharia Sanitária e Ambiental*. **2018**, *23* (3), 527–534. https://doi.org/10.1590/S1413-41522018119310

Rao, M.; George, L. A.; Rosenstiel, T. N.; Shandas, V.; Dinno, A. Assessing the relationship among urban trees, nitrogen dioxide, and respiratory health. *Environmental Pollution*. **2014**, *194*. 96–104. https://doi.org/10.1016/j.envpol.2014.07.011

Richmond-Bryant, J.; R. Chris Owen, R. C.; Graham, S.; Snyder, M.; Mcdow1, S.; Oakes, M.; Kimbrough, S. Estimation of on-road NO_2 concentrations, NO_2/NO_X ratios, and related roadway gradients from near-road monitoring data. *Air Quality, Atmosphere & Health*. **2017**, *10*, 611–625. https://doi.org/10.1007/s11869-016-0455-7

Russo, A.; Trigo, R. M.; Martins, H.; Mendes, M. T. NO_2, PM10 and O_3 urban concentrations and its association with circulation weather types in Portugal. *Atmospheric Environment*. **2014**, *89*, 768–785. https://doi.org/10.1016/j.atmosenv.2014.02.010

Saltzman, B. E. Colorimetric Microdetermination of Nitrogen Dioxide in Atmosphere. *Analytical Chemistry*. **1954**, *26* (12), 1949–1955. https://doi.org/10.1021/ac60096a025

Shaw, J. T. The measurement of nitrogen dioxide in the air. *Atmospheric Environment*. **1967**, *1* (2), 81–85. https://doi.org/10.1016/0004-6981(67)90036-4

Shiraiwa, M.; Selzle, K.; Pöschl, U. Hazardous components and health effects of atmospheric aerosol particles: reactive oxygen species, soot, polycyclic aromatic compounds and allergenic proteins. *Free Radical Research*. **2012**, *46* (8), 927–939. https://doi.org/10.3109/10715762.2012.663084

Souza, A.; Santos, D. A. S. Análise das Componentes Principais no Processo de Monitoramento Ambiental. *Nativa*. **2018**, *6* (6), 639–647. https://doi.org/10.31413/nativa.v6i6.6453

Souza, P. A. F.; Cardoso, A. A.; Karen, F. C. A. Desenvolvimento de Amostrador Passivo Sensível para Monitoramento de Poluição Atmosférica por Dióxido de Nitrogênio. *Quimica Nova*. **2017**, *40*, 1233. https://doi.org/10.21577/0100-4042.20170117

Stricker, M. D.; Onland-Moret, N. C.; Boer, J. M. A.; Van Der Schouw, Y. T.; Verschuren, W. M. M.; May, A. M.; Peeters, P. H. M.; Beulens, J. W. J. Dietary patterns derived from principal component- and k-means cluster analysis: Long-term association with coronary heart disease and stroke. *Nutrition. Metabolism & Cardiovascular Diseases*. **2013**, *23* (3), 250–256. https://doi.org/10.1016/j.numecd.2012.02.006

Ugucione, C.; Gomes Neto, J. A.; Cardoso, A. A. Método Colorimétrico para Determinação de Dióxido de Nitrogênio Atmosférico com Preconcentração em Coluna de C–18; *Química Nova*. **2002**, *25* (3), 353–357. https://doi.org/10.1590/S0100-40422002000300003

World Health Organization (WHO). *Air Quality Guideline for Particulate matter, Ozone, nitrogen dioxide and sulfur dioxide*. Global update 2005. https://iris.who.int/bitstream/handle/10665/69477/WHO_SDE_PHE_OEH_06.02_eng.pdf?sequence=1 (accessed 2018-04-20).

Xu, Q.; Ding, C.; Liu, J.; Luo, B. PCA-guided search for K-means. *Pattern Recognition Letters*. **2015**, *54* (1), 50–55. https://doi.org/10.1016/j.patrec.2014.11.017

Zanetti, P.; Melli, P.; *Environmental Modelling*; WIT Press, 1992.

ECLÉTICA QUÍMICA

Eclet. Quim. 49 | e-1496, 2024

Original Article

https://doi.org/10.26850/1678-4618.eq.v49.2024.e1496

Optimizing sewage water of Perum Pesona Permata Gading with the assistance of Cu/Mg electrodes as public street lighting based on green technology electricity

Deni Ainur **Rokhim**[1,2+], Diana Novel **Smith**[3], Alfredo Radinal **Mukhtar**[4], Azzahra Zafira Putri **Koto**[5]

Abstract

Electricity in Indonesia uses fossil fuels as an energy source. If fossil fuels run out, we will lose our largest source of electrical energy. Therefore, we need a way to reduce dependence on fossil fuels by making good use of renewable energy as a source of electrical energy. One of them is Green Technology Electricity with the utilization of sewage water to convert chemical energy into electrical energy. This study aims to determine the potential of sewage water assisted by Cu/Mg electrodes as a source of street lighting, manufacturing, and testing methods, and the effect of optimizing sewage water on electrical performance as street lighting. Lack of lighting in residential areas is also a supporting factor in this research. The stages used are preparation, incubation, construction assembly, research, and strength testing. Based on research, the sewage water from Perum Pesona Permata Gading can be used as street lighting with the highest potential difference and current strength being 4.4 V and 0.55 A for each 50 mL of the sewage water.

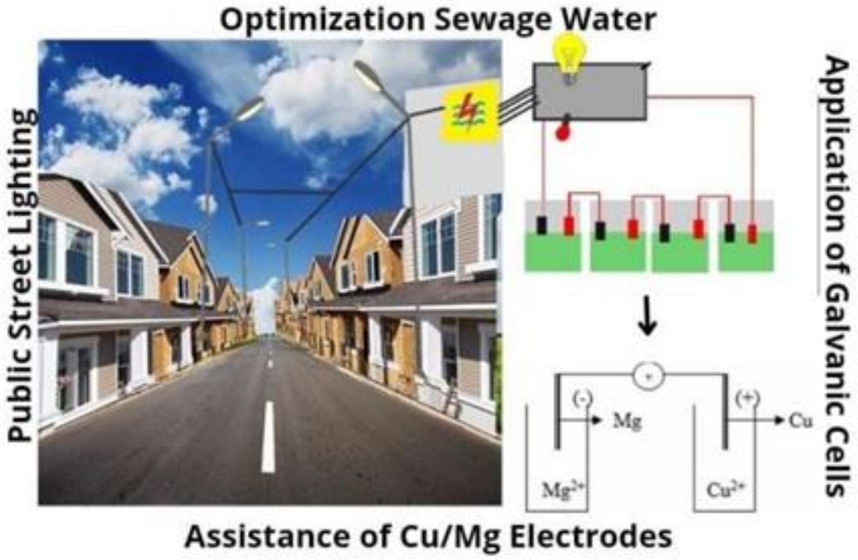

Article History

Received May 31, 2023
Accepted February 27, 2024
Published May 20, 2024

Keywords

1. green technology electricity;
2. alternative energy;
3. sewage water optimization.

Section Editor

Patricia Hatsue Suegama

Highlights

- Green technology applied to sewage water converts chemical energy into electricity.
- Potential of sewage water assisted by Cu/Mg electrodes as a source of street lighting.
- The stages are preparation, incubation, construction, research, and strength testing.
- The highest ΔV and I were 4.4 V and 0.55 A for each 50 mL of sewage water.

[1]State University of Malang, Chemistry, Malang, Indonesia. [2]SMA Negeri 3 Sidoarjo, Sidoarjo, Indonesia. [3]Universitas Airlangga, Pharmacy, Surabaya, Indonesia. [4]Universitas Brawijaya, Computer Science, Malang, Indonesia. [5]Indonesia Defense University, Medical, Bogor, Indonesia.

+Corresponding author: Deni Ainur Rokhim, **Phone:** +6283857257301, **Email address:** deniainurrokhim@gmail.com

1. Introduction

The need for electrical energy in this globalization and modernization era is critical (Hutabarat *et al.*, 2022). Energy is produced by burning non-renewable natural resources. Thus, the amount of natural resource reserves globally is becoming thinner and has an impact on the environment. This is shown by the energy production process that produces gas emissions such as carbon dioxide, methane, and others. The gas then envelops the earth, preventing the sun's heat from evaporating at night. In other words, the energy crisis makes the earth warmer, thus triggering global warming. In addition to having an impact on the environmental sector, the use of non-renewable natural resources has an impact on the economic sector. The higher the energy use, the cost of energy production also increases. Meanwhile, the available natural resources are very limited, so it is very possible that prices will increase many times and can trigger damage to economic stability. One of the logical solutions in dealing with the current energy crisis is to use renewable alternative energy. Therefore, technological innovation and sustainable alternative energy research are urgently needed.

In this era, human beings all around the world are in dire need of renewable alternative energy that will be the new electrical energy source. This is because the availability of electrical energy is not capable of meeting the increasing demand for electricity in Indonesia, there is a division of electrical energy in rotation is the impact of limited electrical energy distributed by PLN (Sintiya and Nurmasyitah, 2019). Alternative energy is an energy source that comes from nature and can be regenerated freely. Electrical energy is a vital need for people worldwide, and Electrical energy is the most economical resource that can be used for our daily needs, jobs, and various activities (Wahid *et al.*, 2014). Almost every aspect of human life cannot be separated from electrical energy (Hamamni *et al.*, 2020). The use of electrical energy is based on cheap supply energy and can be easily used compared to other energy (Priyarsono *et al.*, 2010). Electrical energy generally depends on the availability of natural resources such as fossil-based, solar, wind, and others (Hikmawan and Suprayitno, 2018).

In Indonesia, there are a lot of alternative energy sources that have the potential to be solar power plants, water, and a lot more. Utilization of this natural resource must be developed so that it can become one of the solutions that can be offered to overcome the country's problems, especially in the energy sector. One alternative energy that can be used is sewage water. Sewage water can easily be found across the nation. Sewage is a channel to distribute wastewater and rainwater to be taken to a destination so that it does not bring environmental and health problems. This wastewater can come from households, industrial industries, or other public places that contain materials that can endanger human life and living that can interfere with environmental sustainability (Chandra and Jaya, 2021). Imagine if all the streetlights in the environment are using wastewater as a power for the streetlights. This can result in more available natural resources to store and a lot of wastewaters to be used for something useful. "Public Street Lighting" (PSL) is a lamp used for street lighting at night, making it easier for drivers to see the road in the middle of the night to improve traffic safety.

One of the causes of traffic accidents is the lack of lighting in the area. Based on police data, an average of 3 people die every hour from traffic accidents in Indonesia (Sugiyanto *et al.*, 2017). The data also says that several causes caused many accidents, 61% of accidents were caused by human factors related to the ability and character of the driver, 9% were due to vehicle factors, and 30% were caused by infrastructure and environmental factors (Zulkarnaen *et al.*, 2018). Dark lighting conditions lead to lousy eye-sighting and bad road sense. When doubled with the condition of a sleepy driver, it will be even more dangerous. This condition is threatening for motorists and pedestrians. Furthermore, a dark location can also provoke someone to commit a crime.

The reason why the writer chooses to do this research is that the writer wants to examine how the increasing demand for electrical energy in Indonesia is currently not balanced with the availability of electrical energy supply or the electrical energy crisis is something that cannot be avoided. The control blackouts in Jawa-Bali and planned control blackouts in certain places in Sumatra are sign that the electrical supply within the interconnection routine is able to fulfill the expanding power needs of individuals and industry. The circumstance compounds with the expanding toll of fuel which rises to the moon indeed the larger part of control plants exterior Java which are utilizing diesel as fuel experienced swelling operational costs (Agung, 2013).

After examining these conditions, at least two things have to be considered and assessed. To begin with, how distant is the viability and productivity of the interconnection framework for supplying electrical vitality that includes numerous powerplants accessible to date? It is presently the time to explore an elective, more reasonable electrical vitality supply framework. Both dependences on fuel oil ought to continuously be diminished by utilizing elective vitality based on nearby potential from each locale in Indonesia. Since of this reason, an expansion to the utilization of preliminary vitality sources whose saves are bigger such as gas and coal, too calculated application of naturally inviting renewable vitality, such as geothermal, sun powered vitality, wind, and water (Agung, 2013).

This research was conducted based on the green technology electricity method. Green Technology Electricity is a development of the electrical energy concept that starts from the theories of designing or developing an operating system that integrates modern technology and electrical energy with environmental science, to reduce the negative impacts of human activities. Also, with the help of Cu/Mg electrodes, which will have an impact on the electricity to be used and the lights on public street lighting. The writer wants to use Perum Pesona Permata Gading's sewage water because there are dozens of paths in the area as well as the lack of public street lighting in the area. This is done by testing the strength of the current and voltage, which is intended to analyze the effectiveness of ditch water on the three paths contained in the ditch namely the main line, entrance and exit as a source of electrical energy. The voltage and electric current generated in this study can be explained by adopting the working principle of a voltaic cell. If two different electrodes are placed in an electrolyte solution, they will produce electrical energy from a chemical reaction that takes place spontaneously (Atina, 2015).

2. Experimental

2.1. Tools and Materials

The tools and materials used in this experiment are: AVO Meter commonly called a multimeter which serves to measure more than one electric quantity, 9 pieces of 50 mL beaker as a place to react ingredients, Crocodile clip cable as a connecting circuit, Miniatur LED lights as a measure of the ability of the power to turn on the lights, Cu plate and Mg band 5 cm x 1 cm x 0.1 cm as conductor, Sandpaper which serves to smooth the surface of the Cu plate and Mg band 5 cm x 1 cm x 0.1 cm, Sewage water from 3 different paths as a source of electrical energy.

2.2. Step-step

First, pour the sewage water into the beaker with the provision of sewage water on each line using 3 beakers. Sand the Cu plate and Mg band until you can see the difference in color from the original color. After that, insert the Cu plate and Mg tape that has been sanded into each beaker that has been filled with sewage water. Attach the alligator clip cable to the Cu plate and Mg band. Then, connect it with an AVO Meter or Multimeter analogue and see how much voltage and electrical wear is contained in each sewage line. Repeat the experiment up to 5 times every 30 min with an estimated standard deviation not exceeding the mean.

3. Results and discussion

An electrode is a conductor that can give an electric current from one media to another. Electrodes are generally made from metal—namely copper, silver, tin, and zinc. But there are also electrodes made from Non-metal electrical conductor materials, a kind of graphite. Electrodes can be used in welding, batteries, medicines, as well as manufacturing for processes involving electrolysis (Tanjung, 2021).

In the case of unidirectional electric current, electrodes came hand in hand and were named as anode and cathode. In a battery, or other DC, anode is interpreted as when the electrons emerge from the electrochemical cell, oxidation occurs. On the opposite, a cathode is interpreted as when electrodes at an electron pass through electrochemistry thus resulting in electrodes when electrons pass through an electrochemical cell resulting in reduction. Each electrode can make an anode or cathode depending on the potential differences given to the electrochemical cell. Bipolar electrodes are electrodes that act as anode of an electrochemical cell and cathode for other electrochemical cells (Sumanzaya *et al.*, 2019).

As a result of electrons flowing from the negative electrodes to the positive electrodes, it impacted the electric current in the voltaic cells. This thing was caused by the differences between the potential ratio and the two electrodes. For example, measuring the potential difference between two electrodes using the potentiometer when the electric charge is flowing until it runs out. As a result, this causes potential differences when the electric current reaches zero, named potential cell. The Potential differences are obsessed with various electrode materials and concentrations as well as electrolyte temperatures. For example, if Daniel cells were measured with a voltage potentiometer at 25°C of temperature when the concentration of Zn^{2+} and Cu^{2+} ions is the same the voltage is 1.10 volt. If the electrodes of Cu^{2+} inside Daniell cells were exchanged with Ag/Ag^{+} electrodes, and the cell potential will be 1.56 volt.

This research method will utilize one pair of Cu/Mg electrodes to measure the current and voltage of 3 path's sewage water, the 3 path's are at inlet, outlet, and main way. Utilizing a series of devices such as LED lights and multimeters to measure the current strength and electrical potential differences. The result of this research is that Cu-Mg electrodes can produce a large current value and electric voltage so that the lights using the Cu-Mg electrode become brighter.

The data obtained in this research conducted 5 repetitions in measurement every 30 minutes with an estimated standard deviation not exceeding the mean. If the standard deviation is greater than the mean, it means the data is more diverse. If the standard deviation is smaller than the mean, it means that the data is less diverse. The standard deviation of the electric voltage is 0.00–0.20 and the standard deviation of the current strength is 0.08–0.16. This is in line with expectations, namely, it does not exceed the mean, which means the data is less diverse, so the data is stable. The voltage and current values vary because of different sewage water paths, there may be differences in each sewage water's content. The voltage and current generated at every 5 cm x 1 cm x 0.1 cm Cu/Mg electrode in sewage water can be explained by the working principle of a galvanic cell. Two different electrodes inserted into the electrolyte will produce electrical energy because of chemical reactions, namely the reduction-oxidation reaction. On the anode, namely the Mg band, the oxidation process occurs, meanwhile, on the cathode, the Cu plate occurs a reduction reaction (**Eq. 1**).

$$\begin{array}{l} Mg_{(S)} \rightarrow Mg^{2+}_{(aq)} + 2\,e^{-} \\ Cu^{2+}_{(aq)} + 2\,e^{-} \rightarrow Cu_{(S)} \\ \hline Mg_{(S)} + Cu^{2+}_{(aq)} \rightarrow Cu_{(S)} + Mg^{2+}_{(aq)} \end{array} \tag{1}$$

The electron moves from the anode to the cathode; this reaction keeps repeating until it produces electrical energy. **Table 1** shows the result of sewage water at the inlet with a Cu plate and Mg band.

Table 1. The experiment of sewage water at the inlet with Cu plate and Mg band.

Time	Voltage (V)	Strong Current (A)
First 30 min	3.80	0.29
Second 30 min	3.80	0.35
Third 30 min	3.80	0.50
Fourth 30 min	3.80	0.35
Fifth 30 min	3.80	0.30

Based on **Table 1**, the voltage of the experiment tends to be constant at 3.80 V. Meanwhile, the highest current occurred at the third 30 min which was 0.50 A. The second highest current occurs at the second 30 min and the fourth 30 min, which is 0.35 A. The third highest current occurs at the fifth 30 minutes, which is 0.30 A. The lowest current occurs at the first 30 minutes, i.e., 0.29 A. In conclusion, the average current of sewage water electricity in the entrance path is 0.36 A. The formula for calculating power is P = V x I so the inlet power is 1.37 watts by multiplying the average voltage by the average current strength.

Table 2 presents results obtained from a second path's sewage water.

Table 2. The experiment of sewage water at the outlet with Cu plate and Mg band.

Time	Voltage (V)	Strong Current (A)
First 30 min	4.00	0.45
Second 30 min	4.40	0.55
Third 30 min	4.40	0.75
Fourth 30 min	4.40	0.55
Fifth 30 min	4.00	0.45

Based on **Table 2**, the voltage of the experiments tends to be constant at 4.00 V and 4.40 V, the average from the first to fifth 30 min is 4.24 V. Meanwhile, the highest current occurred at the third 30 min which was 0.75 A. The second highest current occurs at the second 30 min and the fourth 30 min that was 0.55 A. The lowest current occurs at the first 30 min and the fifth 30 min, which is 0.45 A. In conclusion, the average current of sewage water electricity in the entrance path is 0.55 A. The formula for calculating power is P = V x I so the outlet power is 2.33 watts by multiplying the average voltage by the average current strength.

Table 3 presents results obtained from a third path's sewage water.

Table 3. The experiment of sewage water at the main way with Cu plate and Mg band.

Time	Voltage (V)	Strong Current (A)
First 30 min	4.00	0.20
Second 30 min	4.00	0.45
Third 30 min	4.00	0.55
Fourth 30 min	4.00	0.45
Fifth 30 min	4.00	0.20

Based on Table 3, the voltage of the experiments tends to be constant at 4.00 V. While the highest current occurs at the third 30 min which was 0.55 A. The second highest current occurs at the second 30 min and the fourth 30 min, which was 0.45 A. And the lowest current occurs at the first 30 min and the fifth 30 min, which is 0.20 A. In conclusion, the average current of sewage water electricity in the entrance path is 0.37 A. The formula for calculating power is P = V x I so the outlet power is 1.48 watts by multiplying the average voltage by the average current strength.

Figures 1 and 2 show the graphic of the electrical voltage for the three parts.

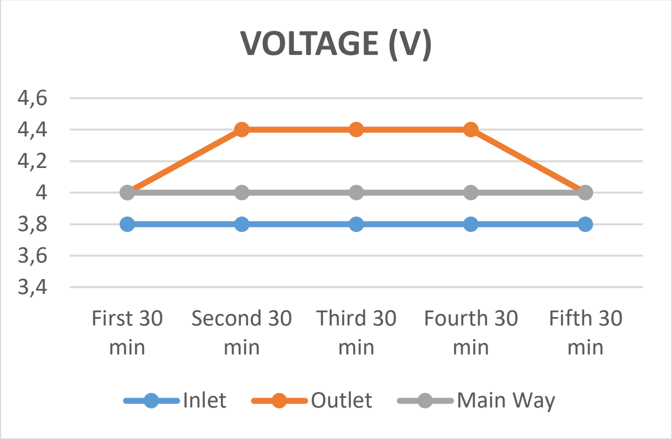

Figure 1. Electrical voltage on the three paths.

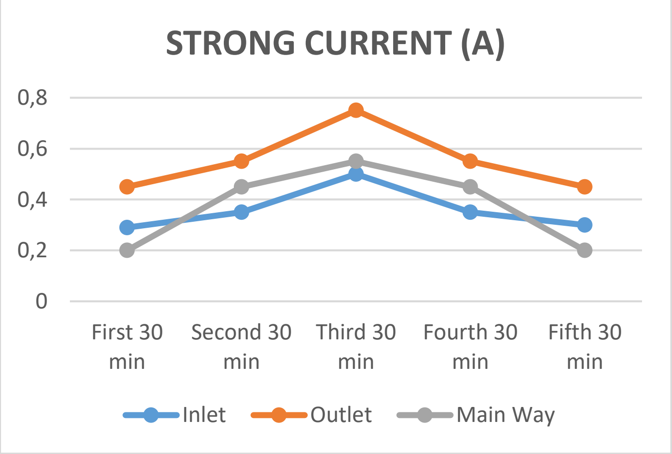

Figure 2. The strong electric current in the three paths.

From the tables and figures, it is evident that every wastewater channel in Perum Pesona Permata Gading has the potential to be a lighting power plant, considering that in Indonesia the average public street lighting lamp has a power of 30 to 60 Watts. Meanwhile, in the research above, for every 5 mL of wastewater, 1.36, 2.33 and 1.48 Watts of power were obtained from the inlet, outlet, and main lines respectively. If the sewer water volume and Cu/Mg area increases the power of the wastewater will also increase and can meet the minimum standards for public street lighting in Indonesia. With the entrance and main path of Perum Pesona Permata Gading is less effective to be the source of electricity in Public Street Lighting. Meanwhile, based on the table above, the exit path of Perum Pesona Permata Gading has high, constant voltage and current strength. So, we can conclude that the sewage water in this path is very effective in water optimization to be used as a source of electrical energy with Cu/Mg electrodes inserted into the wastewater which will later help the ions in the water interact and turn into electrical energy. This is also supported by the conductivity found in wastewater of 10,000. Conductivity is related to the amount of electron flow that is excited due to the content in the wastewater. The exit route of Perum Pesona Permata Gading leads to a river that contains many kinds of household waste so the content in the wastewater is not pure H_2O which causes the voltage and strength of the water flow to be higher and more constant.

Based on the research above, the optimization of sewage water is certainly very influential for electrical performance as an energy source for Public Street Lighting lamps as well as in people's lives. Because the use of this sewage water produces a high, constant voltage and strong electric current so that the lamp can light up brightly. The use of this sewage water as energy source is also included in the use of renewable alternative energy where this energy can be continuously used and will not run out so that it can guarantee the fulfillment of increasing human needs. Furthermore, the increasing demand for electrical energy in Indonesia is currently not balanced with the availability of electrical energy supply. This can also help the government in supplying electrical energy by utilizing wastewater so that it can be more useful, and the use of alternative energy can help the government to store natural resources that are currently in limited availability. This experiment requires further research to realize it in the field with more complex internal and external factors such as the need for greater funds and materials as well as the need for support from residents and local government for the realization of this power plant.

4. Conclusions

Based on the research's data, the experiment proves that the light is better lit on the water exit path of the Perum Pesona Permata Gading sewage than on the other two paths. With the difference of potential of 4.4 V and the current strength of 0.55 A for every 50 mL sewage water of the Perum Pesona Permata Gading. After all that, we can conclude that all 3 paths of Perum Pesona Permata Gading can be used as a source of electricity with the assistance of Cu/Mg electrodes, being able to produce voltage and high current electricity, thus has the potential to be used in Public Street Lighting with brightly lit lights.

Authors' contributions

Conceptualization: Rokhim, D. A.; **Data curation**: Smith, D. N.; **Formal Analysis**: Koto, A. Z. P.; Smith, D. N.; **Funding acquisition**: Rokhim, D. A.; **Investigation**: Smith, D. N.; **Methodology**: Mukhtar, A. R.; **Project administration**: Koto, A. Z. P.; **Resources**: Koto, A. Z. P.; **Software**: Mukhtar, A. R.; **Supervision**: Rokhim, D. A.; **Validation**: Rokhim, D. A.;

Visualization: Mukhtar, A. R.; **Writing – original draft**: Smith, D. N.; **Writing – review & editing**: Rokhim, D. A.

Data availability statement

All data sets were generated or analyzed in the current study.

Funding

Not applicable.

Acknowledgments

Not applicable.

References

Agung, A. I. Potensi Sumber Energi Alternatif Dalam Mendukung Kelistrikan Nasional. *J. Pendidik. Tek. Elektro.* **2013**, *2* (2), 892–897. https://doi.org/10.26740/jpte.v2n2.p%25p

Atina, A. Tegangan dan kuat arus listrik dari sifat asam buah. *Sainmatika* **2015**, *12*, (2) 28–42. https://doi.org/10.31851/sainmatika.v12i2.989

Chandra, A. T. G.; Jaya, A. M. Aplikasi Metoda Arsitektur Inklusif pada Ruang Ekspresi Seni bagi Penyandang Disabilitas. *J. Sains dan Seni ITS.* **2021**, *10* (2) 2337–3520. https://doi.org/10.12962/j23373520.v10i2.74554

Hamamni, K.; Mukhsim, M.; Siswanto, D. Prototipe Sistem Monitoring Biaya Penggunaan Listrik Pada Rumah Kos Berbasis IoT. *Journal of Application and Science on Electrical Engineering.* **2020**, *1* (2) 100–110. https://doi.org/10.31328/jasee.v1i02.12

Hikmawan, S. R.; Suprayitno, E. A. Rancang Bangun Lampu Penerangan Jalan Umum (Pju) Menggunakan Solar Panel Berbasis Android (Aplikasi Di Jalan Parkiran Kampus 2 Umsida). *Elinvo (Electronics, Informatics, Vocat. Educ.* **2018**, *3* (1) 9–17. https://doi.org/10.21831/elinvo.v3i1.15343

Hutabarat, P. H.; Zambak, M. F.; Suwarno, S. Prediksi Kebutuhan Energi Listrik Wilayah Pln Kota Parapat Simalungun Sampai Tahun 2024. *Journal of Electrical and System Control Engineering.* **2022**, *5* (2) 52–58. https://doi.org/10.31289/jesce.v5i2.5757

Priyarsono, E.; Tambunan, D. S.; Muhammad, M. F. Perkembangan Konsumsi dan Penyediaan Energi dalam Perekonomian Indonesia, *Indones. J. Agric. Econ.* **2010**, *2* (1) 97–119.

Sintiya, D.; Nurmasyitah, N. Pengaruh Bahan Elektroda Terhadap Kelistrikan Jeruk Dan Tomat Sebagai Solusi Energi Alternatif, *J. Pendidik. Fis. dan Sains.* **2019**, *2* (1), 1–6.

Sugiyanto, G.; Fadli, A.; Santi, M. Y. Identification of Black Spot and Equivalent Accident. *ARPN J. Eng. Appl. Sci.* **2017**, *12* (2) 528–535.

Sumanzaya, T.; Supriyanto, A.; Pauzi, G. A. Analisis Karakteristik Elektrik Onggok Singkong sebagai Pasta Bio-Baterai. *J. Teor. dan Apl. Fis.* **2019**, *7* (2) 231–238. https://doi.org/10.23960/jtaf.v7i2.1982

Tanjung, A. F. Pengaruh Variasi Elektroda Terhadap Kelistrikan Bio-baterai Berbahan Dasar Sari Buah Tomat (*Solanum lycopersicum*). Thesis, Universitas Islam Negeri Sumatera Utara, 2021.

Wahid, A.; Junaidi, I.; Arsyad, I. H. M. I. Analisis Kapasitas Dan Kebutuhan Daya Listrik Untuk Menghemat Penggunaan Energi Listrik Di Fakultas Teknik Universitas Tanjungpura, *J. Tek. Elektro UNTAN.* **2014**, *2* (1), 10.

Zulkarnaen, Z.; Lestantyo, D.; Ekawati, E. Faktor-Faktor Yang Berhubungan Dengan Praktik Safety Driving Pada Pengemudi Mobil Skid Tank Di Pt X. *J. Kesehat. Easy.* **2018**, *6* (5) 678–686. https://doi.org/10.14710/jkm.v6i5.22112

ECLÉTICA QUÍMICA

Eclet. Quim. 49 | e-1402, 2024

Original Article

https://doi.org/10.26850/1678-4618.eq.v49.2024.e1402

Determination of parameters and kinetic evaluation for chromium (VI) removal using four resins

Stamber Alvaro **Ramírez-Revilla**[1+], Daniela **Camacho-Valencia**[1], Derly **Ortiz-Romero**[1]

Abstract

This research aimed to identify optimal studied variables for chromium (VI) removal using four resins (IRA 96, IRA 400, DOWEX 1x8, and LEWATIT). A 1,5-diphenylcarbazide method was used for the quantification of chromium (VI). A factorial design with triple replication at the center point was used to evaluate pH, resin dose (g/100 mL), and initial chromium (VI) concentration. The optimal values for the four resins were a pH of 3, a resin concentration of 0.15 g/100 mL of solution, and an initial concentration of 10 mg/L of chromium. Then, an ANOVA study was done to compare the resins results using a p-value <0.05. The DOWEX resin presented the highest removal percentage (98.39%) for a reaction period of 45 minutes, with an exponential model that fits a pseudo-first-order kinetics with a coefficient of determination equal to 0.967.

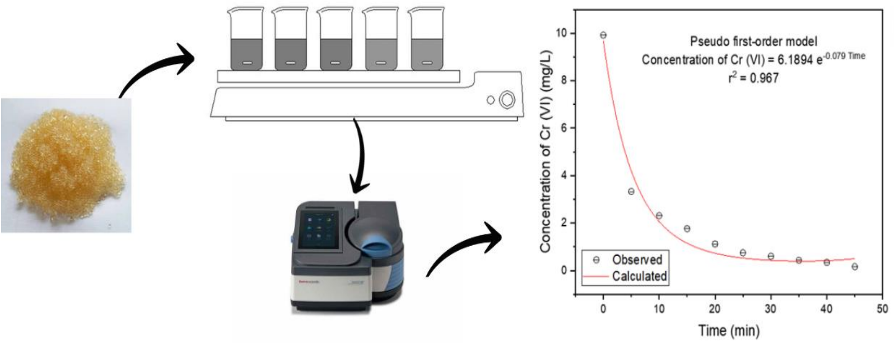

Article History

Received November 11, 2022
Accepted April 24, 2024
Published June 07, 2024

Keywords

1. resins;
2. DOWEX;
3. chromium (VI);
4. pseudo first order;
5. kinetics.

Section Editor

Assis Vicente Benedetti

Highlights

- Dowex resin presented the highest percentage of removal.
- A factorial design with triple replication at the centre point was used.
- The exponential model adjusts to pseudo-first-order kinetics.

[1] Universidad Tecnológica del Perú, Laboratorio de Calidad de Aguas y Medio Ambiente, Arequipa, Perú.

+Corresponding author: Stamber Alvaro Ramírez-Revilla, **Phone:** +51974434314, **Email address:** sramirezr@utp.edu.pe

1. Introduction

Industries such as leather tanning, dyeing and galvanizing release a large amount of untreated chromium-charged water, which constitutes a danger to living beings (Bhatti *et al.*, 2017). Industrial wastewater containing Cr(VI) is a complex threat to the environment (Liu *et al.*, 2015), (Tümer and Edebali, 2019). In these industrial effluents, chromium is present in trivalent and hexavalent forms. The toxicity of each depends on its state of oxidation: it can be carcinogenic, mutagenic and genotoxic (Bhatti *et al.*, 2017; Li *et al.*, 2018). Cr(VI) concentrations in wastewater can range from tenths to hundreds of milligrams per liter (Kahraman and Pehlivan, 2019). There are several methods to reduce chromium concentration in wastewater, such as chemical precipitation (Xie *et al.*, 2017), adsorption (Coşkun *et al.*, 2018), biosorption (Costa, 2017), reverse osmosis (Gaikwad and Balomajumder, 2017), electrocoagulation (Hu *et al.*, 2017), ion exchange (Korak *et al.*, 2017), electrodialysis (Sadyrbaeva, 2016), and photocatalysis (Wang *et al.*, 2016).

Ion exchange is an effective treatment for Cr(VI) removal (Gorman *et al.*, 2016). It has been shown that resins with styrene-divinylbenzene matrix and quaternary ammonium functional groups (Kusku *et al.*, 2014), N-methylglucamine tertiary amine polyamine, and sorption capacity can be used for the efficient removal of hexavalent chromium of wastewater due to their good thermal stability. To optimize the process, several authors use Freundlich and Langmuir isotherms to determine the relationship between the amount of chromium adsorbed by the resin and the concentration of chromium in the solution, together with adsorption kinetics to investigate the mechanism of chromium adsorption (Bajpai *et al.*, 2012; Polowczyk *et al.*, 2016).

This study aims to evaluate different types of ion exchange resins for the adsorption of Cr(VI) in industrial effluents and to determine the efficiency of each. The effect of using each resin, pH and chromium concentration have been studied, as well as the removal kinetics, through direct modelling of the obtained data.

2. Experimental

2.1. Analytical curve preparation

For the quantification of chromium (VI), the standard colorimetric method of 1,5-diphenylcarbazide was used (Pflaum and Howick, 1956) Cr-3500 APHA-AWWA-WEF, using a UV-VIS Genesys 150 spectrophotometer. Analysis grade potassium dichromate obtained from Sigma Aldrich was used as a standard (500 mg/L). The tested concentrations ranged from 0.2 to 1.2 mg/L of chromium (VI), using distilled water for the determinations. Measurements were taken at 540 nm wavelength.

Diphenylcarbazide reacts with Cr(VI) in acidic medium producing the colored complex Cr(III)-diphenylcarbazone **Eq. 1**:

$$2CrO_4^{2-} + 3H_4L + 8H^+ \rightarrow Cr(HL)_2^+ + Cr^{3+} + H_2L + 8H_2O \qquad (1)$$

where, H_4L is 1,5-diphenylcarbazide and H_2L is diphenylcarbazone.

2.2. Experimental design

A factorial design of type 2^2 with triple replication in the central point was configured for each resin in the study. The factors studied were pH, resin concentration (g/100 mL) and initial chromium (VI) concentration. For pH adjustment, concentrated H_2SO_4 and 10% NaOH were used, measuring the entire operation with HANNA HI2211 pH/mV equipment, while all the weighing measurements were performed on a Mettler Toledo ME 204 analytical balance. The factor levels studied are presented in **Table 1**. The experiments were carried out in a pH range of 3 to 5 due to the precipitation of Cr(VI) ions at higher pH. The levels used for resin dosing were set in a range of 0.05 to 0.15 g to optimally evaluate the contact time (Patel *et al.*, 2022), while the Cr(VI) solution concentrations were set in a range where no deviation from Beer's Law is observed.

Table 1. Studied factor levels.

Factor	Low level	Central point	High level
pH	3.00	4.00	5.00
Dose (g/100 mL)	0.05	0.10	0.15
Concentration (mg/L)	10.00	30.00	50.00

2.3. Adsorption experiments

Amberlite IRA 96, Amberlite IRA 400, Dowex 1x8 and Lewatit MP-62, resins were purchased from Sigma Aldrich. For each resin, 7 experiments were configured (4 for the high and low levels, 3 for the central points) following what is indicated in **Table 1**. The experiments were performed in triplicate.

For the determination of the removal percentage, **Eq. 2** was used, where C_0 is the initial concentration and C_f is the final concentration.

$$\text{Remotion } (\%) = \frac{C_0 - C_f}{C_0} \times 100 \qquad (2)$$

2.4. Optimization process

After executing the experimental runs for each resin and identifying the optimal test conditions, five replications were performed for each optimized experiment and an ANOVA was performed to evaluate the existence of significant differences between the resins used in the different experiments.

2.5. Kinetic study

A kinetic study was carried out with the resin that resulted in the highest rate of removal of chromium (VI) in solution. The sampling was carried out by taking 5 mL of solution every 5 minutes until completing 45 min reaction time (total volume 100 mL). The modelling process was carried out using the OriginPro 9.0 software fitting tool.

3. Results and discussion

3.1. Analytical curve

To quantify chromium (VI), a linear regression **Eq. 3** was obtained with a coefficient of determination equal to 0.9997.

$$\text{Absorbance} = 0.7729 * \text{Concentration} \qquad (3)$$

3.2. Adsorption experiments

The results of the different combinations of the factorial design levels are shown in **Tables 2** and **3**. All the experiments were carried out under the same conditions. From **Table 3** it can be inferred that the highest percentage of removal was for the

DOWEX 1x8 resin. To enhance the interaction of resins with Cr(VI), a pH of 3 was chosen to facilitate the contact of H^+ ions with the surface, thus preventing them from becoming negatively charged and consequently reducing their adsorption capacity. On the other hand, low pH prevents the precipitation of Cr(VI), since at high pH, the interaction with OH^- ions favors the negative charge of the resin. Likewise, by increasing the dose of resin and decreasing the concentration of the Cr(VI) solution, an increase in the removal percentage is favored.

Figure 1 presents the Pareto plot for chromium removal. It can be seen that resin concentration, chromium concentration and pH have a significant effect ($p<0.05$) on the removal percentage. In the same way, the double interactions present a significant effect ($p<0.05$).

Table 2. Results obtained from the experimental design for IRA 96 and IRA 400 resins under study.

			IRA 96			IRA 400		
pH	Cc resin (g)	Cc Cr(VI) (mg/L)	Absorbance	Cr final (mg/L)	Cr(VI)% Removal	Absorbance	Cr final (mg/L)	Cr(VI)% Removal
3	0.05	10	0.2677	6.93	30.72	0.2656	6.87	31.27
		50	0.7275	37.65	24.70	0.6219	32.18	35.63
	0.15	10	0.1001	2.59	74.09	0.1099	2.84	71.57
		50	0.4175	21.61	56.79	0.2924	15.13	69.74
4	0.10	30	0.3256	16.85	43.83	0.2759	14.28	52.41
			0.3393	17.56	41.47	0.2723	14.09	53.02
			0.3395	17.57	41.42	0.2719	14.07	53.09
5	0.05	10	0.2859	7.40	26.00	0.2654	6.87	31.33
		50	0.8219	42.54	14.93	0.6691	34.63	30.74
	0.15	10	0.1439	3.73	62.75	0.1147	2.97	70.33
		50	0.6316	32.69	34.62	0.3215	16.64	66.72

Table 3. Results obtained from the experimental design for Dowex and Lewatit resins under study.

			IRA 96			IRA 400		
pH	Cc resin (g)	Cc Cr(VI) (mg/L)	Absorbance	Cr final (mg/L)	Cr(VI)% Removal	Absorbance	Cr final (mg/L)	Cr(VI)% Removal
3	0.05	10	0.1641	4.25	57.54	0.2607	6.75	32.55
		50	0.6527	33.78	32.44	0.6990	36.17	27.65
	0.15	10	0.0336	0.87	91.31	0.1008	2.61	73.93
		50	0.0774	4.00	91.99	0.4300	22.25	55.49
4	0.10	30	0.1304	6.75	77.51	0.4809	24.89	17.04
			0.1352	7.00	76.67	0.4375	22.64	24.52
			0.1251	6.47	78.42	0.4763	24.65	17.84
5	0.05	10	0.1670	4.32	56.80	0.3047	7.88	21.16
		50	0.4278	22.14	55.72	0.8811	45.60	8.80
	0.15	10	0.0355	0.92	90.82	0.1870	4.84	51.61
		50	0.0893	4.62	90.76	0.6581	34.06	31.88

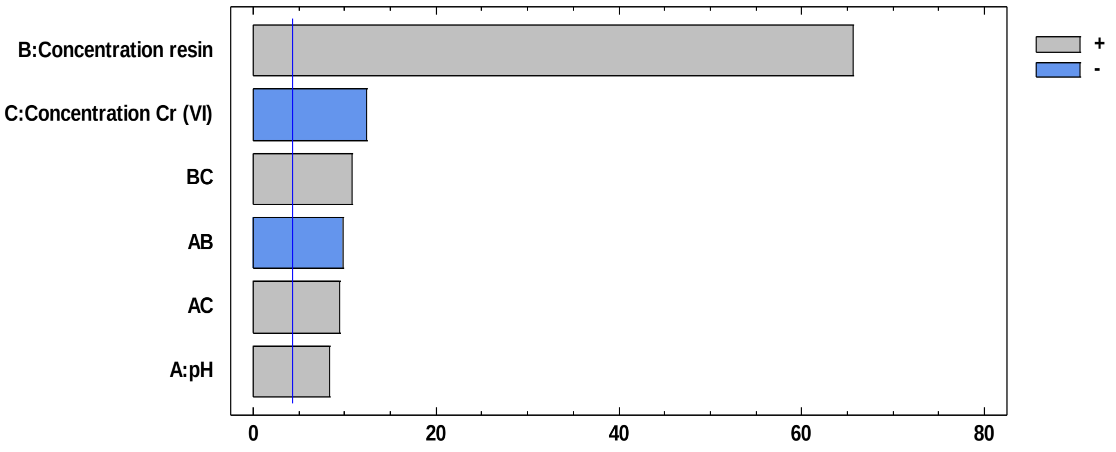

Figure 1. Pareto plot for chromium removal using DOWEX resin.

Figure 2 presents the graph of the main effects where it is observed that as the concentration of the chromium solution increases, the percentage of removal begins to decrease (negative slope). Likewise, as the pH and resin dosage increase, the percentage of removal increases (Patel *et al.*, 2022).

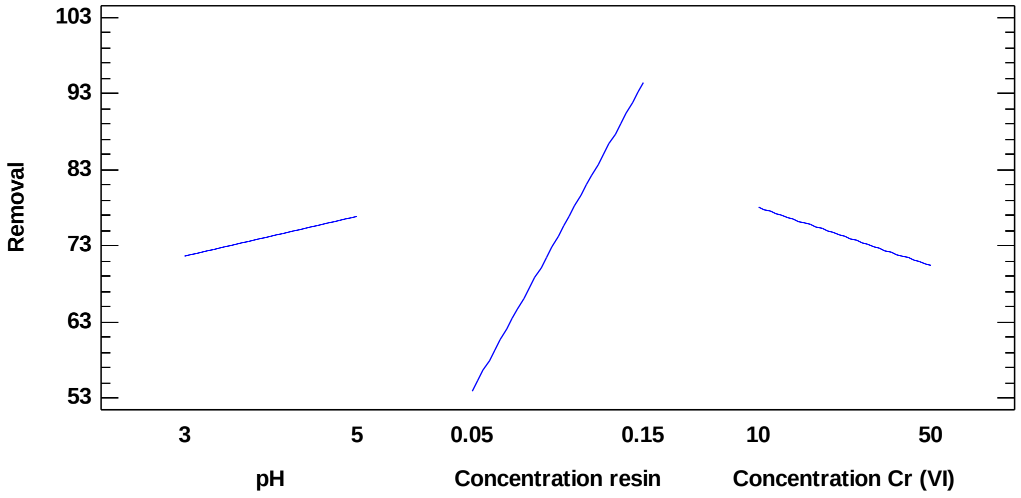

Figure 2. Main effects plot for chromium removal.

3.3. Adsorption studies

Table 4 shows the percentage of chromium removal for each resin in its optimized form. The analysis of variance reports a $p < 0.05$, which indicates a significant statistical difference between the resins under study.

Figure 3 illustrates the box-and-whisker plot for the experiment. The variation of the results for the conditions of each resin is minimal. However, DOWEX resin has the highest chromium (VI) removal percentage (98.40%) from the solution, which is why it could be considered the resin with the most effective chromium decontamination process in different effluent types.

Table 4. Percentage of removal for different resins.

Replicate	IRA 96	IRA 400	DOWEX	LEWATIT
1	84.96	87.28	98.20	76.56
2	84.97	86.83	98.36	75.96
3	84.58	87.17	98.24	75.95
4	84.77	86.75	98.49	76.21
5	84.90	86.72	98.40	75.90

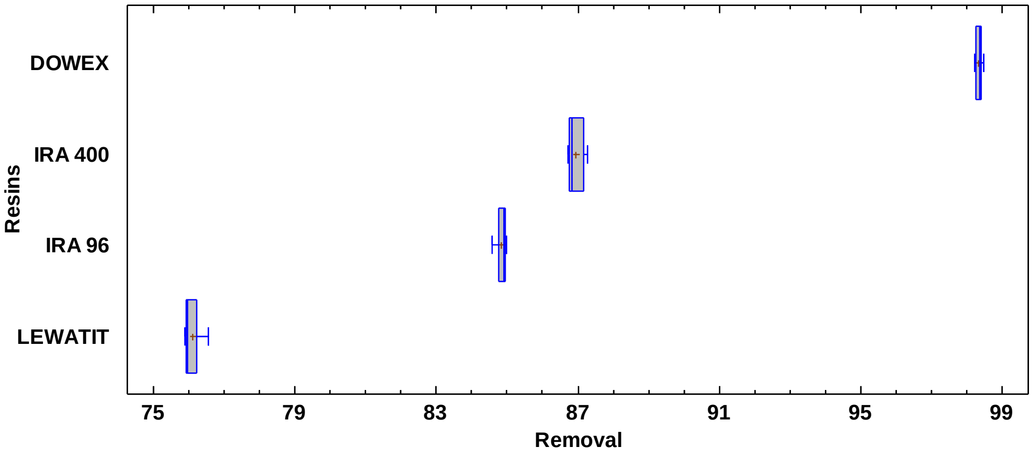

Figure 3. Box-and-whisker plot for chromium removal (%).

To perform the kinetic study, the optimal conditions for working with the DOWEX resin were taken, starting with an aqueous chromium solution of 10 mg/L, taking a sample of 5 mL every 5 min for a period of 45 min. The results are presented in **Table 5**.

Table 5. Removal kinetics data for the DOWEX resin.

Time (min)	Concentration Cr (mg/L)
0	9.92
5	3.33
10	2.31
15	1.76
20	1.12
25	0.75
30	0.60
35	0.43
40	0.34
45	0.16

3.4. Kinetic study

The mathematical model that determines the chromium (VI) adsorption kinetics for DOWEX resin is a pseudo-first-order model (Ok *et al.*, 2014) with an adjusted coefficient of determination of 0.967, a value that explains the variability that the model can estimate. **Equation 4** and **Fig. 4** present the model obtained:

$$\text{Concentration} = 6.1894\text{e}^{-0.079*\text{Time}} \qquad (4)$$

where 6.1894 corresponds to the initial concentration (in mg/L) y 0.079 to the rate constant (in min^{-1}).

In the **Fig. 4** it is observed that around the first 5 min there is a rapid removal of chromium (VI), which is usually found under the forms of $HCrO_4^-$ and $Cr_2O_7^{2-}$, them it slows down after 10 min as pointed out by Xing *et al.* (2022) and Ok *et al.* (2014).

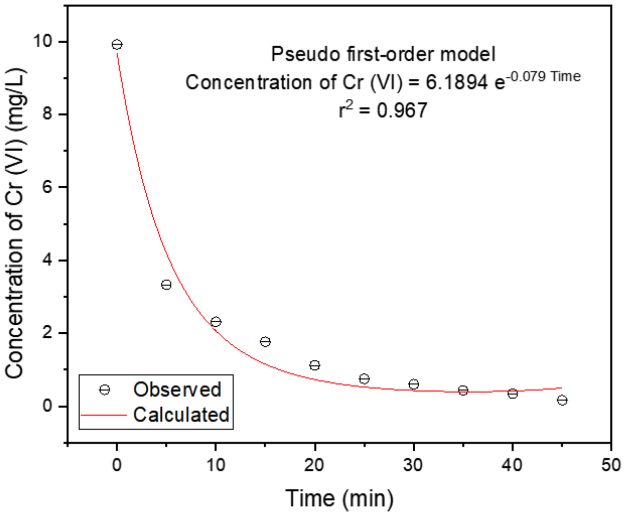

Figure 4. Adsorption kinetics for DOWEX resin.

Research has shown that pH, temperature, resin dose, contact time and initial chromium (VI) concentration are all significant factors in the chromium (VI) adsorption process, using Freundlich, Langmuir and Scatchard adsorption isotherms (Kahraman and Pehlivan, 2019). In this research study, the influence of pH, resin dose and initial chromium (VI) concentration were studied by direct modelling of the data, identifying an exponential model. The direct adaptation of data to mathematical models has been developing increasingly since it allows a clear appreciation of the adsorption behavior (Gaikwad and Balomajumder, 2017).

On the other hand, (Hashem *et al.*, 2018) have reported bioremediation processes for chromium (VI) removal using *Syzygium cumini* bark as an adsorbent, achieving removal rates of 99.9% in 15 min using 3 g of adsorbent. In this study, using DOWEX resin, a removal of 98.39% was obtained in 45 min of reaction time using only 0.15 g of resin with an initial chromium concentration of 10 mg/L.

4. Conclusions

An analytical technique using visible ultraviolet spectroscopy was used to quantify chromium, identifying DOWEX resin as the most appropriate to remove chromium in solution, achieving 98.39% effectiveness when working at a pH of 3 with a dose of 0.15 g/100 mL and an initial chromium (VI) concentration of 10 mg/L in solution. The equation found corresponds to an exponential model that fits a pseudo-first-order kinetics with a coefficient of determination of 0.967 registering a velocity constant equal to 0.079 min^{-1}.

Authors' contributions

Conceptualization: Ramirez-Revilla, S. A.; Ortiz-Romero, D.; **Data curation:** Ramirez-Revilla, S. A.; Ortiz-Romero, D.; **Formal Analysis:** Ramirez-Revilla, S. A.; Camacho-Valencia, D.; Ortiz-Romero, D.; **Funding acquisition:** Not applicable; **Investigation:** Ramirez-Revilla, S. A.; Camacho-Valencia, D.; Ortiz-Romero, D.; **Methodology:** Ramirez-Revilla, S. A.; Ortiz-Romero, D.; **Project administration:** Ramirez-Revilla, S. A.; Ortiz-Romero, D.; **Resources:** Ramirez-Revilla, S. A.; Ortiz-Romero, D.; **Software:** Not applicable; **Supervision:** Ramirez-Revilla, S. A.; Ortiz-Romero, D.; **Validation:** Ramirez-Revilla, S. A.; Ortiz-Romero, D.; **Visualization:** Ramirez-Revilla, S. A.; Ortiz-Romero, D.; **Writing – original draft:** Ramirez-Revilla, S. A.; Camacho-Valencia, D.; Ortiz-Romero, D.; **Writing – review & editing:** Ramirez-Revilla, S. A.; Camacho-Valencia, D.; Ortiz-Romero, D.;

Data availability statement

All data sets were generated or analyzed in the current study.

Funding

Not applicable.

Acknowledgments

Not applicable.

References

Bajpai, S.; Dey, A.; Jha, M. K.; Gupta, S. K.; Gupta, A. Removal of hazardous hexavalent chromium from aqueous solution using divinylbenzene copolymer resin. *Int. J. Environ. Sci. Technol.* **2012**, *9* (4), 683–690. https://doi.org/10.1007/s13762-012-0099-6

Bhatti, A. A.; Memon, S.; Memon, N.; Bhatti, A. A.; Solangi, I. B. Evaluation of chromium(VI) sorption efficiency of modified Amberlite XAD-4 resin. *Arab. J. Chem.* **2017**, *10* (Suppl. 1), S1111–S1118. https://doi.org/10.1016/j.arabjc.2013.01.020

Coşkun, R.; Er, E.; Delibaş, A. Synthesis of novel resin containing carbamothiolylimidamide group and application for Cr(VI) removal. *Polym. Bull.* **2018**, *75* (3), 963–983. https://doi.org/10.1007/s00289-017-2068-1

Costa, A. W. M. C. Produção de biossorvente magnetizado à base de biopolímeros do tipo polissacarídeo, para remoção de cromo (VI) de efluentes industriais. Tese (Doutorado em Biotecnologia), Universidade Federal de Sergipe, São Cristóvão, SE, 2017.

Gaikwad, M. S.; Balomajumder, C. Simultaneous rejection of fluoride and Cr(VI) from synthetic fluoride-Cr(VI) binary water system by polyamide flat sheet reverse osmosis membrane and prediction of membrane performance by CFSK and CFSD models. *J. Mol. Liq.* **2017**, *234*, 194–200. https://doi.org/10.1016/j.molliq.2017.03.073

Gorman, C.; Seidel, C.; Henrie, T.; Huang, L.; Thompson, R. Pilot Testing Strong Base Anion Exchange for CrVI Removal. *Journal AWWA*, **2016**, *108* (4), E240–E246. https://doi.org/10.5942/jawwa.2016.108.0028

Hashem, A.; Momen, A.; Hasan, M.; Nur-A-Tomal, S.; Sheikh, H. R. Chromium removal from tannery wastewater using Syzygium cumini bark adsorbent. *Int. J. Environ. Sci. Technol.* **2018**, *16*, 1395–1404. https://doi.org/10.1007/s13762-018-1714-y

Hu, S.; Li, D.; Huang, C.; Sun, D.; Yuan, X. A continuous electrocoagulation system with pH auto-adjusting by endogenous products to treat Cr(VI)-contaminated soil flushing solution. *Sep. Purif. Technol.* **2017**, *189*, 213–219. https://doi.org/10.1016/j.seppur.2017.07.081

Kahraman, H. T.; Pehlivan, E. Evaluation of anion-exchange resins on the removal of Cr(VI) polluted water: Batch ion-exchange modeling. *Arab. J. Geosci.* **2019**, *12*, 532. https://doi.org/10.1007/s12517-019-4677-5

Korak, J. A.; Huggins, R.; Arias-Paic, M. Regeneration of pilot-scale ion exchange columns for hexavalent chromium removal. *Water Res.* **2017**, *118*, 141–151. https://doi.org/10.1016/j.watres.2017.03.018

Kusku, O.; Rivas, B. L.; Urbano, B. F.; Arda, M.; Kabay, N.; Bryjak, M. A comparative study of removal of Cr(VI) by ion exchange resins bearing quaternary ammonium groups. *J. Chem. Technol. Biotechnol.* **2014**, *89* (6), 851–857. https://doi.org/10.1002/jctb.4320

Li, X.; Shi, S.; Cao, H.; Li, Y.; Xu, D. Comparative Study of Chromium(VI) Removal from Simulated Industrial Wastewater with Ion Exchange Resins. *Russ. J. Phys. Chem. A.* **2018**, *92*, 1229–1236. https://doi.org/10.1134/S0036024418060237

Liu, X.; Li, Y.; Wang, C.; Ji, M. Cr(VI) removal by a new type of anion exchange resin DEX-Cr: Adsorption affecting factors, isotherms, kinetics, and desorption regeneration. *Environ. Prog. Sustain. Energy*. **2015**, *34* (2), 387–393. https://doi.org/10.1002/ep.11998

Ok, Y. S.; Jeon, C. Selective adsorption of the gold–cyanide complex from waste rinse water using Dowex 21K XLT resin. *J. Ind. Eng. Chem.* **2014**, *20* (4), 1308–1312. https://doi.org/10.1016/j.jiec.2013.07.010

Patel, P. K.; Nagireddi, S.; Uppaluri, R. V. S.; Pandey, L. M. Batch adsorption characteristics of Dowex Marathon MSA commercial resin for Au(III) removal from synthetic electroless plating solutions. *Mater. Today. Proc.* **2022**, *68* (4), 824–829. https://doi.org/10.1016/j.matpr.2022.06.258

Pflaum, R. T.; Howick, L. C. The Chromium-Diphenylcarbazide Reaction. *J. Am. Chem. Soc.* **1956**, *78*, 4862–4866. https://doi.org/10.1021/ja01600a014

Polowczyk, I.; Urbano, B. F.; Rivas, B. L.; Bryjak, M.; Kabay, N. Equilibrium and kinetic study of chromium sorption on resins with quaternary ammonium and N-methyl-d-glucamine groups. *Chem. Eng. J.* **2016**, *284*, 395–404. https://doi.org/10.1016/j.cej.2015.09.018

Sadyrbaeva, T. Z. Removal of chromium (VI) from aqueous solutions using a novel hybrid liquid membrane—Electrodialysis process. *Chem. Eng. Process.: Process Intensif.* **2016**, *99*, 183–191. https://doi.org/10.1016/j.cep.2015.07.011

Tümer, A. E.; Edebali, S. Artificial Neural Network Approach for Modeling of Cr(VI) Adsorption from Waste Water by Lewatit MP64 and Dowex 1×8. 2019 IEEE 7th Palestinian International Conference on Electrical and Computer Engineering (PICECE), Gaza, Palestine, 2019. https://doi.org/10.1109/PICECE.2019.8747199

Wang, C.-C.; Du, X.-D.; Li, J.; Guo, X.-X.; Wang, P.; Zhang, J. Photocatalytic Cr(VI) reduction in metal-organic frameworks: A mini-review. *Appl. Catal. B: Environ.* **2016**, *193*, 198–216. https://doi.org/10.1016/j.apcatb.2016.04.030

Xie, B.; Shan, C.; Xu, Z.; Li, X.; Zhang, X.; Chen, J.; Pan, B. One-step removal of Cr(VI) at alkaline pH by UV/sulfite process: Reduction to Cr(III) and in situ Cr(III) precipitation. *Chem. Eng. J.* **2017**, *308*, 791–797. https://doi.org/10.1016/j.cej.2016.09.123

Xing, X.; Alharbi, N. S.; Ren, X.; Chen, C. A comprehensive review on emerging natural and tailored materials for chromium-contaminated water treatment and environmental remediation. *J. Environ. Chem. Eng*. **2022**, *10* (2), 107325. https://doi.org/10.1016/j.jece.2022.107325

Eclet. Quim. **49** | e-1524, 2024

Original Article, Education in Chemistry and Correlated Areas

https://doi.org/10.26850/1678-4618.eq.v49.2024.e1524

Quantum chemistry in public higher education institutions in the Brazilian state of Piauí: an analysis of the perceptions of undergraduate chemistry students

Luís Miguel Pinheiro de **Sousa**[1], Kariny Mery Araujo **Cunha**[1], Luciana Nobre de Abreu **Ferreira**[2], Alexandre Araujo de **Souza**[2+]

Abstract

Quantum chemistry is a challenging required course in undergraduate chemistry. Despite its unconventional concepts, it is crucial for understanding modern chemistry. This study investigated how students perceive certain topics and the learning process. Interviews were conducted using a Likert scale questionnaire and sixteen content-specific questions. Some responses differed from the existing literature, such as students' interpretations of the nature of light. In terms of learning, students acknowledged that the topic was complex due to the lack of mathematical foundations and the elevated level of abstraction. Students were primarily seeking the average grade required for admission. The data underscore the need for a deeper discussion of curriculum development and implementation. The curriculum matrix revision could provide space for more substantive thinking about content delivery and assessment processes.

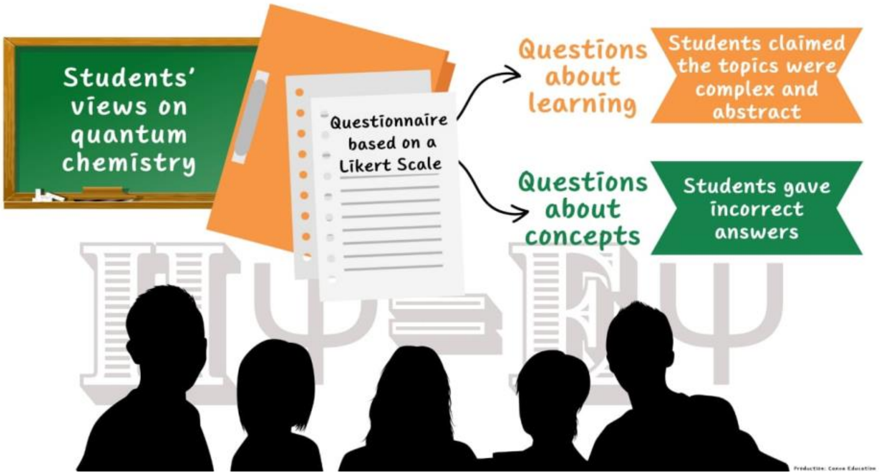

Article History

Received October 05, 2023
Accepted April 02, 2024
Published June 12, 2024

Keywords

1. chemistry education;
2. higher education;
3. quantum chemistry.

Section Editor

Assis Vicente Benedetti

Highlights

- Unconventional concepts challenge students.
- Lack of math background hinders learning.
- Light-nature misconceptions exist.
- Students prioritize grades over understanding.
- Curriculum needs revision for clarity.

[1]Federal University of Piauí, Chemistry Graduate Program, Teresina, Brazil. [2]Federal University of Piauí, Department of Chemistry, Teresina, Brazil.

+Corresponding author: Alexandre Araujo de Souza, **Phone:** +558632155840, **Email address:** alesouza@ufpi.edu.br

ISSN 1678-4618

1. Introduction

Quantum mechanics is one of the most important fundamental theories and one of the pillars of modern and contemporary physics. It emerged and consolidated during the great revolution that took place in physics in the first three decades of the 20th century, based on the need to explain the behavior of submicroscopic systems such as electrons, atoms, and molecules. Classical physics, which includes Newtonian mechanics and Maxwell's classical electromagnetism, proved inadequate to describe such systems. The foundations of quantum mechanics lie in the ideas of energy quantization by Max Planck (1858-1947), the quantum of electromagnetic radiation (photon) by Albert Einstein (1879-1955), the Bohr model of the atom by Niels Bohr (1855-1962), the wave-particle duality by Louis de Broglie (1892-1987), the uncertainty principle by Werner Heisenberg (1901-1976), the statistical interpretation of the wave function by Max Born (1882-1970), the spin-statistics theorem and the Pauli exclusion principle by Wolfgang Pauli (1900-1958), and many others. Currently, quantum mechanics is considered the fundamental physical theory that explains chemical phenomena at the atomic and molecular levels and is essential for discussing the behavior of matter. The application of quantum mechanics in chemistry is called quantum chemistry and is based on Erwin Schrödinger's (1887-1961) equation to determine the wave functions and energies of atoms and molecules. In this way, it becomes possible to predict atomic and molecular structures and spectra, molecular dipole moments, transition states of chemical reactions, thermodynamic properties, etc. Quantum chemistry is practiced with the help of computers using special computational programs and is called computational chemistry. People who have contributed significantly to the development of quantum and computational chemistry includes Douglas Hartree (1897-1958), Erich Hückel (1896-1980), Friedrich Hund (1896-1997), John Pople (1925-2004), Linus Pauling (1901-1994), Robert Mulliken (1896-1986), Vladimir Fock (1898-1974), and Walter Kohn (1923-2016) (Levine, 2014).

Quantum chemistry is a fundamental part of the content covered in an undergraduate or graduate chemistry course. However, most chemistry students have great difficulty understanding the concepts covered in undergraduate courses. This difficulty can be partly attributed to the technical teaching model, characterized by repetition procedures in which the teacher is the owner of the knowledge, and the student does not participate in the teaching-learning process (Libâneo and Pimenta, 1999; Saviani, 2011), and which, although it was overtaken decades ago by other pedagogical theories, is still widely used in teacher education today (Alberto *et al.*, 2020). These difficulties may also be related to deficits in the process of science education resulting from initial conceptions about the structure and understanding of scientific thinking that run throughout the educational process of students and often accompany them until postgraduate studies (Chassot, 2014). Looking specifically at the panorama of undergraduate chemistry courses, the need for a solid mathematical foundation, combined with the elevated level of abstraction of the subject and other factors such as the lack of more efficient teaching methods, leads to a high failure rate in this course, according to Belo *et al.* (2019). As noted by Gregório *et al.* (2019), these claims occur more frequently in undergraduates such as General Chemistry, Inorganic Chemistry, and Physical Chemistry, leading to a discrepancy between the number of first-year students and the number of students who drop out in the first semesters. All these cumulative factors imply a large obstacle to the understanding of topics related to quantum chemistry compared to the first theories of chemical thinking, which do not allow the construction of knowledge using the previously mentioned methods (Costa and Souza, 2017). To overcome these deficiencies, different methods can be applied to improve the relationship between teaching and learning in quantum chemistry, but it is necessary to perform a deeper analysis of the causes of this problem. In the present work, we have tried to identify learning problems related to the content of the subject quantum chemistry, based on the perceptions of students in undergraduate chemistry courses in three public universities in a state in northeastern Brazil.

2. Experimental

This work is conceived as a quantitative study, since it attempts to quantify the modalities of information gathering, and as qualitative research, which allows us to adequately interpret the nature of a social phenomenon (Beuren, 2006). To achieve the above objectives, a literature search on this topic was first conducted to obtain a solid theoretical foundation. The search initially focused on listing the topics considered fundamental to the understanding of quantum chemistry and looked for specific books in the field intended for higher education and cited in the paper. Then, the curricula for the subject of quantum chemistry from two of the three universities that participated in the study were analyzed, considering that the specific subject of quantum chemistry is not part of the compulsory curriculum at one of the universities. A sample for the interview was then conducted, consisting of students in the final phase of their undergraduate studies in chemistry at universities in a state in northeastern Brazil. The following procedure was used to select the students: the coordinators of every institution were requested to compile a roster of students currently enrolled in the 7th semester or beyond of their respective courses. From this pool, a random selection of 10 students was made. Following this selection process, each chosen student was contacted via telephone and provided with a concise overview of the research aims and methodology, subsequently extending an invitation to participate in the study.

Only 9 students were eligible to participate in the study in two of the three institutions, for a total of 28 students. Concerning the study's qualitative aspect, interviews were conducted with the participants. Both recruitment and interviews took place remotely, via the online platform Google Meet, due to the social isolation caused by the COVID-19 pandemic. In the interviews (all of which were recorded), after an appropriate introduction to the project, a Likert-scale questionnaire was used, based on a series of statements about the topic discussed, in which the respondent indicates the extent to which he or she agrees on a 5-point scale: disagree; partially disagree; undecided; partially agree; agree (Silva Júnior and Costa, 2014). At this point, the interviewer read the questions on a shared screen during an online session, and the respondent answered according to his or her point of view. After the participant indicated the extent to which he or she agreed with each statement, a brief discussion took place on the topic addressed, during which respondents were free to express themselves without interference from the interviewer. The discussions began with two questions designed to stimulate the respondents' thinking: "Do you have anything to say about this topic?" and "How would you justify your choice?"

The interview was used as a data collection method because it can more clearly capture issues of subjectivity due to the greater freedom and expressiveness of the participant (Batista *et al.*, 2017) and also because it is qualitative research. Regarding ethical procedures, the standards established by the Comitê de Ética em Pesquisa (CEP) of the Universidade Federal do Piauí (UFPI) were followed, through the Brazillian government website Plataforma Brasil (https://plataformabrasil.saude.gov.br/), whose opinion was approved for the conduct of the study. Considering the protocols established by the agency, all interviews were also approved by the respective heads of the institutions. Finally, the data were analyzed considering the division between the statements in the questionnaire, which are presented below:

- **Specific thematic topics:** The answers to the specific statements were compared with the concepts of quantum chemistry contained in the literature, which will be presented later in the paper. The questions where the answers differed the most from those expected were selected for discussion because the concepts related to quantum chemistry are predetermined and provide less room for subjectivity in the answers.
- **Pedagogically oriented topics:** The responses to the statements related to student learning were all discussed because they had a higher degree of subjectivity. They were analyzed in light of ideas from previous work that were raised in the discussion.

In both cases, the percentage of responses from each higher education institution was presented in a grouped bar graph, with each grouping represented by an alternative indicating the level of agreement and each column representing a higher education institution.

3. Results and discussion

This work is the result of interviews conducted with fourth-year chemistry students at three public higher education institutions (HEI) in the state of Piauí, northeastern Brazil. The HEI were labelled A, B, and C to avoid revealing their identities. Only B does not offer quantum chemistry as a compulsory subject in the chemistry curriculum. The analysis of the results had two foci: **(1)** the analysis of the items related to the specific topics of the subject and **(2)** the analysis of the items related to learning. To find out how HEI addresses the subject of quantum chemistry, they were characterized based on the following criteria: **(I)** subject-specific offering; **(II)** module in which it is offered; **(III)** workload; **(IV)** methodology; and **(V)** resources. Sources for this information are available the institutional website and the subject plan (UFPI, 2022).

When analyzing the two topic plans for quantum chemistry provided by the universities, it was found that both have the following contents in common: **(a)** basic concepts of quantum mechanics; **(b)** free/confined particles; **(c)** harmonic oscillator; **(d)** rigid rotor; **(e)** Schrödinger equation; **(f)** concepts of spectroscopy. All these topics appear in books on quantum chemistry and are also mentioned in the topic plans as bibliographies and supplementary materials (the data will be available upon request). When analyzing the interviews, it is interesting to mention that the questionnaire consisted of 16 statements. Generic names are used to preserve the identity of the students surveyed and their respective institutions. As for the presentation of the results, the selected items were presented in the form of grouped bar graphs, considering the individual responses of each institution, in addition to a calculation of the general percentage of respondents. The questionnaire was organized as follows: a total of 10 questions related to the specific topics of quantum chemistry, with correct and incorrect statements based on concepts of quantum mechanics, such as the nature of light, molecular orbitals and their applications; and a total of 6 questions related to the teaching and learning process of quantum chemistry, based on the main learning problems in chemistry, such as the difficulty of understanding mathematical formalisms, the high degree of abstraction, and others.

3.1. Items related to the specific topics

Considering the structure of the questionnaire based on the Likert scale (Silva Júnior and Costa, 2014), where the first ten items were related to the specific contents of quantum chemistry, the first step was to compare the participants' answers with those expected in the literature. The questionnaire was structured so that the first questions covered basic topics such as the dualistic nature of light and the photoelectric effect, while the complexity of the topics gradually increased. Five questions (3, 5, 8, 9, and 10) were selected for discussion, considering discrepancies and conflicts between respondents' answers and those expected based on the literature.

The first highlight of the respondents' answers relates to statement 3 (**Fig. 1**): "When a beam of light of a certain frequency strikes a metal, electrons are ejected from the surface with a kinetic energy proportional to the intensity of the light". This statement refers to the photoelectric effect and is false since electrons are ejected with kinetic energy regardless of the intensity of the incident light. According to the photon model presented by Albert Einstein in 1905, light consists of particles called photons whose energy E is proportional to the frequency, ν of light, according to the equation $E = h\nu$, where h is Planck's constant. Each incident photon exchanges energy with an electron, which overcomes the potential energy (work function, ω of the metal) that binds it to the surface and detaches from the surface with kinetic energy, K, following the conservation of energy, $K = E - \omega$. (Halliday and Resnick, 2014) This mechanism is fundamental to understanding the quantization of energy, which is paramount in today's discussion of chemistry. Therefore, students must be expected to understand it in quantum chemistry. However, as can be seen in **Fig. 1**, only 8% of respondents disagreed to some extent with statement 3 of the questionnaire, leaving a total of 92% (among those who agree to some extent or declare themselves undecided, like the majority) with no real idea that it is one of the most elementary principles of quantum mechanics, although it is covered at school and in undergraduate subjects such as general chemistry, quantum chemistry, and others. It is also interesting that the few students who disagree with the statement in some aspects belong to Institution C and do so with vehemence.

This difficulty in understanding the nature of light is confirmed by Coelho and Borges (2010) when they conducted a specific analysis of this topic at the beginning of high school. Even after the presentation of current concepts regarding the dualistic nature of light (wave-particle duality) and its interaction with matter, a considerable proportion of students remain with misconceptions that contain elements of errors derived from already disproven concepts or adaptations of quantum theory. This suggests that attempts are made to integrate new concepts that conflict with those already present through a process known as balancing (Piaget, 1977 cited in Mortimer, 2000), but this does not necessarily apply to the specific case. This is because on certain occasions it is necessary to abandon old ideas and make a radical paradigm shift (Mortimer, 2000).

Other problems related to the difficulty of understanding the dualistic nature of light, according to Henriksen *et al.* (2018), are the abstract nature of the concept, the lack of practical experience, and cognitive limitations. About these aspects, the author highlights that it is precisely the lack of a deterministic perspective of quantum knowledge, which is associated with uncertainty and probability, which tends to hinder the construction of new knowledge. This encounters a cognitive limitation on the part of the students, cemented by the previous study of classical physics, which much more often offers some aspects to which the students are more accustomed, such as exact values, macroscopic experimental demonstrations, and simpler mathematical applications.

One can better understand these difficulties by taking the perspective of the student who learns in elementary and high school to relate subatomic particles to spheres (which have a predictable and predictable trajectory in a macroscopic universe), and the principles of wave motion based on wavelength, frequency, intensity, amplitude, and other concepts. The difficulties become clear when one understands that quantum physics combines all these aspects and creates a new body of knowledge without necessarily invalidating earlier ideas.

Another remarkable result relates to statement 5 of the questionnaire (**Fig. 2**): "Molecular orbitals can be found using Newton's laws of mechanics". This is another deliberately false statement about the possibility of finding molecular orbitals using Newton's laws of classical mechanics. Orbitals are wavefunctions, abstract quantum entities that cannot be determined with the formalism of Newtonian mechanics, but only with the Schrödinger equation. However, as shown in **Fig. 2**, only 25% of the respondents disagreed with this statement and about 40% declared themselves undecided. This result shows that most students do not understand the quantum nature of atomic and molecular orbitals. This is one of the most important topics in chemistry, essential for understanding bonding and chemical reactions. However, it is important to highlight the fact that more than half of the Institution C students disagree with the concept in some way, indicating a greater knowledge of the topic addressed.

Although it is a subject that contains mathematical formalisms, as does much of quantum mechanics, it is well known that classical mechanics reaches its limits when trying to explain quantum phenomena, and some students show that they are not aware of this fact: "I agree, I think Newton's laws (sic) have a big impact on explaining orbitals" (Student 1, Institution A).

Several aspects can be seen in Student 1's statement that indicate that the student finds it difficult to comment on what was being discussed at the time of the interview. The first point to discuss in this context is the apparent difficulty in expressing oneself on the topic, as the speech is disjointed and not fluent, and also superficial explanations of the topic are used (Pereira *et al.* 2006). When Newton's laws are cited to justify the choice of answer, an attempt is made to support the explanation with an argumentative strategy known as the argument from authority (from the Latin *argumentum ad verecundiam*), in which a person of notable authority on a particular topic is used to lend validity to an argument (Woods and Walton, 1974). The problem is that Isaac Newton, despite his immense contribution to science, especially physics, did not publish a single paper on the subject of quantum mechanics, as he died in 1727 and the first ideas of this new branch of physics did not appear until the beginning of the 20th century.

In connection with the previous statement, we can now discuss statement 9 (**Fig. 3**): "The molecular orbitals (MO's) are obtained by linear combinations of atomic orbitals (AO's). The number of MO's is equal to half the total number of AO's." This statement has a specific error in the number of molecular orbitals formed, which must be equal to the number of atomic orbitals. Nevertheless, slightly more than 46% of the students reported being undecided and 25% agreed with the statement, as you can see in **Fig. 3**.

It can be highlighted that Institution B performs slightly better, as most respondents disagree with this statement to some extent and also have the lowest number of undecided respondents. However, the indecision of a considerable proportion of respondents on statements 5 and 9, which involve in-depth knowledge of covalent bonds, suggests a relationship with respondents' preference for more elementary concepts taught in undergraduate and introductory courses such as General Chemistry (Fernandes, 2019). This directly affects the understanding of more complex concepts because, according to Bouayad *et al.* (2014), concepts such as atomic orbitals, valence bond and molecular orbital theories, and hybridization are not fully mastered by students because a mathematical formalism and a high level of abstraction are required to understand topics that have no obvious connection to the empirical knowledge used as reference.

We continue the analysis and now focus on statement 8 (**Fig. 4**): "The harmonic oscillator model can, after appropriate adjustments, be used to explain infrared spectra". This is a true statement about the theoretical model used to explain the absorption of infrared light energy by molecular vibrational modes (bendings, stretchings, etc.). This is the process that occurs in infrared spectroscopy, a technique used (in conjunction with other techniques such as NMR spectroscopy) to elucidate molecular structure (Pavia *et al.* 2013). The harmonic oscillator, based on Hooke's law, is one of the most widely used physical models in the exact sciences and has applications in various fields such as engineering, physics, geology, and chemistry. Any oscillatory phenomenon with low amplitude can be explained with this model (Nussenzveig, 2014). In quantum mechanics, the harmonic oscillator model is obtained by solving the Schrödinger equation exactly, which gives its energy levels and the corresponding quantum states (Levine, 2014).

However, as can be seen in **Fig. 4**, about 89% of the respondents answered "undecided", revealing their ignorance of one of the most fundamental topics in undergraduate studies. The fact that Institution B does not offer quantum chemistry as a compulsory subject could serve as a justification for this statement. However, the high number of undecided students at the three universities prompts us to reflect on the influence of the subject on students' actual knowledge.

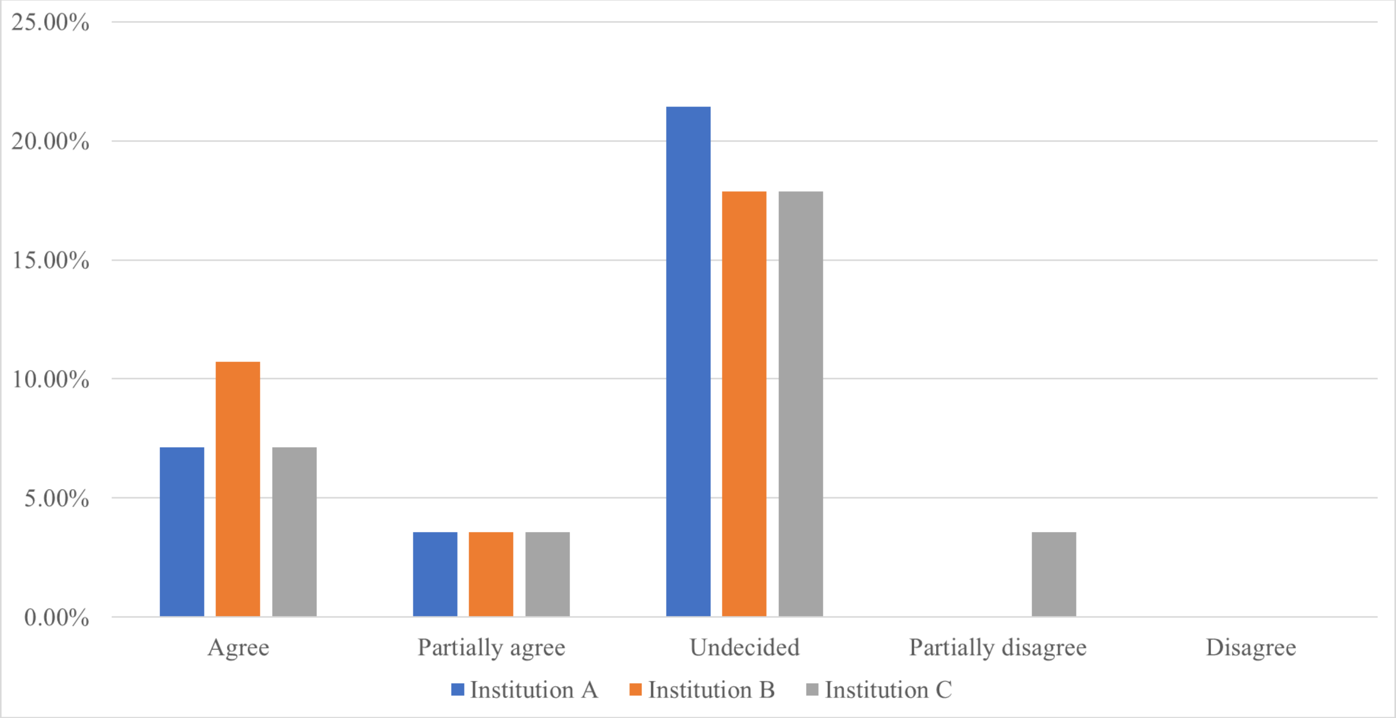

Figure 1. Answering the profile of participants in statement 3.

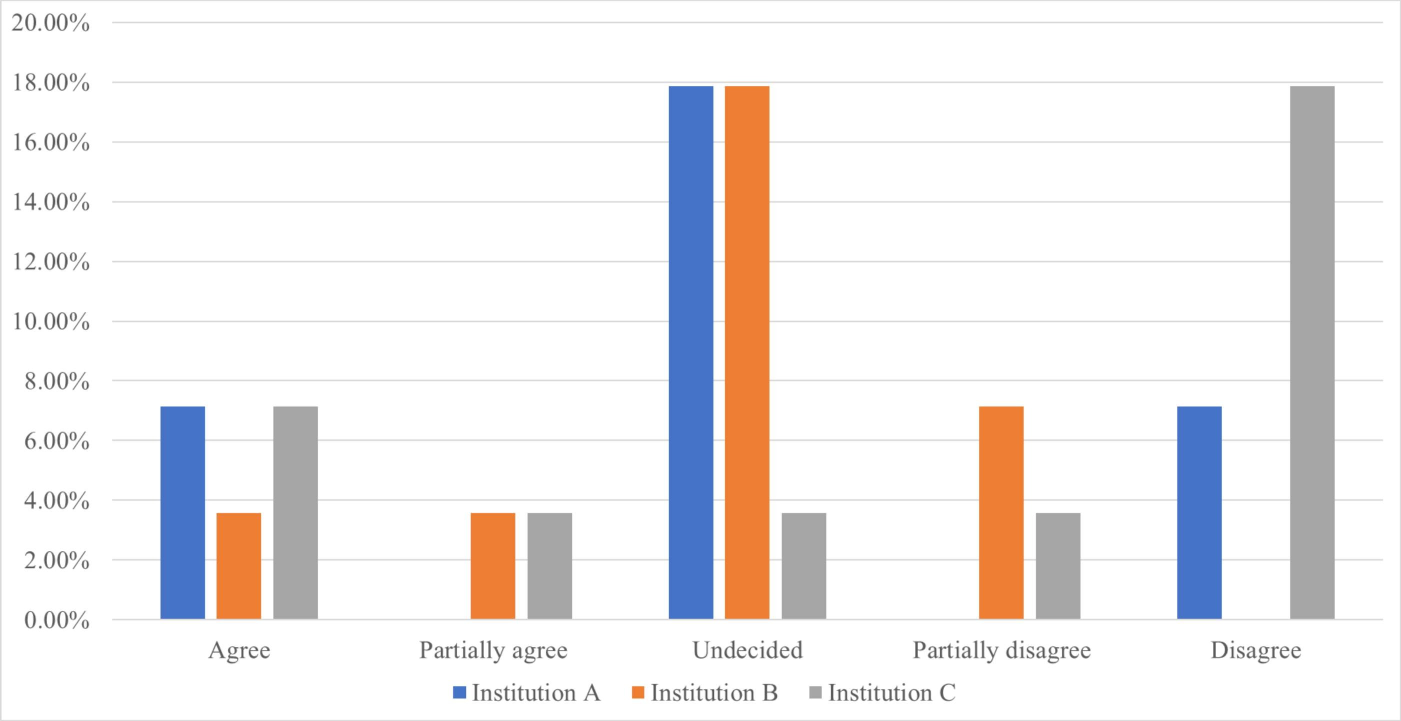

Figure 2. Answering the profile of participants in statement 5.

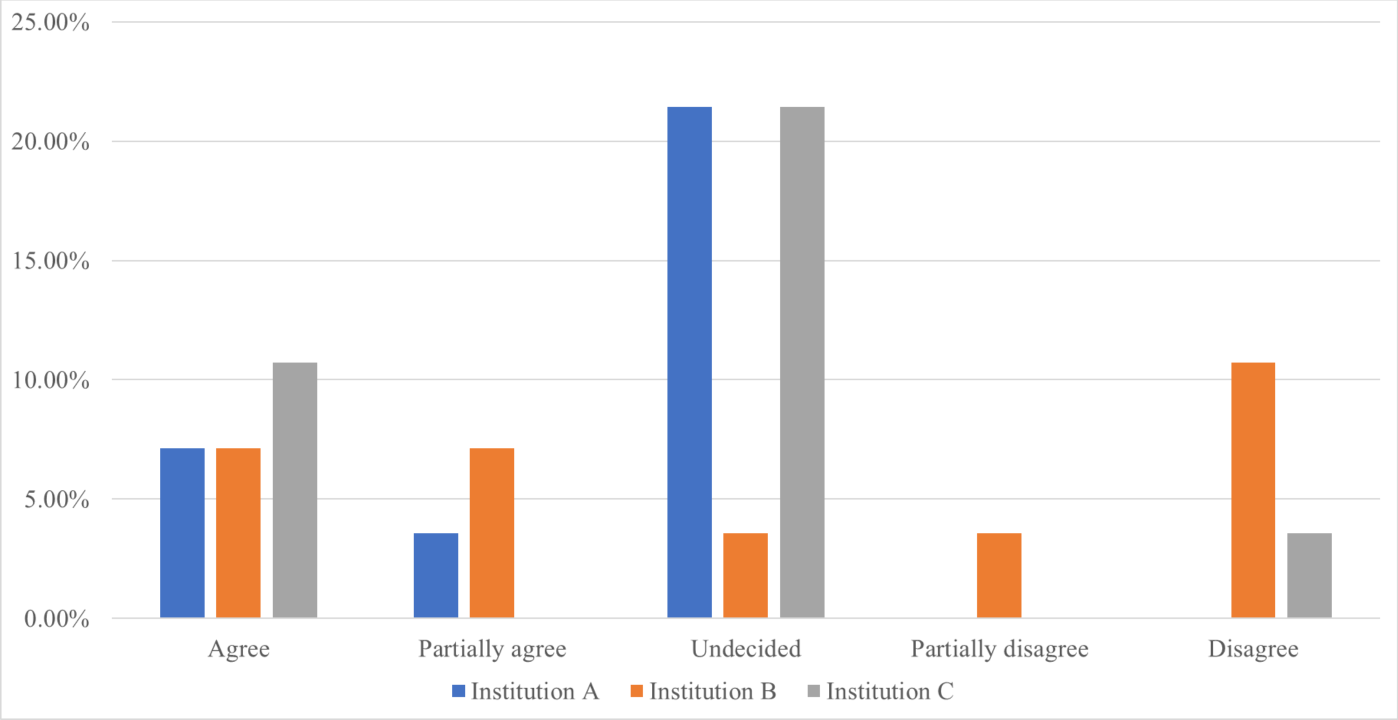

Figure 3. Answering the profile of participants in statement 9.

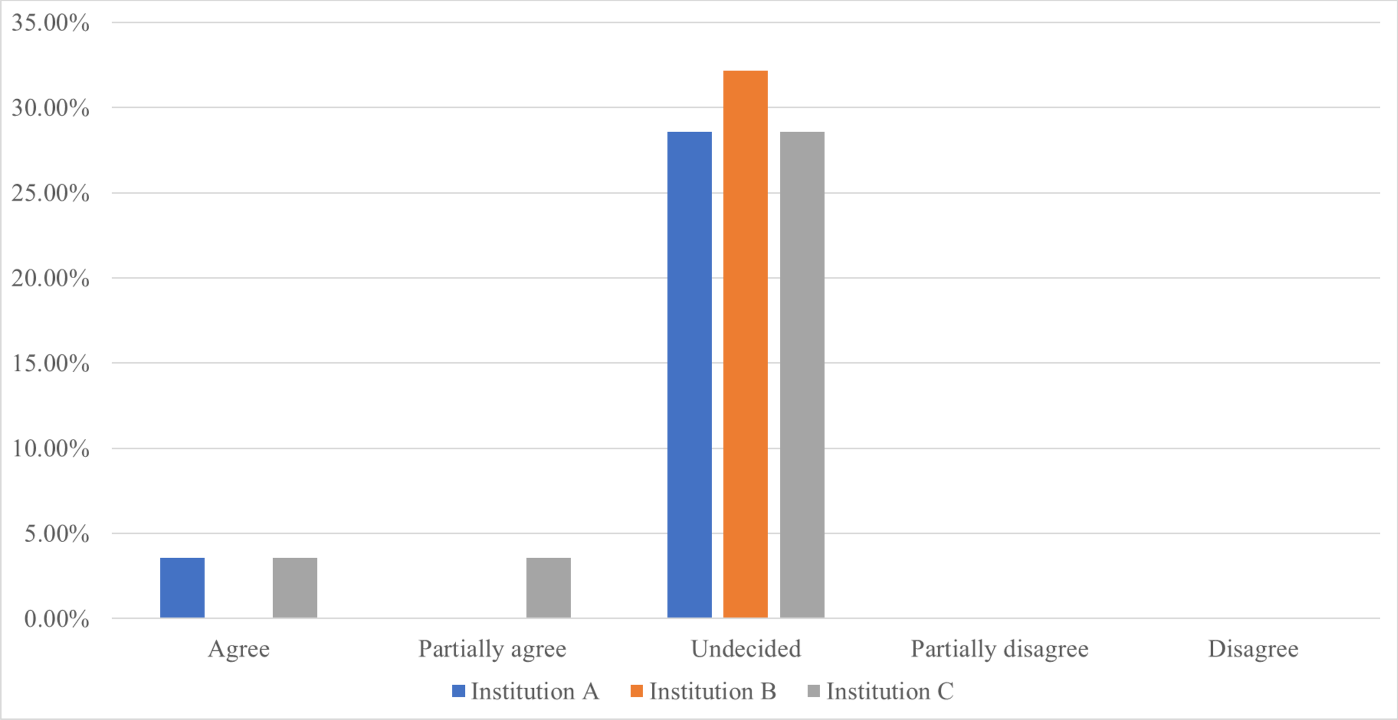

Figure 4. Answering the profile of participants in statement 8.

However, as Parnafes (2010) notes, there are several obstacles to understanding this model. These obstacles include the challenge of correlating physical behavior with mathematical idealizations, which include differential equations, differential and integral calculus, Fourier series, and other mathematical formalisms. Furthermore, there is a lack of macroscopic applicability due to an insufficient understanding of the fundamental processes of spectroscopy. It is not easy to think about harmonic motion at the level of the microscope, and without an understanding of the basic concepts of spectroscopy such as stretching, bending, oscillation and others, students have difficulty relating their knowledge to the appropriate meaning.

This difficulty regarding the relationship between mathematics and physical phenomena can be explained by the lack of meanings of mathematical symbols. Mathematics is a universal language because it has several applications in science. One of them is essential for quantum mechanics, i.e., modelling of complex systems. Differential equations, for example, are used in situations involving rates of change. They describe how physical variables change over time.

As for the second problem, there is a failure in the processes of knowledge construction and the resulting lack of meaning in the new body of knowledge that is taught to students. According to Ausubel (2003), for the assimilation of new concepts by the subject, they must be linked to the structures based on prior knowledge and experiences that serve as the foundation for the new knowledge. This means that solid knowledge of classical physics and its principles is necessary for learning concepts related to quantum mechanics to be meaningful.

The last prominent statement to analyze is number 10 (**Fig. 5**): “The consideration of the atomic nuclei at rest in relation to the electrons simplifies the solution of the electronic problem of the Schrödinger equation”. This excerpt contains a true statement. The Born-Oppenheimer approximation is based on the experimental fact that atomic nuclei are much more massive than electrons and therefore must move at much slower speeds than electrons. Therefore, one can approximate that the electrons in the molecule move in an electric field generated by the set of atomic nuclei at rest. In this way, the two movements, the nuclear and the electronic, can be separated mathematically, which simplifies the problem considerably. This is a good approximation when considering the molecular electronic ground state, i.e. the one with the lower energy (Levine, 2014). This approximation is fundamental and essential to the methods used in quantum chemistry and leads to the concept of molecular geometry, which otherwise, if the approximation were not valid, would have no physical meaning (Cramer, 2004). However, about 57% of the respondents say they have no opinion on this issue and declare themselves undecided, as shown in **Fig. 5**.

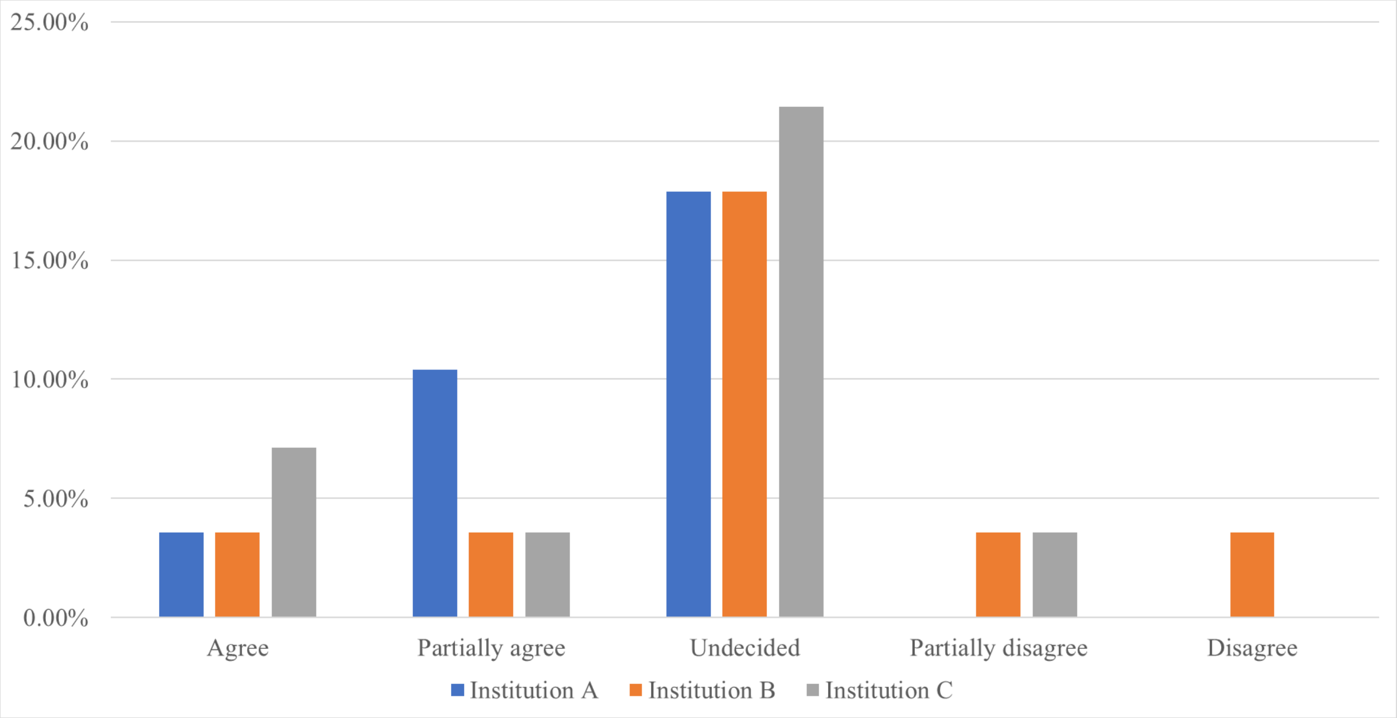

Figure 5. Answering the profile of participants in statement 10.

The last two statements (8 and 10) require a deeper understanding of the elements of quantum mechanics and are usually discussed only in the specialized discipline of quantum chemistry. According to Stefani and Tsaparlis (2009), the understanding of what really constitutes quantum chemistry is very superficial, considering that the construction of specific knowledge in this field has numerous errors, such as calling Bohr’s “atomic model” the “first quantum model” even though it ignores the dualistic behavior of the electron. According to Stefani and Tsaparlis (2009), this excess of misconceptions about quantum chemistry is also due to students’ insistence on basing their ideas on elementary ideas about the atom, as these are more intuitive and more plausible than what is discussed in mechanics.

An objective analysis of the data shows that most responses are inconsistent, e.g., students agree with statement 5 and then disagree with statement 6. Another example of the inconsistency of responses is the fact that only one (statement 8) of the ten questions has a higher percentage (approximately 68%) of respondents agreeing, while the remaining percentages are well distributed among the responses. Considering that the statements deal with ideas that are uniformly established in quantum mechanics and consequently in quantum chemistry, there should not be such divergences between the answers. This panorama reveals a certain weakness in the construction of knowledge about the topic under discussion, thus confirming previous works. (Bouayad *et al.*, 2014; Coelho and Borges, 2010; Cunha, 2022; Fernandes, 2019; Stefani and Tsaparlis, 2009).

At the end of the analysis of responses to specific assertions, it was also noted that many responses were partial, such as "partially agree" or "partially disagree." Although many chose these answers and claimed to partially agree or disagree with the assertions, many justified their choice as an opinion. This shows not only a certain lack of knowledge about the content under discussion but also that at least those participants who justified their answers with opinions do not appear to know the basic procedures of the scientific method, which were introduced over 400 years ago.

According to Silva and Videira (2020), discourses based on opinions and assumptions are extremely harmful, and the importance of the method and scientific knowledge should be made clear, especially for future professionals who are seen as a reference by society. And this view should not be confused with the expectation that respondents will agree or disagree with every assertion, because even if they were unfamiliar with the content, they would be expected to declare themselves undecided. No pedagogical assertions were used in this analysis as these allow for a higher degree of subjectivity.

3.2. Items related to learning

In this section, all six items (11 to 16) were selected for discussion, considering the subjective nature of the answers and the direct connection with the origin of the learning problems in the field of quantum chemistry.

The first statement that we would like to highlight in terms of the respondents' views on the teaching problems of the subject is statement 11 (**Fig. 6**): "The large number of mathematical expressions and symbols makes learning the content of quantum chemistry difficult". Despite the percentage of respondents agreeing with the statement (about 61%), as we can see in **Fig. 6**, there is an unexpected divergence between the answers, considering that historically the disciplines that have more mathematical formalisms are the "bad guys". of undergraduate courses.

This can be partly explained by the opinion of the participants themselves, who stated in the interviews that the problem is not the calculations themselves, but rather the mathematical foundations of most students, which are not solid enough to understand the topics worked on. which the students themselves confirm in statement 14 (**Fig. 7**): "I have a solid foundation in mathematics and am proficient in topics such as linear algebra and differential and integral calculus". For this topic, about 68% disagreed with the statement, as **Fig. 7** shows. The fundamentals of mathematical concepts are extremely important for understanding the content of quantum chemistry. If this part of the respondents states that they do not know this area, this question brings to light one of the main learning problems of the subject.

Below are some comments from research participants on the two topics previously addressed, which we will discuss later: "Mathematics does not make things difficult; its task is to promote understanding. The obstacle is in the teacher's explanations, forgetting that most students don't even know math from high school, let alone college" (Student 3, Institution A, re: Item 11); "I totally disagree, that was one of the most horrible subjects of the course, I haven't learned anything to this day, and not that it's the teacher's fault, but I am not able to learn these things, I don't even know how I passed Calculus 2" (Student 4, Institution B, at 14).

It is important to point out that when looking at the data presented in the previous two graphs, it is noticeable that the students of Institution C have greater difficulties in the mathematical part. We can observe that there is no unanimity among the students of this institution on the last graph (**Fig. 7**); on the contrary, there is a balance between those who agree and those who disagree with this statement. This fact must be considered considering that HEI also has in its curriculum a compulsory course in linear algebra and analytic geometry, offered in the first semester of the program and focused on developing the basic mathematical skills necessary for understanding the disciplines of differential and integral calculus.

According to Ribeiro *et al.* (2019), the subjects in which students have the greatest difficulties are related to mathematics and lead to many failures, including quantum chemistry.

Most of the students' responses agree with Macêdo and Gregor (2020), who state that one of the main obstacles to understanding and learning differential and integral calculus (essential subjects for learning quantum chemistry) is the weak mathematical foundation, much of which is taught in public education. The student's conception of the role of mathematics in quantum chemistry is a critical factor in preventing it from being an obstacle to understanding the subject's topics, because only when individuals become aware of their position in the learning process can they move through the stages of assimilation and accommodation of the new knowledge. (Mortimer, 2000).

This weakness in mathematical concepts can first be explained from the student's point of view. Often the individual does not know which concept or technique he or she should know. In addition, practicing advanced mathematics is not a general behavior, because although the use of simple operations is quite common in everyday life, other important tools such as differential calculus or linear algebra are usually not part of everyday life, i.e., to master this content, intentional and constant practice is required (Lithner, 2011).

An example of this is the application of integrals, which are usually associated with polar coordinates. To understand the application of integrals through polar coordinates, one must know the difference between Cartesian coordinates and trigonometric functions. But before you learn polar coordinates, you need to learn how integrals work, and to do that you first need to know how to use derivatives. Before derivatives, you need to know how to use limits, and before limits, you need to master the concept and use of different types of functions, such as affine, quadratic, exponential, and others. After this analysis, we come to the basic mathematical topics where students also have difficulties, such as operations with fractions, exponentiation properties, scientific notation, and others.

This is related to what was said earlier about how students relate mathematics and physical phenomena. If they have not mastered the basics, they have greater difficulty understanding more advanced topics in mathematics, and consequently, they have difficulty relating mathematical expressions to physical phenomena.

Next, we can mention statement 12 (**Fig. 8**): "Examples of the application of quantum chemistry in daily life are not uncommon". What we can highlight in this topic is the apparent inconsistency between the answers and the actual thinking of the respondents who agreed with the statement (about 67%), as can be seen in **Fig. 8**, because there was significant uncertainty in the answers and the lack of real examples. when the interviewer asked for examples.

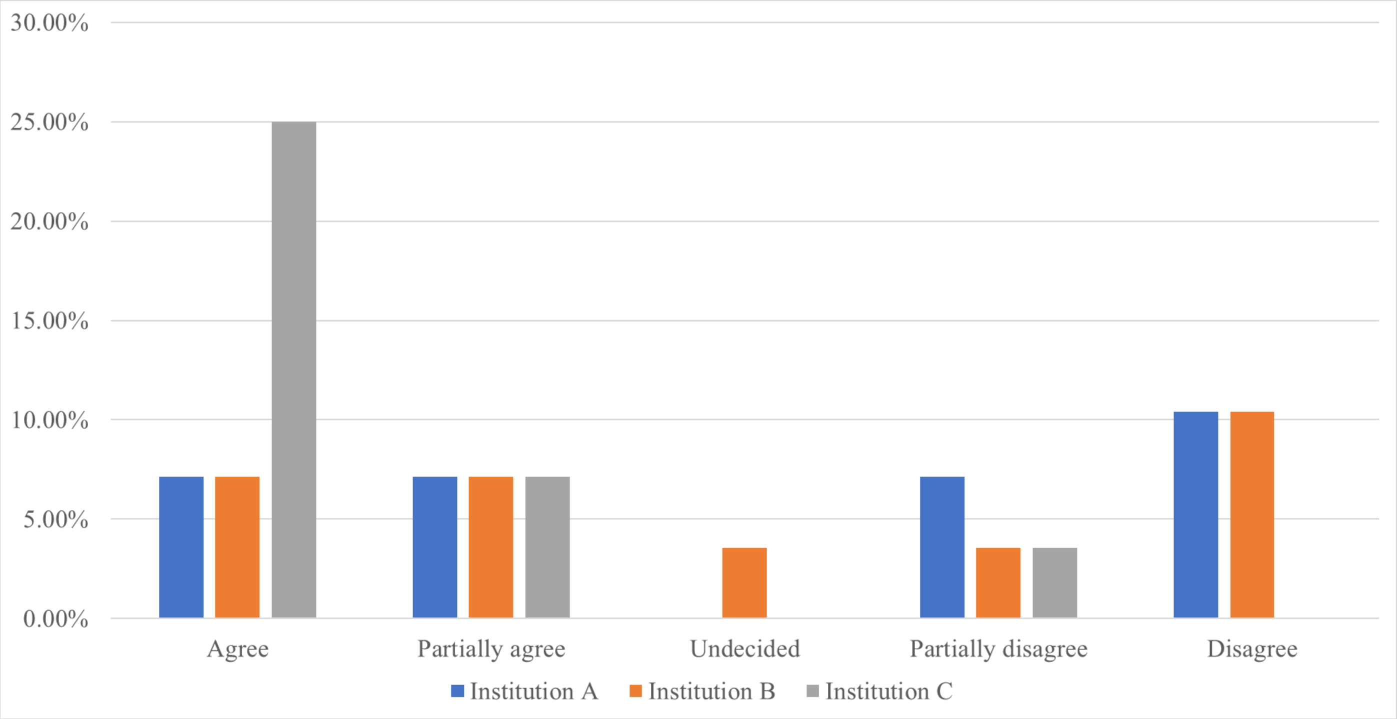

Figure 6. Answering the profile of participants in statement 11.

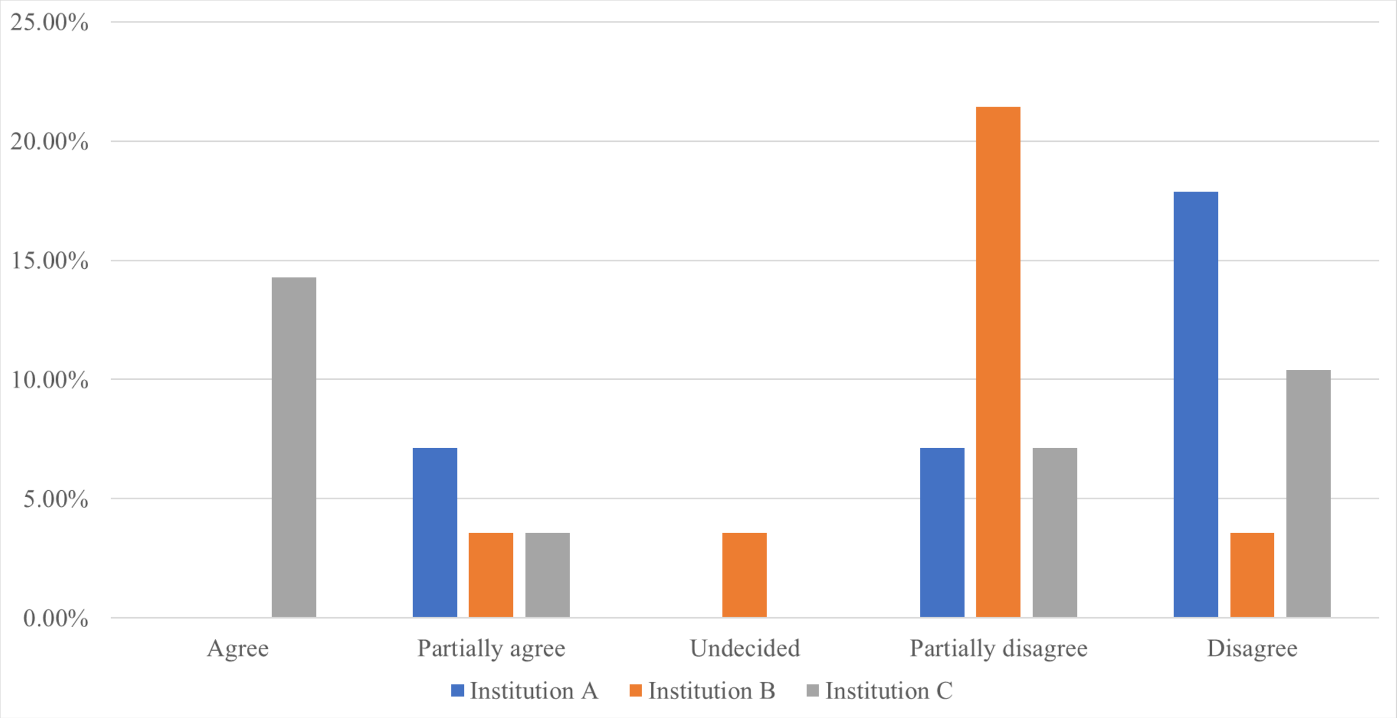

Figure 7. Answering the profile of participants in statement 14.

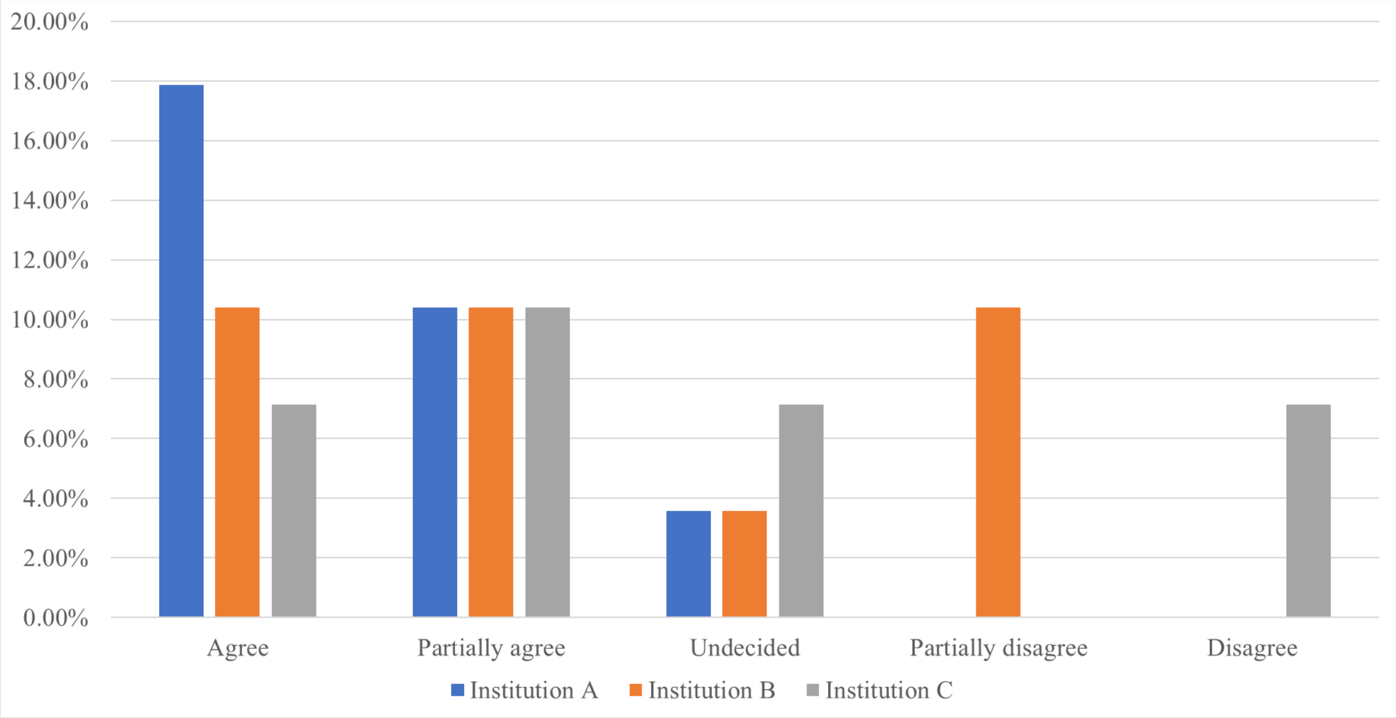

Figure 8. Answering the profile of participants in statement 12.

The difficulty that respondents have in presenting examples of applications is the high degree of abstraction that quantum mechanics, and consequently quantum chemistry, requires for their understanding. For example, automatic doors could be used as an example of a practical application if the photoelectric effect were understood in its essence, but the first statement discussed proves otherwise. In this context, Mortimer (2000) points out that common sense and science use tools such as generalization, induction, and deduction, but science tends to go beyond the limits of common sense and also produce counterintuitive findings. This new perspective acts as a rupture between science and common sense, and only the interference of culture promotes the overcoming of this barrier. Therefore, according to Sagan (1990), it is necessary for scientific knowledge to break through the boundaries of academia and reach people's daily lives, because science is more than a body of knowledge with cold formulas, but a way of thinking.

This is evident in the report of one respondent who, while acknowledging the importance of quantum chemistry, makes a remark that is far removed from what is being discussed in the discipline: "Quantum energy is energy packages that we can't live without, from our breathing to the food we eat. I believe that energy exists because otherwise we wouldn't be living here in the environment" (Student 5, Institution A).

Another respondent who showed that she knew a little more about the subject made a meaningful statement about her experience in the subject that she related to other teaching suggestions:

> I think what makes quantum chemistry difficult is the abstraction, because chemistry in itself is already abstract, and the content often needs to be connected to images or representations from everyday life in order for people to understand the phenomena. When we think of quantum chemistry, we immediately associate it with calculations, and the lack of a solid foundation in mathematics gets in the way, and there are teachers who focus only on that part. My teacher, for example, always talked about theoretical aspects, about how things work, and that helped me a lot. Computer programs make visible what you can't see with the naked eye. So, I think the association of these applications makes students' lives much easier, especially for those who have difficulty abstracting and understanding the phenomena in question (Student 7, Institution C).

Regarding statement 13, which says: "I can well understand the explanations of the teacher of the subject dealing with the contents of quantum chemistry", a look at **Fig. 9** shows a balanced result, as half of the respondents answered positively to this statement. The conclusion from this statement is that many indicated that despite the understanding, it was not a deeper knowledge that remained after the course, but rather something preliminary that served only the purpose of assessment and recognition in the course.

From this point of view, it is important that the teacher reflects on his teaching practice and tries to match the attention he pays to the technical part of his subject with the learning process of the students, which does not always happen automatically, especially in the case of quantum chemistry content. According to Quadros and Mortimer (2014), constant reflection on the teaching practice allows the development of a practice in which the strategies are diversified, and participation is favored, creating a more effective environment. We can highlight the thought of Ausubel (2003) to connect the two previous points. For students to actually learn, the added information must be linked to their prior knowledge to make sense of it. Using conceptual maps, text, pictures, and other tools, such as applying content to daily life, helps make these connections and make science instruction more meaningful, according to Tavares (2008). Another factor that contributes to meaningful learning is reflection on the assessment process. When traditional assessments consider only a numerical value of what is learned, the assessment becomes only an expression of the emotional state at the time of the assessment and ignores all the subjectivity and complexity of the assessment process (Luckesi, 2012). Thus, the student's main goal is to achieve the score required to pass the subject, not the learning itself.

Analyzing statement 15 (**Fig. 10**), which says: "It is possible to understand chemistry today without knowing the basics of quantum chemistry", we can see another problem related to learning the content of this subject, because as shown in **Fig. 10**, about 39% of the respondents agree with a statement that can be considered false. One does not have to go much further than the topics covered in school, such as Bohr's atomic model, to conclude that quantum chemistry was not essential for understanding chemistry at the beginning of the 20th century.

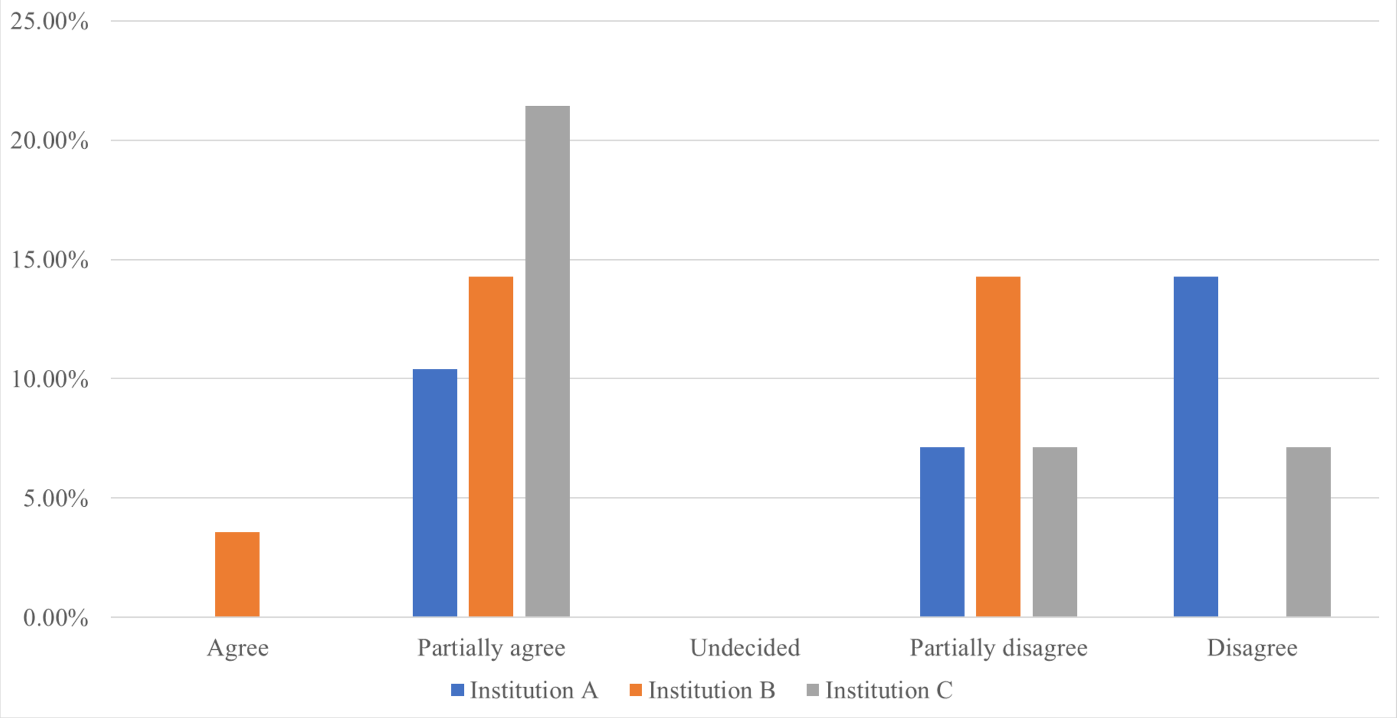

Figure 9. Answering the profile of participants in statement 13.

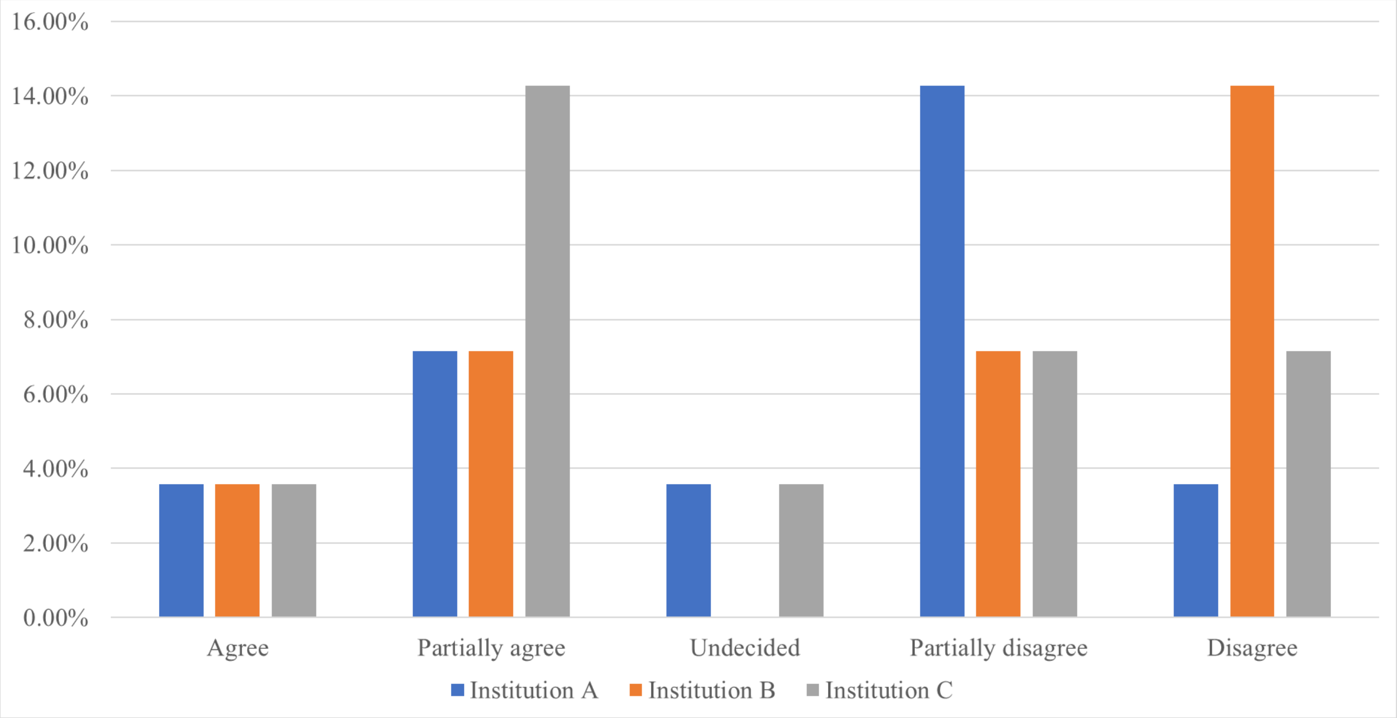

Figure 10. Answering the profile of participants in statement 15.

This perspective explains a gap in the training process of future teachers and the need to re-evaluate the curricular matrices and political-pedagogical projects of institutions, as well as a paradigm shift for higher education institution to recognize their responsibilities in the training process of these professionals (Schnetzler and Corrêa, 2017) since students do not seem to have a comprehensive idea of the scope of chemistry content, especially quantum chemistry, nor of the context in which it is embedded, as well as of its social application (Santos and Schnetzler, 1996). This problem also runs through the training of college teachers. It is important to also focus on the teacher of the teacher who needs training during his or her postgraduate studies that focuses on teaching in a different area of instruction. The teacher must view his or her educational process as a maturation of his or her previous education, rather than as a sum of specific and pedagogical disciplines. Also, there needs to be more dialogue between supervisors and students about teaching practice in addition to reflection on teaching practice (Arroio *et al.* 2006). In this way, according to Arroio (2009), something that traditionally does not appear in discussions would be discussed, namely methodological practices in higher education.

Finally, we see in statement 16: "I know many people who have mastered the basics of quantum chemistry", it is not a problem, but a reflection of learning problems related to the content of quantum chemistry when about impressive 93% of the respondents disagree with the statement, as shown in **Fig. 11**.

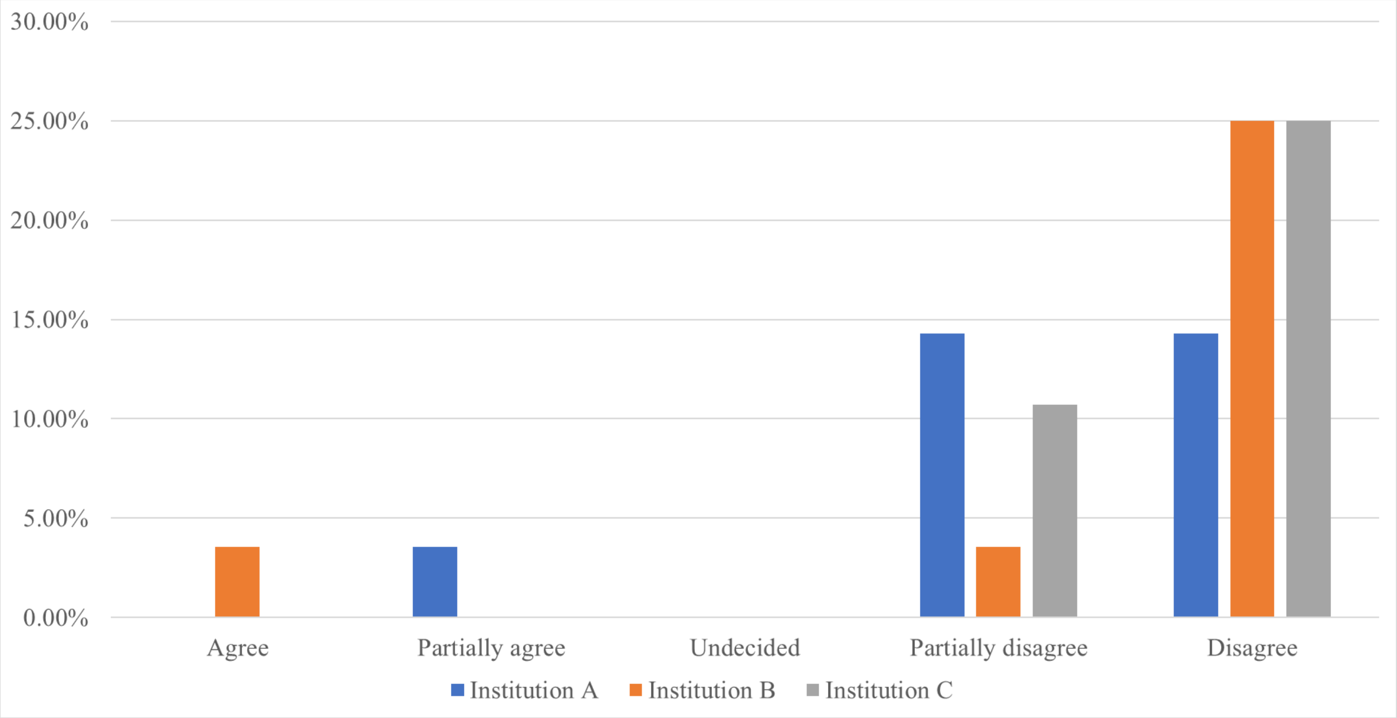

Figure 11. Answering the profile of participants in statement 16.

During their training, prospective chemistry teachers face several problems, such as the weak pedagogical base offered in chemistry curricula (Fernandez, 2018), the excessive focus on the epistemological training of the subject to the detriment of critical sense and reflection on chemistry and teaching practices (Mesquita *et al.*, 2012), and the aforementioned difficulties related to the mathematical base which is essential for the development of chemical knowledge. The answers to statement 16 reflect the result of the synthesis of the problems mentioned above and show the enormous difficulties in teaching and learning quantum chemistry, leading to a series of chain effects, such as a false understanding of the nature of matter, which is one of the most important effects observed.

Furthermore, in teaching practice, the teacher must seek the connection between mathematical theories and formalisms with observed phenomena, or at least with those that can be proven (in the case of submicroscopic phenomena), to minimize the level of abstraction of this content. This facilitates the learning of quantum chemistry as it is, and the student understands that this branch of science is more than just traces, numbers and disconnected forms.

4. Conclusions

Basic knowledge of quantum chemistry is more than necessary for a better understanding of modern chemistry, especially for chemistry students who will be responsible for teaching this field of knowledge in the future.

If we look at the specific part of the questionnaire, we first realize that the students have a misconception of the nature and interactions of matter at the atomic level, linked to the most elementary notions that could be overcome by considering the most appropriate and up-to-date theories. And with increasing difficulty of the tasks, it was found that students do not have a comprehensive idea of the application and performance of quantum chemistry.

These problems can be understood from the answers to the last 6 questions, which relate to learning the subject content. The first point refers to the mathematical basis of the students, which is not solid enough to understand the mathematical formalisms of quantum chemistry, which are essential for the interpretation of the experimentally observed physical phenomena.

The second point is related to the high degree of abstraction of the content, which is mostly counterintuitive. The fact that the observed phenomena are often in apparent contradiction with the ideas of classical physics, such as the lack of an idea of the trajectory of the electron due to its dualistic behavior, promotes a certain resistance and even cognitive blockages caused by the confrontation with these confusing situations, making it difficult for the student to become aware of the new concepts that he/she must assimilate and process.

Another aspect that can be gleaned from the students' responses is their concentration during subject lessons. Given the current assessment model, which is too quantitative, students tend to strive only to pass the subject, regardless of whether they have learned the content.

The fourth impasse is related to the design and implementation of the curricula proposed by universities, which do not make room for discussions such as these in specific disciplines within the matrix, which would be necessary to break down the barriers to learning quantum chemistry.

Discussing this scenario can help to mitigate the problems mentioned above, as universities and their faculties have the autonomy to develop projects and strategies. As Moraes and Teixeira Júnior (2014) point out, it is evident that the difficulties in the use of mathematics in undergraduate studies are inextricably linked to deficiencies in the construction of knowledge, especially in the fundamentals taught in primary and secondary education. Therefore, it is interesting to introduce specialized undergraduate courses in calculus to fill these gaps and provide a solid and reliable foundation for the study of quantum chemistry. Another important aspect, as Raupp *et al.* (2008) argue, is that the use of information and communication technologies (ICT) plays a crucial role in the teaching of quantum chemistry. Molecular modeling and computational chemistry software offer a tangible approach to overcoming the challenges posed by the inherent abstraction of the subject and compensate for the lack of macroscopically observable practical experiments.

Back to the teachers and their practice. Given the constant technological development of the last decades, we must recognize that teachers are not always able to keep up with these changes, as Pretto and Riccio (2010) and Trebien *et al.* (2020) point out. Therefore, it is important to establish professional development programs for teachers. This will ensure that they are adequately prepared to apply the aforementioned methods and adapt their pedagogical practices to today's demands. Finally, as Oliveira (2010) points out, the introduction of alternative forms of assessment such as research and group work is crucial for the development of understanding of quantum chemistry. These approaches encourage social interaction and collaboration between students, allowing for the sharing of experiences, the transmission of knowledge and the exploration of different perspectives on the topics covered, thus enriching the learning experience.

The discussion of this scenario can help to mitigate the problems mentioned above since universities have the autonomy to develop projects that improve the mathematical foundations of students; methods that deal with different ways of presenting the content of the subject; in addition to seeking reformulations of the assessment processes aimed at the meaningful learning proposed by Ausubel (2003), and thus it will be possible to envisage a more effective training of chemistry teachers, with professionals who are better prepared and aware of their social role.

Authors' contributions

Conceptualization: Ferreira, L. N. A.; Souza, A. A.; **Data curation:** Not applicable; **Formal Analysis:** Sousa, L. M. P.; Cunha, K. M. A.; **Funding acquisition:** Not applicable; **Investigation:** Sousa, L. M. P.; **Methodology:** Sousa, L. M. P.; **Project administration:** Not applicable; **Resources:** Not applicable; **Software:** Not applicable; **Supervision:** Souza, A. A.; **Validation:** Not applicable; **Visualization:** Not applicable; **Writing – original draft:** Sousa, L. M. P.; **Writing – review & editing:** Cunha, K. M. A.; Ferreira, L. N. A.; Souza, A. A.

Data availability statement

The data will be available upon request.

Funding

Not applicable.

Acknowledgments

The authors acknowledge the Federal University of Piauí (UFPI).

References

Alberto, S.; Placido, R. L.; Placido, I. T. M. A formação docente e o tecnicismo pedagógico: um desafio para a educação contemporânea. *Rev. Ibe. Est. Ed.* **2020**, *15* (2), 1652–1668. https://doi.org/10.21723/riaee.v15iesp2.13837

Arroio, A. Formação docente para o ensino superior em química. VII Enpec, Florianópolis, Santa Catarina, Brasil, 2009.

Arroio, A.; Rodrigues Filho, U. P.; Silva, A. B. F. A formação do pós-graduando em química para a docência em nível superior. *Quím. Nova.* **2006**, *229* (6), 1387–1392. https://doi.org/10.1590/S0100-40422006000600040

Ausubel, D. *Aquisição e retenção de conhecimentos*: uma perspectiva cognitiva; Plátano, 2003.

Batista, E. C.; Matos, L. A. L.; Nascimento, A. B. A entrevista como técnica de investigação na pesquisa qualitativa. *Revista Interdisciplinar Científica Aplicada.* **2017**, *11* (3), 23–38.

Belo, T. N.; Leite, L. B. P.; Meotti, P. R. M. As dificuldades de aprendizagem de química um estudo feito com alunos da Universidade Federal do Amazonas. *Scientia Naturalis.* **2019**, *1* (3), 1–9.

Beuren, I. M. *Como elaborar trabalhos monográficos*: teoria e prática; Atlas, 2006.

Bouayad, A.; Kaddari, F.; Lachkar, M.; Elachqar, A. Quantum model of chemical bonding: barriers and learning difficulties. *Procedia Soc. Behav. Sci.* **2014**, *116*, 4612–4616. https://doi.org/10.1016/j.sbspro.2014.01.994

Chassot, A. *Alfabetização científica: questões e desafios para a educação*; Unijuí, 2014.

Coelho, G. R.; Borges, O. O entendimento dos estudantes sobre a natureza da luz em um currículo recursivo. *Cad. Bras. Ens. Fís*. **2010**, *27* (1), 63–87.

Costa, H. R.; Souza, A. R. A produção de significados no modelo quântico por meio de ferramentas socioculturais: uma proposta analítica da aprendizagem. *Ensino & Multidisciplinaridade*. **2017**, *3* (1), 17–39.

Cramer, C. J. *Essentials of computational chemistry: theories and models*; Wiley, 2004.

Cunha, S. G.; Dias, D; Streit, L. A estrutura eletrônica do átomo: um estudo sobre o conhecimento de Química Quântica no ensino superior. In 41º Encontro de Debates sobre o Ensino de Química, Pelotas – RS, Brasil, October 14–15, 2022.

Fernandes, L. S. *Conceituação da ligação covalente por licenciandos em Química*; UFBA, 2019.

Fernandez, C. Formação de professores de Química no Brasil e no mundo. *Estud. Av.* **2018**, *32* (94), 205–224. https://doi.org/10.1590/s0103-40142018.3294.0015

Gregório, J. R.; Leite, C. C.; Leal, B. C.; Nitschke, W. K.; Pederzolli, F. R. S.; Nobre, K. M.; Fraga, M. V. B.; Silva, C. B. O programa de apoio à graduação em Química (PAG-Química) e sua contribuição para a democratização e permanência dos estudantes no ensino superior. Authorea. [PREPRINT] May 20, 2019. https://doi.org/10.22541/au.155836336.67356235

Halliday, D.; Resnick, R. *Fundamentals of Physics*; 10. ed. Wiley, 2014.

Henriksen, E. K.; Angell, C.; Vistnes, A. I.; Bungum, B. What is light? *Sci. Educ*. **2018**, *27* (1-2), 81–111. https://doi.org/10.1007/s11191-018-9963-1

Levine, I. N. *Quantum Chemistry*; 7. ed. Pearson Education, 2014.

Libâneo, J. C.; Pimenta, S. G. Formação de profissionais da educação: visão crítica e perspectiva de mudança. *Educ. Soc.* **1999**, *20* (68), 239–277. https://doi.org/10.1590/S0101-73301999000300013

Lithner, J. University mathematics students' learning difficulties. *Educ. Inq.* **2011**, *2* (2), 289–303. https://doi.org/10.3402/edui.v2i2.21981

Luckesi, C. C. *Educação, avaliação qualitativa e inovação*; INEP, 2012.

Macêdo, J. A.; Gregor, I. C. S. Dificuldades nos processos de ensino e de aprendizagem de cálculo diferencial e integral. *Educação Matemática Debate.* **2020**, *4* (10), 1–24. https://doi.org/10.24116/emd.e202008

Mesquita, N. A. S.; Cardoso, T. M. G.; Soares, M. H. F. B. O projeto de educação instituído a partir de 1990: caminhos percorridos na formação de professores de Química no Brasil. *Quím; Nova.* **2013**, *36* (1), 195–200. https://doi.org/10.1590/S0100-40422013000100033

Moraes, C. A.; Teixeira Júnior, J. G. Reflexões sobre o ensino de cálculo diferencial e integral em cursos de graduação em Química. *DiversaPrática.* **2014**, *2* (1), 194–217.

Mortimer, E. F. *Linguagem e formação de conceitos no ensino de ciências*; UFMG, 2000.

Nussenzveig, H. M. *Curso de Física Básica: Fluidos Oscilações e Ondas, Calor*; v. 2, 5. ed., Editora Blücher, 2014.

Oliveira, J. R. S. A perspectiva sócio-histórica de Vygotsky e suas relações com a prática da experimentação no Ensino de Química. *Revista de Educação em Ciência e Tecnologia*. **2010**, *3* (3), 25-45.

Parnafes, O. When simple harmonic motion is not that simple: managing epistemological complexity by using computer-based representations. *J. Sci. Educ. Technol.* **2010**, *19* (6), 565–579. https://doi.org/10.1007/s10956-010-9224-9

Pavia, D. L.; Lampman, G. M.; Kriz, G. S.; Vyvyan, J. R. *Introduction to spectroscopy;* Cengage Learning, 2013.

Pereira, M. E.; Brasileiro, R.; Silva J. F.; Silva, P. B.; Brachi, D.; Albuquerque, F. Esteriótipos, mentiras e videotape: estudos experimentais sobre a acurácia na identificação da mentira. *Psicologia em Estudo.* **2006**, *11* (1), 209–218.

Pretto, N. L.; Riccio, N. C. R. A formação continuada de professores universitários e as tecnologias digitais. *Educ. Rev*. **2010**, *37*, 153–169. https://doi.org/10.1590/S0104-40602010000200010

Quadros, A. L.; Mortimer, E. F. Fatores que tornam o professor de ensino superior bem-sucedido: analisando um caso. *Ciênc. Educ.* **2014**, *20* (1), 259–278. https://doi.org/10.1590/1516-731320140010016

Raupp, D.; Serrano, A.; Martins, T. L. C. A evolução da Química Computacional e sua contribuição para a educação em Química. *Revista Liberato.* **2008**, *9* (12), 13–22. https://doi.org/10.31514/rliberato.2008v9n12.p13

Ribeiro, J. C. A.; Rosa, J. V. A.; Souza, G. A. P.; Haraguchi, S. K.; Silva, A. A. Evasão e retenção na perspectiva de alunos do curso de licenciatura em Química. *South. Am. J. Bas. Edu. Tec. Technol.* **2019**, *6* (2), 609–618.

Sagan, C. Why we need to understand science. *Skeptical Inquirer.* **1990**, *14*, 263–269.

Santos, W. L. P.; Schnetzler, R. P. Função social: o que significa ensino de Química para formar o cidadão? *Química Nova na Escola.* **1996**, *4* (4), 28–34.

Saviani, D. *Pedagogia histórico-crítica*: primeiras aproximações; Autores Associados, 2011.

Schnetzler, R. P.; Corrêa, T. H. B. Da formação à atuação: obstáculos do tornar-se professor de Química. *Revista Debates em Ensino de Química*. **2017**, *3* (1), 28–46.

Silva Júnior, D. S.; Costa, F. J. Mensuração e escalas de verificação: uma análise comparativa das escalas Likert e frase completion. *XVII Seminários em Administração*, São Paulo, Brasil, 2014.

Silva, V. C.; Videira, A. A. P. Como as ciências morrem? Os ataques ao conhecimento na era da pós-verdade. *Cad. Bras. Ens. Fís.* **2020**, *37* (3), 1041–1073. https://doi.org/10.5007/2175-7941.2020v37n3p1041

Stefani, C.; Tsaparlis, G. Students' levels of explanations, models, and misconceptions in basic quantum chemistry: a phenomenographic study. *J. Res. Sci. Teach*. **2009**, *46* (5), 520–536. https://doi.org/10.1002/tea.20279

Tavares, R. Aprendizagem significativa e o ensino de ciências. *Cienc. Cogn.* **2008**, *13* (1), 94–100.

Trebien, M. M.; Souza, W. R.; Oliveira, E. R.; Silva, J. L. Formação continuada de professores: uma epistemologia da prática. *Ambiente: Gestão e Desenvolvimento.* **2020**, *13* (1), 91–102. https://doi.org/10.24979/359

Universidade Federal do Piauí (UFPI). *Sistema Integrado de Gestão de Atividades Acadêmicas – SIGAA.* 2022. https://sigaa.ufpi.br/sigaa/public/home.jsf accessed 2022-12-16).

Woods, J.; Walton, D. Argumentum ad verecundiam. *Philosophy & Rhetoric.* **1974**, *7* (3), 135–153.

ECLÉTICA QUÍMICA

Eclet. Quim. 49 | e-1529, 2024

Review Article

https://doi.org/10.26850/1678-4618.eq.v49.2024.e1529

Last decade insights on cemented carbides: A review on alternative binders, new consolidation techniques and advanced characterization

Daniela Andreina Sandoval **Ravotti**[1], Hortensia Melero **Correas**[1], Núria Cinca **Luis**[1+]

Abstract

Cemented carbide alloys are well known powder metallurgically processed materials used for a wide range of tooling and components that require a good balance of hardness and fracture toughness, together with wear resistance. After 100 years of the first patent, research and development within this area continues to fulfil more demanding applications and adapt to new requirements. The last decade especially has witnessed important advances. In that sense, Co-free compositions are being studied due to the health issues that its use implies and its criticality in the supply chain. Secondly, the steps towards near-net-shape components by means of additive manufacturing technologies to avoid waste of powder and the technological advance of fast sintering processes are promising. Finally, new microstructural and mechanical characterization methods at micro and nanoscale provide helpful insights for a better understanding of these materials under performance.

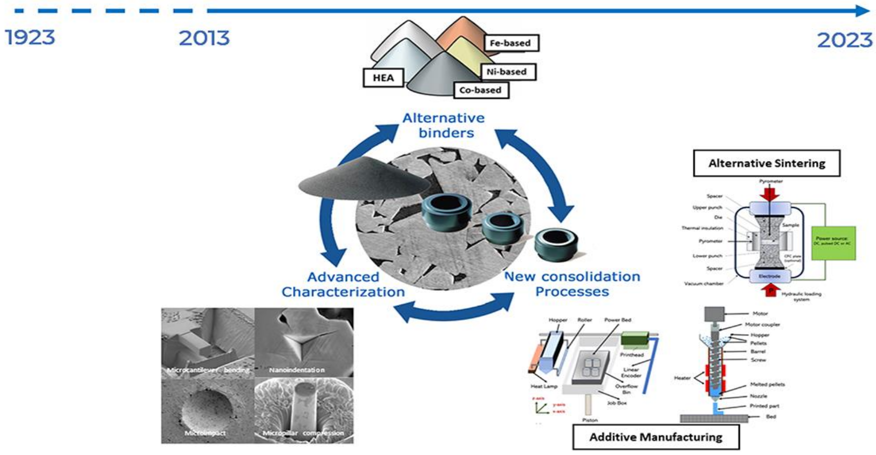

Article History

Received	November 03, 2023
Accepted	April 25, 2024
Published	July 04, 2024

Keywords

1. cemented carbides;
2. alternative binders;
3. consolidation routes;
4. micro mechanical;
5. tribological properties.

Section Editor

Mário Antônio Alves da Cunha

Highlights

- More demanding wear and corrosion resistant applications incentive new developments in tooling industry.
- Novel binders, mainly those based on high entropy alloys, are promising for cobalt substitution.
- New powder metallurgy routes overcome limitations of conventional production methodologies.
- Micro and nano-scale testing characterization increases the understanding of failure mechanisms.

CONTENTS

[1]Hyperion Materials & Technologies, Polígono Industrial Roca, Martorelles, Barcelona, Spain.

+Corresponding author: Núria Cinca Luis, **Phone:** +34935717600, **Email address:** nuria.cinca@hyperionmt.com

1. Introduction

Cemented carbides (also referred to as hardmetals) are a group of composite materials that show outstanding mechanical properties such as hardness and fracture toughness and excellent wear resistance. Such combination of properties makes them suitable to produce component and tool materials capable of working under stringent requirements for high demanding applications.

The microstructure of cemented carbides is heterogeneous. It is constituted by hard, brittle carbides bonded by a soft and tough metallic binder. The first ones are refractory carbides of transition metals (WC, TiC, TaC, Cr_3C_2 or Mo_2C), and the last one is a metal from the iron group, more often cobalt (Co) or nickel (Ni) and their alloys (Exner, 1979).

Refractory carbides of transition metals from the groups IV, V and VI show an interstitial structure that combines metallic, covalent, and ionic bonds, providing them with a high melting point. They also exhibit high hardness and strength with high thermal and chemical stability. The metallic binder phase is a ductile and softer phase that contributes to improve the toughness of cemented carbides (Upadhyaya, 1996).

The unique combination of hardness and toughness given by its constitutive phases (in comparison with other hard materials), positions cemented carbides as the most versatile materials used mainly in the tooling, mining, and oil and gas industries (Hyperion Materials & Technologies, 2019). Figure 1 presents the different application sectors in which cemented carbides are used, according to their Co content and WC grain size, as well as hardness; it can be observed that by tailoring these parameters, cemented carbides can be applied in a broad range of applications.

The development of cemented carbides started during World War I in Germany due to the need to replace diamond drawing dies with a less expensive material in the production of tungsten (W) filaments (Exner, 1979; Ortner *et al.*, 2014). Several attempts were made without success, until 1923, when tungsten carbide (WC) with added Ni was sintered. With time, Ni was replaced by Co, obtaining a good ceramic-metal combination, suitable to produce fine W wires of good quality (Ettmayer *et al.*, 2014; Ortner *et al.*, 2014). The new material was commercialized in 1926 under the name "WIDIA" (from German terminology "wie Diamant" – meaning like diamond).

With the 100th anniversary of its invention (Konyashin, 2023), it became evident that there are many opportunities to improve cemented carbides by tailoring their composition and microstructure through substitution and/or alloying of both carbide and binder phases, as well as by using novel processing and characterization methods. In the following review, we present current industrial knowledge around cemented carbides before focusing on the main developments evidenced during the last decade.

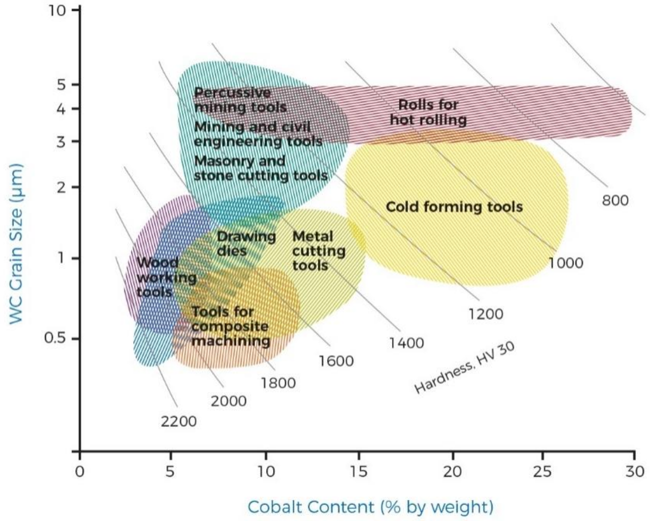

Figure 1. Range of applications in which cemented carbides are used, defined by WC grain size, Cobalt content and hardness.
Source: Adapted from Sandvik (s.d.) and Hyperion Materials & Technologies (2019).

2. General insights on conventional knowledge of cemented carbides

2.1. Common constituents

In cemented carbides, the most used ceramic phase is tungsten carbide (WC) (Upadhyaya, 2001), while the metallic binder is often cobalt (Co), followed by nickel (Ni) and iron (Fe) in order of importance (Prakash, 2008). These are still the most successful composite materials produced by powder metallurgy technologies.

The binder is selected for its wettability on the carbide and interfacial adhesion characteristics. In this regard, Co shows outstanding wetting of WC, resulting in full densification during conventional liquid phase sintering methods, leading to higher values of toughness when comparing with other metallic binders (García *et al.*, 2019; Lay and Missiaen, 2014). The formation of other undesirable phases, such as graphite or eta phase, occurs when the WC-Co system is exceeding or depleting in carbon content, respectively (García *et al.*, 2019; Lay and Missiaen, 2014).

WC particles exhibit a hexagonal close packed (HCP) crystal structure; WC crystals grown from liquid-metal solutions exhibit the shape shown in Fig. 2a, which is also the shape of WC grains in cemented carbides as seen in Fig. 2b and 2c. The shape adopted by WC in cemented carbides owes to the high polarity of the prismatic crystal planes of (1010) type due to the different spacing of the W and C planes of [1010] directions; therefore, there are two sets of equivalents (1010) planes, instead of six ones. Because of its non-centrosymmetric structure of WC, the microhardness is strongly anisotropic, i.e., the hardness of the basal plane (0001), the prismatic plane (1010) and intermediate orientations are different (Exner, 1979).

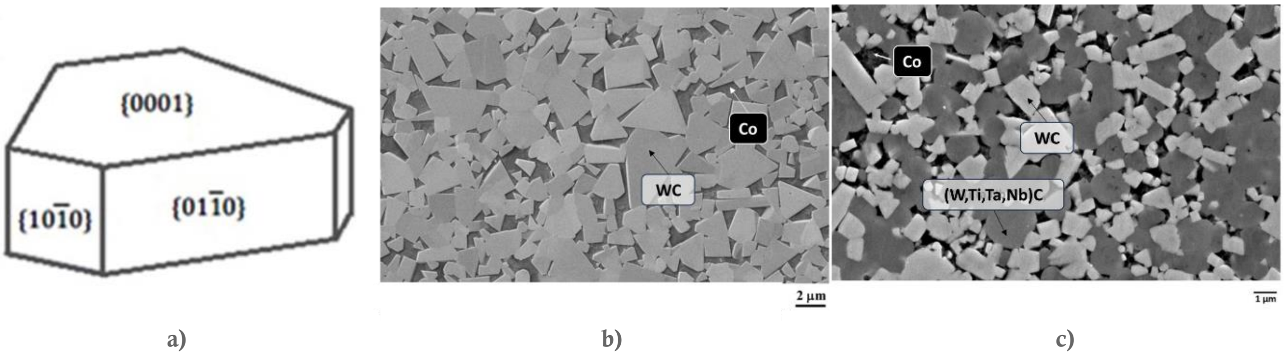

Figure 2. **(a)** Schematic representation of truncated WC grains shape in WC-Co composites; **(b)** a typical microstructure of WC-Co cemented carbides with microstructural parameters commonly determined for cemented carbides; **(c)** microstructure of cemented carbide with gamma phase. The light and dark phases correspond to the carbide and to the metallic binder, respectively.
Source: Adapted from Lay and Missiaen (2014), Roa *et al.* (2015) and Sandoval Ravotti *et al.* (2019).

TiC, ZrC, HfC, VC, NbC and TaC carbides are also used to produce cemented carbides. These carbides are face-centred cubic (FCC), melt congruently, and exhibit higher hardness than WC. When their content is higher than the solubility limit within the metallic binder, these elemental carbides precipitate, combining to form a mixed solid solution along with WC in the final part, which is commonly known as the cubic carbide phase or gamma (γ) phase (Fig. 2c); this phase is more brittle than WC. However, when their nominal content falls below the solubility limit, they behave as WC grain growth inhibitors (Exner, 1979).

Cobalt is the most used material as a metallic binder in cemented carbides. Pure Co shows an allotropic transformation from an HCP structure up to around 415 °C to a cubic structure (FCC) at higher temperatures (Davis, 1995). The prevalence of one form or another may affect the mechanical properties of the composite material. In sintered WC-Co alloys, Co shows a cubic lattice because the stabilization of it by dissolved W and C cannot be transformed by annealing (Exner, 1979; Upadhyaya, 2001).

Both the mechanical and tribological performance of cemented carbides are related to the chemical nature, amount, and size of carbide and binder phases (Chychko *et al.*, 2022; Davis, 1995; Gurland, 1988). The common parameters used to characterize the microstructure of cemented carbides are the mean grain size of the carbide particles ($d_{carbide}$) and the binder content (wt.%). The proportion of the carbide phase is generally between 3-30 wt.% of the total weight of the composite and its grain size averages between 0.4 and 10 µm.

Other important microstructural parameters are the contiguity of the carbide phase ($C_{carbide}$) and the binder's mean free path (λ_{binder}) (Exner, 1979; Roebuck and Almond, 1988; Upadhyaya, 1998), which refer to the interface area fraction of WC carbides that is shared between them and to the mean size of the metallic phase, respectively (Fig. 2c).

2.2. Industrial processing steps

Ammonium-para-tungstate (APT) is the usual starting raw material for standard WC powder production. After a hot reduction of the APT in hydrogen, pure tungsten powder is obtained, with controlled grain size. Tungsten and carbon are mixed in the right proportions, and this mixture is heated at high temperatures in hydrogen, forming tungsten carbide powder (Furberg *et al.*, 2019).

Different WC powder types and binders (Co, Ni) are the raw materials for the conventional manufacturing of cemented carbide, usually through a weigh-in, milling and then spray drying process.

Once the powder is ready, the production of parts follows the traditional powder metallurgy routes, either compaction plus sintering or hot compaction. Finally, the parts are finished in one or several grinding/turning/polishing steps if needed (Raihanuzzaman *et al.*, 2014).

Figure 3 shows the workflow of the entire traditional manufacturing process, starting from the APT, passing through the production of the agglomerated powder, and then compacting the part and densifying it (typically with a liquid phase sintering process). Finally, the part can be finished to provide the required surface roughness.

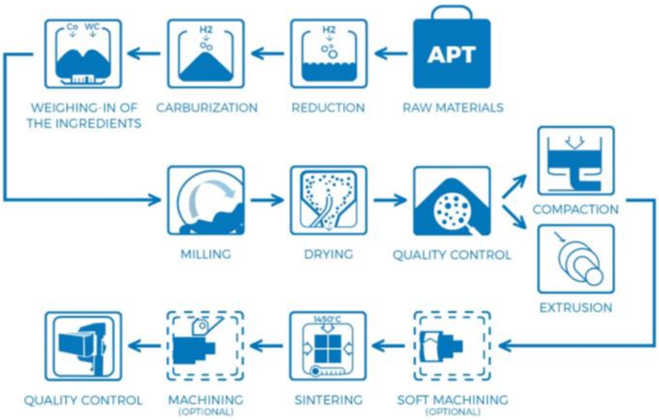

Figure 3. Traditional powder metallurgy process steps to produce parts.
Source: Adapted from Hyperion Materials & Technologies (2019).

2.3. Properties characterization

Cemented carbide products must accomplish some industrial quality checks to satisfy their demands in the application. These are related to the carbon content (through magnetic saturation measurements), carbide grain size (through coercivity values), metallographic examination, density, and hardness.

Due to the heterogeneity of cemented carbides and the cost and complexity of field testing, the development of laboratory-scale testing becomes vital for characterization of microstructure, measurement of properties and response to service-like conditions.

A wide variety of test methods according to specific standards for cemented carbides are available today (Table 1). Among them, hardness and fracture toughness prevail. Vickers hardness HV30 (load corresponding to 30 kg of weight), is the most used measurement. Typical values for WC–Co cemented carbides range from about 700 up to 2200 HV30. Higher values are obtained for binderless and nano–grained grades of WC–Co (Shatov *et al.*, 2014a). Finer carbide grain sizes and lower binder contents result in increased hardness, but decreased fracture toughness.

The higher the hardness, the more resistance to plastic deformation, penetration and thus abrasion wear, whereas high fracture toughness implies better absorption of impact energy by deformation, therefore, delaying crack propagation.

Hardness of cemented carbides was modelled as the sum of the in-situ hardness of the hard phase times the volume fraction of the contiguous carbide skeleton ($V_{WC}C$) and the hardness of the remaining binder times the rest of the volume (**Eq. 1**) (Shatov *et al.*, 2014a):

$$H_{CC} = H_{WC}V_{WC}C + H_{Co}(1 - V_{WC}C) \quad (1)$$

where CC denotes cemented carbides.

On the other hand, the measurement of fracture toughness in cemented carbide can be performed by several methods, with the Palmqvist test being the most accepted one. This method gives a good approximation of toughness for brittle-like cemented carbides, with a good correlation with the Chevron-notched three-point bending method from 10 to 14 MPa $m^{1/2}$. However, Palmqvist method becomes invalid when Chevron-notched three-point bending gives higher than 14 MPa $m^{1/2}$ (Sheikh *et al.*, 2015). A compilation of hardness-toughness relationship data has been recently carried out by Chychko *et al.* (2022). These authors have examined being plotted according to the microstructure, chemical composition, and processing. WC-Co data is very much dependent on particle size of WC and binder phase volume fraction, where the different grain growth inhibitors affect at a different extent the limitation of WC coarsening during conventional liquid phase sintering. The addition of cubic carbides, being present as complex solid solutions, increases the hardness but reduces the fracture toughness; high percentages of those result in cermet-like compositions. The substitution of cobalt by nickel or iron results in tendencies to high toughness/low hardness ratios and high hardness/low toughness ratios respectively. Finally, promising hardness-toughness ratios have been found by new sintering processes, but their industrialization is not yet ready.

Table 1. Standards for testing properties in cemented carbides.

Hardness	ASTM B294-22	Standard Test Method for Hardness Testing of Cemented Carbides
	ISO 3878	Hardmetals – Vickers hardness test
	ISO 3738	Hardmetals – Rockwell hardness test
	ISO 22394	Hardmetals – Knoop hardness test
Strength	ASTM B406	Standard Test Method for Transverse Rupture Strength of Cemented Carbides
	ISO 3327	Hardmetals – Determination of transverse rupture strength
Fracture toughness	ISO 28079	Hardmetals – Palmqvist toughness test
	ASTM B 771	Standard Test Method for Short Rod Fracture Toughness of Cemented Carbides
Stiffness	ISO 3312	Sintered metal materials and hardmetals – Determination of Young modulus
Wear resistance	ASTM B611	Standard Test Method for Abrasive Wear Resistance of Cemented Carbides

Note: Metallographic standards are not included here.

3. Recent advances in cemented carbides

3.1. Alternative binders

Since their discovery in 1922 by Schröter, materials with a predominant phase of WC are known preferably as cemented carbide. However, there is a variety of compositions, including binder-free and those containing TiN, that fall into the 'hardmetal' classification. Another way to refer to cemented carbides is as 'cermet,' understood as a particulate composite consisting of ceramic particles bonded with metallic matrix (German, 2005).

Co is the preferred metallic binder in cemented carbides, but provided that Co is considered carcinogenic, and both Co and W were classified by the European Union as Critical Raw Materials (Grilli *et al.*, 2017; Grohol and Veeh, 2023) (materials that are economically and strategically important for the European economy and have high risk associated with their supply), efforts have been made in the past decade to substitute it either partially or fully as a metallic binder in cemented carbides.

Although alternative binder systems have been explored since the 1980s, it is only recently that efforts have led to new materials, even more with the advances of computational systems that help tailor the properties for specific applications (Long *et al.*, 2017; Nicolás *et al.*, 2020). The most explored elements for substitution of Co are nickel (Ni) and iron (Fe) and their alloys, because they are the closest transition metals in the periodic table, and it is expected for them to have a similar affinity with carbon and tungsten as cobalt.

For applications demanding acidic corrosion resistance, Ni binder is preferred (Prakash, 2014). However, the substitution of Co is not straightforward, and an understanding of the mechanisms for microstructure formation should be well understood. In this sense, Roulon *et al.* (2020) found that for C-rich alloys, WC-Ni cemented carbides show significant grain growth with a major increase of mean intercept length and a widening of distribution, with increasing the sintering time.

In contrast, WC-Fe does not show any significant grain growth with a negligible change in the distribution of intercept length. Consequently, after 8 hours of isothermal sintering, the coarser microstructure was obtained for WC-Ni material followed by WC-Co and finally WC-Fe. In addition, in WC-Ni C-rich alloys, WC grains were more rounded, due to a more uniform precipitation of the solid on the rounded edges of the WC.

The use of alternative binders was first compiled in the review by García *et al.* (2019). Apart from exposing Ni-based and Fe-based binders as they are the closest elements to Co in the periodic table for its potential substitution, they exposed the use of: **(i)** precipitated reinforce binders for increasing hardness, wear resistance, bending strength, **(ii)** aluminide intermetallics for their high oxidation and corrosion resistance, **(iii)** High Entropy Alloys (HEA) for additionally improving hot hardness and fracture toughness, and **(iv)** ruthenium for the increase of hardness of the cemented carbide without losing the corresponding amount of toughness.

To better assess their feasibility, thermodynamic interfacial energy models between WC and liquid binder phase were proposed by Warren (1980), because this parameter is responsible for the resulting microstructure (Lay and Missiaen, 2014). The solid-liquid interfacial energy is composed by two contributing factors: the chemical contribution and the structure contribution. The last one is constant (0.31 J/m^2), as it considers only the melting point of WC grains. On the other hand, the chemical contribution is given by the binder metal, which changes as the composition of metallic alloys changes.

Long *et al.* (2017) evaluated the chemical contribution of WC-50 (Co-Ni-Al) interfacial energy at various Ni_3Al contents. The simulation showed that the chemical contribution increases from a minimum value of 0.215 J/m^2 at the composition of WC-50Co, up to 1.003 J/m^2 at the composition of WC-25Co-25Ni_3Al. Based on this information, phase diagrams can be calculated to determine the two-phase region in which a cemented carbide composed by WC and a metallic binder are the stable phases, the carbon (C) content, and the sintering temperature.

Fe- and Ni-based binders have been explored using thermodynamic simulations made with Thermo-Calc Software. Fe-Cr-Al and Fe-Ni-Cr binders showed good densification and homogeneity in agreement with simulations (Nicolás-Morillas *et al.*, 2020; 2023). Comparable or even improved combination of hardness, toughness and corrosion resistance to acidic media compared to Co binders was obtained (Nicolás-Morillas *et al.*, 2024).

Thermodynamic calculations can also help to explain variations in the grain size of the binder, which is known to be very large in comparison to the carbide phase (Mingard *et al.*, 2011). In the case of WC-50(Co-Ni-Al), alloys containing 0, 11.4 and 15.2 wt.% Ni_3Al, the grain size of the binder phase decreases as the amount of Ni_3Al increases due to the elevated driving forces for nucleation that contribute to the nuclei formation during solidification, resulting in a larger number of grains with smaller sizes (Long *et al.*, 2017). In addition, the interfacial energy between WC particles and liquid Co-Ni-Al binder becomes higher with addition of Ni_3Al, becoming an important obstacle for grain growth of the binder phase.

Another reported feature was the precipitation of the cuboidal γ' phase within the Co-Ni-Al binder, also observed in Co-Al-W superalloys (Suzuki *et al.*, 2015), which can contribute to the superior mechanical properties of the cemented carbide at elevated temperatures. Correspondingly, Konyashin *et al.* (2014; 2015) have shown that reinforced metallic binder with nanoprecipitates dramatically improves wear resistance by avoiding the detachment of the WC grains during wearing.

Besides mechanical properties, corrosion resistance and behaviour can be tailored by modifying the metallic binder. A methodical study of the corrosion behaviour of three groups of cemented carbides (WC-20 wt.% Ni, WC-20 wt.% Ni15Cr and WC-20 wt.% Ni11Cr6Mo), showed that solubility of W in Ni alloys is higher than in Co, greatly affected by the gross carbon content in the material (solubility decreases by increasing the carbon content) (Steinlechner *et al.*, 2022). For cemented carbides with low carbon i.e., high degree of alloying, WC-Ni(Cr,W) and WC-Ni(Cr, Mo, W) showed superior corrosion resistance in pH ranging from 1.5 to 7, as compared to WC-Ni(W), WC-Co(Cr, W) and WC-CoNiCr(W).

More recently, high entropy alloys (HEA) are the focus of study as substitutes for Co binder alloys. HEA are complex metallic alloys with at least five components in which any of them is principal in the composition. The advantage of using HEA is that they increase the hardness (also at elevated temperatures), fracture toughness, wear, oxidation, and corrosion resistance of cemented carbides (Straumal and Konyashin, 2023).

HEAs allow the decrease of the sintering temperature and suppress the WC grain growth during sintering (Zhou *et al.*, 2016). Refinement of WC grains is especially expected in Cr-containing compositions due to its known inhibition effect (Straumal and Konyashin, 2023). However, a two-phase material is difficult to obtain because of segregation and reaction during sintering, allowing the formation of numerous carbide phases (Mueller-Grunz *et al.*, 2019).

Despite difficulties in production of cemented carbides with HEA as binder, the improvement of properties has been demonstrated. Zhou *et al.* (2016) found an improved corrosion resistance of cemented carbides with 10 and 20 wt.% of HEA in a 0.1 M sulphuric acid solution, compared to a 10 wt.% Co material. Additionally, they found that the corrosion resistance depends only on the chemical nature of the binder and not on the binder content. Luo *et al.* (2021) found a decrease in the oxidation rate by increasing the aluminium content in the HEA binder.

Hardness and toughness have been studied more extensively. For several compositions, Zhou *et al.* (2018) found the optimal sintering temperature of 1,400°C, to obtain the highest hardness for 10 and 20 wt.% HEA cemented carbides. Moreover, when the HEA content increased to 20 wt.%, the fracture toughness increased. Dong *et al.* (2020) found that both Vickers hardness and fracture toughness increased with increasing HEA content in WC-Co materials. On the other hand, hot hardness was improved in WC-HEA, as studied by Hering *et al.* (2023).

In the work of R. Chen *et al.* (2022) they obtained increased density of WC-Co_xFeNiCrCu (x= 1, 1.5, 2, 2.5) by increasing the sintering temperature from 1,300°C up to 1450°C, with the corresponding improvement of hardness. Increasing the temperature from 1,400°C to 1,450°C promoted WC grain growth, which translated into an increase in toughness.

Comparison of hardness and fracture toughness ranges obtained for different cemented carbides with HEA as binders, with WC-10 wt.% Co, is shown in **Fig. 4**.

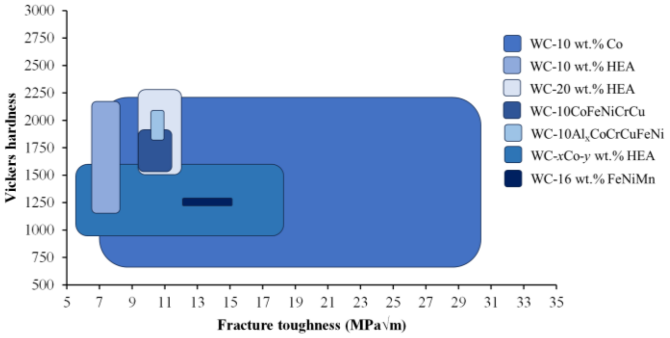

Figure 4. Vickers hardness vs. Fracture Toughness maps for cemented carbides with 10 wt.% Co, compared to cemented carbides with HEA as binders.

Source: Elaborated by the authors using the data from (García *et al.*, 2019; R. Cheng *et al.*, 2022; Dong *et al.*, 2020; Hering *et al.*, 2023; Zhou *et al.*, 2016; 2018).

3.2. New consolidation methods

Traditional powder metallurgy considers two main groups of forming technologies: cold compaction and sintering (or two-step consolidation routes) and hot compaction (or single-step consolidation routes). **Figure 5** presents the main ones for each subdivision.

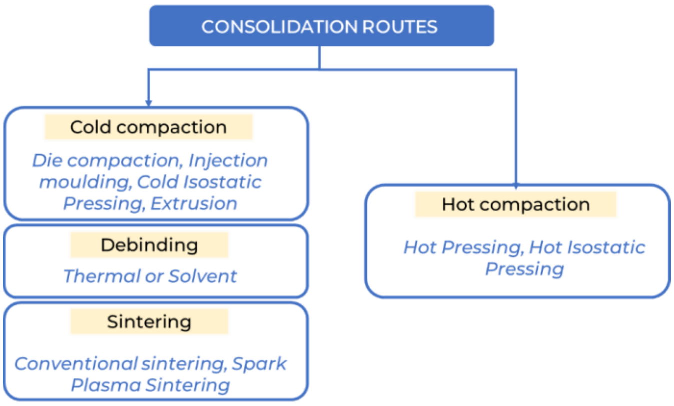

Figure 5. Main consolidation routes used for cemented carbides.

As many of these technologies have been well known for decades, the research conducted in past years has been mainly focused on two topics:

- Additive manufacturing (AM) technologies, as opposed to conventional subtractive technologies;
- Alternative sintering technologies, as opposed to conventional, time-consuming, sintering technologies, or alternative applications for well-known sintering technologies, mainly Spark Plasma Sintering (SPS).

This section will cover these two subjects. However, additionally to those, some research groups have made attempts to bring novelties on traditional technologies: micro-powder injection moulding for micro components (Heng *et al.*, 2014; Fayyaz *et al.*, 2014; 2018), casting processes using complex moulds (Kim *et al.*, 2022), or different film deposition technologies (Hu *et al.*, 2020; Xu and Huang, 2022a; 2022b; Zhao *et al.*, 2020) are examples of it.

3.2.1. Additive manufacturing technologies

The European Powder Metallurgy Association (EPMA) defines additive manufacturing as "The process of joining materials to make objects from 3D model data, usually layer upon layer, as opposed to subtractive manufacturing methodologies" (Booklet, 2019).

Conventional methodologies usually go through forming a blank that will be either green-machined, turned or ground to obtain the desired dimensions. However, these conventional approaches generate important waste and successive manufacturing operations, increasing the production cost of complex geometries.

Due to these limitations of conventional technologies, additive manufacturing provides several advantages: the agility, or capability of acting quickly without manufacturing extra tooling, the flexibility to print single parts or short series without time loss (changeover time), the creation of new complex and optimized geometries, and an important contribution to sustainability avoiding unnecessary waste (Javaid *et al.*, 2021).

There are many different additive manufacturing technologies and several ways to group them (Carreño-Morelli *et al.*, 2020; Yang *et al.*, 2020). A division that works well for cemented carbides is between one-step technologies (also called Melting Processes) and two-step technologies (or Shaping-Debinding-Sintering Processes) (**Fig. 6**) (C. Chen *et al.*, 2023).

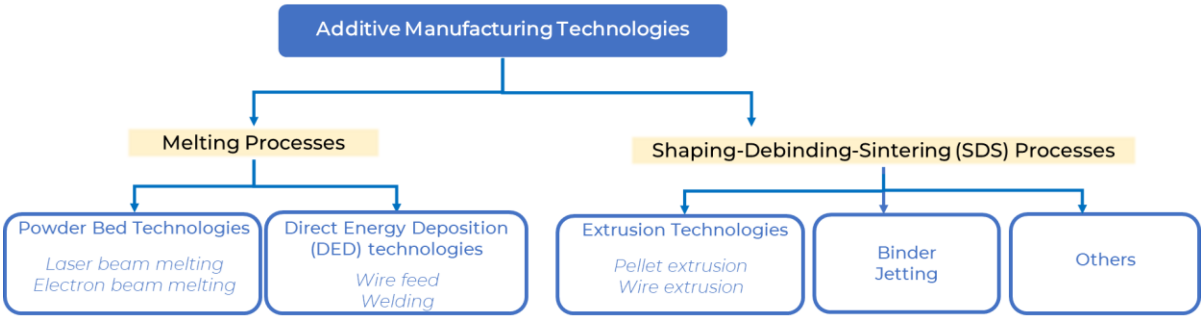

Figure 6. Metal Additive Manufacturing Technologies.

Selective Melting Processes include technologies such as Selective Laser Melting (SLM) or Electron Beam Melting (EBM) that build parts by directly melting the powder (Padmakumar, 2020). In these processes, the melting of the metallic binder is achieved in a very short time, and successive heating-cooling cycles are performed. This usually leads to many defects appearing within the structure: porosity, thermal cracks, grain growth and undesired phases, among others. Some research groups have tried alternative approaches such as higher amounts of Co, optimization of the process parameters or modification of the starting powder, but generally, these studies have not led to mechanical properties comparable to traditional powder metallurgy routes (Padmakumar, 2020; Yang *et al.*, 2020).

Shaping-Debinding-Sintering (SDS) processes are usually more suitable to process hardmetals, as the shaping/forming process is done at low temperatures and does not induce modifications within the material. The following sintering process also contributes to homogenize, remove potential defects, and fully densify the structures (Miyanaji *et al.*, 2018).

Among the different SDS processes, two have proven to give positive results for cemented carbides (WC-Co): Binder Jetting and Extrusion-Based Additive Manufacturing (see **Fig. 7**).

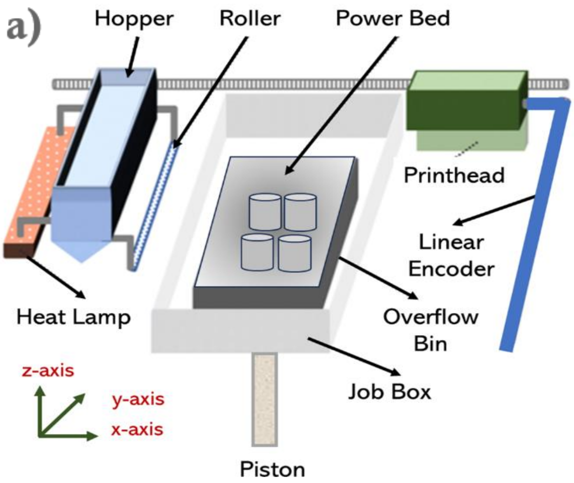

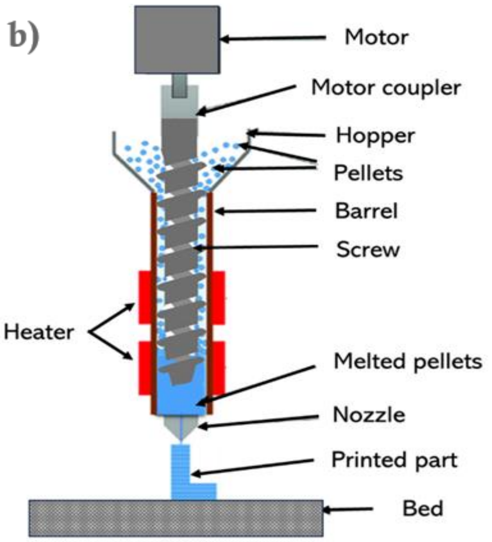

Figure 7. (a) Schematics for binder jetting technology (FFF process, Schematic of the binder-jet 3D printing machine with the printing, 2023); **(b)** extrusion-based AM (pellets extrusion process, 2023).
Source: Adapted from Gupta and Taulik (2021) and Mostafaei *et al.* (2018).

Binder Jetting is based on selectively bonding powder particles and layers together with a binder. After that, the printed parts are cured to improve the green strength and are further subjected to thermal debinding and sintering (Elliott, 2020). Studies with Co contents equal to or higher than 12wt% showed microstructures fully densified after conventional sintering processes, with medium hardnesses and acceptable wear resistances (Cramer *et al.*, 2020; Enneti and Prough, 2019; Wolfe *et al.*, 2023a; 2023b). The feedstock powder characteristics play a crucial role in the process. The possibility of using available commercial powders other than the typical ones used for additive manufacturing has been explored by Berger *et al.* (2023), finding that they can be appropriate for use in binder jetting as well.

On the other hand, extrusion-based AM technologies use as feedstock either pellets or filament manufactured with high polymer content (Altiparmak *et al.*, 2022). The principle of the technology is like commercial home printers: extruding the material (pellets or filament) through a screw and a nozzle to build the part layer-upon-layer. After the printing, the parts need to go through a debinding step (usually solvent for hardmetals) to remove one of the polymers used, then through a thermal debinding plus sintering step to eliminate the backbone binder and fully densify the parts.

These technologies have proven to obtain very good microstructures for 10% Co, although they exhibit some macroporosities due to printing limitations (Lengauer *et al.*, 2018; Yang *et al.*, 2020). An alternative to this extrusion-based AM has been developed by the Fraunhofer IKTS: Thermoplastic 3D printing (T3DP) builds the part using a precise deposition of small droplets of molten thermoplastic hard-metal-containing suspensions. After debinding and sintering, full densities were achieved, no defects were found and homogeneous microstructures were obtained (Scheithauer *et al.*, 2017; Pötschke *et al.*, 2017).

3.2.2. Alternative sintering technologies

Conventional sintering cycles are very well suited to cemented carbides and can be designed to optimize the densification of different grades. However, they also present several drawbacks:

- Time, as they tend to be long cycles, and that makes the process inefficient for short series;
- High energy consumption, leading to an important carbon footprint of these processes;
- Difficulty in sintering some alternative binders using long conventional cycles, as they might react with each other.

All those reasons lead to alternative sintering technologies being evaluated (Guillon *et al.*, 2023).

The commercial alternative technology mostly used in the past years for hardmetals is Field-assisted Sintering Technique/Spark Plasma Sintering (FAST/SPS). This technology, which has been in the market for decades, is a low-voltage, current-activated, pressure-assisted sintering process (**Fig. 8**). This combination of heating and pressure gives high heating rates and short cycle times (5–20 min), making this process very suitable for materials with low sintering activity or high reactivity (Eriksson *et al.*, 2013; Guillon *et al.*, 2014).

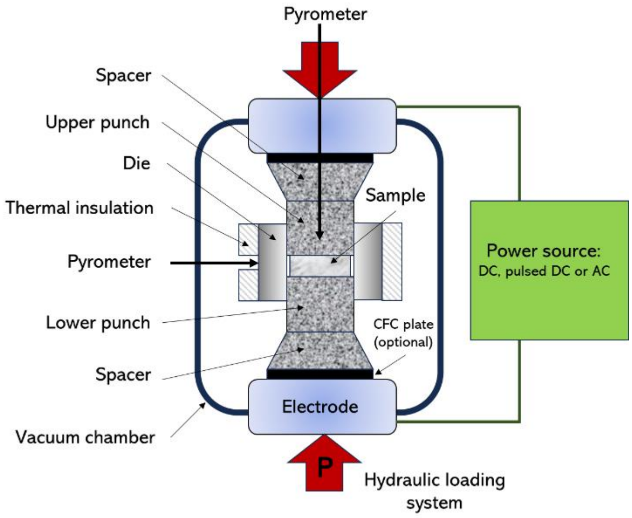

Figure 8. Schematics of the SPS process.
Source: Adapted from Bram *et al.* (2022).

Due to these characteristics, many studies have been conducted using FAST/SPS to sinter binderless powders (Tang *et al.*, 2017), nanopowders (Chuvil'deev *et al.*, 2017) or composites of tungsten carbide with other ceramics (W. Chen *et al.*, 2014; Sribalaji *et al.*, 2017; Wang *et al.*, 2018), leading to interesting results.

In recent years, some research has been dedicated to exploring additional sintering mechanisms that are not present in conventional sintering. Although the physics behind those sintering mechanisms has been shown, it is too soon to implement these processes in the industry (Guillon *et al.*, 2014; 2023). An example of these technologies is flash sintering (applying an electric field to a green body while it is heated in a conventional furnace) (Wachowicz *et al.*, 2023).

3.3. Advanced testing

Cemented carbides face such a wide array of stress-temperature-environment combinations that only a few standard parameters, as exposed in previous section 2.3, cannot describe the performance in all different applications. In terms of macroscale testing of mechanical properties, mechanical strength and abrasion wear resistance are standardized. Strength, typically measured by bending as transverse rupture (TRS), is limited by size, shape, and distribution of flaws (pore, crack, or inclusion), and by the stress distribution in the structure, i.e., the larger the body or test piece, the weaker it is since a large part has a greater chance of having a large flaw (Zak Fang *et al.*, 2014).

The abrasion resistance measured through ASTM B611 is known to be correlated with hardness following an expression of the form V = A $\exp^{(-BH)}$, where V is the wear volume, H is the sample hardness and A and B are constants (Gee *et al.*, 2007).

Although the abrasion resistance is the only wear mode standardized for cemented carbides, it is not the only one that can be found. Other wear modes experienced by these materials are adhesive wear, fatigue, erosion, and cavitation coming from sliding, rolling, impact, fretting or slurry contacts (**Table 2**) (Beste *et al.*, 2001; Bonny *et al.*, 2010; Gee *et al.*, 2007; Lavigne *et al.*, 2022; Perez Delgado *et al.*, 2011). Typical features that result from these wear mechanisms can be binder extrusion and removal, accumulation of plastic strain in WC grains, cracking of individual WC grains and between them, and even WC grain pullout.

A compiled literature about the influence of microstructure and composition around these topics is very scarce given the many different testing parameters that can be considered in each wear test method. **Figure 9** (left side) illustrates some of the morphologic features that can be observed during those tests.

The situation becomes more complex when these mechanical requirements need to accommodate different ranges of temperatures and surrounding media. Therefore, hot hardness, oxidation, creep, and corrosion, as well as wear-corrosion synergy effects have been tested (Boukantar *et al.*, 2021; Fathipour *et al.* 2024; Gant *et al.*, 2004; Guo *et al.* 2018; Lebedev *et al.* 2023; Maier *et al.* 2021; Tang *et al.*, 2023). All these properties are generally evaluated according to the microstructural parameters and binder nature.

Table 2. General standards used to test wear in cemented carbides.

Standard ref	Test
ASTM G65	Standard Test Method for Measuring Abrasion Using the Dry Sand/Rubber Wheel Apparatus
ASTM G133	Standard Test Method for Linearly Reciprocating Ball-on-Flat Sliding Wear
ASTM G99	Standard Test Method for Wear Testing with a Pin-on-Disk Apparatus
ASTM G32	Standard Test Method for Cavitation Erosion Using Vibratory Apparatus
ASTM-G76	Standard Test Method for Conducting Erosion Tests by Solid Particle Impingement Using Gas Jets

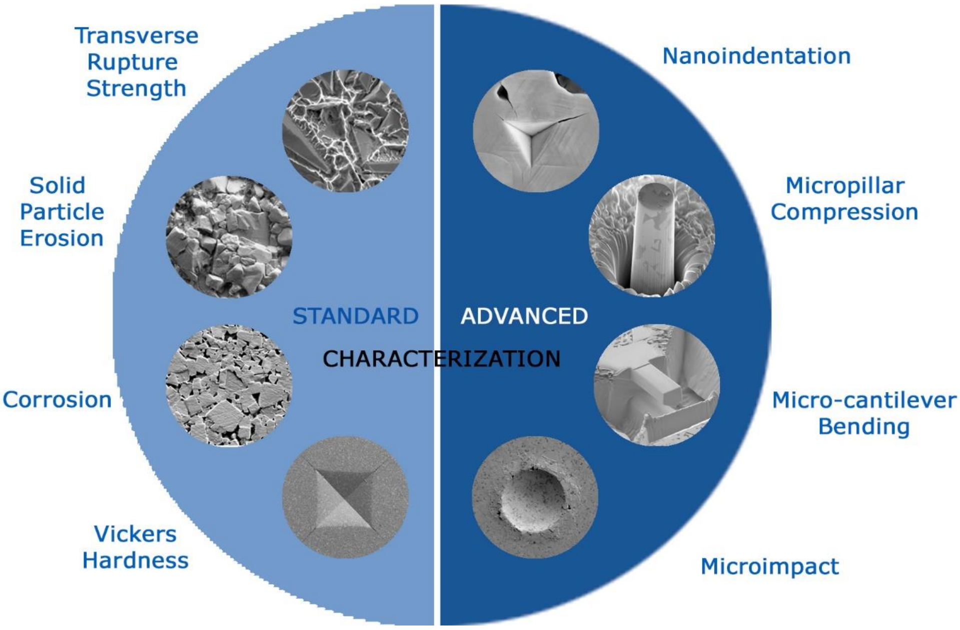

Figure 9. Some morphological features from cemented carbides tested in different conditions; left (standard) and right (advanced) characterization techniques.

Source: Elaborated by the authors using data from Cinca *et al.* (2019), Ortiz-Membrado *et al.* (2021), Sandoval Ravotti (2019), Hyperion Materials & Technologies (2019).

Due to the cost and time-consuming efforts to provide complete characterization, and to facilitate new materials development, machine learning strategies have also been introduced in this sector (Guan *et al.*, 2022). However, their use is not yet of widespread knowledge.

Interestingly, many of the material developments have been linked and helped by emerging advanced testing and characterization methods that appear due to the necessity in materials science to further explore connections between microstructure and bonding with final properties. Hence, in recent years, the use of conventional techniques has been complemented with the use of more sophisticated ones working at the micro and nanoscale.

The understanding of the material performance at small scales is important because the mechanical failure of any bulk material is triggered by the formation, extension, or local accumulation of initial small defects (Naughton-Duszová *et al.*, 2019). Specifically for cemented carbides, classical works focused on the intergranular and intragranular fracture of WC grains, the formation and rupture of Co ligaments and the decohesion of the Co-WC interface, even on crack propagation and plastic deformation of the binder.

In recent years, 3D visualization techniques, such as serial sectioning, Focused Ion Beam /Field Emission Scanning Electron Microscopy (FIB/FESEM) Tomography, X-ray tomography, Transmission Electron Microscopy (TEM) based tomography and atom probe tomography are becoming helpful in providing images of the internal structures, specifically on the spatial distribution of phases, real feature shapes and sizes, and feature connectivity. The FIB/FESEM tomography has been used by some scientists to reveal the complexity of the WC carbide skeleton and binder ligaments in cemented carbides to study crack propagation (Jiménez-Piqué *et al.*, 2017; Tarragó *et al.*, 2015).

Nanoindentation is the most appropriate technique to determine mechanical properties such as hardness and elastic modulus for the constitutive phases. However, intrinsic response of constitutive phases is usually not considered in the overall behavior of the composite material. For example, it has been established that hardness of WC is anisotropic (Naughton-Duszová *et al.*, 2013; Roebuck *et al.*, 2012), with hardness values for WC basal planes significantly higher than for the prismatic orientation.

Focused ion-beam (FIB) has also been used to investigate the morphological features below local phase nanoindentations (Walbrühl *et al.*, 2018). Electron Backscattered Diffraction (EBSD), Scanning Electron Microscopy (SEM) and Atomic Force Microscopy (AFM) have been used to evaluate the dependence of hardness and deformation mechanisms on orientation for WC grains in coarse WC-Co materials (Csanádi *et al.*, 2015).

Furthermore, binder is a Co-W-C alloy in which the amount of the alloying elements plays an important role on the intrinsic hardness and deformation mechanisms. On the other hand, disposition of the surrounding carbide particles, i.e., constraint degree, affects its flow stress in the composite (Roa *et al.*, 2016). All these measurements have been lately complemented by the statistical analysis provided in massive nanoindentation studies on the small scale, reporting hardness values for Co-based binder of around 8 GPa constrained by the WC grains. Around 30 GPa and 22 GPa were measured for the basal and prismatic WC planes, respectively (Roa *et al.*, 2015).

Walbrühl *et al.* (2018) studied thoroughly the hardness of an alternative Ni-based binder in cemented carbides (85Ni15Fe alloy). In their study, they assessed the effect of the WC particles surrounding the indentation made in the metallic binder. According to their results, the measured hardness of the metallic binder first should be corrected to neglect the pile-up effect found in Ni alloys. Moreover, the measured hardness increases with the proximity of WC particles to the indentation, obtaining the maximum value when the indentation touches a carbide particle. After correction, intrinsic hardness of the metallic binder approximates its value, to that of a bulk alloy with similar composition. Such finding is critical as input for FEM simulations.

Regarding small scale, many studies have found estimated data in agreement with experimental data by assuming an effect of the length scale, such as a Hall-Petch relationship in intrinsic hardness of constitutive phases, regardless the constrain factors (Shatov *et al.*, 2014b; Xu and Ågren, 2004). Besides nanoindentation, uniaxial compression of micropillars gives further insights on the local response of cemented carbides.

Samples for uniaxial compression of micropillars are micron-sized pillars prepared by FIB milling. Micropillars are afterwards deformed with a nanoindenter equipped with a flat punch. The failure initiation at WC/Co and WC/WC has been investigated according to the specimen size through in-situ uniaxial compression and FESEM microscopy. Different mechanical responses depend on the ratio of the WC grain size and micropillar diameter (Csanádi *et al.*, 2014; Sandoval Ravotti *et al.*, 2018; 2019).

Material deformation and fracture have also been examined by micro-beam bending through free-standing micro-cantilevers, where also the specimen size is of importance (Csanádi *et al.*, 2020; Elizalde *et al.*, 2018; Klünsner *et al.*, 2011; Ortiz-Membrado *et al.*, 2021; Trueba *et al.*, 2014). Load vs. displacement curves have been reported with the analysis of fractographic behaviours. The technique has contributed to evaluating the role of individual microstructural features in cemented carbides (single WC crystals and single Co ligaments as well as WC/WC and WC/Co boundaries) (Csanádi *et al.*, 2020; Trueba *et al.*, 2014). An average mechanical strength of 6.32 GPa for ultrafine specimens with 8.2 wt.% Co content and 5.46 Gpa for those with 12 wt.% Co content were found (Klünsner *et al.*, 2011). Fracture strength values as high as 20-25 Gpa for WC/WC boundaries in a 6.5 wt.% Co coarse cemented carbide were found (Elizalde *et al.*, 2018). Also, in a coarse specimen but with 16.7 vol.% Co, most of the WC/WC boundaries exhibited brittle failure with an average fracture strength of 4.1 ± 2.5 GPa (Csanádi *et al.*, 2020). Fracture toughness of single WC grains has been also assessed as 5.6 ± 0.8 $\text{MPa}\cdot\text{m}^{1/2}$ by means of the micro-beam bending technique (Ortiz-Membrado *et al.*, 2021).

Additionally, the use of spherical indenters for monotonic and cyclic Hertzian indentation loading has attracted attention with the aim to evaluate plastic deformation features beneath the indenter as well as residual strength.

In the last years, monotonic loading has been used to evaluate the damage tolerance of cemented carbides, i.e., deformation prevailing over fracture as damage mode. This allows the optimization of the microstructural design to improve reliability by mapping the transition from brittle to quasi-plastic damage (Góez *et al.*, 2012; Mahani *et al.*, 2024). On the other hand, the use of cyclic loading is useful to evaluate fatigue sensitivity.

The use of macro, micro and nano-scale impact tests have been useful to test WC-Co specimens with thin coatings where the ratio of coating thickness t to the indenter radius R (t/R), has been explored. Deformation and failure mechanisms depend on applied load and indenter sharpness (Beake, 2022). In nano-impact test for coated specimens, due to force limitations, very sharp probes are used, which can break eventually if testing tough materials. Micro-impact tests (repetitive loads at 1-3N) have been used to avoid probe damage. This test is severe/accelerated even at low forces, and it is an “in situ” test where the impact damage is followed cycle by cycle.

Deformation and cracking of uncoated cemented carbides has been found to be dependent on the H/E and H^3/E^2 ratios (H being the hardness and E the elastic modulus), known as the elastic strain to break and the resistance to plastic deformation, respectively (Cinca *et al.*, 2019).

Wear at the micro and nanoscale also has been examined in the last decade by means of scratch testing. Diamond indenters with different radii have been used while applying different loads and sliding speeds. The friction coefficient is systematically recorded, and the damage mechanisms examined. Intergranular and intragranular WC cracking as well as at WC-Co interfaces have been found (Gee *et al.*, 2017; Gee and Nimishakavi, 2011). As it can be defined as an abrasion wear mode, it has been also found that smaller WC grain sizes lead to better wear resistance.

The same methodology as in a scratch test but with different stylus material has been used to evaluate adhesive wear, concluding that submicrometric surface irregularities have more influence than carbide composition on metal transfer (Olsson and Cinca, 2024).

Finally, nanoindentation, scratch and contact damage tests in aggressive media show evidence of corrosion effects (by removal of the metallic binder) in the mechanical integrity of cemented carbides (Gant *et al.*, 2013; Zheng *et al.*, 2019; 2022a; 2022b). **Figure 9** (right side) illustrates features of tested cemented carbides by means of those micromechanical characterization methods above described.

4. Concluding remarks

Within these 100 years of existence for cemented carbides, progress on new formulations and processing methods has been made. However, the last decade has witnessed an increased challenge given the necessity of substituting Co, not only due to its carcinogenic effects, but to its consideration as a critical raw material by the European Union.

With the necessity to assist more demanding applications, academic and industrial experts have extensively worked to overcome these potential challenges. This has resulted in increased publications where High Entropy Alloys (HEAs) have been explored due to their high hardness at elevated temperatures in addition to high wear and corrosion resistance.

Moreover, the boom in additive manufacturing technologies and the application of Spark Plasma Sintering or Field-assisted Sintering Technique (FAST/SPS) to sinter binderless powders, nanopowders or composites of tungsten carbide with other ceramics has opened new possibilities.

Finally, new, and advanced characterization techniques such as nanoindentation, compression of micropillars and micro-beam bending through free-standing micro-cantilevers, are helping to provide insights into the mechanical properties of cemented carbides and their constitutive phases.

Authors' contributions

Conceptualization: Sandoval Ravotti, D. S.; Melero, H.; Cinca, N.; **Data collection:** Not applicable; **Formal Analysis:** Not applicable; **Funding acquisition:** Not applicable; **Investigation:** Not applicable; **Methodology:** Not applicable; **Project administration:** Not applicable; **Resources:** Not applicable; **Software:** Not applicable; **Supervision:** Cinca, N.; **Validation:** Not applicable; **Visualization:** Not applicable; **Writing – original draft:** Sandoval Ravotti, D. S.; Melero, H.; Cinca, N.; **Writing – review & editing:** Sandoval Ravotti, D. S.; Melero, H.; Cinca, N.

Data availability statement

Data sharing is not applicable.

Funding

Not applicable.

Acknowledgments

The authors want to acknowledge the marketing team at Hyperion Materials and Technologies for providing editing help of internal pictures.

References

Altıparmak, S. C.; Yardley, V. A.; Shi, Z.; Lin, J. Extrusion-based additive manufacturing technologies: State of the art and future perspectives. *J. Manufact. Proc.* **2022**, 83, 607–636. https://doi.org/10.1016/j.jmapro.2022.09.032

Beake, B. D. Nano- and Micro-Scale Impact Testing of Hard Coatings: A Review. *Coatings.* **2022**, *12* (6), 793. https://doi.org/10.3390/COATINGS12060793

Berger, C.; Pötschke, J.; Scheithauer, U.; Michaelis, A. Correlation of Different Cemented Carbide Starting Powders with the Resulting Properties of Components Manufactured via Binder Jetting. *Metals.* **2023**, *13*, 1848. https://doi.org/10.3390/met13111848

Beste, U.; Hammerström, L.; Engqvist, H.; Rimlinger, S.; Jacobson S. Particle erosion of cemented carbides with low Co content. *Wear.* **2001**, *250* (1–12), 809–817. https://doi.org/10.1016/S0043-1648(01)00735-9

Bonny, K.; De Baets, P.; Quintelier, J.; Vleugels, J.; Jiang, D.; VanderBiest, O.; Lauwers, B.; Liu, W. Surface finishing: Impact on tribological characteristics of WC–Co hardmetals. *Tribol. Int.* **2010**, *43* (1–2), 40–54. https://doi.org/10.1016/j.triboint.2009.04.029

Booklet. *ADDITIVE MANUFACTURING TECHNOLOGY A Guide for Designers and Engineers.* EPMA, 2019. https://www.epma.com/european-additive-manufacturing-group (accessed 2024-01-01).

Boukantar, A. R.; Djerdjare, B.; Guiberteau, F.; Ortiz, A. L. A Critical Comparison of the Tribocorrosive Performance in Highly-Alkaline Wet Medium of Ultrafine-Grained WC Cemented Carbides with Co, Co+Ni, or Co+Ni+Cr Binders. *Int. J. Refract. Metals Hard Mater.* **2021**, *95*, 105452. https://doi.org/10.1016/j.ijrmhm.2020.105452

Bram, M.; Beynet, Y.; Van Der Laan, A.; Neubauer, E.; Guillon, O.; Huber, J.; Trapp, J.; Keszler, M.; Luthardt, B.; Hennicke, J. *Introduction to Field-Assisted Sintering Technology/Spark Plasma Sintering (FAST/SPS)*; 2022.

Carreño-Morelli, E.; Alveen, P.; Moseley, S.; Rodriguez-Arbaizar, M.; Cardoso, K. Three-Dimensional Printing of Hard Materials. *Int. J. Refract. Metals Hard Mater.* **2020**, *87*, 105110. https://doi.org/10.1016/j.ijrmhm.2019.105110

Chen, W. H.; Lin, H. T.; Nayak, P. K.; Huang, J. L. Material Properties of Tungsten Carbide-Alumina Composites Fabricated by Spark Plasma Sintering. *Ceram. Int.* **2014**, *40* (9 PART B), 15007–15012. https://doi.org/10.1016/j.ceramint.2014.06.102

Chen, R.; Zheng, S.; Zhou, R.; Wei, B.; Yang, G.; Chen, P.; Cheng, J. Development of Cemented Carbides with CoxFeNiCrCu High-Entropy Alloyed Binder Prepared by Spark Plasma Sintering. *Int. J. Refract. Metals Hard Mater.* **2022**, *103*, 105751. https://doi.org/10.1016/J.IJRMHM.2021.105751

Chen, C.; Huang, B.; Liu, Z.; Li, Y.; Zou, D.; Liu, T.; Chang, Y.; Chen, L. Additive Manufacturing of WC-Co Cemented Carbides: Process, Microstructure, and Mechanical Properties. *Additive Manufacturing.* **2023**, *63*, 103410. https://doi.org/10.1016/j.addma.2023.103410

Chuvil'deev, V. N.; Blagoveshchenskiy, Y. V.; Nokhrin, A. V.; Boldin, M. S.; Sakharov, N. V.; Isaeva, N. V.; Shotin, S. V.; Belkin, O. A.; Popov, A. A.; Smirnova, E. S.; Lantsev, E. A. Spark Plasma Sintering of Tungsten Carbide Nanopowders Obtained through DC Arc Plasma Synthesis. *J. Alloys Compd.* **2017**, *708*, 547–561. https://doi.org/10.1016/j.jallcom.2017.03.035

Chychko, A.; García, J.; Collado Ciprés, V.; Holmström, E.; Blomqvist, A. HV-KIC Property Charts of Cemented Carbides: A Comprehensive Data Collection. *Int. J. Refract. Metals Hard Mater.* **2022**, *103*, 105763. https://doi.org/10.1016/j.ijrmhm.2021.105763

Cinca, N.; Beake, B. D.; Harris, A. J.; Tarrés, E. Micro-Scale Impact Testing on Cemented Carbides. *Int. J. Refract. Metals Hard Mater.* **2019**, *84*, 105045. https://doi.org/10.1016/J.IJRMHM.2019.105045

Cramer, C. L.; Aguirre, T. G.; Wieber, N. R.; Lowden, R. A.; Trofimov, A. A.; Wang, H.; Yan, J.; Paranthaman, M. P.; Elliott, A. M. Binder Jet Printed WC Infiltrated with Pre-Made Melt of WC and Co. *Int. J. Refract. Metals Hard Mater.* **2020**, *87*, 105137. https://doi.org/10.1016/j.ijrmhm.2019.105137

Csanádi, T.; Bl'anda, M.; Naughton-Duszová, A.; Chinh, N. Q.; Szommer, P.; Dusza, J. Deformation Characteristics of WC Micropillars. *J. Eur. Ceram. Soc.* **2014**, *34* (15), 4099–4103. https://doi.org/10.1016/J.JEURCERAMSOC.2014.05.045

Csanádi, T.; Bl'Anda, M.; Chinh, N. Q.; Hvizdoš, P.; Dusza, J. Orientation-Dependent Hardness and Nanoindentation-Induced Deformation Mechanisms of WC Crystals. *Acta Mater.* **2015**, *83*, 397–407. https://doi.org/10.1016/J.ACTAMAT.2014.09.048

Csanádi, T.; Vojtko, M.; Dusza, J. Deformation and Fracture of WC Grains and Grain Boundaries in a WC-Co Hardmetal during Microcantilever Bending Tests. *Int. J. Refract. Metals Hard Mater.* **2020**, *87*, 105163. https://doi.org/10.1016/J.IJRMHM.2019.105163

Davis, J. R. *ASM Specialty Handbook:* Tool Materials; ASM International, 1995.

Dong, D.; Xiang, X.; Huang, B.; Xiong, H.; Zhang, L.; Shi, K.; Liao, J. Microstructure and Properties of WC-Co/CrMnFeCoNi Composite Cemented Carbides. *Vacuum.* **2020**, *179*, 109571. https://doi.org/10.1016/J.VACUUM.2020.109571

Elizalde, M. R.; Ocaña, I.; Alkorta, J.; Sánchez-Moreno, J. M. Mechanical Strength Assessment of Single WC-WC Interfaces Present in WC-Co Hardmetals through Micro-Beam Bending Experiments. *Int. J. Refract. Metals Hard Mater.* **2018**, *72*, 39–44. https://doi.org/10.1016/J.IJRMHM.2017.12.009

Elliot, A.; Cramer, C.; Nandwana, P. *Binder Jetting and Sintering in Additive Manufacturing*; USDOE Office of Energy Efficiency and Renewable Energy (EERE), 2020. https://doi.org/10.31399/asm.hb.v24.a0006569

Enneti, R. K.; Prough, K. C. Wear Properties of Sintered WC-12%Co Processed via Binder Jet 3D Printing (BJ3DP). *Int. J. Refract. Metals Hard Mater.* **2019**, *78*, 228–232. https://doi.org/10.1016/j.ijrmhm.2018.10.003

Eriksson, M.; Radwan, M.; Shen, Z. Spark Plasma Sintering of WC, Cemented Carbide and Functional Graded Materials. *Int. J. Refract. Metals Hard Mater.* **2013**, *36*, 31–37. https://doi.org/10.1016/j.ijrmhm.2012.03.007

Ettmayer, P.; Kolaska, H.; Ortner, H. M. History of Hardmetals. In *Comprehensive Hard Materials Vol. 1-3*; Sarin, V.; Mari, D.; Llanes, L.; Nebel, C. E., Eds.; Elsevier, 2014; pp 3–27. https://doi.org/10.1017/CBO9781107415324.004

Exner, H. E. Physical and Chemical Nature of Cemented Carbides. *Int. Mat. Rev.* **1979**, *4*, 1149–1173. https://doi.org/10.1179/imtr.1979.24.1.149

Fathipour, Z.; Hadi, M.; Maleki, M.R.; Fernandes, F. Effect of Binder on Oxidation Properties of Tungsten Carbides: A Review by a Conceptual Classification Approach. *Ceramics.* **2024**, *7*, 166–191. https://doi.org/10.3390/ceramics7010011

Fayyaz, A.; Muhamad, N.; Sulong, A. B.; Rajabi, J.; Wong, Y. N. Fabrication of Cemented Tungsten Carbide Components by Micro-Powder Injection Moulding. *J. Mater. Process Technol.* **2014**, *214* (7), 1436–1444. https://doi.org/10.1016/j.jmatprotec.2014.02.006

Fayyaz, A.; Muhamad, N.; Sulong, A. B. Microstructure and Physical and Mechanical Properties of Micro Cemented Carbide Injection Moulded Components. *Powder Technol.* **2018**, *326*, 151–158. https://doi.org/10.1016/j.powtec.2017.12.011

Furberg, A.; Arvidsson, R.; Molander, S. Environmental Life Cycle Assessment of Cemented Carbide (WC-Co) Production. *J. Clean Prod.* **2019**, *209*, 1126–1138. https://doi.org/10.1016/j.jclepro.2018.10.272

Gant, A. J.; Gee, M. G.; May, A. T. The Evaluation of Tribo-Corrosion Synergy for WC-Co Hardmetals in Low Stress Abrasion. *Wear.* **2004**, *256* (5), 500–516. https://doi.org/10.1016/j.wear.2003.04.001

Gant, A. J.; Gee, M. G.; Gohil, D. D.; Jones, H. G.; Orkney, L. P. Use of FIB/SEM to Assess the Tribo-Corrosion of WC/Co Hardmetals in Model Single Point Abrasion Experiments. *Tribol. Int.* **2013**, *68*, 56–66. https://doi.org/10.1016/J.TRIBOINT.2012.11.008

García, J.; Collado Ciprés, V.; Blomqvist, A.; Kaplan, B. Cemented Carbide Microstructures: A Review. *Int. J. Refract. Metals Hard Mater.* **2019**, *80*, 40–68. https://doi.org/10.1016/j.ijrmhm.2018.12.004

Gee, M. G.; Gant, A.; Roebuck, B. Wear Mechanisms in Abrasion and Erosion of WC / Co and Related Hardmetals. *Wear.* **2007**, *263*, 137–148. https://doi.org/10.1016/j.wear.2006.12.046

Gee, M. G.; Nimishakavi, L. Model Single Point Abrasion Experiments on WC/Co Hardmetals. *Int. J. Refract. Metals Hard Mater.* **2011**, *29* (1), 1–9. https://doi.org/10.1016/J.IJRMHM.2010.04.009

Gee, M.; Mingard, K.; Nunn, J.; Roebuck, B.; Gant, A. In Situ Scratch Testing and Abrasion Simulation of WC/Co. *Int. J. Refract. Metals Hard Mater.* **2017**, *62*, 192–201. https://doi.org/10.1016/J.IJRMHM.2016.06.004

German, R. M. *A-Z of Powder Metallurgy*; Elsevier, 2005.

Góez, A.; Coureaux, D.; Ingebrand, A.; Reig, B.; Tarrés, E.; Mestra, A.; Mateo, A.; Jiménez-Piqué, E.; Llanes, L. Contact damage and residual strength in hardmetals, *Int. J. Refract. Metals Hard Mater.* **2012**, *30*, 121–127. https://doi.org/10.1016/j.ijrmhm.2011.07.013

Grilli, M. L.; Bellezze, T.; Gamsjäger, E.; Rinaldi, A.; Novak, P.; Balos, S.; Piticescu, R. R.; Ruello, M. L. Solutions for Critical Raw Materials under Extreme Conditions: A Review. *Materials.* **2017**, *10*, 285. https://doi.org/10.3390/ma10030285

Grohol, M; Veeh, C. *Study on the Critical Raw Materials for the EU 2023*; European Comission, 2023. https://op.europa.eu/en/publication-detail/-/publication/57318397-fdd4-11ed-a05c-01aa75ed71a1 (accessed 2024-01-01).

Guan, Z.; Li, N.; Zhang, W.; Wang, J.; Wang, C.; Shen, Q.; Xu, Z.; Peng, J.; Du, Y. A Multiple Loops Machine Learning Framework to Predict the Properties of WC–Co Based Cemented Carbides. *Int. J. Refract. Metals Hard Mater.* **2022**, *104*, 105798. https://doi.org/10.1016/j.ijrmhm.2022.105798

Guillon, O.; Gonzalez-Julian, J.; Dargatz, B.; Kessel, T.; Schierning, G.; Räthel, J.; Herrmann, M. Field-Assisted Sintering Technology/Spark Plasma Sintering: Mechanisms, Materials, and Technology Developments. *Adv. Eng. Mater.* **2014**, *16* (7), 830–849. https://doi.org/10.1002/adem.201300409

Guillon, O.; Rheinheimer, W.; Bram, M. A Perspective on Emerging and Future Sintering Technologies of Ceramic Materials. *Adv. Eng. Mater.* **2023**, *25*, 2201870. https://doi.org/10.1002/adem.202201870

Guo, B.; Zhang, L.; Cao, L.; Zhang, T.; Jiang, F.; Yan, L. The Correction of Temperature-Dependent Vickers Hardness of Cemented Carbide Base on the Developed High-Temperature Hardness Tester. *J. Mater. Process Technol.* **2018**, *255*, 426–433. https://doi.org/10.1016/J.JMATPROTEC.2017.12.041

Gupta, A. K.; Taulik, M. Effect of Process Variables on Performances Measured in Filament and Pellet Based Extrusion Processes. *Materials Today.* **2021**, *47* (15) 5177–5184. https://doi.org/10.1016/j.matpr.2021.05.508

Gurland, J. New scientific approaches to development of tool materials. *Int. Mater. Rev.* **1988**, *33* (1), 151–166. https://doi.org/10.1179/imr.1988.33.1.151

Heng, S. Y.; Raza, M. R.; Muhamad, N.; Sulong, A. B.; Fayyaz, A. Micro-Powder Injection Molding (MPIM) of Tungsten Carbide. *Int. J. Refract. Metals Hard Mater.* **2014**, *45*, 189–195. https://doi.org/10.1016/j.ijrmhm.2014.04.012

Hering, B.; Gestrich, T.; Steinborn, C.; Vornberger, A.; Pötschke, J. Influence of Alternative Hard and Binder Phase Compositions in

Hardmetals on Thermophysical and Mechanical Properties. *Metals.* **2023**, *13*, 1803. https://doi.org/10.3390/met13111803

Hu, D.; Liu, Y.; Chen, H.; Wang, M. Microstructure and Wear Resistance of Ni-Based Tungsten Carbide Coating by Laser Cladding on Tunnel Boring Machine Cutter Ring. *Surf. Coat. Technol.* **2020**, *404*, 126432. https://doi.org/10.1016/j.surfcoat.2020.126432

Hyperion Materials & Technologies. *All about cemented carbide*. http://www.allaboutcementedcarbide.com/ (accessed 2019-08-22).

Javaid, M.; Haleem, A.; Singh, R.; Suman, R.; Rab, S. Role of additive manufacturing applications towards environmental sustainability. *Adv. Ind. Eng. Polym. Res.* **2021**, *4* (4), 312. https://doi.org/10.1016/j.aiepr.2021.07.005

Jiménez-Piqué, E.; Turon-Vinas, M.; Chen, H.; Trifonov, T.; Fair, J.; Tarrés, E.; Llanes, L. Focused ion beam tomography of WC-Co cemented carbides, *Int. J. Refract. Metals Hard Mater.* **2017**, *67*, 9–17. https://doi.org/10.1016/j.ijrmhm.2017.04.007

Kim, H.; Kim, J. I.; Ryu, S. S.; Jeong, H. Cast WC-Co Alloy-Based Tool Manufacturing Using a Polymeric Mold Prepared via Digital Light Processing 3D Printing. *Mater. Lett.* **2022**, *306*. https://doi.org/10.1016/j.matlet.2021.130979

Klünsner, T.; Wurster, S.; Supancic, P.; Ebner, R.; Jenko, M.; Glätzle, J.; Püschel, A.; Pippan, R. Effect of specimen size on the tensile strength of WC–Co hard metal. *Acta Mater.* **2011**, *59*, 4244–4252. https://doi.org/10.1016/j.actamat.2011.03.049

Konyashin, I.; Lachmann, F.; Ries, B.; Mazilkin, A.; Straumal, B.; Kübel, C.; Llanes, L.; Baretzky, B. Strengthening Zones in the Co Matrix of WC–Co Cemented Carbides. *Scr Mater* **2014**, *83*, 17–20. https://doi.org/10.1016/J.SCRIPTAMAT.2014.03.026

Konyashin, I.; Ries, B.; Hlawatschek, D.; Zhuk, Y.; Mazilkin, A.; Straumal, B.; Dorn, F.; Park, D. Wear-Resistance and Hardness: Are They Directly Related for Nanostructured Hard Materials? *Int. J. Refract. Metals Hard Mater.* **2015**, *49* (1), 203–211. https://doi.org/10.1016/J.IJRMHM.2014.06.017

Konyashin, I. Approaching the 100th Anniversary of the Hardmetal Invention: From First WC-Co Samples towards Modern Advanced Hardmetal Grades. *Int. J. Refract. Metals Hard Mater.* **2023**, *111*, 106113. https://doi.org/10.1016/J.IJRMHM.2023.106113

Lavigne, O.; Cinca, N.; Ther, O.; Tarrés, E. Effect of Binder Nature and Content on the Cavitation Erosion Resistance of Cemented Carbides. *Int. J. Refract. Metals Hard Mater.* **2022**, *109*, 105978. https://doi.org/10.1016/j.ijrmhm.2022.105978

Lay, S.; Missiaen, J. M. Microstructure and Morphology of Hardmetals. In *Comprehensive Hard Materials*; Sarin, V. K., Mari, D., Llanes, L., Nebel, C. E., Eds.; Elsevier, 2014; pp 91–117.

Lebedev, A.; Alves, N.; Balbino, N.; Otoni Corrêa, E.; Roque Huanca, D.; Amaury De Freitas Matos, F.; De Carvalho Valeriano, L. Comparative Study of Corrosion Behaviors of WC-NiMo and WC-Co Cemented Carbides. *Materials.* **2023**, *16* (12), 4480. https://doi.org/10.3390/MA16124480

Lengauer, W.; Kukla, C.; Kitzmantel, M.; Duretek, I.; Schwarz, V.; Neubauer, E.; Lieberwirth, C.; Morrison, V. Preparation and properties of extrusion-based 3D-printed hardmetal and cermet parts. In: *Proceedings of the Euro PM2018 Congress & Exhibition Euro PM2018 Proceedings, Bilbao Exhibition Centre (BEC)*, Bilbao, Spain. 2018. p. 14-18.

Long, J.; Zhang, W.; Wang, Y.; Du, Y.; Zhang, Z.; Lu, B.; Cheng, K.; Peng, Y. A New Type of WC–Co–Ni–Al Cemented Carbide: Grain Size and Morphology of Γ′-Strengthened Composite Binder Phase. *Scr. Mater.* **2017**, *126*, 33–36. https://doi.org/10.1016/j.scriptamat.2016.08.007

Luo, W.; Liu, Y.; Liu, X.; Zhou, Z. Oxidation behavior of ultrafine WC-based cemented carbides with AlxCoCrCuFeNi high-entropy alloy binders. *Ceram. Intern.* **2021**, *47*, 8498–8509. https://doi.org/10.3390/met13010171

Mahani, F.; Liu, C.; Sousa Machado, P. V.; Lin, L. L.; Wen, X.; Jiménez-Piqué, E.; Llanes, L.; Contact damage induced by means of conical indentation in hardmetals: Microstructural effects on residual strength. *Int. J. Refract. Metals Hard Mater.* **2024**, *118*, 106446, https://doi.org/10.1016/j.ijrmhm.2023.106446

Maier, K.; Klünsner, T.; Krobath, M.; Pichler, P.; Marsoner, S.; Ecker, W.; Czettl, C.; Schäfer, J.; Ebner, R. Creep Behaviour of WC-12 Wt% Co Hardmetals with Different WC Grain Sizes Tested in Uniaxial Tensile and Compression Step-Loading Tests at 700 °C and 800 °C. *Int. J. Refract. Metals Hard Mater.* **2021**, *100*, 105633. https://doi.org/10.1016/J.IJRMHM.2021.105633

Mingard, K. P.; Roebuck, B.; Marshall, J.; Sweetman, G. Some Aspects of the Structure of Cobalt and Nickel Binder Phases in Hardmetals. *Acta Mater.* **2011**, *59* (6), 2277–2290. https://doi.org/10.1016/J.ACTAMAT.2010.12.004

Miyanaji, H.; Orth, M.; Akbar, J. M.; Yang, L. Process Development for Green Part Printing Using Binder Jetting Additive Manufacturing. *Front. Mech. Eng.* **2018**, *13*, 504–512. https://doi.org/10.1007/s11465-018-0508-8

Mostafaei, A.; Neelapu, S. H. V. R.; Kisailus, C.; Nath, L. M.; Jacobs, T. D. B.; Chmielus, M. Characterizing surface finish and fatigue behavior in binder-jet 3D-printed nickel-based superalloy 625. *Additive Manufacturing.* **2018**, *24*, 200–209. https://doi.org/10.1016/j.addma.2018.09.012

Mueller-Grunz, A.; Alveen, P.; Rassbach, S.; Useldinger, R.; Moseley, S. The Manufacture and Characterization of WC-(Al)CoCrCuFeNi Cemented Carbides with Nominally High Entropy Alloy Binders. *Int. J. Refract. Metals Hard Mater.* **2019**, *84*, 105032. https://doi.org/10.1016/j.ijrmhm.2019.105032

Naughton-Duszová, A.; Csanádi, T.; Sedlák, R.; Hvizdoš, P.; Dusza, J. Small-Scale Mechanical Testing of Cemented Carbides from the Micro-to the Nano-Level: A Review. *Metals.* **2019**, *9* (5), 502. https://doi.org/10.3390/met9050502

Naughton-Duszová, A.; Halgaš, R.; Bl'anda, M.; Hvizdoš, P.; Lofaj, F.; Dusza, J.; Morgiel, J. Nanoindentation of WC–Co Hardmetals. *J. Eur. Ceram. Soc.* **2013**, *33* (12), 2227–2232. https://doi.org/10.1016/J.JEURCERAMSOC.2012.12.018

Nicolás-Morillas, M.; Besharatloo, H.; Alvaredo, P.; Roa, J. J.; Llanes, L.; Gordo, E. Design of alternative binders for hard materials. *Int. J. Refract. Metals Hard Mater.* **2020**, *87*, 105089. https://doi.org/10.1016/j.ijrmhm.2019.105089

Nicolás-Morillas, M.; Llanes, L.; Gordo, E. High-temperature wettability in hard materials: Comparison of systems with different binder/carbide phases and evaluation of C addition. *Int. J. Refract. Metals Hard Mater.* **2023**, *111*, 106081. https://doi.org/10.1016/j.ijrmhm.2022.106081

Nicolás-Morillas, M.; Besharatloo, H.; Cabezas, L.; la Mata, M.; Sales, D. L.; Pereira, L.; Müller-Grunz, A.; Bertalan, C.; Useldinger, R.; Llanes, L.; Gordo, E.; Processing of WC with Fe-based alternative binders: Adjustment of C content and effect of Cr addition. *Int. J. Refract. Metals Hard Mater.* **2024**, *118*, 106444. https://doi.org/10.1016/j.ijrmhm.2023.106444

Olsson, M.; Cinca, N. Mechanisms controlling friction and material transfer in sliding contacts between cemented carbide and aluminum during metal forming. *Int. J. Refract. Metals Hard Mater.* **2024**, *1184*, 106481. https://doi.org/10.1016/j.ijrmhm.2023.106481

Ortiz-Membrado, L.; Cuadrado, N.; Casellas, D.; Roa, J. J.; Llanes, L.; Jiménez-Piqué, E. Measuring the Fracture Toughness of Single WC Grains of Cemented Carbides by Means of Microcantilever Bending and Micropillar Splitting. *Int. J. Refract. Metals Hard Mater.* **2021**, *98*, 105529. https://doi.org/10.1016/j.ijrmhm.2021.105529

Ortner, H. M.; Ettmayer, P.; Kolaska, H. The History of the Technological Progress of Hardmetals. *Int. J. Refract. Metals Hard Mater.* **2014**, *44*, 148–159. https://doi.org/10.1016/j.ijrmhm.2013.07.014

Padmakumar, M. Additive Manufacturing of Tungsten Carbide Hardmetal Parts by Selective Laser Melting (SLM), Selective Laser Sintering (SLS) and Binder Jet 3D Printing (BJ3DP) Techniques. *Lasers in Manufacturing and Materials Processing*. **2020**, *7*, 338–371. https://doi.org/10.1007/s40516-020-00124-0

Perez Delgado, Y.; Bonny, K.; Baets, P.; Neis, P. D.; Rodriguez Fereira, V.; Malek, O.; Vleugels, J.; Lauwers, B. Dry sliding friction and wear response of WC-Co hardmetal pairs in linearly reciprocating and rotating contact. *Sustainable Construction and Design*. **2011**, 12–18.

Pötschke, J.; Berger, C.; Richter, H. J.; Scheithauer, U.; Weingarten, S. Additive manufacturing of hardmetals. In *Proceedings of European Powder Metallurgy*, 2017. https://publica-rest.fraunhofer.de/server/api/core/bitstreams/a474fa1b-4efe-4390-8560-5fd14b276368/content (accessed 2024-01-01).

Prakash, L. *Developments in Tungsten Carbide-Cobalt Cemented Carbides*; Inovar communications, 2008.

Prakash, L. Fundamentals and General Applications of Hardmetals. In *Comprehensive Hard Materials Vol. 1-3*; Sarin, V.; Mari, D.; Llanes, L.; Nebel, C. E., Eds.; Elsevier, 2014; pp 29–90.

Raihanuzzaman, R. M.; Xie, Z.; Hong, S. J.; Ghomashchi, R. Powder Refinement, Consolidation and Mechanical Properties of Cemented Carbides - An Overview. *Powder Technol.* **2014**, *261*, 1–13. https://doi.org/10.1016/j.powtec.2014.04.024

Roa, J. J.; Jimenez-Pique, E.; Verge, C.; Tarragó, J. M.; Mateo, A.; Fair, J.; Llanes, L. Intrinsic Hardness of Constitutive Phases in WC-Co Composites: Nanoindentation Testing, Statistical Analysis, WC Crystal Orientation Effects and Flow Stress for the Constrained Metallic Binder. *J. Eur. Ceram. Soc.* **2015**, *35* (13), 3419–3425. https://doi.org/10.1016/j.jeurceramsoc.2015.04.021

Roa, J. J.; Jiménez-Piqué, E.; Tarragó, J. M.; Sandoval Ravotti, D. A.; Mateo, A.; Fair, J.; Llanes, L. Hall-Petch Strengthening of the Constrained Metallic Binder in WC–Co Cemented Carbides: Experimental Assessment by Means of Massive Nanoindentation and Statistical Analysis. *Materials Science and Engineering: A.* **2016**, *676*, 487–491. https://doi.org/10.1016/J.MSEA.2016.09.020

Roebuck, B.; Almond, E. A. Deformation and Fracture Processes and the Physical Metallurgy of WC–Co Hardmetals. *International Materials Reviews.* **1988**, *33* (2), 90–110. https://doi.org/10.1179/095066088790324094

Roebuck, B.; Klose, P.; Mingard, K. P. Hardness of Hexagonal Tungsten Carbide Crystals as a Function of Orientation. *Acta Mater.* **2012**, *60* (17), 6131–6143. https://doi.org/10.1016/J.ACTAMAT.2012.07.056

Roulon, Z.; Missiaen, J. M.; Lay, S. Carbide Grain Growth in Cemented Carbides Sintered with Alternative Binders. *Int. J. Refract. Metals Hard Mater.* **2020**, *86*, 105088. https://doi.org/10.1016/j.ijrmhm.2019.105088

Sandoval Ravotti, D. A.; Rinaldi, A.; Tarragó, J. M.; Roa, J. J.; Fair, J.; Llanes, L. Scale Effect in Mechanical Characterization of WC-Co Composites. *Int. J. Refract. Metals Hard Mater.* **2018**, *72*, 157–162. https://doi.org/10.1016/J.IJRMHM.2017.12.029

Sandoval Ravotti, D. A. Small-Scale Testing of Micromechanical Response of Cemented Carbides. Thesis (Doctorate), Universitat Politècnica de Catalunya, Barcelona, 2019.

Sandoval Ravotti, D. A.; Roa, J. J.; Ther, O.; Tarrés, E.; Llanes, L. Micromechanical Properties of WC-(W,Ti,Ta,Nb)C-Co Composites. *J. Alloys. Compd.* **2019**, *777*, 593–601. https://doi.org/10.1016/J.JALLCOM.2018.11.001

Sandvik. Understanding cemented carbide. https://pt.scribd.com/document/375993631/SANDVIK-Understanding-cemented-carbide-pdf (accessed 2024-01-01).

Scheithauer, U.; Pötschke, J.; Weingarten, S.; Schwarzer, E.; Vornberger, A.; Moritz, T.; Michaelis, A. Droplet-Based Additive Manufacturing of Hard Metal Components by Thermoplastics 3D Printing. *J. Ceram. Sci. Tech*. **2017**, *8* (1), 155–160. https://doi.org/10.4416/JCST2016-00104

Shatov, A. V.; Ponomarev, S. S.; Firstov, S. A. Hardness and Deformation of Hardmetals at Room Temperature. In *Comprehensive Hard Materials Vol. 1-3*; Sarin, V.; Mari, D.; Llanes, L.; Nebel, C. E., Eds.; Elsevier, 2014a; pp 267–299. https://doi.org/10.1016/B978-0-08-096527-7.00009-X

Shatov, A. V.; Ponomarev, S. S.; Firstov, S. A. Fracture and strength of hardmetals at room temperature. In *Comprehensive Hard Materials Vol. 1-3*; Sarin, V.; Mari, D.; Llanes, L.; Nebel, C. E., Eds.; Elsevier, 2014b; pp 301–343. https://doi.org/10.1016/B978-0-08-096527-7.00010-6

Sheikh, S.; M'Saoubi, R.; Flasar, P.; Schwind, M.; Persson, T.; Yang, J.; Llanes, L. Fracture toughness of cemented carbides: Testing method and microstructural effects. *Int. J. Refract. Metals Hard Mater.* **2015**, *49*, 153–160. https://doi.org/10.1016/j.ijrmhm.2014.08.018

Sribalaji, M.; Mukherjee, B.; Islam, A.; Kumar Keshri, A. Microstructural and Mechanical Behavior of Spark Plasma Sintered Titanium Carbide with Hybrid Reinforcement of Tungsten Carbide and Carbon Nanotubes. *Materials Science and Engineering: A.* **2017**, *702*, 10–21. https://doi.org/10.1016/j.msea.2017.06.108

Steinlechner, R.; Oro Calderon, R.; Koch, T.; Linhardt, P.; Schubert, W. D. A Study on WC-Ni Cemented Carbides: Constitution, Alloy Compositions and Properties, Including Corrosion Behaviour. *Int. J. Refract. Metals Hard Mater.* **2022**, *103*, 105750. https://doi.org/10.1016/j.ijrmhm.2021.105750

Straumal, B.; Konyashin, I. WC-Based Cemented Carbides with High Entropy Alloyed Binders: A Review. *Metals* **2023**, *13*, 171. https://doi.org/10.3390/met13010171

Suzuki, A.; Inui, H.; Pollock, T. M. L12-Strengthened Cobalt-Base Superalloys. *Annu. Rev. Mater. Res.* **2015**, *45*, 345–368. https://doi.org/10.1146/ANNUREV-MATSCI-070214-021043

Tang, W.; Zhang, L.; Zhu, J. fei; Chen, Y.; Tian, W.; Liu, T. Effect of Direct Current Patterns on Densification and Mechanical Properties of Binderless Tungsten Carbides Fabricated by the Spark Plasma Sintering System. *Int. J. Refract. Metals Hard Mater.* **2017**, *64*, 90–97. https://doi.org/10.1016/j.ijrmhm.2017.01.010

Tang, T.; Xiao, X.; Xu, K.; Lou, M.; Hu, X.; Li, S.; Zhang, W.; Fan, Z.; Chang, K. Corrosion-Resistant WC-Co Based Cemented Carbides: Computational Design and Experimental Verification. *Int. J. Refract. Metals Hard Mater.* **2023**, *110*, 106044. https://doi.org/10.1016/J.IJRMHM.2022.106044

Tarragó, J. M.; Jiménez-Piqué, E.; Schneider, L.; Casellas, D.; Torres, Y.; Llanes, L. FIB/FESEM Experimental and Analytical Assessment of R-Curve Behavior of WC-Co Cemented Carbides. *Materials Science and Engineering: A.* **2015**, *645*, 142–149. https://doi.org/10.1016/j.msea.2015.07.090

Trueba, M.; Aramburu, A.; Rodríguez, N.; Iparraguirre, I.; Elizalde, M. R.; Ocaña, I.; Sánchez, J. M.; Martínez-Esnaola, J. M. “In-Situ” Mechanical Characterisation of WC–Co Hardmetals Using Microbeam Testing. *Int. J. Refract. Metals Hard Mater.* **2014**, *43*, 236–240. https://doi.org/10.1016/J.IJRMHM.2013.12.005

Upadhyaya, G. S. *Nature and Properties of Refractory Carbides*; Nova Science Publishers, 1996.

Upadhyaya, G. S. *Cemented Tungsten Carbides: Production, Properties and Testing*; Noyes Publications, 1998.

Upadhyaya, G. S. Materials Science of Cemented Carbides—an Overview. *Mater. Des.* **2001**, *22* (6), 483–489.

Wachowicz, J.; Kruzel, R.; Bałaga, Z.; Ostrowska, A.; Dembiczak, T. Application of U-FAST Technology in Sintering of Submicron WC-Co Carbides. *Materials.* **2023**, *16* (6), 2450.

Walbrühl, M.; Linder, D.; Ågren, J.; Borgenstam, A. Alternative Ni-Based Cemented Carbide Binder – Hardness Characterization by Nano-Indentation and Focused Ion Beam. *Int. J. Refract. Metals Hard Mater.* **2018**, *73*, 204–209. https://doi.org/10.1016/j.ijrmhm.2018.02.017

Wang, J.; Zuo, D.; Zhu, L.; Li, W.; Tu, Z.; Dai, S. Effects and Influence of Y2O3 Addition on the Microstructure and Mechanical Properties of Binderless Tungsten Carbide Fabricated by Spark Plasma Sintering. *Int. J. Refract. Metals Hard Mater.* **2018**, *71*, 167–174. https://doi.org/10.1016/j.ijrmhm.2017.11.016

Warren, R. Solid-Liquid Interfacial Energies in Binary and Pseudo-Binary Systems. *J. Mater. Sci.* **1980**, *15* (10), 2489–2496. https://doi.org/10.1007/BF00550752/METRICS

Wolfe, T. A.; Shah, R. M.; Prough, K. C.; Trasorras, J. L. Binder Jetting 3D Printed Cemented Carbide: Mechanical and Wear Properties of Medium and Coarse Grades. *Int. J. Refract. Metals Hard Mater.* **2023a**, *113*. https://doi.org/10.1016/j.ijrmhm.2023.106197

Wolfe, T.; Shah, R.; Prough, K.; Trasorras, J. L. Coarse Cemented Carbide Produced via Binder Jetting 3D Printing. *Int. J. Refract. Metals Hard Mater.* **2023b**, *110*, 106016. https://doi.org/10.1016/j.ijrmhm.2022.106016

Xu, Z. H.; Ågren, J. A Modified Hardness Model for WC–Co Cemented Carbides. *Materials Science and Engineering: A.* **2004**, *386*(1–2), 262–268. https://doi.org/10.1016/J.MSEA.2004.07.061

Xu, H.; Huang, H. Microstructure Evolution and Mechanical Properties of Thermally Sprayed Coating Modified by Laser Remelting and Injection with Tungsten Carbide. *Ceram. Int.* **2022a**, *48* (16), 22854–22868. https://doi.org/10.1016/j.ceramint.2022.04.189

Xu, H.; Huang, H. Plasma Remelting and Injection Method for Fabricating Metal Matrix Composite Coatings Reinforced with Tungsten Carbide. *Ceram. Int.* **2022b**, *48* (2), 2645–2659. https://doi.org/10.1016/j.ceramint.2021.10.048

Yang, Y.; Zhang, C.; Wang, D.; Nie, L.; Wellmann, D.; Tian, Y. Additive Manufacturing of WC-Co Hardmetals: A Review. *Int. J. Adv. Manuf. Tech.* **2020**, *108* (5–6), 1653–1673. https://doi.org/10.1007/s00170-020-05389-5

Zak Fang, Z.; Koopman. M. C. Cemented Tungsten Carbide Hardmetal-An Introduction. In *Comprehensive Hard Materials*; Sarin, V. K., Mari, D., Llanes, L., Nebel, C. E., Eds.; Elsevier, 2014; pp 123-137. https://doi.org/10.1016/B978-0-08-096527-7.00004-0

Zhao, Z.; Liu, F.; Zhao, M.; Zhong, L.; Xu, Y.; Li, J. A New Strategy to Efficiently Fabricate Tungsten Carbide Coating on Tungsten: Two-Step Interstitial Carburization. *Surf. Coat. Technol.* **2020**, *389*, 125579. https://doi.org/10.1016/j.surfcoat.2020.125579

Zheng, Y. F.; Fargas, G.; Besharatloo, H.; Serra, M.; Roa, J. J.; Armelin, E.; Lavigne, O.; Llanes, L.; Assessment of corrosion-induced changes on the mechanical integrity of cemented carbides at small length scales. *Int. J. Refract. Metals Hard Mater.* **2019**, *84*, 105033, https://doi.org/10.1016/j.ijrmhm.2019.105033

Zheng, Y.F.; Fargas, G.; Lavigne, O.; Serra, M.; Coureaux, D.; Zhang, P.P.; Yao, Z.H.; Zhang, Q.L.; Yao, J.H.; Llanes, L. Contact fatigue of WC-6%wtCo cemented carbides: Influence of corrosion-induced changes on emergence and evolution of damage, *Ceram. Int.* **2022a**, *48*, 5766-5774. https://doi.org/10.1016/j.ceramint.2021.11.124

Zheng, Y.; Fargas, G.; Armelin, E.; Lavigne, O.; Zhang, Q.; Yao, J.; Llanes, L. Influence of Corrosion-Induced Damage on Mechanical Integrity and Load-Bearing Capability of Cemented Carbides. *Metals.* **2022b**, *12*, 2104. https://doi.org/10.3390/met12122104

Zhou, P. F.; Xiao, D. H.; Yuan, T. C. Comparison between Ultrafine-Grained WC–Co and WC–HEA-Cemented Carbides. *Powder Metallurgy.* **2016**, *60* (1), 1–6. https://doi.org/10.1080/00325899.2016.1260903

Zhou, P. L.; Xiao, D. H.; Zhou, P. F.; Yuan, T. C. Microstructure and Properties of Ultrafine Grained AlCrFeCoNi/WC Cemented Carbides. *Ceram. Int.* **2018**, *44* (14), 17160–17166. https://doi.org/10.1016/J.CERAMINT.2018.06.171

Eclet. Quim. 49 | e-1514, 2024

Original Article

https://doi.org/10.26850/1678-4618.eq.v49.2024.e1514

Study of the impact of irradiation and temperature on physical and chemical characteristics of paracetamol

Hussein Manaa Ali **Al-Maydama**[1], Adlia Ahmad Mohammad **Abduljabbar**[2+]

Abstract

Pure paracetamol samples were subjected to temperature (40 °C) and light (sunlight, UV-lamp, and γ-ray) for time intervals. Treatment impact on the extent of chemical and physical impairments in the treated samples was pursued by comparing the results obtained from thermogravimetric analysis and differential scanning calorimeter (TGA/DSC), scanning electron microscopy (SEM), X-ray diffraction (XRD), high-performance liquid chromatography (HPLC), and photocatalytic decomposition process. Thermal analysis behavior, lifetime prediction, thermal stability, kinetics (i.e., E_a, Z, n), and thermodynamic (ΔG^*, ΔH^*, and ΔS^*) parameters were investigated for samples before and after exposure to heat and light from curves of the non-isothermal gravimetric analysis (TGA) at a heating rate of 10 °C min^{-1} and with an association of Coats-Redfern and the other standard equations. Changes in crystallinity percentage were calculated relative to the untreated sample using measurements of DSC and XRD. In some treated samples, changes in morphology and purity were observed in SEM images and HPLC results. Kinetic parameters were determined, and the photocatalytic degradation percentage was discussed.

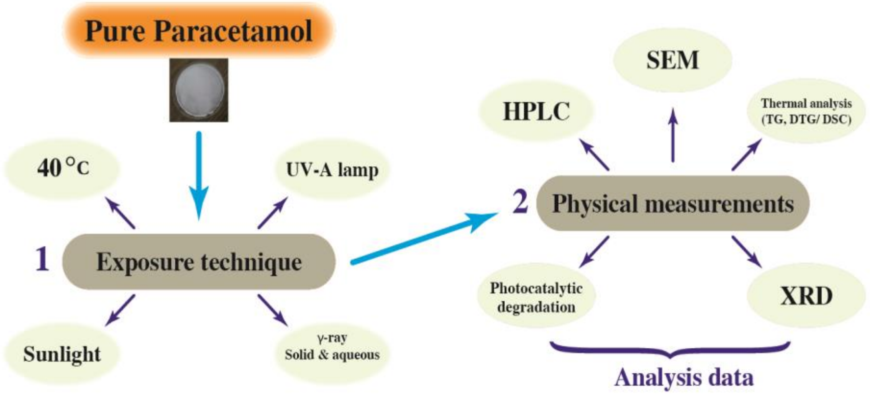

Article History

Received August 22, 2023
Accepted May 08, 2024
Published July 22, 2024

Keywords

1. Paracetamol;
2. Treatments;
3. TGA/DSC;
4. XRD;
5. SEM.

Section Editor

Irlon Maciel Ferreira

Highlights

- Thermal behavior of paracetamol allows for obtaining thermodynamic data.
- Changes in crystallinity and purity were observed by different techniques.
- Kinetic parameters and photocatalytic decomposition percentage were discussed.

[1] Sana'a University, Faculty of Science, Sana'a, Yemen. [2] Amran University, Faculty of Applied Sciences and Humanities, Amran, Yemen.
+Corresponding author: Adlia Ahmad Abduljabbar, **Phone:** +967736966503, **Email address:** dr.adlia@amu.edu.ye

1. Introduction

The chemical changes, physical state, or form, of Active Pharmaceutical Ingredients (API), as well as other performance characteristics of pharmacological products (such as dissolution, particle changes, and surface modifications), all have a substantial impact on product efficacy and safety (Huynh-Ba, 2010). The efficacy, safety, and quality of pharmaceutical products may be affected by various environmental factors, particularly those distributed in harsh climates or entering commerce abroad. Most environmental impact factors on stability are caused by insufficient storage (in heat, moisture, or sunlight), which can cause the medicine to degrade and lose its therapeutic properties (Akyar, 2011).

Acetaminophen, often known as paracetamol, is a popular analgesic and antipyretic used to treat fever and acute pain. Some studies (Lusina *et al.*, 2005) focused on how the characteristics of analgesics varied when exposed to normal and accelerated conditions (above 50 °C and 80% relative humidity). The studies that documented the decomposition of analgesics caused by radiation impacts were greatly improved, and each of these studies addresses the impact of long-term storage conditions (2 weeks - 3 months) (Suno *et al.*, 2015; Vermeire and Remon, 1999). In our paper published elsewhere (Al-Maydama *et al.*, 2018), such changes have been observed in the treated Aspirin samples by sunlight, UV-lamp, and γ-ray when compared with the untreated one.

When thermally evaluated utilizing single and multiple heating rates techniques with a change in its heat of fusion value, the thermal degradation of the paracetamol study was previously a topic of interest (Oliveira *et al.*, 2017; Schnitzler *et al.*, 2002; Tomassetti *et al.*, 2005). Studies on the photocatalytic degradation of the analgesics (paracetamol) under investigation were conducted using UV and sunlight systems in the presence of TiO_2, and their efficacy was dependent on the intensity of the light (Aguilar *et al.*, 2011; Méndez-Arriaga *et al.*, 2008; Moctezuma *et al.*, 2012; Trujillano *et al.*, 2022). The described photocatalytic decomposition studies utilized different methodologies and aspects than this work.

In this work, the analgesic acetaminophen (paracetamol) has been exposed to temperature (40 °C) and irradiation (sunlight, UV-lamp, and γ-ray) to observe their effects. The purpose of this study is to investigate how temperature and irradiation affect the chemical and physical properties of paracetamol. To determine the purity, crystal properties, and decomposition of both treated and untreated paracetamol samples, various techniques such as high-performance liquid chromatography (HPLC), X-ray diffraction (XRD), scanning electron microscopy (SEM), thermal analysis, and photocatalytic degradation were used.

The thermal analysis behavior, lifetime prediction, decomposition kinetics, and thermodynamic parameters from a single heating rate (10 °C min^{-1}) using a technique of the non-isothermal thermogravimetric analysis (TG/DTG) and differential scanning calorimeter (DSC) were processed by the Coats-Redfern (CR) method (Coats and Redfern, 1964) with the assistance of relevant standard equations. The chemical or physical changes due to temperature and irradiation exposure were compared to the results of the standard sample (untreated) obtained from the relevant measurements of the study and hence discussed.

2. Experimental

2.1. Reagents and solutions

The Modern Pharmaceutical Company (Yemen) provided the analytical standard grade (≥ 99%) paracetamol compound for use in pharmaceutical products (also known as acetaminophen). Chemicals suitable for HPLC such as methanol and water, are offered by Sharlua. 99% purity of TiO_2 (anatase) is available from Sigma-Aldrich.

According to the British Pharmacopeia (2009), paracetamol has the following structure and physical characteristics.

Acetaminophen (paracetamol)
Acetamide, N-(4-hydroxyphenyl)-.4′-Hydroxyacetanilide
M.Wt: 151.16 g mol^{-1}
Chemical Formula: $C_8H_9NO_2$
M.P.: 168–172 °C

2.2. Preparing sample

2.2.1. Exposure strategy

A specific quantity of the standard paracetamol took place over 8 days in vials at a temperature of 40 °C in a digital oven (Memert GmbH Co. KG, Germany). A nearly identical amount of the pharmaceutical was exposed to a 300 W UV-A lamp (λ=365 nm) for 12 h at far from 18 cm. Approximately the same amount of the drug was exposed to sunlight for 8 days. A total of 80 Gy of γ-ray radiation (source Co^{60}) was administered to two Petri plates, each of which contained an equal amount of solid and aqueous samples of paracetamol.

2.2.2. Sampling for photocatalytic study

The sunlight photocatalytic decomposition of the samples of standard and treated paracetamol was conducted by combining 20 ppm of the sample with 1 mg mL^{-1} aqueous solution of TiO_2 catalyst (anatase- purity 99%, Sigma-Aldrich) to make up a reacting mixture. A 300-minute direct sunlight exposure of 15 min time intervals per aliquot collection was considered. Therefore, for each paracetamol sample, fifteen samples of 25 mL reacting mixture were prepared to correspond to the consecutive 15 min time intervals each individually. The samples were exposed to sunlight in open beakers on a sunny day from 10:00 am to 2:00 pm (winter). An aliquot of 10 mL of the reaction mixture was placed into a covered test tube at every consecutive 15 min interval of sunlight exposure and centrifuged to separate the catalyst residue for 30 min (4000 r.p.m.). The pH of the solution used in the photocatalytic experiment was measured at 6.5. At the same concentration of the interest of paracetamol samples, the photocatalytic decomposition processes were individually investigated.

2.3. Methods and physical measurements

2.3.1. Thermal analysis

The TGA and DSC curves of paracetamol-treated and untreated were analyzed using non-isothermal Netzsch, STA 449 F3. All measurements employed highly sintered Al_2O_3 as a reference material and sample masses ranging from 6.4 to 9.2 mg. The samples under investigation were subjected to thermal analysis measures at a heating rate of 10 °C min^{-1}, nitrogen flow rates of 25 mL min^{-1}, and temperature ranges of 25–650 °C.

The relevant TGA curves were used to derive quantitative data. The kinetic parameters of the decomposition processes before and after treatments were calculated using the Coats-Redfern method (Coats and Redfern, 1964).

2.3.2. X-ray diffraction

The instrumentation, Shimadzu ED-720 XD-2 powder X-ray diffractometer at 20 mA current and a voltage of 35 kV with a CuK(U) radiation generator at 1° min^{-1} scanning rate in the range of $5° < 2θ < 65°$ and a wavelength of 1.54056 Å was used to obtain the powder X-ray diffraction patterns of the paracetamol samples.

2.3.3. High-performance liquid chromatography (HPLC)

For separation and detection of paracetamol, the HPLC system (HPLC Jasco, UV2075 UV/Vis detector, and Pump 2089 plus) was employed. The mobile phase was a 30:70 mixture of methanol and water. Before and after treatments, 100 mg of paracetamol samples were dissolved in 100 mL of the mobile phase. 10 mL of this solution was diluted with the mobile phase to a concentration of 0.1 mg mL^{-1}. At room temperature (25 °C), the analysis was performed at a flow rate of 2 mL min^{-1}.

The BDS Hypersil C18 column (200 mm × 4.6 mm) was employed. A UV-visible detector was used to record chromatograms at 245 nm, and the retention time ranged from 5.27 to 5.33 min.

2.3.4. Scanning electron microscope (SEM)

The surface morphology and form of the particles were examined using a scanning electron microscope. Using an instrumental Jeol Jem-1200 EX II electron microscope and gold-coated samples, SEM pictures took place at a 20 kV acceleration voltage.

2.3.5. Electronic spectra

The absorbance of the treated and untreated paracetamol was measured at various time intervals for the photocatalytic decomposition using a UV-VIS Spectrophotometer (Specord200, Analytik Jena). Paracetamol has maximum absorbance ($λ_{max}$) at 254 nm. The Beer-Lambert law was applied to compute the relevant data at $λ_{max}$ from the electronic spectra curves.

3. Results and discussion

3.1. Thermal analysis of paracetamol

The TG and DTG curves recorded for the paracetamol before and after treatments are shown in **Fig. 1**. These curves describe and evaluate the thermal decomposition behavior of paracetamol samples at a given experimental condition. The results of the thermal degradation behavior of these samples are summarized in **Table 1**. It is noteworthy that the DSC curves in **Fig. 2** exhibit a prominent single endothermic peak for all paracetamol samples almost within the range of their single degradation steps. These endothermic peaks are attributed to the samples' heat of fusion as shown in **Fig. 1**.

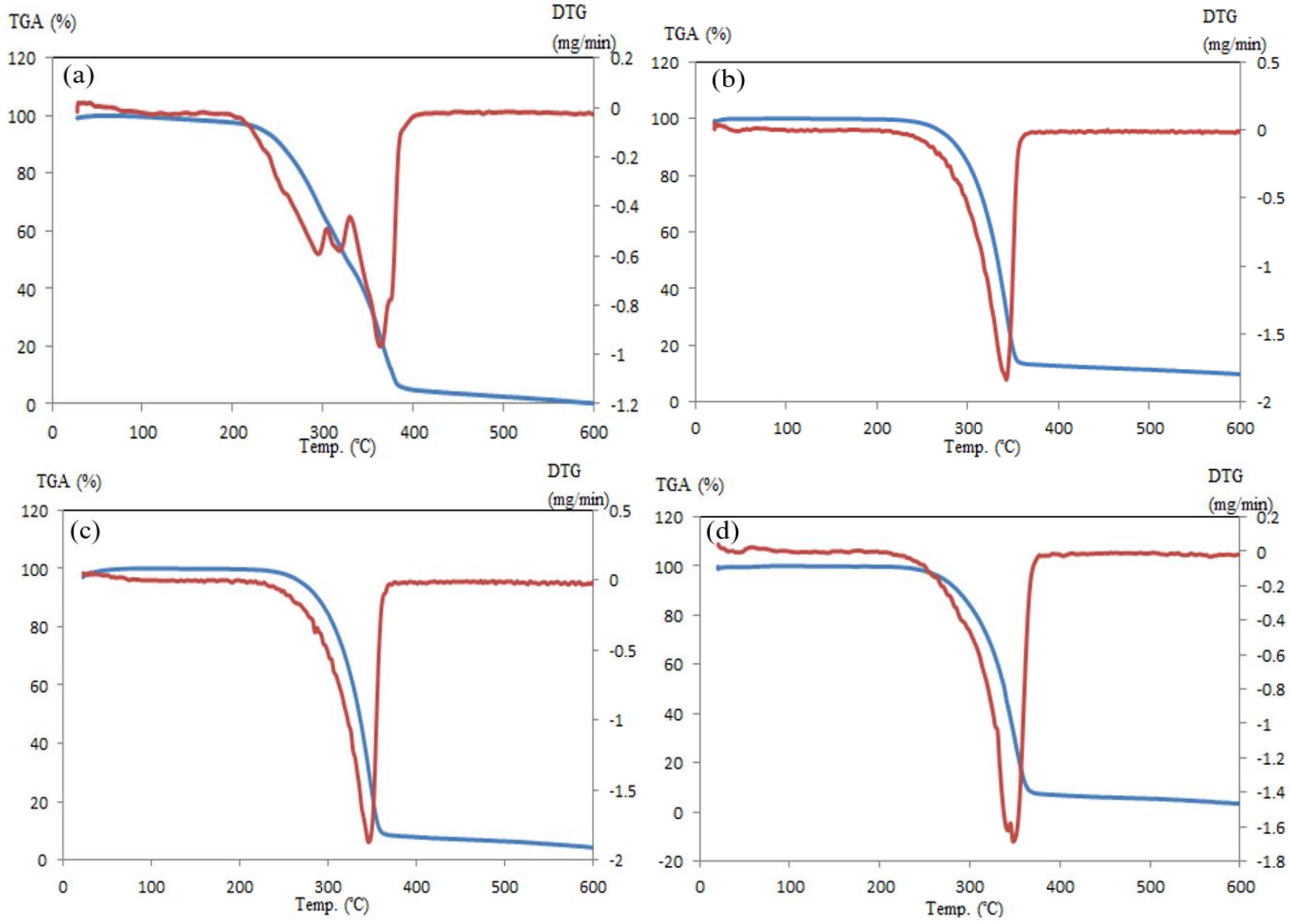

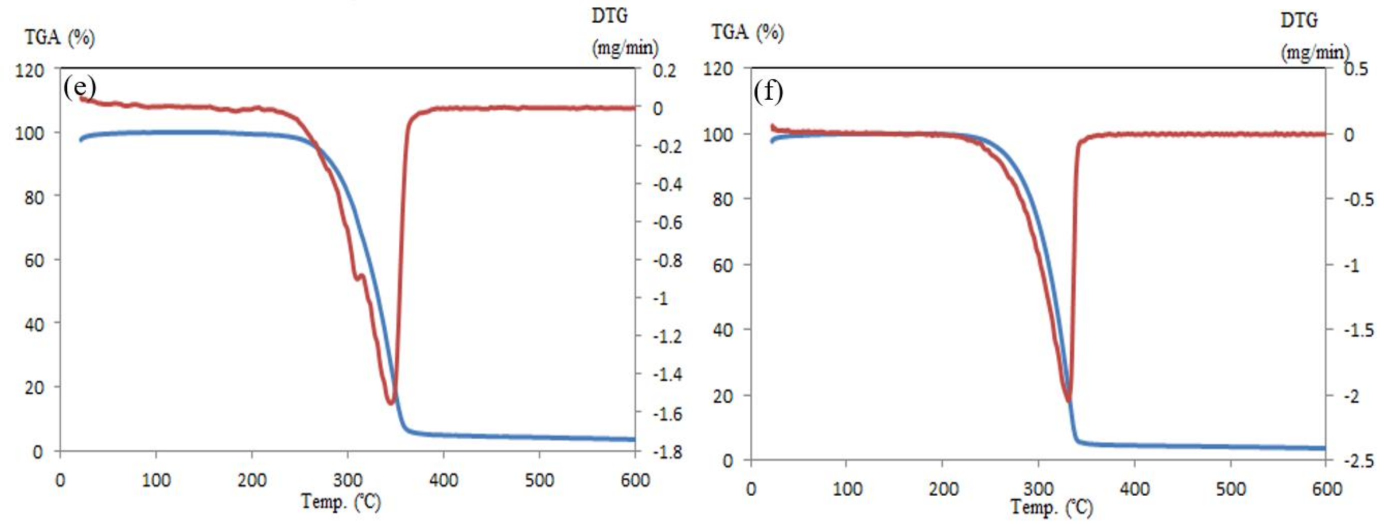

Figure 1. TG and DTG curves of paracetamol before and after treatments **(a)** standard, **(b)** 40 °C-8d, **(c)** UV-12 h, **(d)** γ-solid, **(e)** γ-aq, **(f)** Sun-8d.

Table 1. Thermodynamic and kinetic parameters of thermal decomposition of the paracetamol samples before and after exposure to irradiation and temperature.

Paracetamol samples	Step	*n*	Ea kJ mol^{-1}	TGA			*Log Z* at T_{DTG}	Δm %	ΔG* kJ mol^{-1}	ΔH* kJ mol^{-1}	ΔS* kJ mol^{-1}	Final residue
				T_i °C	T_f °C	T_{DTG} °C						
Standard	1	3.6	126.2	211.1	398.2	354.1	11.16	95	144	121	-37.5	**5%**
40 °C-8d	1	0.7	118.4	227.8	360.2	338	9.74	86.2	152.7	113.3	-64.5	**13.8%**
UV-12h	1	0.75	111.3	227.8	367.5	345.3	9.04	91.3	154.4	106.2	-78	**8.7%**
γ-solid	1	0.7	104.7	232.7	372.5	342.9	8.39	92.3	155.2	99.54	-90.3	**7.7%**
γ-aqueous	1	1.1	122.3	230.2	370.1	340.5	10.16	94.4	151.8	117.2	-56.4	**5.6%**
Sunlight-8d	1	0.6	116.8	221.1	344.1	326.8	9.82	94.5	149.4	111.8	-62.7	**5.5%**

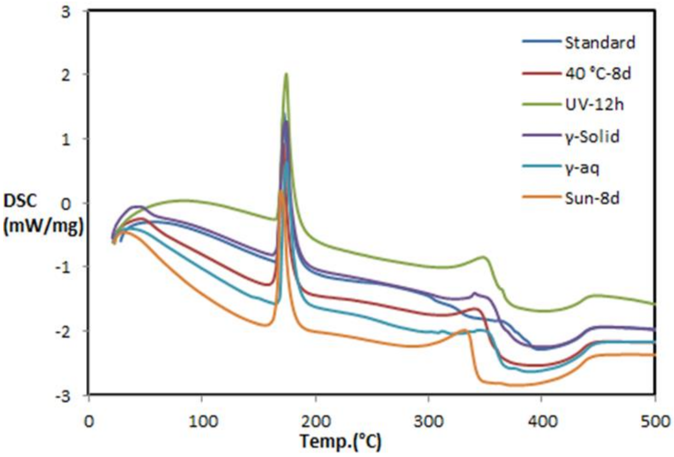

Figure 2. DSC profiles of the paracetamol samples before and after exposure to irradiation and temperature.

3.1.1. Assessment of thermal decomposition kinetics

The activation energy (E_a) and pre-exponential factor (Z) are calculated using the CR method (Coats and Redfern, 1964) for the proper order of reaction (n) to assess the decomposition of the thermal kinetics parameters at (10 °C min^{-1}) single heating rate. The Coats-Redfern equation is linearized for a well-selected order of reaction, and the activation energy (E_a) is determined from the slope of **Eqs. 1** and **2**:

$$\log\frac{1-(1-\alpha)^{1-n}}{T^2\,(1-n)} = \log\left[\frac{ZR}{q\,E_a}\left(1-\frac{2RT}{E_a}\right)\right] - \frac{E_a}{2.303RT} \qquad for \quad n \neq 1 \tag{1}$$

$$\log\left[\frac{-\log\,(1-\alpha)}{T^2}\right] = \log\left[\frac{ZR}{q\,E_a}\left(1-\frac{2RT}{E_a}\right)\right] - \frac{E_a}{2.303RT} \qquad for \quad n = 1 \tag{2}$$

where: T = temperature (K), α = fraction of weight loss, Z = pre-exponential factor, q = heating rate, n = order of reaction, and R = molar gas constant.

For a temperature of maximum mass loss rate (TDTG), the pre-exponential factor (Z) is computed from the intercept. In general, one step of the decomposition process for the samples of standard and treated paracetamol can be seen by attentively examining the TG/DTG curves (**Fig. 1**).

3.1.2. Thermal decomposition behavior of paracetamol

The thermal studies of paracetamol at single and multiple heating rates were mentioned elsewhere (Schnitzler *et al.*, 2002; Tomassetti *et al.*, 2005). It showed a single-step (214–357 °C) degradation behavior at a T_{DTG} peak at 326 °C with various heat of fusion values (22.8–35.7 kJ mol^{-1}). This agrees fairly with the results obtained for the samples with interest. Unlike the treated samples, although the TG curve of the untreated paracetamol sample shows one degradation step, its DTG curve appears with two immature peaks followed by one principal peak at 354.1 °C. This may indicate rate variation due to competitive degradation reaction. The standard paracetamol (untreated sample) loses 95% in a single step at 211.1 – 398.2 °C at a maximum temperature (T_{DTG}) of 354.1 °C and 5% residue. According to the order of reaction (n = 3.6), the activation energy is determined to be 126.2 kJ mol^{-1}. The parameters of thermodynamic ΔH^*, ΔS^*, and

ΔG^* are 121 kJ mol^{-1}, –37.5 J K^{-1} mol^{-1}, and 144.6 kJ mol^{-1}, respectively.

For paracetamol exposed to 40 °C temperature, the single step (227.8 – 360.2 °C) at T_{DTG} of 338 °C is accompanied by a mass loss of 86.2% and 13.8% residue. The activation energy E_a for the single step (n = 0.7) is 118.4 kJ mol^{-1} and the thermodynamic parameters (ΔH^*, ΔS^*, and ΔG^*) calculated for this step are –113.3 kJ mol^{-1}, –64.5 J K^{-1} mol^{-1}, and 152.7 kJ mol^{-1}, respectively.

The UV-lamp irradiated paracetamol shows a single step of degradation (227.8 – 367.5 °C) at T_{DTG} of 345.3 °C with mass loss of 91.3% and residue of 9.7%. The value of activation energy of the single (n = 0.75) step is 111.3 kJ mol^{-1} and the values of ΔH^*, ΔS^*, and ΔG* of this step are 106.2 kJ mol^{-1}, –78 J K^{-1} mol^{-1}, and 154.4 kJ mol^{-1}, respectively.

The single degradation steps of the treated paracetamol with γ-ray in solid and aqueous states are observed at (232.7 – 372.5 °C) and (230.2 – 370.1 °C) range at T_{DTG} of 243.9 °C and 340.5 °C with mass losses of 92.3% and 94.4%, and residues of 7.7% and 5.6%, respectively. Values of E_a, ΔH^*, ΔS^*, and ΔG^* for the single decomposition step of paracetamol irradiated with γ-ray in solid (n = 0.7) and aqueous (n = 1.1) states are (104.7 kJ mol^{-1}, 99.5 kJ mol^{-1}, –190.3 J K^{-1} mol^{-1}, and 155.2 kJ mol^{-1}) and (122.3 kJ mol^{-1}, 117.2 kJ mol^{-1}, –56.4 J K^{-1} mol^{-1}, and 151.8 kJ mol^{-1}), respectively.

The degradation of paracetamol treated with sunlight shows single-step (221.1 – 344.1 °C) at T_{DTG} of 326.8 °C with mass loss of 94.5% and residue of 5.5%. The activation energy for the single (n = 0.6) step is found to be 116.8 kJ mol^{-1}. The values of ΔH^*, ΔS^*, and ΔG^* are 111.8 kJ mol^{-1}, –62.7 J K^{-1} mol^{-1}, and 149.4 kJ mol^{-1}, respectively.

Typically, for all the samples, the positive values of ΔH^* and ΔG^* for the transition-state reaction indicate an extremely small equilibrium constant and the reactants are stable concerning the formation of the activated complex and there are insignificant variations in values of the samples before and after treatments. The changes in activation entropy values for the individual steps of the paracetamol samples' decomposition are negative, reflecting the corresponding reduction in degrees of freedom for rotation in the reactants and generating the new degrees of freedom for vibration in the activated complex, which is more ordered than the reactants (Al-Maydama, 2004).

3.1.3. Estimating the lifetime (tf)

From the TGA observed curves for the paracetamol samples before and after treatments, the lifetime was estimated for various temperatures (25, 40, 100, 150, and 200 °C). The estimated lifetime of the paracetamol samples can be defined as the time when 5% of the degradation was reached (Prime *et al.*, 2009), and for n ≠1 be obtained from the **Eq. 3**:

$$t_f = \frac{(1-0.95^{1-n})}{Z(1-n)} exp \frac{E_a}{RT} \tag{3}$$

According to the data for kinetics collected by applying the CR method (**Tables 1** and **2**) and **Eq. 3**, the predicted lifetime for the decomposition of the paracetamol samples at a conversion of 5% and a variety of temperatures are summarized in **Table 2**. Values of the estimated lifetime for the decomposition vary consistently with the temperatures of (25, 40, 100, 150, and 200 °C). A lifetime ($t_{5\%,\ 25°C}$) is typically estimated using the time for 5% conversion of the samples of treated and untreated paracetamol at 25 °C (Prime *et al.*, 2009). All the samples show almost the same lifetime except for the value (4.7×10^8 s) of γ-ray in the solid state, as given in **Table 2**.

Table 2. The standard and treated paracetamol samples' DSC characteristics and calculated values of a lifetime at different temperatures of the decomposition based on weight loss (α = 5%).

Variable	**DSC**			**t_f (sec) at 5% conversion**					***Log Z* at 5%**
	M.P. (°C)	ΔH_f kJ mol^{-1}	X$_c$ (%)	25 °C	40 °C	100 °C	150 °C	200 °C	
Standard	171.5	18.9	100	5.1 × 10^9	4.4 × 10^8	1.8 × 10^5	1.5 × 10^3	33.3	11.15
40 °C-8d	154.5	15.3	81	5.2 × 10^9	5.3 × 10^8	3.5 × 10^5	3.9 × 10^3	110.1	9.74
UV-12h	174.5	19.5	103.1	1.6 × 10^9	1.8 × 10^8	1.9 × 10^5	2.7 × 10^3	93.6	9.03
γ-solid	174.7	19.8	104.7	4.7 × 10^8	6.1 × 10^7	9.5 × 10^4	1.8 × 10^3	75.8	8.39
γ-aqueous	174.5	19.1	100.9	9.9 × 10^9	9.3 × 10^8	4.8 × 10^5	4.6 × 10^3	115.4	10.16
Sunlight-8d	169.2	17	90.02	2.3 × 10^9	2.4 × 10^8	1.8 × 10^5	2.1 × 10^3	61.4	9.82

3.1.4. Thermal stability of paracetamol

Based on temperature fluctuation at the maximum degradation rate (T_{DTG}), the thermal stability of decomposition is measured (Al-Maydama *et al.,* 2009; Donia *et al.*, 1992). As the paracetamol samples before and after treatments show almost incomparable differences in their temperature of the maximum degradation rates (T_{DTG}) the increase in thermal stability of the paracetamol samples can be listed in the following order:

Standard (354.1 °C) > UV-sample (345.3 °C) > γ-solid (342.9 °C) > γ-ray-aqueous (340.5 °C) > 40 °C-sample (338 °C) > sunlight (326.8 °C).

The decomposition rate consequently decreases as the slope of the CR method plot increases because the activation energy increases. It follows that the activation energies (kJ mol^{-1}) of the treated and untreated paracetamol samples rise in the following order:

Standard (126.2) > γ-ray-aqueous (124.1) > 40 °C-sample (120.4) > sunlight (116.8) > UV-sample (111.3) > γ-solid (104.7).

Consequently, the decomposition rates are increasing in the following order:

γ-solid > UV-sample > sunlight > 40 °C-sample > γ-aqueous > Standard

3.1.5. DSC technique

The curves of DSC for the treated and untreated paracetamol samples are shown in **Fig. 2**. According to the DSC curves, the melting point of the standard paracetamol is 171.5 °C which agrees with the literature values of 168 – 172 °C, indicating the extremely pure of the standard paracetamol (British Pharmacopeia, 2009). The results indicate that when the melting points of the standard paracetamol and the treated samples are compared, the melting point of the paracetamol exposed to sunlight (169.2 °C) is within the range of values reported in the literature, while that exposed to 40 °C exhibits the lowest melting point value (154.5 °C). However, the melting points of paracetamol treated with UV-lamp and γ-ray in solid and aqueous states (174.4 – 174.8 C) are noticeably higher than the literature values. Various fusion heat values (22.8 – 35.7 kJ mol^{-1}) were reported for paracetamol (Oliveira *et al.*, 2017; Schnitzler *et al.*, 2002; Tomassetti *et al.*, 2005). Some of these values are fairly comparable to the value obtained (18.9 kJ mol^{-1}) for the untreated sample.

The ratio of the treated paracetamol sample's enthalpy of fusion to that of the standard paracetamol was applied to determine the relative crystallinity of the treated paracetamol samples (i.e., 40 °C, UV, sunshine, and -ray) as given in the **Eq. 4**:

$$X_c(\%) = \frac{\Delta H_f}{\Delta H_f^{\circ}} \times 100 \qquad (4)$$

where X_c is the relative crystallinity, ΔH_f is the enthalpy of fusion for the treated sample and ΔH_f° is that of the 100 % crystalline standard, i.e., of the standard paracetamol sample.

The relative crystallinity and fusion heat of the standard and treated paracetamol samples were evaluated using **Eq. 4**, as given in **Table 2**. When compared to the greatest crystallinity value (100%) estimated for the standard paracetamol, the treated paracetamol samples' extent of crystallinity reduction is measured (Varshny and Patel, 1994).

The lowest values of the relative crystallinity (81 and 90%) and consequently that of the enthalpy of fusion (15.3 and 17 kJ mol^{-1}) are reported for the paracetamol samples exposed to the temperature of 40 °C and sunlight, respectively.

3.2. X-ray diffraction

Figure 3 displays the paracetamol XRD patterns before and after being exposed to radiation and temperature. These patterns demonstrate that paracetamol has a polycrystalline phase (five principal peaks at 15° ≤ 2θ ≥ 45.5°). Comparing the apparent sublattice peaks with the crystallographic data available in the crystallographic information file no: 2103465. cif, the crystal structures of all paracetamol samples except sunlight-treated samples belong to the orthorhombic symmetry, space group Pbca. While the XRD pattern of the sunlight-treated paracetamol sample matches essentially with the monoclinic symmetry, space group *P2/a* (Druzhbin *et al.*, 2015; Jendrzejewska *et al.*, 2020), mixed with the original orthorhombic polymorph as a minor component. The occurrence of some crystal lattice inversion for the paracetamol samples treated with UV, γ-ray both solid and aqueous states, and at 40 °C, can be evidenced by the interchange of relative intensities of the sublattice peaks observed at 2θ ~ 15° and ~20°, as indicated by asterisks (*) in the relevant patterns. This crystallographic inversion represents one of some lattice disorders, as expected from DSC results, particularly those samples treated with sunlight and at 40 °C, behind which both ΔH_f and M.P. are greatly dropped.

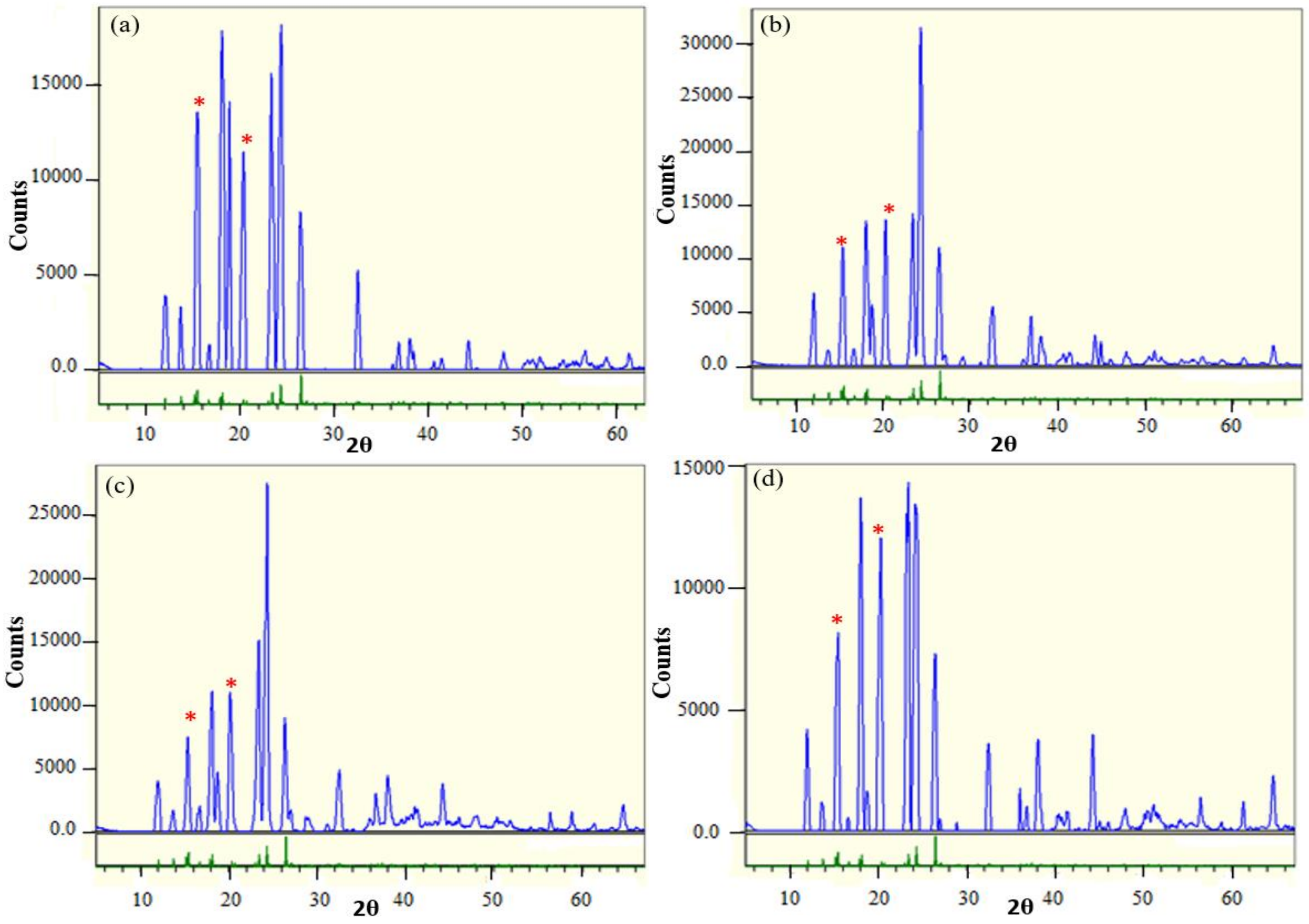

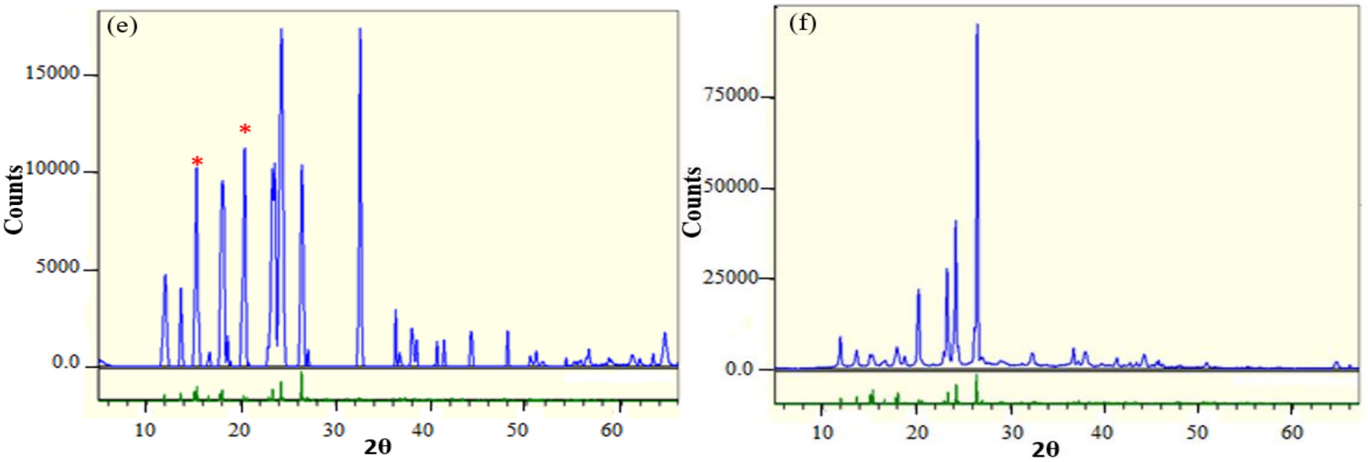

Figure 3. XRD patterns for paracetamol before and after exposure to irradiation and temperature: **(a)** standard, **(b)** 40 °C-8 d, **(c)** UV-12 h, **(d)** γ-solid, **(e)** γ-aq, **(f)** Sun-8 d.
Source: Elaborated by the authors using data from MDI Jade 5.

The Debye-Scherrer and Williamson-Hall (W-H) **Eqs. 5** and **6** can be used for calculating the average crystal size (Yousaf *et al.*, 2021):

$$D = \frac{k\lambda}{\beta_{hkl}\cos\theta} \qquad (5)$$

$$\beta_{hkl}\cos\theta = \frac{k\lambda}{D} + 4\varepsilon\sin\theta \qquad (6)$$

where β is full width at half maximum (FWHM in radians), λ is the wavelength (λ=1.54056 Å), D is the particle size (nm), *k* is Scherer constant (0.94), and θ is the diffraction angle, and ε is the micro strain.

The slope of the fitted line indicating the strain can be used to calculate the effective particle size.

Table 3 shows a comparison of the particle size of paracetamol samples using Scherrer and Williamson-hall (W-H) equations. Due to variation in averaging particle distribution, the values of the average crystalline size gained for the W-H equation showed significant fluctuation. The crystalline size (10.34-57.93 nm) that was observed for the W-H equation is inconsistent with Scherrer's equation.

Table 3. The properties of lattice crystalline and relative purity of the standard and treated paracetamol samples using XRD and HPLC techniques.

Paracetamol samples	**HPLC**	**XRD**					
	Purity%	2θ	β	D (nm) Scherrer	D (nm) W-H	Microstrain	X_c%
Standard	100	15.46	0.006178	23.54	28.39	0.0009	100
		18.08	0.006754				
		23.32	0.005917				
		24.36	0.006423				
		26.38	0.006126				
40 °C-8d	98.7	15.4	0.006388	22.61	24.54	0.0004	113.8
		18.06	0.006999				
		23.42	0.006423				
		24.3	0.006301				
		26.42	0.006562				
UV-12h	98.9	15.36	0.005864	23.78	26.33	0.0007	93.9
		18.1	0.006754				
		23.4	0.006545				
		24.34	0.005969				
		26.34	0.005986				
γ-solid	101.4	15.48	0.006353	20.32	57.93	0.0068	99.4
		18	0.005655				
		23.4	0.011083				
		24.38	0.009809				
		26.44	0.006144				
γ-aqueous	101.3	15.32	0.00473	23.75	42.59	0.0037	83.9
		18.06	0.006632				
		23.54	0.010489				
		24.24	0.006597				
		26.4	0.005096				
Sunlight-8d	99.5	15.099	0.008255	24.08	10.34	-0.01	126.5
		17.959	0.006266				
		23.279	0.003857				
		24.201	0.003665				
		26.48	0.003019				

According to the integrated areas of the five principal peaks as a ratio to those of the standard samples, crystallinity calculation is given in **Table 3**. According to the results reported in **Table 3**, paracetamol treated with -ray in the aqueous state (83.9%) and with UV light (93.9%) significantly decreased crystallinity. The nanoparticle size in the literature ranges between 1-100 nm (Boverhof *et al.*, 2015). The particle size obtained from XRD (**Table 3**) for the untreated sample is 23.54 nm. The particle size of treated paracetamol samples calculated by XRD exhibits no effects on their size of nanoparticles (20.3 – 24.08 nm) due to radiation and temperature treatments. This means that, as the particle size depends only on the crystallinity degree and phase transformations, it seems that the treatments of the samples were not able to affect the bulk of particles.

3.3. High-performance liquid chromatography (HPLC) analysis

Typical chromatograms of HPLC for the paracetamol samples' purity analyses are shown in **Fig. 4**, and all samples were analyzed using the British Pharmacopoeia standard method. HPLC profiles of the samples of standard and treated paracetamol have a ranging retention time (R_t) of (5.27 – 5.33 min). The insignificant changes in the absolute purity values determined by HPLC are due to the absence of chemical changes in the composition of the paracetamol samples. Nevertheless, no unusual peaks in HPLC chromatograms of the paracetamol-treated samples are seen under the studied conditions. In general, the results in **Table 3** show no significant changes in the purity of the paracetamol exposed to temperature and radiation.

However, under the investigated circumstances there are no unexpected peaks in the HPLC chromatograms of the treated samples of paracetamol. The results in **Table 3** generally demonstrate no appreciable variations in the purity of the paracetamol subjected to heat and radiation.

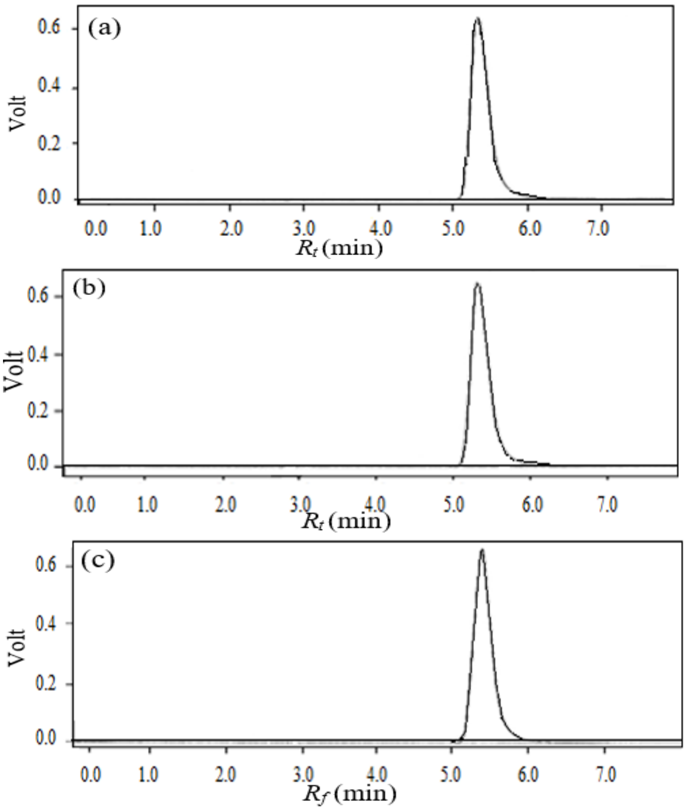

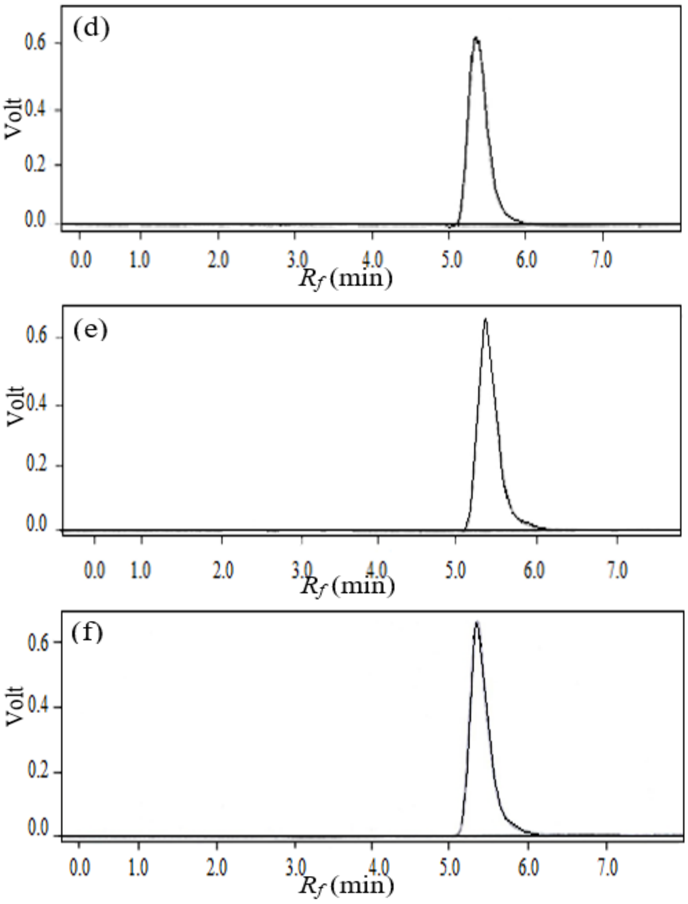

Figure 4. HPLC profiles of the paracetamol samples before and after exposure to radiation and temperature: **(a)** standard, **(b)** 40 °C-8 d, **(c)** UV-12 h, **(d)** γ-solid, **(e)** γ-aq, **(f)** Sun-8 d.
Source: Elaborated by the authors using data from HPLC.

3.4. Scanning electron microscopy (SEM)

Figure 5 displays the images of SEM of paracetamol microparticles before and after having undergone heating to 40 °C temperature and being subjected to UV, sunlight, and γ-ray in both solid and liquid states. The range of particle size for the untreated paracetamol sample is approximately (14.1 – 27.7 µm), and the particles have an irregular crystal form with sharp edges. The morphology of the treated paracetamol particles shows quite distinct alterations. The UV-treated particles exhibit an agglomeration of large rectangular-like particles (19.2 – 49.7 µm) with small ridges growth of the surface ridges. The particles of irradiated by γ–solid have an irregular shape with few small ridges on the surface.

However, the γ–irradiated sample in the aqueous state shows an acicular shape due to the scatter of smaller shape particles.

Exposing the sample to 40 °C for 8 days shows small cylindrical rod-like shape particles with smooth surfaces. The sunlight-irradiated sample has a flakey shape of a very large texture plate.

Although crystallinity from DSC and XRD show few significant changes, SEM images show obvious changes in the morphology and shapes of the treated samples. Some consistency is observed in the particle size from XRD and SEM images.

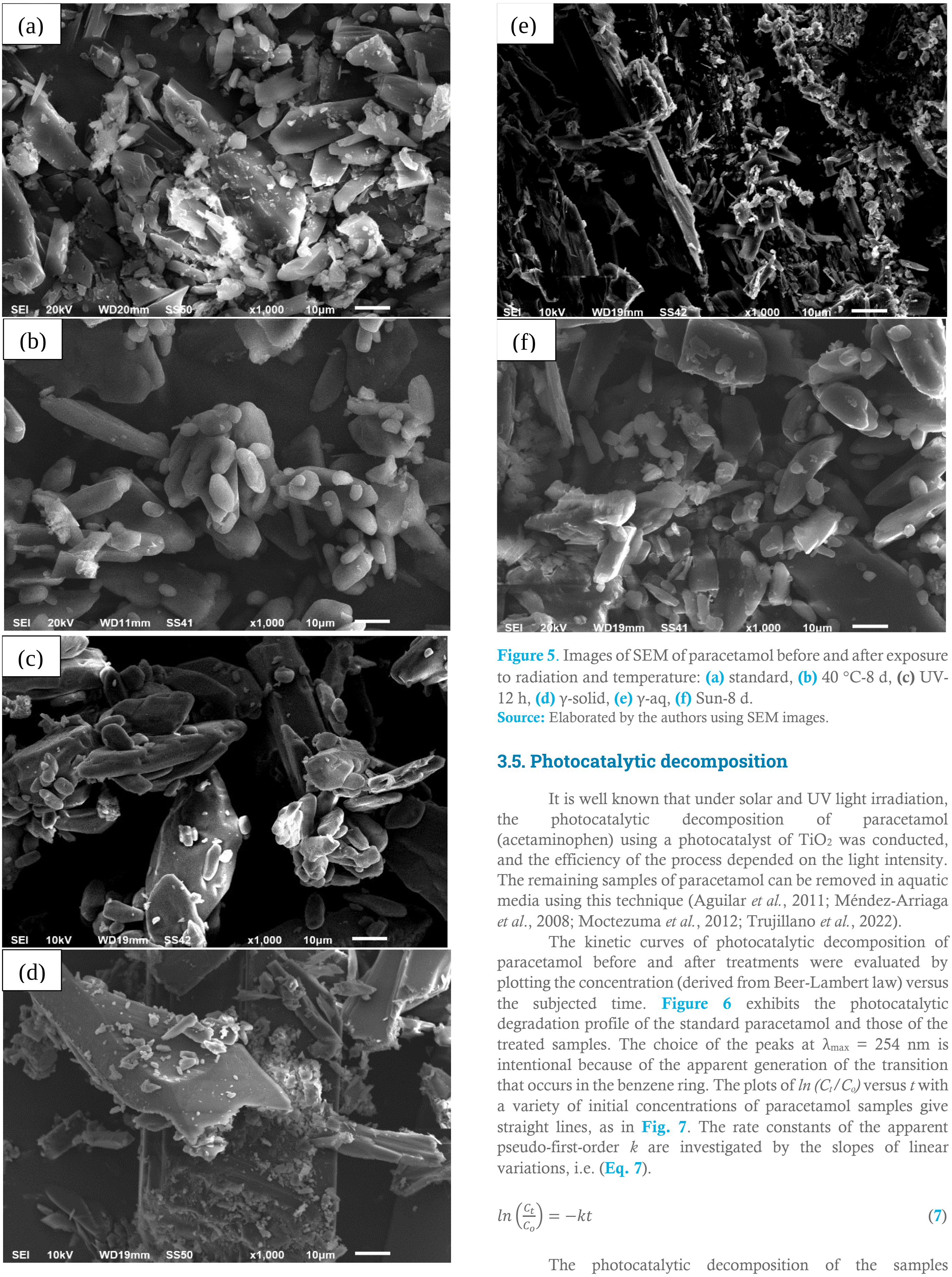

Figure 5. Images of SEM of paracetamol before and after exposure to radiation and temperature: **(a)** standard, **(b)** 40 °C-8 d, **(c)** UV-12 h, **(d)** γ-solid, **(e)** γ-aq, **(f)** Sun-8 d.
Source: Elaborated by the authors using SEM images.

3.5. Photocatalytic decomposition

It is well known that under solar and UV light irradiation, the photocatalytic decomposition of paracetamol (acetaminophen) using a photocatalyst of TiO_2 was conducted, and the efficiency of the process depended on the light intensity. The remaining samples of paracetamol can be removed in aquatic media using this technique (Aguilar *et al.*, 2011; Méndez-Arriaga *et al.*, 2008; Moctezuma *et al.*, 2012; Trujillano *et al.*, 2022).

The kinetic curves of photocatalytic decomposition of paracetamol before and after treatments were evaluated by plotting the concentration (derived from Beer-Lambert law) versus the subjected time. **Figure 6** exhibits the photocatalytic degradation profile of the standard paracetamol and those of the treated samples. The choice of the peaks at λ_{max} = 254 nm is intentional because of the apparent generation of the transition that occurs in the benzene ring. The plots of $ln\ (C_t/C_o)$ versus t with a variety of initial concentrations of paracetamol samples give straight lines, as in **Fig. 7**. The rate constants of the apparent pseudo-first-order k are investigated by the slopes of linear variations, i.e. (**Eq. 7**).

$$ln\left(\frac{C_t}{C_o}\right) = -kt \qquad (7)$$

The photocatalytic decomposition of the samples paracetamol before and after treatments is illustrated in **Fig. 6** as influenced significantly by the TiO_2 and sunlight system. The percentage of degradation is determined from the absorbance spectra by applying the **Eq. 8** (Şayan, 2006):

$$\text{Degradation } \% = \frac{C_o - C_t}{C_o} \times 100 \qquad (8)$$

where $C_\circ$ is the initial concentration, and C_t is the concentration at a given exposure time.

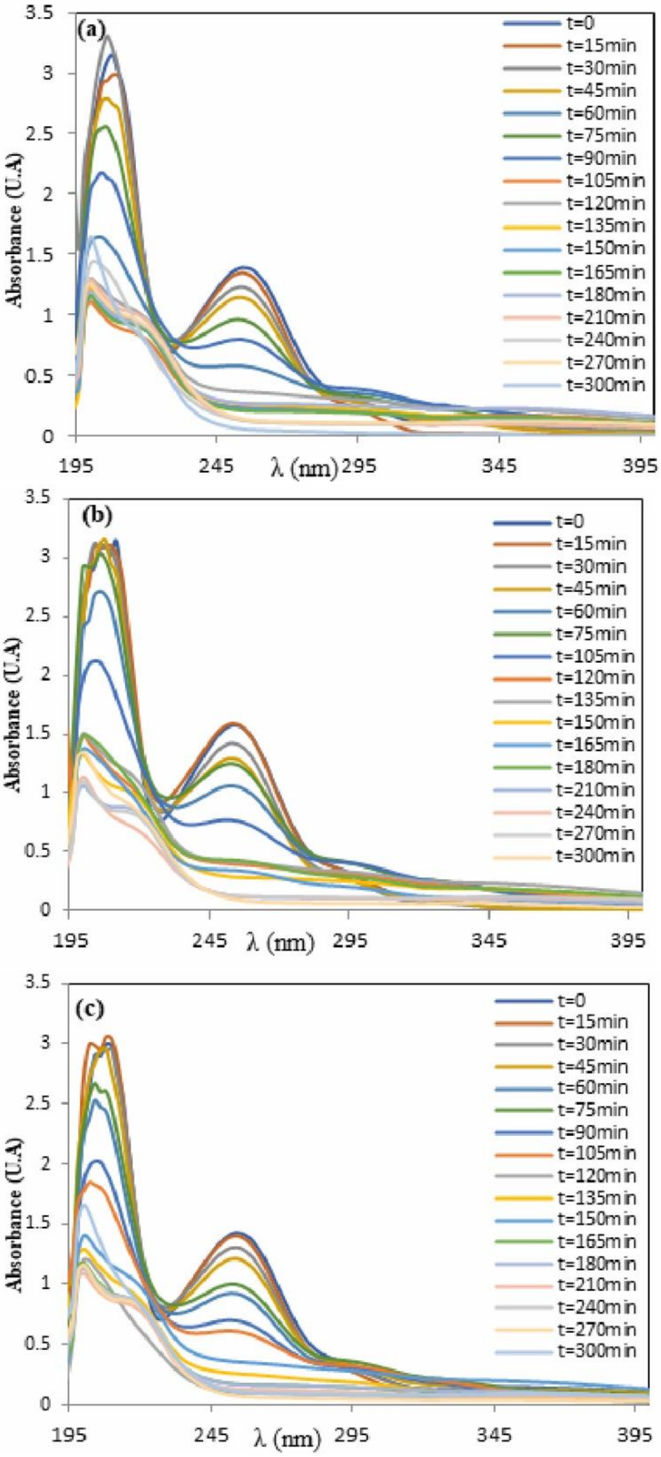

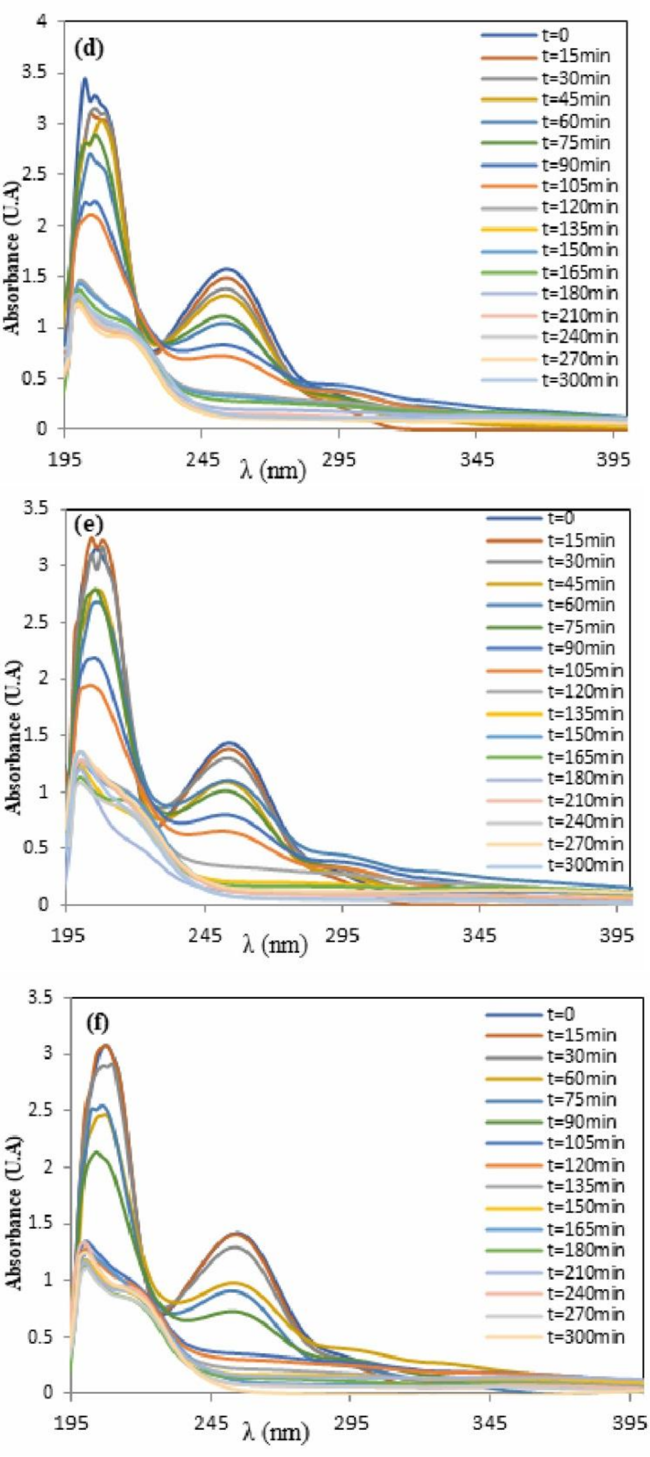

Figure 6. Effect of sunlight on paracetamol before and after exposure to irradiation and temperature: **(a)** standard, **(b)** 40 °C-8 d, **(c)** UV-12 h, **(d)** γ-solid, **(e)** γ-aq, **(f)** Sun-8 d.

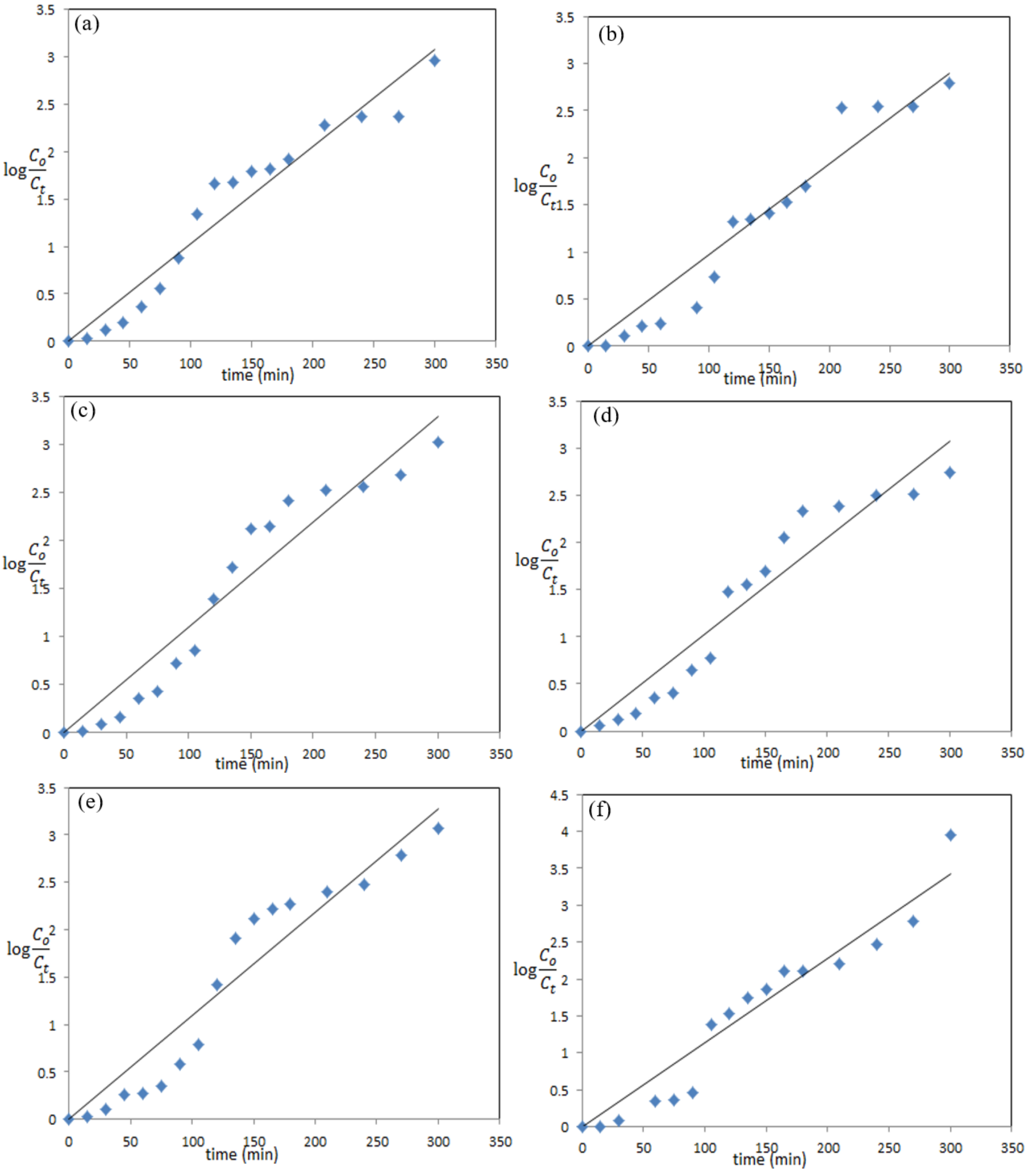

Figure 7. Kinetics of pseudo-first order reaction of the photocatalytic degradation of the paracetamol samples: **(a)** standard, **(b)** 40 °C-8 d, **(c)** UV-12 h, **(d)** γ-solid, **(e)** γ-aq, **(f)** Sun-8 d.

For five hours of sunlight exposure, the decomposition percentage of the samples of paracetamol in **Table 4** has been calculated. The variations in the percentage of the decomposition for the paracetamol samples before and after treatments (**Table 4**) are not vast. The highest degradation percentage (93.8%) appears for the sample exposed to the temperature of 40 °C, whereas the lowest one (98.1%) is for the sample of sunlight.

Table 4. Half-life, lifetime, rate constant, and percentage of degradation of photocatalytic decomposition of the treated paracetamol.

Paracetamol samples	k (min^{-1})	$t_{1/2}$ (min)	R^2	Degradation%	$t_{10\%}$ (min)
Standard	0.0102	67.9	0.9417	94.8	10.3
40 °C-8d	0.0097	71.4	0.9433	93.8	10.8
UV-12h	0.0109	63.6	0.9264	95.1	9.6
γ-solid	0.0102	67.9	0.9258	94	10.3
γ-aqueous	0.0109	63.6	0.9176	95.4	9.6
Sunlight	0.0114	60.8	0.9296	98.1	9.2

The half-life of the decomposition of the paracetamol exposed to sunlight exhibits the lower value (60.8 min), whereas the sample treated at 40 °C exhibits the highest value (71.4 min). When a pharmaceutical product is stored under specific conditions, its shelf-life ($t_{10\%}$) is anticipated to be stable or preserve at least 90% of its initial concentration in most circumstances (Carstensen, 1974). It is possible to calculate the photocatalytic decomposition's shelf life from the rate constant by **Eq. 9** (Fubara and Notari, 1998):

$$t_{10\%} = \frac{0.105}{k} \tag{9}$$

where $t_{10\%}$ is shelf-life which is the time 10% of the active ingredient of the pharmaceutical product is reduced and k is the rate constant of reaction.

When this equation is applied to the rate constant of photocatalytic decomposition of the samples of standard and treated paracetamol, **Table 4** reveals that the shelf-life values dropped dramatically, from 10.8 to 9.2 min. This is because of the influence of TiO_2 catalyst on the decomposition of the samples of paracetamol.

Generally, it has been found that the decomposition percentage has an inverse association with the half-life and shelf-life, indicating that the higher the decomposition percentage, the lower the half-life and shelf-life values.

4. Conclusions

In general, all treated and untreated paracetamol samples undergo a single degradation step. The untreated sample appears to be more thermally stable than the others. Crystallinity from DSC and XRD show few significant changes, however, SEM images exhibit obvious changes in the morphologies and shapes of the treated samples compared to the untreated ones. Some consistency is observed in the particle size from the XRD and the SEM images. HPLC results show almost no purity changes due to chemical degradation associated with the temperature and irradiation treatments. From the outcomes of the photocatalytic degradation, the TiO_2 catalyst proves high efficiency in degrading all the paracetamol samples almost equally (93.8 – 98.1%).

Authors' contributions

Conceptualization: Al-Maydama, H. M.; **Data curation:** Abduljabbar, A. A.; **Formal Analysis:** Abduljabbar, A. A.; **Funding acquisition:** Not applicable; **Investigation:** Al-Maydama, H. M.; **Methodology:** Abduljabbar, A. A.; **Project administration:** Al-Maydama, H. M.; **Resources:** Abduljabbar, A. A.; **Software:** Not applicable; **Supervision:** Al-Maydama, H. M.; **Validation:** Al-Maydama, H. M.; **Visualization:** Abduljabbar, A. A.; **Writing – original draft:** Abduljabbar, A. A.; **Writing – review & editing:** Al-Maydama, H. M.

Data availability statement

The data will be available upon request.

Funding

Not applicable.

Acknowledgments

Not applicable.

References

Aguilar, C. A.; Montalvo, C.; Ceron, J. G.; Moctezuma, E. Photocatalytic degradation of Acetaminophen. *Int. J. Environ. Health Res.* **2011**, *5* (4), 1071–1078. https://doi.org/10.22059/IJER.2011.465

Akyar, I. *Wide spectra of Quality Control*. În: Tella, A. C.; Salawu, M. O.; Philips, I. M.; Olabemiwo O. M.; and Adediran, G. O. Quality assessment of solid pharmaceuticals and intravenous fluid manufacturing in Sub-Saharan Africa. Intech Open (CCBY 3.0 license. Nigeria) 2011.

Al-Maydama, H. M.; Abduljabbar, A. A.; Al-Maqtari, M. A.; Naji, K. M. Study of temperature and irradiation influence on the physicochemical properties of Aspirin. *J. Mol. Struct.* **2018**, *1157*, 364–373. https://doi.org/10.1016/j.molstruc.2017.12.062

Al-Maydama, H. M.; El-Shekeil, A. G.; Al-Karbouly, A.; Al-Ikrimawy, W. Thermal degradation behavior of some Poly[4-amino-2,6-pyrimidnodithiocarbamate] metal complexes. *Arab. J. Sci. Eng.* **2009**, *34* (1), 67–75.

Al-Maydama, H. M. A. Comments on "The effect of UV radiation on the thermal parameters of collagen degradation". *Polym. Degrad. Stab.* **2004**, *84*, 363–365. https://doi.org/10.1016/j.polymdegradstab.2003.06.002

Boverhof, D. R.; Bramante, C. M.; Butala, J. H.; Clancy, S. F.; Lafranconi, M.; West, J.; Gordon, S. C. Comparative assessment of nanomaterial definitions and safety evaluation considerations. *Regul. Toxicol. Pharmacol.* **2015**, 73, 137–150. https://doi.org/10.1016/j.yrtph.2015.06.001

British Pharmacopeia, Vol. I & II. Her Majesty's stationary office, London, UK, 2009.

Carstensen, J. T. Stability of solids and solid dosage forms. *J. Pharm. Sci.* **1974**, *63* (1), 1–14. https://doi.org/10.1002/jps.2600630103

Coats, A. W.; Redfern, J. P. Kinetic parameters from thermogravimetric data. *Nature.* **1964**, *201* (4914), 68–69. https://doi.org/10.1515/zna-1979-0523

Donia, A. M.; Gouda, M. M.; Ayad, M. I.; El-Boraey, H. A. Thermal behavior of some aromatic diamine complexes. *Thermochim. Acta.* **1992**, *194*, 155–163. https://doi.org/10.1016/0040-6031(92)80014-N

Druzhbin, D.; Drebushchak, T.; Min Kov, V.; Boldyneva, E. Crystal structure of two Paracetamol polymorphs at 20 K: A search for the 'structure-property' relationship. *J. Struct. Chem.* **2015**, *52*, 317–323. https://doi.org/10.1134/S002247661502016X

Fubara, O. J. and Notari, R. Influence of pH, temperature, and buffers on Cefepime degradation kinetics and stability predictions in aqueous solutions. *J. Pharm. Sci.* **1998**, *87* (12), 1572–1576. https://doi.org/10.1021/js980170y

Huynh-Ba, K. An Overview of Physical Stability of Pharmaceuticals. In: Pharmaceutical Stability Testing to Support Global Markets. 2010, p. 145–152. https://doi.org/10.1007/978-1-4419-0889-6_19

Jendrzejewska, I.; Goryczka, T.; Pietrasik, E.; Klimontko, J.; Jampilek, J. X-ray and Thermal Analysis of Selected Drugs Containing Acetaminophen. *Molecules.* **2020**, *25* (24), 5909. https://doi.org/10.3390/molecules25245909

Lusina, M.; Cindrić, J.; Peko, M.; Pozaić, L.; Musulin, N. Stability study of losartan/hydrochlorothiazide tablets. *Int. J. Pharm.* **2005**, *291*, 127–137. https://doi.org/10.1016/j.ijpharm.2004.07.050

Méndez-Arriaga, F.; Esplugas, S.; Giménez, J. Photocatalytic degradation of non-steroidal anti-inflammatory drugs with TiO_2 and simulated solar irradiation. *Water Research.* **2008**, *42*, 585–594. https://doi.org/10.1016/j.watres.2007.08.002

Moctezuma, E.; Leyva, E.; Aguilar, C. A.; Luna, R. A.; Montalvo, C. Photocatalytic degradation of paracetamol: Intermediates and total reaction mechanism. *J. Hazard. Mater.* **2012**, *243*, 130–138. https://doi.org/10.1016/j.jhazmat.2012.10.010

Oliveira, G. G. G.; Feitosa, A.; Loureiro, K.; Fernandes, A. R.; Souto, E. B.; Severino, P. Compatibility study of paracetamol, chlorpheniramine maleate and phenylephrine hydrochloride in physical mixtures. *Saudi Pharmaceutical Journal.* **2017**, *25* (1), 99-103. https://doi.org/10.1016/j.jsps.2016.05.001

Prime, R. B.; Bair, H. E.; Vyazovkin, S.; Gallagher, P. K.; Riga, A. *Thermogravimetric analysis (TGA).* In: thermal analysis of polymers: Fundamentals and Applications, eds. J. D. Menczel and R. B. Prime. Hoboken: Willey, 2009. https://doi.org/10.1002/9780470423837.ch3

Şayan, E. Optimization, and modeling of decolorization and COD reduction of reactive dye solutions by ultrasound-assisted adsorption. *Chem. Eng. J.* **2006**, *119*, 175–181. https://doi.org/10.1016/j.cej.2006.03.025

Schnitzler, E.; Lençone, K.; Kobelnik, M. Characterization of pharmaceuticals by thermal analysis. *Ciências Exatas e da Terra, C. Agrárias e Engenharias.* **2002**, *8* (1), 91–100.

Suno, M.; Ichihara, H.; Ishino, T.; Yamamoto, K.; Yoshizaki, Y. Photostability studies on (±)-tramadol in a liquid formulation. *J. Pharm. Health Care Sci.* **2015**, *1* (5), 1–6. https://doi.org/10.1186/s40780-014-0003-2

Tomassetti, M.; Catalanib, A.; Rossib, V.; Vecchio, S. Thermal analysis study of the interactions between acetaminophen and excipients in solid dosage forms and in some binary mixtures. *J. Pharm. Biomed. Anal.* **2005**, *37*, 949–955. https://doi.org/10.1016/j.jpba.2004.10.008

Trujillano, R.; Rives, V.; García, I. Photocatalytic Degradation of Paracetamol in Aqueous Medium Using TiO_2 Prepared by the Sol-Gel Method. *Molecules.* **2022**, *27* (9), 2904. https://doi.org/10.3390/molecules27092904

Varshny, L. and Patel, K. M. Effects of ionizing radiation on the pharmaceutical compound, Chloramphenicol. *Radiat. Phys. Chem*. **1994**, *43* (5), 471–480. https://doi.org/10.1016/0969-806X(94)90064-7

Vermeire, A.; Remon, J. P. Stability and compatibility of morphine: Review. *Int. J. Pharm.* **1999**, *187*, 17–51. https://doi.org/10.1016/S0378-5173(99)00181-7

Yousaf, M.; Nazir, S.; Hayat, Q.; Akhtar, M. N.; Akbar, M.; Lu, Y.; Noor, A.; Zhang, J.; Shah, M.A.K.; Wang, B. Magneto-optical properties and physical characteristics of M-type hexagonal ferrite ($Ba_{1-x}Ca_xFe_{11.4}Al_{0.6}O_{19}$) nanoparticles (NPs). *Ceram. Int*. **2021**, *47* (8), 11668–11676. https://doi.org/10.1016/j.ceramint.2021.01.006

ECLÉTICA QUÍMICA

Eclet. Quim. 49 | e-1526, 2024

Original Article

https://doi.org/10.26850/1678-4618.eq.v49.2024.e1526

Evaluation of the effectiveness of new mixed ligand complexes against the vector of Dengue fever *Aedes aegypti* (Diptera; Culicidae)

Nedhal Abdulmawla **Al–Selwi**[1], Abbas Mohamed **Al–Azab**[1], Yasmin Mosa'd Saeed **Jamil**[1+], Fathi Mohamed **Al–Azab**[1], Anwar Mohamed **Al–Ryami**[1]

Abstract

Chloroquine phosphate with ibuprofen and sulphamethoxazole were used as mixed ligands with Ni(II), Co(II), Cu(II), and Zn(II) to prepare new transition metal complexes. Metal analysis, IR, and X-ray diffraction (XRD) spectrum analyzes were used to describe them, with some modifications to the World Health Organization (WHO) standard susceptibility test under laboratory conditions. The biological effects of ligands and new complexes against *Aedes aegypti* mosquito larvae were evaluated at various concentrations. To assess larvicidal efficacy, late third or early fourth instar larvae were exposed to multiple concentrations of the examined compounds, ranging from 50 to 1000 ppm. Cu(II) complexes revealed significant high activity (LC$_{50}$ = 100 ppm against *Ae. Aegypti* was compared with the rest of the metal complexes. On the other hand, the Co(II) complex showed no activity against *Ae. aegypti*. These mixed ligand complexes seemed to be an alternative method for manufactured insecticides to control larvae of this medically important mosquito vector *Ae. aegypti*. Further research on other metal complex compounds responsible for larvicidal efficacy will be required.

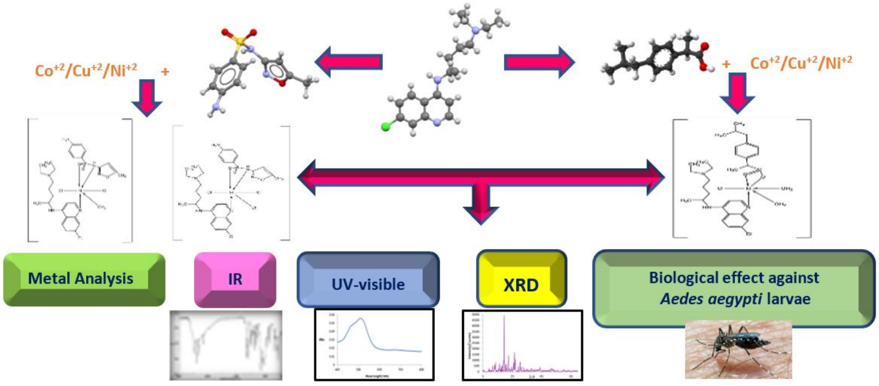

Article History

Received October 20, 2023
Accepted May 10, 2024
Published August 21, 2024

Keywords

1. complex;
2. mixed ligands;
3. XRD;
4. *Aedes aegypti*;
5. dengue fever.

Section Editor

Rogéria Rocha Gonçalves

Highlights

- Chloroquine phosphate was used with ibuprofen and sulphamethoxazole as mixed ligands.
- The mixed ligands were complexed with Ni(II), Co(II), Cu(II), and Zn(II).
- The biological effects against *Aedes aegypti* mosquito larvae were evaluated.
- The Cu(II) complexes revealed higher activity against *Aedes aegypti* than others.

[1]Sana'a University, Faculty of Science, Sana'a, Yemen. **+Corresponding author:** Yasmin Mosa'd Saeed Jamil, **Phone:** +967771952842, **Email address:** y.jamil@su.edu.ye

ISSN 1678-4618

1. Introduction

Mosquitoes belong to the order Diptera presented worldwide in most ecosystems. They are widely distributed around the world and can transmit viral, protozoal, and helminth diseases to human beings, such as dengue fever, chikungunya, West Nile virus, yellow fever, Rift Valley fever, malaria and elephantiasis in almost all tropical and subtropical countries, as well as many other parts of the world (Chew *et al.*, 2019; Netoi *et al.*, 2018).

Aedes aegypti Linnaeus was described in 1762 (Bar *et al.*, 2013). In most of the world, it is the primary vector for dengue (WHO, 2009), yellow fever (Al–Azab *et al.*, 2020), zika (Fauci and Morens, 2016; Marcondes and Ximenes, 2015; Schrauf *et al.*, 2020), chikungunya (Charrel *et al.*, 2014). Due to its strong ties to people, *Aedes aegypti* is significant. Unlike other animals, females attack people. They lay their eggs near human habitations in man-made containers, typically breeding grounds that are not completely covered with many organic resources for larval nutrition. *Aedes aegypti* has become more adapted to urban surroundings all over the world due to unchecked urbanization, rising temperatures, and a lack of long–term vector control measures (David *et al.*, 2021; Leandro *et al.*, 2023; Maciel-de-Freitas *et al.*, 2007; Scott *et al.*, 1993).

In some tropical and subtropical countries in the past 30 years, dengue fever outbreaks have grown ten times (Simmons and Farrar, 2009; WHO, 2009). The dengue virus has infected more than 3 billion people around the world and is responsible for more than 20,000 deaths annually. A total of 128 countries are in danger (Bhatt *et al.*, 2013; Rajaganesh *et al.*, 2016; Suresh *et al.*, 2015).

Dengue fever (DF) is a common local endemic infectious disease that mainly affects underdeveloped areas of Yemen and has high mortality and severity rates. This prevalence and geographic expansion of epidemic dengue have hurt Yemen, and the number of reported cases has increased in lockstep with the nation's social upheaval and civil war (Alyousefi *et al.*, 2016; Gutu *et al.*, 2021). Since 2000, there have been regular outbreaks of DF in Yemen, where it was initially identified in the Shabwah governorate in 1994. Aden and Taiz (2010; 2020), Hadramout and Mulalla (2005), and Al-Hudeidah Governorate, Yemen (1994, 2000, 2004, and 2005), outbreaks have been detected in Shabwah Governorate in 2001, 2002, 2005, 2018, 2019, and 2020 (unpublished reports) (Bin Ghouth *et al.*, 2012; Gutu *et al.*, 2021).

Chloroquine (CQ), an antimalarial drug, was first developed in the 1930s. It is produced by a convergent synthesis in which the aliphatic components (novaldiamine, 2–amino–5–dimethylaminopentane) and the quinoline parts (4,7–dichloroquinoline) are combined in the final stage of aromatic nucleophilic displacement. Although affordable and widely available, chloroquine is no longer highly effective against *P. falciparum*, the most lethal strain of the malaria parasite, due to drug resistance (Kucharski *et al.*, 2022; V. Singh, 2019).

The bacteriostatic agent sulfamethoxazole (SMX) is an antibiotic ften used for the treatment of many infections. Due to its common use, humans and animals can develop active and unmetabolized metabolites that have a variety of biological effects (Jasim *et al.*, 2022). In both human and veterinary medicine, is a frequently prescribed antibiotic that is also used as a sulfonamide in aquatic and terrestrial environments. In a European assessment of medicine and personal hygiene items, it was also included in the top 10 lists of essential drugs (Rauseo *et al.*, 2019).

One non–steroidal anti-inflammatory medicine (NSAID) that has therapeutic effects is Ibuprofen, which inhibits both the COX1 and COX2 isoforms of the cyclooxygenase enzyme. The production of prostaglandins, which are endogenous mediators implicated in the start of pain, inflammation, and fever, is catalyzed by this enzyme (Singh, 2019; Kucharski *et al.*, 2022).

Metals have always attracted researchers in modern medicine because of their significant involvement in physiological and pathological processes, and their antibacterial, antifungal, anti-inflammatory, and antimalarial capabilities. In many fields as molecular biology, photochemistry, bioinorganic chemistry, medicine, and chemistry, mixed ligand–metal complexes are essential (Muthuppalani *et al.*, 2022; A. Singh *et al.*, 2020). The biological features of these compounds and their inherent chemical value as multidentate ligands have been influenced by specific central metals, particularly Cu(II), Zn(II), Fe(III), Ni(II), Co(II), etc. This has led to a substantial improvement in the research on their coordination behavior (Kumar *et al.*, 2021). One of the main goals of modern inorganic coordination chemists and pharmaceutical research is to find and produce more effective pharmaceuticals to treat ailments. This has led to several investigations of drug–metal complexes (Adediji *et al.*, 2018), and researchers are exploring the therapeutic potential of metal-based antimalarial agents, especially since the discovery of ferroquine, once the most potent organometallic antimalarial drug (Biot *et al.*, 2011).

In this work, the potential larvicidal activities of these compounds are evaluated together with the production and characterization of complexes from chloroquine phosphate, ibuprofen and sulphamethoxazole with transition–metal ions.

2. Experimental

2.1. Materials

High–purity chemicals were used by many companies. Chloroquine phosphate, ibuprofen (Ibu), and sulphamethoxazole were obtained from Shaphaco Pharmaceutical Company. Other chemicals, solvents, indicators, and metal (II) chlorides (nickel chloride hexahydrate, cobalt chloride hexahydrate, copper chloride dehydrate, and zinc chloride hexahydrate) from BDH were used without further purification.

2.2. Preparation of metal complexes

In general, aqueous solutions of hydrated metal chlorides, chloroquine phosphate, and (10% ammonia solution of ibuprofen or 10% potassium hydroxide solution of sulphamethoxazole) in 1:1:1 mole ratio are prepared. The combination of the corresponding three solutions was refluxed on a hot plate for 3 h at 60–80 °C with constant stirring to obtain colored precipitates. Filters were used to obtain the solid precipitates, then carefully cleaned in hot water and dried by air (Muthuppalani *et al.*, 2022).

2.3. Physical Measurements

The Central Laboratory of the Faculty of Science of Cairo University, Giza, Egypt, used a Vario EL Fab. CHNS Nr to conduct the C, H, N, and S element analysis. At the Global Pharmaceutical Company, the metal content was evaluated using an atomic absorption spectrophotometer with standard solutions of metal chlorides used for calibration. A definite weight of the solid complexes was digested with 10 mL of concentrated HNO_3. This was repeated several times until all the organic matter was completely decomposed. The reaction mixture was evaporated just to dryness. After being cooled, the residue complex was dissolved in distilled water (Bader, 2011). At the Global

Pharmaceutical Company, a Sartorius conductivity meter model pp20 was used to measure the molar conductance of 10^{-3} mol L^{-1} solutions of metal complexes in 10% DMSO (dimethylsulfoxide) solvent. For the freshly produced solutions, all measurements were made at room temperature. At Sana'a University, the infrared spectra of the complexes were measured using an FT/IR–140 spectrophotometer with a KBr disc (4000–400 cm^{-1}) from Jasco, Japan.

A magnetic susceptibility balance from the Johnson–Metthey and Sherwood model was used to measure magnetic susceptibilities using Gouy's approach (Szafran *et al.*, 1991). The effective magnetic moment (μ_{eff}) values were obtained using the **Eqs. 1–3**).

$$X_g = \frac{C_{Bal} L\,(R - R_0)}{10^9 M} \quad (1)$$

where R_o=Reading of empty tube, L=Sample length (cm), M=Sample mass (g), R=Reading for the tube with sample, C_{Bal}=balance calibration constant=2.086

$$X_M = X_g .\ MWt \quad (2)$$

The values of X_M as calculated from **Eq. 2** are corrected for the diamagnetism of the ligands using Pascal's constants, then used in Curie's **Eq. 3**.

$$\mu_{eff} = 2.84\sqrt{X_M .\ \ T} \quad (3)$$

where T = t (°C) + 273

All melting points for the compounds are given in degrees Celsius and are measured in glass capillary tubes. Silver nitrate was used to determine chloride using a gravimetric method (Jamil *et al.*, 2022a). The weight loss approach allowed us to gravimetrically calculate the number of coordinated and uncoordinated water molecules (Refat *et al.*, 2014). TLC was carried out on Silica Gel GF_{254} plates (mn–kieselgel G., 0.2 mm thickness) with acetone solution as mobile eluent at room temperature (25 °C), plates were scanned using an ultraviolet 254 nm lamp. XRD patterns were obtained using an XD–2 powder X-ray diffractometer (Shimadzu ED–720) at a voltage of 35 kV and a current of mA using CuK(α) radiation in the range of $5^o < 2\theta < 70^o$ at 1^o min^{-1} scanning rate and a wavelength 1.54056 Å, in Yemen Geological Survey and Mineral Resources Board.

2.4. Crystallinity and particle size from XRD

The percentage of crystallinity, XC (%) was calculated based on the integrated peak areas of the principal peaks (Jamil *et al.*, 2023a). The crystallinity of the complexes is calculated relative to the crystallinity of the ligands as a ratio (**Eq. 4**):

$$XC\ (\%) = \left[\frac{(A_{ligand})}{(A_{complex})}\right] \times 100 \quad (4)$$

where $A_{complex}$ and A_{ligand} are the areas under the principal peaks of the complex and ligand sample, respectively.

XRD was also used to determine the average particle size (D), which was estimated by the Scherrer equation (**Eq. 5**) (Patterson, 1939; Saeed *et al.*, 2015).

$$D = \frac{K\lambda}{\beta\, cos\theta} \quad (5)$$

where K is Scherrer constant and equals 0.94, λ is the X-ray wavelength of Cu–Kα radiations (1.5405 Å), β is the full width at half maximum (FWHM) and θ is the Bragg diffraction angle in degrees.

2.5. Source of mosquito strain and rearing

2.5.1. Insects: mosquitoes

Aedes aegypti (Diptera; Culicidae) were obtained from untreated sites using insecticides from Sana'a city.

2.5.2. Mosquito strain rearing

The larvae of *Ae. aegypti* were reared under laboratory conditions of medical entomology, Department of Biological Sciences, Faculty of Science – Sana'a University for over several generations using fish food diet medium, larvae from culture.

2.5.3. Bioassay of mixed ligand complexes against *Ae. aegypti* (L.)

The larvicidal bioassay followed the WHO (2008) standard protocols with some modifications. Individual ligands and metal complexes were dissolved in 3% DMSO and the results were recorded 24 h later.

3. Results and discussion

After being washed with hot water, the Ni(II), Co(II), Cu(II), and Zn(II) complexes produced with the ligands were collected. Because of this, the complexes on their thin–layer chromatography displayed single spots with acceptable Rf values, indicating their pure condition. Insoluble in water, ethanol, methanol, acetone, $CHCl_3$, 0.1 mol/L NaOH, and dimethylformamide (DMF), all complexes were pigmented and stable in the presence of air but were all soluble in DMSO 10% and 0.1 mol/L HCl. The new complexes have melting points higher than those of the pure ligands. The melting points of Ni(II), Co(II) and Cu(II) complexes with the complex (CQ)(Ibu) and $[Zn(CQ)(SMX)Cl_3]$ were (> 350 °C). The melting temperatures of the other materials ranged from 204 to 254 °C. The complexes of Ni(II), Co(II), Cu(II) and Zn(II) exhibited molar conductivity values between 7 and 15 Ω^{-1} mol^{-1} cm^2, indicating the non–electrolytic nature of these complexes (Jamil *et al.*, 2022b). Some physical properties and analytical data of these complexes are listed in **Tables 1** and **2**.

Table 1. Some physical properties of the complexes.

Compound	Color (Yield%)	M.P. (°C)	Λm (Ω^{-1} cm^2 mol^{-1})	μeff (B.M.)	F.Wt (g/mol)	TLC	
						No. of Spots	R_f*
[Ni(CQ)(Ibu)(H_2O)$_2$Cl]	Light yellow (21)	>350	9	3.09	655.343	One	0.81
[Co(CQ)(Ibu)(H_2O)$_2$Cl]	Dark purple (26)	>350	7	4.75	655.583	One	0.71
[Cu(CQ)(Ibu)(H_2O)$_2$Cl]	Light green (20)	>350	8	1.68	660.199	One	0.54
[Zn (CQ)(Ibu)(H_2O)$_2$Cl]	White (22)	240	7	–	662.033	One	0.67
[Ni (CQ)(SMX)(H_2O)Cl_2]	Light green (36)	204	15	3.01	720.791	One	0.85
[Co (CQ)(SMX)(H_2O)Cl_2]	Pink (22)	254	14	5.05	721.001	One	0.74
[Cu (CQ)(SMX)Cl_3]	Sky blue (25)	220	12	1.73	743.055	One	0.49
[Zn (CQ)(SMX)Cl_3]	White (28)	>350	14	–	744.889	One	0.61

Note: *R_f = retention factor in Thin Layer Chromatography

Table 2. Elemental analysis of the complexes.

Complex (Molecular formula)	Element Analysis, Found (Calculated)%					
	C	H	N	S	M	Cl
[Ni(CQ)(Ibu)(H_2O)$_2$Cl]	56.82	7.21	6.42	–	8.98	10.83
($C_{31}H_{47}Cl_2NiN_3O_4$)	(56.81)	(7.23)	(6.41)	–	(8.96)	(10.82)
[Co(CQ)(Ibu)(H_2O)$_2$Cl]	56.79	7.25	6.44	–	8.94	10.85
($C_{31}H_{47}Cl_2CoN_3O_4$)	(56.75)	(7.23)	(6.41)	–	(8.99)	(10.82)
[Cu(CQ)(Ibu)(H_2O)$_2$Cl]	56.43	7.16	6.38	–	9.67	10.75
($C_{31}H_{47}Cl_2CuN_3O_4$)	(56.40)	(7.18)	(6.36)	–	(9.63)	(10.74)
[Zn(CQ)(Ibu)(H_2O)$_3$]	56.28	7.14	6.37	–	9.86	10.73
($C_{31}H_{47}Cl_2ZnN_3O4$)	(56.24)	(7.16)	(6.35)	–	(9.88)	(10.71)
[Ni(CQ)(SMX)(H_2O)Cl_2]	46.61	5.40	11.58	4.47	8.10	14.72
($C_{28}H_{37}Cl_3CuO_4N_6S$)	(46.66)	(5.45)	(11.66)	(4.45)	(8.14)	(14.76)
[Co(CQ)(SMX)(H_2O)Cl_2]	46.61	5.43	11.67	4.42	8.19	14.79
($C_{28}H_{39}Cl_3CoN_6SO_4$)	(46.64)	(5.45)	(11.66)	(4.45)	(8.17)	(14.75)
[Cu(CQ)(SMX)Cl_3]	45.31	5.09	11.27	4.30	8.60	19.01
($C_{28}H_{37}Cl_4CuO_3N_6S$)	(45.25)	(5.02)	(11.31)	(4.32)	(8.55)	(19.06)
[Zn(CQ)(SMX)Cl_3]	45.21	4.97	11.62	4.33	8.81	14.71
($C_{28}H_{37}Cl_4ZnN_6O_4S$)	(45.15)	(5.01)	(11.66)	(4.30)	(8.78)	(14.76)

3.1. The infrared spectra

The infrared spectrum of chloroquine was compared with that of the metal complex. It is reported (Otuokere *et al.*, 2019) that the vibration frequencies of NH and C=N of chloroquine occur at 3260 and 1580 cm^{-1}. Chloroquine in these complexes behaves as a neutral monodentate molecule, due to the nitrogen atom in the quinoline ring.

3.1.1. Infrared spectra of nickel (II), cobalt (II), copper (II) and zinc (II) complexes with chloroquine and ibuprofen

Ibuprofen was bidentate through the oxygen atoms in the carboxyl group. As a result, in these complexes (**Figs. S1–S4**), a metal ion is coordinated with each of the two ligands, ibuprofen and chloroquine (**Table S1**) summarizes the bonding site assignments, which are based on the following pieces of evidence. A wide band that was present in all complexes within the 3467–3195 cm^{-1} range has been assigned to ν(OH) and *ν*(NH), with ν(OH) appearing at 3388–3467 cm^{-1} and ν(NH) appearing at 3195–3220 cm^{-1} (Otuokere *et al.*, 2019). At 3451 cm^{-1}, ν(OH) in the ibuprofen–free ligand is visible. The coordination is confirmed by the absence of ν(OH) vibration (Abbas *et al.*, 2022). According to (Bamigboye *et al.*, 2020), coordinated water can be distinguished by the appearance of 880 and 522 cm^{-1}, respectively. The peak at 1709 cm^{-1}, previously ascribed to the free ibuprofen band of C=O stretching (Abbas *et al.*, 2022), has been shifted to 1722 cm^{-1}, indicating that coordination occurred at this position.

The stretch of C=N in free chloroquine is linked to the peak at 1580 cm^{-1} (Mohammad and Abdullah, *et al.*, 1984). This peak moved to 1458 cm^{-1}, indicating that the C=N functional group was involved in coordination. The C=N bond length grew because of the falling electron density, which in turn caused the vibration frequency to decrease. This change implies that the location of the quinoline ring in chloroquine caused coordination. For each of the M–O vibrations at 416–445 cm^{-1}, the Ni(II), Co(II), Cu(II), and Zn(II) complexes displayed a single weak band. The current evidence of υ(M–N) could not be brought into the IR data due to instrumental limitations in the 219–297 cm^{-1} region (Nakamoto, 1978).

3.1.2. Infrared spectra of nickel(II), cobalt(II), copper(II), and zinc(II) complexes with chloroquine and sulfamethoxazole

Using KBr discs to examine the infrared bands of free sulfamethoxazole, three distinct and strong bands were found at 3466, 3377, and 3298 cm^{-1}. These bands are the result of symmetric and asymmetric stretching vibrations of the aromatic amino group (NH_2) and sulfonamide (NH), respectively (Al–Noor *et al.*, 2014; Alosaimi, 2022; Chavda *et al.*, 2021). According to Torre *et al.* (2005) and Jamil *et al.* (2017), stretching vibrations of the S=O group were found at 1365 cm^{-1} and 1091 cm–^{1}, respectively. By stretching the phenyl ring (C=C) strong and sharp bands are generated at 1596 cm^{-1} and 1503 cm^{-1}. As shown in **Figs. S5 and S6**, the complexes have the same bands in the same location with the same wave number without shifting. However, the complex in **Fig. S7** shows only one band at 3443 cm^{-1}, with the other bands disappearing. Three bands overlap, resulting in the formation of a broadband and the elimination of the other bands.

The complex in **Fig. S8** contains a single broadband at 3453cm^{-1} for the same reason.

The S=O group stretching vibrations are asymmetric and symmetric at 1365 and 1091 cm^{-1}, respectively. Asymmetric and symmetric were found at 1383 cm^{-1} and 1076 cm^{-1}, respectively, for the molecule shown in **Fig. S5**. **Table S2** contains the remaining items. The M–O stretching vibrations in the 421–483 cm^{-1} region are responsible for the new bands in the complex spectra. Current evidence of υ(M–N) was not included in IR data due to an experimental limitation in the 219–297 cm^{-1} range (Nakamoto, 1978).

3.2. X–ray diffraction

3.2.1. X–ray diffraction of the chloroquine, ibuprofen ligands, and their complexes

Figure S9–S14 represent the XRD patterns for chloroquine, ibuprofen, and its complexes. From these figures, a notable shifting of the main peak toward higher diffraction angles (**Table S3**) is observed for the complexes, suggesting the reduction of the unit cell dimensions and consequently contracting the crystal lattice (Aroyo, 2016). In addition, significant changes in intensities of the main peaks of ligands and their complexes are observed in these figures, which are attributed to the reduction in crystallinity. The crystallinity calculations are based on the ratio of the principal peak area of the complex sample to that of the ligand sample, obtaining a relative crystallinity (Shah *et al.*, 2006). The results in **Table S3** show significant changes in crystallinity between chloroquine, ibuprofen, and its complexes that exhibit low relative crystallinity (3.201, 4.600, 23.017 and 24.366%). In the literature, the range between 1–100 nm is reported to be of nanoparticle size (Boverhof *et al.*, 2015). The particle size of the complexes obtained from XRD shows effects on their nanoparticle size (4.422, 2.99, 4.821 and 4.4054 nm).

3.2.2. X–ray diffraction of the chloroquine, sulphamethoxazol ligands, and their complexes

The XRD patterns for chloroquine, sulfamethoxazole, and their compounds are shown in **Fig. S15– S19**. According to these figures, a notable shift of the primary peak for the complexes towards higher diffraction angles (**Table S4**) suggests that the dimensions of the unit cells have decreased, which has caused the crystal lattice to constrict (Aroyo, 2016). Calculations of relative crystallinity are also based on the ratio of the primary peak area of the complex sample to that of the ligand sample (Shah *et al.*, 2006). The findings shown in **Table S4** demonstrate considerable variations in the relative crystallinity of chloroquine, sulfamethoxazole and their complexes (61.386, 23.513, 92.978 and 32.538%). The literature reports that the sizes of nanoparticles fall within the range of 1 to 100 nm (Boverhof *et al.*, 2015). The complexes discovered by XRD had nanoparticle–sized particles (5.058, 4.789, 3.5754 and 4.9042 nm). The proposed structure of the complexes in **Figs. 1** and **2**.

3.3 Biological effect of metal complexes against *Aedes aegypti* larvae

The larvicidal bioassay adhered to the established guidelines by the WHO (Abbott, 1925). Concentrations of 50, 100, 150, 300, 500, and 1000 ppm were prepared in 3% DMSO for each chemical. The late third or early fourth instar larvae were constantly exposed to different concentrations of chemicals for the duration of the treatments. Following these tests, the larvae were given their regular diet. The fatality percentage was reported after a 24–hour exposure period.

The compounds were carefully stored according to the recommended conditions by periodic measurements to assess their pH, solubility, and dissolution stability. DMSO solvent was employed to ensure the integrity of the compounds, avoiding any solvent that could potentially affect their properties. The compounds' physical appearance, including color and odor, were examined in addition to the physicochemical assessments. Comprehensive biological tests took place to evaluate their properties during the storage period. These experiments involved a wide range of concentrations at the beginning of the evaluation, and to determine the stability and shelf–life of these compounds high (1000 ppm) and low (50 ppm) concentrations were utilized. These concentrations were chosen after four months of storage, reflecting real–life conditions. By employing this approach, the compounds' long–term stability could be assessed and established their suitability for practical applications.

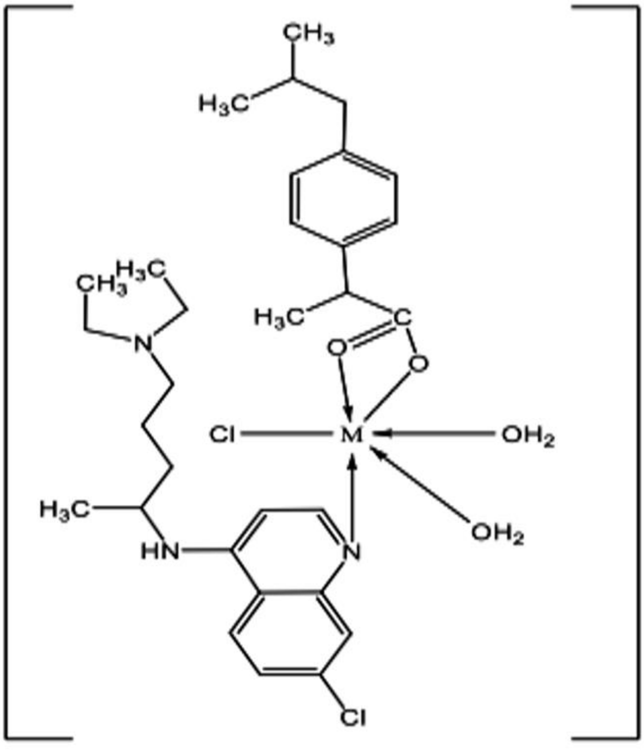

Where: M= Ni(II), Co(II), Cu(II), or Zn(II)

Figure 1. Proposed structure of (CQ)(Ibu) complexes.

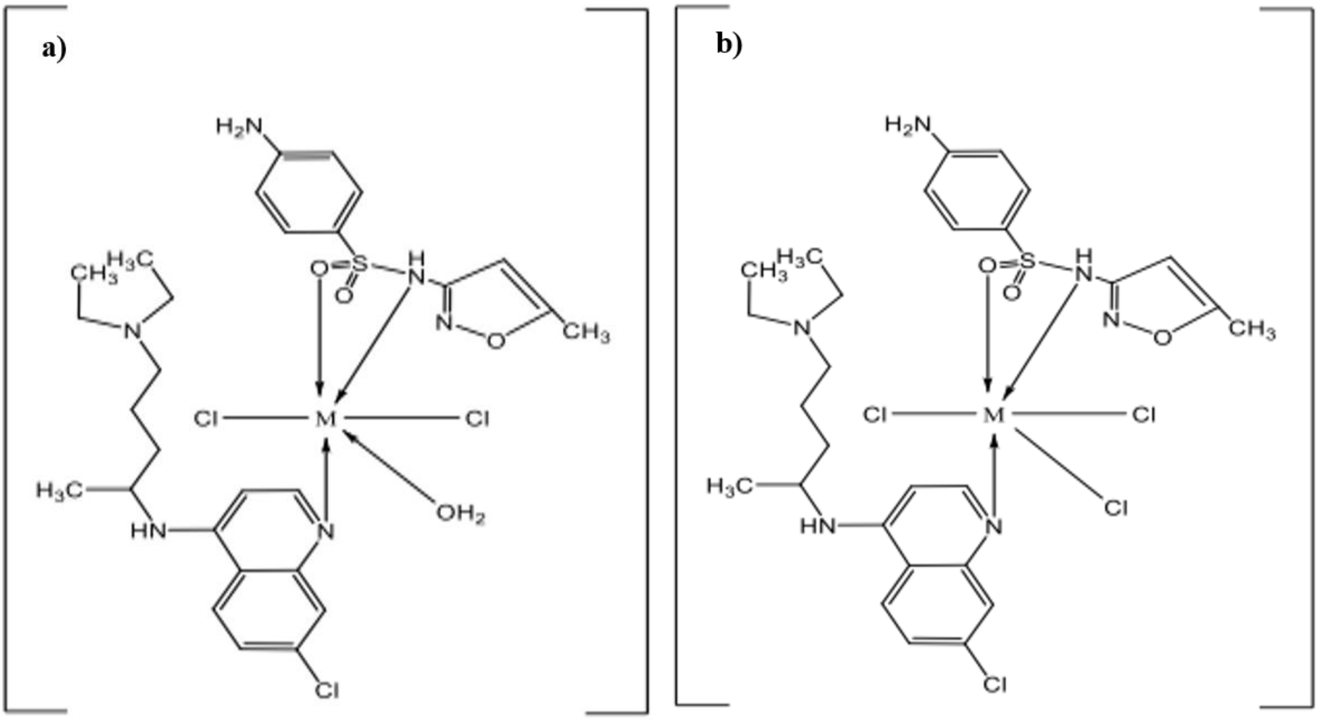

Where: M = Ni(II) or Co(II)

Where: M = Cu(II) or Zn(II)

Figure 2. Proposed structure of (CQ)(SMX)complexes.

3.3.1 Statistical analysis

A complete randomized design (CRD) was used in a factorial experiment design. Using the Minitab application, the statistical analysis of the data was performed using analysis of variance (ANOVA) tools, and the averages were compared by Least Significance Difference LSD at $p \leq 0.05$. According to the Probit analysis program, LC_{50} (concentration that kills 50% of mosquito larvae) and LC_{95} (concentration that kills 95% of mosquito larvae) were determined (Abbott, 1925; Tisgratog *et al.*, 2016). According to an automated log–probit analysis, the 95% confidence interval.

3.3.2. Biological effect of the complexes nickel (II), cobalt (II), copper (II) and zinc (II) with chloroquine phosphate, and ibuprofen against larvae mosquito (*Aedes aegypti*)

As given in **Table S5** chloroquine, ibuprofen and their complexes with nickel (II), cobalt (II), copper (II) and zinc (II) were less effective in larvae mortality compared to the ibuprofen compound at concentrations of 1000 ppm and 300 ppm. For copper and zinc metal complexes, the percentage of mosquito larvae mortality was higher than that of the nickel (II) complex, and the cobalt (II) complex did not affect mosquito larvae. The acidic effect of the chloroquine diphosphate ligand resulting from the two phosphate groups is the main reason for the effectiveness, where the pH is (3.8 to 4.3). The effect of free Ibuprofen may be due to the carboxylic acid group of the acidic effect. It was also assumed that complexes with endogenous metals (Ni, Co, Cu, and Zn) could be less toxic than those with nonessential metals (WHO, 1999). Copper–containing coordination compounds were found to be promising therapeutic agents in a diverse range of diseases, including malaria, due to their ability to act by various mechanisms, such as inhibition of proteasome activity (WHO, 2003), telomerase activity (Meshnick and Dobson, 2001), and formation of reactive oxygen species (ROS) (Wells, 2011), DNA degradation (Stork *et al.*, 2001), and DNA intercalation (Wongsrichanalai *et al.*, 2002). All complexes are less acidic than their ligands due to chelation and changing of the –COOH group in ibuprofen into the –COO– group but, may have a high effect of some complexes against *Ae. aegypti.* depend on the toxicity of the metal (Rayms–Keller *et al.*, 1998).

The effectiveness of CQ,Ibu–Cu complexes increases with concentration (**Table 3**). The high effect of this complex against *Ae. aegypti* depends on the toxicity of the metal (Rayms–Keller *et al.*, 1998). Then, the toxicity line was drowned to calculate LC_{50} and LC_{95} (**Table 4** and **Fig. S20**).

Table 3. Toxicity effect of CQ,Ibu–Cu complex against *Ae. aegypti* larvae.

Compound	Conc. (ppm)	Larval Mortality (%)
CQ,Ibu–Cu complex	50	10
	100	17
	150	26
	300	70
	500	88
	1000	100
Control	3% DMSO	0

Table 4. Statistical parameters of CQ,Ibu –Cu complex.

Statistical parameters	CQ, Ibu–Cu complex
LC_{50} (ppm)	209.73
95% (*F. L)	198.48 – 221.09
LC_{95} (ppm)	609.12
95% (*F. L)	565.26 – 662.08
Slope	1.37
R^2	0.98

3.3.3. Biological effect of nickel (II), cobalt (II), copper (II) and zinc (II) complexes with chloroquine phosphate and sulfamethoxazole against larvae mosquito (*Aedes aegypti*)

Chloroquine, sulfamethoxazole and their complexes with nickel (II), cobalt (II), copper (II) and zinc (II) were less efficient in causing mortality in larvae than their complexes at concentrations of 1000 and 300 ppm, as shown in **Table S6**. Sulphamethoxazole ligand may have a basic effect in situations where it was not effective against larvae, and the effects of all subsequent ligands and complexes rely on acidity. The effectiveness of the CQ,SMX–Cu complex increased with concentration (**Table 5**). Depending on the metal's toxicity, this combination has a strong anti–*Aedes aegypti* action (Wongsrichanalai *et al.*, 2002). Then, the toxicity line was drowned to calculate LC_{50} and LC_{95} (Jamil *et al.*, 2023b) (**Table 6** and **Fig. S21**).

Table 5. Toxicity effect of CQ,SMX–Cu complex against *Ae. aegypti* larvae.

Compound	Concentration (ppm)	Larval Mortality (%)
CQ SMX–Cu Complex	50	30
	100	50
	150	68
	300	80
	500	85
	1000	100
Control	3% DMSO	0

Table 6. Statistical parameters of CQ,SMX–Cu complex.

Statistical parameters	CQ,SMX–Cu complex
LC_{50} (ppm)	103.12
95% (*F. L)	92.56 – 113.51
LC_{95} (ppm)	699.39
95% (*F. L)	622.64 – 799.36
Slope	0.76
R^2	0.94

4. Conclusions

The novel compounds have been produced by mixing chloroquine phosphate with ibuprofen and sulfamethoxazole, individually with the metals Ni(II), Co(II), Cu(II) and Zn(II). This research has looked at how the ligands and their complexes affect *Ae. aegypti* mosquito larvae biologically. Based on these findings, it was determined that the mixed ligand complexes have beneficial effects against the larval stage of *Ae. aegypti*. The most effective compounds were Cu(II) complexes, followed by Ni(II), Co(II), and Zn(II) complexes. The Cu(II) complexes may offer other strategies for limiting the *Ae. aegypti* mosquito, the dengue vector, according to this study's findings. These findings could motivate researchers to look for new active substances that could be effective substitutes for the present pesticides.

Authors' contributions

Conceptualization: Jamil, Y. M.; Al–Azab, F. M.; Al–Ryami, A. M.; **Data curation:** Al–Ryami, A. M.; **Formal Analysis:** Jamil, Y. M.; Al–Ryami, A. M.; Al–Selwi, N. A.; **Funding acquisition:** Not applicable; **Investigation:** Jamil, Y. M.; Al–Azab, A. M.; Al–Ryami, A. M.; **Methodology:** Jamil, Y. M.; Al–Azab, A. M.; Al–Ryami, A. M.; **Project administration:** Jamil, Y. M.; **Resources:** Jamil, Y. M.; Al–Azab, F. M.; Al–Azab, A. M.; **Software:** Jamil, Y. M.; Al–Azab, A. M.; Al–Ryami, A. M.; **Supervision:** Jamil, Y. M.; Al–Azab, F. M.; **Validation:** Jamil, Y. M.; Al–Azab, F. M.; **Visualization:** Jamil, Y. M.; Al–Azab, F. M.; Al–Selwi, N. A.; **Writing – original draft:** Al–Ryami, A. M.; Al–Selwi, N. A.; **Writing – review & editing:** Jamil, Y. M.

Data availability statement

The data will be available upon request.

Funding

Not applicable.

Acknowledgments

Not applicable.

References

Abbas, A. M.; Aboelmagd, A.; Kishk, S. M.; Nasrallah, H. H.; Boyd, W. C.; Kalil, H. and Orabi, A.S. A Novel Ibuprofen Derivative and Its Complexes Physicochemical Characterization, DFT Modeling, Docking, In Vitro Anti–Inflammatory Studies, and DNA Interaction. *Molecules*. **2022**, *27* (21), 7540. https://doi.org/10.3390/molecules27217540

Abbott, W. S. A Method of Computing the Effectiveness of an Insecticide. *Journal of Economic Entomology*. **1925**, *18* (2), 265–267. https://doi.org/10.1093/jee/18.2.265a

Adediji, J. F.; Olayinka, E. T.; Adebayo, M. A.; Babatunde, O. A study of the mode of coordination of mixed antimalarial metal complexes. *African Journal of Malaria and Tropical Diseases*. **2018**, *6* (10), 444–449.

Al–Azab, A. M.; Zaituon, A. A.; Al–Ghamdi, K. M.; Abd Al–Galil, F. M. Effect of Four Indigenous Medicinal Plants on Dengue Fever, Vector *Aedes aegypti* from Jeddah, Saudi Arabia. *Biosc. Biotech. Res. Comm*. **2020,** *13* (1), 212–218. https://doi.org/10.21786/bbrc/13.1/37

Al–Noor, T. H.; Mahdi, R. T.; Ismael, A. H. Preparation, characterization, and antibacterial properties of mixed ligand complexes of L–aspargine and sulfamethoxazole(antibiotic) with Mn(II), Co(II), Ni(II), Cu(II), Zn(II), Cd(II) and Hg(II) ions. *Journal of Chemical and Pharmaceutical Research*. **2014**, *6* (5), 1286–1294. https://doi.org/10.18488/journal.65/2014.1.6/65.6.109.120

Alosaimi, E. H. Spectroscopic Characterization, Thermogravimetry and Biological Studies of Ru(III), Pt(IV), Au(III) Complexes with Sulfamethoxazole Drug Ligand. *Crystals*. **2022**, *12* (3), 340. https://doi.org/10.3390/cryst12030340

Alyousefi, T. A. A.; Abdul–Ghani, R.; Mahdy, M. A. K.; Al–Eryani, S. M. A.; Al–Mekhlafi, A. M.; Raja Y. A.; Shah, S. A.; Beier, J. C. A household–based survey of knowledge, attitudes and practices towards dengue fever among local urban communities in Taiz Governorate, *Yemen. BMC Infect Dis*. **2016**, *16* (1), 543. https://doi.org/10.1186/s12879–016–1895–2

Aroyo, M. I. *International Tables for Crystallography Volume A*: Space–Group Symmetry. John Wiley and Sons, 2016. https://doi.org/10.1107/97809553602060000114

Bader, N. R. Sample preparation for flame atomic absorption spectroscopy: an overview. RJC. **2011**, *4* (1), 49–55.

Bamigboye, O. M.; Ejidike, I. P.; Ahmed, R. N.; Lawal, M.; Nnabuike, G. G. Medubi, K. Chelation, characterization, and antibacterial activities of some mixed isonicotinic acid hydrazide–Paracetamol metal drug complexes. *Suranaree J. Sci. Technol.* **2020,** *27* (3), 030026.

Bar, A.; Andrew, J. Morphology and Morphometry of *Aedes aegypti* Larvae. *Annual Review & Research in Biology*. **2013**, *3* (1), 1–21.

Bhatt, S.; Gething, P. W.; Brady, O. J.; Messina, J. P.; Farlow, A. W.; Moyes, C. L.; Drake, J. M.; Brownstein, J. S.; Hoen, A. G.; Sankoh, O.; Myers, M. F.; George, D. B.; Jaenisch, T.; Wint, G. R. W.; Simmons, C. P.; Scott, T. W.; Farrar, J. J.; Simon I. Hay, S. I. The global distribution and burden of dengue. *Nature*. **2013**, *496*, 504–507. https://doi.org/10.1038/nature12060

Bin Ghouth A. S. B.; Amarasinghe, A.; Letson, G. W. Dengue outbreak in Hadramout, Yemen, 2010: an epidemiological perspective. *Am J Trop Med Hyg*. **2012**, *86* (6),1072. https://doi.org/10.4269/ajtmh.2012.11–0723

Biot, C.; Nosten, F.; Fraisse, L.; Ter–Minassian, D.; Khalife, J.; Dive, D. The antimalarial ferroquine: From bench to clinic. *Parasite*, **2011**, *18*, 207–214. https://doi.org/10.1051/parasite/2011183207

Boverhof, D. R.; Bramante, C. M.; Butala, J. H.; Clancy, S. F.; Lafranconi, M.; West, J.; Gordon, S. C. Comparative assessment of nanomaterial definitions and safety evaluation considerations. *Regulatory Toxicology and Pharmacology*. **2015**, *73* (1), 137–150. https://doi.org/10.1016/j.yrtph.2015.06.001

Charrel, R. N.; Leparc–Gofart, I.; Gallian, P.; Lamballerie, X. Globalization of chikungunya: 10 years to invade the world. *Clin Microbiol Infect*. **2014**, *20* (7), 662–663. https://doi.org/10.1111/1469-0691.12694

Chavda, B. R.; Socha, B. N.; Pandya, S. B.; Chaudhary, K. P.; Padariya, T. J.; Alalawy, M. D.; Patel, M. K.; Dubey, R. P.; Patel, U. H. Coordination behavior of dinuclear silver complex of sulfamethoxazole with solvent molecule having static rotational d isorder: Spectroscopic characterization, crystal structure, Hirshfeld surface and antimicrobial activity. *J. Mol. Struct*. **2021**, *1228*, 129777. https://doi.org/10.1016/j.molstruc.2020.129777

Chew, T.; Pakasi, T.; Taylor–Robinson, A**.** Dengue Infection in Indonesia: Improved Clinical Profiling is Needed to Better Inform Patient Management and Disease Outbreak Control. *Journal of Tropical Medicine and Health*. **2019,** *3*, 142. https://doi.org/10.29011/2688-6383.000042

David, M. R.; Dantas, E. S.; Maciel–de–Freitas, R.; Codeço, C. T.; Prast, A. E.; Lourenço–de–Oliveira, R. Influence of Larval Habitat Environmental Characteristics on Culicidae Immature Abundance and Body Size of Adult Aedes Aegypti. *Front. Ecol. Evol*. **2021**, *9*, 626757. https://doi.org/10.3389/fevo.2021.626757

Fauci, A. S.; Morens, D. M. Zika virus in the Americas—yet another arbovirus threat. *New Eng Jour Med.* **2016**, *374* (7), 601–604. https://doi.org/10.1056/nejmp1600297

Gutu, M. A.; Bekele, A.; Seid, Y.; Mohammed, Y.; Gemechu, F.; Woyessa, A. B.; Tayachew, A.; Dugasa, Y.; Gizachew, L.; Idosa, M.; Tokarz, R. E.; Sugerman, D. Another dengue fever outbreak in eastern Ethiopia—an emerging public health threat. *PLOS Negl Trop Dis*. **2021**, *15* (1), e0008992. https://doi.org/10.1371/journal.pntd.0008992

Jamil, Y. M. S.; Al–Maqtari, M. A.; Al–Qadasi, M. K. Ligational and Spectroscopic On Some Sulfamethoxazole Metal Complexes As Antimicrobial Agents, *European Journal Of Pharmaceutical And Medical Research*. Ejpmr. **2017**, *4* (7), 95–105.

Jamil, Y. M. S.; Al–Azab, F. M.; Al–Selwi, N. A.; Alorini, Th. and Al–Hakimi, A. N. P. Preparation, physicochemical characterization, molecular docking and biological activity of a novel schiff–base and organophosphorus schiff base with some transition metal(II) ions. *Main Group Chemistry*. **2022a**, 1–26. https://doi.org/10.3233/MGC-220101

Jamil, Y. M. S.; Al–Azab, F.; Al–Selwi, N.; Al–duais, F.; Al–Hakimi, A.; Alhagri, I.; El–Sayed, S. Synthesis, Spectroscopic and Antibacterial Studies of New Schiff–base and Organophosphorus Schiff–base with Some Transition Metal (II) Ions. *Journal of Qassim University for Science*. **2022b**, *1* (1), 129–153.

Jamil, Y. M. S.; Al–Azab, F. M.; Al–Selwi, N. A. Novel organophosphorus schiff base ligands: synthesis characterization, ligational aspcts, XRD and biological activity studies. *Eclét. Quím*. **2023a**, *48* (3), 36–53. https://doi.org/10.26850/1678-4618eqj.v48.3.2023.p36-53

Jamil, Y. M. S.; Al–Azab, A.; Al–Azab, F.; Al–Selwi, N. A. Larvicidal Effects of New Organophosphorus Schiff base compounds against Dengue Fever Vector Aedes aegypti (Diptera; Culicidae). *Sana'a University Journal of Applied Sciences and Technology* **2023b**, 1(1) 78 – 87. https://doi.org/10.59628/jast.v1i1.156

Jasim, D. J.; Abbas, A. K. Synthesis, identification, antibacterial, medical and dying performance studies for azosulfamethoxazole metal complexes. *Eurasian Chem. Commun*. **2022**, *4*, 16–40. https://doi.org/10.22034/ecc.2022.310593.1251

Kucharski, D. J.; Jaszczak, M. K.; Przemysław Boraty´nski, J. A. Review of Modifications of Quinoline Antimalarials Mefloquine and (hydroxy)Chloroquine. *Molecules*. **2022**, *27* (3), 1003. https://doi.org/10.3390/molecules27031003

Kumar, K. S.; Reena, V. N.; Aravindakshan, K. K. Synthesis, anticancer and larvicidal activities of a novel Schiff base ligand, 3–((2–((1–(4–hydroxyphenyl)ethylidene)amino)ethyl)imino)–N–(p–tolyl) butanamide and its Mn(II), Fe(III), Co(II), Ni(II) and Zn(II) complexes. *Results in Chemistry*, **2021**, *3*, 100166. https://doi.org/10.1016/j.rechem.2021.100166

Leandro, A. D. S.; Ayala, M. J. C.; Lopes, R. D.; Martins, C. A.; Maciel–de–Freitas R.; Villela, D. A. M. Entomo–Virological *Aedes aegypti* Surveillance Applied for Prediction of Dengue Transmission: A SpatioTemporal Modeling Study. *Pathogens*. **2023**, *12* (1), 4. https://doi.org/10.3390/pathogens12010004

Maciel-de-Freitas, R.; Marques, W. A.; Peres, R. C.; Cunha, S. P.; Lourenço-de-Oliveira, R. Variation in *Aedes aegypti* (Diptera: Culicidae) Container Productivity in a Slum and a Suburban District of Rio de Janeiro during Dry and Wet Seasons. *Mem. Inst. Oswaldo Cruz*. **2007**, *102*, 489–496. https://doi.org/10.1590/s0074–02762007005000056

Marcondes, C. B.; Ximenes, F. F. M. Zika virus in Brazil and the danger of infestation by *Aedes (Stegomyia)* mosquitoes. *Rev. Soc. Bras. Med. Trop*. **2015**, *49* (1), 4–10. https://doi.org/10.1590/0037-8682-0220-2015

Meshnick, S. R.; Dobson, M. J. The history of antimalarial drugs. Antimalarial chemotherapy. *P. J. Rosenthal (ed.)*. **2001**, 15–26. https://doi.org/10.1385/1-59259-111-6:15

Mohammad, T.; Abdullah, A. *Analytical profiles of drug substances*. King Saud University, 1984.

Muthuppalani, M.; Al Otaibi, A.; Balasubramaniyan, S.; Manikandan, S.; Manimaran, P.; Mathubala, G.; Manikandan, A.; Arshad, M. N.; Puttegowda, M.; Alorfi, H. S.; Khan, A.; Asiri, A. M.; Rahman, M. M. Synthesis, Characterization and Bio–Potential Activities of Co(II) and Ni(II) Complexes with O and N Donor Mixed Ligands. *Crystals*, **2022**, *12* (3), 326. https://doi.org/10.3390/cryst12030326

Nakamoto, K. *Infrared and Raman Spectra of Inorganic and Coordination Compounds*. John Wiley and Sons, 1978.

Netoi, A.; Junior, P.; Silva, M.; Lima, S.; Yara, R.; Guimavaes, E.; Santana, E.; Selva, L.; Delira, E.; Vieir, J. Evaluation of Embryotoxic and Embryostatic Effects of the Aqueous Extract of Rhizophora mangle and Tannic Acid on Eggs and Larvae of *Aedes aegypti*. *Anais da Academia Brasileira de Ciencias*. **2018**, *2* (1), 2141–2148. https://doi.org/10.1590/0001–3765201720170297

Otuokere, I. E.; Okpara, L. O.; Amadi, K. C.; Alisa,C. O.; Okoyeag, A.; Nwadire, F. C. Synthesis, Characterization and Complexation Behaviour of Chloroquine towards Ti (II) Ion. *Journal of Pharmaceutical Research International*. **2019**, *27* (3), 1–6. https://doi.org/10.9734/jpri/2019/v27i330168

Patterson, A. The Scherrer formula for X–ray particle size determination. *Phys. Rev*. **1939**, *56*, 978. https://doi.org/10.1103/PhysRev.56.978

Rajaganesh, R.; Murugan, K.; Panneerselvam, C.; Jayashanthini, S.; Roni, M.; Suresh, U.; Trivedi, S.; Rehman, H.; Higuchi, A.; Nicoletti, M.; Benelli, G. Fern–synthesized silver nanocrystals: Towards a new class of mosquito oviposition deterrents. *Res. Vet. Sci*. **2016**, *109*, 40–51. https://doi.org/10.1016/j.rvsc.2016.09.012

Rauseo, J.; Barra Caracciolo, A.; Ademollo, N.; Cardoni, M.; Di Lenola, M.; Gaze, W.; Stanton, I.; Grenni, P.; Pescatore, T.; Spataro, F.; Patrolecco, L. Dissipation of the antibiotic sulfamethoxazole in a soil amended with anaerobically digested cattle manure. *Mater*. **2019**, *378*, 120769. https://doi.org/10.1016/j.jhazmat.2019.120769

Rayms–Keller, A.; Olson, K. E.; McGaw, M.; Oray, C.; Carlson, J. O.; Beaty, B. J. Effect of Heavy Metals on Aedes aegypti (Diptera: Culicidae) Larva. *Ecotoxicology and environmental safety*. **1998,** *39* (1), 41–47. https://doi.org/10.1006/eesa.1997.1605

Refat, M. S.; Al-Azab F. M.; Al-Maydama H. M.; Amin R. R.; Jamil, Y.M.S. Synthesis and in vitro microbial evaluation of La(III), Ce(III), Sm(III) and Y(III) metal complexes of vitamin B6 drug. *Spectrochim. Acta - A: Mol. Biomol. Spectrosc.* **2014** *127* (2014) 196–215. https://doi.org/10.1016/j.saa.2014.02.043

Saeed, M.; Alenad, A. A.; Malik, M. A. Synthesis of mackinawite FeS thin films from acidic chemical baths. *Materials Science in Semiconductor Processing*. **2015**, *32*, 1–5. https://doi.org/10.1016/j.mssp.2014.12.073

Schrauf, S.; Tschismarov, R.; Tauber, E.; Ramsauer, K. Current eforts in the development of vaccines for the prevention of Zika and chikungunya virus Infections. *Front Immunol*. **2020**, *11*, 592. https://doi.org/10.3389/fimmu.2020.00592

Scott, T. W.; Chow, E.; Strickman, D.; Kittayapong, P.; Wirtz, R. A.; Lorenz, L. H.; Edman, J. D. Blood–Feeding Patterns of *Aedes aegypti* (Diptera: Culicidae) Collected in a Rural Thai Village. *J. Med. Entomol*. **1993**, *30*, 922–927. https://doi.org/10.1093/jmedent/30.5.922

Shah, B.; Kakumanu, V. K.; Bansal, A. K. Analytical techniques for quantification of amorphous/crystalline phases in pharmaceutical solids. *J. Pharm Sci*. **2006**, *95* (8), 1641–1665. https://doi.org/10.1002/jps.20644

Simmons, C.; Farrar, J. Changing Patterns of Dengue Epidemiology and Implications for Clinical Management and Vaccines. *PLoS Med*. **2009**, *6* (9), e1000129. https://doi.org/10.1371/journal.pmed.1000129

Singh, V. Metal complexes as antimalarial potential: A review. *The Pharma Innovation Journal.* **2019**, *8* (5), 403–406.

Singh, A.; Sharma, J.; Paichha, M.; Chakrabarti, R. *Achyranthes aspera* (prickly chaff flower) leaves- and seeds-supplemented diets regulate growth, innate immunity, and oxidative stress in *Aeromonas hydrophila*-challenged *Labeo rohita*. *J. Appl. Aquacult*. **2020**, 32 (3), 250-267. https://doi.org/10.1080/10454438.2019.1615594

Stork, G.; Niu, D.; Fujimoto, A.; Koft, E. R.; Balkovec, J. M.; Tata, J. R.; Dake, G. R. The first stereoselective total synthesis of quinine. *Journal of the American Chemical Society.* **2001**, *123* (14), 3239–3242. https://doi.org/10.1021/ja004325r

Suresh, U.; Murugan, K.; Benelli, G.; Nicoletti, M.; Barnard, D. R.; Panneerselvam, C.; Kumar, P. M.; Subramaniam, J.; Dinesh, D.; Chandramohan, B. Tackling the growing threat of dengue: Phyllanthus nirurimediated synthesis of silver nanoparticles and their mosquitocidal properties against the dengue vector *Aedes aegypti* (Diptera: Culicidae). *Parasitol Res.* **2015**, *114* (4), 1551–1562. https://doi.org/10.1007/s00436–015–4339–9

Szafran, Z.; Pike, R. M.; Singh, M. M. *Microscale inorganic chemistry*. John Wiley & Sons, 1991.

Tisgratog, R.; Sanguanpong, U, Grieco, J. P.; Ngoen–Kluan, R.; Chareonviriyaphap, T. Plants traditionally used as mosquito repellents and the implication for their use in vector control. *Acta Tropica.* **2016**, *157*, 136–144. https://doi.org/10.1016/j.actatropica.2016.01.024

Torre, M.; Calvo, S.; Pardo, H.; Mombru, A. W. Synthesis, spectroscopic characterization and crystal structure of disulfamethoxazole diaquo Ni(II) monohydrate. *J. Coord. Chem*. **2005**, *58* (6), 513–520. https://doi.org/10.1080/00958970500037516

Wells, T. N. C. Natural products as starting points for future anti–malarial therapies: going back to our roots. *Malaria Journal*. **2011**, *10* (1), 1–12. https://doi.org/10.1186/1475–2875–10–S1–S3

Wongsrichanalai, C.; Pickard, A. L.; Wernsdorfer, W. H.; Meshnick, S. R. Epidemiology of drug–resistant malaria. *The Lancet Infectious Diseases*. **2002**, *2* (4), 209–218. https://doi.org/10.1016/s1473–3099(02)00239–6

World Health Organization [WHO]. Weekly Epidemiological Record – Malaria, (1982–1997); Technical Report Number 32. Geneva: WHO, 1999. http://www.who.int/wer. Accessed 9 Sept. 2021

World Health Organization [WHO]. UNICEF. The Africa Malaria Report. Geneva: WHO, 2003. https://iris.who.int/handle/10665/67869. Accessed 9 Sept. 2021

World Health Organization [WHO]. Dengue and dengue haemorrhagic fever. Factsheet N°117. Geneva: WHO, 2008.

World Health Organization [WHO]. Dengue Guidelines for diagnosis, treatment, prevention and control 2009. Geneva: WHO, 2009. https://iris.who.int/handle/10665/44188. Accessed 9 Sept. 2021

Supplementary Material

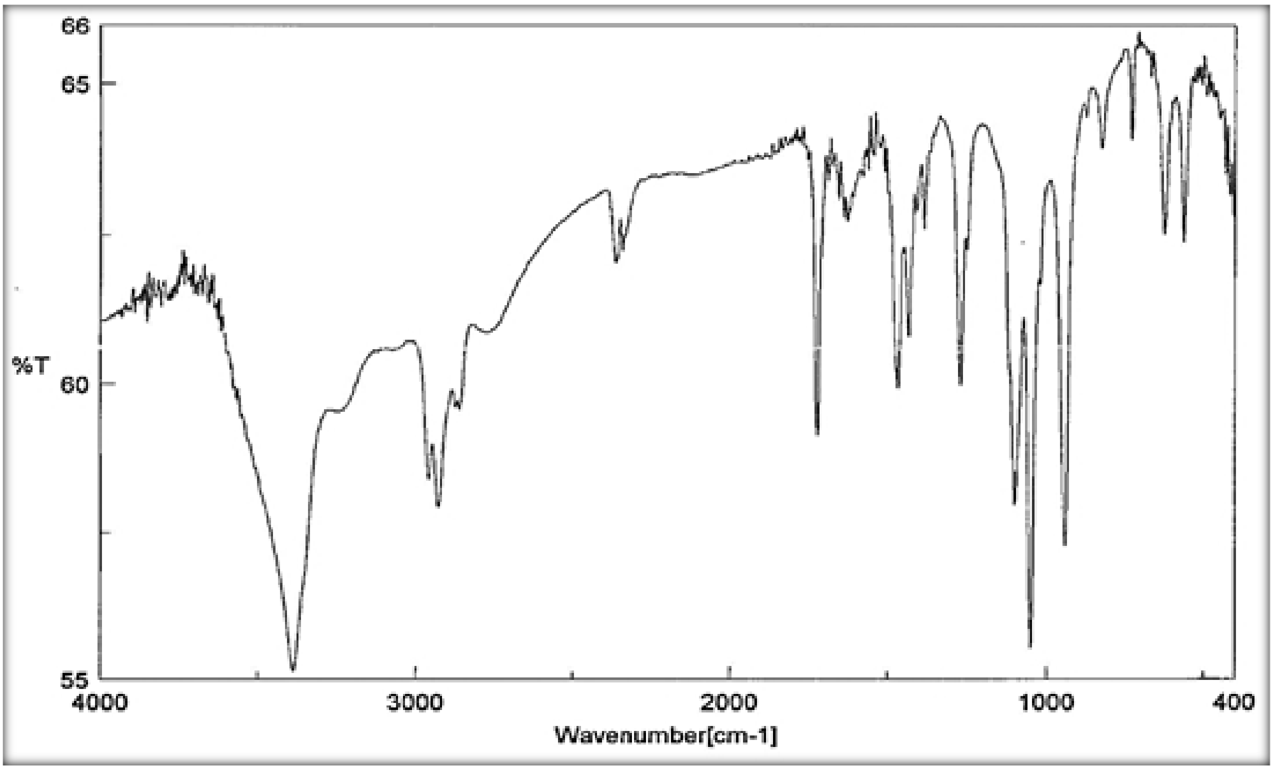

Figure S1. Infrared Spectrum of [Ni(CQ)(Ibu)(H_2O)$_2$Cl]complex.

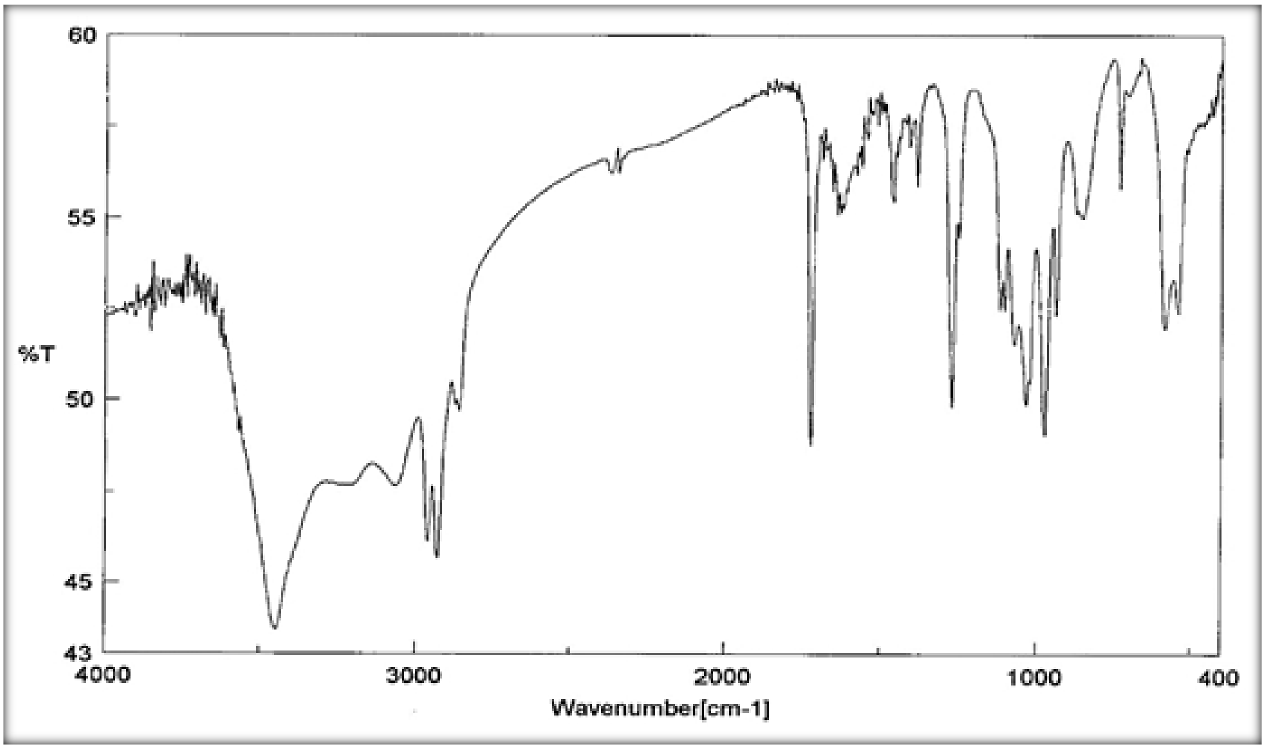

Figure S2. Infrared Spectrum of [Co(CQ)(Ibu)(H_2O)$_2$Cl]complex.

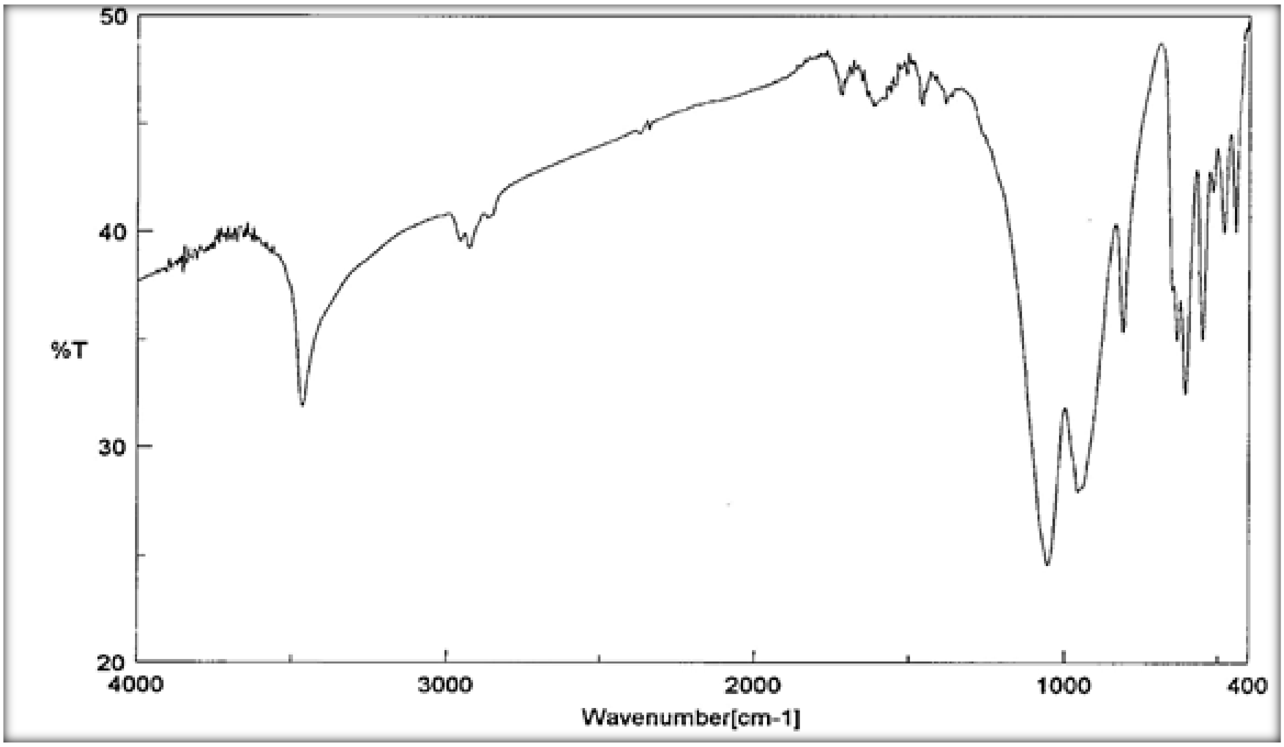

Figure S3. Infrared Spectrum of [Cu(CQ)(Ibu)(H_2O)$_2$Cl]complex.

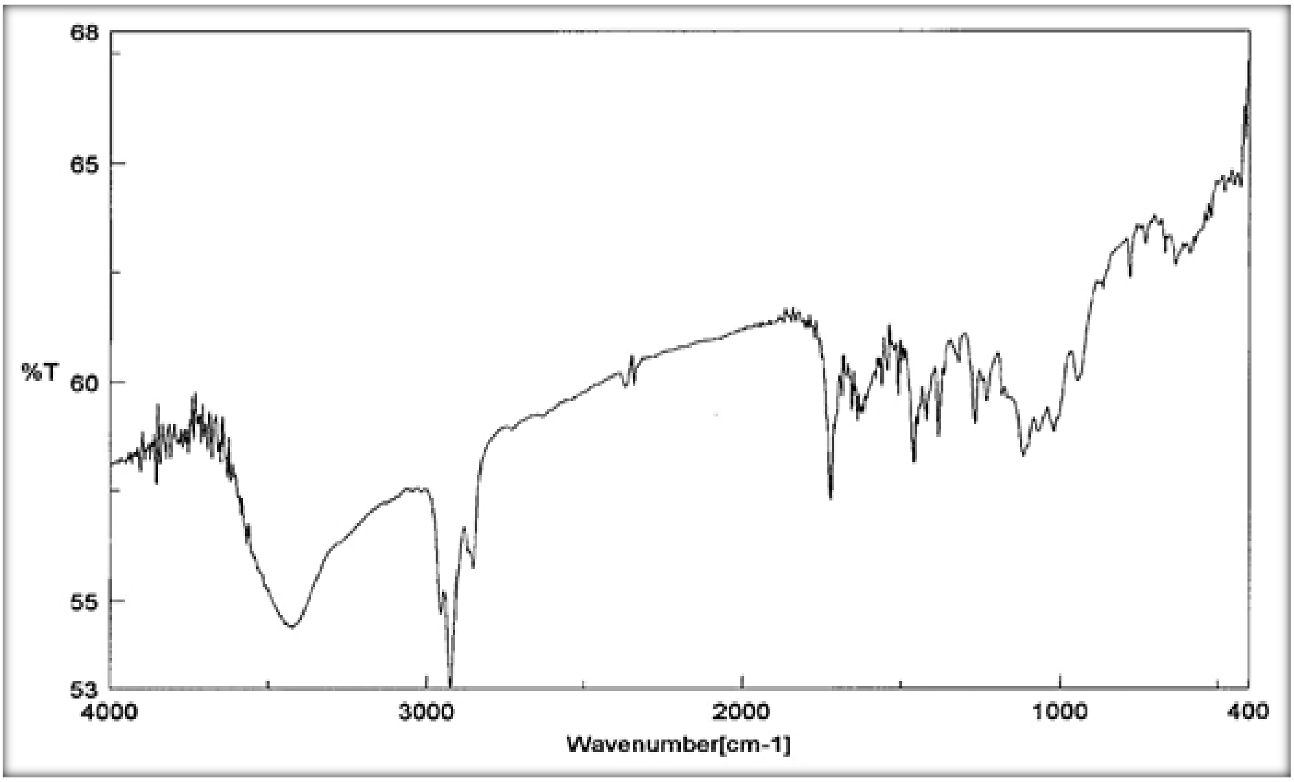

Figure S4. Infrared Spectrum of [Zn(CQ)(Ibu)(H_2O)$_2$Cl]complex.

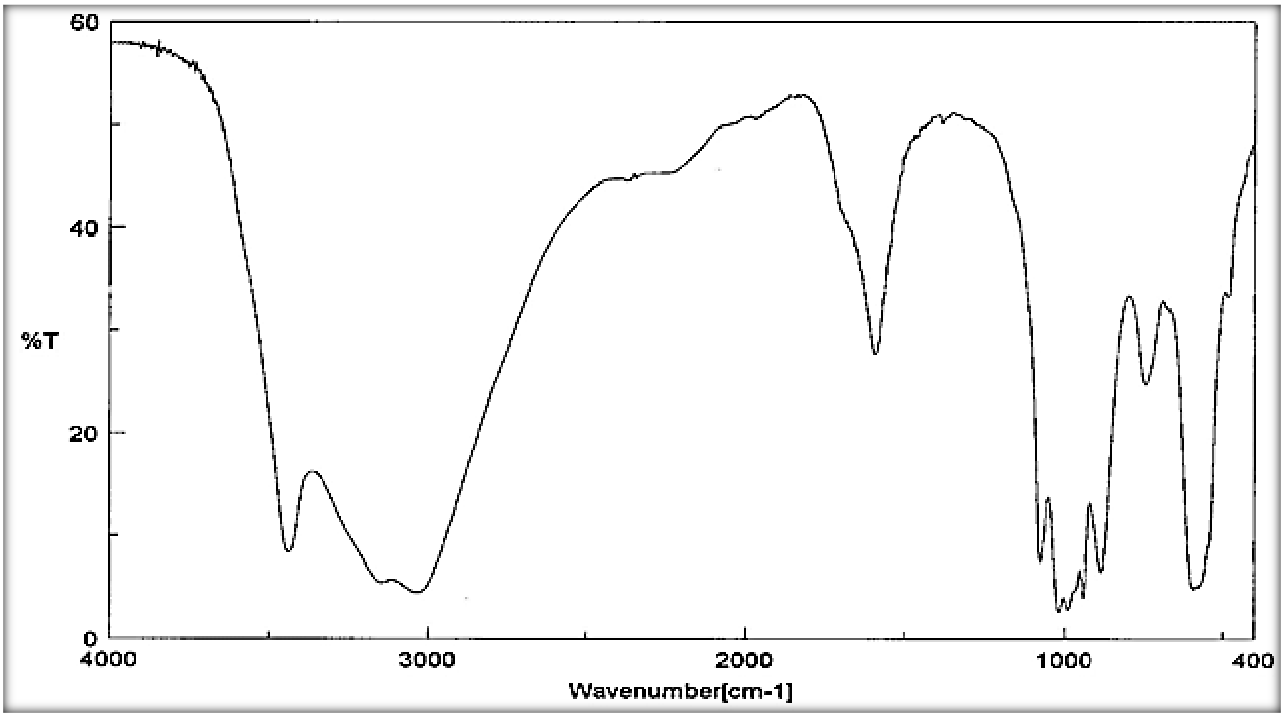

Figure S5. Infrared Spectrum of [Ni(CQ)(SMX)(H_2O)Cl_2] complex.

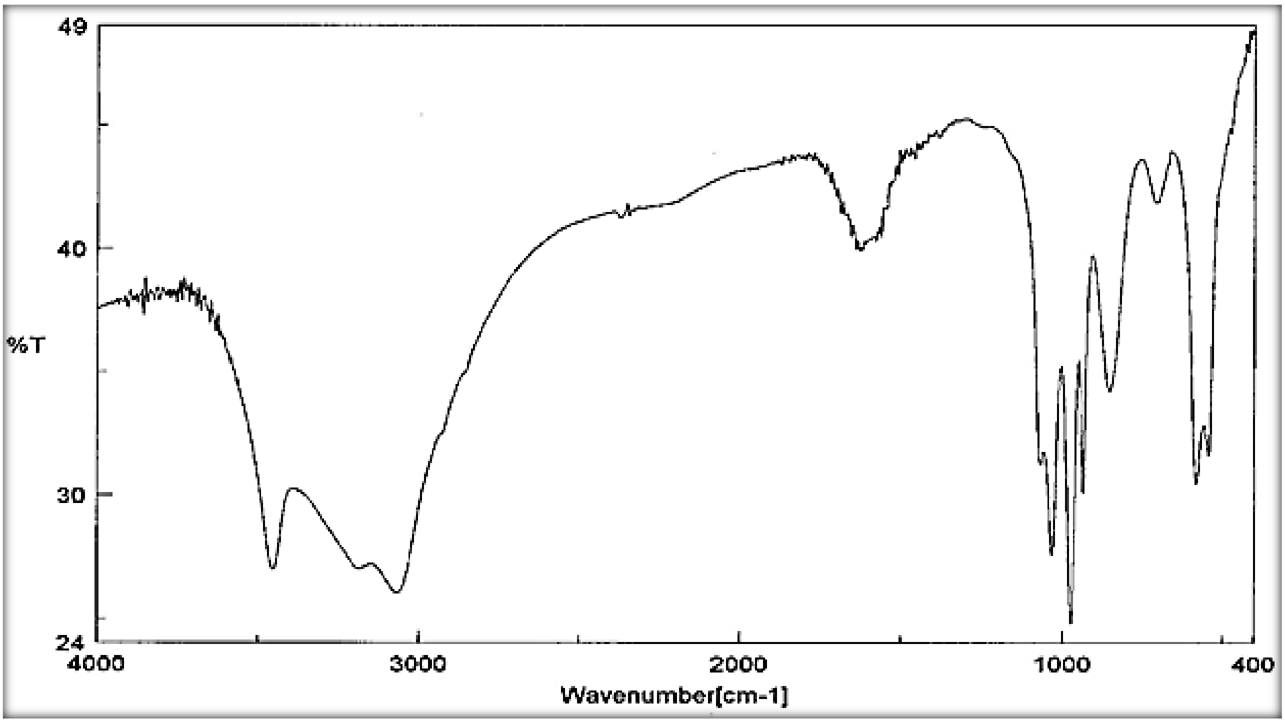

Figure S6. Infrared Spectrum of [Co(CQ)(SMX)(H_2O)Cl_2] complex.

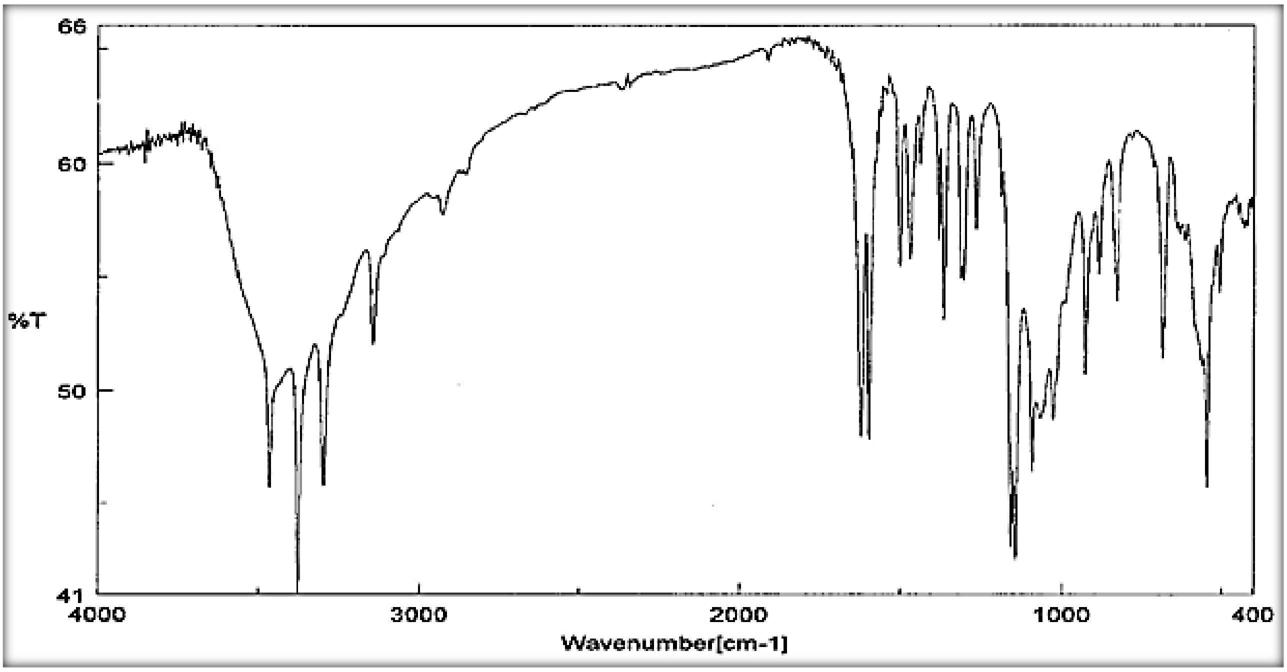

Figure S7. Infrared Spectrum of [Cu(CQ)(SMX)Cl_3] complex.

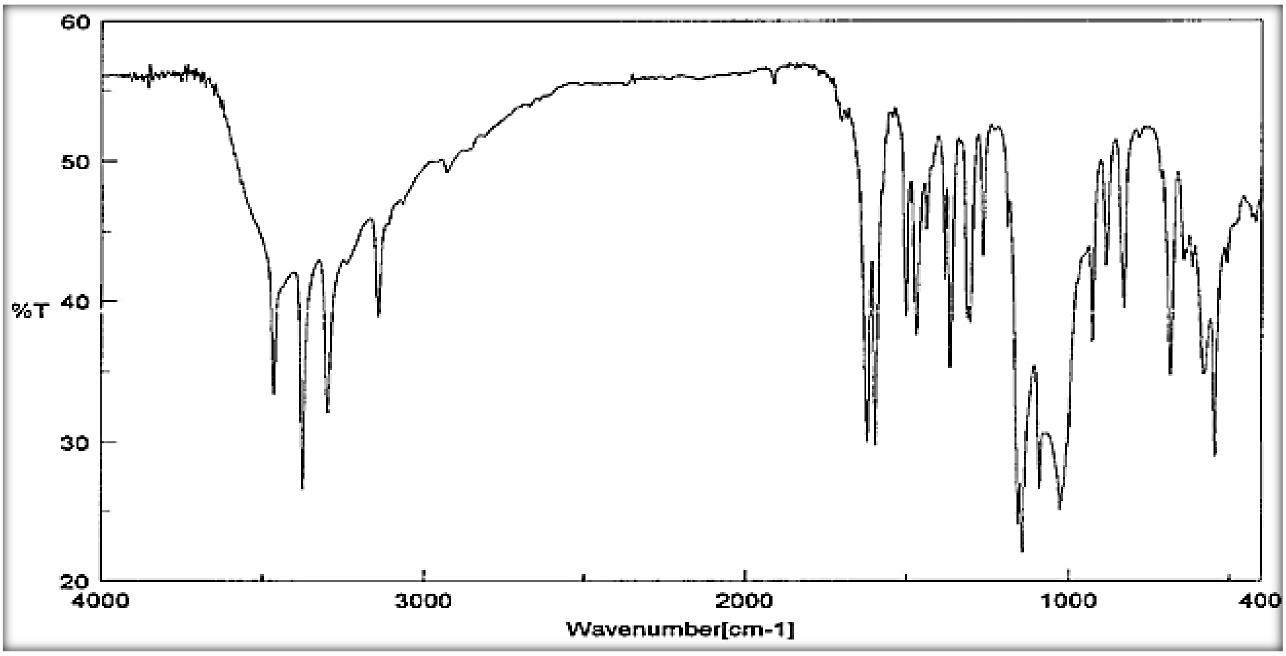

Figure S8. Infrared Spectrum of [Zn(CQ)(SMX)Cl_3] complex.

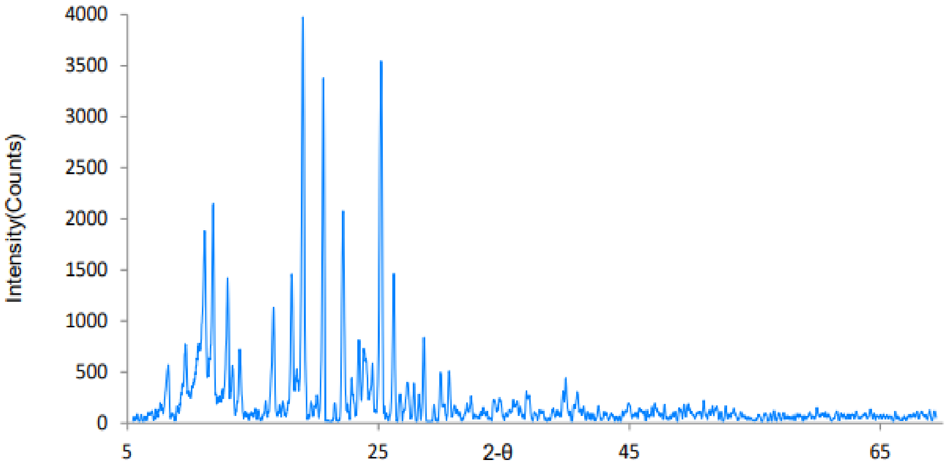

Figure S9. XRD pattern for chloroquine phosphate.

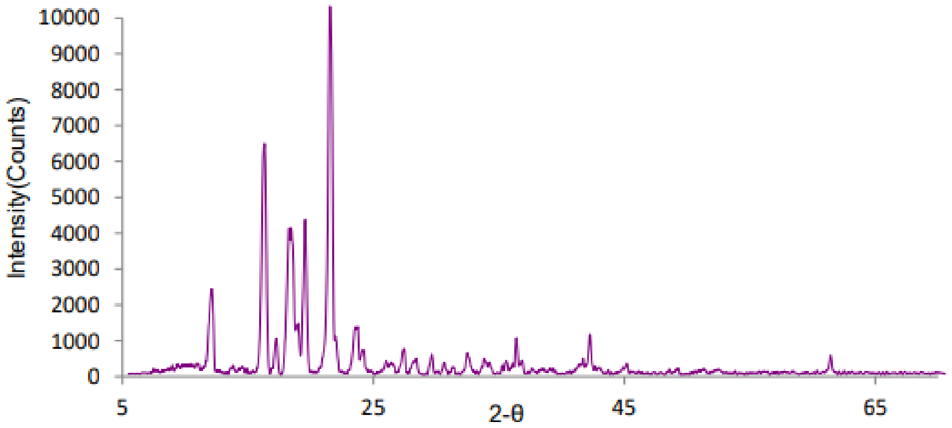

Figure S10. XRD pattern for ibuprofen.

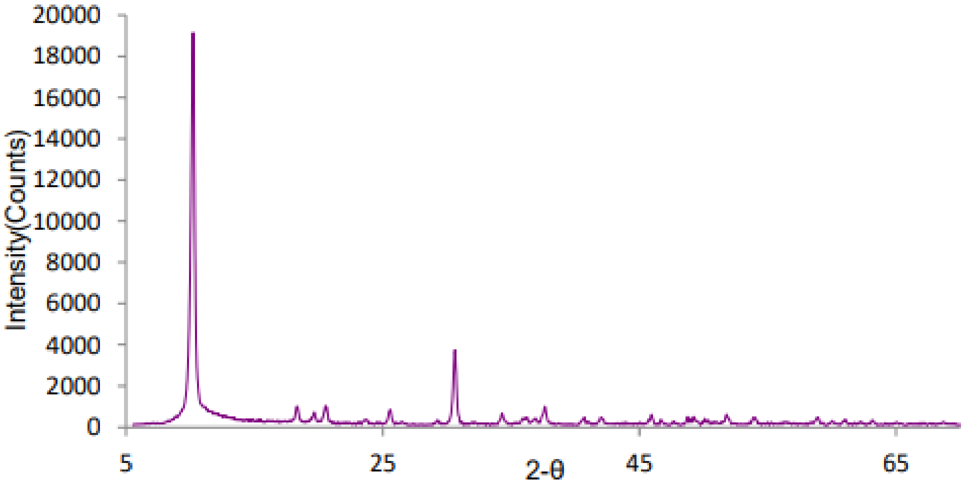

Figure S11. XRD pattern for CQ,Ibu-Ni complex.

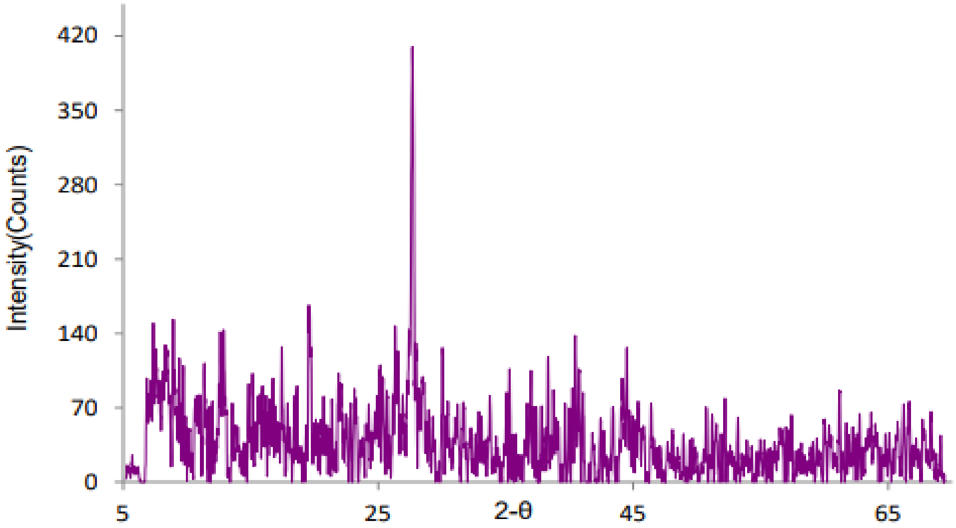

Figure S12. XRD pattern for CQ,Ibu-Co.complex.

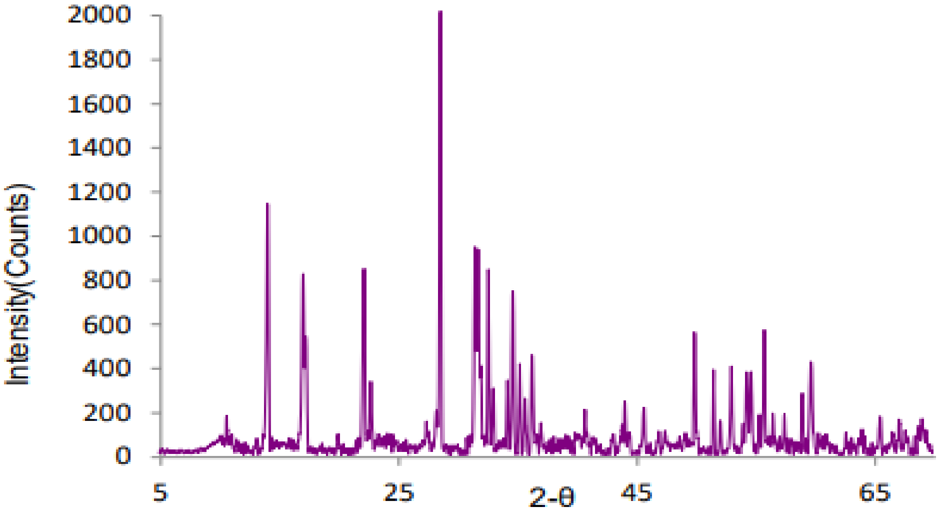

Figure S13. XRD pattern for CQ,Ibu-Cu.complex.

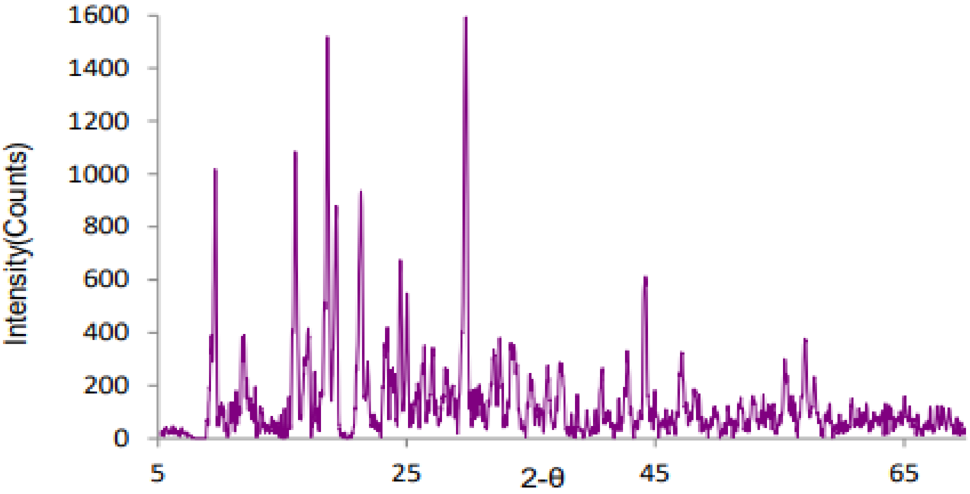

Figure S14. XRD pattern for CQ,Ibu-Zn.complex.

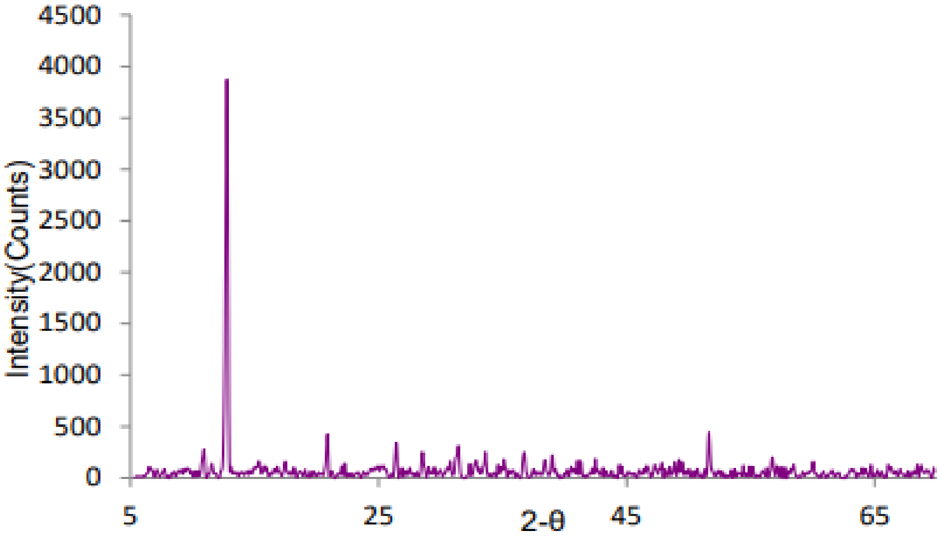

Figure S15. XRD pattern for CQ,SMX-Co complex.

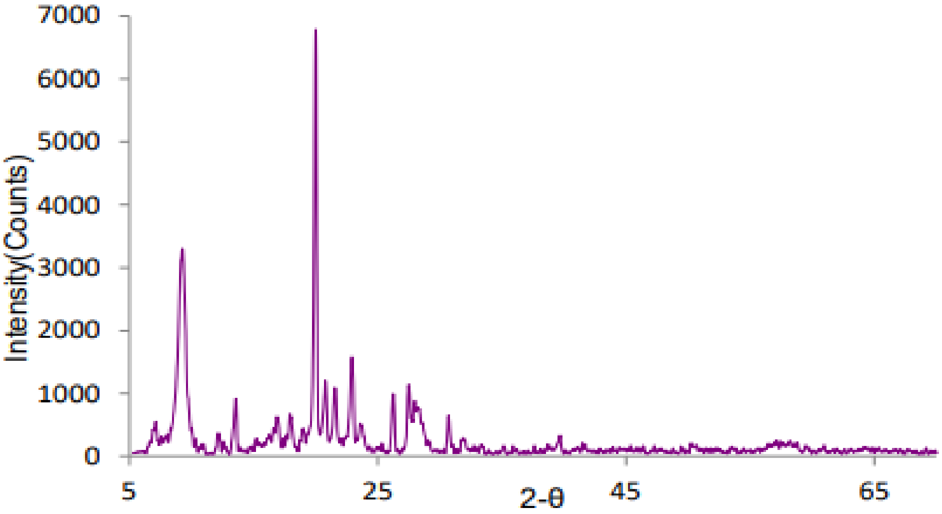

Figure S16. XRD pattern for CQ,SMX-Cu complex.

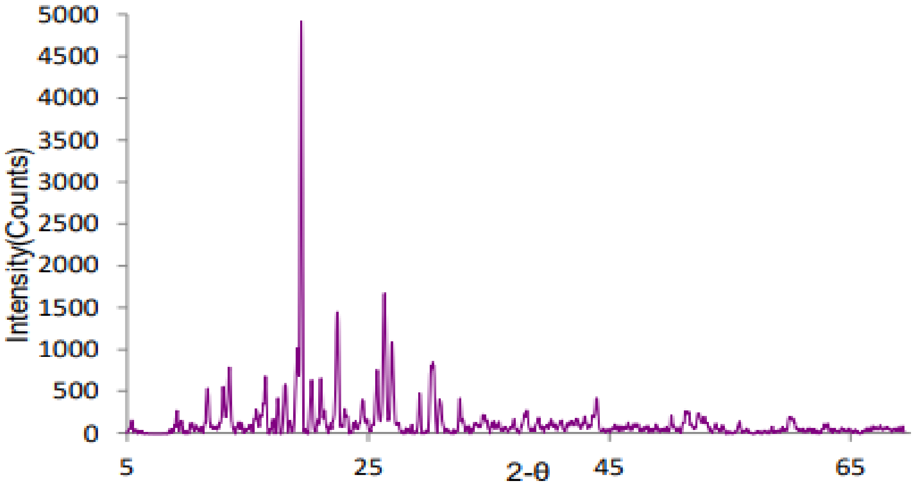

Figure S17. XRD pattern for CQ,SMX-Zn complex.

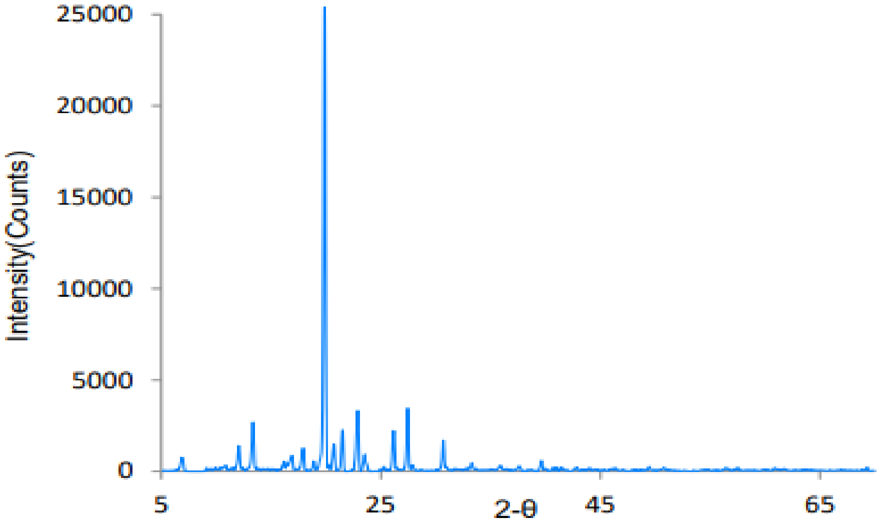

Figure S18. XRD pattern for sulphamethoxazole.

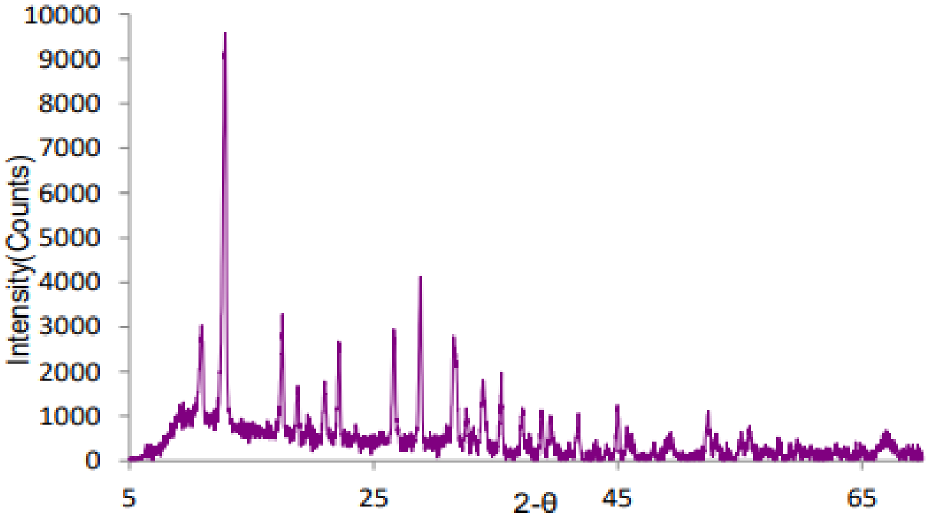

Figure S19. XRD pattern for CQ,SMX-Ni complex.

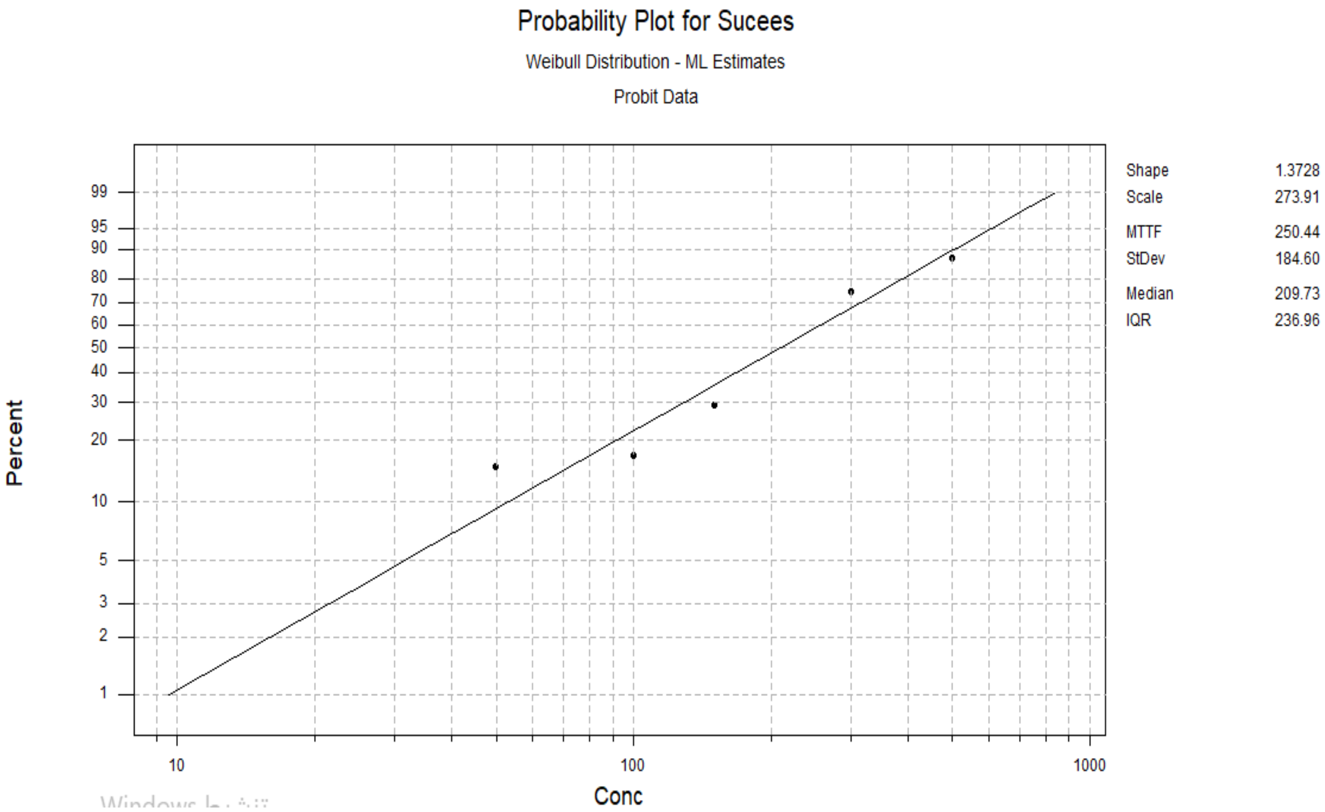

Figure S20. The relationship between concentration of CQ,Ibu-Cu complex and mortality percentage of *Ae. aegypti* larvae.

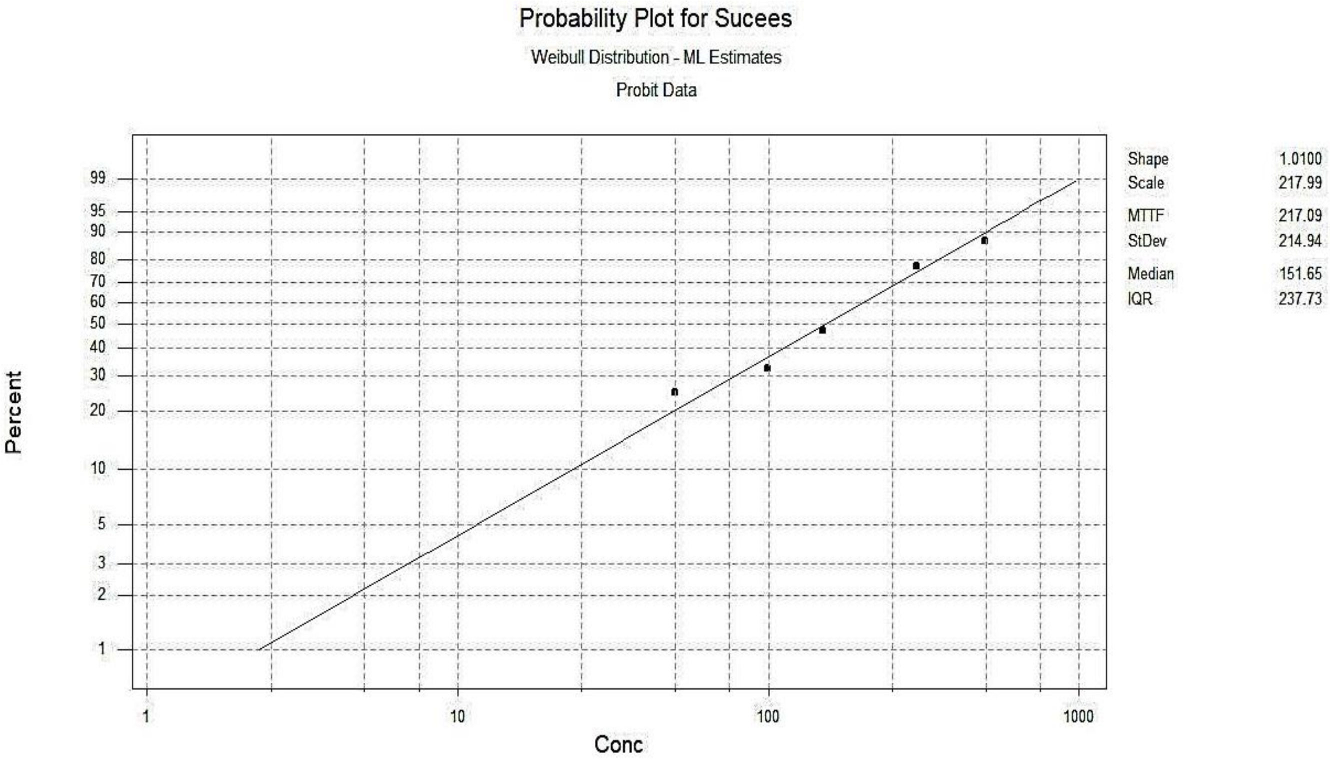

Figure S21. The relationship between concentration of CQ,SMX-Cu complex and mortality percentage of *Ae. aegypti* larvae.

Table S1. Significant IR spectral bands (cm^{-1}) of complexes with chloroquine and ibuprofen.

[Ni(CQ)(Ibu)(H_2O)$_2$Cl]	[Co(CQ)(Ibu)(H_2O)$_2$Cl]	[Cu(CQ)(Ibu)(H_2O)$_2$Cl]	[Zn(CQ)(Ibu)(H_2O)$_2$Cl]	Assignment
$3215^{\text{br \&w}}$	$3210^{\text{br \& w}}$	$3195^{\text{br \& w}}$	$3220^{\text{br \& w}}$	v(NH)
$3388^{\text{br \&s}}$	$3448^{\text{br \& w}}$	$3467^{\text{br \& w}}$	$3422^{\text{br \& w}}$	v(OH) of H_2O
$1626^{\text{sh\&w}}$	$1633^{\text{sh \& w}}$	$1637^{\text{sh \& w}}$	$1638^{\text{sh \& w}}$	Benzene ring +pyridine ring stretch
$2959^{\text{sh\&w}}$	$3064^{\text{sh \& w}}$	$2954^{\text{sh \& m}}$	$2955^{\text{sh \& w}}$	vCH–arom
$2859^{\text{sh\&w}}$	$2859^{\text{sh \& w}}$	$2867^{\text{br \& w}}$	$2853^{\text{sh \& w}}$	vCH–aliph
$1101^{\text{sh\&m}}$	$1102^{\text{sh \& m}}$	$1053^{\text{sh \& m}}$	$1115^{\text{sh \& m}}$	v(C–N)
$1722^{\text{sh\&m}}$	$1723^{\text{sh \& m}}$	$1720^{\text{sh \& w}}$	$1720^{\text{sh \& m}}$	v(C=O)
$1467^{\text{sh\&w}}$	$1459^{\text{sh \& w}}$	$1462^{\text{sh \& w}}$	$1458^{\text{sh \& w}}$	v(C=N)
$416^{\text{sh\&w}}$	$420^{\text{sh \& w}}$	$445^{\text{sh \& w}}$	$419^{\text{sh \& w}}$	v(M–O)

Note: w = weak; m = medium; s = strong; br = broad; sh= short.

Table S2. Significant IR spectral bands (cm^{-1}) of complexes with chloroquine and sulfamethoxazole.

[Ni(CQ)(SMX)(H_2O)Cl_2]	[Co(CQ)(SMX)(H_2O)Cl_2]	[Cu(CQ)(SMX)Cl_3]	[Zn(CQ)(SMX)Cl_3]	Assignment
Overlab with v(OH) of H_2O	Overlab with v(OH) of H_2O	$3298^{\text{sh \& s}}$	$3298^{\text{sh \& s}}$	v(NH)
$3440^{\text{br \& m}}$	$3453^{\text{br \& m}}$	–	–	v(OH) of H_2O
$1591^{\text{br \& m}}$	$1578^{\text{sh \& w}}$	$1596^{\text{sh \& w}}$	$1502^{\text{sh \& m}}$	Benzene ring +pyridine ring stretch
$3147^{\text{br \& s}}$	$3187^{\text{br \& s}}$	$3239^{\text{sh \& s}}$	$3143^{\text{sh \& m}}$	vCH–arom
$3030^{\text{br \& w}}$	$3068^{\text{br \& s}}$	$3066^{\text{sh \& s}}$	$2958^{\text{sh \& s}}$	vCH–aliph
$1076^{\text{sh \& w}}$	$1068^{\text{sh \& w}}$	$1091^{\text{sh \& s}}$	$1091^{\text{br \& w}}$	v(C–N)
$1383^{\text{sh \& w}}$	$1383^{\text{sh \& w}}$	$1382^{\text{sh \& s}}$	$1366^{\text{sh \& s}}$	v(O=S=O)
$1483^{\text{sh \& w}}$	$1490^{\text{sh \& w}}$	$1502^{\text{sh \& w}}$	$1502^{\text{sh \& w}}$	v(C=N)
$483^{\text{sh \& w}}$	$410^{\text{sh \& w}}$	$419^{\text{sh \& w}}$	$421^{\text{sh \& w}}$	v(M–O)

Note: w = weak; m = medium; s = strong; br = broad; sh= short.

Table S3. XRD spectra data of the principal intensity values of the ligands chloroquine, ibuprofen, and their complexes with (Ni,Co,Cu, and Zn).

Compound	2θ	β	D (nm)	Mean D	X_C (%)
CQ.	19.581	0.223	6.5895	7.056	100
	26.259	0.231	6.4369		
	21.321	0.181	8.1409		
Ibu	12.16	0.422	3.451	3.658	100
	16.70	0.389	3.762		
	20.16	0.301	4.886		
	22.30	0.397	3.718		
	24.64	0.600	2.470		
CQ,Ibu–Ni complex	10.16	0.357	4.0725	4.422	3.201
	32.26	0.316	4.7704		
CQ,Ibu–Co complex	7.121	0.622	2.3327	2.998	4.600
	7.379	0.620	2.3405		
	7.62	0.620	2.3407		
	8.40	0.387	3.7519		
	13.101	0.345	4.2247		
CQ,Ibu–Cu complex	14.841	0.216	6.761	4.821	23.017
	18.04	0.379	3.869		
	18.30	0.422	3.476		
	30.459	0.174	8.625		
	33.60	0.331	4.569		
	33.88	0.408	3.710		
	34.101	0.553	2.739		
CQ,Ibu–Zn complex	9.780	0.364	3.9929	4.4054	24.366
	16.740	0.298	4.9119		
	19.539	0.314	4.6795		
	20.319	0.303	4.8553		
	22.440	0.408	3.6183		
	31.56	0.344	4.3744		

Table S4. XRD spectra data of the principal intensity values of the ligand's chloroquine, sulphamethoxazole and their complexes with (Ni, Co, Cu, and Zn).

Compound	2θ	β	D (nm)	Mean D	X_C (%)
CQ.	19.581	0.223	6.5895	7.056	100
	26.259	0.231	6.4369		
	21.321	0.181	8.1409		
SMX.	13.98	0.247	5.9066	6.570	100
	20.98	0.205	7.1839		
	24.22	0.253	5.8539		
	29.121	0.204	7.3339		
CQ, SMX –Ni complex	11.4	0.334	4.3571	5.058	61.386
	13.46	0.332	4.3919		
	18.5	0.216	6.7924		
	22.259	0.261	5.6545		
	28.342	0.271	5.5111		
	30.682	0.248	6.0547		
	33.602	0.403	3.7534		
	36.22	0.351	4.3408		
	37.837	0.203	7.5409		
	39.699	0.28	5.4983		
	44.484	0.895	1.7480		
CQ, SMX –Co complex	13.1	0.244	5.9737	4.789	23.513
	21.9	0.279	5.2864		
	26.34	1.111	1.3386		
	33.339	0.323	4.6798		
	55.24	0.245	6.6706		
CQ, SMX –Cu complex	9.3	0.696	2.0874	3.5754	92.978
	20.88	0.237	6.2128		
	28.98	0.341	4.3860		
	29.52	0.927	1.6154		
CQ, SMX –Zn complex	14.279	0.308	4.7382	4.9042	32.538
	20.4	0.505	2.9135		
	20.759	0.2	7.3608		
	24.00	0.274	5.4029		
	28.24	0.269	5.5509		
	28.901	0.325	4.6011		
	32.58	0.401	3.7621		

Table S5. Date mortality of larvae after 24 h for chloroquine, Ibuprofen, and their complex.

Compound	Percentage of mortality of *Aedes aegypti* after 24 h
Water	0
DMSO 3%	0
CQ1000ppm	50
Ibu 1000ppm	100
CQ,Ibu–Ni 1000ppm	50
CQ,Ibu–Co 1000ppm	0
CQ,Ibu–Cu 1000ppm	100
CQ,Ibu–Zn 1000ppm	80
CQ300ppm	20
Ibu 300 ppm	70
CQ,Ibu–Ni 300ppm	40
CQ,Ibu–Co 300ppm	0
CQ,Ibu–Cu 300ppm	70
CQ,Ibu–Zn 300ppm	20

Table S6. Date mortality of larvae after 24 h for chloroquine, sulphamethoxazole and their complex.

Compound	Percent mortality of larvae after 24 h
DMSO 3%	0
CQ1000 ppm	50
CQ300 ppm	20
SMX 1000 ppm	0
SMX 300 ppm	0
CQ,SMX–Ni 1000ppm	0
CQ,SMX–Co 1000ppm	0
CQ,SMX–Cu 1000ppm	100
CQ,SMX–Zn 1000ppm	40
CQ,SMX–Ni 300ppm	0
CQ,SMX–Co 300ppm	0
CQ,SMX–Cu 300ppm	80
CQ,SMX–Zn 300ppm	20

Eclet. Quim. 49 | e-1515, 2024

Original Article

https://doi.org/10.26850/1678-4618.eq.v49.2024.e1515

Development and validation of a green spectrophotometric method for simultaneous determination of combined pharmaceutical dosage form (paracetamol and caffeine) using chemometrics technique in comparison with HPLC

Bushra **Alattab**[1], Fares Abdullah **Alarbagi**[1+], Maher Ali **Almaqtari**[1], Entesar **Alhuraishi**[1], Hussein **Al-Maydama**[1]

Abstract

A green analytical method, a simple, fast, and cost-effective simultaneous spectrophotometric method using two chemometric techniques, the partial least square regression (PLS) and principal component regression (PCR), for determining a combination of paracetamol and caffeine in pharmaceutical formulations was developed. Pretreatment and separation steps are not required in the proposed method. For model construction and validation, various drug concentrations and instrumental spectra of 25 mixed solutions of paracetamol and caffeine were analyzed. The UV analysis of the prepared mixtures was recorded for a selected solvent blank in the wavelength range of 210-300 nm. The digitized absorbance was sampled at 0.2-nm intervals. R^2 values of 0.9993 and 0.9994 assigned for the PLS of paracetamol and caffeine and 0.9995 and 0.9991 for the PCR of paracetamol and caffeine, respectively, exhibited greater prediction efficiencies. The obtained results were statistically compared with the results of the HPLC reference method. Concerning accuracy and precision, the statistical comparison revealed no significant differences between the suggested and reference HPLC approaches.

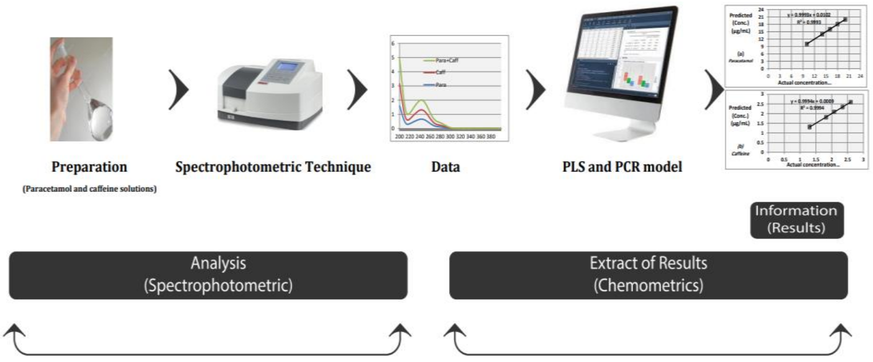

Article History

Received September 06, 2023
Accepted June 11, 2024
Published September 17, 2024

Keywords

1. paracetamol;
2. caffeine;
3. green method;
4. validation;
5. spectrophotometric method.

Section Editor

María Natalia Besil Arismendi

Highlights

- Development and validation of a new eco-friendly chemometric spectrophotometric.
- The proposed methods are statistically compared with reported HPLC method.
- Can be used for the routine quality control of paracetamol and caffeine analysis.

[1]Sana'a University, Faculty of Science, Sana'a, Yemen. **+Corresponding author:** Fares Abdullah Alarbagi, **Phone:** +967773698413, **Email address:** f.ghaleb@su.edu.ye

1. Introduction

The combination of paracetamol and caffeine is commonly used as a pain reliever and antipyretic agent in pharmaceutical formulations (Uddin *et al.*, 2019). Chemically, paracetamol is (N-(4-hydroxyphenyl) acetamide (**Scheme 1a**). Paracetamol, also known as paracetamol, is one of the most popular medications commonly used to treat fever (antipyretic) and mild to moderate pain (analgesic agent) (Drugbank, 2005a; Glavanović *et al.*, 2016; Yehia and Mohamed, 2016). Caffeine is 1,3,7-Trimethyl-3,7-dihydro-1H-purine-2,6-dione and its chemical structure (**Scheme 1b**). It is one of the drugs mostly used worldwide as a Central Nervous System (CNS) stimulant of the methylxanthine class (Drugbank, 2005b; Uddin *et al.*, 2019).

1,3,7-Trimethylpurine-2,6-dione
Caffeine

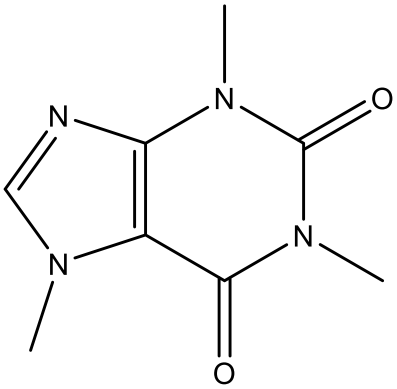

a)

n-(4-hydroxyphenyl)acetamide
paracetamol

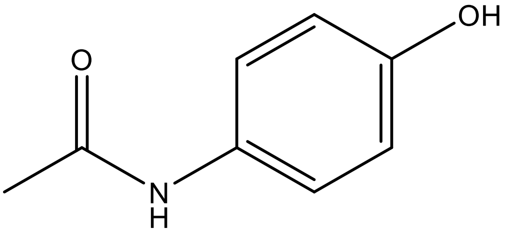

b)

Scheme 1. Chemical structure of paracetamol **(a)** and caffeine **(b)**.
Source: Adapted from Drugbank (2005a; b).

The field of chemometrics has had a significant impact on analytical chemistry, particularly in the area of spectral analysis, which is important in the quality control of mixed drugs and pharmaceutical formulations involving two or more medications of overlapping spectra (Eticha *et al.*, 2018; Glavanović *et al.*, 2016; K. Patel *et al.*, 2013a).

Chemometric methods depend on multivariate analysis, which means considering more than one variable at a time in UV Spectrophotometry techniques (Riddhi and Rajashree, 2019). Many wavelengths are taken as variables, and the absorbance at each wavelength is considered (Gandhi *et al.*, 2017; Riddhi and Rajashree, 2019). The most important chemometric methods used in multivariate analysis are Principal Component Regression (PCR) and Partial Least Squares (PLS). These methods use multivariate calibration using spectrophotometric data along with statistical tools, mathematical models, and software for the determination of combined drugs in pharmaceutical formulations (Riddhi and Rajashree, 2019). These methods also rely on the calibration of the mathematical model by using absorbance data of calibration standards with known concentrations and then predicting the concentration of unknown samples from their absorbance data (Gandhi *et al.*, 2017; Riddhi and Rajashree, 2019).

Chemometrics has multiple applications in spectroscopy, including UV-visible spectrophotometry (Ashour *et al.*, 2015; Attia *et al.*, 2018; Belal *et al.*, 2018; Darbandi *et al.*, 2020; Elfatatry *et al.*, 2016; Gholse *et al.*, 2022; Manouchehri *et al.*, 2016; Mattar and Sobhy, 2022; Moussa *et al.*, 2021; M. Patel *et al.*, 2013b; Phechkrajang *et al.*, 2015; Putri *et al.*, 2021; Sebaiy *et al.*, 2020; V. D. Singh and V. K. Singh, 2021; Vichare *et al.*, 2010), fluorescence spectroscopy (Manouchehri *et al.*, 2016; Salem *et al.*, 2019; Shinde and Divya, 2015; Walash *et al.*, 2011; Zhu *et al.*, 2016), NIR spectroscopy (Manouchehri *et al.*, 2016; Moroni *et al.*, 2022; Muntean *et al.*, 2021; Muntean *et al.*, 2017; Rahman *et al.*, 2020; Sun *et al.*, 2021), and FTIR spectroscopy (Rahman *et al.*, 2020). In addition, chromatography techniques such as Liquid Chromatography (Aminu *et al.*, 2019; Mohammed *et al.*, 2021; Tsvetkova *et al.*, 2012; Vu Dang *et al.*, 2020) as well as a variety of other analytical chemistry techniques, such as flow-injection analysis (Ortega-Barrales *et al.*, 2002; Silva *et al.*, 2011).

Uddin *et al.* (2019) reported that the classic UV spectral assay could not be used to determine most analytes of interest because they are accompanied in their dose forms by other substances that absorb in the same spectral area. Traditional procedures, such as extraction, are difficult to employ because they require a lot of solvent, which comes with hazards of analyte loss or contamination, as well as the likelihood of incomplete separation, which is costly and time-consuming. However, when paired with chemometric methods for determining a combined mixture in pharmaceutical quality control, spectrophotometry as a simple, precise, rapid, and low-cost method may be a great option. They provide benefits when the quality monitoring of pharmaceutical products demands reliable, accurate, and fast analytical procedures. This process avoids prior separation processes and is fast, accurate, and easy to use.

One of the tools used to assess the greenness of analytical procedures is the analytical Greenness Calculator, which is based on the 12 principles of Green Analytical Chemistry. It is a tool for assessing the environmental and occupational risks connected with a certain analytical technique applied in this study (Gałuszka *et al.*, 2013), as shown in **Scheme 2**. The criteria scores and the Analytical Greenness score are linked to a "traffic lights" red-yellow-green sequential color map, with red assigned to the lowest values and green to the highest values, and its value ranges from 0.0 (the lowest score) to 1.0 (perfect score) (Tobiszewski *et al.*, 2017), as shown in **Scheme 3**.

To the best of our knowledge, no published work has been conducted on developing and validating spectrophotometric methods for the examination of some combined pharmacological compounds using a chemometrics approach in the Yemeni market (The Republic of Yemen). Therefore, the present study aims to develop and validate an adequate and green simultaneous spectrophotometric assay method for the determination of paracetamol and caffeine in a combined pharmaceutical formulation-assisted chemometric technique.

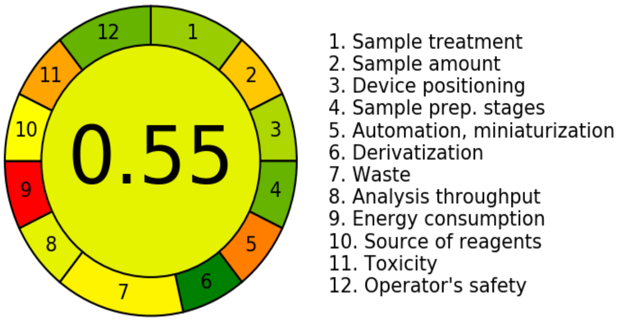

Scheme 2. Annotated result of the generic assessment.

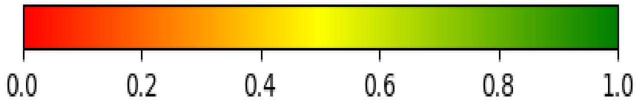

Scheme 3. The span of the colour map used in the graph and the corresponding values.

2. Materials and methods

2.1. Materials and reagents

The reference standard paracetamol and caffeine were obtained from Global Pharma Company, Sana'a, Yemen. All reagents and chemicals used for the spectrophotometric methods were of analytical grade, and HPLC grade was used for the HPLC method. Deionized water (with a specific conductance of 0.05 µS cm^{-1}) was in-house produced and used for the preparation of all sample solutions. Hydrochloric acid, sodium hydroxide, and benzoic acid were obtained from Shiba'a Pharma Company, Sana'a, Yemen.

- ***Preparation of standard stock solution:*** Stock solutions of 1000 µg mL^{-1} of paracetamol and 130 µg mL^{-1} of caffeine were individually prepared in a 100 mL volumetric flask by dissolving 100 mg paracetamol and 13 mg caffeine separately in water.
- ***Preparation of hydrochloric acid solution:*** it was prepared by diluting appropriate amounts of reagent in deionized water to make 0.1 mol L^{-1}.
- ***Preparation of sodium hydroxide solution:*** This solution was prepared by dissolving 4.00 g of NaOH pellet into a 1000 mL volumetric flask in deionized water to obtain a final concentration of 0.1 mol L^{-1}.
- ***Preparation of the benzoic acid solution:*** it was prepared by dissolving appropriate amounts of benzoic acid in methanol.

2.2. Instrumentation

A double beam UV-Vis spectrophotometer (analytik jena), Model (SPECORD 200) at Sana'a University-Faculty of Science was used for the absorbance measurements. The HPLC system was from JASCO and included a UV detector (UV-2070 Plus), pump (PU-2089), autosampler (AS-2055 Plus), column oven (CO-2067 Plus), and a C18 column (10 cm × 4.6 mm, 5 µm). Electronic balance (AA-160), Denver Instrument. Electronic balance (GH-252), AND. Electronic balance (GR-120), AND. pH meter (3520), Jenway. A centrifuge (Z326 K) and Hermle were also used.

2.3. Development procedures

To develop accurate, precise, and reliable simultaneous spectrophotometric methods assisted with the chemometrics technique, analytical methods were established and developed to obtain the intended results for quantifying the targeted components. The suitability of the proposed and developed method was decided based on the results of the validation method. This method was studied and experimented for the paracetamol determination with caffeine in marketed pharmaceutical formulations. They were compared to the results of the reference method.

2.3.1. Selection of the solvent

The effect of the solvent on solubility was studied to choose a suitable solvent. Solubility was checked in water, methanol, 0.1 mol L^{-1} NaOH, and 0.1 mol L^{-1} HCl. The targeted combined active pharmaceutical ingredients in this study were dissolved in volumetric flasks by adding appropriate amounts of selected solvents for the dissolution of the desired active pharmaceutical components without excipients.

2.3.2. Selection of the spectral zone analysis

After the solvent selection step and before pre-processing the data, the individual pure and mixture absorbance spectra of the targeted pharmaceutical components in an appropriately selected solvent were recorded in the range of 200–400 nm with 0.2 nm intervals. UV spectra of the mixtures analysis were selected among a suitable wavelength range against a solvent blank, providing the greatest amount of information about the two components (Shah and Jasani, 2017).

2.3.3. Construction of the training set

Twenty-five different concentrations of paracetamol and caffeine binary mixtures were prepared as the training set (calibration set) to construct the model. The absorbencies of these mixtures were measured between 200 and 400 nm at 0.2-nm intervals against a blank.

2.4. Validation of the chemometric analysis

2.4.1. Construction of the chemometric models

The two multivariate calibration models; the partial least square (PLS) and principal component regression (PCR), were developed as follows:

- The absorbencies of binary mixtures were measured against a blank, and the spectra were saved and extracted into MS Excel for model generation and merit figures to evaluate the obtained results;
- The PCR and PLS models were developed using absorption data at selected spectral zones for analysis at intervals of 0.2 nm using the Minitab 17 program;
- The leave-one-out (LOO) cross-validation method was used to obtain the necessary number of latent variables (optimum number of the principal factors);
- The calibration samples, constant, and coefficients at each wavelength were calculated to obtain the predicted concentrations;

- Finally, the predicted concentrations of the components were compared with the actual concentrations in each sample and the binary mixture was calculated for each sample;
- To determine the precision and accuracy of predictions for the models, the root mean square error of cross-validation (RMSECV), which must be as low as possible for a particular model, was calculated for each method using the following **Eq. 1** (Shah and Jasani, 2017):

$$\mathrm{RMSECV} = \sqrt{\frac{\sum(C\mathrm{act}-C\mathrm{pre})^2}{I\mathrm{c}}} \quad (1)$$

where:
RMSECV = Root means square error of cross-validation
C_{act} = Actual concentration of the calibration set
C_{pre} = predicted concentration of the calibration set
I_{c} = Total number of samples in the calibration set

2.4.2. Validation method and construction of the validation set

To validate and evaluate the performance of the proposed and developed spectrophotometric methods assisted by chemometric models, these methods were applied to the validation set. In addition, the performance criteria of the developed methods, including linearity, accuracy, precision (repeatability), and specificity, were validated as per the recommendations of International Conference Harmonization (ICH) and hence determined.

2.5. Analytical method procedures

2.5.1. Construction of the calibration (training) set

Several 25 binary mixtures of paracetamol and caffeine were prepared by transferring different aliquots of their standard stock solutions into a series of 50 mL volumetric flasks (**Table 1**). The absorbencies of these mixtures were measured between 200 and 400 nm at 0.2 nm intervals against water as a blank.

2.5.2. Construction of the validation set

A set of 12 binary mixtures of paracetamol and caffeine was prepared by transferring different volumes into 50 mL volumetric flasks, and the procedure for the construction of the training set was repeated (**Table 2**).

2.5.3. Preparation of the test sample

Approximately 20 tablets of a commercial pharmaceutical formulation tablet containing 500/65 mg of paracetamol/caffeine, respectively, were analysed using the proposed chemometric methods. The sample 500/65 were weighed and finely powdered in a mortar. A quantity of powdered tablets equivalent to 100 mg of paracetamol and 13 mg of caffeine was accurately weighed and transferred into a 100 mL volumetric flask containing 50 ml of water. The mixture was shaken for 5 min, and with frequent shaking, the volume was completed to 100 mL with the selected solvent. The solution was then filtered through 0.45 µm filter paper. 0.8 mL of the filtrate was transferred into a 50 mL volumetric flask and then diluted by completion to 50 mL with water. The absorbance was measured between 200 and 400 nm at 0.2-nm intervals against water as a blank.

2.5.4. Preparation of spiked samples

Powdered tablets of 100 mg paracetamol and 13 mg caffeine in triplicates were accurately weighed and transferred to a 100 mL volumetric flask. Then, 50 mL of water was added, and the calculated amount of paracetamol and caffeine from standard solutions was spiked into the sample solution. The mixture was shaken for 5 min, and with frequent shaking the volume completion to 100 mL with the selected solvent was carried out. The solution was then filtered. A total of 0.8 mL of the filtrate was transferred into a 50 mL volumetric flask and then diluted with water up to 50 mL. The absorbance was then measured.

2.5.5. Analysis of the marketed formulations

The developed method was applied to the measurement of three commercially available samples. It was performed using the marketed formulation with a concentration of 500 mg paracetamol and 65 mg caffeine. The tablet solution prepared in the sample preparation section was diluted with water to prepare solutions with a concentration of 16 µg mL^{-1} paracetamol and 2.08 µg mL^{-1} caffeine. The spectra of the prepared solutions were recorded, and then the developed multivariate models PCR and PLS were applied to determine the concentrations of paracetamol and caffeine.

2.6. Comparing the suggested method with the reference method

Comparison was carried out with the recovery results of the newly developed methods and that of reference method for each of paracetamol with caffeine according to the United States Pharmacopeia (USP, 43). 100 µg mL^{-1} paracetamol with 13 µg mL^{-1} caffeine and 360 µg mL^{-1} of benzoic acid as internal standard solution were prepared by dissolving 100 mg paracetamol with 13 mg caffeine in methanol: glacial acetic acid (95:5) in a 100 mL volumetric flask as standard stock solution. The internal standard solution was prepared in a 100 mL volumetric flask by dissolving 600 mg of benzoic acid in methanol. 5 mL of paracetamol with the caffeine of the standard stock solution and 3 mL of internal standard solution were transferred in methanol: glacial acetic acid (95:5) in a 50 mL volumetric flask. A test sample was prepared by transferring a portion of the powder equivalent to 250 mg paracetamol with 32.5 mg caffeine from NLT 20 finely powdered tablets to a 100 mL volumetric flask. 75 mL of methanol: glacial acetic acid (95:5) as solvent was added as solvent and the solution was shaken for 30 min and then diluted with solvent. Two milliliters of this solution and 3 mL of internal standard solution were transferred into 50 mL volumetric flask and diluted with solvent. The standard and test samples of paracetamol with caffeine were injected through an HPLC system with a mixture of methanol: glacial acetic acid: and water (28: 3: 69) as the mobile phase at a flow rate of 2 mL/min. UV detection of paracetamol and caffeine was then carried out at 275 nm (United States Pharmacopeia and the National Formulary (USP 43 - NF 38). The United States Pharmacopeial Convention; 2020).

Table 1. Composition of the calibration set.

Mixture No.	Paracetamol (µg mL^{-1})	Caffeine (µg mL^{-1})	Mixture No.	Paracetamol (µg mL^{-1})	Caffeine (µg mL^{-1})
1	10	1.3	14	16	2.34
2	10	1.82	15	16	2.6
3	10	2.08	16	18	1.3
4	10	2.34	17	18	1.82
5	10	2.6	18	18	2.08
6	14	1.3	19	18	2.34
7	14	1.82	20	18	2.6
8	14	2.08	21	20	1.3
9	14	2.34	22	20	1.82
10	14	2.6	23	20	2.08
11	16	1.3	24	20	2.34
12	16	1.82	25	20	2.6
13	16	2.08	--	--	--

Table 2. Results of the predicted concent vrations with the recovery of paracetamol and caffeine in the binary mixture in each sample for the PLS model.

Name		Paracetamol			Caffeine	
Constant		-0.20039			-0.02079	
Mixture NO.	Actual Conc. (µg mL^{-1})	Predicted Conc. (µg mL^{-1})	%Recovery	Actual Conc. (µg mL^{-1})	Predicted Conc. (µg mL^{-1})	%Recovery
1	10	10.07	100.70	1.3	1.30	100.00
2	10	10.01	100.10	1.82	1.82	100.00
3	10	9.84	98.40	2.08	2.08	100.00
4	10	10.09	100.90	2.34	2.35	100.43
5	10	9.92	99.20	2.6	2.60	100.00
6	14	14.02	100.14	1.3	1.30	100.00
7	14	13.96	99.71	1.82	1.80	98.90
8	14	14.02	100.14	2.08	2.08	100.00
9	14	13.98	99.86	2.34	2.35	100.43
10	14	14.04	100.29	2.6	2.59	99.62
11	16	15.98	99.88	1.3	1.29	99.23
12	16	15.90	99.38	1.82	1.81	99.45
13	16	16.05	100.31	2.08	2.09	100.48
14	16	15.91	99.44	2.34	2.33	99.57
15	16	16.15	100.94	2.6	2.61	100.38
16	18	18.01	100.06	1.3	1.30	100.00
17	18	18.11	100.61	1.82	1.80	98.90
18	18	18.00	100.00	2.08	2.08	100.00
19	18	18.06	100.33	2.34	2.34	100.00
20	18	18.19	101.06	2.6	2.59	99.62
21	20	20.09	100.45	1.3	1.33	102.31
22	20	19.82	99.10	1.82	1.81	99.45
23	20	20.00	100.00	2.08	2.10	100.96
24	20	19.87	99.35	2.34	2.34	100.00
25	20	19.89	99.45	2.6	2.60	100.00
		Mean%	99.99		Mean%	99.99
		RSD%	0.64		RSD%	0.68
		RMSECV	0.093		RMSECV	0.011

3. Results and Discussion

3.1. Development procedures for paracetamol and caffeine determination

3.1.1. Selection of the solvent

To choose a suitable solvent, solubility was checked in water, methanol, 0.1 mol L^{-1} NaOH, and 0.1 mol L^{-1} HCl. The drug was found to be soluble in methanol, water, 0.1 mol L^{-1} NaOH, and 0.1 mol L^{-1} HCl. Therefore, water was selected as a diluent that has striking advantages such as being easily available, easy to handle, cheap, and environmentally friendly for implementing the spectrophotometric method, and Fig. 1 shows the spectra of paracetamol and caffeine in water.

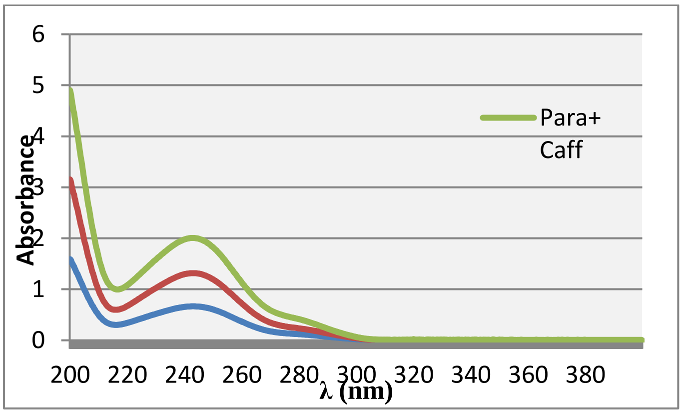

Figure 1. UV Absorbance spectra of pure and mixed samples of paracetamol and caffeine in water solvent.

3.1.2. Selection of the spectral zones for analysis

To determine the overlap spectral zones, the absorbance spectra of the pure paracetamol and caffeine samples and that of the sample of the mixed paracetamol with caffeine in water were recorded in the range of 200–400 nm with 0.2 nm intervals. For the analysis, the UV spectra of the mixtures were selected for a suitable wavelength range (210-300 nm) against the water blank. This range provided a great amount of information about the two components, as shown in the paracetamol and caffeine spectra (**Fig. 1**).

3.1.3. Construction of the training set

To determine the linear range from measuring the absorbance at different concentrations for paracetamol with caffeine, the response was found to be linear in the range of 10–20 μg mL^{-1} for paracetamol and 1.3–2.6 μg mL^{-1} for caffeine using 25 different concentrations of paracetamol and caffeine mixtures, as shown in **Table 1**.

3.2. Validation of the chemometric analysis for paracetamol and caffeine determination

3.2.1. Construction of chemometric models

The spectra were saved and extracted into MS Excel for model generation. The PCR and PLS models were developed using the absorption data for the selected spectral zones using the Minitab 17 software. After the PCR and PLS models were constructed, the optimum number of principal components of paracetamol and caffeine were obtained and given in **Table S1–S4 (Supplementary Material)**.

3.2.1.1. Determination of the optimum number of principal components of paracetamol and caffeine for PLS

Choosing the proper number of principal components for the development of the model was necessary to obtain good predictions. The leave-one-out (LOO) cross-validation method was used to obtain the necessary optimum number of principal factors for the PLS model. It was found that the optimum number of principal components was three for paracetamol and four for caffeine, as mentioned above and given in **Tables S1 and S2**.

3.2.1.2. Determination of constants and coefficients obtained at each wavelength of paracetamol and caffeine for PLS models

The constant and coefficients at each wavelength were calculated using the Minitab 17 program, as illustrated in **Table S3**.

3.2.1.3. Determination of predicted concentrations and recovery of paracetamol and caffeine in PLS models

The predicted or calculated concentrations in μg mL^{-1} of the paracetamol and caffeine were calculated from the multiple regression **Eq. 2**.

The predicted or calculated concentrations of the components were compared with the actual concentrations, and the assay of the binary mixture was performed. The root mean square error of cross-validation (RMSECV) was calculated and found to be low. The low values of RMSECV in **Table 2**indicate that both the precision and accuracy of the PLS model for paracetamol and caffeine were very high, and the R^2 values in **Fig. 2** were also of high linearity.

The linearity of the developed method of the PLS model was tested by constructing a cross-validation of the data in **Table 2**. The results obtained in **Fig. 2** indicate that the developed method possessed high linearity with $R^2 = 0.9993$ within the method linear range (10–20 μg mL^{-1}) for paracetamol and $R^2 = 0.9994$ within the method linear range (1.3–2.6 μg mL^{-1}) for caffeine. In comparison, Uddin *et al.* (2019) revealed less linearity with R^2 values of 0.9928 and 0.9933 assigned for the PLSR of paracetamol and caffeine in methanol solvent, respectively. In contrast, the other study (Aktaş and Kitiş, 2014) that was carried out in 0.1 mol L^{-1} HCl revealed linearity almost similar to our eco-friendly developed method.

$$\text{Predicted (Calculated)} = \text{Constant} + \sum (\text{Coefficient} \times \text{Absorbance}) \qquad (2)$$

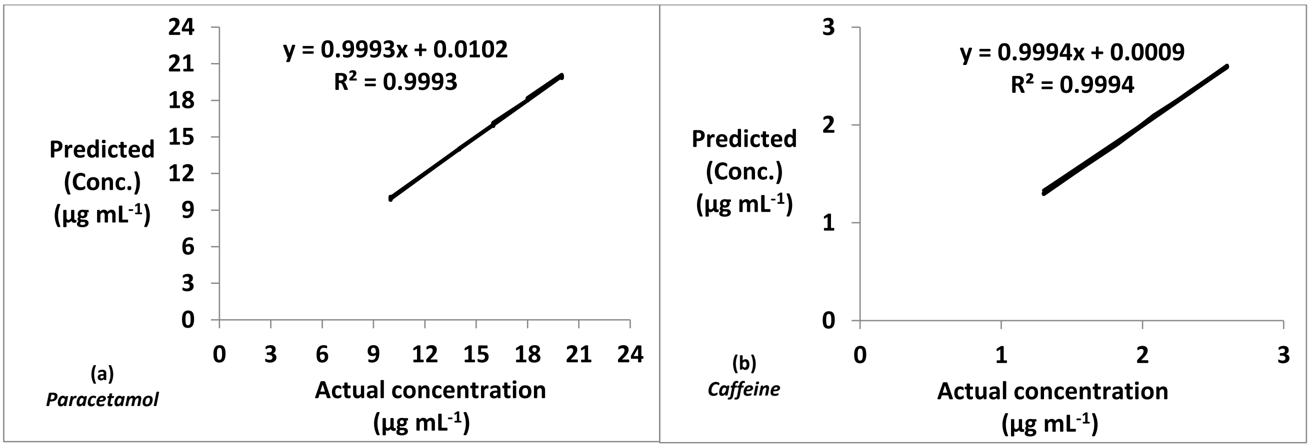

Figure 2. PLS cross-validation for the calibration set of the actual vs. predicted concentration.

3.2.1.4. Determination of the optimum number of principals components and their coefficients of paracetamol and caffeine for PCR

The PCR was computed using six principal components (PCs) and a regression analysis of these PCs with a concentration was performed to determine the PC coefficients of paracetamol and caffeine for the PCR model, as shown in **Table S4**. From the treatment of the principal component's coefficients in (**Table S4**) using the Minitab 17 program. Regression equations for paracetamol and caffeine were obtained and used to calculate the predicted concentrations, as shown below.

Response variable (Predicted concentration) of paracetamol

$$-0.177 + 1.23301\,Z1 + 1.1417\,Z2 + 3.102\,Z3 + 0.81\,Z4 + 2.94\,Z5 + 16.91\,Z6 \tag{3}$$

Response variable (Predicted concentration) of caffeine

$$0.0284 + 0.01374\,Z1 + 1.5390\,Z2 + 3.531\,Z3 + 1.016\,Z4 + 1.491\,Z5 + 1.30\,Z6 \tag{4}$$

where: Z is the principal component coefficients.

3.2.1.5. Determination of the predicted concentrations and recovery of paracetamol and caffeine in the PCR models

The predicted or calculated concentrations in μg mL^{-1} of the paracetamol and caffeine were calculated from the above regression equations.

The predicted or calculated concentrations of paracetamol and caffeine were compared with the actual concentrations, and the assay for binary mixture was performed for each sample. The root mean square error of cross-validation (RMSECV) was calculated and found to be minimal. The small RMSECV values in **Table 3** indicate that both the precision and accuracy of the PCR model for paracetamol and caffeine were very great, with the R^2 values in **Fig. 3** showing very strong linearity.

3.2.2 Validation procedures and construction of the validation set for paracetamol and caffeine determination

3.2.2.1 Linearity method

The linearity of the developed methods for both the PLS and PCR models was tested by constructing a cross-validation of the data, as shown in **Table 4**. The results obtained (**Figs. 4** and **5**) indicated that the developed method possessed high linearity: $R^2 = 0.9989$ and 0.9988 for the PLS and PCR models, respectively, within the method linear range (10 – 20 μg mL^{-1}) of paracetamol. Whereas $R^2 = 0.9989$ and 0.9987 for the PLS and PCR models, respectively, within the method linear range (1.3–2.6 μg mL^{-1}) of caffeine. The linearity of the developed method was better than that of the method in Uddin *et al.* (2019). In addition, another study by Alam *et al.* (2022) showed less linearity with R^2 values of 0.9970 and 0.9928 assigned for the linear regression analysis of paracetamol and caffeine using the greener normal-phase HPTLC technique, respectively, and with R^2 values of 0.9966 and 0.9976 assigned for the linear regression analysis of paracetamol and caffeine using the greener reversed-phase HPTLC technique, respectively.

3.2.2.2. Construction of validation set

The results of the prediction and the percentage recoveries are presented in **Table 4**. The predictive abilities of the models were evaluated by plotting the actual known concentrations against the predicted concentrations shown in **Figs. 4** and **5**. A tremendous agreement between the predicted (calculated) and actual paracetamol and caffeine concentrations for the PLS and PCR models can be observed in **Figs. 4** and **5**.

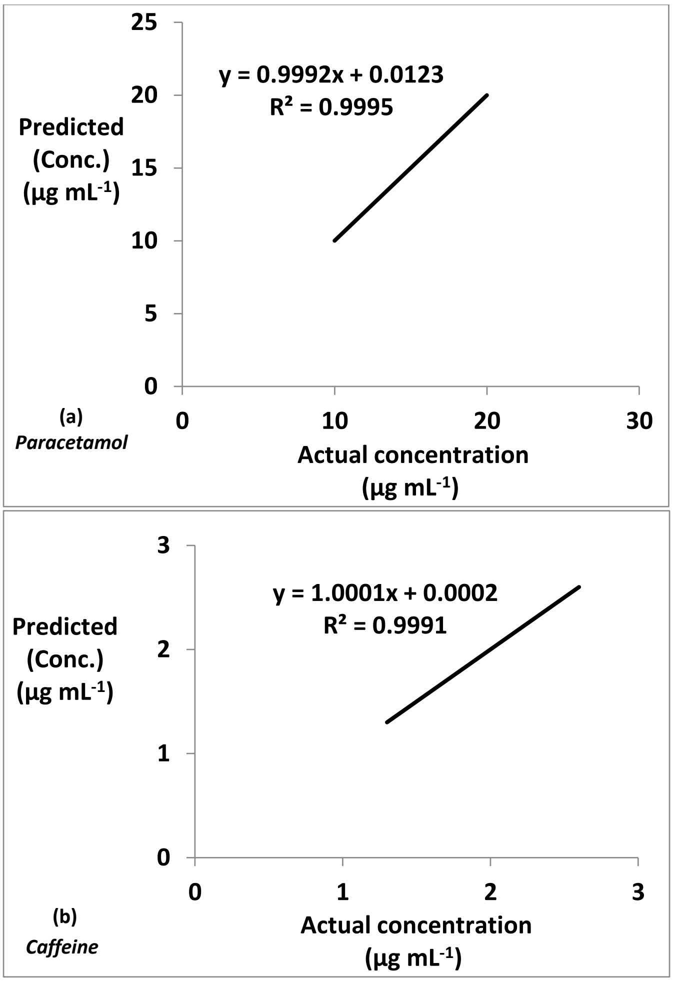

Figure 3. PCR cross-validation for the calibration set of the actual vs. predicted concentrations.

Table 3. Results of the predicted concentrations with the recovery of paracetamol and caffeine in the binary mixture in each sample for the PCR models.

Name		Paracetamol			Caffeine	
Constant		-0.177			0.0284	
Mixture NO.	Actual Conc. (μg mL^{-1})	Predicted Conc. (μg mL^{-1})	%Recovery	Actual Conc. (μg mL^{-1})	Predicted Conc. (μg mL^{-1})	%Recovery
1	10	10.09	100.90	1.3	1.30	100.00
2	10	10.04	100.40	1.82	1.82	100.00
3	10	9.85	98.50	2.08	2.08	100.00
4	10	10.10	101.00	2.34	2.35	100.43
5	10	9.93	99.30	2.6	2.60	100.00
6	14	13.97	99.79	1.3	1.31	100.77
7	14	13.94	99.57	1.82	1.80	98.90
8	14	14.02	100.14	2.08	2.09	100.48
9	14	13.99	99.93	2.34	2.35	100.43
10	14	14.07	100.50	2.6	2.59	99.62
11	16	15.99	99.94	1.3	1.30	100.00
12	16	15.88	99.25	1.82	1.81	99.45
13	16	16.05	100.31	2.08	2.10	100.96
14	16	15.90	99.38	2.34	2.32	99.15
15	16	16.15	100.94	2.6	2.61	100.38
16	18	18.01	100.06	1.3	1.30	100.00
17	18	18.05	100.28	1.82	1.78	97.80
18	18	17.91	99.50	2.08	2.08	100.00
19	18	18.04	100.22	2.34	2.34	100.00
20	18	18.11	100.61	2.6	2.59	99.62
21	20	20.08	100.40	1.3	1.32	101.54
22	20	20.00	100.00	1.82	1.81	99.45
23	20	19.98	99.90	2.08	2.10	100.96
24	20	19.87	99.35	2.34	2.35	100.43
25	20	19.96	99.80	2.6	2.61	100.38
		Mean%	100.00		Mean%	100.03
		RSD%	0.60		RSD %	0.75
		RMSECV	0.079		RMSECV	0.014

Table 4. Results of the validation set of paracetamol and caffeine for the PLS and PCR models.

NO.	METHOD				PLS				PCR	
	Para.		Caff.	Para.		Caff.		Para.		Caff.
	Actual (μg mL^{-1})	Predicted (μg mL^{-1})	%R	Predicted (μg mL^{-1})	%R		Predicted (μg mL^{-1})	%R	Predicted (μg mL^{-1})	%R
1	10	2.34	10.178	101.78	2.344	100.17	10.247	102.47	2.312	98.80
2	10	2.60	10.030	100.30	2.610	100.38	10.096	100.96	2.573	98.96
3	16	1.82	15.912	99.45	1.800	98.90	15.900	99.38	1.784	98.02
4	16	2.08	15.876	99.23	2.056	98.85	15.896	99.35	2.040	98.08
5	20	1.30	19.798	98.99	1.257	96.69	19.746	98.73	1.248	96.00
6	20	2.60	19.905	99.53	2.575	99.04	19.893	99.47	2.545	97.88
7	12	2.808	11.806	98.38	2.864	101.99	11.852	98.77	2.837	101.03
8	12	3.12	11.802	98.35	3.155	101.12	11.829	98.58	3.136	100.51
9	19.2	2.184	18.847	98.16	2.181	99.86	18.812	97.98	2.162	98.99
10	19.2	2.496	19.445	101.28	2.470	98.96	19.431	101.20	2.444	97.92
11	24	1.56	23.865	99.44	1.530	98.08	23.795	99.15	1.514	97.05
12	24	3.12	23.946	99.78	3.129	100.29	23.895	99.56	3.094	99.17
			Mean%	99.55	--	99.53	Mean%	99.63	--	98.54
			RSD%	1.12	--	1.42	RSD%	1.29	--	1.40

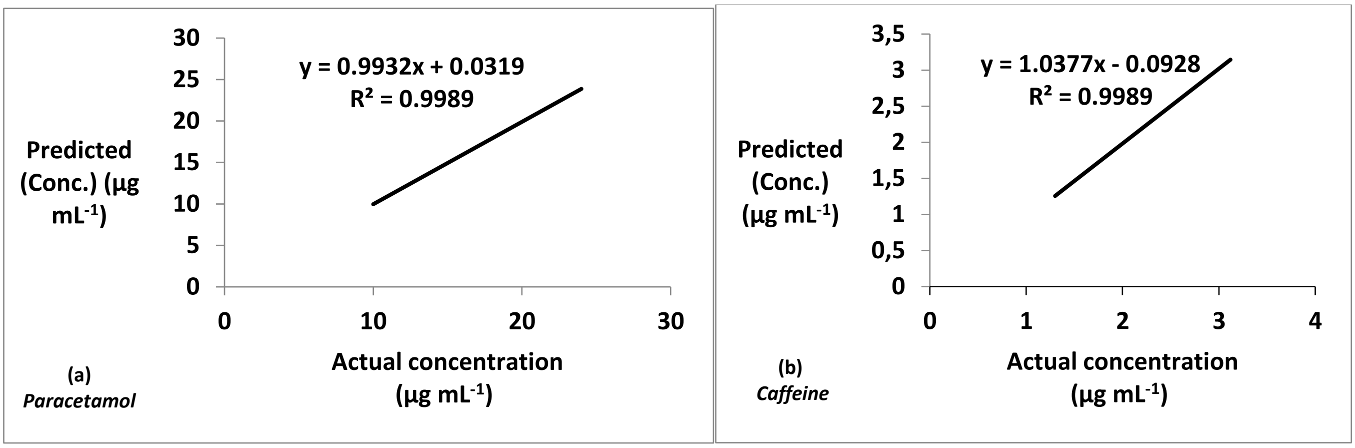

Figure 4. PLS cross-validation for the validation set of the actual vs. predicted concentrations.

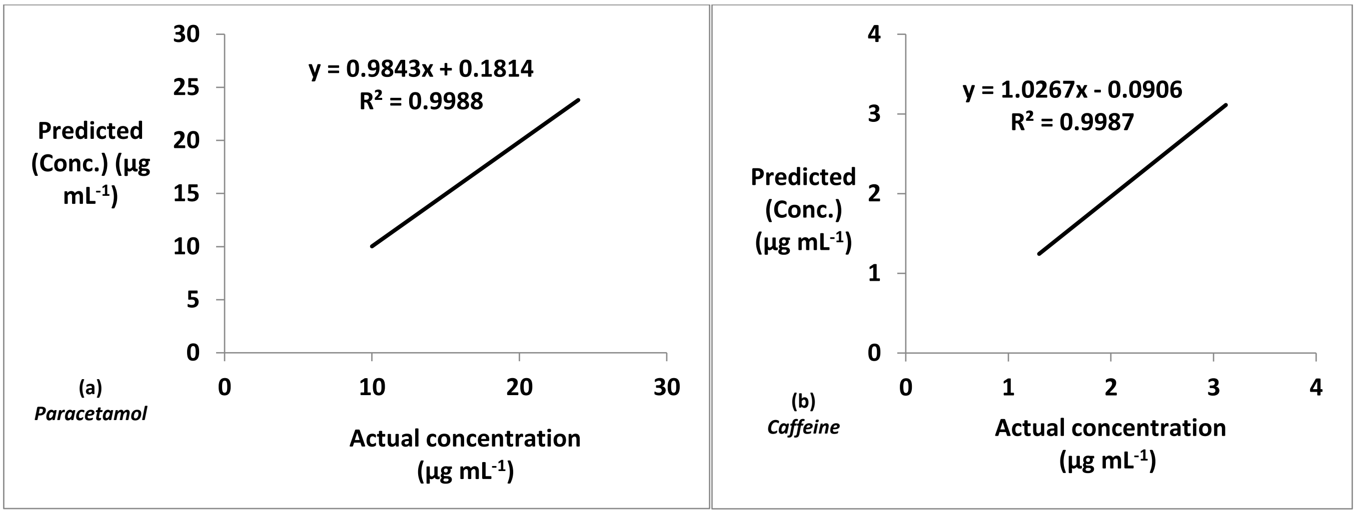

Figure 5. PCR cross-validation for the validation set of the actual vs. predicted concentrations.

3.2.2.3. Precision (Repeatability)

The repeatability (intraday precision) of the developed method was determined by determining the binary mixture at three different concentrations for paracetamol and caffeine in bulk using three different concentrations (i.e., 10/1.3, 16/1.82 and 20/2.6 µg mL^{-1} of paracetamol/caffeine, respectively) sequentially in triplicates. The results are reported as percentage RSD. The low values of percentage RSD indicated the high precision of the method. The %RSD values of the developed method were within the acceptable limit as suggested by the USP pharmacopeia, and the results are presented in **Table 5**.

3.2.2.4. Accuracy

The accuracy of the method was investigated using the standard addition method for three different percentage levels (i.e., 80, 100, and 120%) by recovery experiments. Known amounts of standard solutions containing paracetamol and caffeine were added to sample solutions under investigation to make up solutions of 80%, 100%, and 120% levels in triplicate and scanned in the range 200–400 nm. The quantity of drugs recovered at each percentage level was determined using the developed PCR and PLS models. The mean percentage recovery for each percentage level showed low values of percentage RSD, and the percentage recovery was within the acceptable limit (90–110%) as suggested by the USP pharmacopeia. This indicates a high accuracy method at all three levels, and the accuracy data are given in **Tables 6** and **7**.

3.2.2.5. Specificity (spiking method)

The specificity of the method was checked by adding a certain amount of paracetamol and caffeine standard into a known amount of the marketed sample solution, as described earlier (i.e., Methodology). Specificity data are shown in **Tables 8** and **9**.

As can be seen from these data, recovery for paracetamol and caffeine using the developed PCR and PLS models are within the acceptable limit (90-110%). This suggests that the methods are free from interference due to the excipients used in the commercial formulation.

The above validation indicates the method is simple, rapid, economical, precise, and accurate in addition to being eco-friendly. Therefore, it can be used for routine analysis in the quality control of mixtures and commercial products containing paracetamol and caffeine.

Table 5. Results of repeatability and Intraday precision using the developed PLS and PCR models.

Amount taken (Actual Conc.) µg/ml		Predicted Conc. µg mL^{-1}				% Recovery				Acceptable % RSD NMT 2%			
Para.	Caff.	PLS		PCR		PLS		PCR		PLS		PCR	
		Para.	Caff.	Para.	Caff.	Para.	Caff.	Para.	Caff.	Para.	Caff.	Para.	Caff.
10	1.3	9.973	1.291	10.059	1.281	99.73	99.31	100.59	98.54	0.12	0.32	0.08	0.28
10	1.3	9.984	1.299	10.048	1.286	99.84	99.92	100.48	98.92				
10	1.3	9.996	1.297	10.063	1.288	99.96	99.77	100.63	99.08				
16	1.82	16.382	1.912	16.358	1.91	102.39	105.05	102.24	104.95	0.08	0.28	0.04	0.30
16	1.82	16.396	1.914	16.357	1.91	102.48	105.16	102.23	104.95				
16	1.82	16.370	1.904	16.347	1.90	102.31	104.62	102.17	104.40				
20	2.6	20.365	2.721	20.282	2.715	101.83	104.65	101.41	104.42	0.16	0.41	0.11	0.50
20	2.6	20.387	2.707	20.275	2.714	101.94	104.12	101.38	104.38				
20	2.6	20.324	2.699	20.239	2.691	101.62	103.81	101.20	103.50				

Note: % Recovery = Predicted Conc. (µg/ml) / Actual Conc. (µg/ml) ×100.

Table 6. Accuracy data for paracetamol by PCR and PLS models.

%Level	Sample Conc. µg mL^{-1}	Amount of standard paracetamol µg mL^{-1}	Total Conc. µg mL^{-1}	Predicted Conc. µg mL^{-1}		% Recovery		% RSD	
				PLS	PCR	PLS	PCR	PLS	PCR
80%	10	8	18	18.427	18.549	102.37	103.05	0.16	0.12
				18.464	18.547	102.58	103.04		
				18.487	18.586	102.71	103.26		
100%	10	10	20	20.291	20.302	101.46	101.51	0.21	0.17
				20.367	20.361	101.84	101.81		
				20.362	20.366	101.81	101.83		
120%	10	12	22	22.465	22.416	102.11	101.89	0.08	0.14
				22.429	22.403	101.95	101.83		
				22.445	22.358	102.02	101.63		

Table 7. Accuracy data for caffeine by PCR and PLS models.

%Level	Sample Conc. µg mL^{-1}	Amount of standard caffeine µg mL^{-1}	Total Conc. µg mL^{-1}	Predicted Conc. µg mL^{-1}		% Recovery		% RSD	
				PLS	PCR	PLS	PCR	PLS	PCR
80%	1.3	1.04	2.34	2.377	2.333	101.58	99.70	0.49	0.68
				2.395	2.355	102.35	100.64		
100%	1.3	1.3	2.6	2.399	2.364	102.52	101.03	0.37	0.52
				2.690	2.670	103.46	102.69		
				2.692	2.683	103.54	103.19		
				2.708	2.698	104.15	103.77		
120%	1.3	1.56	2.86	2.981	2.970	104.23	103.85	0.26	0.28
				2.966	2.965	103.71	103.67		
				2.971	2.981	103.88	104.23		

Table 8. Results of specificity for paracetamol using the developed PCR and PLS models.

Name of the marketed sample	Sample Conc. µg mL^{-1}	Amount added µg mL^{-1}	Total Conc. µg mL^{-1}	Predicted Conc. µg mL^{-1}		% Recovery		% RSD	
				PLS	PCR	PLS	PCR	PLS	PCR
Panadol	16	16	32	31.590	31.524	98.72	98.51	1.64	1.5
				32.329	32.206	101.03	100.64		
Ramol	16	16	32	32.478	32.451	101.49	101.41	1.85	2.0
				31.639	31.532	98.87	98.54		
Amol	16	16	32	31.625	31.514	98.83	98.48	1.58	1.8
				32.339	32.332	101.06	101.04		

Table 9. Results of specificity for caffeine using the developed PCR and PLS models.

Name of the marketed sample	Sample Conc. μg mL^{-1}	Amount added μg mL^{-1}	Total Conc. μg mL^{-1}	Predicted Conc. μg mL^{-1}		% Recovery		% RSD	
				PLS	PCR	PLS	PCR	PLS	PCR
Panadol	2.08	2.08	4.16	4.125	4.044	99.16	97.21	1.17	0.21
				4.194	4.056	100.82	97.50		
Ramol	2.08	2.08	4.16	4.130	4.039	99.28	97.09	0.20	0.47
				4.142	4.066	99.57	97.74		
Amol	2.08	2.08	4.16	4.171	4.091	100.26	98.34	0.73	0.36
				4.214	4.112	101.30	98.85		

3.3. Analysis of the marketed formulations

The applicability of the developed methods for the quantification of paracetamol and caffeine in marketed formulations was evaluated using the marketed formulation of 500 mg paracetamol with 65 mg caffeine concentration collected from the local pharmacies in the capital Sana'a. **Tables 10** and **11** summarize the data obtained for paracetamol and caffeine in the analyzed marketed formulations.

As can be seen from these data, the paracetamol and caffeine concentrations were within the acceptable limit (90-110%) according to the United States Pharmacopeia (USP).

3.4. Comparison with the reference method

A comparison was carried out with the aid of the SPSS program using F-Test to ensure a non-significant difference between the recovery results of the newly developed methods and that of the reference method for both paracetamol and caffeine. The significance level indicated that the null hypothesis was acceptable because the P-value was greater than the significance level (**Table 12**). As for reference methods, paracetamol and caffeine were determined according to the United States Pharmacopeia (USP), as described earlier in the methodology.

In addition, the chromatograms in **Fig. 6** show the results of the analysis for the reference method for the determination of paracetamol and caffeine.

Table 10. Assay results for paracetamol and caffeine in tablets (marketed sample) using the proposed PLS method.

Name of the marketed sample	METHOD		PLS					
	Para.	Caff.	Para.			Caff.		
	Actual (μg mL^{-1})		Predicted (μg mL^{-1})	% Recovery	% RSD	Predicted (μg mL^{-1})	% Recovery	% RSD
Panadol	16	2.08	16.135	100.84	1.30	2.088	100.38	2
	16	2.08	16.434	102.71		2.023	97.26	
Amol	16	2.08	15.654	97.84	0.03	2.053	98.70	0
	16	2.08	15.660	97.88		2.053	98.70	
Ramol	16	2.08	15.597	97.48	2	2.039	98.03	2
	16	2.08	16.132	100.83		2.098	100.87	

Table 11. Assay results for paracetamol and caffeine in tablets (Marketed Sample) by the PCR proposed method.

Name of the marketed sample	METHOD		PCR					
	Para.	Caff.	Para.			Caff.		
	Actual (μg mL^{-1})		Predicted (μg mL^{-1})	% Recovery	% RSD	Predicted (μg mL^{-1})	% Recovery	% RSD
Panadol	16	2.08	16.253	101.58	0.93	2.007	96.49	1.21
	16	2.08	16.469	102.93		1.973	94.86	
Amol	16	2.08	15.653	97.83	0.01	2.024	97.31	0.03
	16	2.08	15.656	97.85		2.025	97.36	
Ramol	16	2.08	15.620	97.63	2.6	1.996	95.96	1.40
	16	2.08	16.215	101.34		2.036	97.88	

Table 12. Results of statistical comparison between the newly developed and reference methods.

Name of the marketed sample	Components	paracetamol			Caffeine		
	Methods	Reference method (HPLC)	PLS	PCR	Reference method (HPLC)	PLS	PCR
Panadol	Mean%	102.12	100.84	101.58	99.27	100.38	96.49
		101.67	102.71	102.93	99.32	97.26	94.86
		101.90	101.78	102.26	99.30	98.82	95.68
	Significance level		0.912	0.663	--	0.790	0.047
Ramol	Mean%	100.08	97.48	97.63	97.75	98.03	95.96
		100.02	100.83	101.34	97.35	100.87	97.88
		100.05	99.16	99.49	97.55	99.45	96.92
	Significance level (α)		0.647	0.789	--	0.316	0.586

Note: p-value = 0.01.

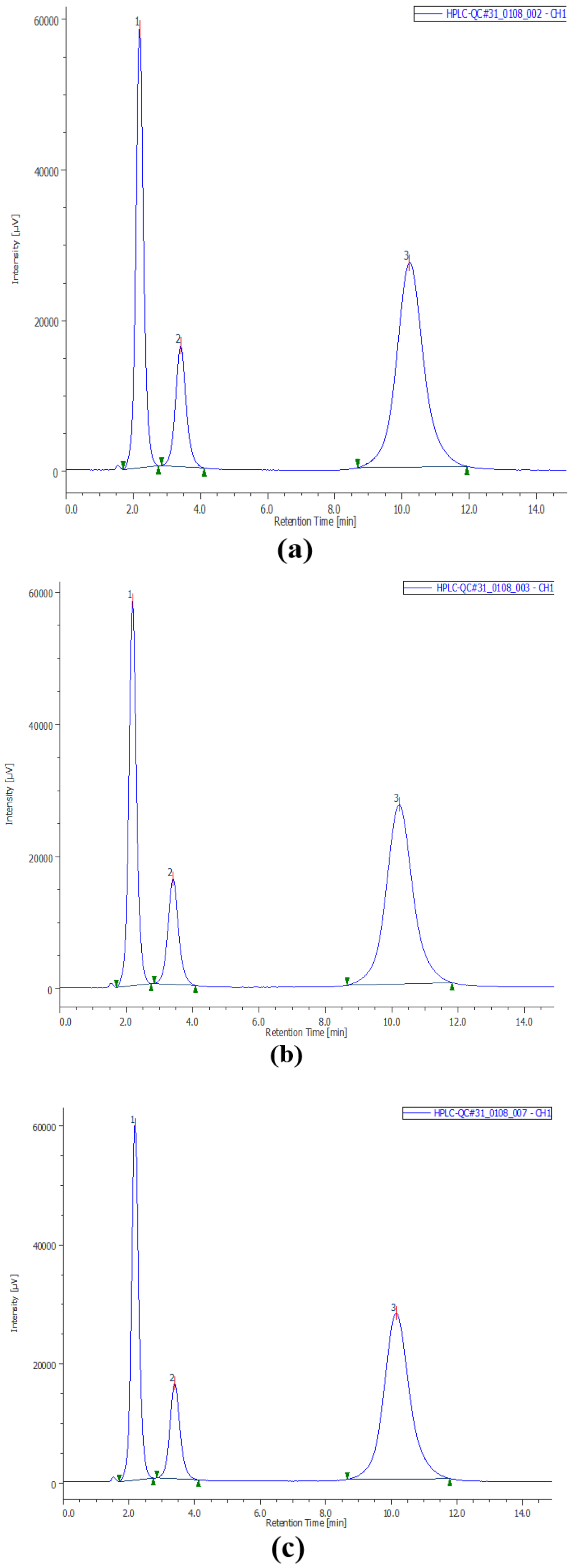

(a)

(b)

(c)

Figure 6. Chromatogram of paracetamol and caffeine standard with Benzoic acid as the internal standard and commercial samples. **(a)** Standard paracetamol and caffeine with benzoic acid as the internal standard; **(b)** Panadol Extra Sample (commercial); **(c)** Ramol Extra Sample (commercial).

3.5. Greenness evaluation of the developed methods

Modern analytical chemistry provides various methods and tools for identifying a specific analyte in various samples. The main objectives of greening analytical methods are to minimize energy consumption, eliminate or reduce the use of chemical substances (solvents, reagents, preservatives, additives for pH adjustment, and others), and properly manage analytical waste while increasing operator safety. Most of these problems demand reductions, e.g., sample number, reagents, energy, waste, risk, and hazard (Gałuszka *et al.*, 2013). This study introduces green analytical methods in the field of pharmaceutical analysis. In this study, water was used as a solvent to prepare the stock solution of one of the analytes and further dilutions to determine paracetamol with caffeine. Water is a safe solvent for health, safety, and environmental hazards. The instrument used was a spectrophotometer; hence, the energy used by these methods is safe. The proposed method in this study generates only a small volume of waste compared with the reference HPLC method. Another important issue is that the toxicity of waste was negligible. In general, AGREE considers UV-chemometrics methods to be the greenest methods compared to HPLC methods. According to the AGREE scale, the UV-chemometrics method shows a very intense greenness of 0.87. However, the HPLC method is less green and shows a very weak intense greenness, 0.45. This comparison is based on the 12 green analytical chemistry principles as follows:

1. Sample treatment;
2. Sample amount;
3. Device Positioning;
4. Sample pre. Stages;
5. Automation, miniaturization;
6. Derivization;
7. Waste;
8. Analysis throughput;
9. Energy consumption;
10. Source of the reagents;
11. Toxicity;
12. Operator's safety;

A comparison of the results obtained by UV chemometrics and those obtained by HPLC methods for the AGREE program scale is shown in **Fig. 7**.

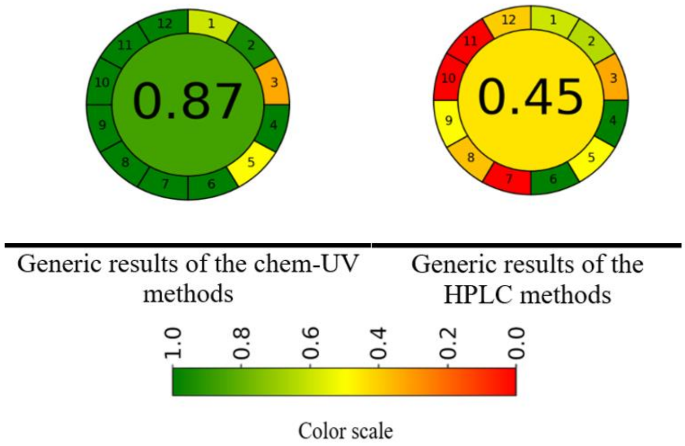

Figure 7. Generic result of assessment (left) and the corresponding color scale for reference for the comparison of the developed UV-chemometrics and reference HPLC methods of paracetamol with caffeine according to the 12 principles of green analytical chemistry, performed using the AGREE program.

4. Conclusions

The use of dangerous chemicals has been discouraged using green analytical chemistry. To determine the combined amounts of caffeine and paracetamol in pharmaceutical formulations, a green spectrophotometric method for simultaneous determination-assisted chemometrics that is simple, quick, and cost-effective has been developed. The proposed chemometric models (PLS and PCR) can be used to simultaneously determine paracetamol and caffeine in binary mixtures in pharmaceutical dosage forms without excipient interference or from each other, and there is no need for prior physical separation of the two drugs. Multivariate calibration models were generated using spectral and concentration matrices. Validation of the two models and their application to a commercial pharmaceutical dosage form gave excellent results. As a result, the suggested techniques can be applied to regular quality control of the specified medications in their combination dosage form in standard laboratories.

Authors' contributions

Conceptualization: Bushra Alattab; Fares Abdullah Alarbagi; **Data curation:** Maher Ali Almaqtari; Entesar Alhuraishi; **Formal Analysis:** Bushra Alattab; Fares Abdullah Alarbagi; **Funding acquisition**: Not applicable; **Investigation**: Bushra Alattab; Fares Abdullah Alarbagi; **Methodology**: Fares Abdullah Alarbagi; **Project administration**: Bushra Alattab; Fares Abdullah Alarbagi; **Resources**: Not applicable; **Software**: Entesar Alhuraishi; Hussein Al-Maydama; **Supervision**: Bushra Alattab; Fares Abdullah Alarbagi; **Validation**: Bushra Alattab; Fares Abdullah Alarbagi; Maher Ali Almaqtari; **Visualization**: Fares Abdullah Alarbagi; **Writing – original draft**: Fares Abdullah Alarbagi; **Writing – review & editing**: Hussein Al-Maydama.

Data availability statement

All data sets were generated or analyzed in the current study.

Funding

Not applicable.

Acknowledgments

The authors would like to thank the Chemistry Department-Factuality of Science, Sana'a University, Global Pharma and Shiba'a pharma Companies, Sana'a, Yemen for providing the laboratory facilities and the reference standards of the samples drugs as gift samples.

References

Aktaş, A. H.; Kitiş, F. Spectrophotometric simultaneous determination of caffeine and paracetamol in commercial pharmaceutical by principal component regression, partial least squares and artificial neural networks chemometric methods. *Croat. Chem. Acta*. **2014**, *87* (1), 69–74. https://doi.org/10.5562/cca2214

Alam, P.; Shakeel, F.; Ali, A.; Alqarni, M. H.; Foudah, A. I.; Aljarba, T. M.; Alkholifi, F. K.; Alshehri, S.; Ghoneim, M. M.; Ali, A. Simultaneous determination of caffeine and paracetamol in commercial formulations using greener normal-phase and reversed-phase HPTLC methods: A contrast of validation parameters. *Molecules*. **2022**, *27* (2), 405. https://doi.org/10.3390/molecules27020405

Aminu, N.; Chan, S.-Y.; Khan, N. H.; Farhan, A. B.; Umar, M. N.; Toh, S.-M. A simple stability-indicating HPLC method for simultaneous analysis of paracetamol and caffeine and its application to determinations in fixed-dose combination tablet dosage form. *Acta Chromatogr*. **2019**, *31* (2), 85–91. https://doi.org/10.1556/1326.2018.00354

Ashour, A.; Hegazy, M. A.; Abdel-Kawy, M.; ElZeiny, M. B. Simultaneous spectrophotometric determination of overlapping spectra of paracetamol and caffeine in laboratory prepared mixtures and pharmaceutical preparations using continuous wavelet and derivative transform. *J. Saudi Chem. Soc*. **2015**, *19* (2), 186–192. https://doi.org/10.1016/j.jscs.2012.02.004

Attia, K. A.-S. M.; Abdel-Aziz, O.; Magdy, N.; Mohamed, G. F. Development and validation of different chemometric-assisted spectrophotometric methods for determination of cefoxitin-sodium in presence of its alkali-induced degradation product. *Futur. J. Pharma. Sci*. **2018**, *4* (2), 241–247. https://doi.org/10.1016/j.fjps.2018.08.002

Belal, F.; Ibrahim, F.; Sheribah, Z.; Alaa, H. New spectrophotometric/chemometric assisted methods for the simultaneous determination of imatinib, gemifloxacin, nalbuphine and naproxen in pharmaceutical formulations and human urine. *Spectrochim. Acta A. Mol. Biomol. Spectrosc*. **2018**, *198*, 51–60. https://doi.org/10.1016/j.saa.2018.02.048

Darbandi, A.; Sohrabi, M. R.; Bahmaei, M. Development of a chemometric-assisted spectrophotometric method for quantitative simultaneous determination of Amlodipine and Valsartan in commercial tablet. *Optik*. **2020**, *218*, 165110. https://doi.org/10.1016/j.ijleo.2020.165110

Drugbank online. *Acetaminophen*. Drug created at June 13, 2005a 13:24 / Updated at September 07, 2024. https://go.drugbank.com/drugs/DB00316. Accessed on 18 Jan 2023.

Drugbank online. *Caffeine*. Drug created at June 13, 2005b 13:24 / Updated at September 07, 2024. https://go.drugbank.com/drugs/DB00201. Accessed on 18 Jan 2023.

Elfatatry, H. M.; Mabrouk, M. M.; Hammad, S. F.; Mansour, F. R.; Kamal, A. H.; Alahmad, S. Development and validation of chemometric-assisted spectrophotometric methods for simultaneous determination of phenylephrine hydrochloride and ketorolac tromethamine in binary combinations. *J. AOAC Int*. **2016**, *99* (5), 1247–1251. https://doi.org/10.5740/jaoacint.16-0106

Eticha, T.; Kahsay, G.; Asefa, F.; Hailu, T.; Gebretsadik, H.; Gebretsadikan, T.; Thangabalan, B. Chemometric-Assisted spectrophotometric method for the simultaneous determination of ciprofloxacin and doxycycline hyclate in pharmaceutical formulations. *J. Anal. Methods Chem*. **2018**, *2018*, 9538435. https://doi.org/10.1155/2018/9538435

Gałuszka, A.; Migaszewski, Z.; Namieśnik, J. The 12 principles of green analytical chemistry and the SIGNIFICANCE mnemonic of green analytical practices. *TrAC, Trends Anal. Chem*. **2013**, *50*, 78–84. https://doi.org/10.1016/j.trac.2013.04.010

Gandhi, S. V.; Abhilash, D.; Waghmare, N. Y.; Mutha, A. S. Chemometrics-assisted UV spectrophotometric method for determination of ciprofloxacin and ornidazole in pharmaceutical formulation. *ARC J. Pharm. Sci*. **2017**, *3* (1), 19–25. https://doi.org/10.20431/2455-1538.0301005

Gholse, Y. N.; Chaple, D. R.; Kasliwal, R. H. Development and Validation of Novel Analytical Simultaneous Estimation Based UV Spectrophotometric Method for Doxycycline and Levofloxacin Determination. *Biointerface Res. Appl. Chem*. **2022**, *12* (4) 5458–5478. https://doi.org/10.33263/BRIAC124.54585478

Glavanović, S.; Glavanović, M.; Tomišić, V. Simultaneous quantitative determination of paracetamol and tramadol in tablet formulation using UV spectrophotometry and chemometric methods. *Spectrochim. Acta A. Mol. Biomol. Spectrosc*. **2016**, *157*, 258–264. https://doi.org/10.1016/j.saa.2015.12.020

Manouchehri, F.; Izadmanesh, Y.; Aghaee, E.; Ghasemi, J. B. Experimental, computational and chemometrics studies of BSA-vitamin B6 interaction by UV-Vis, FT-IR, fluorescence spectroscopy, molecular dynamics simulation and hard-soft modeling methods. *Bioorg. Chem*. **2016**, *68*, 124–136. https://doi.org/10.1016/j.bioorg.2016.07.014

Mattar, A. A.; Sobhy, M. UV-Chemometric Method Development for Resolving The Overlapped Spectra of Aspirin, Caffeine and Orphenadrine Citrate in Their Ternary Pharmaceutical Dosage Form. **Preprint from** *Research Square*, Jan. 31 2022. https://doi.org/10.21203/rs.3.rs-1262160/v1

Mohammed, O. J.; Hamzah, M. J.; Saeed, A. M. RP-HPLC Method Validation for Simultaneous Estimation of Paracetamol and Caffeine in Formulating Pharmaceutical Form. *Res. J. Pharm. Technol*. **2021**, *14* (9), 4743–4748. https://doi.org/10.52711/0974-360X.2021.00825

Moroni, A. B.; Vega, D. R.; Kaufman, T. S.; Calvo, N. L. Form quantitation in desmotropic mixtures of albendazole bulk drug by chemometrics-assisted analysis of vibrational spectra. *Spectrochim. Acta A. Mol. Biomol. Spectrosc.* **2022**, *265*, 120354. https://doi.org/10.1016/j.saa.2021.120354

Moussa, B. A.; Mahrouse, M. A.; Fawzy, M. G. Smart spectrophotometric methods for the simultaneous determination of newly co-formulated hypoglycemic drugs in binary mixtures. *Spectrochim. Acta A. Mol. Biomol. Spectrosc*. **2021**, *257*, 119763. https://doi.org/10.1016/j.saa.2021.119763

Muntean, D. M.; Alecu, C.; Tomuta, I. Simultaneous quantification of paracetamol and caffeine in powder blends for tableting by NIR-chemometry. *J. Spectrosc*. **2017**, *2017*, 160675. https://doi.org/10.1155/2017/7160675

Muntean, D.; Porfire, A.; Alecu, C.; Iurian, S.; Casian, T.; Gâvan, A.; Tomuta, I. A non-destructive NIR spectroscopic method combined with chemometry for simultaneous assay of paracetamol and caffeine in tablets. *Ro. J. Pharm. Pract.* **2021**, 14 (2), 68–75. https://doi.org/10.37897/RJPhP.2021.2.2

Ortega-Barrales, P.; Padilla-Weigand, R.; Molina-Díaz, A. Simultaneous determination of paracetamol and caffeine by flow injection-solid phase spectrometry using C18 silica gel as a sensing support. *Anal. Sci.* **2002**, *18* (11), 1241-1246. https://doi.org/10.2116/analsci.18.1241

Patel, K. R.; Prajapati, L. M.; Joshi, A. K.; Kharodiya, M. L.; Patel, J. R. Application of Chemometrics in Simultaneous Spectrophotometric Quantification of Etophylline and Theophylline: The Drugs with Same Chromophore. *Iran. J. Pharm. Sci*. **2013a**, *9* (3), 17–28. https://doi.org/10.22037/ijps.v9.40870

Patel, M. N.; Alvi, S. N.; Savalia, M. D.; Kathiria, P. B.; Patel, B. A.; Parmar, S. J. Development and Validation of First Order Derivative Spectrophotometric Method for Simultaneous Estimation of Paracetamol and Caffeine in Tablet Dosage Form. *Inventi Rapid: Pharm Analysis & Quality Assurance*. **2013b**, *5* (5), 213–218.

Phechkrajang, C.; Siriratawan, W.; Narapanich, K.; Thanomchat, K.; Kantanawat, P.; Srikajhondei, W.; Khajornvanitchot, V.; Sakchaisri, K. Development and validation of chemometrics-assisted spectrophotometric method for determination of clotrimazole in the presence of betamethasone valerate. *Mahidol Univ. J. Pharm. Sci*. **2015**, *42*, 1–7.

Putri, D. C. A.; Gani, M. R.; Octa, F. D. Chemometrics-Assisted UV Spectrophotometric Method for Simultaneous Determination of Paracetamol and Tramadol in Divided Powder Dosage Form. *Inter. J. Pharm. Res.* **2021**, *13* (01), 1901–1907. https://doi.org/10.31838/ijpr/2021.13.01.075

Rahman, A.; Sravani, G. J.; Srividya, K.; Priyadharshni, A. D. R.; Narmada, A.; Sahithi, K.; Sai, T. K.; Padmavathi, Y. Development and Validation of Chemometric Assisted FTIR Spectroscopic Method for Simultaneous Estimation of Valsartan and Hydrochlorothiazide in Pure and Pharmaceutical Dosage Forms. *J. Young Pharm.* **2020**, *12* (2s), s51–s55. https://doi.org/10.5530/jyp.2020.12s.46

Riddhi, P.; Rajashree, M., Development and Validation of Chemometric Assisted Methods and Stability Indicating RP-HPLC Method for Simultaneous Estimation of Rasagiline Mesylate and Pramipexole in Synthetic Mixture. *Acta Sci. Pharm. Sci.* **2019**, *3* (8), 154–168. https://doi.org/10.31080/ASPS.2019.03.0359

Salem, Y. A.; Hammouda, M. E.; El-Enin, M. A. A.; El-Ashry, S. M. Application of derivative emission fluorescence spectroscopy for determination of ibuprofen and phenylephrine simultaneously in tablets and biological fluids. *Spectrochim. Acta A. Mol. Biomol. Spectrosc.* **2019**, *210*, 387–397. https://doi.org/10.1016/j.saa.2018.11.054

Sebaiy, M. M.; Sobhy, M.; Mattar, A. A. Different techniques for overlapped UV spectra resolution of some co-administered drugs with paracetamol in their combined pharmaceutical dosage forms. *Spectrochim. Acta A. Mol. Biomol. Spectrosc.*. **2020**, *224*, 117429. https://doi.org/10.1016/j.saa.2019.117429

Shah, U. H.; Jasani, A. H. Chemometric assisted spectrophotometric methods for simultaneous determination of paracetamol and tolperisone hydrochloride in pharmaceutical dosage form. *Eurasian J. Anal. Chem*. **2017**, *12* (3), 211–222. https://doi.org/10.12973/ejac.2017.00164a

Shinde, M. A.; Divya, O. Simultaneous quantitative analysis of a three-drug combination using synchronous fluorescence spectroscopy and chemometrics. *Curr. Sci.* **2015**, 1348–1354.

Silva, W. C.; Pereira, P. F.; Marra, M. C.; Gimenes, D. T.; Cunha, R. R.; Da Silva, R. A.; Munoz, R. A.; Richter, E. M. A simple strategy for simultaneous determination of paracetamol and caffeine using flow injection analysis with multiple pulse amperometric detection. *Electroanalysis*. **2011**, *23* (12), 2764-2770. https://doi.org/10.1002/elan.201100512

Singh, V. D.; Singh, V. K. Chemo-metric assisted UV-spectrophotometric methods for simultaneous estimation of Darunavir ethanolate and Cobicistat in binary mixture and their tablet formulation. *Spectrochim. Acta A. Mol. Biomol. Spectrosc.* **2021**, *250*, 119383. https://doi.org/10.1016/j.saa.2020.119383

Sun, X.; Li, H.; Yi, Y.; Hua, H.; Guan, Y.; Chen, C. Rapid detection and quantification of adulteration in Chinese hawthorn fruits powder by near-infrared spectroscopy combined with chemometrics. *Spectrochim. Acta A. Mol. Biomol. Spectrosc.* **2021**, *250*, 119346. https://doi.org/10.1016/j.saa.2020.119346

Tobiszewski, M.; Namieśnik, J.; Pena-Pereira, F., A derivatisation agent selection guide. *Green Chem*. **2017**, *19* (24), 5911–5922. https://doi.org/10.1039/C7GC03108D

Tsvetkova, B.; Kostova, B.; Pencheva, I.; Zlatkov, A.; Rachev, D.; Peikov, P. Validated LC method for simultaneous analysis of paracetamol and caffeine in model tablet formulation. *Int. J. Pharm. Pharm. Sci*. **2012**, *4* (4), 680–684.

Uddin, M.; Mondal, A.; Karim, M.; Jahan, R.; Rana, A. Chemometrics assisted spectrophotometric method for simultaneous determination of paracetamol and caffeine in pharmaceutical formulations. *Bangladesh J. Sci. Ind. Res.* **2019**, *54* (3), 215–222. https://doi.org/10.3329/bjsir.v54i3.42673

United States Pharmacopeia and the National Formulary (USP 43 - NF 38). The United States Pharmacopeial Convention; 2020.

Vichare, V.; Mujgond, P.; Tambe, V.; Dhole, S. Simultaneous spectrophotometric determination of paracetamol and caffeine in tablet formulation. *Int. J. Pharmtech Res*. **2010**, *2* (4), 2512–2516.

Vu Dang, H.; Truong Thi Thu, H.; Dong Thi Ha, L.; Nguyen Mai, H. RP-HPLC and UV Spectrophotometric Analysis of Paracetamol, Ibuprofen, and Caffeine in Solid Pharmaceutical Dosage Forms by Derivative, Fourier, and Wavelet Transforms: A Comparison Study. *J. Anal. Methods Chem*. **2020**, *2020*, 8107571. https://doi.org/10.1155/2020/8107571

Walash, M. I.; Belal, F. F.; El-Enany, N. M.; El-Maghrabey, M. H. Synchronous fluorescence spectrofluorimetric method for the simultaneous determination of metoprolol and felodipine in combined pharmaceutical preparation. *Chem. Cent. J.* **2011**, *5* (1), 70. https://doi.org/10.1186/1752-153X-5-70

Yehia, A. M.; Mohamed, H. M. Chemometrics resolution and quantification power evaluation: application on a pharmaceutical quaternary mixture of Paracetamol, Guaifenesin, Phenylephrine and p-aminophenol. *Spectrochim. Acta A. Mol. Biomol. Spectrosc.* **2016**, *152*, 491–500. https://doi.org/10.1016/j.saa.2015.07.101

Zhu, L.; Wu, H.-L.; Xie, L.-X.; Fang, H Xiang, S.-X.; Hu, Y.; Liu, Z.; Wanga, T.; Yu, R.-Q. A chemometrics-assisted excitation-emission matrix fluorescence method for simultaneous determination of arbutin and hydroquinone in cosmetic products. *Anal. Methods.* **2016**, *8* (24), 4941–4948. https://doi.org/10.1039/C6AY00821F

Supplementary Material

Table S1. Results of the optimum number of principal factors of paracetamol for PLS models.

Method	Components to evaluate	Number of components evaluated	Number of components selected		
Cross-validation (Leave-one-out)	Set	10	3		
Model selection and validation for paracetamol					
Components	**X Variance**	**Error**	**R-sq**	**Press**	**R-sq (Pred)**
1	0.966084	14.5473	0.95085	17.0743	0.942316
2	0.990946	0.4642	0.99843	0.6627	0.997761
3	0.999871	0.2161	0.99927	0.3068	0.998964
4	--	0.0555	0.99981	0.3730	0.998740
5	--	0.0308	0.99990	0.3141	0.998939
6	--	0.0126	0.99996	0.3219	0.998913
7	--	0.0032	0.99999	0.3245	0.998904
8	--	0.0007	1.00000	0.3327	0.998876
9	--	0.0002	1.00000	0.3332	0.998874
10	--	0.0000	1.00000	0.3298	0.998886

Table S2. Results of the optimum number of principal factors of caffeine for PLS models.

Method	Components to evaluate	Number of components evaluated	Number of components selected		
Cross-validation (Leave-one-out)	Set	10	4		
Model selection and validation for caffeine					
Components	**X Variance**	**Error**	**R-sq**	**Press**	**R-sq (Pred)**
1	0.952542	4.50078	0.10028	4.98888	0.002703
2	0.990880	0.14035	0.97194	0.18389	0.963240
3	0.999871	0.00689	0.99862	0.00937	0.998128
4	0.999899	0.00334	0.99933	0.00779	0.998442
5	--	0.00097	0.99981	0.00858	0.998285
6	--	0.00029	0.99994	0.00821	0.998359
7	--	0.00012	0.99998	0.00840	0.998320
8	--	0.00002	1.00000	0.00834	0.998332
9	--	0.00001	1.00000	0.00848	0.998304
10	--	0.00000	1.00000	0.00846	0.998310

Table S3. The constant and coefficients at each wavelength of paracetamol and caffeine for PLS models.

Paracetamol				Caffeine			
Constant			-0.20039	Constant			-0.02079
Wavelength (nm)	**Coefficients**	**Wavelength (nm)**	**Coefficients**	**Wavelength (nm)**	**Coefficients**	**Wavelength (nm)**	**Coefficients**
300	-3.17198	254.8	0.11817	300	-2.54573	254.8	-0.06339
299.8	-2.62108	254.6	0.11705	299.8	-0.88698	254.6	-0.06383
299.6	-2.39074	254.4	0.11657	299.6	-2.97845	254.4	-0.05558
299.4	-1.71683	254.2	0.11665	299.4	5.04438	254.2	-0.05372
299.2	-1.9243	254	0.11566	299.2	-0.38125	254	-0.06811
299	-1.97862	253.8	0.11516	299	-4.09387	253.8	-0.05123
298.8	-1.58562	253.6	0.11491	298.8	-3.29	253.6	-0.05448
298.6	-1.20244	253.4	0.11407	298.6	0.94618	253.4	-0.07226
298.4	-1.25856	253.2	0.11396	298.4	1.81124	253.2	-0.06115
298.2	-1.0679	253	0.11314	298.2	-0.54598	253	-0.05667
298	-0.98847	252.8	0.11242	298	-2.58962	252.8	-0.057
297.8	-0.77672	252.6	0.1115	297.8	-1.24952	252.6	-0.05138
297.6	-0.77833	252.4	0.1115	297.6	-2.48049	252.4	-0.05338
297.4	-0.55081	252.2	0.11087	297.4	-0.1358	252.2	-0.05592
297.2	-0.51919	252	0.11071	297.2	-0.67162	252	-0.05017
297	-0.51479	251.8	0.10941	297	-1.30059	251.8	-0.06055
296.8	-0.47054	251.6	0.10994	296.8	-0.95739	251.6	-0.06112

296.6	-0.30712	251.4	0.10891	296.6	-1.44424	251.4	-0.04166
296.4	-0.27819	251.2	0.10796	296.4	-0.45932	251.2	-0.06577
296.2	-0.29218	251	0.1086	296.2	-0.49553	251	-0.04374
296	-0.06107	250.8	0.10768	296	0.76776	250.8	-0.04445
295.8	-0.29063	250.6	0.10673	295.8	-0.9825	250.6	-0.05228
295.6	-0.2163	250.4	0.1067	295.6	-0.64288	250.4	-0.04955
295.4	-0.18514	250.2	0.10583	295.4	-0.70114	250.2	-0.05665
295.2	-0.19596	250	0.10582	295.2	-0.68644	250	-0.05365
295	-0.09683	249.8	0.10498	295	-0.74669	249.8	-0.04801
294.8	-0.12287	249.6	0.10461	294.8	-1.46849	249.6	-0.05607
294.6	-0.04307	249.4	0.10457	294.6	-1.12768	249.4	-0.04357
294.4	-0.13292	249.2	0.10466	294.4	-1.62163	249.2	-0.04086
294.2	-0.11608	249	0.10343	294.2	0.36611	249	-0.04269
294	-0.02925	248.8	0.10342	294	0.5644	248.8	-0.04174
293.8	-0.05058	248.6	0.10329	293.8	-0.12767	248.6	-0.0353
293.6	-0.09462	248.4	0.10269	293.6	-0.13326	248.4	-0.05478
293.4	-0.01126	248.2	0.1022	293.4	-0.80982	248.2	-0.04107
293.2	-0.03762	248	0.1018	293.2	0.19936	248	-0.03153
293	-0.0456	247.8	0.10148	293	-0.32957	247.8	-0.03954
292.8	-0.06734	247.6	0.10127	292.8	-0.09365	247.6	-0.04458
292.6	-0.08343	247.4	0.10153	292.6	-0.31811	247.4	-0.05439
292.4	-0.07732	247.2	0.10077	292.4	0.18434	247.2	-0.06205
292.2	-0.07333	247	0.09953	292.2	0.08145	247	-0.04007
292	-0.0856	246.8	0.10028	292	-0.59123	246.8	-0.04153
291.8	-0.06925	246.6	0.09982	291.8	-0.50905	246.6	-0.03187
291.6	-0.08663	246.4	0.09978	291.6	0.40509	246.4	-0.04485
291.4	-0.0139	246.2	0.09973	291.4	0.41079	246.2	-0.03161
291.2	-0.05657	246	0.09897	291.2	-0.09501	246	-0.04129
291	-0.09089	245.8	0.09884	291	-0.18023	245.8	-0.0361
290.8	-0.11682	245.6	0.09866	290.8	0.12179	245.6	-0.02679
290.6	-0.11116	245.4	0.09886	290.6	-0.19209	245.4	-0.03814
290.4	-0.12019	245.2	0.09797	290.4	0.1637	245.2	-0.04417
290.2	-0.10109	245	0.09785	290.2	0.13566	245	-0.04607
290	-0.13797	244.8	0.09808	290	-0.13265	244.8	-0.04249
289.8	-0.13573	244.6	0.09791	289.8	-0.12967	244.6	-0.03722
289.6	-0.13253	244.4	0.0977	289.6	0.02555	244.4	-0.02913
289.4	-0.15148	244.2	0.0972	289.4	-0.21064	244.2	-0.03327
289.2	-0.16285	244	0.09755	289.2	-0.41242	244	-0.03707
289	-0.14923	243.8	0.0974	289	-0.25736	243.8	-0.03062
288.8	-0.14669	243.6	0.09711	288.8	0.24968	243.6	-0.02654
288.6	-0.158	243.4	0.09708	288.6	0.12284	243.4	-0.03557
288.4	-0.17086	243.2	0.09676	288.4	0.1785	243.2	-0.02865
288.2	-0.1695	243	0.09642	288.2	0.19158	243	-0.03372
288	-0.17493	242.8	0.09652	288	0.10924	242.8	-0.03226
287.8	-0.15086	242.6	0.09603	287.8	0.37266	242.6	-0.0202
287.6	-0.18811	242.4	0.09645	287.6	-0.04277	242.4	-0.03252
287.4	-0.1742	242.2	0.09654	287.4	0.21131	242.2	-0.03506
287.2	-0.17609	242	0.09626	287.2	0.24657	242	-0.02784
287	-0.17017	241.8	0.09619	287	0.12559	241.8	-0.02424
286.8	-0.20714	241.6	0.09668	286.8	0.0962	241.6	-0.02498
286.6	-0.18553	241.4	0.0959	286.6	0.3877	241.4	-0.03212
286.4	-0.18549	241.2	0.0963	286.4	0.42973	241.2	-0.02749
286.2	-0.19396	241	0.09613	286.2	0.42634	241	-0.0204
286	-0.18352	240.8	0.09632	286	0.2337	240.8	-0.02946
285.8	-0.20782	240.6	0.09636	285.8	0.40371	240.6	-0.01848
285.6	-0.19629	240.4	0.09577	285.6	0.27051	240.4	-0.02891
285.4	-0.19592	240.2	0.09586	285.4	0.40861	240.2	-0.02316
285.2	-0.19647	240	0.09622	285.2	0.2303	240	-0.02554
285	-0.20083	239.8	0.0961	285	0.45941	239.8	-0.02212
284.8	-0.1987	239.6	0.09582	284.8	0.49869	239.6	-0.02385
284.6	-0.18508	239.4	0.09597	284.6	0.43238	239.4	-0.02365
284.4	-0.19714	239.2	0.09633	284.4	0.3339	239.2	-0.02832
284.2	-0.20147	239	0.09659	284.2	0.36469	239	-0.0268
284	-0.20639	238.8	0.09663	284	0.38612	238.8	-0.01485
283.8	-0.20381	238.6	0.09651	283.8	0.34181	238.6	-0.01829
283.6	-0.19359	238.4	0.09665	283.6	0.38542	238.4	-0.01225
283.4	-0.21951	238.2	0.09657	283.4	0.16936	238.2	-0.01526
283.2	-0.19123	238	0.09689	283.2	0.40077	238	-0.02151
283	-0.2012	237.8	0.09708	283	0.56637	237.8	-0.01965
282.8	-0.19456	237.6	0.097	282.8	0.32709	237.6	-0.02355
282.6	-0.21331	237.4	0.09702	282.6	0.18173	237.4	-0.01789

282.4	-0.20475	237.2	0.09722	282.4	0.20358	237.2	-0.01263
282.2	-0.20026	237	0.09784	282.2	0.36444	237	-0.00706
282	-0.20709	236.8	0.0974	282	0.37242	236.8	-0.02062
281.8	-0.20313	236.6	0.09773	281.8	0.19249	236.6	-0.02412
281.6	-0.20848	236.4	0.098	281.6	0.22699	236.4	-0.00733
281.4	-0.2103	236.2	0.09772	281.4	0.2773	236.2	-0.01646
281.2	-0.19703	236	0.09784	281.2	0.32308	236	-0.01026
281	-0.20881	235.8	0.09841	281	0.22468	235.8	-0.0138
280.8	-0.19285	235.6	0.0985	280.8	0.16909	235.6	-0.01194
280.6	-0.19189	235.4	0.09848	280.6	0.30375	235.4	-0.0138
280.4	-0.20417	235.2	0.09878	280.4	0.15414	235.2	-0.01678
280.2	-0.19544	235	0.09894	280.2	0.26435	235	-0.02103
280	-0.1989	234.8	0.09934	280	0.23919	234.8	-0.01126
279.8	-0.19093	234.6	0.099	279.8	0.29626	234.6	-0.00774
279.6	-0.17525	234.4	0.09917	279.6	0.51439	234.4	-0.00784
279.4	-0.18638	234.2	0.09925	279.4	0.29315	234.2	-0.00805
279.2	-0.18813	234	0.10003	279.2	0.21955	234	-0.01253
279	-0.18442	233.8	0.09998	279	0.30854	233.8	-0.01755
278.8	-0.18587	233.6	0.10022	278.8	0.30478	233.6	-0.01027
278.6	-0.19019	233.4	0.10092	278.6	0.23387	233.4	-0.0081
278.4	-0.18618	233.2	0.10075	278.4	0.35055	233.2	-0.00561
278.2	-0.18654	233	0.10136	278.2	0.29053	233	0.00352
278	-0.18201	232.8	0.10152	278	0.4192	232.8	-0.00622
277.8	-0.18923	232.6	0.10141	277.8	0.26233	232.6	-0.00823
277.6	-0.17961	232.4	0.1018	277.6	0.31118	232.4	-0.00879
277.4	-0.17806	232.2	0.10175	277.4	0.36514	232.2	-0.00428
277.2	-0.17741	232	0.10261	277.2	0.31819	232	-0.00043
277	-0.16926	231.8	0.10291	277	0.3386	231.8	-0.00164
276.8	-0.17351	231.6	0.10292	276.8	0.30991	231.6	-0.00177
276.6	-0.17669	231.4	0.10296	276.6	0.33439	231.4	0.0056
276.4	-0.17355	231.2	0.10333	276.4	0.33753	231.2	-0.00369
276.2	-0.17091	231	0.10374	276.2	0.34312	231	0.00428
276	-0.16386	230.8	0.10418	276	0.37346	230.8	0.0035
275.8	-0.1659	230.6	0.10479	275.8	0.21794	230.6	-0.00563
275.6	-0.16337	230.4	0.10472	275.6	0.35442	230.4	0.00489
275.4	-0.16673	230.2	0.10542	275.4	0.24724	230.2	-0.00581
275.2	-0.15572	230	0.10552	275.2	0.27426	230	0.00595
275	-0.15385	229.8	0.10596	275	0.33961	229.8	0.0065
274.8	-0.15432	229.6	0.10618	274.8	0.27547	229.6	0.00228
274.6	-0.15271	229.4	0.10638	274.6	0.28833	229.4	-0.00461
274.4	-0.14574	229.2	0.10656	274.4	0.33196	229.2	-0.00303
274.2	-0.14712	229	0.10721	274.2	0.18674	229	-0.00132
274	-0.1453	228.8	0.10755	274	0.26149	228.8	0.00793
273.8	-0.13354	228.6	0.10785	273.8	0.27242	228.6	0.01306
273.6	-0.12801	228.4	0.10842	273.6	0.32901	228.4	0.00594
273.4	-0.12673	228.2	0.10859	273.4	0.27983	228.2	0.00814
273.2	-0.11965	228	0.10872	273.2	0.29935	228	0.0032
273	-0.11852	227.8	0.10924	273	0.25227	227.8	0.0105
272.8	-0.1106	227.6	0.10905	272.8	0.31885	227.6	0.00853
272.6	-0.10752	227.4	0.1093	272.6	0.21985	227.4	0.00929
272.4	-0.10465	227.2	0.10985	272.4	0.24164	227.2	0.00172
272.2	-0.09522	227	0.11046	272.2	0.25001	227	0.01777
272	-0.09216	226.8	0.1106	272	0.26687	226.8	0.01083
271.8	-0.08578	226.6	0.11071	271.8	0.24861	226.6	0.00384
271.6	-0.08373	226.4	0.1115	271.6	0.21936	226.4	0.00374
271.4	-0.0755	226.2	0.11167	271.4	0.26732	226.2	-0.00048
271.2	-0.07275	226	0.11182	271.2	0.19673	226	0.01165
271	-0.0614	225.8	0.11199	271	0.16119	225.8	0.00911
270.8	-0.06158	225.6	0.11254	270.8	0.18653	225.6	0.00852
270.6	-0.05443	225.4	0.11265	270.6	0.14512	225.4	0.01667
270.4	-0.05089	225.2	0.11323	270.4	0.14119	225.2	0.01592
270.2	-0.04055	225	0.11303	270.2	0.17367	225	0.0127
270	-0.03647	224.8	0.11357	270	0.20174	224.8	0.02353
269.8	-0.03366	224.6	0.11363	269.8	0.09564	224.6	0.00963
269.6	-0.03094	224.4	0.11357	269.6	0.17085	224.4	0.01553
269.4	-0.02401	224.2	0.11429	269.4	0.15675	224.2	0.00863
269.2	-0.01523	224	0.11355	269.2	0.1152	224	0.01504
269	-0.00982	223.8	0.11403	269	0.12943	223.8	0.0105
268.8	-0.00526	223.6	0.11424	268.8	0.102	223.6	0.02661
268.6	-0.00312	223.4	0.11402	268.6	0.06177	223.4	0.01975
268.4	0.00565	223.2	0.11427	268.4	0.06742	223.2	0.0261

268.2	0.01076	223	0.11387	268.2	0.04745	223	0.03155
268	0.01655	222.8	0.11357	268	0.03964	222.8	0.02794
267.8	0.02367	222.6	0.1138	267.8	0.02999	222.6	0.02827
267.6	0.02674	222.4	0.11355	267.6	0.04151	222.4	0.0255
267.4	0.03211	222.2	0.11266	267.4	0.06309	222.2	0.03409
267.2	0.03769	222	0.11243	267.2	0.00752	222	0.03115
267	0.04393	221.8	0.11142	267	0.02221	221.8	0.03609
266.8	0.04813	221.6	0.11134	266.8	0.02363	221.6	0.02762
266.6	0.0536	221.4	0.11087	266.6	0.03962	221.4	0.03691
266.4	0.05645	221.2	0.1096	266.4	0.01931	221.2	0.04239
266.2	0.06129	221	0.10846	266.2	-0.01085	221	0.04582
266	0.06514	220.8	0.10765	266	0.02409	220.8	0.04515
265.8	0.06951	220.6	0.10606	265.8	-0.00922	220.6	0.03088
265.6	0.07342	220.4	0.10516	265.6	0.00656	220.4	0.04215
265.4	0.07518	220.2	0.1038	265.4	-0.05403	220.2	0.05323
265.2	0.07984	220	0.10136	265.2	0.00241	220	0.05013
265	0.0856	219.8	0.10028	265	-0.03753	219.8	0.05219
264.8	0.08882	219.6	0.09751	264.8	0.02459	219.6	0.04387
264.6	0.09165	219.4	0.09576	264.6	-0.02507	219.4	0.04725
264.4	0.09424	219.2	0.09329	264.4	-0.03678	219.2	0.04766
264.2	0.09598	219	0.09091	264.2	-0.0252	219	0.04726
264	0.09936	218.8	0.08817	264	-0.04011	218.8	0.0572
263.8	0.10157	218.6	0.08536	263.8	-0.02593	218.6	0.0517
263.6	0.10486	218.4	0.08192	263.6	-0.03444	218.4	0.06626
263.4	0.10778	218.2	0.08004	263.4	-0.02858	218.2	0.05415
263.2	0.10915	218	0.07485	263.2	-0.03984	218	0.05407
263	0.11181	217.8	0.07177	263	-0.05378	217.8	0.07554
262.8	0.1132	217.6	0.06893	262.8	-0.05115	217.6	0.06741
262.6	0.11405	217.4	0.06297	262.6	-0.06987	217.4	0.0635
262.4	0.11492	217.2	0.05933	262.4	-0.06584	217.2	0.06013
262.2	0.11651	217	0.05469	262.2	-0.05916	217	0.05869
262	0.11885	216.8	0.05017	262	-0.05737	216.8	0.06929
261.8	0.11934	216.6	0.04544	261.8	-0.04062	216.6	0.06265
261.6	0.12013	216.4	0.04113	261.6	-0.06852	216.4	0.06484
261.4	0.12107	216.2	0.03564	261.4	-0.07011	216.2	0.06679
261.2	0.12092	216	0.03101	261.2	-0.07297	216	0.07003
261	0.1224	215.8	0.02575	261	-0.07327	215.8	0.06925
260.8	0.12341	215.6	0.02124	260.8	-0.04862	215.6	0.06546
260.6	0.12328	215.4	0.01721	260.6	-0.06958	215.4	0.07782
260.4	0.12459	215.2	0.01193	260.4	-0.07804	215.2	0.06201
260.2	0.12375	215	0.00741	260.2	-0.07093	215	0.05706
260	0.12403	214.8	0.00206	260	-0.07518	214.8	0.05957
259.8	0.12459	214.6	-0.00082	259.8	-0.07188	214.6	0.05726
259.6	0.12496	214.4	-0.00438	259.6	-0.09861	214.4	0.05672
259.4	0.12614	214.2	-0.00753	259.4	-0.04769	214.2	0.05022
259.2	0.12568	214	-0.01116	259.2	-0.08026	214	0.04857
259	0.12558	213.8	-0.01397	259	-0.07046	213.8	0.03835
258.8	0.12502	213.6	-0.01572	258.8	-0.05786	213.6	0.05278
258.6	0.12489	213.4	-0.01956	258.6	-0.06397	213.4	0.0418
258.4	0.12508	213.2	-0.02124	258.4	-0.08428	213.2	0.03143
258.2	0.1246	213	-0.02194	258.2	-0.07583	213	0.02191
258	0.12487	212.8	-0.02278	258	-0.06488	212.8	0.03108
257.8	0.12414	212.6	-0.02329	257.8	-0.07595	212.6	0.0144
257.6	0.12361	212.4	-0.02442	257.6	-0.07015	212.4	0.00553
257.4	0.12398	212.2	-0.02323	257.4	-0.06395	212.2	0.01013
257.2	0.12308	212	-0.02229	257.2	-0.06097	212	-0.0053
257	0.12292	211.8	-0.02257	257	-0.06829	211.8	0.00233
256.8	0.12224	211.6	-0.02102	256.8	-0.07187	211.6	-0.01371
256.6	0.12199	211.4	-0.01973	256.6	-0.07402	211.4	-0.01745
256.4	0.12101	211.2	-0.01759	256.4	-0.07965	211.2	-0.02744
256.2	0.12101	211	-0.01646	256.2	-0.06801	211	-0.0351
256	0.12132	210.8	-0.01478	256	-0.07327	210.8	-0.03423
255.8	0.12035	210.6	-0.01303	255.8	-0.06154	210.6	-0.03908
255.6	0.11904	210.4	-0.00943	255.6	-0.06224	210.4	-0.06083
255.4	0.11973	210.2	-0.00852	255.4	-0.05225	210.2	-0.04575
255.2	0.1186	210	-0.00525	255.2	-0.0549	210	-0.02839
255	0.11763			255	-0.06462		

Table S4. Results of the principal components coefficients of paracetamol and caffeine for the PCR model.

Mixture No.	Paracetamol (μg mL^{-1})	Caffeine (μg mL^{-1})	Z1	Z2	Z3	Z4	Z5	Z6
1	10	1.3	9.146716	0.922621	0.11385	0.218591	0.064549	-0.00164
2	10	1.82	9.338489	1.227304	0.100951	0.223531	0.066993	-0.00205
3	10	2.08	9.354737	1.388513	0.100658	0.224171	0.060107	-0.00185
4	10	2.34	9.754932	1.57956	0.107429	0.220398	0.058897	-0.0019
5	10	2.6	9.74823	1.72816	0.099278	0.214642	0.059679	-0.0013
6	14	1.3	12.40446	0.933764	0.141302	0.260088	0.057792	0.001265
7	14	1.82	12.64458	1.256145	0.142028	0.25596	0.062195	-0.00074
8	14	2.08	12.89527	1.456187	0.143263	0.240196	0.066623	-0.00077
9	14	2.34	13.23925	1.710256	0.17538	0.204584	0.056079	-0.00052
10	14	2.6	13.279	1.804253	0.149894	0.224501	0.067227	-0.0009
11	16	1.3	14.17486	0.998982	0.167127	0.211254	0.059428	8.95E-05
12	16	1.82	14.41187	1.337918	0.166771	0.208607	0.064014	0.00127
13	16	2.08	14.67569	1.505969	0.163074	0.221245	0.063982	0.000802
14	16	2.34	14.5841	1.607437	0.143083	0.228941	0.070436	0.001214
15	16	2.6	14.91319	1.774835	0.141138	0.240823	0.070132	7.25E-05
16	18	1.3	15.72434	0.95616	0.156724	0.231376	0.065447	0.000162
17	18	1.82	15.91465	1.176127	0.109593	0.212343	0.065423	0.004414
18	18	2.08	15.9445	1.334762	0.10192	0.225312	0.058374	0.005089
19	18	2.34	16.1327	1.493542	0.099248	0.231075	0.058385	0.001423
20	18	2.6	16.36708	1.642257	0.095751	0.233073	0.055706	0.004384
21	20	1.3	17.24382	0.860645	0.108718	0.209636	0.062819	0.002135
22	20	1.82	17.25686	1.14882	0.104635	0.221209	0.063474	-0.01031
23	20	2.08	17.59386	1.363286	0.105134	0.217987	0.079396	0.003633
24	20	2.34	17.55533	1.472502	0.08927	0.228363	0.06883	0.001512
25	20	2.6	17.82869	1.683043	0.114235	0.230266	0.062232	-0.00376

Eclet. Quim. 49 | e-1531, 2024

Original Article

https://doi.org/10.26850/1678-4618.eq.v49.2024.e1531

Analyzing essential oils: extraction and characterization from fresh and dry leaves of *Pinus elliottii*

Leonardo Pratavieira **Deo**[1+], Gabriela Aguiar **Campolina**[2], Cassia Duarte **Oliveira**[2], Kassy Jhones **Garcia**[3], Maria das Graças **Cardoso**[4]

Abstract

Exploration of secondary metabolites, particularly essential oils, reveals diverse properties in antimicrobial, biological, and pharmaceutical contexts, including antibacterial, antifungal, and antiviral attributes, and applications in pest control and insect repellents. In the present work, essential oils were extracted from both fresh and dry leaves of *Pinus elliottii*, using hydrodistillation, followed by meticulous chemical characterization via gas chromatography coupled with a mass spectrometer. The plant leaves, sourced from a reforested area in the southern part of Minas Gerais, Brazil, formed the study's foundation. The main constituents identified in both essential oils were Germacrene D and β-Pinene. Germacrene D dominated in the essential oil from fresh foliage (47.71%), while β-Pinene prevailed in the essential oil from dry foliage (30.06%). Literature indicates that heightened Germacrene D levels may confer antibacterial and repellent properties, while elevated β-Pinene content aligns with various biological, medicinal, and pharmacological activities. Integrating our findings with existing literature, this work highlights potential applications for essential oils derived from both fresh and dry leaves of *Pinus elliottii*.

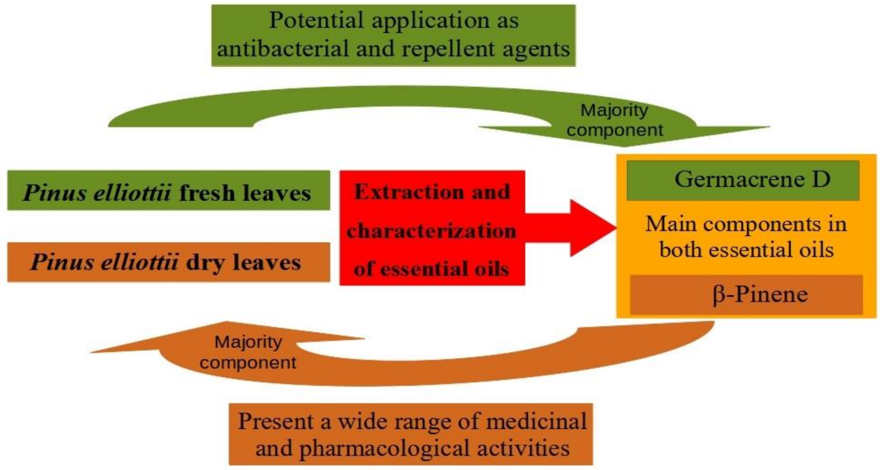

Article History

Received November 20, 2023
Accepted July 12, 2024
Published Octobre 03, 2024

Keywords

1. pines;
2. natural compounds;
3. chemical composition;
4. germacrene D;
5. β-Pinene.

Section Editor

Irlon Maciel Ferreira

Highlights

- Germacrene D and β-Pinene are key compounds in *Pinus elliottii* essential oils.
- Fresh leaves of *Pinus elliottii* show high Germacrene D with antibacterial potential.
- Dry leaves of *Pinus elliottii* are rich in β-Pinene, linked to diverse bioactivities.

[1]Federal University of Lavras, Engineering Department, Lavras, Brazil. [2]Federal University of Lavras, Food Sciences Department, Lavras, Brazil. [3]Federal University of Lavras, Environmental Engineering Department, Lavras, Brazil. [4]Federal University of Lavras, Chemistry Department, Lavras, Brazil. **+Corresponding author:** Leonardo Pratavieira Deo, **Phone:** +553538291860, **Email address:** leonardo.deo@ufla.br

1. Introduction

Essential oils have gained renewed significance across various domains. As natural products, they proudly exhibit attractive physicochemical characteristics coupled with environmentally friendly characteristics (El Asbahani *et al.*, 2015). These oils exhibit evident biological activities, finding application in the medical field for their fungicidal, virucidal, and bactericidal properties. Multiple studies underscore their antimicrobial efficacy, even against multi-resistant bacteria (Burt, 2004; Mayaud *et al.*, 2008). Furthermore, essential oils have been deployed in combating nosocomial infections. They are used as aerosols in operating blocks and waiting rooms to purify the air and minimize contamination (El Asbahani *et al.*, 2015). Additionally, these oils serve as cleaning agents for disinfecting medical equipment and surfaces (Warnke *et al.*, 2009). Beyond their medicinal applications, essential oils contribute to a sense of mental comfort for patients, thanks to their pleasant aroma. Notably, these oils have been explored for their potential as food preservatives as well (Burt, 2004; Tiwari *et al.*, 2009).

Due to their intricate chemical composition, which frequently comprises over 100 distinct terpenic compounds, essential oils exhibit an extensive spectrum of antimicrobial and biological activities. In the pharmaceutical field, the use of products with essential oils is constantly growing and usually is addressed mainly by local applications and inhalation. They are incorporated into the formulation of numerous pharmaceutical products, including capsules, ointments, creams, syrups, suppositories, aerosols, and sprays (El Asbahani *et al.*, 2015). In nature, essential oils are synthesized by over 17,500 aromatic plant species and are stored in various plant organs. These include flowers (e.g., *Citrus bergamia*, bergamot orange), leaves (e.g., *Cymbopogon citratus*, lemon grass), wood (e.g., *Santalum acuminatum*, sandalwood), roots (e.g., *Chrysopogon zizanioides*, vetiver), rhizomes (e.g., *Zingiber officinale*, ginger; *Curcuma longa*, turmeric), fruits (e.g., *Pimpinella anisum*, anise), and seeds (e.g., *Myristica fragrans*, nutmeg) (Baptista-Silva *et al.*, 2020). In special, the essential chemical composition of oil leaves (also called needles) for more than 40 pine species (genus *Pinus*) is known (Ioannou *et al.*, 2014). *Pinus* and *Eucalyptus* species are the most common trees used for reforestation.

In contemporary society, deforestation has become prevalent to meet the demand for various structural components in civil engineering, furniture, charcoal production, and other applications. To equilibrate this trend, plantation forestry is widely employed to expedite reforestation, mitigate greenhouse gas emissions, and alleviate the pressure on timber resources from native forests. Exotic tree species, particularly fast-growing and high-yielding ones like *Pinus* and *Eucalyptus*, are extensively cultivated in monocultures, often beyond their native habitats (Ning *et al.*, 2019). Pine, the largest genus in the *Pinaceae* family, encompasses over 110 species globally (Richardson *et al.*, 2007). Although primarily found in the Northern Hemisphere, this species adapts to various forest types, including temperate, sub-tropical, tropical, and boreal regions (Imanuddin *et al.*, 2020).

In the early 20th century, Brazil initiated its first economic reforestation efforts, primarily involving the introduction of *Eucalyptus* species. By the late 1940s and early 1950s, coniferous species, particularly those of the genus *Pinus*, were introduced. The introduction of conifers was largely driven by the substantial decline in the natural population of *Araucaria angustifolia* (Parana pine). Reforestation operations gained significant momentum in the 1960s, reaching full operational levels during that decade. Starting in 1966, government-led fiscal incentives led to a substantial increase in reforestation activities in Brazil. Reforestation projects covered approximately 6.2 million hectares, with 52 percent dedicated to Eucalyptus, 30 percent to Pinus, and 18 percent to other species (Jesus, 1990). In 2021, the reforestation area reached around 9.5 million hectares, with 7.3 million hectares of Eucalyptus and 1.8 million hectares of *Pinus*. 45.4% percent of *Eucalyptus* area is located in the Brazilian southeast region, while 83.9 percent of *Pinus* forest is established in the Brazilian south region (IBGE, 2021).

Given the abundant presence of *Pinus elliottii* in our region, this study aims to extract essential oils from both fresh and dried leaves of the mentioned *Pinus* species and analyze their chemical compositions. This characterization together with literature data give some support in order to clear up potential applications to the analyzed essential oils.

2. Experimental

2.1. Plant material

Gathering fresh and dried leaves of *Pinus elliottii* took place in a public area situated in *Bueno Brandão*, a city in the southern region of *Minas Gerais*, Brazil, at an elevation of 1,184 meters above sea level. The precise coordinates for the collection site were latitude 22°25'56.91"S and longitude 46°21'15.03"W. The collection occurred in the morning on September 6th, 2021, under mild temperature conditions with no precipitation. Fresh leaves were directly collected from the trees, while dry leaves were gathered from the ground. Post-collection, both fresh and dry leaves underwent careful selection based on imperfections, dirt, and foreign bodies. Subsequently, they were cut into smaller portions in preparation for the subsequent extraction of essential oils.

2.2. Extraction and yield of essential oils

The Organic Chemistry-Essential Oils Laboratory at the Chemistry Department of the Federal University of Lavras conducted the extraction of essential oils from both fresh and dry leaves of *Pinus elliottii*. The extraction process employed hydrodistillation and utilized a modified Clevenger apparatus connected to a 5 L flask, following the method outlined by Teixeira *et al.* (2014). Each batch of approximately 200 g of plant material underwent hydrodistillation for a duration of two hours. Post-extraction, the essential oils were separated from the hydrolytic solution through centrifugation, employing a benchtop centrifuge with a horizontal crosspiece (FANEM BabyRI Model 206 BL) at 965 g and room temperature for 15 minutes. Subsequently, the essential oils were carefully transferred to amber bottles using a Pasteur pipette and stored at a temperature of 5 °C. The yields of the essential oils were 0.82 ± 0.06% and 1.60 ± 0.08% on a fresh and on a dry-weight basis respectively for the species *Pinus elliottii*. The extractions were performed in triplicate.

2.3. Chemical characterization of the essential oils

The identification of the compounds in the essential oil was performed according to those described in the literature (Adams, 2007; NIST, 2010) by gas chromatography coupled to a mass spectrometer, employing a Shimadzu QP model 5050A GC/MS equipped with a J&W Scientific fused-silica capillary column (5% phenyl 95% dimethylpolysiloxane;

30 m × 0.25 mm id, 0.25 µm film). Helium served as the carrier gas with a flow rate of 1.0 mL min^{-1}. The sample injection volume was 0.5 µL, diluted in hexane (1%). The split ratio was 1:20. The column temperature program initiated at 60 °C for 1 minute, followed by a gradual increase to 246 °C at a rate of 3 °C min^{-1}. Subsequently, there was a further increase of 10 °C min^{-1} to 300 °C, where the temperature was maintained for 7 minutes. The injector and detector temperatures were set at 220 and 240 °C, respectively.

Quantitative analysis was conducted through gas chromatography with a flame ionization detector (GC-FID), utilizing a Shimadzu model GC–2010 chromatograph (Shimadzu Corporation, Kyoto, Japan). The experimental conditions mirrored those employed in qualitative analysis, except for the detector temperature set at 300 °C. Relative percentages of each constituent were determined using the normalization of area method. To establish the retention indices of the constituents, a comparison was made with those reported in the literature (Lunguinho *et al.*, 2021). These retention indices were calculated using the Van Den Dool and Dec Kratz (1963) relative to a homologous series of n-alkanes (C9-C18). For comparison of mass spectra, two libraries, NIST107 and NIST21, were employed. The chemical characterization was performed in triplicate.

3. Results and discussion

Table 1 presents the chemical composition average related to the triplicate chemical characterization and the standard deviation of essential oils derived from fresh and dry leaves of *Pinus elliottii*, highlighting the key components in each kind of essential oil. The chromatograms of the essential oils from fresh and dry leaves of *Pinus elliottii*, along with their indexed substances, are illustrated in **Figs. 1** and **2**, respectively. Only one chromatogram of each kind of essential oil is shown due to their similarity in the triplicate analyses.

Table 1. The essential oil constituents are derived from the fresh and dry leaves of *Pinus elliottii*.

N°. in the Chromatogram from Fig. 1	N°. in the Chromatogram from Fig. 2	$\text{RI}_{\text{calc}}^{1}$	$\text{RI}_{\text{lit}}^{2}$	Constituents	Percent of constituent in the fresh leaves	Percent of constituent in the dry leaves
1	1	933	932	α-Pinene	6 ± 1	10 ± 2
-	2	950	964	Camphene	-	0.63 ± 0.09
2	3	979	974	β-Pinene	22 ± 2	30 ± 2
3	-	988	988	Myrcene	1.8 ± 0.9	-
4	4	1196	1186	α-Terpineol	0.22 ± 0.09	2.8 ± 0.2
-	5	1280	1284	Bornyl acetate	-	2.0 ± 0.7
5	6	1420	1417	β-Caryophyllene	7 ± 2	5 ± 2
6	7	1491	1484	Germacrene D	48 ± 3	27 ± 3
7	8	1496	1500	Bicyclogermacrene	2.2 ± 0.8	2.4 ± 0.8
8	9	1493	1500	α-Muurolene	0.47 ± 0.07	0.7 ± 0.1
9	10	1503	1513	γ-Cadinene	2.0 ± 0.7	3.2 ± 0.9
10	11	1518	1522	δ-Cadinene	8 ± 1	9 ± 1
-	12	1577	1577	Spathulenol	-	3 ± 1
11	13	1638	1640	Epi-α-Muurolol	2.8 ± 0.7	4 ± 1
		Total			100.49	99.73

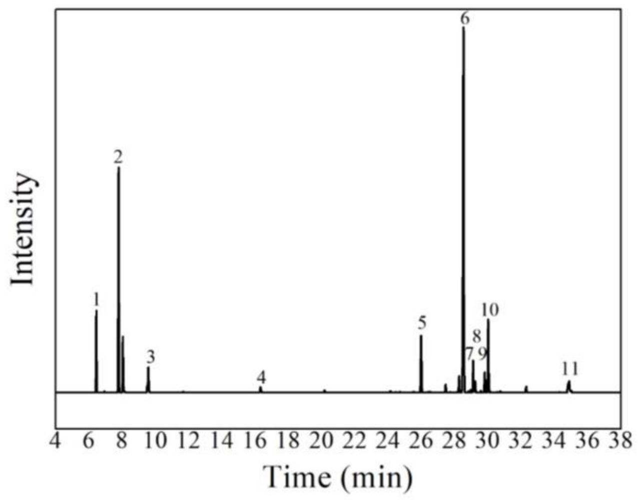

Figure 1. Chromatogram of the essential oil of the fresh leaves of *Pinus elliottii*.

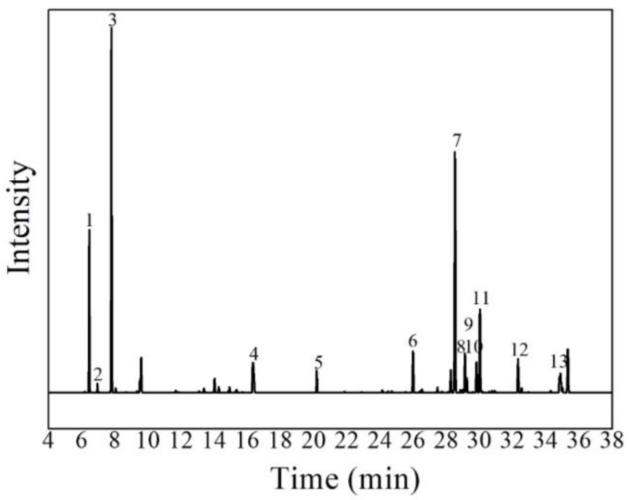

Figure 2. Chromatogram of the essential oil of the dry leaves of *Pinus elliottii*.

The data presented in **Table 1** and **Fig. 1** reveal that Germacrene D (47.71%) predominated as the primary component in the essential oil extracted from fresh *Pinus elliottii* foliage, followed by β-Pinene (21.80%), δ-Cadinene (8.09%), (E)-Caryophyllene (6.86%), and α-Pinene (6.01%). Conversely, in the essential oil derived from dry foliage, the key constituents were β-Pinene (30.06%), Germacrene D (26.77%), α-Pinene (10.26%), δ-Cadinene (9.32%), and (E)-Caryophyllene (5.03%) (**Fig. 3**). Limited literature data exists on the chemical composition of *Pinus elliottii* leaf oil. Ioannou *et al.* (2014) provided the initial report on this type of essential oil. According to their findings, the essential oil from fresh *Pinus elliottii* foliage contained four compounds, with Germacrene D (24.5%), β-Pinene (12.9%), α-Pinene (10.6%), and β-Caryophyllene (6.6%) identified as the main constituents. Notably, there is currently no available literature data on the chemical composition of the essential oil from dry foliage of the analyzed plant.

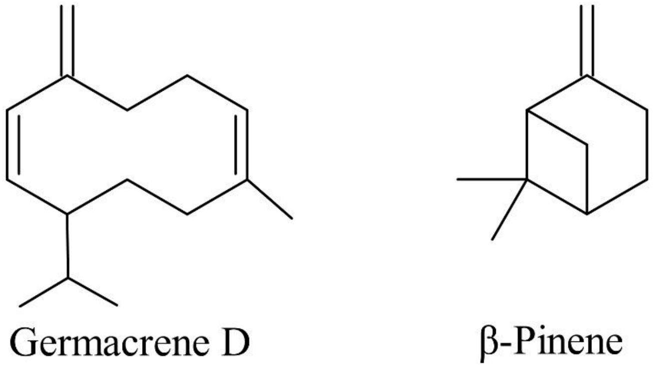

Figure 3. The majority of constituents of essential oils are from fresh and dry leaves of *Pinus elliottii.*

Some discrepancies were evidenced between Ioannou *et al.* (2014) results and those found in the present work, mainly related to the compound amounts in the analyzed fresh foliage essential oil. The variations in the chemical compositions of essential oils derived from plants of identical species can be elucidated through various factors such as geographical location and time of harvest, the nature of the soil and its nutrients. This is because the secondary metabolites are prone to alterations depending on the season during which the collection takes place. Furthermore, factors such as the plant's age, seasonal patterns, temperature, and others exert an influence on virtually all categories of secondary metabolites, including essential oils. Monoterpenes (whether oxygenated or not) and sesquiterpenes (whether oxygenated or not) were found to exhibit a higher concentration in the essential oils (Gobbo-Neto and Lopes, 2007). The discussion below is concerned to the majority of substances found in each analyzed essential oil.

The primary component discovered in the essential oil derived from the fresh leaves of *Pinus elliottii* is Germacrene D, constituting 47.71% of the composition. In the essential oil extracted from dry leaves, Germacrene D is the second most prevalent substance, constituting 26.77% of the composition. The Germacrene D percentage decrease in the essential oil from dry leaves may be explained by the following reasons: Germacrene D, like many other compounds in essential oils, is volatile. During the extraction process, especially if heat is involved, some of the volatile compounds can evaporate or degrade, leading to a decrease in their concentration. Some compounds may undergo chemical reactions during the extraction process, leading to the formation of different compounds or degradation products. This could result in a decrease in the percentage of Germacrene D in the extracted oil derived from the dry leaves compared to the essential oil extracted from fresh leaves. In addition, different compounds have different solubilities in the extraction solvent. The extraction process may selectively extract certain compounds more efficiently than others, leading to a change in the relative concentrations of compounds in the extracted oil compared to the fresh plant material (Chakravarty *et al.*, 2023; Kurti *et al.*, 2019).

Germacrene D falls under the category of sesquiterpenoids or sesquiterpenes, characterized by a group of 15-carbon compounds formed from three isoprene units. These sesquiterpenoids are predominantly found in higher plants and manifest in various acyclic, mono-, bi-, tri-, and tetracyclic systems (Modzelewska *et al.*, 2005). They exist in nature as hydrocarbons or in oxygenated forms like lactones, alcohols, acids, aldehydes, and ketones. Sesquiterpenes present in essential oils and aromatic elements of plants exhibit diverse fundamental structures with distinct nomenclatures (Awouafack *et al.*, 2013). Many of these sesquiterpenes showcase biological activities, including antimicrobial, antitumor, and cytotoxic properties. Within plants, they play crucial ecological roles in interactions with insects and microbes, functioning as attractants, deterrents, antifeedants, and phytoalexins (Modzelewska *et al.*, 2005).

Numerous investigations have delved into the antibacterial and repellent potentials of plant essential oils abundant in Germacrene D, aiming to combat microbial resistance to antibiotics and traditional drugs. The objective is to circumvent the use of expensive synthetic crop protection chemicals by promoting the commercialization of insecticides based on these essential oils (El Mokni *et al.*, 2019). The essential oil, enriched with a significant amount of the aforementioned sesquiterpene, demonstrates moderate antimicrobial activity, particularly against Gram-positive bacteria such as *S. aureus*, *B. subtilis*, and *C. albicans*. In contrast, Gram-negative bacteria like *E. coli*, *P. aeruginosa*, and *S. enterica* inherently exhibit resistance to the antimicrobial effects of essential oils. The efficacy of this type of essential oil is more pronounced against Gram-positive bacteria, attributed to the inherent characteristics of the bacterial cell membrane (Kilani *et al.*, 2005). The limited antibacterial effectiveness against Gram-negative bacteria is associated with the presence of a hydrophilic outer membrane, hindering the penetration of hydrophobic compounds into the target cell membrane (Inouye *et al.*, 2001). In contrast, Gram-positive bacteria boast proteins, mucopolysaccharides, and a lower quantity of phospholipids in their cell membrane. This composition facilitates the permeability, entry, and reaction of most antibiotics and/or antimicrobial agents through the cell envelope (Al-Saimary *et al.*, 2006).

In addition, the insecticidal potential of some essential oils is also related to the presence of high amounts of terpenes, such as Germacrene D and its volatility acts as chemical messengers for insects (Al-Ghanim *et al.*, 2023; Chaieb *et al.*, 2018). Earlier research has also suggested that Germacrene D exhibits impact on herbivores and insecticidal properties, notably against mosquitoes. Additionally, it demonstrates repellent activity against aphids, as highlighted in prior studies by Noge *et al.* (2009). The biological effects of numerous essential oils are linked to their primary biologically active components, thus from our results, the fresh foliage oil from *Pinus elliottii* is a natural source of Germacrene D, a sesquiterpene with high application potential due to its biological activities as aforementioned, such as antimicrobial and insecticidal potentials. Additional biological effects of essential oils abundant in sesquiterpenes are also delineated, encompassing activities like an anti-arthritic, anti-inflammatory, antiviral, antimutagenic, local anesthetic, and anticarcinogenic properties (Oliveira-Tintino *et al.*, 2018). It is crucial to acknowledge that essential oils constitute phytocomplexes, emphasizing the significance of interactions between both minor and major constituents. Each individual compound operates synergistically with others, a fact that shouldn't be overlooked (El Mokni *et al.*, 2019).

β-pinene stands out as the predominant component identified in the essential oil extracted from dry leaves, constituting 30.06% as depicted in **Table 1** and **Fig. 2**. It also holds the position of the second most abundant substance in the essential oil derived from fresh leaves, accounting for 21.80%, as illustrated in **Table 1** and **Fig. 1**, of *Pinus elliottii*. Pinene ($C_{10}H_{16}$) is characterized as a bicyclic, double-bonded terpenoid hydrocarbon, as outlined by Winnacker (2018). α- and β-pinene represent a pair of isomers present in the coniferous trees (pines) essential oils and they belong to the vast family of monoterpenes (Salehi *et al.*, 2019). α-pinene can be detected in more than 40 different essential oils (Vespermann *et al.*, 2017) and β-pinene is commercially acquired through distillation or the conversion of α-pinene (Salehi *et al.*, 2019). Both α- and β-pinene showcase a range of biological activities, some like the biological effects of Germacrene D. These shared activities include fungicidal, antiviral, and antimicrobial properties. Moreover, pinenes find applications in the production of components contributing to aroma, flavor, and fragrance, as discussed in studies by Silva *et al.* (2012), Salehi *et al.* (2019), Van Der Werf *et al.* (1997) and Arya *et al.* (2022). α- and β-pinenes are integral elements in renal and hepatic medications. Their utilization as antibacterials stems from their detrimental impact on membranes (Alma *et al.*, 2004). Additionally, research has uncovered their inhibitory effects on breast cancer and leukemia (Zhou *et al.*, 2004). Some polymers can be synthesized from pinenes (Thomsett *et al.*, 2019) and these materials can present better quality than other conventional polymers (Satoh *et al.*, 2014).

Still related to pinenes, numerous pharmacological effects have been documented, spanning antibiotic resistance modulation, anticoagulant properties, antitumor activity, antimicrobial action, antimalarial effects, antioxidant capabilities, anti-inflammatory responses, anti-Leishmania effects, and analgesic effects. Other prominent effects are also reported, such as cytogenetic, gastroprotective, anxiolytic, cytoprotective, anticonvulsant, and neuroprotective properties have been observed. Additionally, these substances exhibit efficacy against oxidative stress induced by H_2O_2, pancreatitis, hyperthermia triggered by stress, and pulpal pain. Although pinenes showcase various biological activities, their swift metabolism and elimination from the body, attributed to their volatile nature, result in their brief presence at low concentrations within organisms. Despite the acknowledged positive properties of α-pinene and β-pinene, the bioavailability of these terpenes in the human body remains understudied in most investigations. While some in vivo and clinical studies have linked the biological effects of pinenes, additional endeavors are essential to deepening our understanding in this domain, as emphasized by Salehi *et al.* (2019).

Therefore, from our results, the essential oils from fresh and dry foliage from *Pinus elliottii* are natural sources of Germacrene D and β-Pinene. According to the literature data, as mentioned before, Germacrene D has more potential in applications such as antimicrobial and insecticidal activities, while β-Pinene has more potential in applications related to pharmacological activities, although some biological activities are coincident for both substances, such as antimicrobial and antitumor properties. Our results also point that essential oil from fresh leaves of *Pinus elliottii* may be applied mainly as antimicrobial and insecticide, due its majority component Germacrene D, while the essential oil from dry leaves may be applied mainly in a wide range of pharmacological activities due to its majority component β-pinene. However further studies are needed to support these hypotheses. In addition, many other *Pinus elliottii* essential oils' possibilities of application can be investigated, due to the chemical composition complexity of each essential oil, once there are chemical interactions between minor and major constituents, as well as, each compound works together synergistically with the others, creating a combined effect that enhances their overall impact.

4. Conclusions

The findings show that the majority of compounds from fresh foliage essential oil are Germacrene D (47.71%), followed by β-Pinene (21.80%), in addition to minor compounds, such as δ-Cadinene (8.09%), (E)-Caryophyllene (6.86%) and α-Pinene (6.01%). The results also show that the majority of compounds from dry foliage essential oil are β-Pinene (30.06%), followed by Germacrene D (26.77%), in addition to minor compounds, such as α-Pinene (10.26%), δ-Cadinene (9.32%) and (E)-Caryophyllene (5.03%).

Due to the essential oils' chemical compositions found, the present investigation opens the possibility of finding potential applications to essential oils extracted from the fresh and dry leaves of *Pinus elliottii*. The literature points to Germacrene D with excellent antimicrobial and insecticidal properties and β-Pinene with several pharmacological activities. Many other possibilities of application also can be explored because the characterized compounds can interact with each other.

Authors' contributions

Conceptualization: Leonardo Pratavieira Deo; Kassy Jhones Garcia; Maria das Graças Cardoso; **Data curation**: Kassy Jhones Garcia; Maria das Graças Cardoso; Gabriela Aguiar Campolina; Cassia Duarte Oliveira; **Formal Analysis**: Maria das Graças Cardoso; Gabriela Aguiar Campolina; Cassia Duarte Oliveira; **Funding acquisition**: Maria das Graças Cardoso; **Investigation**: Kassy Jhones Garcia; Maria das Graças Cardoso; Gabriela Aguiar Campolina; Cassia Duarte Oliveira; **Methodology**: Kassy Jhones Garcia; Maria das Graças Cardoso; Gabriela Aguiar Campolina; Cassia Duarte Oliveira; **Project administration**: Leonardo Pratavieira Deo; Maria das Graças Cardoso; **Resources**: Maria das Graças Cardoso; **Software**: Maria das Graças Cardoso; **Supervision**: Leonardo Pratavieira Deo; Maria das Graças Cardoso; **Validation**: Maria das Graças Cardoso; Gabriela Aguiar Campolina; Cassia Duarte Oliveira; **Visualization**: Leonardo Pratavieira Deo; Maria das Graças Cardoso; **Writing – original draft**: Leonardo Pratavieira Deo; **Writing – review & editing**: Maria das Graças Cardoso; Gabriela Aguiar Campolina; Cassia Duarte Oliveira;

Data availability statement

All data sets were generated or analyzed in the current study.

Funding

Fundação de Amparo à Pesquisa do Estado de Minas Gerais (FAPEMIG). Grant No: 02390/2018.

Conselho Nacional de Desenvolvimento Científico e Tecnológico (CNPq). Grant No: 311183/2022.

Acknowledgments

Not applicable.

References

Adams, R. P. *Identification of Essential Oils Components by Gas Chromatography/Mass Spectroscopy*. Allured Publishing Corporation, 2007.

Al-Ghanim, K. A.; Krishnappa, K.; Pandiyan, J.; Nicoletti, M.; Gurunathan, B.; Govindarajan, M. Insecticidal Potential of Matricaria chamomilla's Essential Oil and Its Components (E)-β-Farnesene, Germacrene D, and α-Bisabolol Oxide A against Agricultural Pests, Malaria, and Zika Virus Vectors. *Agric.* **2023**, *13*, 779. https://doi.org/10.3390/agriculture13040779

Alma, M. H.; Nitz, S.; Kolmannsberger, H.; Digrak, M.; Efe, F. T.; Yilmaz, N. Chemical composition and antimicrobial activity of the essential oils from the gum of Turkish Pistachio (Pistacia vera l.). *J. Agric. Food Chem.* **2004**, *52* (12), 3911–3914. https://doi.org/10.1021/jf040014e

Al-Saimary, I.; Bakr, S.; Khudaier, B.; Abass, Y. Efficiency of antibacterial agents extracted from Thymus vulgaris L. (Lamiaceae). *Int. J. Nutr. Wellness.* **2006**, *4* (1), 1–5. https://doi.org/10.5580/269

Arya, S.; Kumar, R.; Prakash, O.; Rawat, A.; Mahawer, S. K.; Rawat, D. S.; de Oliveira, M. Hedychium coronarium J. Koenig: Traditional Uses, Phytochemistry, Biological Activities and Future Aspects. *Curr. Org. Chem.* **2022**, *26* (18), 1676–1690. https://doi.org/10.2174/1385272827666221212161320

Awouafack, M. D.; Tane, P.; Kuete, V.; Eloff, J. N. 2 - Sesquiterpenes from the Medicinal Plants of Africa. In: Kuete, V., Ed., *Medicinal plant research in Africa: pharmacology and chemistry*. Elsevier, 2013; pp. 33–103. https://doi.org/10.1016/B978-0-12-405927-6.00002-3

Baptista-Silva, S.; Borges, S.; Ramos, O. L.; Pintado, M.; Sarmento, B. The progress of essential oils as potential therapeutic agents: a review. *J. Essent. Oil Res.* **2020**, *32* (4), 279–295. https://doi.org/10.1080/10412905.2020.1746698

Burt, S. Essential oils: their antibacterial properties and potential applications in foods - a review. *Int. J. Food Microbiol.* **2004**, *94* (3), 223–253. https://doi.org/10.1016/j.ijfoodmicro.2004.03.022

Chaieb, I.; Ben Hamouda, A.; Tayeb, W.; Zarrad, K.; Bouslema, T.; Laarif, A. The Tunisian Artemisia Essential Oil for Reducing Contamination of Stored Cereals by Tribolium castaneum. *Food Technol. Biotechnol.* **2018**, *56* (2), 247–256. https://doi.org/10.17113/ftb.56.02.18.5414

Chakravarty, I.; Parmar, V. M.; Mandavgane, S. A. Current trends in essential oil (EO) production. *Biomass Conv. Bioref.* **2023**, *13*, 15311–15334. https://doi.org/10.1007/s13399-021-01963-3

El Asbahani, A.; Miladi, K.; Badri, W.; Sala, M.; Addi, E. H. A.; Casabianca, H.; El Mousadik, A.; Hartmann, D.; Jilale, A.; Renaud, F. N. R.; Elaissari, A. Essential oils: From extraction to encapsulation. *Int. J. Pharm.* **2015**, *483* (1–2), 220–243. https://doi.org/10.1016/j.ijpharm.2014.12.069

El Mokni, R.; Majdoub, S.; Chaieb, I.; Jlassi, I.; Joshi, R. K.; Hammami, S. Chromatographic analysis, antimicrobial and insecticidal activities of the essential oil of Phlomis floccosa D. *Don. Biomed Chromatogr.* **2019**, *33* (10). https://doi.org/10.1002/bmc.4603

Gobbo-Neto, L.; Lopes, N. P. Plantas medicinais: fatores de influência no conteúdo de metabólitos secundários. *Quim Nova.* **2007**, *30* (2), 374–381. https://doi.org/10.1590/S0100-40422007000200026

Imanuddin, R.; Hidayat, A.; Rachmat, H. H.; Turjaman, M.; Pratiwi, P.; Nurfatriani, F.; Indrajaya, Y.; Susilowati, A. Reforestation and Sustainable Management of Pinus merkusii Forest Plantation in Indonesia: A Review. *Forests.* **2020**, *11* (12), 1235. https://doi.org/10.3390/f11121235

Inouye, S.; Takizawa, T.; Yamaguchi, H. Antibacterial activity of essential oils and their major constituents against respiratory tract pathogens by gaseous contact. *J. Antimicrob. Chemoth.* **2001**, *47* (5), 565–573. https://doi.org/10.1093/jac/47.5.565

Instituto Brasileiro de Geografia e Estatística (IBGE). *Produção da Extração Vegetal e da Silvicultura (Pevs)*. IBGE, 2021.

Ioannou, E.; Koutsaviti, A.; Tzakou, O.; Roussis, V. The genus Pinus: a comparative study on the needle essential oil composition of 46 pine species. *Phytochem. Rev.* **2014**, *13* (4), 741–768. https://doi.org/10.1007/s11101-014-9338-4

Jesus, R. M. The Need for Reforestation. In: *International Workshop Large-Scale Reforestation*. Corvallis, Oregon, United States, 1990.

Kilani, S.; Abdelwahed, A.; Ben Ammar, R.; Hayder, N.; Ghedira, K.; Chraief, I.; Hammami, M.; Chekir-Ghedira, L. Chemical composition, antibacterial and antimutagenic activities of essential oil from (Tunisian) Cyperus rotundus. *J. Essent. Oil Res.* **2005**, *17* (6), 695–700. https://doi.org/10.1080/10412905.2005.9699035

Kurti, F.; Giorgi A.; Beretta, G.; Mustafa, B.; Gelmini, F.; Testa, C.; Angioletti, S.; Giupponi, L.; Zilio, E.; Pentimalli, D.; Hajdari, A. Chemical composition, antioxidant and antimicrobial activities of essential oils of different Pinus species from Kosovo. *J. Essent. Oil Res*. **2019**, *31* (4), 263–275. https://doi.org/10.1080/10412905.2019.1584591

Lunguinho, A. D.; Cardoso, M. D.; Ferreira, V. R. F.; Konig, I. F. M.; Goncalves, R. R. P.; Brandao, R. M.; Rodrigues Silva Caetano, A.; Nelson, D. L.; Remedio, R. N. Acaricidal and repellent activity of the essential oils of Backhousia citriodora, Callistemon viminalis and Cinnamodendron dinisii against Rhipicephalus spp. *Vet. Parasitol.* **2021**, *300*, 109594. https://doi.org/10.1016/j.vetpar.2021.109594

Mayaud, L.; Carricajo, A.; Zhiri, A.; Aubert, G. Comparison of bacteriostatic and bactericidal activity of 13 essential oils against strains with varying sensitivity to antibiotics. *Lett. Appl. Microbiol.* **2008**, *47* (3), 167–173. https://doi.org/10.1111/j.1472-765X.2008.02406.x

Modzelewska, A.; Sur, S.; Kumar, S. K.; Khan, S. R. Sesquiterpenes: natural products that decrease cancer growth. *Curr. Med. Chem. Anticancer Agents.* **2005**, *5* (5), 477–499. https://doi.org/10.2174/1568011054866973

National Institute of Standards and Technology (NIST). *Mass Spectral Library and Search/ Analysis Programs*. NIST/EPA/NIH, 2010.

Ning, C.; Mueller, G. M.; Egerton-Warburton, L. M.; Xiang, W. H.; Yan, W. D. Host Phylogenetic Relatedness and Soil Nutrients Shape Ectomycorrhizal Community Composition in Native and Exotic Pine Plantations. *Forests*. **2019**, *10* (3), 263. https://doi.org/10.3390/f10030263

Noge, K.; Becerra, J. X. Germacrene D, a common sesquiterpene in the genus Bursera (Burseraceae). *Molecules.* **2009**, *14* (12), 5289–5297. https://doi.org/10.3390/molecules14125289

Oliveira-Tintino, C. D. M.; Pessoa, R. T.; Fernandes, M. N. M.; Alcântara, I. S.; Silva, B. A. F.; Oliveira, M. R. C.; de Menezes, I. R. A. Anti-inflammatory and anti-edematogenic action of the Croton campestris A. St.-Hil (Euphorbiaceae) essential oil and the compound β-caryophyllene in in vivo models. *Phytomedicine*. **2018**, *41*, 82–95. https://doi.org/10.1016/j.phymed.2018.02.004

Richardson, D. M.; Rundel, P. W.; Jackson, S. T.; Teskey, R. O.; Aronson, J.; Bytnerowicz, A.; Proches, S. Human impacts in pine forests: Past, present, and future. *Annual Review of Ecology Evolution and Systematics*. **2007**, *38*, 275–297. https://doi.org/10.1146/annurev.ecolsys.38.091206.095650

Salehi, B.; Upadhyay, S.; Erdogan Orhan, I.; Kumar Jugran, A.; Sharifi-Rad, J. Therapeutic Potential of α- and β-Pinene: A Miracle Gift of Nature. *Biomol.* **2019**, *9* (11), 738. https://doi.org/10.3390/biom9110738

Satoh, K.; Nakahara, A.; Mukunoki, K.; Sugiyama, H.; Saito, H.; Kamigaito, M. Sustainable cycloolefin polymer from pine tree oil for optoelectronics material: living cationic polymerization of beta-pinene and catalytic hydrogenation of high-molecular-weight hydrogenated poly(beta-pinene). *Polym Chem-UK.* **2014**, *5* (9), 3222–3230. https://doi.org/10.1039/C3PY01320K

Silva, A. C. R.; Lopes, P. M.; de Azevedo, M. M. B.; Costa, D. C. M.; Alviano, C. S.; Alviano, D. S. Biological Activities of alpha-Pinene and beta-Pinene Enantiomers. *Molecules.* **2012**, *17* (6), 6305–6316. https://doi.org/10.3390/molecules17066305

Teixeira, M. L.; Cardoso, M. d. G.; Figueiredo, A. C. S.; Moraes, J. C.; Assis, F. A.; de Andrade, J.; de Albuquerque, L. R. M. Essential Oils from Lippia origanoides Kunth. and Mentha spicata L.: Chemical Composition, Insecticidal and Antioxidant Activities. *Am. J. Plant. Sci.* **2014**, *5* (9), 1181–1190. https://doi.org/10.4236/ajps.2014.59131

Thomsett, M. R.; Moore, J. C.; Buchard, A.; Stockman, R. A.; Howdle, S. M. New renewably-sourced polyesters from limonene-derived monomers. *Green Chem.* **2019**, *21* (1), 149–156. https://doi.org/10.1039/C8GC02957A

Tiwari, B. K.; Valdramidis, V. P.; O'Donnell, C. P.; Muthukumarappan, K.; Bourke, P.; Cullen, P. J. Application of Natural Antimicrobials for Food Preservation. *J. Agr. Food Chem.* **2009**, *57* (14), 5987–6000. https://doi.org/10.1021/jf900668n

Van Den Dool, H.; Dec. Kratz, P. A generalization of the retention index system including linear temperature programmed gas-liquid partition chromatography. *J. Chromatogr A.* **1963**, *11*, 463–471. https://doi.org/10.1016/S0021-9673(01)80947-X

Van Der Werf, M. J.; de Bont, J. A. M.; Leak, D. J. Opportunities in microbial biotransformation of monoterpenes. In: Berger, R. G., *et al. Biotechnology of Aroma Compounds*: Advances in Biochemical Engineering/Biotechnology, vol 55. Springer, 1997; pp. 147–177. https://doi.org/10.1007/BFb0102065

Vespermann, K. A. C.; Paulino, B. N.; Barcelos, M. C. S.; Pessoa, M. G.; Pastore, G. M.; Molina, G. Biotransformation of alpha- and beta-pinene into flavor compounds. *Appl. Microbiol. Biot.* **2017**, *101* (5), 1805–1817. https://doi.org/10.1007/s00253-016-8066-7

Warnke, P. H.; Becker, S. T.; Podschun, R.; Sivananthan, S.; Springer, I. N.; Russo, P. A. J.; Sherry, E. The battle against multi-resistant strains: Renaissance of antimicrobial essential oils as a promising force to fight hospital-acquired infections. *J. Cranio. Maxill. Surg.* **2009**, *37* (7), 392–397. https://doi.org/10.1016/j.jcms.2009.03.017

Winnacker, M. Pinenes: Abundant and Renewable Building Blocks for a Variety of Sustainable Polymers. *Angew Chem Weinheim Bergstr Ger.* **2018**, *57* (44), 14362–14371. https://doi.org/10.1002/anie.201804009

Zhou, J. Y.; Tang, F. D.; Mao, G. G.; Bian, R. I. Effect of alpha-pinene on nuclear translocation of NF-kappa B in THP-1 cells. *Acta Pharm Sinic.* **2004**, *25* (4), 480–484.

ECLÉTICA QUÍMICA

Eclet. Quim. **49** | e-1508, 2024

Review Article

https://doi.org/10.26850/1678-4618.eq.v49.2024.e1508

Identification of learning difficulties and misconceptions of chemical bonding material: A review

Hayuni Retno **Widarti**[1+], Dian **Nuriyanti**[1], Meyga Evi Ferama **Sari**[1], Antuni **Wiyarsi**[2], Sri **Yatimah**[3], Deni Ainur **Rokhim**[1,4]

Abstract

Chemical bonds are one of the materials in chemistry that are abstract in nature so that many students have difficulty learning chemical bonding material. This study aims to identify the learning difficulties frequently faced by students in understanding chemical bonding materials and various misconceptions that commonly occur in their understanding. Data collection was carried out using a systematic literature review method with several predetermined criteria. The result is that the learning difficulties experienced by students are caused by many factors, one of which is conceptual error or misconception. At present, many methods have been developed to identify students' misconceptions about chemical bonding material such as diagnostic tests such as two-tier, three-tier and four-tier diagnostics.

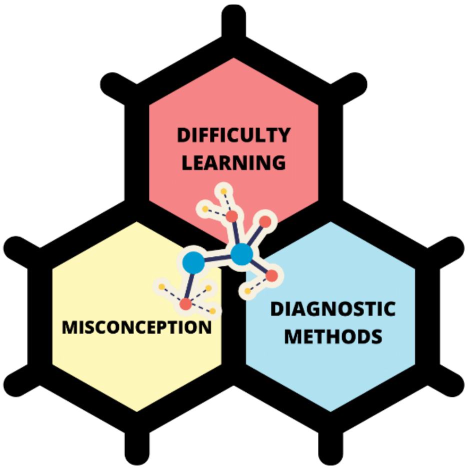

Article History

Received	August 10, 2023
Accepted	June 14, 2024
Published	October 11, 2024

Keywords

1. chemical bonding;
2. difficulty learning;
3. misconception.

Section Editor

Natany Dayani de Souza Assai

Highlights

- Misconceptions about chemical bonding include mastery of concepts and introduction media.
- The difficulty in chemical bonds lies in the abstract complexity of the material.
- Identify misconceptions in chemical bonding using two-, three-, and four-level diagnostics.

CONTENTS

[1]State University of Malang, Faculty of Science and Mathematics, Malang, Indonesia. [2]Yogyakarta State University, Faculty of Science and Mathematics, Yogyakarta, Indonesia. [3]Sebelas Maret University, Faculty of Science and Mathematics, Surakarta, Indonesia. [4]SMAN 3 Sidoarjo, Chemistry and PKWU, Sidoarjo, Indonesia.
+Corresponding author: Hayuni Retno Widarti, **Phone:** +081232458494, **Email address:** hayuni.retno.fmipa@um.ac.id

1. Introduction

Chemistry is a science focused on matter, structure, properties, changes and reactions accompanying it. The scope of scientific studies tends to be invisible and abstract, making it difficult to understand a concept. Chemistry learning has an important role in forming students' understanding and competence in complex concepts. However, along the way, many students face difficulties in understanding and applying basic concepts such as chemical bonds. If the concepts in chemistry are not well understood, students will experience learning difficulties, one of the impacts of which is the occurrence of conceptual errors commonly called misconceptions (Margaretha *et al.*, 2022). The initial knowledge or concept that students have based on an individual's understanding is called conception. Concepts that do not follow scientific concepts are referred to as misconceptions (Rokhim *et al.*, 2023b). The misconception is one of the obstacles to concept mastery that needs to be minimalized (Widarti *et al.*, 2016). Misconceptions are still a problem in the learning process because they can reduce the effectiveness of student learning and hinder students from understanding new knowledge. If misconceptions continue to develop and are not immediately resolved, it will result in students' difficulties in understanding subsequent concepts (Muchtar and Harizal, 2012).

This article aims to provide an in-depth review of the learning difficulties that are often faced by students in understanding chemical bonding material, as well as to analyze various misconceptions that are common in their understanding. Through a comprehensive review, it is hoped that this article can provide better insight into the sources of learning difficulties and conceptual errors that may arise at the learning stage of chemical bonding. By understanding the root causes that often arise, a more effective and appropriate learning approach can be designed to help students overcome obstacles in understanding chemical bonds.

2. Experimental

This study uses the method of Systematic Literature Review (SLR). A systematic literature review aims to identify and understand relevant research with implications for the topics studied (Synder, 2019). This method is carried out by searching for academic publications in national and international journals using online academic publications databases on ERIC and Google Scholar. The search uses the keywords "Difficulty Learning of Chemical Bonding" and "Misconception of Chemical Bonding".

The academic publications obtained are then reduced based on the abstract and title by considering the suitability of the content. The academic publications were selected based on predetermined criteria including (1) academic publications on the analysis of misconceptions and learning difficulties in chemical bonding material; (2) Publication between 2018 and 2023; (3) Full text and accessible. From the selection process, 11 academic publications met all the criteria.

3. Results and discussion

From the findings of the academic publications, the topic of discussion in this review article is divided into 3 parts, including difficulty learning chemical bonds, development of chemical bonding misconception diagnostic methods, and identification of chemical bonding misconceptions.

3.1. Difficulty learning chemical bonds

Difficulty is a difficult situation, difficulty or distress (Big Indonesian Dictionary). Difficulty is a condition that shows the characteristics of obstacles in activities to achieve goals so that a greater effort is needed to overcome them. Learning difficulties are obstacles or challenges faced by students in mastering learning material or concepts. According to Subini (2012), learning difficulties are synonymous with students' difficulties in receiving or absorbing lessons at school. This can cover various aspects, both in terms of understanding the concept, applying it, and developing skills. Learning difficulties can be temporary or more chronic, depending on certain factors such as the complexity of the material, student learning styles, learning environment, and so on. Some academic publications related to learning difficulties in chemical bonding material are presented in **Table 1**.

Based on the results of the research above, the learning difficulties experienced by students in chemical bonding material were caused by several factors. Lack of student interest in learning because of the assumption that chemical bonding material is complicated, the learning process is less interesting and not suitable for students, students' weak ability to remember concepts due to lack of practice questions, lack of student understanding regarding prior knowledge that supports understanding of chemical bonding material, and there are still many concept errors or misconceptions that students experience in chemical bonding material. The learning difficulties experienced by these students certainly hurt student learning outcomes if an effective solution is not immediately given. Low student learning outcomes can be caused by learning problems, for example, lack of understanding of a concept and misconceptions experienced by most students (Warsito *et al.*, 2020).

3.2. Development of chemical bonding misconception diagnostic methods

Misconception is a term used when students' ideas are not relevant to a scientific perspective. Misconceptions should be identified and corrected immediately, so as not to interfere with the further learning process (Margaretha *et al.*, 2022). Misconceptions can be an obstacle for students to acquire complete knowledge, therefore this problem must be addressed (Arslan *et al.*, 2012). Misconception analysis requires instruments that can reveal the causes of misconceptions in depth (Rokhim *et al.*, 2023a). According to Firman, misconceptions can be diagnosed using standardized tests that use valid and reliable instruments (Utami *et al.*, 2019). Various studies have used multiple-choice diagnostic tests to analyze students' misconceptions (Sen and Yilmaz, 2017). Diagnostic tests can help teachers to identify students' misconceptions (Uyulgan *et al.*, 2014).

The high level of students' learning difficulties in chemical bonding material is caused by one of the misconceptions experienced by students. Chemical bonds are one of the subject matter with abstract concepts. Chemical bonding is a difficult concept for students that can lead to misconceptions (Meltafina *et al.*, 2019). To find out the level of students' misconceptions about chemical bonding material, a diagnostic test to analyze and identify misconceptions about chemical bonding is a must (Utami *et al.*, 2019). Several multiple-choice-based diagnostic tests currently being developed include: four-tier multiple-choice, three-tier multiple-choice, and two-tier multiple-choice. The instrument is considered effective because students can give students freedom to describe the representations that exist in their minds (Rokhim *et al.*, 2023b). Some academic publications regarding the diagnostic methods for chemical bond misconceptions are presented in **Table 2**.

From the several studies showed in **Table 2**, it is known that the multiple-choice diagnostic tests currently being developed are in the form of four-tier multiple-choice, three-tier multiple-choice, and two-tier multiple-choice. The difference between the three lies in the division of categories to analyze student misconceptions. Diagnostic test results using four-tier multiple choice have a higher level of sensitivity than diagnostic tests using three-tier multiple choice and two-tier multiple choice so they will be more thorough in identifying misconceptions in students (Qodriyah *et al.*, 2020). The two-tier diagnostic test was unable to distinguish between students who lacked knowledge and those who had misconceptions, however, the three-tier diagnostic test had an unequal score ratio between students who had misconceptions and students who lacked knowledge (Kaltakci-Gurel *et al.*, 2017).

3.3. Identification of chemical bonding misconceptions

Misconceptions or conceptual errors are defined as an erroneous understanding of a concept so that it does not follow scientific concepts or those that are understood and approved by experts in a particular field (Suparno, 2013). Misconception is a condition where students' understanding deviates from the correct concept, but students tend to maintain the wrong understanding (Margaretha *et al.*, 2022). Misconceptions can prevent students from obtaining correct concepts and have the potential to hinder progress in further learning (Horton, 2007). Misconceptions experienced by students have been identified in most of the concepts studied in chemistry, especially at the atomic and molecular level concepts which are indeed abstract (Taber, 2009), such as one of the chemical concepts that often causes misconceptions in students, namely the concept of Chemical Bonds. The concept of chemical bonds underlies most of the concepts in advanced sciences in chemistry such as inorganic chemistry, organic chemistry, and physical chemistry (Gudyanga and Madambi, 2014).

More than 50% of students experience misconceptions about chemical bonding materials (Fadillah and Salirawati, 2018). Misconceptions have been recognized as the main factor influencing understanding of the material, and teachers also have misconceptions about certain concepts (Utomo *et al.*, 2018). Misconception can affect learning effectiveness and significantly impact learning achievement (Chen *et al.*, 2020).

From the studies in **Table 3**, misconceptions about chemical bonding identified by researchers are presented in **Table 4**.

Based on the data described in **Table 4**, many misconceptions about chemical bonds among students occur in all material sub-chapters, especially in ionic and covalent bonds. This is in line with several research results which show a high percentage of misconceptions about ionic bonds and covalent bonds (Rohmah *et al.*, 2022; Setiawan *et al.*, 2017). Most higher education students still have difficulty distinguishing the two types of bonds due to misunderstanding the concept of the formation of the two bonds.

3.4. Future perspectives

Misconceptions can become difficulties for students in the future. Misconceptions allow students to instil wrong concepts and be unable to accept correct concepts. Chemical bonding is one of the basic materials in chemistry. When students experience misconceptions about chemical bonding material, it will cause mistakes and difficulties in understanding further chemical material. After identifying and finding several misconceptions that are still often experienced by students, it is hoped that there will be a solution to reduce the risk of misconceptions or even solve the problem. A complete understanding of chemical bonding is very important to reduce the percentage of misconceptions among students (Safitri *et al.*, 2018).

The solutions offered can be in the form of developing models, media, or other learning tools. The innovations carried out are expected to be able to direct students to build the correct concept so that students will not experience learning difficulties and obstacles to obtaining learning outcomes that follow expectations.

4. Conclusions

Chemical bonds are one of the materials that form the basis of advanced chemical materials. As with chemistry, chemical bonding material is also abstract so many students experience learning difficulties in this material. Learning difficulties experienced are caused by many factors such as a lack of interest in student learning, an inappropriate learning process, a lack of practice questions, a lack of student understanding regarding prior knowledge that supports understanding of chemical bonding material, and there are still many conceptual errors or misconceptions. Based on the results of the last 5 years of studies, many students still find learning difficulties due to misconceptions about chemical bonding material.

There have been many developments in methods for identifying students' misconceptions about chemical bonding material such as diagnostic tests such as two-tier, three-tier, and four-tier diagnostics. As a result, it is known that there are many students' misconceptions that spread to all chemical bonding sub-materials, especially in ionic bonding and covalent bonding materials.

After identifying and finding several misconceptions that are still often experienced by students, it is hoped that there will be a solution to reduce the risk of misconceptions or even solve the problem.

Table 1. Difficulty learning chemical bonds.

No	Author, Title, Journal	Research purposes	Research methods	Research result
1.	Sahriani (2019) Analysis of Learning Difficulties of Class X MIPA Students of SMA Negeri 3 Tanjungpinang on Chemical Bonding Material. Raja Ali Haji Maritime University Thesis	The purpose of this study was to see the learning difficulties of class X students on chemical bonds.	Student learning difficulties are measured from the results of student test questions and are supported by interviews, while the questionnaire aims to look at the factors that cause student learning difficulties.	The study showed that students had difficulty understanding high-category terms with a percentage of 70%, students had difficulty understanding high-category calculations with percentage of 68%, and students had difficulty understanding high-category concepts with a percentage of 71%. The factors that influence student learning difficulties are (1) internal factors in the sufficient category with a percentage of 57.5% including aspects of interest (57%) and aspects of motivation (58%), (2) external factors in the sufficient category with a percentage of 59, 5% includes aspects of teacher teaching methods/methods (5.9%), facilities and infrastructure (60%).
2.	Haris and Wahidah (2018) Analysis of Difficulties in Learning Chemical Bonds in View of Misconceptions of Grade X Students of SMA Negeri 3 Mataran. MIPA Incandescent Journal	This study aims to identify and explain the conceptual errors of class X SMA Negeri 3 Mataram in studying chemical bonding.	Data collection uses a test that contains 12 concepts of chemical bonding.	This research showed that very few students (1-20%) had conceptual errors of electron configuration, ion formation, metals / non-metals, ionic bonds / covalent bonds covalent compounds, and chemical formulas for chloride compounds. Few students (21-40%) experienced misconceptions about the compounds formed and the chloride ion formula. Quite students (41-60%) experienced misconceptions about Lewis structures and ionic compounds. Many students (61-80%) experienced misconceptions about covalent compounds and the atomic numbers of the elements. In general, 62.5% of students experienced difficulty in studying chemical bonds, 20% experienced quite difficulty and 17,5% experienced less difficulty.
3.	Sabrina (2018) Identification of Student Learning Difficulties in Chemical Bonding Material at SMAS Muslimat Samalanga Bireuen. UIN Ar-Raniry Banda Aceh	To analyze students' learning difficulties in chemical bonding material at SMAS Muslimat Samalanga Biruen.	Data was collected through tests and interviews, then the data was analyzed through student mastery and student difficulties.	The results showed that class X students of SMAS Muslimat Samalanga Bireuen still experienced mistakes and difficulties in solving chemical bond problems, namely 80% of students had difficulty distinguishing between covalent and metallic physical properties, 76% of students had difficulty estimating the polarity of a molecule, and 37% of students had difficulty distinguishing between ionic bonds, covalent bonds, coordinate covalent bonds, and metallic bonds. This is caused by material that is difficult for students to understand, low student abilities, and a lack of practice working on questions. As well as students have a weak ability to remember the concept of the material being taught.
4.	Yani (2018) Diagnostics of the Relationship of Prior Knowledge with Learning Difficulties in Class X High School Chemical Bonds, Solok City. Padang State University	Aims to reveal the relationship between learning difficulties and students' prior knowledge of chemical bonding material at SMAN Kota Solok.	The research was conducted through two two-tier diagnostic tests for initial knowledge of chemical bonding and chemical bonding.	The results showed that students at SMAN Kota Solok had learning difficulties in understanding the concept of chemical bonding material with very high learning difficulty criteria in (1) bond formation, (2) ionic bonds, (3) covalent bonds, single bonds, double bonds, double bonds triple, (4) coordinate covalent bonds, (5) polar and non-polar bonds, (6) ionic and covalent bonds. Initial knowledge that most influences students' learning difficulties in chemical bonding material is (1) electron configuration, (2) group and period, (3) periodic properties of an element based on radius, ionization energy, electron affinity and electronegativity. Students' initial knowledge that does not follow scientific understanding causes students' learning difficulties in understanding the concept of chemical bonds.

Table 2. Diagnostic methods of misconception.

No	Author, Title, Journal	Research purposes	Research methods	Research result
1.	Mahmudah *et al.* (2020) Identification of students' misconceptions in chemical bonding topic using the four-tier diagnostic test. Journal of Physics: Conference Series	Identifying misconceptions by measuring students' level of understanding in the topic of chemical bonds using a four-tier multiple choice diagnostic test.	The research method is descriptive and involves 77 students from SMA Tangerang Selatan.	The results of the study stated that the overall level of students' misconceptions about chemical bonds was in the low category (15.14%). Misconceptions on the concept of determining ionic and covalent bonds microscopically results in the moderate category (41.56%), and metallic bonds in the moderate category (37.66%).
2.	Setiawan and Ilahi (2022) Identification of Misconceptions in Chemical Bonding Materials Using Three Tier Diagnostic Tests. Journal of Natural Science of Integration	Knowing whether there is, and the percentage of misconceptions about chemical bonding materials using three tier diagnostic test.	Qualitative research with a descriptive approach using purposive sampling technique	Research on students of SMA Negeri 1 Teluk Kuantan class X on chemical bonding material showed that 72.53% of students experienced misconceptions, 14.98% of students did not understand the concept, and the remaining 12.48% of students understood the concept of chemical bonds.
3.	Ebiati *et al.* (2020) Sensitivity of two-tier and three-tier tests in detecting student's misconceptions of chemical bonding. Journal of Chemistry Education	Knowing how the two-tier and three-tier test sensitivity is on detect students' misconceptions about chemical bonding material.	This research is a quantitative study with a total sampling technique measured using three-tier multiple-choice with modified certainty of response index (CRI).	This study concluded that the three-tier multiple-choice was more sensitive than the two-tier multiple-choice in detecting students' misconceptions about chemical bonds.
4.	Utami *et al.* (2019) Development of a computer based two-tier multiple choice diagnostic test to identify misconceptions on chemical bonding. Journal of Physics: Conference Serie	This study aims to find a computer-based multiple-choice diagnostic test for students' misconceptions about chemical bonding material.	The development process is carried out by analyzing literature, identifying targets, analyzing misconceptions through essays, and analyzing misconceptions through two-tier multiple choice.	A computer-based two-tier multiple-choice diagnostic test was produced on chemical bonding materials which include ionic bonds, covalent bonds, metallic bonds, and coordination bonds. The effectiveness of the developed diagnostic tests will then be tested by conducting trials, identifying misconceptions about feedback and being retested again.

Table 3. Identification of chemical bonding misconceptions.

No	Author, Title, Journal	Research purposes	Research methods	Research result
1.	Warsito *et al.* (2020) Identification of Students' Misconceptions on the Topic of Chemical Bonds and Their Improvements with the ECIRR Learning Model (Elicit, Confront, Identify, Resolve, Reinforce). Journal of Education: Theory, Research, and Development	The purpose of this study was to (1) identify and analyze students 'misconceptions on the topic of chemical bonding with the Three-Tier diagnostic test (2) to determine the effectiveness of the ECIRR model in improving student misconceptions (3) to determine the retention of students' conceptual understanding 3 weeks after remedies.	This research is a descriptive and quasi-experimental study with the design of One Group Pre - Test Post - Test Design. The research subjects were 33 students of class X IPA in a high school outside Java.	The results showed that (1) found 41 types of misconceptions on the topic of chemical bonding (2) remedial learning with the ECIRR model was able to reduce student misconceptions from 61.5% to 22.4%, and (3) retention of students' understanding of remedial results by 82.5 % with very good criteria.
2.	Islami *et al.* (2019) Identification of Students' Misconceptions on the Concept of Chemical Bonds using the Four-Tier Multiple-Choice Test (4TMC). JRPK: Research Journal of Chemistry Education	This study aims to identify student misconception on the concept of Chemical Bonding.	The method used in this research is quantitative descriptive. The misconception identification was performed using a four-tier multiplechoice (4TMC) test instrument.	The results showed the existence of a misconception of 30.31% (low category). Significant misconceptions are identified as 8 out of 13 sub-concepts of Chemical Bonding they are Lewis Structure and the Octet Rule (33.33%), Metal Bond and Metal Properties (20.83%), Ionic Compounds and Covalent Compounds (27.08%), Theory of VSEPR (20.83%), Electron Domain-Theory (18.75%), Polarity of Molecul (27.08%), Van der Waals Forces (14.58%), and Hydrogen Bond (29.17%).
3.	Rohmah *et al.* (2022) Analysis of Student's Chemical Bonding Misconception with A Four-Tier Diagnostic Test. Journal Tadris Chemistry	This study aimed to investigate basic chemistry students' misconceptions of chemical bonding.	This study used a descriptive research design with a four-tier diagnostic test. The research subjects were basic chemistry students.	The results showed that students who had misconceptions about ionic, covalent, and coordinate covalent bonding were 48.9%, 53.0%, and 37.5%, respectively. The misconception in this course is that students need to learn about ionic bonds formed by electrostatic forces between cations and anions. As a result, students cannot determine the difference in electronegativity values in ionic and covalent bonds and the number of valence electrons of each atom in a chemical bonding. Therefore, the misconception is in the moderate category.

Table 4. Misconceptions of chemical bonding.

Sub Matter of Chemical Bonds	Misconception Analysis	References
Lewis Structure and the Octet Rule	The Lewis structure of the molecule before electron transfer is written by adding the charge of the ion.	Warsito *et al.* (2020)
	In the Lewis structure of the HCl molecule, Lone pair of electrons is balanced between the H and Cl atoms.	Islami *et al.* (2019)
Ionic Bonds	Determining the type of bond that is formed is due to referring to the type of bonding elements, namely metals and non-metals.	Warsito *et al.* (2020)
	Ionic bonds are formed from metal and non-metal elements.	Rohmah *et al.* (2022)
	The formation of ionic bonds involves the transfer of electrons between atoms.	Rohmah *et al.* (2022)
	The calcium atom donates its valence electrons to the oxygen atom, then bonds.	Rohmah *et al.* (2022)
Covalent Bonds	Coordinate covalent bonding is the same as the process by which ionic bonds occur, namely the handover of electrons.	Warsito *et al.* (2020)
	NaCl has covalent bonds because the sodium atom donates valence electrons to the chlorine atom.	Rohmah *et al.* (2022)
	$AlCl_3$ compounds are derived from cations and anions.	Rohmah *et al.* (2022)
Metal Bond	The larger the metal atomic radius, the stronger the metallic bond so that the melting point is low.	Warsito *et al.* (2020)
Molecular Polarity	The bonds between atoms in water are polar covalent bonds but the molecules are non-polar.	Warsito *et al.* (2020)
	The CF bond is nonpolar so that the CF_4 molecule is nonpolar.	Islami *et al.* (2019)
Molecular Shape	The molecular shape of XeF_4 is tetrahedral due to the presence of four bonding pairs of electrons.	Warsito *et al.* (2020)
Intermolecular Forces	H_2O and HF have hydrogen bonds because there is a bond between the positive dipole of the H atom and the negative dipole of the very electronegative atom, namely O and group 17.	Warsito *et al.* (2020)
	Hydrogen bonds are formed when the N atoms of one molecule interact with the H atoms of another molecule.	Islami *et al.* (2019)

Authors' contributions

Conceptualization: Dian Nuriyanti; **Data curation**: Dian Nuriyanti; **Formal Analysis**: Antuni Wiyarsi; **Funding acquisition**: Hayuni Retno Widarti; **Investigation**: Dian Nuriyanti; Meyga Evi Ferama Sari; **Methodology**: Deni Ainur Rokhim; **Project administration**: Hayuni Retno Widarti; **Resources**: Hayuni Retno Widarti; **Software**: Deni Ainur Rokhim; **Supervision**: Hayuni Retno Widarti; **Validation**: Sri Yatimah; **Visualization**: Dian Nuriyanti; **Writing – original draft**: Dian Nuriyanti; **Writing – review & editing**: Deni Ainur Rokhim.

Data availability statement

All data sets were generated or analyzed in the current study.

Funding

Not applicable.

Acknowledgments

Not applicable.

References

Arslan, H. O.; Cigdemoglu, C.; Moseley, C. A three-tier diagnostic test to assess pre-service teachers' misconceptions about global warming, greenhouse effect, ozone layer depletion, and acid rain. International journal of science education. **2012**, *34* (11), 67–86. https://doi.org/10.1080/09500693.2012.680618

Chen, C.; Sonnert, G.; Sadler, P. M.; Sasselov, D.; Fredericks, C. The impact of student misconceptions on student persistence in a MOOC. J. Res. Sci. Teaching. **2020**, *57* (6), 879–910. https://doi.org/10.1002/tea.21616

Ebiati, E.; Asrial, A.; Hasibuan, M. Sensitivity of two-tier and three-tier tests in detecting student's misconceptions of chemical bonding. *J. Chem. Educ.* **2020**, *12* (2), 79–87. https://doi.org/10.24114/jpkim.v12i2.19405

Fadillah, A.; Salirawati, D. Analysis of misconceptions of chemical bonding among tenth grade senior high school students using a two-tier test. *AIP Conf. Proc.* **2018**, *2021* (1), 080002. https://doi.org/10.1063/1.5062821

Gudyanga, E.; Madambi, T. Students' misconceptions about bonding and chemical structures in chemistry. Dyke. **2014**, *8* (1), 24–40.

Haris, M.; Wahidah, S. Analysis of Difficulties in Learning Chemical Bonds in View of Misconceptions of Class X Students of SMA Negeri 3 Mataran. *MIPA Incandescent Journal.* **2018**, *6* (2). https://doi.org/10.29303/jpm.v6i2.127

Horton, C. Student alternative conception in chemistry. *Calif J. Sci Educ.* **2007**, *7*, 18–28. https://doi.org/10.1080/03057269508560050

Islami, D.; Suryaningsih, S.; Bahriah, E. S. Identification of Students' Misconceptions on the Concept of Chemical Bonds using the Four-Tier Multiple-Choice Test (4TMC). *JRPK: Res. J. Chem. Educ.* **2019**, *9* (1), 21–29. https://doi.org/10.21009/JRPK.091.03

Kaltakci-Gurel, D.; Eryilmaz, A.; McDermott, L. C. Development and application of a fourtier test to assess pre-service physics teachers' misconceptions about geometrical optics. *Res. Sci. Technol. Educ.* **2017**, *35* (2), 238–60. https://doi.org/10.1080/02635143.2017.1310094

Mahmudah, A.; Nahadi, N.; Firman, H. Identification of student's misconceptions in chemical bonding topic using four-tier diagnostic test. *J. Phys.: Conf. Ser.* **2020**, *1521*, 042059. https://doi.org/10.1088/1742-6596/1521/4/042059

Margaretha, B. P.; Muchson, M.; Hakimah, N.; Rokhim, D.A.; Herunata, H.; Yahmin, M. dan. Identification of Misconceptions on Chemical Equilibrium Material in High School Students Using a Web-Based Three Tier Test. *J. Chem. Educ. Innov*. **2022**, *16* (1), 12615.

Meltafina, M.; Wiji, W.; Mulyani, S. Misconceptions and threshold concepts in chemical bonding. *J. Phys.: Conf. Ser.* **2019**, *1157*, 042030. https://doi.org/10.1088/1742-6596/1157/4/042030

Muchtar, Z.; Harizal. Analyzing of Students' Misconceptions on Acid-Base Chemistry at Senior High Schools in Medan. *Journal of Education and Practice*. **2012**, *3* (15), 65–74.

Qodriyah *et al.* Identification of Misconceptions Of Class XI Students of Sma Negeri 4 Malang on Hydrocarbon Materials Using Three Tier Diagnostic Instruments. *Journal of Chemical Education Innovatio*. **2020**, *14* (2). https://doi.org/10.36987/jpbn.v8i3.2919

Rohmah, R. S.; Sholichah, N.; Pratiwi, Y. N.; Analita, R. N. Analysis of Student's Chemical Bonding Misconception with A Four-Tier Diagnostic Test. *Journal Tadris Chemistry*. **2022**, *7* (2), 166–174. https://doi.org/10.15575/jtk.v7i2.20343

Rokhim, D. A., Rahayu, S.; Dasna, I. W. Analysis of Chemical Misconceptions and Its Diagnostic Instruments: Literature Review. *J. Chem. Educ. Innov.* **2023a**, *17* (1), 13697. https://doi.org/10.15294/jipk.v17i1.34245

Rokhim, D. A.; Widarti, H. R.; Sutrisno, S. Five-Tier Instrument to Identify Students' Misconceptions and Representation: A Systematic Literature Review. *Orbital: Electron. J. Chem.* **2023b**, *15*, 202–207. https://doi.org/10.17807/orbital.v15i4.17709

Safitri A. F.; Widarti H. R.; Sukarianingsih D. Identify understanding of the concept of chemical bonds. *J. Chem. Learning.* **2018**, *3* (1), 41–50. https://doi.org/10.17977/um026v3i12018p041

Sen, S.; Yilmaz, A. The development of a three-tier chemical bonding concept test. *J. Turk. Sci. Educ.* **2017**, *14* (1), 111–126. https://doi.org/10.12973/tused.10193a

Setiawan, D.; Cahyono, E.; Kurniawan, C. Identification and Analysis of Misconceptions in Chemical Bonding Material Using a Three-Tier Diagnostic Test Instrument. *J. Innov. Sci. Educ.* **2017**, *6* (2), 197–204. https://doi.org/10.15294/JISE.V6I2.15580

Setiawan, N. C. E.; Ilahi, P. R. Identification of Misconceptions in Chemical Bonding Materials Using Three Tier Diagnostic Tests. *J. Nat. Sci. Integr.* **2022**, *5* (1), 77–89. https://doi.org/10.24014/jnsi.v5i1.16860

Subini, N. *Learning Psychology*; Mentari Pustaka, 2012.

Suparno, P. *Misconceptions & Changes in the Concept of Physics Education*; Grasindo, 2013.

Synder, H. Literature Review As a Research Methodology: An Overview and Guidelines. *J. Bus. Res.* **2019**, *104*, 333–339. https://doi.org/10.1016/j.jbusres.2019.07.039

Taber, K. S. Challenging Misconceptions inthe Chemistry Classroom: Resources to Support Teachers. *Educació Química*. **2009**, *4*, 13–20. https://doi.org/10.2436/20.2003.02.27

Utami, G. R.; Firman, H.; Nahadi, N. Development of a computer based two-tier multiple choice diagnostic test to identify misconceptions on chemical bonding. *J. Phys. Conf. Ser.* **2019**, *1157*, 042033. https://doi.org/10.1088/1742-6596/1157/4/042033

Utomo, A. P.; Narulita, E.; Yuana, K.; Fikri, K.; Wahono, B. Students' errors in solving science reasoning-domain of trends in international mathematics and science study (TIMSS). *Indonesian Sci. Educ. J.* **2018**, *7* (1), 48–53. https://doi.org/10.15294/jpii.v7i1.11352

Uyulgan, M. A.; Akkuzu, N.; Alpat, S. Assessing the students' understanding related tomolecular geometry using a two-tier diagnostic test. *J. Balt. Sci. Educ.* **2014**, *13* (1), 839–841. https://doi.org/10.33225/jbse/14.13.839

Warsito, J. Subandi, S.; Parlan, P. Identification of Students' Misconceptions on the Topic of Chemical Bonds and Their Improvements with the ECIRR Learning Model (Elicit, Confront, Identify, Resolve, Reinforce). *Journal of Education: Theory, Research, and Development*. **2020**, *5* (11), 1563–1572. https://doi.org/10.17977/jptpp.v5i11.14158

Widarti, H. R.; Permanasari, A.; Mulyani, S. Student misconception on redox titration (a challenge on the course implementation through cognitive dissonance based on the multiple representations). *Indonesian Science Education Journal*. **2016**, *5* (1), 54–62. https://doi.org/10.15294/jpii.v5i1.5790

Sabrina, R. Identification of Student Learning Difficulties in the Material of Chemical Bonds at SMAS Muslimat Samalanga Bireuen. Thesis, UIN Ar-Raniry Banda Aceh. 2018. https://repository.ar-raniry.ac.id/id/eprint/4610

Sahriani, C. Analysis of Learning Difficulties of Class X Mathematics and Natural Sciences Students of SMA Negeri 3 Tanjungpinang on Chemical Bonding Material. Thesis, Raja Ali Haji Maritime University. 2019. http://repositori.umrah.ac.id/id/eprint/1863

Yani, S.N.W. Diagnostics of the Relationship of Prior Knowledge with Learning Difficulties in Class X High School Chemistry Materials in Solok City. Thesis, Padang State University; 2018. http://repository.unp.ac.id/id/eprint/24849

Eclet. Quim. 49 | e-1561, 2024

Original Article, Education in Chemistry and Correlated Areas

https://doi.org/10.26850/1678-4618.eq.v49.2024.e1561

Effects of small-scale chemistry STEM integrated with local contexts for enhancing grade 11 students' learning achievement and learning and innovation skills

Ratanaphun **Utmeemang**[1], Khajornsak **Buaraphan**[2+]

Abstract

This study aimed to; a) create the context-based small-scale chemistry STEM (CSSC-STEM) Model; and b) examine the effects of the CSSC-STEM model on students' learning achievements and learning and innovation skills. The research methodology was Research and Development (R&D). In R1D1, 60 chemistry teachers and 136 students responded to reflect problems and needs about teaching and learning chemistry. In R2D2, 43 and 41 Grade 11 students were in an experiment and control groups, respectively. In R3D3, 40 and 36 students were in the experiment and control groups, respectively. The results showed that the experiment group had higher learning achievement in Rate of Chemical Reactions ($t = 7.599$, $p < 0.05$) than the control group. In addition, the experimental group had higher critical problem-solving skills ($t = 20.968$, $p < 0.05$) and creative thinking skills ($t = 23.168$, $p < 0.05$) than control group. The experiment group also gradually improved communication and teamwork skills throughout the model. The R3D3 results aligned with R2D2 showing the reliability of the CSSC-STEM model.

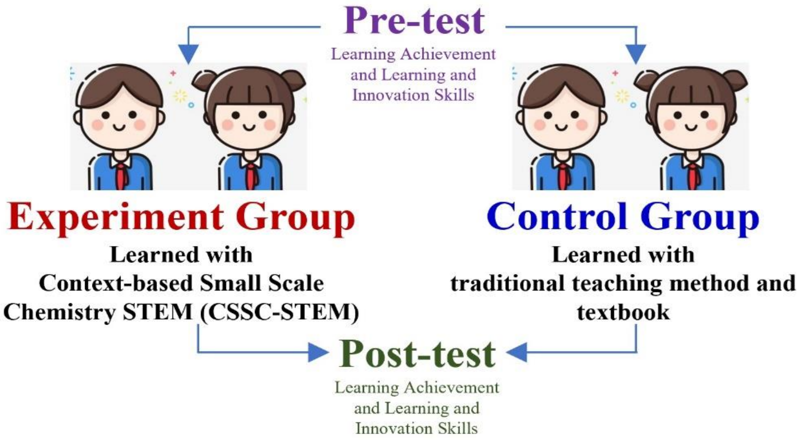

Article History

Received May 05, 2024
Accepted August 07, 2024
Published October 15, 2024

Keywords

1. STEM education;
2. small scale laboratory;
3. educational strategies;
4. educational needs;
5. learning and innovation skills

Section Editor

Habiddin Habiddin

Highlights

- CSSC-STEM is a new model.
- CSSC-STEM enhanced student learning and innovation skills.

CONTENTS

[1]Srisawatwittayakarnchangwatnan School, Nan, Thailand. [2] Mahidol University, Institute for Innovative Learning, Nakhon Pathom, Thailand. +Corresponding author: Khajornsak Buaraphan, Phone: +66829235156, Email address: khajornsak.bua@mahidol.ac.th

1. Introduction

From the past to the present, science has held a pivotal role in our societies, encompassing various aspects of our everyday lives. The synergy between scientific advancement and human creativity has led to the emergence of technologies that enhance our efficiency and effectiveness in both our personal and professional endeavors. The body of scientific knowledge equips individuals with a heightened understanding of natural phenomena, fostering greater awareness. Furthermore, the scientific process fosters the development of diverse cognitive skills such as logical, creative, analytical, and critical thinking, while also nurturing practical proficiencies including problem-solving, inquiry, and decision-making capabilities.

Science plays a crucial role, particularly in enhancing our capacity to make well-informed decisions grounded in reliable and empirical evidence. It contributes to the formation of a modern societal culture referred to as the "Knowledge-based Society". Given the paramount significance of science as highlighted earlier, it is imperative that everyone strives to become scientifically literate. A scientifically literate individual not only possesses foundational scientific knowledge about natural phenomena and human-made technologies but also can logically and ethically apply this scientific knowledge to their everyday life, thus enabling them to navigate the complexities of the world. These attributes of scientific literacy within individuals contribute to the responsible application, sustainable upkeep, and progressive development of both the natural environment and its resources. This comprehensive perspective nurtures a harmonious and enduring coexistence with our environment (Institute for the Promotioin for Promotion of Teaching Science and Technology (Chanprasert, 2014)).

The paramount importance of science accentuates the crucial need for effective science education. However, the process of teaching and learning science in Thailand is still confronted by various difficulties and obstacles. The results of the Ordinary National Education Test (O-NET) in Grades 10-12 science subjects throughout the academic years of 2014-2016 remained persistently below the expected threshold, registering at 32.54%, 33.40%, and 31.62% respectively, all falling short of the established standard (National Institute of Educational Testing Service (Public Organization) (NIETS), 2017). The National Education Plan B.E. 2560-2579 (A.D. 2017-2036) further highlights the ongoing dissatisfaction with the outcomes of educational advancement, given that students' learning achievements continue to fall below both established standards and the performance of other Asian countries. Despite a growing inclination among students to seek out additional knowledge, there remains a deficit in their capacity to effectively organize and synthesize the gathered information (Office of the Education Council (ONEC), 2002). Relying solely on lecture-based instruction might prove inadequate in enabling students to fully grasp the intended subject matter, potentially resulting in both inadequate content acquisition and a sense of disinterest towards science learning (Passakchai and Kuno, 2015). This, in turn, can contribute to a diminished enthusiasm for pursuing further studies in the domains of science and mathematics.

The aforementioned phenomenon highlights an issue within science education in schools, potentially resulting in a deficiency of motivation for students to engage in science learning. Additionally, this situation can hinder the establishment of connections between scientific knowledge and its practical applications in daily life, as well as its relevance to future pursuits and careers. Hence, the Ministry of Education is actively engaged in revising the Basic Education Core Curriculum, with the aim of aligning it more effectively with the development and preparation of students as valuable human resources for the 21st-century global landscape. The focus lies in fostering a meaningful comprehension of science among students while nurturing the essential 21st-century skills vital for both their personal and professional lives.

To achieve these objectives and enhance the country's competitiveness in the face of evolving science and technology, an integrative curriculum has been proposed. This curriculum, designed to span both individual subjects and their intersections, presents a strategic solution for addressing the aforementioned goals (Ministry of Education, 2017). One of the prominent approaches within the integrative curriculum is STEM (Science, Technology, Engineering, and Mathematics) education. Various studies indicate that STEM education has demonstrated a notable enhancement in students' learning achievements when compared to conventional teacher manual-based teaching approaches (Khammamung, 2017; Wicheansang *et al.*, 2018; Khonchaiyapham, 2017; Poonruang, 2016; Saengpromsri, 2015). Consequently, an imperative step is to encourage science educators to embrace and implement STEM education not only in the realm of teaching science but also in related subjects.

Numerous research studies corroborate the assertion that STEM education ignites a heightened enthusiasm for learning, fostering a willingness to tackle challenges, and bolstering students' self-assurance as they engage with science at advanced levels and in subsequent educational endeavors (Pornthip Siripithrachai, 2017: 50). Notably, Khammamung (2017) examined the impact of STEM education on Grade 10 students' comprehension and critical thinking in the context of chemistry reactions was examined. Her findings unveiled that STEM education contributed to a heightened eagerness for learning and facilitated the interlinking of science, technology, engineering, and mathematics knowledge. Additionally, students demonstrated increased engagement with the subject matter and a propensity for collaborative work within groups. This approach resulted in a statistically significant elevation in students' learning achievement and critical thinking skills at a level of significance of .01. Furthermore, Poonruang (2016) found that Grade 11 students, upon exposure to STEM education, exhibited greater advancements in learning achievement and problem-solving prowess within the realm of chemical life topics, compared to their previous achievements at a .05 statistical significance level. Additionally, STEM education was instrumental in elevating Grade 11 students' learning achievement, science process skills, and positive attitudes toward learning chemistry to a level significantly surpassing the outcomes of traditional teaching methods (Saengpromsri, 2015). Furthermore, in the research by Ketsrisakda *et al.* (2017), the experiment group of students who received instruction through STEM education demonstrated superior learning achievement compared to their previous levels at a 0.05 statistical significance level. Importantly, the same experiment group outperformed the control group, which was taught through conventional methods, in terms of learning achievement, also reaching a 0.05 statistical significance level.

Among the myriad skills encompassed by the 21st-century repertoire, learning and innovation skills take a pivotal stance for students in this era, as these proficiencies prove essential for navigating the complexities of contemporary lives and future careers. The evolving landscape demands a skill set that transcends the conventional, an exigency aptly addressed by learning and innovation skills. Nevertheless, the revelations drawn from the ONET (Ordinary National Education Test), and PISA (Programme for International Student Assessment) assessments of Thai students highlight a concerning trend. Students' ONET scores manifest a deficiency, while their PISA scores left behind those of other countries with similar Gross Domestic Product (GDP) standings (National Education Plan B.E. 2560-2579 (A.D. 2017-2036). The roots of these challenges are multi-fold. One significant contributor lies in the students' disproportionate focus on university entry facilitated by tutoring, which might inadvertently undermine self-regulated learning, problem-solving capabilities, as well as communication and creativity skills. The curriculum and learning systems also merit scrutiny, as they tend to disproportionately emphasize content absorption and the rote memorization of information. Consequently, this emphasis tends to overlook the holistic development of skills. The result is a student body lacking proficiencies in creative thinking, innovative approaches, analytical and synthetic reasoning, and effective learning strategies. A noteworthy contributing factor lies in the students' disproportionate concentration on university admission, often facilitated by tutoring, inadvertently eroding their self-regulated learning, problem-solving abilities, and even communication and creativity skills. Moreover, the scrutiny of curricula and learning systems is warranted, as they tend to place undue emphasis on mere content assimilation and rote memorization. Consequently, this emphasis undermines the comprehensive development of skills. The outcome is a student populace deficient in essential proficiencies, encompassing creative thinking, innovative approaches, analytical and synthetic reasoning, as well as effective learning strategies (Chulawattanatol, 2013).

Penratanahiran and Thongkham (2011) explored the challenges faced by primary school students in relation to the 4Cs: Critical thinking, Communication, Collaboration, and Creativity. The findings illuminated several areas of concern. Specifically, in the domain of Critical thinking, it was evident that students displayed shortcomings in observation and problem-solving skills. Their grasp of analytical, logical, and critical thinking was also deficient. This deficiency was exemplified by students' inability to assess the reliability of data sources and their tendency to overlook the search for pertinent information, thus culminating in decisions that were not well informed. Furthermore, the students demonstrated a lack of proficiency in systematic problem planning and resolution, as well as an inability to conceive fresh approaches when addressing the challenges at hand.

In terms of Communication, a notable deficiency was observed among students, particularly in their understanding and practical application of effective communication techniques. They exhibited challenges in employing suitable language for reading, writing, and speaking contexts. Furthermore, they struggled with competently receiving and comprehending the nuances of conveyed messages. A distinct lack of self-assuredness was evident when expressing themselves to others, notably during classroom presentations. Moreover, it was apparent that students sometimes intertwined their viewpoints with factual data, inadvertently leading to misunderstandings among their audience about the intended message.

In the realm of Collaboration, students displayed a tendency towards self-centeredness, often at the expense of acknowledging and respecting their peers' opinions and capabilities. Their capacity to engage effectively in group dynamics was notably compromised. They struggled when it came to cooperative endeavors such as joint planning, decision-making, and task execution within teams. While a subset of students exhibited some proficiency in teamwork, their ability to adapt or seamlessly transition into diverse situations or groups remained a challenge. Additionally, certain students encountered communication barriers stemming from differences in racial backgrounds and languages, further complicating the collaborative process. Additionally, certain students encountered communication barriers stemming from differences in racial backgrounds and languages, further complicating the collaborative process.

Addressing creativity, a prevalent trend was the students' deficiency in generating novel ideas, which often stemmed from their limited reservoir of supporting knowledge and experiences. Furthermore, they exhibited an insufficiency in self-efficacy related to creative thinking, frequently experiencing uncertainty due to their perceived inadequacy and apprehensions about encountering failure. The classroom environment, largely characterized by its teacher-centric nature, also exerted an influence on students' creative tendencies. In such settings, students frequently awaited instructions from the teacher instead of independently contemplating solutions. Consequently, students often retreated to the safety of their comfort zones, foregoing ventures into imaginative and creative thinking. This inadvertently hindered their capacity to think outside the conventional framework and inhibited the demonstration of their creativity and innovative ideas.

In the present era, our society is undergoing profound and constant transformations, primarily driven by the rapid progress of information and communication technology. This advancement has catalyzed the swift dissemination of new information and knowledge on a global scale. Consequently, a significant responsibility rests upon the government's shoulders: that of nurturing a human resource equipped with the vital 21st-century skills, essential for thriving in an ever-evolving landscape. Recognized as a potent pedagogical approach, STEM education has garnered widespread acceptance for its capacity to cultivate the 21st-century skills among students (Gonzalez and Kuenzi, 2012; Samahito, 2014; Siriphatrachai, 2013; Chulawattanatol, 2013; Seneewong, 2013; Acharry, 2019; Chanprasert, 2014).

In Thailand, STEM education has gained prominent recognition as a pedagogical approach integral to preparing young Thais for the future. Since 2013, it has been progressively integrated into science education across the nation (Siriphatrachai, 2013). STEM education is centered on fostering a cohesive approach to teaching, amalgamating the disciplines of Science, Technology, Engineering, and Mathematics. Students engaged in STEM education are proactively encouraged to tackle real-world challenges, applying the engineering design process to create innovative solutions and construct knowledge autonomously (Pudcha, 2016).

The essence of STEM education lies in nurturing an active and inquisitive mindset within students, emboldening them to embrace challenges and cultivate the self-assurance required to pursue advanced scientific learning (Siriphatrachai, 2013). As an educational paradigm, STEM education stands as a catalyst for the development of creative thinking, higher-order cognition, and 21st-century skills (Chanprasert, 2014). The implementation of STEM education commences by immersing students in locally relevant issues they are familiar with. This approach allows for the construction of new knowledge by challenging existing perspectives and prior experiences. Moreover, it empowers students to seamlessly integrate newfound knowledge into their daily lives, thus imparting a profound sense of meaning to their learning.

Regarding the teaching and learning of chemistry within the educational context of Thailand, a prevalent issue persists in most chemistry classrooms concerning laboratory activities. This predicament stems from the scarcity of laboratory equipment and the overwhelming student-to-classroom ratio. With laboratory resources often only accommodating two to three student groups, the limitations in equipment hinder the practical aspect of learning. In response, educators commonly resort to demonstrations and lectures to convey laboratory concepts. Regrettably, this approach gives rise to subsequent complications, notably a deficiency in students' hands-on experience with chemistry experiments and a lack of proficiency in scientific processes. Additionally, the majority of chemistry experiments featured in textbooks adhere to traditional methodologies, emphasizing stringent procedures to save time during experimentation.

A solution to this challenge emerges in the form of Small-Scale Chemistry (SSC) (Tamuang *et al*., 2017), a novel approach to conducting chemistry experiments. SSC offers several advantages, primarily centered around safety, cost-effectiveness, convenience, and efficiency. By utilizing smaller quantities of chemicals and repurposing containers, SSC utilizes familiar substances and materials drawn from students' daily lives. This approach also minimizes the exposure to hazardous chemicals like acids and bases, subsequently reducing the potential risks associated with their usage. Notably, SSC enables teachers to better manage situations involving potential chemical leaks, given the diminished quantities employed. Embracing SSC empowers chemistry educators with heightened control over laboratory proceedings, cultivating an environment that seamlessly combines efficiency with enhanced safety measures (Loei Rajabhat University, 2018; Acharry, 2019). Through SSC, the barriers posed by limited resources and large classroom sizes are mitigated, empowering educators to provide students with a more engaging and practical chemistry education.

The existing challenges in the realm of chemistry education in Thailand underscore the need for a fresh approach that can truly align with the intended educational objectives. In light of this, chemistry educators should embark on an exploration of diverse and impactful teaching methodologies that place student-centered learning at the forefront. Vital to this transformation is the provision of direct experiences and opportunities for self-directed learning and the active construction of knowledge, employing the scientific method and its associated processes. To raise the bar of chemistry education, the cultivation of innovative teaching strategies becomes paramount within the field.

Given the aforementioned challenges, a pedagogical breakthrough in chemistry education manifests in the context-based small scale chemistry STEM (CSSC-STEM) model. This innovative framework advocates for the seamless integration of SSC with STEM education, harnessing real-world scenarios and localized contextual challenges as effective conduits for learning and understanding. Through this model, the barriers to engaging chemistry education are dismantled, paving the way for a more dynamic and meaningful learning journey.

The challenges associated with teaching and learning chemistry in Thailand indicate that past efforts have not successfully met the established goals. To address this, chemistry educators should explore a range of effective teaching methods that prioritize student-centered learning. It is imperative to offer students more direct experiences and occasions for autonomous learning and knowledge construction, employing the scientific method and processes. To elevate the standard of chemistry education, the development of innovative teaching methods in the field is essential. Given the previously highlighted challenges, a pedagogical innovation for chemistry education emerges in the form of the context-based small scale chemistry STEM (CSSC-STEM) model. This model advocates the integration of SSC with STEM education, utilizing real-life situations and local contextual problems to facilitate effective learning.

2. Literature review

2.1. STEM education

The National Education Act of 1999, Section 24(1), emphasizes that educators must align the content and activities with the interests and aptitudes of students, taking into consideration individual differences. It underscores the need for teachers to cultivate skills, thinking processes, management strategies, problem-solving abilities, and the application of knowledge through real-life situations. Additionally, it encourages a focus on hands-on learning, practical exercises, critical thinking, action-based learning, cultivating a love for reading, and fostering continuous curiosity (National Education Act, 1999: 8).

Further elaborated in the revised version (Edition 2) of the National Education Act of 2002, Section 22 states that education must be founded on the principle that every student possesses the capability to learn and develop themselves to the best of their potential (National Education Act, 2002). IPST (2017) recognizes the significance of science education and acknowledges its paramount aim to achieve the most substantial impact on learners. Accordingly, it has established measurement criteria and core learning content for the science curriculum, following the 2008 Basic Education Core Curriculum (B.E. 2551). This curriculum outlines the objectives of science education, emphasizing a focus on self-discovery for learners, aiming to derive knowledge primarily through processes such as observation, investigation, experimentation, followed by the systematic organization of acquired results into principles, concepts, and foundational knowledge. The goal of science education is to integrate knowledge and understanding into beneficial applications for society and daily life, while also nurturing critical thinking, imaginative capabilities, problem-solving skills, communication skills, and decision-making abilities (Ministry of Education, 2017: 3).

Numerous pedagogical approaches align with the student-centered approach, and all of them are crafted to cultivate the growth of 21st-century skills. STEM education stands out as one of these approaches. STEM education is a learning approach that arises from the integration of knowledge in the fields of science, technology, engineering, and mathematics, employing engineering processes. It emphasizes having learners apply theoretical knowledge to solve real-life problems and develop novel processes or products for the benefit of society. This method encourages learners to recognize the significance of science and technology knowledge, which forms essential foundational skills for daily life, occupational pursuits, and national development (Ministry of Education, 2013: 16; Saneewong, 2013: 30; Siriphatrachai, 2013: 49; Thongchai, 2013; Chanprasert, 2014; Somahito, 2014).

Implementing education based on the STEM approach involves various concepts and characteristics. It integrates different disciplines, including science (S), technology (T), engineering (E), and mathematics (M), by synergizing the strengths of each field's nature and teaching methodologies. This aids students in creating connections between the content of these four subjects and everyday life and professional practices. It places emphasis on skill development for the 21st-century, challenges students' thinking, provides opportunities for students to express their opinions, and prioritizes the learner. The teaching format encourages thinking and planning, employing a step-by-step process. This teaching methodology promotes comprehensive development in various aspects among students, aligning with the direction of developing quality individuals in the 21st-century (Siriphatrachai, 2013; Thongchai, 2013).

Many educators have proposed steps in teaching by STEM education (Lou *et al*., 2011; National Research Council, 2012; Schachter, 2012; National Center for STEM Education of Institute for the Promotion of Teaching Science and Technology, 2015; Thongchai, 2013). The authors analyzed the common teaching steps of STEM education, and the outcome has been summarized in **Table 1**.

Table 1. Common teaching steps of STEM education.

Lou *et al*. (2010)	**Schachter (2012)**	**National Institute for STEM Education (2014)**	**National Research Council (2012)**	**Apisit Thongchai (2013)**	**Common teaching stepts of STEM education**
Identify a problem	Pose a question	Identify a problem	Identify a problem	Identify a problem or need	Identification of the problem in local context
Explain the problem	Imagine	Gather data and relevant ideas related to the problem	Explore correct idea	Gather information	Gather data and relevant ideas
Plan	Plan	Plan to solve the problem	Plan and develop	Desigan and choose method	Problem-solving Design
Follow the plan	Construct	Desigan a method to solve the problem		Act	Practice
Evaluate	Revise	Test, evaluate and refine problem-solving methods to improve results	Test and evaluate	Test, revise, and evaluate	Test, improvement and evaluation
		Present problem-solving methods and the results	Present problem-solving results		Presentation

2.2. Small scale chemistry

Small scale chemistry (SSC) has been developed from Microscale experiments, which originated in 1983 and were first introduced at the college level. It was initially applied to organic chemistry experiments for students. Subsequently, its utilization expanded across college and university levels in more than 400 institutions in the United States. SSC is, therefore, a modern instructional method for conducting chemical experiments, focusing on safety, cost-efficiency, convenience, and speed. This approach involves utilizing smaller quantities of chemicals and repurposing containers, which are reusable materials that hold the chemicals during experimentation. These containers are portable, and many of the materials used for chemical reactions are ones that students encounter in their daily lives. By employing minimal amounts of chemicals, the chances of students and teachers coming into contact with hazardous substances are significantly reduced. In the event of a spill or leakage, the impact is relatively mild compared to experiments that involve larger quantities of chemicals. This allows for quicker mitigation of any situations that may arise. Kellly and Finlayson (2022) mentioned that SSC involves minimizing the quantity of chemicals used in experiments while still yielding satisfactory results. This practice aims to maintain environmental sustainability and prevent pollution by utilizing minimal quantities of chemicals without compromising quality, accuracy, and precision. This approach can reduce chemical usage by up to 80-90%. As a result, SSC offer a higher level of safety compared to traditional chemical experiments and require less time for experimentation. This method has been endorsed by various sources (Rajabhat Loei University, 2021) as a safer and more time-efficient alternative to current chemical experimentation practices. Furthermore, it contributes to a reduction in the volume of hazardous chemical waste (Wood, 1990). The instructional technique concerning SSC Presently, SSC is increasingly incorporated into high school-level experimentations due to the advantages it offers. SSC is recognized for its time efficiency, safety, and reduced costs since it requires minimal quantities of chemicals. (Tontayanon, 2011; Singhet *et al*., 1999).

The application of SSC techniques can be effectively integrated into teaching chemistry at both the secondary and tertiary education levels. This approach offers various advantages, including reduced experimentation time and ease of equipment cleanup. Consequently, educators can incorporate experiments more frequently, allowing more time for collaborative classroom discussions of experimental outcomes. Safety during experimentation is enhanced, while costs associated with chemical procurement and disposal are minimized. Notably, every student in the classroom has the opportunity to conduct experiments individually, eliminating the need for group-based experiments. This method is adaptable to students of all ages and aptitudes, resulting in significant learning outcomes comparable to traditional laboratory experiments. Therefore, SSC has the potential to yield numerous benefits, including the development of scientific process skills and analytical thinking in students, providing them with direct experiential learning.

3. Methodology

This study employed a Research and Development (R&D) methodology in three cycles, namely R1D1, R2D2, and R3D3. R1D1 was conducted during the academic year 2019, from October 2019 to March 2020. R2D2 took place in the first semester of the academic year 2020, from July to August 2020. Finally, R3D3 was carried out in the first semester of the academic year 2021, from July to August 2021. The details of R1D1, R2D2, and R3D3 can be illustrated as follows.

3.1. R1D1

3.1.1. R1

The first R&D cycle has been occurred in the 2nd semester of 2019 academic year at Srisawatwittayakarnchangwatnan School, Nan Province, Thailand. This cycle aimed to explore teachers' and students' perspectives on current state, problems and needs of teaching and learning about chemistry.

3.1.2. Population and sample

3.1.2.1. Teachers

The population consisted of 60 chemistry teachers within the Nan Educational Area Office's jurisdiction, located in Nan Province, Thailand. Data were gathered from the entire population.

3.1.2.2. Students

The population comprised 204 Grade 11 students who were enrolled in the 2nd semester of the 2019 academic year at Srisawatwittayakarnchangwatnan School in Nan Province, Thailand. The sample consisted of 136 Grade 11 students who had previously studied chemistry using the SSC approach on chemical reaction rates during the 1st semester of the 2019 academic year.

3.1.3. Data collection

The questionnaires investigating the viewpoints of both teachers and students regarding the current state, problems and needs of teaching and learning chemistry comprised three main sections: a) background; b) perspectives on the current state, problems and needs of teaching and learning chemistry; and c) Suggestion for improving teaching and learning chemistry. The perspectives on the current state of teaching and learning chemistry were consisted of 8 items; the perspectives on the problems of teaching and learning chemistry were consisted of 7 items; and the perspectives on the needs of teaching and learning chemistry were consisted of 8 items.

The questionnaires exploring the teachers' and students' perspectives on the current state, problems and needs of teaching and learning chemistry utilized a five-point survey scale, encompassing options from strongly disagree (1), disagree (2), neutral (3), agree (4) to strongly agree (5).

The teachers' and students' perspective on current state, problems and needs of teaching and learning about chemistry questionnaires was validated the congruence between the questions and the objectives (Index of Item-Objective Congruence: IOC) by a panel of five experts. The IOC of questionnaire items related to current state, problems and needs of teaching and learning about chemistry was 1.00 that were acceptable. The researcher has revised and improved the questionnaire according to the recommendations of experts. Subsequently, the researchers tried out the current state, problems and needs of teaching chemistry questionnaire (Teacher Version) with 60 teachers. Then, the analysis was conducted to find reliability by calculating Cronbach's alpha coefficient, which equals 0.83, that was acceptable. In addition, the researchers tried out the current state, problems and needs of learning chemistry questionnaire (Student Version) with 136 individuals, who had previously learned through STEM education or had experience with SSC. The analysis was conducted to find reliability by calculating Cronbach's alpha coefficient, which equals 0.81, that was acceptable.

3.1.4. Data analysis

The data derived from the questionnaires exploring the teachers' and students' perspectives on the current state, problems and needs of teaching and learning chemistry were analyzed for frequency, percentage, mean and standard deviation (SD). Then, the authors interpreted the mean range of each item and the overall in three dimensions, i.e., current state, problems and needs.

3.1.5. D1

The authors developed the Context-based Small Scale Chemistry STEM (CSSC-STEM) model and asked five experts to validate its Suitability, Correspondence, Feasibility, and Potential Benefits. The results affirmed that the CSSC-STEM model was qualified. Therefore, the CSSC-STEM model was implemented with the experiment group and examined its effects on their learning achievement and learning and innovation skills in the R2D2 loop.

3.2. R2D2

3.2.1. R2

In this R&D loop, the independent variable was the utilization of the Context-based Small Scale Chemistry STEM (CSSC-STEM) model. The dependent variables were students' learning achievements as well as learning and innovation skills. The content used in this study is the chemical reaction rate in the chemistry subject at the Grade 11 level, according to the Basic Education Core Curriculum B.E. 2551 (Revised Version, B.E. 2560). The instruction time for teaching this content was a total of 24 hours.

3.2.2. Population and sample

The population consisted of 224 Grade 11 students who were enrolled in the second semester of the 2019 academic year at Srisawatwittayakarnchangwatnan School, Nan Province, Thailand. A sample of 84 Grade 11 students was randomly selected from two classrooms. The sample was chosen through Cluster Random Sampling, with classrooms as the sampling units. One classroom was randomly designated as the experimental group, while the other was randomly assigned as the control group. The experimental group, which engaged in learning through the Context-based small-scale chemistry STEM (CSSC-STEM) model, consisted of 43 students from Classroom 5/7. On the other hand, the control group, who followed the conventional approach using chemistry textbooks and manuals, was comprised of 41 students from Classroom 5/5.

3.2.3. Data collection

The authors created two major research instruments called the Learning Achievement Test and the Learning and Innovation Skills Test.

The Learning Achievement Test was a multiple-choice exam consisting of four options (a, b. c and d). It comprised the questions related to the rate of chemical reactions, totaling 40 questions. The exam duration is 45 minutes. It is administered both before and after each CSSC-STEM lesson. The exams for pre-lesson and post-lesson were the same set but with questions and options shuffled. The IOC of the learning achievement test ranged from 0.60 to 1.00 that was in acceptable level. In addition, the learning achievement test was piloted with 40 students, who had completed Chemistry. The item difficulty (p) and item discrimination (r) were calculated for each item. Only items with difficulty values between 0.20 and 0.80 and discrimination values above 0.20 were selected. Pre- and post-test exams consisted of 10 items each. In total, the Learning Achievement Test were consisted of 40 items. In addition, the researchers utilized

Lovett's method to establish the reliability of the test and found that the reliability of learning achievement test was 0.87, that was acceptable.

The learning and innovation skills test consisted of three major parts: a) critical thinking skills; b) creative thinking for innovation skills; and c) communication and collaboration skills. The details of each part were as follows.

The critical thinking skills (Learning Skills) test was in the form of an essay exam. Students were required to read the provided situations and answer questions based on them. The assessment of critical thinking skills is conducted both before and after each lesson, and the situations provided for each assessment were different. There were two situations, each with four essay questions, 16 questions in total. Each question is worth 4 points, with a maximum score of 32 points. The test duration is 30 minutes.

The creative thinking for innovation (Learning Skills) test was in the form of an essay exam. Students were required to read the provided situations and answer questions based on them. The assessment of creative thinking skills for innovation was conducted both before and after the lesson, and the situations provided for assessment were different. There were two situations, each with three essay questions, six questions in total. Each question is worth four points, with a maximum score of 24 points. The test duration is 30 minutes.

The communication and teamwork skills (Innovation Skills) test focused on assessing student behaviors in communication and teamwork practices. It included questions related to communication skills in speaking, writing, and comprehension (5 questions), and behaviors of collaboration with others emphasizing teamwork (6 questions). These are measured on a 5-level Likert scale ranged from consistently demonstrating the behavior, often demonstrating the behavior, sometimes demonstrating the behavior, rarely demonstrating the behavior, and never demonstrating the behavior (11 items in total).

The IOC of critical thinking skills test was 0.80 that was in acceptable level. The IOC of creative thinking for innovation skills test was 0.80 that was in acceptable level. Also, the IOC of communication and teamwork skills test ranged from 0.60 to 0.80 that was in acceptable level.

3.2.4. Data analysis

The researcher analyzed quantitative data using both descriptive statistics, including frequency, percentage, mean, standard deviation, and inferential statistics as independent t-test and dependent t-test.

3.2.5. D2

In the Development phase, the researchers employed the data from research 2 (R2) to improve the CSSC-STEM model and its associated lesson plans for improving Grade 11 students' academic achievement and their learning and innovation skills in the context of chemical reaction rates.

3.3. R3D3

The R3D3 cycle aimed to assess the consistency of the CSSC-STEM model in fostering students' academic achievements and enhancing their learning and innovation skills. As a result, the procedure of R3D3 replicated that of R2D2, albeit taking place in the subsequent academic year.

3.3.1. Population and sample

The study population included 216 Grade 11 students enrolled in the second semester of the 2021 academic year at Srisawatwittayakarnchangwatnan School, Nan Province, Thailand. A sample of 76 Grade 11 students was randomly selected from two classrooms through Cluster Random Sampling, using classrooms as the sampling units One classroom was randomly chosen to serve as the experimental group, while the other was randomly assigned as the control group. The experimental group comprised 40 students from Classroom 5/7, and the control group consisted of 36 students from Classroom 5/5.

3.3.2. Data collection and analysis

The R3D3 cycle aimed to assess the consistency of the CSSC-STEM model in fostering students' academic achievements and enhancing their learning and innovation skills. As a result, the procedure of data collection and analysis in R3D3 loop was replicated that of R2D2.

4. Results

4.1. Current state, problems and needs of teaching and learning chemistry

The teachers expressed their opinions about the current state, problems and needs of teaching and learning chemistry as Table 2.

Table 2. Teachers' opinions about the current state, problems and needs of teaching and learning chemistry.

Aspects	Mean	SD	Interpretation
Current state	3.98	0.86	High
Problems	3.95	0.88	High
Needs	4.43	0.59	High

The chemistry teachers expressed their opinions about the current state, problems and needs of teaching chemistry in the high (mean = 4.17, SD = 0.74), high (mean = 4.20, SD = 0.97) and very high (mean = 4.55, SD = 0.50) levels, respectively.

The students expressed their opinions about the current state, problems and needs of teaching and learning chemistry as Table 3.

Table 3. Students' opinions about the current state, problems and needs of teaching and learning chemistry.

Aspects	Mean	SD	Interpretation
Current state	3.51	0.92	High
Problems	3.63	0.94	High
Needs	3.77	0.90	High

The responding students reflected the high level of current state (mean = 3.67, SD = 0.91), problems (mean = 3.76, SD = 0.92) and needs (mean = 3.81, SD = 0.96) concerning learning chemistry.

4.2. Development of context-based small-scale chemistry STEM (CSSC-STEM) model

In this study, the researchers blended SSC and STEM education, incorporating various real-life situations within the students' local contexts through context-based learning (CBL). The researchers chose to incorporate chemistry content by aligning with chemicals, materials, and scenarios that closely relate to students' lives, such as cooking, baking, rusting, burning and so on. The laboratory activities created were partly restructured and partly refined from existing ones. The researcher chose to employ chemicals commonly found in daily life and utilized locally available materials and equipment. For instance, transparent drinking straws that had been used were repurposed as experimental tubes, and eggshells and seashells were used as substitutes for calcium carbonate. These materials were safe, cost-effective, and eco-friendly. They were adapted to suit the local context of the students. The teaching steps of CSSC-STEM model can be shown as **Table 4**.

Table 4. Summarized teaching steps of CSSC-STEM model.

Concept and Principle of STEM Education	STEM education is an approach that integrates knowledge from science, technology, engineering, and mathematics through engineering processes. It emphasizes having students apply theoretical knowledge to solve real-life problems and develop new processes or beneficial products. This leads to students recognizing the significance of scientific and technological knowledge, which are fundamental skills for sustainable living, professional careers, and national development.
Concept and Principle of SSC	SSC is a new teaching method for conducting chemical experiments that are highly safe, cost-effective, convenient, and fast. They make chemical experiments easily accessible, using minimal chemicals while maintaining quality, accuracy, and precision. The containers used to hold chemicals in these experiments are reusable materials that can be used again. They are easily transportable. Various materials used in conducting chemical reactions in these experiments are common items that students encounter in their daily lives.
Concept and Principle of context-based learning	CBL refers to the integration of various situations or events closely related to the students' real-life contexts. These connections aim to bridge classroom learning with real-life situations and challenges, thereby enhancing the students' abilities. By learning from diverse contexts that are interconnected with the chemistry knowledge to be imparted, students are encouraged to fully utilize their knowledge and thinking abilities. Moreover, they can effectively transfer these understandings to other situations or events.
Summarized teaching steps of CSSC-STEM Model	Identification of the problem in local context Gather data and relevant ideas Problem solving design Practice Test, improvement and evaluation Presentation

The following are descriptions of each teaching step of CSSC-STEM model.

Teaching step 1: Identification of the problem in local context

The teacher begins by evaluating students' existing knowledge through appropriate methods, ensuring they possess a solid foundation for upcoming material. Subsequently, the teacher introduces practical real-world challenges aligned with students' environment, employing captivating and fitting media or technology tailored to each unique problem context. Next, students individually pinpoint issues within situations that intrigue them, devising potential solutions before assembling into groups according to their preferences. In these groups, they collaboratively compile and evaluate problems, ultimately selecting a shared area of interest to tackle together.

Teaching step 2: Gather data and relevant ideas

Each student group collaboratively compiles relevant information and scientific ideas that pertain to problem-solving methodologies in science, mathematics, and technology, which are applicable to the selected issue. Concurrently, they establish the problem's objectives and scope, while also scrutinizing the conditions and limitations that come with solving it. Diverse educational materials, such as textbooks, online resources, and informational sheets, can be utilized for data collection. Additionally, the teacher employs concise chemical experiments to enhance students' comprehension, thereby contributing to the development of forthcoming problem-solving strategies.

Teaching step 3: Problem-solving design

In each student group, they collaboratively devise potential problem-solving methodologies by applying the information collected from the preceding steps. This involves considering locally available materials, situational constraints, and conditions, while also evaluating the feasibility of each approach. Eventually, the best problem-solving approach is selected for designing the project. Subsequently, the groups jointly establish a sequence of steps for crafting the project, followed by individual student presentations to the class. This allows the teacher and peers to inquire, provide suggestions, and offer additional problem-solving insights. Students then take this feedback to refine and enhance their problem-solving method design.

Teaching step 4: Practice

Students in each group proceed to create projects or develop methods according to the problem-solving steps they have designed. The teacher supervises the group work and provides guidance if students encounter challenges while crafting their projects or refining methods for problem-solving.

Teaching step 5: Test, improvement, and evaluation

Students conduct testing on their projects or problem-solving methods and subsequently evaluate the outcomes to pinpoint opportunities for enhancement and growth, ensuring the efficacy of their problem-solving endeavors. The iterative process of testing and refining projects or problem-solving methods can be executed multiple times within the allocated timeframe. The teacher underscores the significance of carefully recording testing outcomes and the specifics of each modification undertaken, facilitating the utilization of this data for forthcoming presentations.

Teaching step 6: Presentation

Each group of students presents their projects or problem-solving methods along with the relevant principles or design concepts. After the presentation, classmates collectively ask questions, discuss, and provide suggestions to enhance the projects or problem-solving methods. The teacher encourages an interactive and creative presentation atmosphere.

The researchers presented the CSSC-STEM model to a panel of five experts to evaluate its quality in four aspects: suitability, correspondence, feasibility, and potential benefits. The results of expert evaluation of the CSSC-STEM model are shown in Table 5.

Table 5. Assessment of the CSSC-STEM Model's quality by a panel of experts.

Item	Statement	Mean	SD	Interpretation
	Suitability			
1.	The CSSC-STEM model is aligned with the utilized concepts/theories in its development.	4.40	0.49	High
2.	The CSSC-STEM model is suitable for improving learning outcomes.	4.40	0.49	High
3.	The CSSC-STEM model is suitable in developing students' learning and innovation skills.	4.20	0.75	High
4.	The component of CSSC-STEM mode is suitable.	4.40	0.49	High
5.	The CSSC-STEM model is suitable for further development and dissemination on a broader scale.	4.60	0.49	Very high
6.	The teaching steps of CSSC-STEM model are undertaken through appropriate analysis and synthesis.	4.60	0.49	Very high
	Overall average in suitability	**4.43**	**0.56**	**High**
	Correspondence			
7.	The CSSC-STEM model is corresponded with the current state of instructional management issues.	5.00	0.00	Very high
8.	The CSSC-STEM model is corresponded with the needs of current teaching management.	4.40	0.49	High
9.	The CSSC-STEM model is corresponded to the development of learning quality according to the curriculum.	4.40	0.49	High
10.	All components of the CSSC-STEM model have internal correspondence.	4.60	0.49	Very high
11.	The synthesized teaching steps of CSSC-STEM model are aligned with the CSSC-STEM conceptual framework.	4.20	0.40	High
	Overall average in correspondence	**4.52**	**0.50**	**Very high**
	Feasibility			
12.	The CSSC-STEM model shows its creativity.	5.00	0.00	Very high
13.	The CSSC-STEM model is possible for application.	4.40	0.49	High
14.	The CSSC-STEM model is possible in developing students' learning achievement.	4.20	0.40	High
15.	The CSSC-STEM model is possible in developing learning and innovation skills.	5.00	0.00	Very high
16.	The CSSC-STEM model has its potential for application in other educational institutions.	4.20	0.75	High
	Overall average in feasibility	**4.56**	**0.57**	**Very high**
	Potential benefits			
17.	The CSSC-STEM model is beneficial for improving the quality of instructional management.	4.20	0.75	High
18.	The CSSC-STEM model is beneficial for developing students' learning achievement.	4.40	0.49	High
19.	The CSSC-STEM model is beneficial for developing learning and innovation skills.	4.60	0.49	Very high
20.	The CSSC-STEM model is beneficial for other teachers in the same subject.	4.60	0.49	Very high
21.	The CSSC-STEM model is beneficial for other teachers in the different subjects.	4.40	0.49	High
	Overall average in potential benefits	**4.44**	**0.57**	**High**

The experts evaluated the quality of CSSC-STEM model regarding its suitability, correspondence, feasibility, and potential benefits in High (mean = 4.43, SD = 0.56), Very high (mean = 4.52, SD = 0.50), Very high (mean = 4.56, SD = 0.57) and high (mean = 4.44, SD = 0.57) levels, respectively.

The researchers utilized the CSSC-STEM model to create four instructional plans, totaling 24 teaching hours, i.e., meaning of the rate of chemical reaction (6 h), concepts and energy involved in chemical reactions (4 h), factors affecting the rate of chemical reactions (6 h), and fermented pork sausage: like and sure (8 h).

In translating the CSSC-STEM model into practice, the researchers would like to present an example of lesson plan on the factors affecting the rate of chemical reactions as follows.

Teaching step 1: Identification of the problem in local context

The teacher presents video clips relevant to student contexts, illustrating the factors that influence the rate of chemical reactions.

From Video Clip 1, two individuals are washing dishes. Person 1 takes dishwashing liquid from a bottle using a teaspoon and adds it to a foam of water. They use it to remove grease from a plastic dish. Person 2 also takes dishwashing liquid from a bottle using a teaspoon and mixes it with water. They pour the mixture onto the foam to clean the greasy residue from the plastic dish. Students predict the outcome of the cleaning process, considering the differences in how person 1 and person 2 washed the dish, and explain the reasons behind it.

In Video Clip 2, there are two bundles of "Cha-om" (in Thai) or Chinese chives (garlic chives). One bundle was placed inside a refrigerator, while another placed outside the refrigerator. Students are asked to predict the outcome after leaving them for one day and explain the reasons behind it.

From Video Clip 3, salt crystals and finely ground salt are placed in two plastic glasses. Students are asked to predict the outcome of the experiment and explain the reasons behind it.

Students should be able to conclude that factors affecting the rate of chemical reactions include increasing concentration, increasing surface area, and raising the temperature. These are important factors that contribute to the faster occurrence of chemical reactions. However, sometimes following these methods can lead to time and cost inefficiencies. For instance, in reactions that require acids as starting materials in a production process, increasing the reaction rate by enhancing the acid concentration would result in higher costs. Additionally, dealing with the excess acid left after the reaction would require neutralization before disposal, leading to increased expenses. Similarly, if the reaction rate is increased by raising the temperature, it could lead to increased fuel consumption, making it impractical. Therefore, enhancing the concentration of starting materials or raising the temperature might not always be suitable for promoting rapid reaction rates.

Teaching step 2: Gather data and relevant ideas

The teacher sets the context for students to identify problems and define the requirements for problem-solving.

Student A will prepare a meal which is pineapple curry with boiled meat and eggs. Before starting, she prepares the ingredients in two separate bowls for convenience in cooking. In a small bowl, she puts pineapple juice, and in a larger bowl, she places chopped pineapple and sliced meat, with some parts of the meat mixed with the pineapple. While waiting for the cooking time, she peels the boiled eggs to prepare for consumption. By chance, the eggshell pieces fall into the pineapple juice in the bowl prepared to be used in the curry. She notices that gas bubbles start to form rapidly, and within a minute, the smaller eggshell pieces disappear. When she eats the pineapple curry, she notices that some meat pieces are tender while others are chewy, even though they come from the same meat. Curious about these two events, the students wonder why the smaller eggshell pieces disappeared in the pineapple juice in a shorter time compared to the larger pieces, and why some meat pieces are tender while others are chewy. She speculates that there might be something causing the eggshell to react differently in the pineapple juice and that mixing pineapple with the meat might influence the tenderness. To address these questions, the students plan to conduct experiments using household materials to investigate both scenarios.

The teacher instructs each student group to practice identifying problems and conditions on Activity Sheet related to finding factors affecting the rate of chemical reactions. The following is one example.

Identify the problem: How can the eggshell undergo a reaction in orange juice, resulting in varying rates of reaction, and why do certain pieces of the egg have different levels of firmness and stickiness?

Factors or Conditions: Conduct an experiment using household materials to address both suspected scenarios. There must be certain elements that cause the eggshell to react differently in orange juice, resulting in varying rates of reaction. Additionally, examine whether the presence of pineapple mixed with the egg has an impact on the texture and stickiness of the eggshell or if other factors influence the texture of the eggshell.

Each student group collaboratively gathers information and scientific ideas related to problem-solving approaches in chemistry, mathematical principles, and relevant technologies. These are pertinent to the selected problem-solving strategies derived from the contextual factors that influence chemical reactions. This enables students to comprehend the issues they have chosen and determine the objectives of problem-solving, problem scope, and analyze conditions or constraints involved. Each group is tasked with researching information from various sources such as the internet, textbooks, library resources, and knowledge sheets. They should outline the sequence of study for each activity and knowledge sheet to extract relevant data while indicating the sequence for effective learning.

The teacher distributes the experiment sheet: Calcium carbonate ($CaCO_3$) and acetic acid (CH_3COOH) affecting the chemical reaction. The purpose of this activity is to guide students in planning the experiment and ensuring they have all the necessary apparatuses ready.

The students are directed to follow the steps outlined in the experiment sheet and conduct the experiment regarding the factors influencing the chemical reaction between calcium carbonate ($CaCO_3$) and acetic acid (CH_3COOH). After completing the experiment, students are required to record their findings focusing on the factors affecting the chemical reaction between calcium carbonate ($CaCO_3$) and acetic acid (CH_3COOH). Additionally, students should establish the experiment's objectives, independent variables, dependent variables, controlled variables, and formulate hypotheses before proceeding with the experiment.

Students in each group should summarize the experimental results as follows.

Calcium carbonate ($CaCO_3$) and acetic acid (CH_3COOH) affecting the chemical reaction rate of eggshell with orange juice, resulting in varied time of gas bubble formation in Tubes 1-4:

Tube 1. Initial Surface Area of Reactants: In this tube, the calcium carbonate ($CaCO_3$) and acetic acid (CH_3COOH) reaction was observed to produce gas bubbles within a certain time frame;

Tube 2. Comparative Control Tube: This tube served as a control to compare the results of the other tubes. The reaction between calcium carbonate ($CaCO_3$) and acetic acid (CH_3COOH) was allowed to occur naturally;

Tube 3. Concentration of Reactants: In this tube, a different concentration of reactants (calcium carbonate and acetic acid) was used to determine its effect on the rate of gas bubble formation;

Tube 4. Temperature: This tube investigated the impact of temperature on the reaction rate by experimenting with a different temperature from the other tubes.

The results of this experiment show that various factors, including the initial surface area of reactants, concentration of reactants, and temperature, play a significant role in influencing the rate of chemical reactions. The differences observed in the time taken for gas bubble formation suggest that manipulating these factors can either accelerate or decelerate the reaction process. Furthermore, the eggshell and orange juice experiment also demonstrated how the reaction rate can be affected by the nature of the materials involved in the reaction.

The teacher distributed the experiment sheet titled "Effects of adding potassium iodide (KI) on the decomposition rate of hydrogen peroxide (H_2O_2)". This chemistry experiment aims to engage student groups in a concise chemical investigation. Collaboratively, students are tasked with gathering scientific concepts from the realm of chemistry, mathematical principles, and relevant technology. The chosen problem-solving approach stems from a specific scenario. The students then proceed to devise an experimental plan and ensure that all necessary apparatus is prepared. Upon completion of the experiment following the steps outlined in Activity Sheet, students are required to record their experimental results on the same sheet.

Students in each group should conclude that when adding KI solution to hydrogen peroxide (H_2O_2), the decomposition rate of H_2O_2 increases. The KI solution returns to its original state after the reaction concludes. Further explanation by the teacher: The catalyst participates in the reaction, but once the reaction is complete, the catalyst returns to its original state. This can be observed from the experiment, where the decomposition of hydrogen peroxide is accelerated upon adding potassium iodide. The chemical equations for the reactions are as follows (**Eq. 1** and **2**):

$$H_2O_2\,(aq) + I^-\,(aq) \rightarrow H_2O\,(l) + OI^-\,(aq) \qquad (1)$$

$$OI^-\,(aq) + H_2O_2\,(aq) \rightarrow I^-\,(aq) + H_2O_2\,(l) + O_2\,(aq) \qquad (2)$$

The acceleration of the reaction will lower the activation energy of the reaction, but the overall energy change of the reaction remains unchanged. The delayed reaction will also lower the activation energy of the reaction, but, like the acceleration, the overall energy change of the reaction remains unchanged.

Teaching step 3: Problem-solving design

The teacher instructs the students to collaborate in designing an experiment to create a model for testing the effects of slow reaction rates. Each group is provided with one sheet of graph paper and a simplified chemistry experiment kit. The students are tasked with collectively designing a problem-solving method by applying the information gathered from the previous steps. In this design process, each student group should consider using locally available materials and equipment. They are required to brainstorm and outline their plan on the paper before proceeding to draw a draft of the experimental setup.

Part 1: How can we induce different reaction rates of eggshell dissolution in vinegar?

Part 2: Testing the tenderness and stickiness of meat.

The teacher instructs each student group to present their design for the experiment to test the effects of reaction rate alteration. The teacher will randomly select each group to present using the PiliApp program.

Teaching step 4: Practice

Students proceed learning through the CSSC-STEM model based on their devised plans to address the aforementioned issues. Students record the step-by-step process of problem-solving as they work to test the impact of slow reaction rates. During the activity, the teacher will provide guidance and suggestions if students encounter difficulties.

Teaching step 5: Test, improvement, and evaluation

After designing and conducting the experiment, students may encounter challenges. What problems did the students encounter, and how did they suggest improving or modifying the experimental design? For groups that didn’t achieve the expected outcomes or faced issues during the experiment, they can address the shortcomings and then proceed to experiment again. The students should have refined their models until they are successfully completed.

Teaching step 6: Presentation

Each student group present the relationship between S-T-E-M in their designed plan and process as well as the results of their plan to test the effect of the reaction rate of a chemical reaction. After the presentation, classmates should engage in questioning, discussion, and offering suggestions to enhance the project or problem-solving methods. An example of integrating knowledge from S-T-E-M (Science, Technology, Engineering, and Mathematics) is as follows:

Science: Scientific knowledge about factors affecting chemical reactions, including substance concentration, surface area, temperature, catalysts, and reaction accelerators;

Technology: Technologies help the experiment from planning to execution, obtaining results, and data collection e.g. using photography and video recording during the experiment;

Engineering: Using Engineering Design Process in designing problem-solving processes and products;

Mathematics: Measurement and calculation e.g. measuring time, counting gas bubbles, etc.

The teacher and students together summarize the knowledge gained from the lesson.

Chemical reactions in daily life can occur more rapidly or slowly when changing factors affecting the rate of reaction, as follows:

Nature of Reactants: Different types of reactants have varying reaction rates. Some substances react easily, while others react less readily;

Surface Area: Increasing the surface area of reactants leads to more collisions and faster reaction rates;

Concentration: Increasing the concentration of reactants speeds up the reaction, while decreasing it slows it down;

Temperature: Higher temperatures increase the kinetic energy of molecules, resulting in more frequent collisions and faster reactions;

Catalysts: Catalysts lower the activation energy, making the reaction proceed faster, and are not consumed in the process;

Inhibitors: Inhibitors raise the activation energy, leading to slower reactions.

Finally, the teacher encourages students to apply their constructed knowledge in providing examples of activities or everyday life events that are related to factors influencing the rate of chemical reactions.

4.3. Effects of CSSC-STEM model on students’ learning achievement and learning and innovation skills: R2D2

The researchers evaluated the normal distribution of students' learning achievement scores through the Kolmogorov-Smirnov test. The analysis indicated that the data adhered to a normal distribution, enabling to proceed with inferential statistics. The comparison between the experiment and control groups’ learning achievement was as follows.

Table 6. Independent t-test of learning achievement scores between the experiment and control groups.

Group	n	Mean	SD	t	p
Experiment group	43	28.79	4.378	7.599	0.000
Control group	41	21.63	4.247		

Table 6 showed that the Grade 11 students in the experimental group, who were taught using the CSSC-STEM model, demonstrated significantly higher learning achievement ($t = 7.599$, $p < 0.05$) in the rate of chemical reactions topic compared to the students in the control group.

Table 7. Dependent t-test of learning achievement scores of experiment group at the beginning and the end of CSSC-STEM model.

Group	n	Mean	SD	t	p
Pre-test	43	9.42	2.21	34.242	0.000
Post-test	43	28.79	4.38		

Table 7 showed that the Grade 11 students in the experimental group, who learned with the CSSC-STEM model, exhibited notably enhanced learning achievement in the post-test

($t = 34.242$, $p < 0.05$) for the topic of Rate of Chemical Reactions in comparison to their pre-test performance.

Table 8. Independent t-test of critical problem-solving skills between the experiment and control groups.

Group	n	Mean	SD	t	p
Experiment group	43	27.12	2.701	20.968	0.000
Control group	41	14.32	2.893		

Table 8 showed that the Grade 11 students in the experimental group, who received instruction through the CSSC-STEM model, exhibited markedly improved critical problem-solving skills ($t = 20.968$, $p < 0.05$) in the rate of chemical reactions, surpassing the performance of students in the control group.

Table 9. Dependent t-test of critical thinking skills scores of experiment group at the beginning and the end of CSSC-STEM model.

Group	n	Mean	SD	t	p
Pre-test	43	5.40	1.256	50.459	0.000
Post-test	43	27.12	2.701		

From Table 9, the Grade 11 students in the experimental group, who received instruction through the CSSC-STEM model, demonstrated significantly improved critical problem-solving skills in the post-test ($t = 50.459$, $p < 0.05$) related to rate of chemical reactions topic, compared to their performance in the pre-test.

Table 10. Independent t-test of creativity and innovation skills between the experiment and control groups.

Group	n	Mean	SD	t	p
Experiment group	43	19.60	2.461	23.168	0.000
Control group	41	8.71	1.778		

From Table 10, the Grade 11 students in the experimental group, who received instruction through the CSSC-STEM model, exhibited markedly improved creativity and innovation skills ($t = 23.168$, $p < 0.05$) in rate of chemical reactions, surpassing the performance of students in the control group.

Table 11. Dependent t-test of creativity and innovation skills of experiment group at the beginning and the end of CSSC-STEM model.

Group	n	Mean	SD	t	p
Pre-test	43	5.67	1.304	36.843	0.000
Post-test	43	19.60	2.461		

From Table 11, the Grade 11 students in the experimental group, who received instruction through the CSSC-STEM model, demonstrated significantly improved creativity and innovation skills in the post-test ($t = 36.843$, $p < 0.05$) related to rate of chemical reactions, compared to their performance in the pre-test.

Table 12. Development of students' communication and teamwork skills from instructional plans 1 to 4 of the CSSC-STEM model.

Lesson Plan	Total score	Mean	SD
1	55	46.09	2.068
2	55	49.26	2.094
3	55	50.65	1.660
4	55	51.91	1.211
Average	55	49.48	2.680

From Table 12, the experimental group, which learned through the CSSC-STEM model, exhibited a gradual enhancement in their communication and collaboration skills across instructional Plans 1 to 4.

4.4. Effects of CSSC-STEM model on students' learning achievement and learning and innovation skills: R3D3

The researchers evaluated the normal distribution of students' learning achievement scores through the Kolmogorov-Smirnov test. The analysis indicated that the data adhered to a normal distribution, enabling to proceed with inferential statistics. The comparison between the experiment and control groups' learning achievement was as follows.

Table 13. Independent t-test of learning achievement scores between the experiment and control groups.

Group	n	Mean	SD	t	p
Experiment group	40	33.50	4.358	13.342	0.000
Control group	36	22.50	2.408		

From Table 13, the Grade 11 students in the experimental group, who were taught using the CSSC-STEM model, demonstrated significantly higher learning achievement ($t = 13.342$, $p < 0.05$) in rate of chemical reactions compared to the students in the control group.

Table 14. Dependent t-test of learning achievement scores of experiment group at the beginning and the end of CSSC-STEM model.

Group	n	Mean	SD	t	p
Pre-test	40	9.55	2.087	36.658	0.000
Post-test	40	33.50	4.385		

From Table 14, the Grade 11 students in the experimental group, who were instructed using the CSSC-STEM model, exhibited notably enhanced learning achievement in the post-test ($t = 36.658$, $p < 0.05$) for rate of chemical reactions in comparison to their pre-test performance.

Table 15. Independent t-test of critical problem-solving skills between the experiment and control groups.

Group	n	Mean	SD	t	p
Experiment group	40	26.93	2.693	19.058	0.000
Control group	36	14.14	3.155		

From Table 15, the Grade 11 students in the experimental group, who received instruction through the CSSC-STEM model, exhibited markedly improved critical problem-solving skills ($t = 19.058$, $p < 0.05$) in rate of chemical reactions, surpassing the performance of students in the control group.

Table 16. Dependent t-test of critical thinking skills scores of experiment group at the beginning and the end of CSSC-STEM model.

Group	n	Mean	SD	t	p
Pre-test	40	9.80	1.556	52.079	0.000
Post-test	40	26.93	2.693		

From **Table 16**, the Grade 11 students in the experimental group, who received instruction through the CSSC-STEM model, demonstrated significantly improved critical problem-solving skills in the post-test ($t = 52.079$, $p < 0.05$) related to rate of chemical reactions, compared to their performance in the pre-test.

Table 17. Independent t-test of creativity and innovation skills between the experiment and control groups.

Group	n	Mean	SD	t	p
Experiment group	40	19.98	2.178	19.065	0.000
Control group	36	9.97	2.396		

Table 17 showed that the Grade 11 students in the experimental group, who received instruction through the CSSC-STEM model, exhibited markedly improved creativity and innovation skills ($t = 19.065$, $p < 0.05$) in rate of chemical reactions, surpassing the performance of students in the control group.

Table 18. Dependent t-test of creativity and innovation skills of experiment group at the beginning and the end of CSSC-STEM model.

Group	n	Mean	SD	t	p
Pre-test	40	6.33	1.118	38.018	0.000
Post-test	40	19.98	2.178		

Table 18 showed the Grade 11 students in the experimental group, who received instruction through the CSSC-STEM model, demonstrated significantly improved creativity and innovation skills in the post-test ($t = 38.018$, $p < 0.05$) related to rate of chemical reactions, compared to their performance in the pre-test.

Table 19. Development of students' communication and teamwork skills from instructional plans 1 to 4 of the CSSC-STEM model.

Lesson Plan	Total score	Mean	SD
1	55	46.38	1.547
2	55	49.45	1.377
3	55	50.88	1.090
4	55	52.05	0.986
Average	55	49.46	1.230

Table 19 showed the experimental group, which learned through the CSSC-STEM model, exhibited a gradual enhancement in their communication and collaboration skills across instructional plans 1 to 4.

5. Discussion

The researchers found that the teachers expressed a high level of demand for the CSSC-STEM model, which combines SSC with STEM and context-based learning (CBL), because they perceive the potential benefits of SSC with STEM and CBL for developing learning and innovation skills. This is consistent with previous works (Thongchai, 2013; Siriphatraichai, 2013; Chaolumbua, 2013; Siriphatrachai, 2013; Loei Rajabhat University, 2018; Acharry, 2019). The integrative teaching approach in STEM, which incorporates four different disciplines, including Science (S), Technology (T), Engineering (E), and Mathematics (M). This amalgamation blends the strengths and teaching methods of each discipline to enable students to establish connections between the four subjects and their daily lives and future careers. This approach emphasizes the development of 21st-century skills, challenges students' thinking, and encourages them to voice their opinions, placing learner-centeredness at its core. The instructional design focuses on training students to think and plan using a step-by-step process. It aims to foster comprehensive growth across various domains and aligns with the development of quality skills for the 21st-century. Additionally, it corresponds with Chaiyasit Chanchaikaew's work in 2013 and Mahasarakham University in 2018, as well as the Chemical Society of Thailand and the Dow Group in 2019. They noted that SSC offer a safe, cost-effective, convenient, and efficient method for teaching chemistry. This method minimizes the use of chemicals and encourages the reuse of containers, allowing for easy transport. Utilizing various materials in chemistry experiments that students encounter in their daily lives with small quantities of chemicals reduces the risk of exposure, making it less dangerous. If an accident occurs, it can be quickly rectified compared to experiments that involve a large quantity of chemicals. SSC thus offer a safer alternative to current chemical experiments, requiring less time. Students' desire for integrative learning and SSC stems from the current context, problems, and educational needs, all of which are substantial. Their demand arises from a preference for engaging learning that goes beyond theoretical study. As Passakchai (2015) stated, relying solely on chemistry theories and lectures can lead to some students misunderstanding, causing genuine frustration and disinterest in chemistry.

The CSSC-STEM model is qualified in views of experts. It is appropriate for enhancing students' learning outcomes, learning and innovation skills, the researchers incorporated SSC into the process of gathering data related to a problem. They integrated situations inf SSC are close to the students in identifying contextualized problems within the local context, resulting in increased student engagement in learning. As noted by Siripatharachai (2013), SSC facilitates comprehensive development in various aspects, aligned with the 21st-century human development approach. This includes enhancing students' understanding of subject matter, higher-ordered thinking skills such as analysis and creative thinking, as well as fostering qualities such as effective teamwork, communication skills, leadership, and the ability to accept constructive criticism from others.

The CSSC-STEM model promotes self-directed learning among students through a diverse range of activities. These activities align with the guidelines for organizing science learning activities specified in the curriculum. Additionally, the approach involves studying and analyzing students to understand their potential and needs. It follows a systematic process for creating a well-structured learning plan, incorporating appropriate and accurate steps. This includes analyzing foundational data related to the current situation and challenges in teaching and learning chemistry at the Grade 11. The curriculum, theories, principles, ideas, documents, and research related to SSC, STEM and CBL are considered. A panel of expert also provide comments and suggestions to various aspects such as content, language use, activity design, and assessment methods.

The CSSC-STEM model significantly promotes students critical problem-solving skills, creativity and innovation skills and communication and collaboration skills.

In alignment with Chaolumbua (2015), STEM education can foster learners' skills such as critical thinking, systematic scientific learning, and the creation of new generations of innovators. It supports sustainable innovation and new processes, adapting to the rapidly changing economic landscape. These innovations are fundamentally rooted in knowledge from science, technology, engineering, and mathematics (STEM), particularly through STEM content learning. This occurs via engineering design processes (EDP), which help cultivate desired habits of mind and essential skills for the 21st-century. In accordance with the mentioned context, the EDP serves as an accelerator for integrating STEM content, aiding the development of essential skills for national progress.

In accordance with Acharry (2009), the utilization of SSC in learning activities involves the use of minimal quantities of chemicals and reuses containers for chemical experimentation, enhancing portability. Various materials employed in chemical reactions are common in everyday life, and students' personal involvement in conducting hands-on experiments fosters curiosity and enthusiasm for learning. This approach, SSC, enables students to develop scientific process skills and swiftly and clearly observe experimental outcomes. Simultaneously, teachers' instructional strategies, punctuated with periodic questioning, stimulate greater classroom participation. Students become more confident in expressing their doubts and findings, promoting an environment that supports the contextualized learning format of combining chemical experimentation with local contexts. This is congruent with the topic of chemical reaction rates, which the researchers developed, exhibiting significantly higher effectiveness compared to the standard criteria. After learned with SSC combined with STEM education, students had significantly higher learning achievement than students undergoing conventional instruction ($t = 7.599$, $p < .05$).

Aligned with the research findings (Khammamung, 2017; Wicheansang *et al*., 2018; Khonchaiyapham, 2017; Poonruang, 2016; Saengpromsri, 2015), this is due to the systematic evaluation of the tool's efficacy before its application within the sample group. The researchers recognized the significance of student-centered instructional activities, emphasizing the use of engaging teaching materials. These materials are derived from items close to students' daily lives, enhancing accelerated learning. Once students successfully design and implement their projects, they are able to consume their creations, such as pork jerky and marinated meat with pineapple. The designed learning activities also consider individual differences, and the experiences students engage in, resulting in interconnected knowledge acquisition. This interaction fosters students' critical thinking and deepens their understanding, consequently elevating the quality of their learning outcomes. Based on these reasons, it can be concluded that employing the CSSC-STEM model and its lesson plans significantly contributes to students' learning achievement development. It affirms that the CSSC-STEM learning activities play a vital role in advancing students' learning quality.

The CSSC-STEM model significantly promotes students learning and innovation skills. Siripithayachai (2013) suggests that teachers should employ a science teaching approach aligned with the constructivist concept, which can generate student interest, excitement, challenge, and confidence in learning. This leads to an increased inclination among students to study science at higher levels and achieve success in their studies. Pholchayachaya (2014) stated that organizing learning through inquiry-based activities is a method that helps students develop more creative thinking skills. Furthermore, creative thinking is a crucial skill for learning in the 21st-century. Chanprasert (2014) stated that contemporary teaching must be aligned with the rapidly changing 21st-century society. Learners need to develop various skills necessary for the 21st-century. Organizing learning in the 21st-century is guided by key principles, such as learner-centeredness, hands-on activities, and objectives aimed at enhancing students' learning capabilities, including advanced thinking skills. The researcher has designed activities in the CSSC-STEM model that correspond to various skills necessary in the 21st-century. As a result, students' learning and innovation skills are higher compared to those learning through conventional methods.

In R3D3, the CSSC-STEM model still constantly continues to produce positive impacts on Grade 11 students' learning achievement and learning and innovation skills. This phenomenon underscores the consistency and reliability of the newly developed model in this study i.e., the CSSC-STEM model.

6. Conclusions

The CSSC-STEM model developed in this study has been demonstrated as an innovative and effective teaching approach for enhancing Grade 11 students' academic performance and fostering their learning and innovation skills in the field of chemical reaction rates in chemistry. The research and development (R&D) methodology progressed from the development phase (R1D1) through the implementation phase (R2D2) and replication phase (R3D3) yield the completed version of CSSC-STEM model, which is ready to be implemented in other chemistry classroom settings. The challenge lies in determining whether the CSSC-STEM model is effective for teaching topics beyond chemical reactions, extending to other areas of chemistry or even other scientific subjects such as physics and biology. Furthermore, the examination of the impacts of the CSSC-STEM model on other dependent variables awaits further research conducted by other researchers.

Authors' contributions

Conceptualization: Ratanaphun Utmeemang; Khajornsak Buaraphan; **Data curation:** Ratanaphun Utmeemang; **Formal Analysis:** Ratanaphun Utmeemang; **Funding acquisition:** Ratanaphun Utmeemang; **Investigation:** Ratanaphun Utmeemang; **Methodology:** Ratanaphun Utmeemang; Khajornsak Buaraphan; **Project administration:** Ratanaphun Utmeemang; Khajornsak Buaraphan; **Resources:** Ratanaphun Utmeemang; **Software:** Khajornsak Buaraphan; **Supervision:** Khajornsak Buaraphan; **Validation:** Ratanaphun Utmeemang; Khajornsak Buaraphan; **Visualization:** Ratanaphun Utmeemang; Khajornsak Buaraphan; **Writing – original draft:** Ratanaphun Utmeemang; **Writing – review & editing:** Khajornsak Buaraphan.

Data availability statement

The data will be available upon request.

Funding

Not applicable.

Acknowledgments

The authors would like to express their sincere gratitude to all the participants involved in the data collection, the school director for permitting this project, and Dr. Jirutthitikan Pimvichai for her valuable suggestions.

References

Acharry, S. *The Development of Chemistry Curriculum Via Microscale Experiments for Vocational Learners*. Doctor of Education Thesis in Science Education, Srinakharinwirot University, Bangkok, 2009.

Chamrat, S. The Definition of STEM and Key Features of STEM Education Learning Activity. *STOU Education Journal.* **2017**, *10* (2), 13–34. [in Thai].

Chanprasert, S. STEM education and Teaching and Learning in the 21st Century. *IPST Magazine.* **2014**, *42* (186), 3-5. [In Thai].

Chaolumbua, S. Development of STEM Education Curriculum on Sugar Cane for Grade 9 Students. Doctor of Education Thesis, Srinakharinwirot University, Bangkok, 2015. [In Thai].

Chulawattanatol. M. STEM Education Thailand and STEM Ambassadors. *Institute for the Promotion of Teaching Science and Technology: IPST Magazine.* **2013**, *42* (185), 14–18. [In Thai].

Jong, O .Context-based Chemical Education :How to Improve it? *Chemical Education International.* **2006**, *8*) 1(, 1–7.

Faikhamta, C. *Strategies for Teaching Chemistry*. Chulalongkorn University Press, 2020. [In Thai].

Gilbert, J .K .On the Nature of “context” in Chemical Education . *International Journal of Science Education.* **2006**, *28*) 9(, 957–976. https://doi.org/10.1080/09500690600702470

Gonzalez, H .B.; Kuenzi, J .J. *Science, Technology, Engineering, and Mathematics)STEM (Education :A Primer*; Congressional Research Service, 2012.

Kelly, O.; Finlayson, O .E“ .*Small-Scale Chemistry in the School Laboratory – Small is Beautiful, Green is more Beautiful* ”2022.

Khammamung, A .The Study of Learning Achievement in Chemistry on Chemical Reaction and Critical Thinking for Matthayomsueksa 4 on STEM Education. Rangsit University, Bangkok, 2017.

Ketsrisakda, N.; Noin, J.; Tunreun, K.; Poolprasert, P. Learning Achievement and Science Process Skill of Fifth Grade Students Using STEM Education. In *Proceedings of the National Research Conference Northern College*, Northern College, 2017; Tak, pp. 272–276.

Khonchaiyapham, P. Development of Activity-Based Learning Conceptual Approach with the STEM Education on the Photosynthesis Issue at the 11th Grade Level to Promote Students' Learning Achievement and their Systems Thinking Abilities. Rajabhat Maha Sarakham University, Maha Sarakham, 2017. [In Thai].

Laohapiboon. P. *Science Teaching Approaches*; Thai Watthanaphanit, 1999. [In Thai].

Loei Rajabhat University. *Training Materials for the Comprehensive Teacher Development Program. Faculty of Science and Technology*. Loei Rajabhat University, Loei, 2018. [In Thai].

Lou, S. J.; Shih, R. C.; Diez, C. R.; Tseng, K. H. The impact of problem-based learning strategies on STEM knowledge integration and attitudes: An exploratory study among female Taiwanese senior high school students. *International Journal of Technology and Design Education.* **2011**, *21* (2), 195–215. https://doi.org/10.1007/s10798-010-9114-8

Ministry of Education. *The Basic Education Core Curriculum B.E. 2551* (*BE. 2560 revised edition (A.D. 2017);* The Printing House of Express Transportation Organization of Thailand, 2017. [In Thai].

National Center for STEM Education of Institute for the Promotion of Teaching Science and Technology. *Introduction to STEM Education. STEM Education Thailand*, IPST, Bangkok, 2015.

National Research Council. *A Framework For K-12 Science Education: Practices, Crosscutting Concept, and Core Ideas*. Committee on New Science Education Standards, Board on Science Education, Division of Behavioral and Social Science and Education National Academy Press, 2012.

Office of the Education Council. *National Education Act B.E. 2542 (1999) and Amendments (Second National Education Act B.E. 2545 (2002))*; Office of the Education Council, Bangkok, 2002. [In Thai].

Pudcha, W. *A Comparative Study of Learning Achievement on Trigonometry Ratios Between the Use of Stem Education and IPST Method for Mathayom Suksa 5 Wathuaichorakhe Wittayakhom School*. Master of Science Thesis in Mathematics Study, Silpakorn University, Nakhon Pathom, 2016.

Passakchai, P.; Kuno, M. The Development of Computer-Assisted Instruction on the Topic of Chemical Reaction For Matthayomsuksa 2 Students. *Veridian E-Journal, Silpakorn University*. **2015**, *8* (2), 483–492. [In Thai].

Penratanahiran, R.; Thongkham, K. A Survey of Soft Skills Needed in the 21st Century Workplace. *Rajabhat Rambhai Barni Research Journal.* **2011**, *15* (1), 59–69. [In Thai].

Penrattanahiran, R. An Analysis of Problems and Guidelines for Enhance 4Cs Skills of Primary School Students under Chiang Mai Primary Educational Service Area Office 3. *Journal of MCU Peace Studies.* **2021**, *10* (2), 675–692. [In Thai].

Poonruang, A. A Development of Learning Achievement and Ability in Problem-Solving in Science through STEM Education Approach in Enzyme. Master of Education Thesis in Biology, Srinakharinwirot University, Bangkok (2016). [In Thai].

Prakun, C. *Integrated Design of Reading, Analytical Thinking, and Writing Instruction. 2nd Edition*. Chulalongkorn University Press (Cuprint), 2009. [In Thai].

Saengpromsri. P. Comparisons of Learning Achievement, Integrated Science Process Skills, and Attitude Towards Chemistry Learning for Matthayomsueksa 5 Students between STEM education and Conventional Method. Mahasarakham University, Mahasarakham 2015. [In Thai].

Samahito, C. Training Material for Practical Training, Integrating Science, Technology, Engineering, and Mathematics (STEM) Activities for Early Childhood Education. Pre-school Education Association of Thailand Under the Royal Patronoge of Her Royal Highness Maha Chakri Sirindhorn "P.E.A.T", 2014. [In Thai].

Seneewong, S. STEM Education through Origami Frog. *IPST Magazine.* **2013**, *42* (185), 10–13. [In Thai].

Shi-Jer Lou; Ru-Chu Shih; C .Ray Diez; Kuo-Hung Tseng .The Impact of Problem-Based Learning Strategies on STEM Knowledge Integration and Attitudes :An Exploratory Study among Female Taiwanese Senior High School Students .*Int. J. Technol. Des. Educ.* **2011**, *10*) 1007(, 195–215. https://doi.org/10.1007/s10798-010-9114-8

Singh, M. M.; Szanfran, Z.; Pike, R. M. Microscale Chemistry and Green Chemistry: Complementary Pedagogies. *J. Chem. Educ.* **1999**, *12* (76), 1684–1686. https://doi.org/10.1021/ed076p1684

Siriphatrachai. P. STEM Education and 21st Century Skills Development. *Executive Journal.* **2013**, *33* (2), 49–56. [In Thai].

Sombatsri; Kantadong, P.; Chankaew, C.; Asavasukhee, A. Green Chemistry. *Journal of Science and Technology*. *Ubon Ratchathani University.* **2016**, *18* (3), 1–15. [In Thai]. https://doi.org/10.30574/ijsra.2023.8.2.0225

Tamuang, S.; Wuttisela, K.; Supasorn, S. Development of 11th Grade Students' Conceptual Understanding of Chemical Reaction Rate by using Inquiry Experiments. *CMU Journal of Education*. **2017**, *1* (2), 1–15. [In Thai].

Thongchai, A. STEM Education and Development of Education in Science, Technology, engineering and Mathematics in USA. *Association of Science, Mathematics and technology Teachers of Thailand.* **2013**, *19* (1), 15–18.

Tontayanon, S. *Green Chemistry: Theory and Practice*. Bangkok: STC Media and Maketing, 2011.

Wicheansang, K.; Mophan, N.; Lateh, A. Effect of STEM Education on Chemistry Achievement, Problem-Solving Ability and Instructional Satisfaction of Grade 12 Students. *Prince of Songkhla University Pattani Campus.* **2018**, *29* (3), 148–158. [In Thai].

Wood, C. G. Microchemistry. *J. Chem. Educ.* **1990**, *67* (7), 596–597. https://doi.org/10.1021/ed067p596

Wooster, M. Microscale Chemistry. *Educ. Chem.* **2007**, *44* (2), 45–47.

ECLÉTICA QUÍMICA

Eclet. Quim. 49 | e-1528, 2024

Original Article

https://doi.org/10.26850/1678-4618.eq.v49.2024.e1528

In vitro and *in silico* evaluation of the antimicrobial potential of *Celtis zenkeri* roots volatile metabolites

Ejike Onwudiegwu **Okpala**[1+], William Ojoniko **Anthony**[1], Godfrey Okechukwu **Eneogwe**[1], Oluwakayode Olubunmi **Odeja**[2], Michael Gabriel **Ibok**[3], Joel Ojogbane **Onoja**[4], Samuel Akinniyi **Odewo**[5], Shedrach Ndubuisi **Ike**[6], Olusimbo Adesegun **Onanuga3**, Banjo **Semire**[1,7]

Abstract

This study is aimed at investigating the volatile constituents of the air-dried roots of *Celtis zenkeri*. The volatile oil was extracted using hydro-distillation method and characterised using gas chromatography-mass spectrometry (GC-MS). The volatile oil was screened against six selected bacteria and four fungi strains using the agar diffusion method. The molecular docking study of the identified compounds was conducted to investigate their binding pattern with the substrate and nucleotide complexes of *Enterococcus faecium* aminoglycoside-2''-phosphotransferase-IIa [APH(2'')-IIa] (PDB ID: 3HAM) and full-length Lanosterol 14 alpha-Demethylases of Prominent fungal pathogens *Candida albicans* (PDB ID: 5V5Z). The yield of the volatile oil (% w/w) root of *C. zenkeri* was 0.79%. Six compounds were identified in the root essential oil representing 80.07% of the volatile oil. 2-methyl-1-pentene (40.01%) was the most abundant compound in the root essential oil. The volatile oil from roots of the *C. zenkeri* exhibited good activity against all the screened bacteria and fungi strains at a concentration of 12.5-100 mg/mL when compared with Gentamicin for bacteria and Tioconazole for fungi.

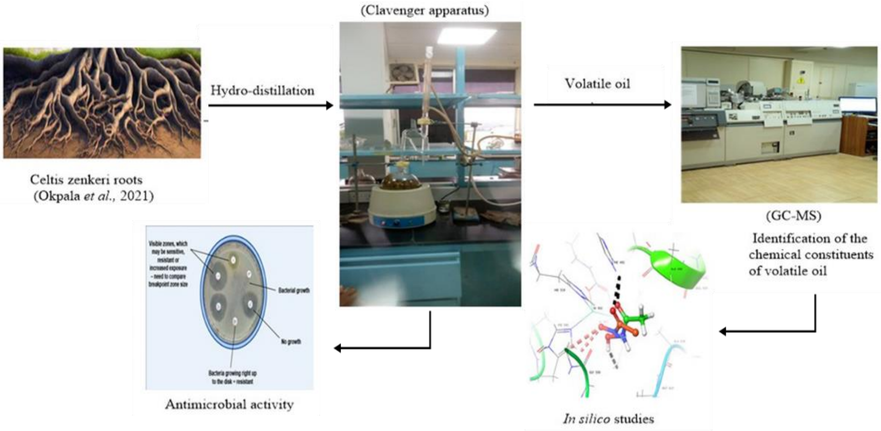

Article History

Received October 30, 2023
Accepted August 14, 2024
Published November 04, 2024

Keywords

1. *Celtis zenkeri*;
2. volatile oil;
3. gas chromatography-mass spectrometry;
4. antimicrobial activity.

Section Editor

Rogéria Rocha Gonçalves

Highlights

- The chemical components of *Celtis zenkeri* roots' volatile oil are first reported.
- The antimicrobial potential of the identified chemical constituents was evaluated.
- Molecular docking studies were made on the oil volatile identified compounds-STEM is a new model.

[1]Federal University Lokoja, Faculty of Science, Lakoja, Nigeria. [2]Federal University of Petroleum Resources, Department of Chemistry, Effurun, Nigeria. [3]University of Ibadan, Department of Chemistry, Ibadan, Nigeria. [4]University of Nigeria, Faculty of Pharmaceutical Sciences, Nsukka, Nigeria. [5]Forestry Research Institute of Nigeria, Ibadan, Nigeria. [6]Federal Polytechnic Oko, Department of Science Laboratory Technology, Aguata, Nigeria. [7]Ladoke Akintola University of Technology, Department of Pure and Applied Chemistry, Ogbomoso, Nigeria. **+Corresponding author:** Ejike Onwudiegwu Okpala, **Phone:** +2347031835599, **Email address:** ejike.okpala@fulokoja.edu.ng

1. Introduction

About 80% of the world's population, according to the World Health Organisation (WHO, 2008), primarily receives their primary healthcare from traditional medicine. Plant-based products are also a major component of the healthcare systems of the remaining 20% of the world's population, which is mostly found in wealthy nations. The 44th World Health Assembly adopted a resolution in 1991 that promoted the use of "traditional, safe, effective, and scientifically approved medicines" (Pamplona-Roger, 2014).

The WHO encourages the study of medicinal plants throughout all its geographic zones. WHO funds and organizes seminars on the development of drugs from medicinal plants to accomplish this. The African Union has independently established centres in Cairo, Dakar, Ile-Ife, Kampala, and Tananarive for the coordination of research on African medicinal plants. Furthermore, several African nations have contributed to the development of traditional medicine in distinctive ways (WHO, 2008). The Universal Education, Social, and Cultural Organisation (UNESCO) stated that one of the safest ways to guarantee complete health care for the world's rapidly growing population is through conventional treatments (UNESCO, 1994). In essence, chemicals derived from plant extracts have remained the focus of natural products.

As per the findings of Hamburger and Hostettmann (1991), the crude extract is a diverse mixture comprising various compounds that are by-products of metabolism. They are metabolites, either primary or secondary. It has been proposed that secondary metabolites in plants are what give them their therapeutic properties because they comprise most biologically active compounds (Fabeku, 2006; Neumann and Hirsch, 2000).

Organic compounds play a major role in the drug research initiatives of the pharmaceutical industry (Ata *et al.*, 2007; Hanazki *et al.*, 2000). There are hundreds of plant species that have not yet been investigated for their phytochemicals and, consequently, their biological potential. For this reason, the importance of continued research into plant phytochemicals cannot be overemphasized (Fadipe, 2014; Rates, 2001). Likewise, the development of resistance to most known antimicrobial drugs and the resulting high cost of treatment have led to the search for novel, safe, efficient, and effective ways to manage infectious diseases (El-Mahmood and Doughari, 2008).

Fragrant liquids with an oily uniformity, essential oils are extracted from a wide variety of plant parts, such as flowers, roots, leaves, seeds, fruits, and bark (Ibok *et al.*, 2023; Odeja *et al.*, 2023). They are also referred to as volatile odoriferous oils. They can be extracted from plant materials in a variety of ways, such as steam distillation, expression, and hydro-distillation. Among all the techniques, for example, steam distillation has been used a lot, especially for large-scale production (Cassel and Vargas 2006; Di Leo Lira *et al.*, 2009). According to Masango (2005), plant essential oils are frequently a complex mixture of polar and non-polar natural compounds. The main ingredients of various essential oils are terpenes (monoterpenes and sesquiterpenes), aromatic compounds (aldehydes, alcohols, phenols), and terpenoids (Bakkali *et al.*, 2008; Mohamed *et al.*, 2010).

According to ethnobotanical reports, *Celtis zenkeri*, a member of the Ulmaceae family, has a variety of medicinal uses, including the treatment of skin infections, cancer, arthritis, and coughs. It is acknowledged that ligand- and structure-based computational studies are useful tools for hastening the drug design process (Lapa *et al.*, 2012). This study reports the volatile secondary metabolites from the roots of *Celtis zenkeri*, its antimicrobial activity, and molecular docking analysis of the identified compounds in the roots of the volatile oil of *C. zenkeri* as part of our continuous investigation of this medicinal plant (Okpala *et al.*, 2021; 2022).

2. Material and methods

2.1. Plant collection and preparation

In August 2016, *Celtis zenkeri* was collected at an elevation of 305 metres in Ikire, Osun State, Nigeria (7°22′20′′N; 4°11′14′′E), identified, and authenticated at the Ibadan, Nigeria. Forestry Research Institute Herbarium, where a voucher specimen was placed under the accession number FHI-110554. The fresh plant materials were air-dried for a while to shield them from the sun's direct rays. The plant materials were first ground up to increase surface area, and then, to keep any volatile components from evaporating before use, they were sealed in airtight bags.

2.2. Extraction of volatile oils

Hydro-distillation methods were employed using the Clevenger apparatus for the extraction of essential oil from the roots of the *Celtis zenkeri*. The pulverised sample was weighed and carefully loaded into a 10 L round-bottomed flask, and water was added until the sample was fully immersed. The flask was placed on a heating mantle and fitted with the all-glass Clevenger distillation unit designed according to the British pharmacopoeia specification (Paterson, 1982). The extraction process was carried out for a minimum of 3 h at a temperature of 50 °C. The volatile oils trapped in 2.0 ml of hexane were carefully collected using a syringe and put in a pre-weighed sample vial. The weight of the volatile oil was recorded, and the yield was calculated for each of the samples. The sample vial containing the oil was carefully corked and stored in the refrigerator for further analysis.

The percentage yield for the oil sample was calculated using the **Eq. 1**:

$$\%\ \text{Yield} = \frac{Mass\ of\ oil}{Mass\ of\ sample}\ \text{X}\ 100 \qquad (1)$$

2.3. Gas chromatography-mass spectrometry (GC-MS) analysis

The volatile oil was analysed using a GC-MS Agilent Technologies, Model-7890A Gas Chromatograph, coupled with a 5975C mass spectrometer. The gas chromatograph capillary column type was an HP-5MS, with a column length of 30m, an internal diameter of 0.320 mm, and a film thickness of 0.25 µm. The volume of the sample injected was 1 µL, the split ratio was 50:1, and the split flow was 70.615 mL/min. The carrier gas, helium, had a flow rate of 1 mL/min. The pressure, linear velocity, and injection volume were set at 56.2 kPa, 362 cm/s, and 1.0 µL, respectively. The oven temperature was adjusted to 60 °C, held for 1 minute, increased to 180 °C for 3 min at 10 °C/min, and finally reached 280 °C for 2 min at 10 °C/min. The temperatures of the injector and detector were set at 250 °C. The constituents were identified by comparing the published mass spectral database (NIST 11.L) and literature data with the total chromatogram that had been auto integrated.

2.4. Antimicrobial assay

2.4.1. Preparation of graded concentration of the samples

A solution of volatile oil was prepared by dissolving 200 µg of the oil in 2.0 mL of dimethylsulfoxide (DMSO) to give 100 µg/mL. From the 100 mg/mL solution, 1 mL was taken into another sample bottle and 1 mL of solvent (DMSO) was added to give 50 µg/mL. This was serially diluted until a 6.25 µg/mL concentration was obtained. Two other sample bottles contained the negative control (DMSO solvent) and the positive control (gentamicin 10 µg/mL for bacteria and tioconazole 0.07 µg/mL for fungi).

2.4.2. Agar diffusion: pour plate method for bacteria

The volatile oil was screened against two gram-positive bacteria: *Staphylococcus aureus* and *Bacillus subtilis*; four gram-negative bacteria: *Pseudomonas aeruginosa, Escherichia coli, Klebsiella pneumonia,* and *Salmonella typhi*; obtained from the Department of Pharmaceutical Microbiology, University of Ibadan. An overnight culture of each microorganism was prepared by taking a loop full of the microorganisms from stock (slope) and inoculating each into a sterile nutrient broth of 5 mL each, incubated for 18-24 h at 37 °C. From overnight culture, 0.1 mL of each microorganism was taken and put into 9.9 mL of sterile distilled water to get 1:100 (10^{-2}) dilution of the microorganisms.

From the molten diluent (10^{-2}), 0.2 mL was taken into the 20 mL of freshly prepared sterile nutrient agar, then shaken gently for uniformity and aseptically poured into sterile Petri dishes, allowed to solidify for about 30-50 minutes. Using a sterile cork borer of 6 mm diameter, the wells were made in the set nutrient agar plate according to the number of graded concentrations of the samples.

In each well, 0.02 mL of the different graded concentrations of the sample were introduced using a Pasteur pipette. This was done in triplicate. The plates were allowed to stay on the bench for 1 h for pre-diffusion. The plates were incubated uprightly in the incubator for 18-24 h at 37 °C. Then the observed zones of inhibition were measured.

2.4.3. Agar diffusion: surface plate method for fungi

The antifungal potential of the volatile oil was determined against four fungi strains: *Candida albicans, Aspergillus niger, Rhizopus stolonifer,* and *Penicillum notatum;* obtained from the Department of Pharmaceutical Microbiology. A sterile Sabouraud Dextrose Agar (62 g/L) was prepared accordingly and aseptically poured into the sterile plate in triplicates and allowed to set properly, 0.2 mL of the 10^{-2} of the agar was then spread using a sterile spreader to cover the surface of the agar. The wells were made using a sterile cork borer 8 mm in diameter. In each well, the graded concentrations of the oil were introduced, including the controls. The plates were left on the bench for 120 min to allow the oil to diffuse properly into the agar, i.e., pre-diffusion. The plates were incubated uprightly in the incubator for 48 h at 26-28 °C.

2.5. Molecular docking of the identified compounds in the volatile oil

The AutoDockTools (ADT), a free graphic user interface (GUI) for the AutoDockVina program, was used to conduct molecular docking investigations (Tanchuk *et al.*, 2015). The compounds were docked against the protein's active site (PDB ID: 3HAM and 5V5Z) using AutoDockVina using the usual methodology (Bottomley *et al.,* 2007; Narramore *et al.,* 2019; Tanchuk *et al.*, 2015). With suitable 2D orientation assigned, the ChemOffice program (ChemDraw 16.0) was used to build the chemical structures of the compounds. Spartan 14's graphical user interface was used to reduce the energy of each molecule (**Table 1**). The docking simulation was then performed using the input provided by the energy-minimized ligand molecules to AutoDock Vina (Zeleke *et al.*, 2020). The crystal structures of substrate and nucleotide complexes of *Enterococcus faecium* aminoglycoside-2''-phosphotransferase-IIa [APH(2'')-IIa] (PDB ID: 3HAM) and the crystal structures of full-length Lanosterol 14 alpha-demethylases of the prominent fungal pathogen, *Candida albicans* (PDB ID: 5V5Z) were downloaded from the protein data bank. The target protein file was prepared by leaving the associated residue with the protein using auto preparation of the target protein file AutoDock 4.2 (MGLTools 1.5.6), and the protein preparation was carried out using the reported standard protocol (Narramore *et al.*, 2019). The grid box for the docking simulations was set using the graphical user interface application. The macromolecule's region of interest was put up in the grid so that it is encircled by it. The best-docked configuration between the ligand and protein was sought using the docking algorithm offered by AutoDock Vina (Narramore *et al.,* 2019; Seeliger and de Groot, 2010; Zeleke *et al.*, 2020). For each ligand, a maximum of 9 conformers were considered throughout the docking procedure. The post-docking evaluations were conducted using **PyMOL** and Discovery Studio.

Table 1. The chemical compounds identified in the volatile oil of C. *zenkeri.*

S/N	PubChem No.	Name	3D Structure
1	28021	2,2,3-trimethylhexane	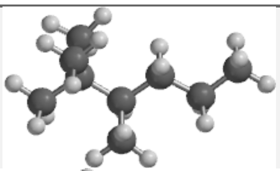
2	12986	2-methyl-1-pentene	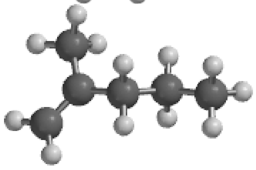

3	6432308	γ-murolene	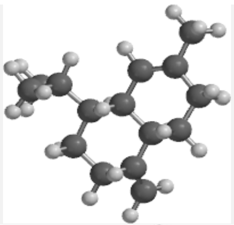
4	638072	Squalene	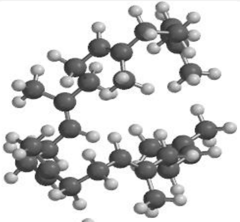
5	91699505	Velerenol	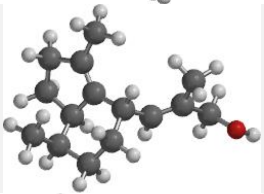
6	74764030	Gremacrene D	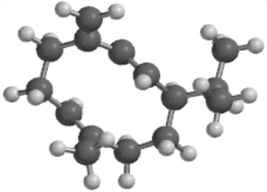

3. Results and discussion

3.1. Yield of the oil

The weight of roots of *C. zenkeri* used during hydro-distillation extraction, and the weight of the essential oils obtained, and the corresponding percentage yield are presented in **Table 2**. **Figure 1** is the GC-MS chromatogram of the root volatile oil of *C. zenkeri.* Plant material (200 g) was used in the extraction process, resulting in 1.58 g of colourless oil, which equates to a yield of 0.79%.

3.2. Identification of the chemical constituents of the volatile oil

The GC-MS result of the chemical constituents of the volatile oil is given in **Table 3** and **Fig. 2**. The 6 identified compounds are responsible for 80.07% of the root's volatile oil. The major compounds in root volatile oil include 2-methyl-1-pentene (40.01%), Gremacrene D (19.68%) and Squalene (10.95%). The root volatile oil of *C. zenkeri* was of different classes of compounds: alkene (40.01%), sesquiterpenes (20.35%) and triterpene (10.95%), oxygenated sesquiterpenes (2.71%) and alkane (6.05%). Terpenoids are known for their antimicrobial activity (Ogunnusi *et al*., 2010).

In the GC-MS analysis of the *n*-hexane extract of *Bambusa nrundinaceae* leaves and *Trigonell tehranica* essential oils, 2, 2, 3-trimethylhexane and 2-methyl-1-pentene were identified as one of the main chemical constituents in the extract and essential oils of both plants. The *B. nrundinaceae* leaf extract and *T. tehranica* oil exhibited strong antimicrobial properties (Kiashi *et al*., 2017; Zubair *et al*., 2013). In the *Hypericum perforatum* plant, volatile oils rich in germacrene D and other sesquiterpenes have been found to have anti-radical and anti-proliferative effects on tumour cell lines (Mockute, *et al.,* 2008; Casigilia *et al*., 2017). Similarly, the germacrene D dominant essential oils of *Siparuna aspera, Siparuna macrotepala, piper leticianum, piper augustum* possess significant antimicrobial activity (Noriege *et al*., 2019), *Ocotea silvestris* and *Ocotea indecora* leaves exhibit good antifungal activity against *candida parapsilosis* (Rambo *et al*., 2022). Studies have shown that the squalene-rich acetone fraction of *Stichopus hermanni* extract is a potent antibacterial and antifungal agent. Squalene is a well-known dietary supplement that has been shown to be effective in the treatment of cancer (Nazemi *et al*., 2022).

Table 2. Yields and properties of the volatile oil.

S/N	Plants name & parts	Weight of plant material (g)	Weight of oil (g)	Percentage (%) Yield of oil	Colour of oil
1	*C. zenkeri*, root	200	1.58	0.79	Colourless

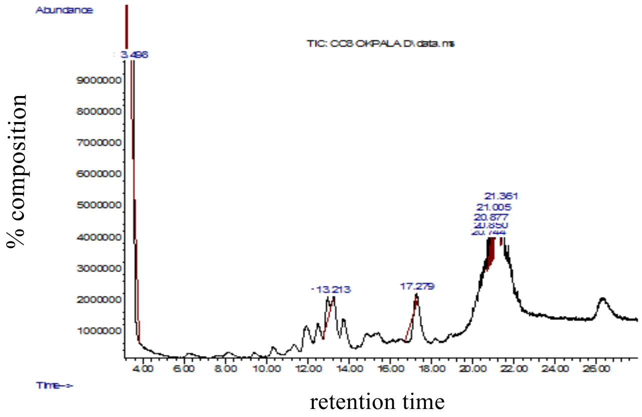

Figure 1. GC-MS Chromatogram of components of *Celtis zenkeri* roots volatile oil.

Table 3. Chemical composition of the roots volatile oil of *C. zenkeri*.

S/N	RI	Compounds	% Composition
1	91	2,2,3-trimethylhexane	6.05
2	321	2-methyl-1-pentene	40.01
3	447	Germacrene D	19.68
4	1302	γ- muurolene	0.67
5	1725	Velerenol	2.71
6	1825	Squalene	10.95
		Total % Composition	80.07

Note: RI = Calculated Retention Index; Compounds = Compounds listed in order of elution from a HP-5MS column; % Composition = Percentage composition.

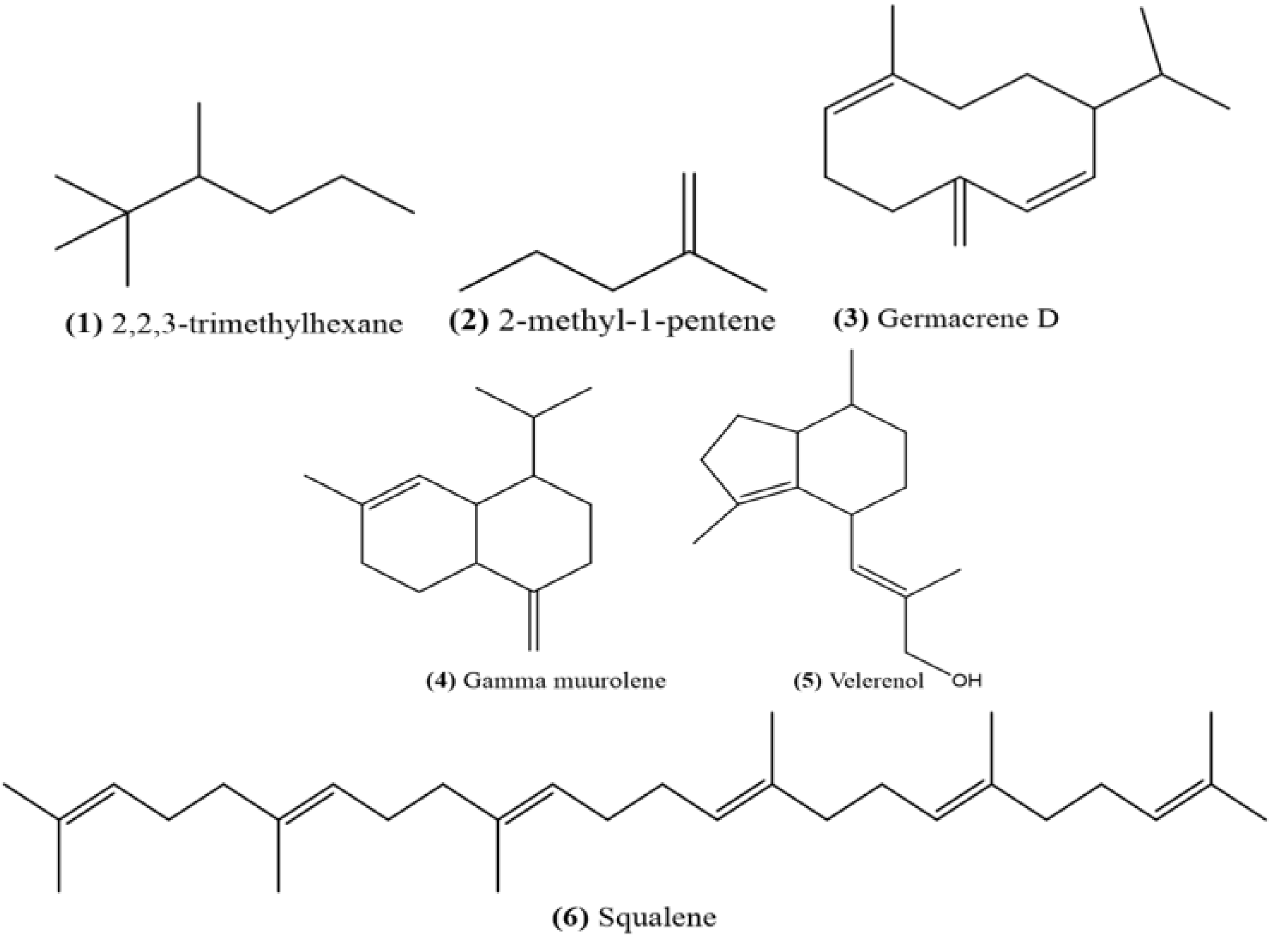

Figure 2. Structures of the compounds identified in roots volatile oil of *C. zenkeri*.

3.3. Antimicrobial activity of the volatile oil

The antimicrobial activity of the volatile oil from the roots of *C. zenkeri* is presented in **Table 4**. Comparing the volatile oil to the positive control (gentamicin 10 µg/mL for bacteria and tioconazole 0.07 µg/mL for fungi), the volatile oil showed a broad spectrum of activity against all microorganisms at 125-1000 µg/mL concentrations. Both gentamicin and ticonazole are well-known antibiotics that are frequently prescribed in healthcare facilities to treat infections (Ngoupayo *et al*., 2015; Okpala *et al*., 2019). In every tested concentration, they demonstrated better growth inhibition than the volatile oil. This investigation revealed that, despite significant variations in the recorded zone of inhibition when compared to the controls, which are well-known antibacterial and antifungal medications, the volatile oil exhibits moderate to good activity at higher concentrations (Lima-Filho *et al*., 2002; Obame *et al*., 2008; Sohail *et al*., 2018).

The oil's zone of inhibition against gram-positive and gram-negative bacteria ranged from 24-10 mm, while Gentamicin's ranged from 40-38 mm at concentrations of 125-1000 µg/mL. The most susceptible bacteria strains to volatile oil were *Pseudomonas aeruginosa and Staphylococcus aureus*. At concentrations ranging from 125 to 1000 µg/mL, the oil demonstrated growth inhibition against the fungi with a zone of inhibition between 18 and 10 mm whereas, the zone of inhibition of tioconazole was between 28 and 26 mm. At lower concentrations, there is either no activity or no significant inhibition. According to Kaur *et al*. (2011), a combination of compounds in essential oils is responsible for the antifungal activity of essential oils.

The volatile oil was generally found to be more effective against fungi than bacteria. This finding supports the traditional use of *C. zenkeri* for treating skin infections, including scabies and eczema, particularly those caused by *Rhizopus stolonifer*, *Penicillum notatum,* and *Candida albicans* (Burkill, 1995; Olaoluwa and Olapeju, 2015). Essential oils containing aldehydes or phenols as major constituents have been reported to exhibit the highest level of antimicrobial activity, with terpene alcohol-containing essential oils following closely behind. Other essential oils with ketones or ester had far less activity than volatile oils with terpene-hydrocarbons, which are usually inactive. However, the interaction of the different components may result in negative, positive, or advantageous effects (Janssen *et al*., 1987).

3.4. Molecular docking analysis

The binding affinities calculated from the docking simulation of compounds found in the volatile oil of *C. zenkeri* are presented in **Table 5**. The identified compounds in the volatile oil were docked against the substrate and nucleotide complexes of *Enterococcus faecium* aminoglycoside-2''-phosphotransferase-IIa [APH(2'')-IIa] (PDB ID: 3HAM) and full-length Lanosterol 14 alpha-demethylases of the prominent fungal pathogen, *Candida albicans* (PDB ID: 5V5Z), and the interacting modes (hydrogen bonding, hydrophobic and Van der Waal interactions) of the compounds with promising affinities are displayed in **Tables 6** and **7**.

Molecular docking results of the substrate and nucleotide complexes of *Enterococcus faecium* aminoglycoside-2''-phosphotransferase-IIa [APH(2'')-IIa] (PDB ID: 3HAM) compared with the clinical drugs (Gentamicin) docked with compounds identified in the roots oil of *Celtis zenkeri.* The compounds were found to have minimum binding energies ranging from –17.6 to –29.7 kJ/mol (**Table 5**), with the best results achieved using compounds gremacrene D and γ-muurolene (–29.7 kJ/mol). According to Adepoju *et al*. (2022), the lower the binding affinity value of any compound, the better the inhibiting ability of such compound; thus, compounds: gremacrene D and γ-muurolene were observed to have the highest tendency to inhibit the studied receptor than other identified compounds.

Similarly, results from docking lanosterol 14 alpha-demethylases of the prominent fungal pathogen, *Candida albicans* (**PDB ID: 5V5Z**) with the ligands showed that two of the identified compounds in the oil have higher inhibitory activities than tioconazole (**Table 5**) vis-à-vis γ-muurolene (–32.2 kJ/mol) and squalene (–38.1 kJ/mol). Thus, these identified compounds can be better drug candidates than Tioconazole (–31.4 kJ/mol) for the treatment of fungi infections. When a compound's binding affinity decreases, its drug-likeness increases, and its inhibitory potency increases (Omotayo *et al*., 2022; Oyewole *et al*., 2020).

Table 4. Antimicrobial activity of the volatile root oil of *C. zenkeri.*

	Test microorganisms / Zones of Inhibition (mm)									
Conc. (µg/mL)	*S. auerus*	*B. subtilis*	*E. coli*	*P. aeruginosa*	*S. typhil*	*K. pneumona*	*C. albican*	*A. niger*	*P. notatum*	*R. stolonifer*
1000	24	18	20	24	22	20	18	16	16	18
500	20	16	18	20	18	18	16	14	14	14
250	18	14	16	18	16	16	14	12	12	12
125	14	12	12	14	14	14	12	10	10	10
62.5	10	10	10	12	12	12	10	-	-	-
31.25	-	-	-	10	10	10	-	-	-	-
DMSO	-	-	-	-	-	-	-	-	-	-
Gen. (+ve)	38	38	38	40	38	38	-	-	-	-
Tio. (+v)	-	-	-	-	-	-	28	28	26	28

Note: DMSO: negative control (Dimethylsulphoxide); Gen. (+ve): positive control (Gentamicin at 10µg/ml for bacteria); Tio. (+ve): positive control (Tioconazole 70% for fungi); *S. aureus: Staphylococcus aureus; E. coli: Escherichia coli; B. subtilis= Bacillus subtilis; P. aeruginosa: Pseudomonas aeruginosa; S. typhil: Salmonella typhi; K. pneumonae: Klebsiellae pneumona; C. albicans: Candida albicans; A. niger: Aspergillus niger; P. notatum= Penicillum notatum; R. stolonifer: Rhizopus stolonifer;* **-**: no inhibition.

Table 5. Binding Affinities of the Receptors PDB ID: 3HAM and PDB ID: 5V5Z with the identified compounds (ligands) in the volatile oil.

S/N	Ligand Number	PDB ID: 3HAM		PDB ID: 5V5Z	
		Binding Affinity (kJ/mol)	Inhibitory constant (Ki, µM)	Binding Affinity (kJ/mol)	Inhibitory constant (Ki, µM)
1	3467	−30.5	4.43		
2	5482	–	–	−31.4	3.16
3	28021	−19.7	357.40	−20.9	215.24
4	12986	−17.6	831.46	−17.2	984.41
5	6432308	−29.7	6.21	−32.2	2.25
6	638072	−23.8	66.00	−38.1	0.21
7	91699505	−27.6	14.44	−28.9	8.70
8	74764030	−29.7	6.21	−31.4	3.16

Table 6. Docking ligand-receptor complexes of selected ligands with the binding affinity (PDB ID: 3HAM).

	3D representation	2D representation
3467	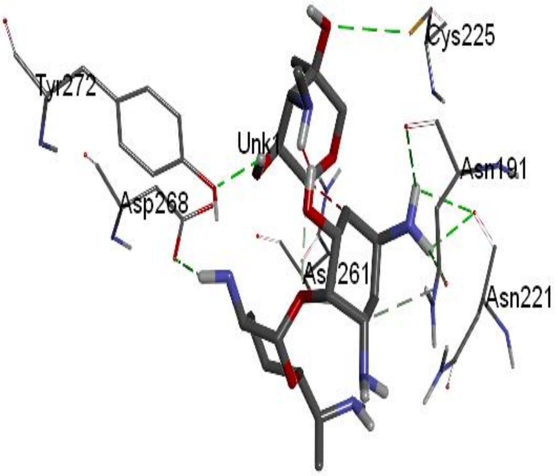	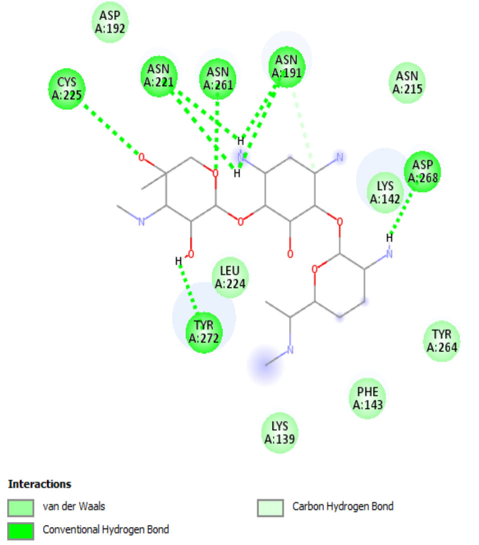
28021	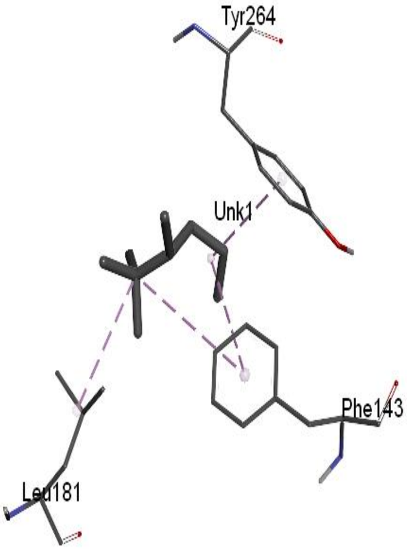	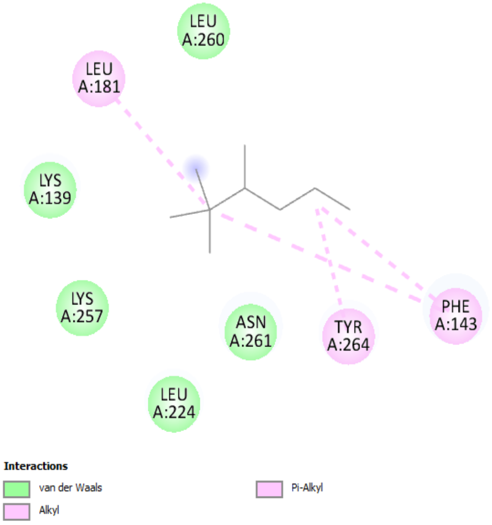
12986	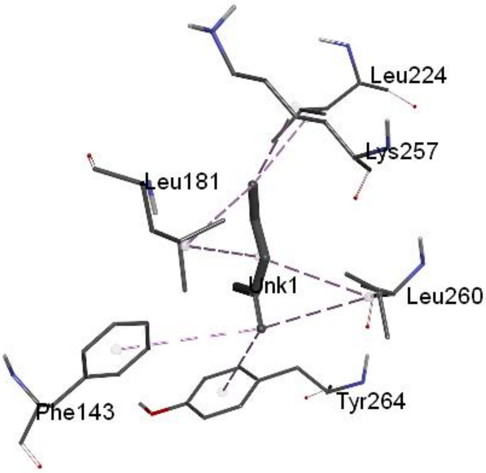	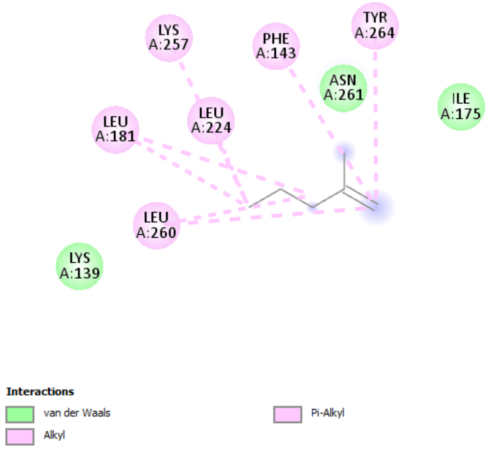

6432308

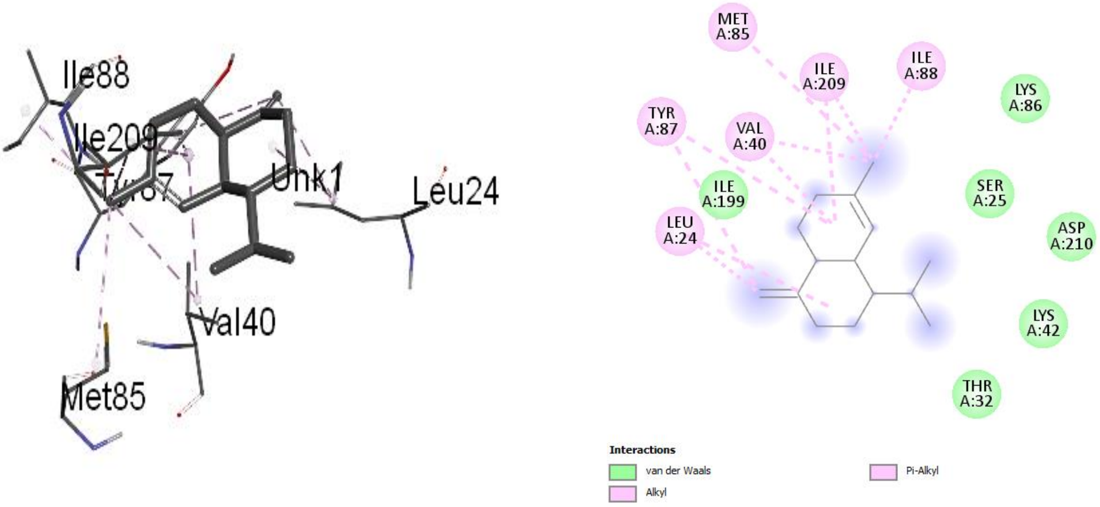

638072

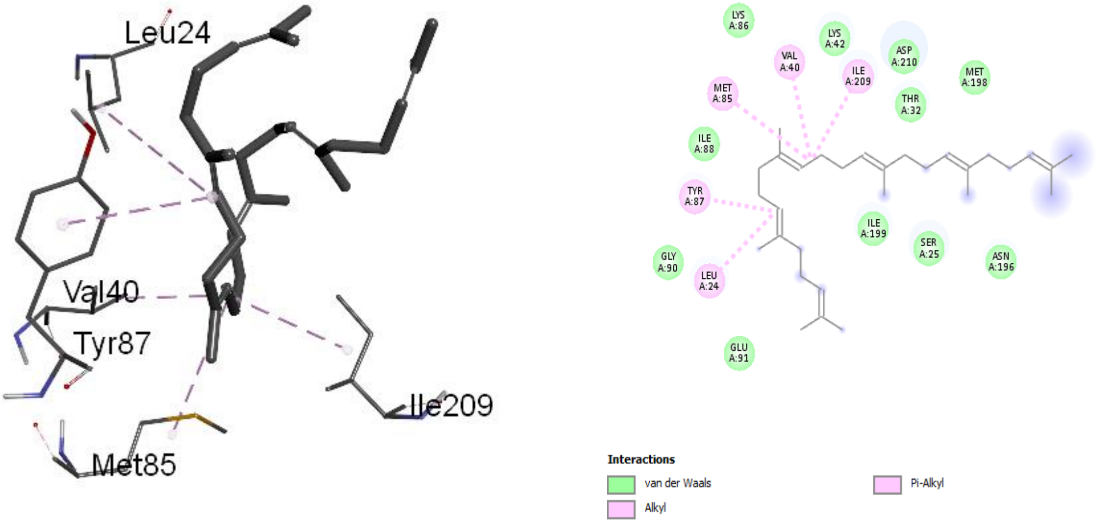

91699505

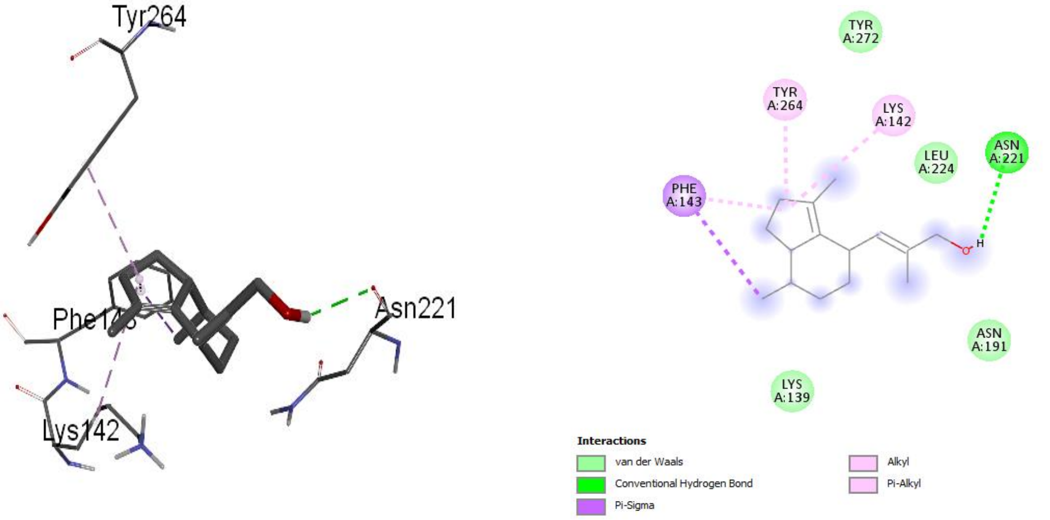

74764030	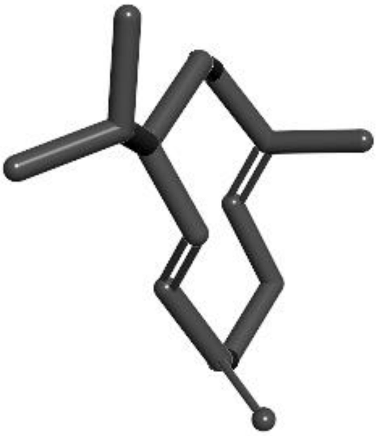	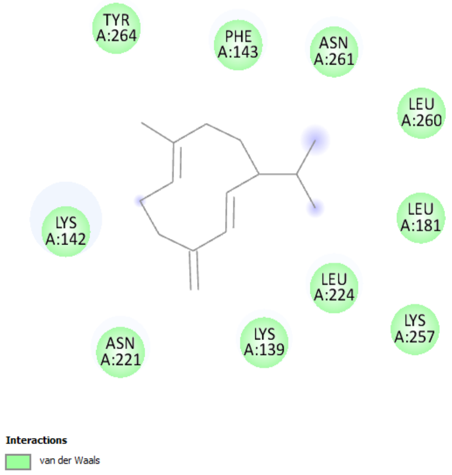

Table 7. Docking ligand-receptor complexes of selected ligands with the binding affinity (PDB ID: 5V5Z).

	3D representation	2D representation
5482	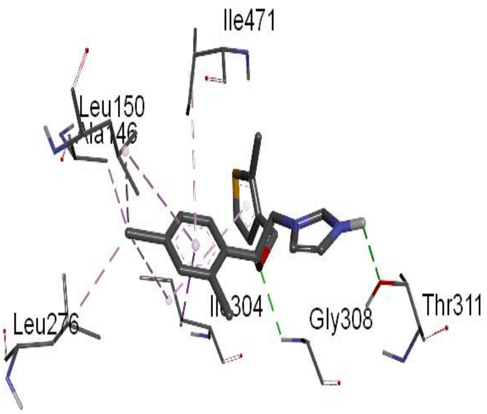	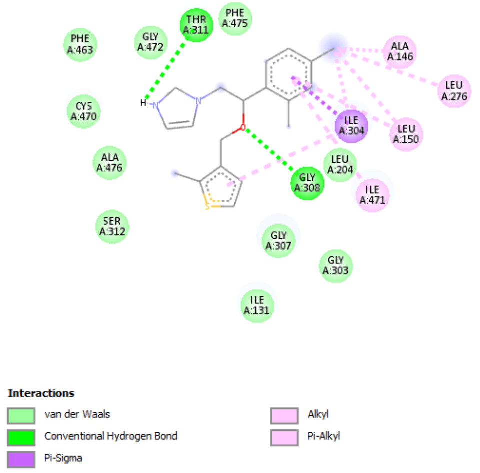
28021	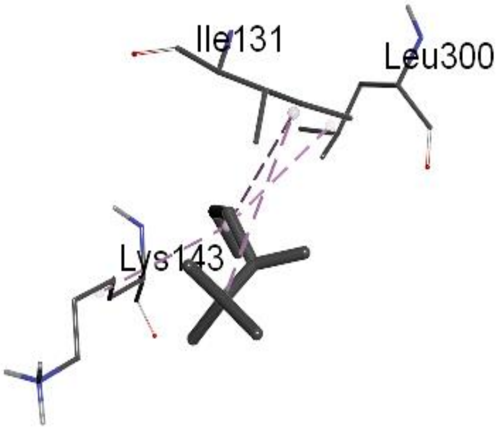	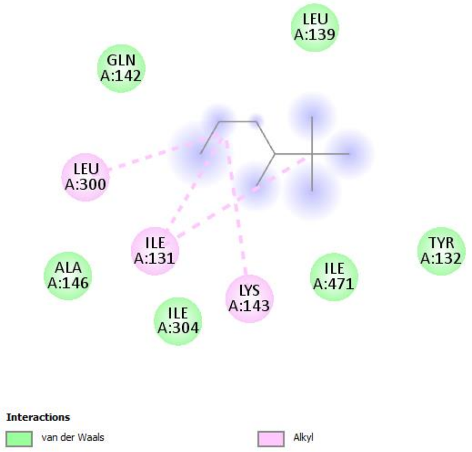

12986

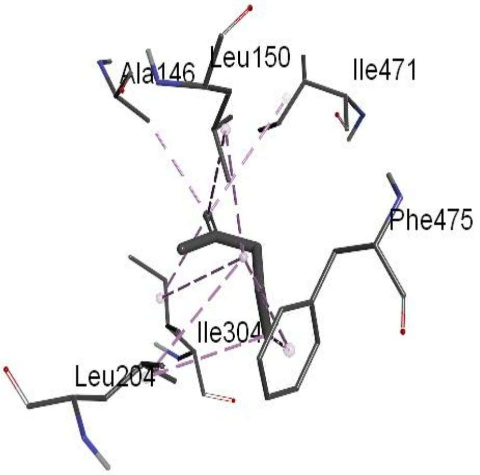

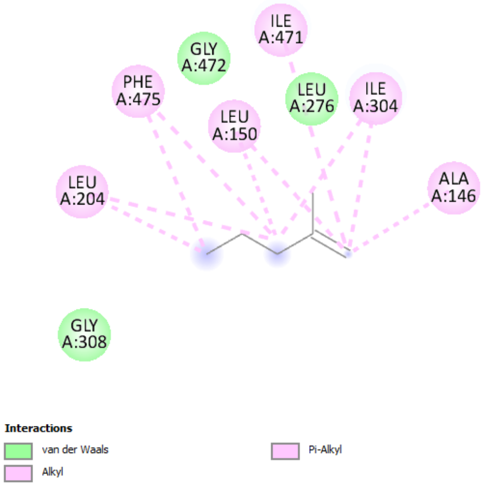

6432308

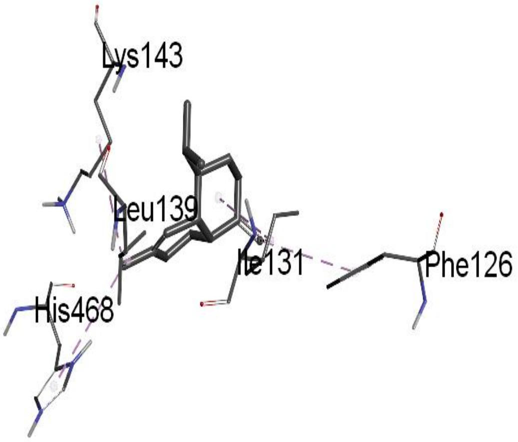

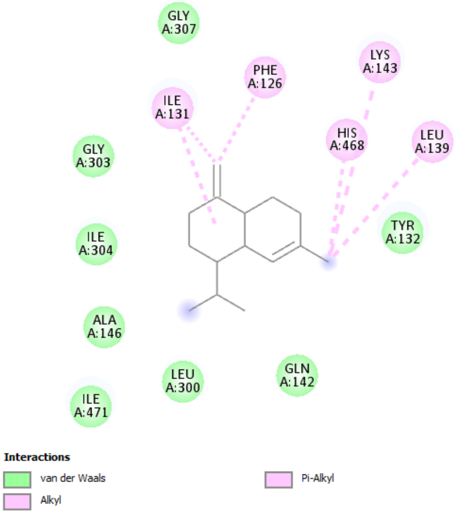

638072

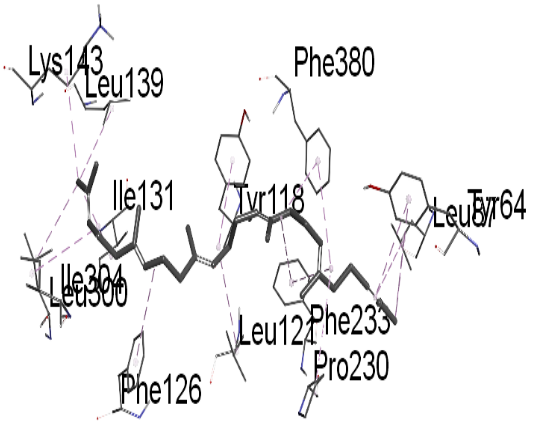

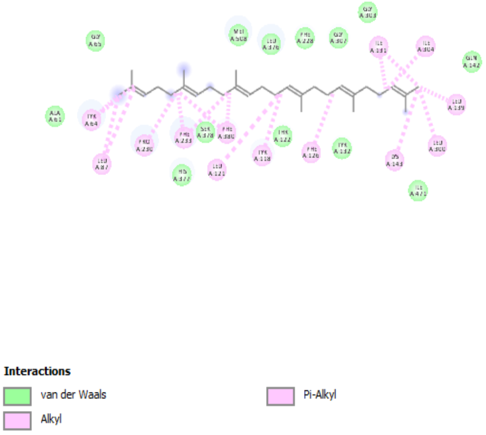

91699505	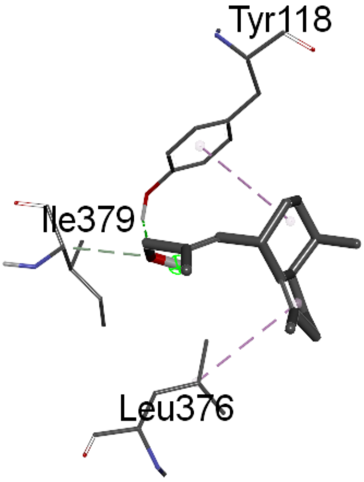	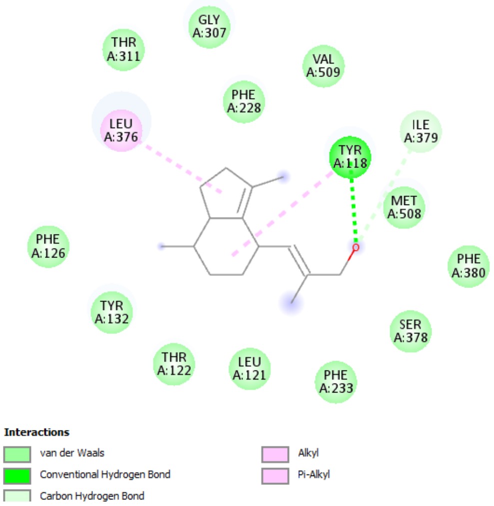
74764030	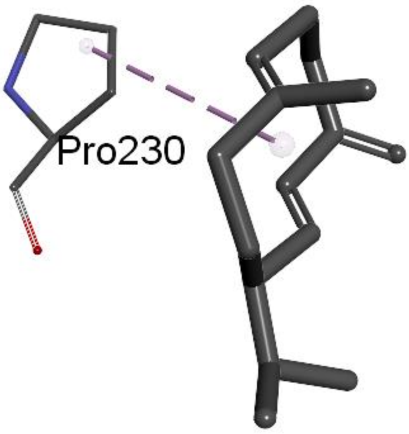	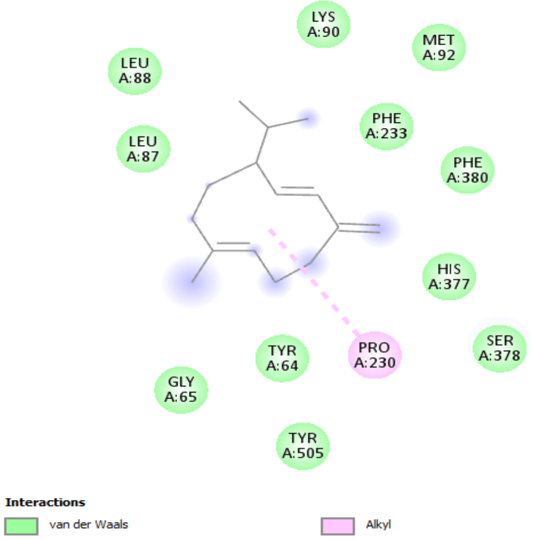

4. Conclusions

For the first time, chemical components, antibacterial and antifungal properties of the volatile oil from the roots are reported. This study is the first attempt to accurately characterize the volatile oil from the roots of *C. zenkeri* and conduct antibacterial and antifungal tests on it. The volatile oil is a potential candidate for the development of antibiotic drugs due to its antimicrobial activity against various tested strains of bacteria and fungi. Our study is the first report on the antimicrobial properties of the essential oil from *C. zenkeri*. The *in silico* molecular docking analysis of the volatile oil-identified compounds revealed good agreement with the outcomes of the *in vitro* antibacterial assay, when a compound's binding affinity decreases, its drug-likeness increases, and its inhibitory potency increases. The components of the volatile oil from *C. zenkeri* roots were also shown by the molecular docking analysis to be potential good sources for protein targeted antimicrobial compounds. This supports the use of *C. zenkeri* in folklore remedies for infections caused by microorganisms.

Authors' contributions

Conceptualization: Ejike Onwudiegwu Okpala; William Ojoniko Anthony; Godfrey Okechukwu Eneogwe; **Data curation:** Ejike Onwudiegwu Okpala; William Ojoniko Anthony; Godfrey Okechukwu Eneogwe; **Formal Analysis:** Ejike Onwudiegwu Okpala; William Ojoniko Anthony; Godfrey Okechukwu Eneogwe; **Funding acquisition:** Not Applicable; **Investigation:** Ejike Onwudiegwu Okpala; William Ojoniko Anthony; Godfrey Okechukwu Eneogwe; **Methodology:** Ejike Onwudiegwu Okpala; Oluwakayode Olubunmi Odeja; Michael Gabriel Ibok; **Project administration:** Joel Ojogbane Onoja; Samuel Akinniyi Odewo; Shedrach Ndubuisi Ike; **Resources:** Olusimbo Adesegun Onanuga; Samuel Akinniyi Odewo; Shedrach Ndubuisi Ike; **Software:** Ejike Onwudiegwu Okpala; William Ojoniko Anthony; Godfrey Okechukwu Eneogwe; **Supervision:** Banjo Semire; **Validation:** Ejike Onwudiegwu Okpala; William Ojoniko Anthony; Godfrey Okechukwu Eneogwe; **Visualization:** Ejike Onwudiegwu Okpala; William Ojoniko Anthony; Godfrey Okechukwu Eneogwe; **Writing – original draft:** Ejike Onwudiegwu Okpala; William Ojoniko Anthony; **Writing – review & editing:** Oluwakayode Olubunmi Odeja; Michael Gabriel Ibok.

Data availability statement

All data sets were generated or analyzed in the current study.

Funding

Not applicable.

Acknowledgments

The authors acknowledge the Department of Chemistry and Central Research Laboratory, University of Ibadan, Nigeria for facilities utilized in conducting the research.

References

Adepoju, A. J.; Latona, D. F.; Olafare, O. G.; Oyebamiji, A. K.; Abdul-Hammed, M.; Semire, B. Molecular docking and pharmacokinetics studies of *Curcuma longa* (Curcumin) potency against Ebola virus. *Ovidius Univ. Ann. Chem*. **2022**, *33* (1), 22–35. https://doi.org/10.2478/auoc-2022-0004

Ata, A.; Van Den Bosch, S. A.; Harwannik, D. J.; Pidsinski, G. E. Gluthathione-S transferase and acetylcholinesterase inhibiting natural products from medicinally important plants. *Pure Appl. Chem*. **2007**, *70*, 2269–2279. https://doi.org/10.1351/pac200779122269

Bakkali, F.; Averbeck, S.; Averbeck, D.; Idaomar, M. Biological effects of essential oils- a review. *Food Chem. Toxicol.* **2008**, *46* (2), 446–4475. https://doi.org/10.1016/j.fct.2007.09.106

Bottomley, M. J.; Muraglia, E.; Bazzo, R.; Carfi, A. Molecular Insights into Quorum Sensing in the Human Pathogen *Pseudomonas aeruginosa* from the Structure of the Virulence Regulator LasR Bound to Its Autoinducer. *J. Biol. Chem.* **2007**, *282* (18), 13592–13600. https://doi.org/10.1074/jbc.m700556200

Paterson, G. R. (1982). British Pharmacopoeia 1980. Can. Med. Assoc. J. **1982**, *126* (5), 514.

Burkill, H. M. The useful plants of West tropical Africa. Royal Botanic garden Kew. **1995**, *2*, 160–163.

Casigilia, S.; Bruno, M.; Bramucci, M.; Quassinti, L.; Lupidi, G.; Fiorini D.; Maggi, F. *Kundmannia sicula* (L.) DC: a rich source of germacrene D. *J. Essent. Oil Res*. **2017**, *29* (6) 437-442. https://doi.org/10.1080/10412905.2017.1338625

Cassel, E.; Vargas R. M. F. Experiments and modeling of the *Cymbopogon winterianus* essential oil extraction by steam distillation. *J. Mexican Chem. Soc.* **2006**, *50*, 126–129.

Di Leo Lira, P.; Retta, D.; Tkacik, E.; Ringuelet, J.; Coussio, J. D.; Van Baren, C.; Bandoni A. L. Essential oil and by-products of distillation of bay leaves (*Laurusnobilis* L.) from Argentina. *Ind. Crops Prod.* **2009**, *30* (2), 259–264. https://doi.org/10.1016/j.indcrop.2009.04.005

El-Mahmood, A. M.; Doughari, J. H. Phytochemical Screening and Antibacterial evaluation of the leaf and root extracts of *Cassia alata* Linn. *Afr. J. Pharm. Pharmacol.* **2008**, *2* (7), 124–129.

Fabeku, P. O. Traditional Medicine: the art, ways and practice. *In*: Odugbemi, T. (Ed.). *Outlines and Pictures of Medicinal Plants from Nigeria*; University of Lagos Press, **2006**, p. 13–24.

Fadipe, A. L. Some fatty acids ester of the ripe fruits of *Nauclea latifolia* (family: Rubiacea). *Inter. J. Res. Pharm. Chem.* **2014**, *4* (4), 783–788.

Hamburger, M.; Hostettmann, K. Bioactivity in plants: the link between phytochemistry and medicine. *Phytochemistry.* **1991**, *30* (12), 3864–3874. https://doi.org/10.1016/0031-9422(91)83425-K

Hanazki, N.; Tamishoro, J. Y.; Leitao-Filho, H.; Gegossi, A. Diversity of Plant use in Caicaras Communities from the Atlantic forest coast, Brazil. *Biodiversity and Conservation*. **2000**, *9*, 597–615.

Ibok, M. G.; Odeja, O. O.; Okpala, E. O.; Eghwubare, J. E.; Anifalaje E. O. *Eremomastax speciosa* (Hochst.): GC/MS Profiling, Antioxidant and Antimicrobial Activities of Stem Essential oil. *Futur. J. Pharm. Sci.* **2023**, *9*, 51. https://doi.org/10.1186/s43094-023-00501-4

Janssen, A. M.; Scheffer, J. J. C.; Baerheim-Svendsen, A. Antimicrobial activities of essential oils. A 1976-1986 literature review on possible applications. *Pharm. Weekblad Sci. Edu.* **1987**, *9*, 193–197. https://doi.org/10.1007/BF02029329

Kaur, S.; Singh, H. P.; Batish, D. R.; Kohli, R. K. Chemical characterization, antioxidant and antifungal activity of essential oil from *Eucalytus tereticornis*. *Journal of medicinal plants Research.* **2011**, *5* (19), 4788–4793.

Kiashi, F.; Momeni-nasab, F.; Akhbar, M.; Hadjiakhoondi, A.; Aghaahmeddi M.; Tavakoli S.; Tofighi Z. Phytochemicals and antimicrobial activities of aerial parts and roots of *Trigonella tehranica L.* essential oils. *Res. J. Pharmacogn.* **2017**, *4* (4) 29–30.

Lapa, G. B.; Bekker, O. B.; Mirchink, E. P.; Danilenko, V. N.; Preobrazhenskaya, M. N. Regioselective acylation of congeners of 3-amino-1H-pyrazolo[3,4-b]quinolines, their activity on bacterial serine/threonine protein kinases and in vitro antibacterial (including antimycobacterial) activity. *J. Enzyme Inhib. Med. Chem.* **2012**, *28* (5), 1088–1093. https://doi.org/10.3109/14756366.2012.716056

Lima-Filho, J. V. M.; Carvalho, A. F. F. U.; Freitas, S. M.; Melo, V. M. M. Antibacterial activity of extracts of six macroalgae from the North-eastern Brazillian coast. *Braz. J. Microbiol*. **2002**, *33* (4), 311–313. https://doi.org/10.1590/S1517-83822002000400006

Masango, P. Cleaner production of essential oils by steam distillation. *J. Cleaner Prod.* **2005**, *13* (8) 833–839. https://doi.org/10.1016/j.jclepro.2004.02.039

Mohamed, A. A.; El-Emary, G. A.; Ali, H. F. Influence of some citrus essential oils on cell viability, glutathione-s-transferase and lipid peroxidation in *Ehrlich ascites* Carcinoma cells. *J. Am. Sci.* **2010**, *6*, 820–826.

Mockute, D.; Bernotiene, G.; Judzentiene, A. The essential oils with dominant germacrene D of *Hypericum perforatum* L. growing wild in Lithuania. *J. Essent. Oil Res.* **2008**, *20* (2), 128–131. https://doi.org/10.1080/10412905.2008.9699973

Narramore, S.; Stevenson, C. E.; Maxwell, A.; Lawson, D. M.; Fishwick, C. W. New insights into the binding mode of pyridine-3-carboxamide inhibitors of E. coli DNA gyrase. *Bioorganic & Medicinal Chemistry*. **2019**, *27* (16), 3546–3550. https://doi.org/10.1016/j.bmc.2019.06.015

Nazemi, M.; Motallebi A.; Abbasi Z.; Khaledi M.; Zare, M. Antibacterial, antifungal and cytotoxic activity of the fraction contains squalene in the acetone extract of a sea cucumber, *Stichopus hermanni*. *Iran. J. Fish. Sci.* **2022**, *21* (6) 1495–1507.

Neumann, R. R.; Hirsch, E. *Commercialization of Non-Timber Forest Products*: Review and Analysis for Research; CIFOR, 2000.

Ngoupayo, J.; Kasali F. M.; Djiele N. P.; Turibio T. K.; Ali, M. S. Antimicrobial of extract and compounds from the bark of *Drypetes afzelii* (pax) Hutch. *J. Pharmacogn. Phytochem.* **2015**, *4* (4), 250–255.

Noriege P.; Guerrini, A.; Sacchetti G.; Grandini, A.; Ankuash E.; Manfredini, S. Chemical composition and biological activity of five essential oils from Ecuadorian Amazon rain forest. *Molecule.* **2019**, *24* (8), 1637. https://doi.org/10.3390/molecules24081637

Obame, L. C.; Edou P.; Bassole I. H. N.; Koudou, J.; Agnaniet, H.; Eba, F.; Traore, A. S. Chemical composition, antioxidant and antimicrobial properties of essential oil of *Dacryodes edulis* (G. Don) H. J. Lam from Gabon. *African J. Microbiol. Res.* **2008**, *2*, 146–152.

Odeja O. O.; Okpala E. O.; Ibok, M. G.; Okoro, E. E.; Onoja J. O. Essential oil Composition, Antioxidant and Antibacterial Activities of *Jatropha tanjorensis* (Euphorbiaceae). *Ann. Rev. Resear.* **2023**, *9* (1), 55575. https://doi.org/10.19080/arr.2023.09.555751

Ogunnusi, T. A.; Oso, B. A.; Dosumu, O. O. Isolation and antibacterial activity of triterpeme from *Euphorbia kamerunica* pax. *Int. J. Biol. Chem. Sci.* **2010**, *4* (1), 158–167. https://doi.org/10.4314/ijbcs.v4i1.54241

Okpala, E. O.; Oloyede, G. K.; Onocha, P. A. Chemical Composition, Antimicrobial and Antioxidant Activities of Volatile oil of *Euphorbia graminea* JACQ from Nigeria. *Int. J. Adv. Sci. Eng. Inf. Techno.* **2019**, *7* (4), 50–54.

Okpala, E. O.; Onocha, P. A.; Ali, M. S.; Zikr-Ur-Rehmen, S.; Lateef, M. Zenkeramide: a new iso-benzofuranone propanamide and urease inhibitory constituents of *Celtis zenkeri* Engl stem bark (Ulmaceae). *Nat. Prod. Res.* **2021**, *37* (1) 93–98. https://doi.org/10.1080/14786419.2021.1954643

Okpala, E. O.; Onocha, P. A.; Ali, M. S. Antioxidant activity of phytol dominated stem bark and leaf essential oils of *Celtis zenkeri* Engl. *Trends Phytochem. Res.* **2022**, *6* (2), 137–144. https://doi.org/10.30495/tpr.2022.1952985.1246

Olaoluwa, O. O.; Olapeju, A. O. Phytochemical investigation and antimicrobial screening of *Cardiospermun grandiflorum* (Sweet), Sapindaceae. *Int. J. Pharm. Sci. Res.* **2015**, *6* (2), 348–351.

Omotayo, I. A.; John, A. A.; Gbenga, O. O.; Misbaudeen, A.-H.; Felix, L. D.; Kolawole, O. A.; Banjo, S. *In-silico* assessment via molecular docking and ADMET profile of Botanical drugs (bergamottin and casticin) against trial drugs for Lassa virus. *Int. J. Pharm. Sci. Res.* **2022**, *13* (9), 3494–3518. https://doi.org/10.13040/IJPSR.0975-8232.13(9).3494-18

Oyewole, R. O.; Oyebamiji, A. K.; Semire, B. Theoretical calculations of molecular descriptors for anticancer activities of 1,2,3-triazole-pyrimidine derivatives against gastric cancer cell (MGC-803): DFT, QSAR and docking approaches. *Heliyon.* **2020**, *6* (5), e03926. https://doi.org/10.1016/j.heliyon.2020.e03926

Pamplona-Roger, G. D. *Encylopedia of medicinal plants*; Education and Health Library, 2004.

Rambo, A.-M.; Soares, K. D.; Danielli, J. L.; Lana, D. F. D.; Bordignon, L. A. S.; Fuentefria, M. A.; Apel, M. A. *Biological Activities of Essential Oils from Six Genotypes of Four ocotea Species. Braz. J. Pharm. Sci.* **2022**, *58*, e181097. https://doi.org/10.1590/s2175-97902022e181097

Rates, S. M. Plants as source of drugs. *Toxicon.* **2001**, *39* (5), 603–613. https://doi.org/10.1016/S0041-0101(00)00154-9

Seeliger, D.; Groot, B. L. Ligand docking and binding site analysis with PyMOL and Autodock/Vina. *J. Comput. Aided Mol. Des.* **2010**, *24* (5), 417–422. https://doi.org/10.1007/s10822-010-9352-6

Sohail, T.; Ferheen, S.; Imran, H.; Yaqueen Z.; Rehma, A.; Khan, R. A. Phytochemical and antibacterial screening of different fractions of root part *Ipomea Turpethum*. *Bangladesh J. Med. Sci.* **2018**, *17* (1), 93–97. https://doi.org/10.3329/bjms.v17i1.35288

Tanchuk, V. Y.; Tanin, V. O.; Vovk, A. I.; Poda, G. A. New, Improved Hybrid Scoring Function for Molecular Docking and Scoring Based on AutoDock and AutoDock Vina. *Chem. Biol. Drug Des.* **2015**, *87* (4), 618–625. https://doi.org/10.1111/cbdd.12697

United Nations Educational, Scientific and Cultural Organization (UNESCO). Traditional Knowledge into the twenty-first century: Nature and Resources; UNESCO, 1994.

World Health Organization (WHO). World Malaria Report; WHO, 2008.

Zeleke, D.; Eswaramoorthy, R.; Belay, Z.; Melaku, Y. Synthesis and Antibacterial, Antioxidant, and Molecular Docking Analysis of Some Novel Quinoline Derivatives. *J. Chem.* **2020**, *2020*, 1324096. https://doi.org/10.1155/2020/1324096

Zubair, M.; Bibi, Z.; Rizwan, K.; Rasool, N.; Zahoor F.A.; Riaz, M. In-vitro antimicrobial and Haemolytic Studies of *Bambusa nrundinaceae* leaves. *J. App. Pharm. Sci.* **2013**, *3* (4), 111–115. https://doi.org/10.7324/JAPS.2013.3420

ECLÉTICA QUÍMICA

Eclet. Quim. 49 | e-1534, 2024

Review Article

https://doi.org/10.26850/1678-4618.eq.v49.2024.e1534

Technology-enhanced learning influence on chemical literacy: A systematic review

Ananta **Ardyansyah**[1], Sri **Rahayu**[1+]

Abstract

Chemical literacy is essential to address socio-scientific issues arising today. Technology plays a key role in increasing students' chemical literacy. Understanding how technology improves chemical literacy can help teachers choose appropriate learning tools and strategies. A systematic review with PRISMA guidelines was conducted to map the technology widely used in current chemistry learning and know-how technology influences the development of chemical literacy based on the PISA framework. A total of 15 articles were identified as meeting the review criteria. The results show that based on the literature review, E-modules are the most commonly used technology to improve chemical literacy. Technologies such as augmented reality, Canva, e-modules, mobile apps, and websites are important for the ability to "explain phenomena scientifically". Adobe Flash Interactive Media and Virtual Laboratories are particularly effective for "constructing and evaluating designs for scientific investigation and critical interpretation of scientific data and evidence." Finally, search engine technology has a significant impact on the ability to "research, evaluate, and use scientific information for decision-making and action".

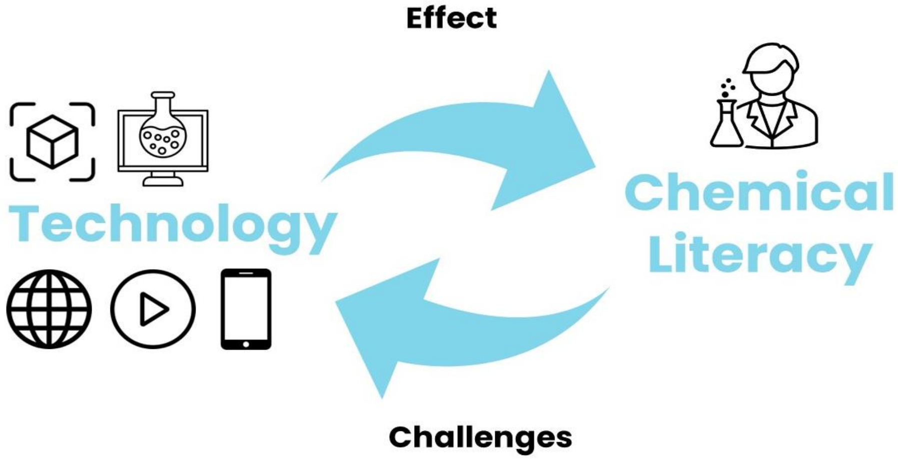

Article History

Received December 28, 2023
Accepted August 23, 2024
Published December 10, 2024

Keywords

1. chemical literacy;
2. influence of technology;
3. PISA framework;
4. systematic literature review;
5. technology-enhanced learning.

Section Editor

Assis Vicente Benedetti

Highlights

- The e-module is the most widely used technology to improve chemical literacy.
- The influence of each technology in improving chemical literacy is explained.
- Potential research gaps in using technology to improve chemical literacy are noted.

[1]Universitas Negeri Malang, Faculty of Mathematics and Science, Malang, Indonesia. **+Corresponding author:** Sri Rahayu, **Phone:** +62 8123394825, **Email address:** sri.rahayu.fmipa@um.ac.id

1. Introduction

Science education aims not only to produce young scientists but also to benefit society in general (Reiss *et al.*, 1999). Everyone should have the necessary scientific knowledge and be able to use the knowledge to explain phenomena scientifically, evaluate and design scientific inquiry, and interpret data and evidence scientifically (OECD, 2023). These competencies are part of scientific literacy, which is important nowadays. Although widely used in science education literature, the term "scientific literacy" has no specific consensus on its definition. The term is used in research, discussions, and analyses of science education goals, assessment programs, curriculum policies, programs, and learning resources. However, everyone agrees that students cannot be scientifically literate if they know nothing about the science. Scientific literacy has several other terms, but scientific literacy is the most widely recognized (Roberts, 2007).

Regardless of its meaning, scientific literacy is important because it influences various meanings, assessment methods, and topics of interest (Laugksch, 2000). Increased scientific literacy improves students' intellect, character, communication, positive behavior, and responsible citizenship (Holbrook and Rannikmae, 2007). Studies show that scientific literacy can foster the principles of democratic education and involve the community in decision-making on socioscientific issues (Yacoubian, 2018). With mathematical literacy, scientific literacy is a means to prepare for adult life, which is expected to involve public discussions related to science, technology, environment, and society, thus creating a democratic society (Yore *et al.*, 2007). Scientific literacy also plays a role in improving communication skills, critical thinking, metacognitive awareness, and understanding of culture and practices in science (Cavagnetto, 2010). Some other studies mention that scientific literacy can build a better society (Roth and Barton, 2004), accelerate the realization of sustainable development goals (SDGs) (Queiruga-Dios *et al.*, 2020), and develop 21st-century transferable skills (Rahayu, 2017). Given the importance of scientific literacy, it has become one of the key learning objectives that education, teachers, and policies focus on today.

In the chemistry field, scientific literacy is referred to as chemical literacy, which is defined as students' ability to recognize, define, conceptualize, and analyze chemical concepts at a higher level (Shwartz *et al.*, 2006b). Chemical literacy is a crucial component of scientific literacy (Mozeika and Bilbokaite, 2011; Stašević *et al.*, 2023), and essential for addressing today's socio-scientific issues. It encompasses a broad chemistry-related context and is connected to other sciences (Shwartz *et al.*, 2006a). Improved chemical literacy enables students to use chemical knowledge and skills to solve everyday problems (Stašević *et al.*, 2023) and socio-scientific issues (Wiyarsi *et al.*, 2021). Chemical literacy is not only about understanding chemistry but also about implementing it in daily life (Primadianningsih *et al.*, 2023). Additionally, it involves the ability to understand and communicate chemical concepts effectively among scientists and chemistry teachers (Kohen *et al.*, 2020). Understanding chemical literacy has significant implications for distinguishing between basic and advanced chemical learning (Shwartz *et al.*, 2005). Therefore, developing chemical literacy should be considered one of the primary objectives in chemistry education.

A key understanding of chemical literacy is required to develop it. While there is no specific consensus on chemical literacy, it can be defined within a scientific framework because it is part of scientific literacy. The most widely used scientific literacy framework today is the PISA framework. The PISA framework focuses on developing the competencies of a science-literate person, namely explaining phenomena scientifically, constructing and evaluating designs for scientific inquiry and interpreting scientific data and evidence critically, and researching, evaluating, and using scientific information for decision-making and action (OECD, 2023). In developing this, students must also understand knowledge (content, procedural, and epistemic) context (personal, local, and global) and have a scientific identity. This concept can be applied to chemical literacy so that the improvement of chemical literacy can be more directed.

Technology is a significant contributor to the quality of education. Thus, there is a growing practice and research on technology-enhanced learning (TEL). Technology-enhanced learning refers to using information and communication technology in learning and teaching, using various approaches and ways to measure improvement (Kirkwood and Price, 2014). It also refers to how to design and evaluate effective technology for learning (Duval *et al.*, 2017). With the utilization of technology, learning can be more optimal. In addition to learning outcomes, TEL supports collaborative learning (Tawafak *et al.*, 2018) and increases the satisfaction of the learning process (Memon *et al.*, 2022). By understanding the role of technology in a learning objective, it can be understood how technology contributes to achieving learning objectives, including chemical literacy.

Technologies like videos, simulations, and student response systems in chemistry learning can help reduce cognitive load, encourage discussion and debate, and improve students' problem-solving skills (Seery and McDonnell, 2013). Digital technologies, especially digital applications, and virtual reality, are widely used in chemistry learning because they help provide visualizations, show chemical structures and models, and provide hands-on activities (Ali *et al.*, 2023; Bellou *et al.*, 2018). The role of technology in chemistry learning is not only as a medium that helps students access material but also as a learning companion that helps students learn in various contexts and use what they learn in everyday life. For example, virtual laboratories can perform experiments in certain contexts (Wu *et al.*, 2021). Thus, it is important to understand how technology plays a role in improving chemistry learning objectives, especially chemical literacy, which is a fundamental goal in much of world education.

Overall, this systematic review is essential for informing educators, policymakers, and researchers about the potential of technology-enhanced learning in promoting chemical literacy. By synthesizing the current evidence, this review aims to advance educational practices that effectively cultivate chemical literacy among students, preparing them to engage with the complexities of the modern world. Therefore, this systematic literature review aims to map the technology widely used in current chemistry learning and analyze its influence on chemistry learning in the context of chemical literacy.

2. Experimental

The framework for preferred reporting items for systematic reviews and meta-analyses (PRISMA) is applied in this literature review. The PRISMA method follows the guidelines provided by Moher *et al.* (2009).

2.1. Eligibility criteria

The study only used peer-reviewed papers from multiple indexed databases. The articles we selected had to satisfy the following requirements: (1) they had to address the use of technology in chemistry education or learning; (2) they had to discuss the chemistry literacy component (competencies aspect); and (3) they had to address the direct effects of the use of technology on chemical literacy (4) the selected articles are those published above the year 2000 (this year was chosen because it was the first time the PISA survey was conducted). This review excluded articles that only mentioned scientific literacy without measuring its components. Articles that lacked a clear explanation of their methodology were likewise excluded. We do not use review papers; only original, English-language articles are used.

2.2. Search query

Several keywords were combined using the Boolean operators and OR to search for articles that met the chosen parameters. To identify articles that discuss the use of technology in learning to improve chemical literacy, a series of word combinations were employed, as shown in **Table 1**. These were then entered into a database to retrieve the relevant articles with Boolean operators, those keywords are used.

Table 1. The following keywords were utilized in the article search.

Technology related keyword	Chemical literacy related keyword	Additional keyword
Technology	Chemical literacy	
Learning Media		Chemistry
ICT	Scientific literacy	Chemistry Learning
Digital		

The databases Taylor & Francis, semantic scholar, and ERIC were searched for articles using these keywords. To refine the search results, the search also made use of the attributes that were offered. For example, in the Taylor & Francis database, we could select "chemical literacy" in the title. We employed quotations on the term "chemical literacy" to further refine the results.

2.3. Study selection

From the initial search of 503 articles, 85 were sourced from ERIC, 316 from Semantic Scholar, and 102 from Taylor & Francis. Following the removal of duplicates, articles were selected based on the presence of technology and chemical literacy aspects. Titles and abstracts were reviewed, and some articles were excluded for not addressing chemical literacy, lacking technological elements, or not being in English. This process yielded 114 items meeting the initial criteria. These articles underwent a detailed analysis, focusing particularly on the methods and results sections. However, some articles were deemed ineligible due to inaccessible full texts or failure to integrate chemical literacy with technology. Consequently, 24 articles met the criteria. A subsequent review of these 24 articles revealed issues such as lack of clarity in results, inadequate description of chemical literacy, and insufficient incorporation of technology in learning. This refinement resulted in 15 articles that fully met the criteria (**Fig. 1**). These selected articles were then subjected to coding analysis and grouped based on similar themes. To facilitate this, Excel 365's Pivot Table was employed to summarize data, such as the number of articles in each category. Additionally, VosViewer provided an overview of the most popular keywords and terms used in the articles.

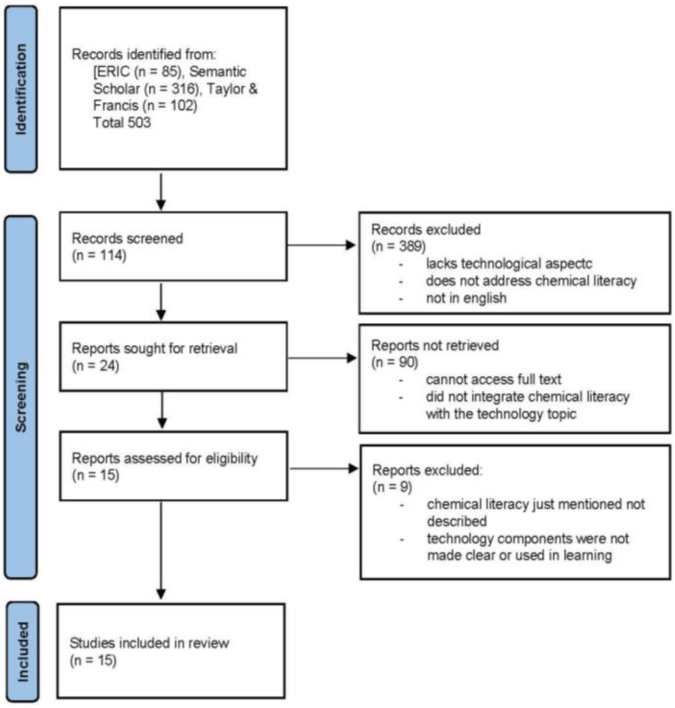

Figure 1. Flowchart of the literature selection process by PRISMA method.

3. Results and discussion

3.1. An overview of the empirical research included in the review

An overview of the 15 publications that are part of this study is provided in **Table 2**. The author and year, journal, subjects, type of research, and technology are all discussed in these articles. Here is the summary.

Most of the articles reviewed were published in 2022, totaling four articles. The research predominantly focused on senior high school students (n = 8). Regarding the research type, the articles were primarily characterized by "two-group experiment" studies (n = 5). In terms of technology, the most widely used technology was the E-module (n = 4). In detail, **Table 3** displays the technologies used in the selected articles.

Table 2. Overview of 15 articles that included on systematic review.

No.	Author	Journal	Subject	Type of research	Technology
1	Schultz *et al.* (2022)	Assess. Eval. High. Educ.	Undergraduate Student	Case Study	Search Engine
2	Frailich *et al.* (2007)	Res. Sci. Technol. Educ.	Senior High School Student	Two Group Experiment	Website
3	Sulistina and Hasanah (2024)	Int. J. Interact. Mob. Technol.	Senior High School Student	R&D One Group Pre-Post	Augmented Reality
4	Bortnik *et al.* (2017)	Res. Learn. Technol.	Undergraduate Student	Two Group Experiment	Virtual laboratory
5	Pulungan and Simamora (2024)	J. Inov. Pemb. Kim.	Senior High School Student	Two Group Experiment	Canva
6	Subarkah *et al.* (2020)	Proc. 1st Bandung Engl. Lang. Teach. Int. Conf.	Undergraduate Student	R&D Only	E-Module
7	Suliono *et al.* (2023)	J. Penelit. Pendidik.	Senior High School Student	R&D One Group Pre-Post	Mobile Apps
8	Techakosit and Wannapiroon (2015)	Procedia Soc. Behav. Sci.	Expert	R&D Only	Augmented Reality
9	Khery *et al.* (2020)	Int. Conf. Math. Sci. Educ.	Undergraduate Student	Two Group Experiment (Postest Only)	Mobile Apps
10	Sutiani and Pasaribu (2023)	J. Tadris Kimiya	Senior High School Student	R&D One Group Pre-Post	E-Module
11	Novitasari *et al.* (2022)	Eduvest J. Univ. Stud.	Senior High School Student	One Group Pretest-Postest	E-Module
12	Khairi and Ikhsan (2022)	J. Kimia Dan Pendidik. Kimia	Senior High School Student	Two Group Experiment (Postest Only)	E-Module
13	Yuendita and Dina (2024)	J. Penelit. Pendidik. IPA	Senior High School Student; Teacher	R&D Only	Augmented Reality
14	Heliawati *et al.* (2022)	J. Pendidik. IPA Indones.	Undergraduate Student	Two Group Experiment	Adobe Flash Interactive Media
15	Cahyana *et al.* (2019)	Int. J. Instr.	Senior High School Student	Two Group Experiment	Website

Table 3. Technologies were used in 15 articles that included on systematic review.

Technology	Frequency
Adobe Flash Interactive Media	1
Augmented Reality	3
Canva	1
E-Module	4
Mobile Apps	2
Search Engine	1
Virtual laboratory	1
Website	2

Another study found that the most widely used technology in chemistry learning is virtual reality. Virtual reality is considered essential in chemistry education because it meets students' needs for visualization, understanding chemical structures, and engaging in hands-on activities (Ali *et al.*, 2023). However, in this review, virtual reality was not one of the technologies examined, suggesting a gap in the utilization of virtual reality for enhancing chemical literacy. Another study indicates that the technologies widely used in chemistry learning include simulation-assembled technology, animation, and virtual labs. These three technologies are deemed effective in helping students understand abstract chemical concepts (Wu *et al.*, 2021). These technologies have either directly or indirectly been included in this review.

Based on an analysis using VosViewer (**Fig. 2**), the following is a comprehensive overview of the terminology used in the topic "effects of technology-enhanced learning on chemical literacy". In general, "chemical literacy," "scientific literacy", and "augmented reality" are the dominant keywords in the papers.

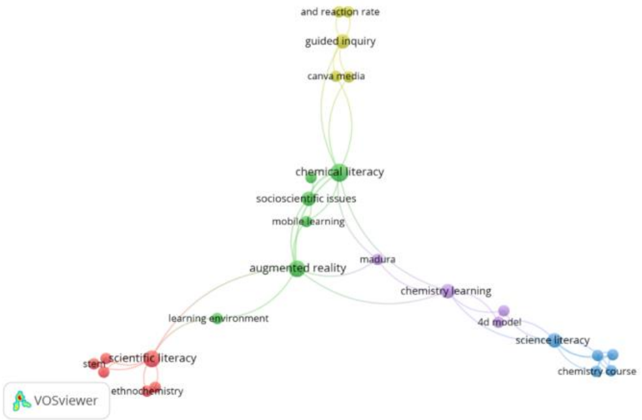

Figure 2. VosViewer Result of keywords of "effects of technology-enhanced learning on chemical literacy".

3.2. Technology's influence on chemical literacy based on PISA frameworks

To explain how technology impacts chemical literacy, the program for international student assessment (PISA) framework is used as the primary guide (OECD, 2023). The PISA framework is globally recognized, making it suitable for clarifying chemical literacy, which can be interpreted differently by various researchers. Moreover, PISA measurements have been conducted for a long time and encompass "scientific literacy," which is closely related to chemical literacy. According to this framework, chemical literacy is divided into three main competencies: (1) explaining phenomena scientifically, (2) constructing and evaluating designs for scientific inquiry and interpreting scientific data and evidence critically, and (3) researching, evaluating, and using scientific information for decision-making and action. The impact of TEL on chemical literacy (CL) will be discussed based on these competencies. The impact of technology will be linked to one of the most affected chemical literacy competencies, as explained in the reviewed articles. A summary of the effects of technology used in learning on chemical literacy is provided in **Table 4**.

Table 4. The impact of technology use on chemical literacy based on the reviewed articles.

No.	Technology	The role of technology	CL aspect	Effect
1	Adobe flash interactive media	Adobe flash technology has become an interactive learning media such as smartphone applications. Provides a variety of material presentations in various forms and is equipped with a virtual laboratory (Heliawati *et al.*, 2022)	CE	Adobe flash, designed as an app, allows students to access materials in various forms (video, text, audio) that facilitate comprehension. Furthermore, the virtual lab enables students to perform simulations, thereby reinforcing their inquiry skills, applying the concepts they have learned, and grasping the fundamental principles of science in everyday life.
2	Augmented reality	• AR enables the representation of submicroscopic objects on chemical bonding materials. AR represents a potential tool that allows users to represent and manipulate three-dimensional chemical structures (Techakosit and Wannapiroon, 2015). • AR facilitates the visualization of abstract chemical material, such as molecular shapes, thereby enabling students to readily comprehend the diverse representations of chemical compound shapes presented (Yuendita and Dina, 2024). • AR facilitates learning, and collaboration, and facilitates learning through technology easily, thereby enabling the development of students' understanding (Sulistina and Hasanah, 2024).	EP	• AR provides a visual representation of chemical 3D structures, which enables learners to explore and identify structures that facilitate the understanding of chemical phenomena. • AR provides a visual representation of chemical processes, allowing students to comprehend abstract chemical compounds in a more accessible manner. This facilitates the comprehension of chemical phenomena. • AR offers a more meaningful learning experience, facilitating the development of student comprehension and enabling them to grasp a phenomenon more easily.
3	Canva	The utilization of Canva as a pedagogical tool can facilitate the transfer of knowledge and enhance the ability of educators to engage students in the subject matter (Pulungan and Simamora, 2024).	EP	The increased interest in learning and the more organized materials provided by Canva have the potential to facilitate the development of student understanding.
4	E-module	• Electronic modules about the study of chemistry and its applications in everyday life may incorporate a multitude of forms of written, visual, and auditory content (Novitasari *et al.*, 2022) • The systematic publication of modules presents certain discourses in the form of scientific social issues sourced from electronic media, such as news and newspapers, which are accurate and reliable (Khairi and Ikhsan, 2022). • The objective of this learning resource is to assist students in comprehending the subject matter more effectively, provide contextualization, and enhance their reading abilities through an aesthetically pleasing design. The incorporation of visualizations, including images, videos, and graphs, in conjunction with factual examples, encourages students to develop and hone their science literacy skills (Sutiani and Pasaribu, 2023). • The e-module is designed to enhance student engagement and motivation by incorporating a range of engaging multimedia elements, including animated videos, images, and summary materials. This approach fosters a more enthusiastic and active participation in the learning process, which is crucial for facilitating deeper understanding and meaningful learning outcomes (Subarkah *et al.*, 2020).	EP	• E-modules can be utilized to summarize phenomena in a multimedia format (audio, video, images) that allows students to gain a comprehensive understanding of the context of a phenomenon. • The e-module presents a variety of real-world contexts through everyday media (news and articles) in a systematic manner that allows students to learn more effectively and comprehend science in the context of everyday life. • The incorporation of structured materials with diverse graphical representations allows students to gain deeper contextual insight, thereby facilitating their comprehension of the phenomenon in question. • E-modules present materials in a visually appealing manner, accompanied by instructions tailored to a specific model. This approach has been shown to enhance student motivation and facilitate comprehension of the material.
5	Mobile apps	• The results indicate that students appreciate the interactivity, accessibility, and convenience of mobile learning. The implementation of a mobile learning system as a supplement to the learning process is relatively straightforward and cost-effective. In designing mobile learning, it is essential to consider motivational factors such as interactivity and attractiveness (Suliono *et al.*, 2023). • The application is equipped with a variety of menus, including learning videos and special calculators. These resources allow students to enhance their factual, conceptual, procedural, and metacognitive knowledge about acid-base material through learning videos from the Acid-Base Multimedia. Consequently, students can comprehend scientific statements in various conceptual and contextual frameworks (Khery *et al.*, 2020).	EP	• With its various conveniences and interactivity, students become motivated to learn and make it easier to understand chemical concepts, enabling an increased understanding of a phenomenon. • In the application, problems are presented in various forms of visual and audio media that allow students to understand the phenomenon better.
6	Search Engine	The Internet offers a vast array of information, fostering an active capacity to assess data. The Internet can disseminate both accurate and inaccurate information in various formats, necessitating the critical examination and selection of such information (Schultz *et al.*, 2022).	RE	Students become trained in researching and finding the information they want. The veracity of information becomes important to determine an action. thus the importance of evaluating information.

7	Virtual laboratory	Virtual laboratories serve as a simulation medium that is learner-centered and inquiry-based, promoting higher levels of critical thinking and retention (Bortnik *et al.*, 2017).	CE	Virtual labs enable learners to perform simulations that enhance their comprehension during hands-on experiments and contribute to a deeper understanding of the material.
8	Website	• The use of web-based media encourages students to construct their knowledge, thereby enhancing their problem-solving and critical-thinking skills (Cahyana *et al.*, 2019). • The web can address the overly theoretical nature of current learning by providing more relevant, context-specific instruction. It offers interactive multimedia that surpasses the limitations of static resources like textbooks in conveying broad, complex, and dynamic subject matter (Frailich *et al.*, 2007).	EP	• Self-directed learning using the web requires students to actively construct their knowledge, which leads to a comprehensive understanding and enables them to explain phenomena scientifically. • The context presented on websites can train students to explain phenomena through interactive learning, thereby enhancing their understanding.

Note: EP = explaining phenomena scientifically; CE = constructing and evaluating designs for scientific inquiry and interpreting scientific data and evidence critically; RE = researching, evaluating, and using scientific information for decision-making and action.

In **Table 4**, the influence of technology on chemical literacy is explained based on three main competencies. The first competency, explaining phenomena scientifically, is the most impacted by TEL. Technologies such as augmented reality, Canva, E-modules, mobile apps, and websites contribute to the development of this competency. The details of the role of each of these technologies in enhancing chemical literacy will be discussed as follows. First, augmented reality plays a significant role by providing visualizations of compounds, molecules, or atoms at the submicroscopic level, enabling students to gain a more complete and concrete understanding. This enhanced visualization allows students to observe phenomena more effectively, thereby improving their ability to explain phenomena scientifically. Similarly, other studies have demonstrated that augmented reality (AR) can provide visualization of chemical structures, enabling students to develop a deeper understanding of the material (Abdinejad *et al.*, 2021; Fombona-Pascual *et al.*, 2022). This visualization capability can reduce cognitive load and enhance spatial ability (Habig, 2020).

Second, Canva can also contribute to the first competency of chemical literacy by increasing learning motivation and helping to present materials in a more organized manner, thereby enhancing student understanding. In general, Canva is useful for increasing motivation, understanding, active participation, and functionality (Vargas *et al.*, 2022). The attractively presented materials in Canva make it easier for students to grasp concepts, which aids in learning chemistry (Fatihah and Ruhiat, 2023). The engaging features of Canva are a crucial factor in its ability to improve students' chemical literacy competencies.

Furthermore, E-modules are the most widely used technology for improving chemical literacy. E-modules enhance students' ability to explain phenomena scientifically by providing comprehensive training through written, visual, and audio content. Their ease of creation and modification allows them to be associated with specific contexts, approaches, and learning models, enabling students to learn in various situations and stages. Another study explained that E-modules in chemistry learning make students more active participants, thereby improving their learning outcomes (Logan *et al.*, 2021; Nainggolan *et al.*, 2023). The use of E-modules has been shown to produce better learning outcomes and increase motivation compared to conventional media (Harefa and Silalahi, 2020). This increase in scientific literacy competence through E-modules is likely due to the enhanced student engagement stemming from the visual, written, and audio representations that capture their interest. Additionally, the use of specific models or approaches further encourages active student participation.

Furthermore, mobile apps are closely related to the first competency of chemical literacy. They offer high interactivity, which can increase student motivation. Additionally, mobile apps can be equipped with diverse menus and content, facilitating well-rounded learning and contributing to enhanced student understanding. These factors collectively improve students' ability to explain phenomena scientifically. Interactivity is the primary feature that supports the use of mobile apps in chemistry (Ewais *et al.*, 2021; Kim *et al.*, 2014; Sadykov *et al.*, 2021). Another study noted that mobile apps make materials more accessible and visible (Ekins *et al.*, 2013). Therefore, the high interactivity provided by mobile apps is a crucial factor in developing and improving scientific literacy.

Finally, is the website, which significantly influences the first competency of chemical literacy. Like E-modules and mobile apps, websites can be customized according to user needs. In terms of explaining phenomena scientifically, websites provide a variety of contexts, allowing students to practice applying their knowledge to different situations independently. Websites enhance student understanding, encourage self-learning, and offer resources that help students stay focused on their studies (Cole and Todd, 2003). Other research also emphasizes the web's ability to support student self-learning (Chamimmah *et al.*, 2023). Thus, the most notable role of websites is their ability to foster self-directed learning, which in turn increases students' active involvement in constructing their knowledge.

The second competency involves constructing and evaluating designs for scientific inquiry and critically interpreting scientific data and evidence. Based on the review of the selected articles, Adobe Flash Interactive Media and Virtual Laboratories can significantly enhance this competency. Adobe Flash Interactive Media contributes to this competency primarily due to its virtual laboratory feature. Although it is often compared to mobile apps, the virtual laboratory aspect is the most prominent. Virtual laboratories allow students to perform simulations, thereby strengthening their inquiry skills. Consistent with this, the research on virtual laboratories discussed in this review indicates that they act as simulation media that facilitate student learning. This ultimately improves their understanding of scientific inquiry and hands-on experimental techniques. This is reinforced by research showing that virtual laboratories can improve students' understanding of basic techniques and concepts (Martínez-Jiménez *et al.*, 2003). This technology facilitates the practice of chemistry fundamentals by allowing students to visualize, navigate, and simulate related processes and real laboratory environments (Almazaydeh *et al.*, 2016). Virtual labs are considered the best alternative for equipping students with essential laboratory knowledge and skills (Kartimi *et al.*, 2022). Thus, the simulation aspect is crucial for developing the second competency of scientific literacy. Virtual labs provide a means for students to explore the research process virtually, making them more familiar with real laboratory practices.

The third competency is researching, evaluating, and using scientific information for decision-making and action. This is the most recent addition to the PISA framework, emerging in response to the surge of information and the increasing importance of assessing this information critically. Search engines are a key technology that contributes to improving this competency (OECD, 2023). Search engines present a wide variety of information quickly, requiring students to assess the validity, accuracy, and appropriateness of the information they encounter. Research shows that search engines motivate students to gain navigational experience and increase their desire to learn chemistry by providing interesting, relevant, and challenging information (Murov, 2001). In chemistry education, students should be encouraged to search and read literature and to use online databases effectively (Gawalt and Adams, 2011). Thus, search engines that offer abundant data can effectively train students in the third competency of chemical literacy.

Each technology discussed has a unique role in enhancing chemical literacy. Based on this review, we can see how these technologies contribute to improving chemical literacy competencies as defined by the PISA framework. The results of this study can inform the implementation of TEL to improve chemical literacy. However, this study has several limitations. First, it only includes English articles, which may exclude other technologies developed to improve chemical literacy. Second, this review focuses solely on the technology used, potentially overlooking other factors that contribute to improving science literacy, such as learning models or specific approaches. Future research should examine the extent to which each technology affects chemical literacy, considering moderating variables to provide a more comprehensive understanding. Thirdly, although the research methodology was designed following established guidelines, the study's results predominantly feature articles from Indonesia. This geographical concentration suggests that the conclusions drawn may be most applicable to the Indonesian context. There is a potential for bias, necessitating caution when generalizing findings to other national contexts. Readers should take this into account. Nevertheless, the research provides valuable insights into how technology influences chemical literacy.

4. Conclusions

Based on the literature review, it is evident that the most widely used technology for improving chemical literacy is the E-module, especially in Indonesia, where most of the articles reviewed were from. E-modules are easy to develop and can be tailored to specific needs, making them the most prevalent technology for enhancing chemical literacy. For improving the competency of "explaining phenomena scientifically", technologies such as augmented reality, Canva, E-modules, mobile apps, and websites play a significant role. In enhancing the second competency, "constructing and evaluating designs for scientific inquiry and critically interpreting scientific data and evidence", Adobe Flash Interactive Media and Virtual Laboratories are particularly effective. Finally, for the competency of "researching, evaluating, and using scientific information for decision-making and action", search engine technology has a notable impact.

With this knowledge, educators can better address their students' needs by identifying specific deficiencies in chemical literacy and selecting the appropriate technology. Additionally, practitioners can proportionally combine different technologies in their teaching strategies based on these findings. The results of this study also highlight a gap in the use of certain technologies for improving chemical literacy. For example, the impact of virtual reality on chemical literacy has not been directly studied, indicating an area for future research.

Authors' contributions

Conceptualization: Ananta Ardyansyah; Sri Rahayu; **Data curation:** Ananta Ardyansyah; Sri Rahayu; **Formal Analysis:** Ananta Ardyansyah; **Funding acquisition:** Sri Rahayu; **Investigation:** Ananta Ardyansyah; **Methodology:** Ananta Ardyansyah; Sri Rahayu; **Project administration:** Ananta Ardyansyah; **Resources:** Sri Rahayu; **Software:** Ananta Ardyansyah; **Supervision:** Sri Rahayu; **Validation:** Ananta Ardyansyah; Sri Rahayu; **Visualization:** Ananta Ardyansyah; **Writing – original draft:** Ananta Ardyansyah; **Writing – review & editing:** Ananta Ardyansyah; Sri Rahayu.

Data availability statement

All data sets were generated or analyzed in the current study.

Funding

Kementerian Pendidikan, Kebudayaan, Riset, dan Teknologi Republik Indonesia. Grant No: 066/E5/PG.02.00.PL/2024.

Acknowledgments

We extend our gratitude to the Indonesian Ministry of Education, Culture, Research, and Technology for their support in funding this research through grant 066/E5/PG.02.00.PL/2024.

Conflict of interest

The authors declare that there is no conflict of interest.

References

Abdinejad, M.; Talaie, B.; Qorbani, H. S.; Dalili, S. Percepciones de los estudiantes utilizando tecnologías de realidad aumentada y visualización 3D en la educación química. *J. Sci. Educ. Technol.* **2021**, *30* (1), 87–96. https://doi.org/10.1007/s10956-020-09880-2

Ali, S. B.; Abdul Talib, C.; Jamal, A. M. Digital technology approach in chemistry education: A systematic literature review. *J. Nat. Sci. Integr.* **2023**, *6* (1), 1. https://doi.org/10.24014/jnsi.v6i1.21777

Almazaydeh, L.; Younes, I.; Elleithy, K. An interactive and self-instructional virtual chemistry laboratory. *Int. J. Emerg. Technol. Learn.* **2016**, *11* (7), 70–73. https://doi.org/10.3991/ijet.v11i07.5853

Bellou, I.; Papaschritos, N. M.; Mikropoulos, T. A. Digital learning technologies in chemistry education: A review. In *Digital Technologies: Sustainable Innovations for Improving Teaching and Learning*, **2018**, 57–80. Springer. https://doi.org/10.1007/978-3-319-73417-0_4

Bortnik, B.; Stozhko, N.; Pervukhina, I.; Tchernysheva, A.; Belysheva, G. Effect of virtual analytical chemistry laboratory on enhancing student research skills and practices. *Res. Learn. Technol.* **2017**, *25*, 1063519, 1–20. https://doi.org/10.25304/rlt.v25.1968

Cahyana, U.; Supatmi, S.; Erdawati, E.; Rahmawati, Y. The influence of web-based learning and learning independence toward student's scientific literacy in chemistry course. *Int. J. Instr.* **2019**, *12* (4), 655–668. https://doi.org/10.29333/iji.2019.12442a

Cavagnetto, A. R. Argument to foster scientific literacy: A review of argument interventions in k-12 science contexts. *Rev. Educ. Res.* **2010**, *80* (3), 336–371. https://doi.org/10.3102/0034654310376953

Chamimmah, N.; Indriani, L.; Mariono, M. A. The influence of web-based learning on students ' self-regulated learning in high school chemistry learning. *Int. J. Educ. Res. Rev.* **2023**, *8* (2), 257–267. https://doi.org/10.24331/ijere.1249689

Cole, R. S.; Todd, J. B. Effects of web-based multimedia homework with immediate rich feedback on student learning. *J. Chem. Educ. Res.* **2003**, *80* (11), 1338–1343. https://doi.org/10.1021/ed080p1338

Duval, E.; Sharples, M.; Sutherland, R. Technology enhanced learning: Research themes. In *Springer Nature*, **2017**, pp. 180. https://doi.org/10.1007/978-3-319-02600-8_4

Ekins, S.; Clark, A. M.; Williams, A. J. Incorporating green chemistry concepts into mobile chemistry applications and their potential uses. *ACS Sustainable Chem. Eng.* **2013**, *1* (1), 8–13. https://doi.org/10.1021/sc3000509

Ewais, A.; Hodrob, R.; Maree, M.; Jaradat, S. Mobile learning application for helping pupils in learning chemistry. *Int. J. Interact. Mobile Technol.* **2021**, *15* (1), 105–118. https://doi.org/10.3991/ijim.v15i01.11897

Fatihah, W.; Ruhiat, Y. Pengembangan konten pembelajaran berbasis canva pada pokok bahasan asam-basa. *J. Inov. Educ. Quim.* **2023**, *17* (1), 57-61. https://doi.org/10.15294/jipk.v17i1.36674

Fombona-Pascual, A.; Fombona, J.; Vicente, R. Augmented reality, a review of a way to represent and manipulate 3d chemical structures. *J. Chem. Inf. Model.* **2022**, *62* (8), 1863–1872. https://doi.org/10.1021/acs.jcim.1c01255

Frailich, M.; Kesner, M.; Hofstein, A. The influence of web-based chemistry learning on students' perceptions, attitudes, and achievements. *Int. J. Phytoremediation* **2007**, *25* (2), 179–197. https://doi.org/10.1080/02635140701250659

Gawalt, E. S.; Adams, B. A Chemical information literacy program for first-year students. *J. Chem. Educ.* **2011**, *88* (4), 402–407. https://doi.org/10.1021/ed100625n

Habig, S. Who can benefit from augmented reality in chemistry? Sex differences in solving stereochemistry problems using augmented reality. *Br. J. Educ. Technol.* **2020**, *51* (3), 629–644. https://doi.org/10.1111/bjet.12891

Harefa, N.; Silalahi, N. F. D. Improvement of student's learning outcomes and motivation with chemical practicum e-module. *J. Pendidikan Kimia* **2020**, *12* (1), 10–19. https://doi.org/10.24114/jpkim.v12i1.17708

Heliawati, L.; Lidiawati, L.; Adriansyah, P. N. A.; Herlina, E. Ethnochemistry-Based adobe flash learning media using indigenous knowledge to improve students' scientific literacy. *J. Pendidikan IPA Indonesia* **2022**, *11* (2), 271–281. https://doi.org/10.15294/jpii.v11i2.34859

Holbrook, J.; Rannikmae, M. The nature of science education for enhancing scientific literacy. *Int. J. Sci. Educ.* **2007**, *29* (11), 1347–1362. https://doi.org/10.1080/09500690601007549

Kartimi, K.; Yunita, Y.; Addiin, I.; Shidiq, A. S. A bibliometric analysis on chemistry virtual laboratory. *Educ. Quím.* **2022**, *33* (2), 194–208. https://doi.org/10.22201/fq.18708404e.2022.2.80579

Khairi, M. A.; Ikhsan, J. Development of guided inquiry-based electronic modules and its effects on students' chemical literacy. *JKPK (J. Kim. Dan Pend. Kim.)* **2022**, *7* (2), 181. https://doi.org/10.20961/jkpk.v7i2.62319

Khery, Y.; Nufida, B. A.; Suryati, S. The influence of mobile-NOS model on students understanding on Nature of Science (NOS) and scientific literacy. *J. Phys.: Conf. Ser.* **2020**, *1521* (4), 042091. https://doi.org/10.1088/1742-6596/1521/4/042091

Kim, H.; Chacko, P.; Zhao, J.; Montclare, J. K. Using touch-screen technology, apps, and blogs to engage and sustain high school students' interest in chemistry topics. *J. Chem. Educ.* **2014**, *91* (11), 1818–1822. https://doi.org/10.1021/ed500234z

Kirkwood, A.; Price, L. Technology-enhanced learning and teaching in higher education: what is "enhanced" and how do we know? A critical literature review. *Learn. Media Technol.* **2014**, *39* (1), 6–36. https://doi.org/10.1080/17439884.2013.770404

Kohen, Z.; Herscovitz, O.; Dori, Y. J. How to promote chemical literacy? On-line question posing and communicating with scientists. *Chem. Educ. Res. Pract.* **2020**, *21* (1), 250–266. https://doi.org/10.1039/C9RP00134D

Laugksch, R. C. Scientific Literacy: A conceptual overview. In *Scientific Literacy*: An International Symposium; John Wiley & Sons: 2000; pp. 71–94.

Logan, R. M.; Johnson, C. E.; Worsham, J. W. Development of an e-learning module to facilitate student learning and outcomes. *Teach. Learn. Nurs.* **2021**, *16* (2), 139–142. https://doi.org/10.1016/j.teln.2020.10.007

Martínez-Jiménez, P.; Pontes-Pedrajas, A.; Polo, J.; Climent-Bellido, M. S. Learning in chemistry with virtual laboratories. *J. Chem. Educ.* **2003**, *80* (3), 346–352. https://doi.org/10.1021/ed080p346

Memon, M. Q.; Lu, Y.; Memon, A. R.; Memon, A.; Munshi, P.; Shah, S. F. A. Does the impact of technology sustain students' satisfaction, academic and functional performance: An analysis via interactive and self-regulated learning? *Sustainability* **2022**, *14* (12), 1–19. https://doi.org/10.3390/su14127226

Moher, D.; Liberati, A.; Tetzlaff, J.; Altman, D. G.; Antes, G.; Atkins, D.; Barbour, V.; Barrowman, N.; Berlin, J. A.; Clark, J.; Clarke, M.; Cook, D.; D'Amico, R.; Deeks, J. J.; Devereaux, P. J.; Dickersin, K.; Egger, M.; Ernst, E.; Gøtzsche, P. C.; Grimshaw, J.; Guyatt, G.; Higgins, J.; Ioannidis, J. P. A.; Kleijnen, J.; Lang, T.; Liberati, A.; Magrini, N.; McNamee, D.; Moja, L.; Moher, D.; Mulrow, C.; Napoli, M.; Oxman, A.; Ba' Pham; Rennie, D.; Sampson, M.; Schulz, K. F.; Shekelle, P. G.; Tetzlaff, J.; Tovey, D.; Tugwell, P. Preferred reporting items for systematic reviews and meta-analyses: The PRISMA statement. *PLoS Med.* **2009**, *6* (7), e1000097. https://doi.org/10.1371/journal.pmed.1000097

Mozeika, D.; Bilbokaite, R. Teaching and learning method for enhancing 15-16 years old students' knowledge as one of scientific literacy aspect in chemistry: Results based on research and approbation. *Int. J. Educ. Res.* **2011**, *2010* (1), 1–16.

Murov, S. Exploring chemistry resources on the internet. *J. Chem. Educ.* **2001**, *78* (10), 1429–1432. https://doi.org/10.1021/ed078p1429

Nainggolan, B.; Juniar, A.; Silaban, R. Development of project-based interactive e-modules in accordance with the IQF integrated curriculum concept in learning organic chemical reactions to improve student chemistry learning outcomes. *J. Pendidikan Kimia* **2023**, *15* (3), 281–291. https://doi.org/10.24114/jpkim.v15i3.47366

Novitasari, R.; Waluyo, J.; Nuriman, N. Chemistry e-module based on socio scientific issues (SSI) for reaction rate material to increase senior high school students' chemical literacy. *Eduvest - J. Univ. Stud.* **2022**, *2* (9), 1811–1816. https://doi.org/10.59188/eduvest.v2i9.588

Organização para Cooperação e Desenvolvimento Econômico (OECD). *PISA 2025 Science Framework*. OECD; **2023**, 1–93.

Primadianningsih, C.; Sumarni, W.; Sudarmin, S. Systematic literature review: Analysis of ethno-STEM and student's chemistry literacy profile in 21st century. *J. Penelitian Pendidikan IPA* **2023**, *9* (2), 650–659. https://doi.org/10.29303/jppipa.v9i2.2559

Pulungan, E. N.; Simamora, K. F. Influence of canva media based on guided inquiry model on students' critical thinking ability and chemical literacy. *J. Inovasi Pembelajaran Kimia* **2024**, *6* (1), 100–1010. https://doi.org/10.24114/jipk.v6i1.57379

Queiruga-Dios, M. Á.; López-Iñesta, E.; Diez-Ojeda, M.; Sáiz-Manzanares, M. C.; Dorrío, J. B. V. Citizen science for scientific literacy and the attainment of sustainable development goals in formal education. *Sustainability* **2020**, *12* (10), 4283. https://doi.org/10.3390/su12104283

Rahayu, S. Promoting the 21st century scientific literacy skills through innovative chemistry instruction. *AIP Conf. Proc.* **2017**, *1911* (1), 020025. https://doi.org/10.1063/1.5016018

Reiss, M. J.; Millar, R.; Osborne, J. Beyond 2000: Science/biology education for the future. *J. Biol. Educ.* **1999**, *33* (2), 68–70. https://doi.org/10.1080/00219266.1999.9655644

Roberts, D. A. Scientific Literacy/Science Literacy. In S. K. Abell & N. G. Lederman (Eds.), *Handbook of Research on Science Education*. **2007**, *25*, 729–781.

Roth, W.-M.; Barton, A. C. Rethinking scientific literacy. Routledge, 2004. https://doi.org/10.4324/9780203463918

Sadykov, T. M.; Ctrnactova, H.; Kokibasova, G. T. Students' opinions toward interactive apps used for teaching chemistry. *Bull. Karaganda Univ. Chem. Ser.* **2021**, *103* (3), 103–114. https://doi.org/10.31489/2021CH3/103-114

Schultz, M.; Lim, K. F.; Goh, Y. K.; Callahan, D. L. OK google: what's the answer? characteristics of students who searched the internet during an online chemistry examination. *Assess. Eval. Higher Educ.* **2022**, *47* (8), 1458–1474. https://doi.org/10.1080/02602938.2022.2048356

Seery, M. K.; McDonnell, C. The application of technology to enhance chemistry education. *Chem. Educ. Res. Pract.* **2013**, *14* (3), 227–228. https://doi.org/10.1039/c3rp90006a

Shwartz, Y.; Ben-Zv, R.; Hofstein, A. The importance of involving high-school chemistry teachers in the process of defining the operational meaning of 'chemical literacy.' *Int. J. Sci. Educ.* **2005**, *27* (3), 323–344. https://doi.org/10.1080/0950069042000266191

Shwartz, Y.; Ben-Zvi, R.; Hofstein, A. Chemical literacy: What does this mean to scientists and school teachers? *J. Chem. Educ.* **2006**, *83* (10), 1557–1561. https://doi.org/10.1021/ed083p1557

Shwartz, Y.; Ben-Zvi, R.; Hofstein, A. The use of scientific literacy taxonomy for assessing the development of chemical literacy among high-school students. *Chem. Educ. Res. Pract.* **2006**, *7* (4), 203–225. https://doi.org/10.1039/B6RP90011A

Stašević, F.; Miletić, N.; Nikolić, J. Đ.; Gutman, I. Do Serbian high school students possess knowledge of basic chemical facts related to real life as a prerequisite for chemical literacy? *J. Serb. Chem. Soc.* **2023**, *88* (3), 343–354. https://doi.org/10.2298/JSC211126083S

Subarkah, C. Z.; Gunawan, A.; Irwansyah, F. S.; Ruswandi, U. The development of chemical-literacy-oriented electronic module on battery topic. *Proc. 1st Bandung Engl. Lang. Teach. Int. Conf. (BELTIC)* **2020**, *2018*, 105, 504–509. https://doi.org/10.5220/0008221505040509

Suliono, S.; Enawaty, E.; Astuti, I. Development of acid-base multimedia (ABM) in chemistry learning to empower students' scientific literacy. *J. Pen. Pendidik. IPA* **2023**, *9* (11), 10395–10402. https://doi.org/10.29303/jppipa.v9i11.4445

Sulistina, O.; Hasanah, S. M. Improving chemical literacy skills: integrated socio-scientific issues content in augmented reality mobile. *Int. J. Interact. Mob. Technol. (IJIM)* **2024**, *18* (5), 135–147. https://doi.org/10.3991/ijim.v18i05.47923

Sutiani, A.; Pasaribu, C. J. T. Fostering scientific literacy through integrated STEM teaching materials on basic laws of chemistry. *JTK (Jurnal Tadris Kimiya)* **2023**, *8* (1), 95–103. https://doi.org/10.15575/jtk.v8i1.25833

Tawafak, R. M.; Romli, A. B. T.; Arshah, R. bin A.; Almaroof, R. A. S. Assessing the impact of technology learning and assessment method on academic performance: Review paper. *Eur. J. Math. Sci. Tech. Educ.* **2018**, *14* (6), 2241–2254. https://doi.org/10.29333/ejmste/87117

Techakosit, S.; Wannapiroon, P. Connectivism learning environment in augmented reality science laboratory to enhance scientific literacy. *Procedia - Soc. Behav. Sci.* **2015**, *174* (2), 2108–2115. https://doi.org/10.1016/j.sbspro.2015.02.009

Vargas, I. M.; Cabrera, C. I. G.; Cortez, C. A. A.; Apaza, I. M. A.; Reátegui, M. D. The Canva platform and meaningful learning in regular basic education. *Int. J. Health Sci.* **2022**, *6*, 643–658. https://doi.org/10.53730/ijhs.v6ns7.11213

Wiyarsi, A.; Prodjosantoso, A. K.; Nugraheni, A. R. E. Promoting students' scientific habits of mind and chemical literacy using the context of socio-scientific issues on the inquiry learning. *Front. Educ.* **2021**, *6*, 1–12. https://doi.org/10.3389/feduc.2021.660495

Wu, S. H.; Lai, C. L.; Hwang, G. J.; Tsai, C. C. Research trends in technology-enhanced chemistry learning: a review of comparative research from 2010 to 2019. *J. Sci. Educ. Technol.* **2021**, *30* (4), 496–510. https://doi.org/10.1007/s10956-020-09894-w

Yacoubian, H. A. Scientific literacy for democratic decision-making. *Int. J. Sci. Educ.* **2018**, *40* (3), 308–327. https://doi.org/10.1080/09500693.2017.1420266

Yore, L. D.; Pimm, D.; Tuan, H. L. The literacy component of mathematical and scientific literacy. *Int. J. Sci. Math. Educ.* **2007**, *5* (4), 559–589. https://doi.org/10.1007/s10763-007-9089-4

Yuendita, D.; Dina, D. Development of chemical literacy book on local wisdom of madura culture based on augmented reality (AR). *J. Pen. Pendidik. IPA* **2024**, *10* (1), 346–359. https://doi.org/10.29303/jppipa.v10i1.5689

Eclet. Quim. 49 | e-1497, 2024

Original Article

https://doi.org/10.26850/1678-4618.eq.v49.2024.e1497

Electrochemical sensing of uric acid using bismuth-silver bimetallic nanoparticles modified sensor

Charlton Van der **Horst**[1], Eric de Souza **Gil**[2], Vernon **Somerset**[1+]

Abstract

We showcase in this investigation a GCE/Bi–Ag electrochemical nanosensor for uric acid (UA) detection in commercial fruit juice samples. These GCE/Bi–Ag nanosensor electrochemical performances were studied using cyclic voltammetry (CV) and differential pulse voltammetry (DPV) modes showing excellent electrochemical properties toward UA detection in contrast with the clean GCE. Using the fabricated nanosensor, we exploited DPV measurements to detect UA at a meager limit of detection (0.6 µmol/L, S/N = 3) and linearity between 5.0 and 80 µmol/L UA. Furthermore, the GCE/Bi–Ag nanosensor illustrates good repeatability and reproducibility with 3.80% and RSDs of 3.22%, respectively. The GCE/Bi–Ag nanosensor was effectively exploited to determine UA in actual fruit juice samples showing excellent recoveries, indicating that it can be a promising alternative sensor for food analytical applications.

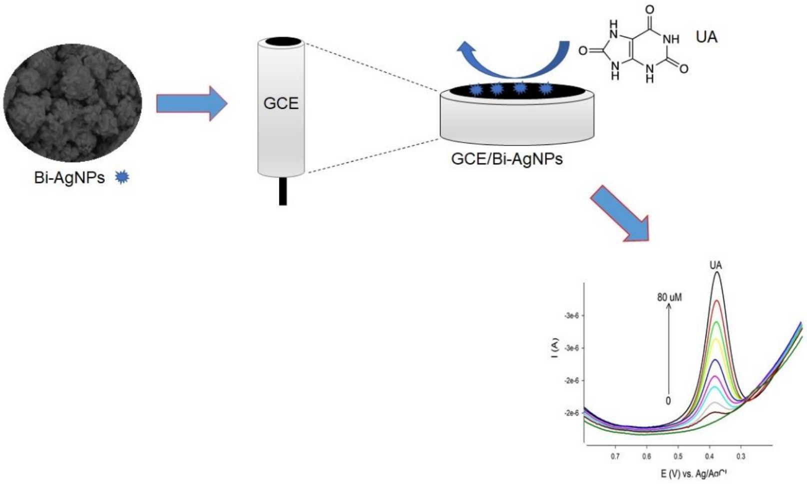

Article History

Received June 04, 2023
Accepted August 23, 2024
Published December 24, 2024

Keywords

1. GCE/Bi–AgNPs;
2. electrochemical sensor;
3. uric acid;
4. fruit juice samples.

Section Editors

Paulo Clairmont Feitosa Lima Gomes
Patricia Hatsue Suegama

Highlights

- Novel GCE/Bi–Ag nanosensor constructed for the individual detection of uric acid.
- Sensor successfully applied for electroanalysis of fruit juices.
- Nanomaterials of Bi–AgNPs have highly dispersed active sites with high surface area.
- The nanosensor obtained a detection limit of 0.6 µmol/L (S/N = 3).
- GCE/Bi–Ag nanosensor illustrates good repeatability and reproducibility.

[1]Cape Peninsula University of Technology, Faculty of Applied Sciences, Cape Town, South Africa. [2]Federal University of Goiás, Faculty of Pharmacy, Goiás, Brazil.
+Corresponding author: Vernon Somerset, **Phone:** +2721959 6116, **Email address:** vsomerset@gmail.com

1. Introduction

Uric acid (UA) or (2,6,8–trihydroxypurine) is in the human body the vital end product for the metabolism of purine and is present in blood serum and urine (Erden and Kilic, 2013; Lakshmi *et al.*, 2011). The correct levels of UA in blood samples are between 0.13 to 0.46 mM and in urine between 2.49 to 4.46 mM (Huang *et al.*, 2004; Raj and Ohsaka, 2001). An excess of UA in blood serum causes hypertension, gout, renal disease, and cardiovascular disease (Choi *et al.*, 2005; Kanbay *et al.*, 2016; Papavasileiou *et al.*, 2016; Riches *et al.*, 2009; Wan *et al.*, 2015), whereas low levels can cause Parkinson's disease, optic disease, and Alzheimer's disease (Lakshmi *et al.*, 2011; Misra *et al.*, 2013). So, the rapid determination of uric acid (UA) with high accuracy and sensitivity using low–cost sensors in serum, urine, fruit juices, and other food products with abnormal levels of UA. It will alert concerned persons to the abnormal levels of UA and take immediate action (therapy). Medical check-ups always involve laboratory setup, bulky instrumentation, trained technicians, pre–treatment, and time do not meet this requirement.

Many analytical methods detect UA in different samples, such as chromatography (Li *et al.*, 2015; Luo *et al.*, 2013) and spectroscopy (Boroumand *et al.*, 2017). However, those methods require bulky instrumentation, harmful solvent, sample pre–treatment, skilled technicians, time, and cost. To overcome these drawbacks of conventional analytical methods, biosensors and electrochemical sensors have received much attention due to the advantages of high selectivity, sensitivity, and rapid response (Raj and Ohsaka, 2001). Many reports have applied various types of modified electrodes in to analyse UA samples. These various types of modified electrodes include graphene nanocomposites (Bai *et al.*, 2017; Yue *et al.*, 2015; Zhang *et al.*, 2016), modified carbon paste electrodes (Beitollahi and Sheikhshoaie, 2011; Ganesh *et al.*, 2015), multi–walled carbon nanotubes (Wayu *et al.*, 2016), quantum dots (Abbas *et al.*, 2019), polymers (Sadikoglu *et al.*, 2012), and gold nanoparticles (Ali *et al.*, 2017).

Bai *et al.* (2017) described the fabrication of a biosensor for UA detection in urine samples that includes cationic poly(diallyldimethylammonium chloride) functionalized reduced graphene oxide and polyoxometalates clusters combined with anionic Au nanoparticles. This biosensor has provided acceptable analytical features such as excellent linearity with a low detection limit. Mahmoudian *et al.* (2019) synthesized α–Fe_2O_3/polyaniline nanotube (PAnNTs) composite to construct an electrochemical nanosensor for the determination of UA in urine samples. This sensor also showed good linearity with a low detection limit. The anti–interference of the nanosensor was good by adding interfering acids such as citric acid and ascorbic acid (AA). Recently, Fukuda *et al.* (2020) have exploited a thin film biosensor that consists of carboxymethylcellulose/ uricase dispersed gold/carbon nanotube for UA detection in blood and urine samples. The constructed biosensor exhibited a low limit of detection, wide linear range, and excellent sensitivity. This report is the first individual determination of UA with other biomolecules as interferences in commercial fruit juice samples by the electrochemical measurement with GCE/Bi–Ag nanosensor.

In literature, a research group synthesized novel bismuth–silver bimetallic nanoparticles and successfully applied them in the construction of an electrochemical nanosensor and a biosensor for the detection of platinum group metals (PGMs) (Van der Horst, 2015; Van der Horst *et al.*, 2015a; 2015b; 2016a; 2017a; 2018), AA (Van der Horst *et al.*, 2016b; Van der Horst and Somerset, 2022), and hydrogen peroxide (Van der Horst *et al.*, 2017b), respectively. Recently, they also used the GCE/Bi–AgNPs nanosensor in the individual and simultaneous detection of caffeine, AA, and paracetamol in pharmaceutical formulae (Van der Horst *et al.*, 2020). These studies make the GCE/Bi–AgNPs nanosensor attractive for the individual determination of UA in commercial fruit juice samples. To date, there's no investigation reported for detecting UA in commercial fruit juice samples by the electrochemical method using Bi–AgNPs drop coated onto a glassy carbon electrode. Only AA detection in commercial fruit juice samples was reported in the literature (Brainina *et al.*, 2020; Das and Sharma, 2020).

This investigation showcases that the GCE/Bi–AgNPs nanosensor exhibited good electrocatalytic activity towards UA detection in model solutions. This GCE/Bi–AgNPs nanosensor obtained a low detection limit, excellent selectivity, wide linearity range, and high sensitivity for the detection of UA. Further, this fabricated nanosensor was utilized for UA determination with satisfactory results using commercial fruit juice samples.

2. Experimental

2.1. Materials

This investigation used analytical–grade chemicals, and we didn't purify them further. Bismuth–silver nanoparticles were prepared by adding ($Bi(NO_3)_3$) and $AgNO_3$ to HNO_3 solution. Citric acid was added to reduce the two salts to Bi–AgNPs. We prepared phosphate buffer (PB) solutions by adding NaH_2PO_4 to Na_2HPO_4, and we adjusted the pH with NaOH and H_3PO_4. UA's stock solutions were prepared by weakly dissolving UA in a freshly PB solution. Throughout this investigation, the diluting of stock solutions in freshly PB (pH = 5.0) to prepare diluted standard solutions.

2.2. Instrumentation

We performed voltammetric measurements with an Epsilon electrochemical analyzer (BASi Instruments, USA). The instrument was equipped with a conventional system of three electrodes, including a GCE/Bi–AgNPs fabricated by drop coating the Bi–AgNPs on a 1.6 mm diameter BASi disc GCE, a platinum wire that acts as the auxiliary electrode, and an Ag/AgCl/$KCl_{sat.}$ reference electrode, respectively. All experiments were performed at conditioned room temperature and in an electrochemical cell (20 mL).

2.3. Working electrode preparation

The bimetallic nanoparticles of Bi–Ag were synthesized based on the experimental procedure of our previous work (Van der Horst *et al.*, 2015a). We fabricated the GCE/Bi–AgNPs nanosensor by polishing a bare GCE in a water surrey consisting of alumina (Al_2O_3) (1.0, 0.3, and 0.05 μm) using a polishing pad. We used deionized water to rinse the clean GCE and ethanol with double distilled water for sonication. The bare GCE was further cleaned using deoxygenated aqueous H_2SO_4 (0.5 mol/L) in an electrochemical cell by applying cyclic voltammetry (CV) for 11 cycles at 100 mV/s scan rates to obtain a stable CV profile (Silwana *et al.*, 2016). Ultrasonic vibrations were used to form a suspension by dispersed bimetallic bismuth–silver nanoparticles (Bi–AgNPs) in deionized water. A small amount of Bi–AgNPs was dropped onto a clean GCE, resulting in an even Bi–AgNPs film by drying it at ambient temperature. The dried modified GCE/Bi–AgNPs sensor was slightly rinsed with deionized water, and submerged in PB (pH = 5.0), and its reproducibility was increased by scanning it for 13 cycles (Van der Horst *et al.*, 2016b).

2.4. Preparation of commercial samples

Two commercial fruit juice samples (apple and orange) were obtained at a local supermarket and the preparation was done by filtering 100 mL of the fruit juice samples in a 250 mL Erlenmeyer flask. The filtered fruit juice samples were diluted by taking 1 mL of filtered fruit juice samples in 9 mL 0.1 mol/L PB solution (pH = 5.0) in a 20 mL electrochemical cell. The diluted fruit juice samples were used for UA analysis using DPVs as the analysis mode (Benjamin *et al.*, 2015).

2.5. Determination procedure of uric acid

Phosphate buffer solution aliquots (0.1 mol/L, pH 5.0) were transferred into an electrochemical cell. Different differential pulse voltammograms were recorded by increasing concentrations from 5 to 80 μmol/L of UA in the aliquots. The cyclic voltammograms were obtained using a scan rate of 100 mV/s from −0.4 to +1.0 V (vs. Ag/AgCl) ranges. The parameters for the DPV analysis were 4 s pulse width and 50 mV pulse amplitude (Benjamin *et al.*, 2015; Van der Horst *et al.*, 2016b).

3. Results and discussion

3.1. Electrochemical characterization of constructed sensor

The electrochemical property studies of the GCE/Bi–AgNPs nanosensor were performed by using cyclic voltammetry (CV) and scan rates studies with $[Fe(CN)_6]^{3-/4-}$ solution as the electrochemistry probe. A transmission electron microscope was employed to determine the particle size of the Bi–AgNPs with diameters between 10 and 25 nanometers in **Fig. 1a**. The particle size distribution indicates that most nanoparticles were 10 and 15 nanometers (Van der Horst *et al.*, 2015a). **Figure 1b** illustrates that the modification with Bi–AgNPs increases the peak currents of the clean GCE. These phenomena may result from a large surface area and thus increase the electronic conductivity. These results illustrate that Bi–AgNPs were deposited onto the clean GCE surface by drop coating (Fukuda *et al.*, 2020; Mahmoudian *et al.*, 2019). Curve (a) (in **Fig. 1b**) of the clean GCE demonstrates a pair of redox peaks with a 142 mV peak separation.

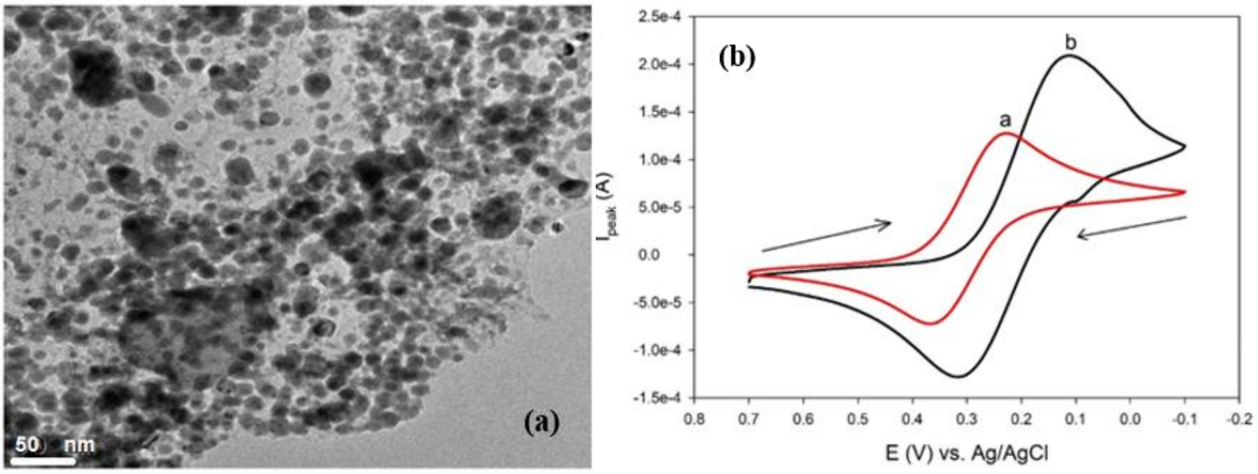

Figure 1. (a) TEM image for Bi–AgNPs; **(b)** curve a: CV curves of clean GCE; curve b: GCE/Bi–AgNPs.

Furthermore, curve (b) (in **Fig. 1b**) of the GCE/Bi–AgNPs showcases a very intense redox peak with an approximately 207 mV ΔE_p ($\Delta E_p = E_{pa} - E_{pc}$; where E_{pc} and E_{pa} stands for cathodic and anodic peak potentials) value greater than the clean GCE. These cathodic, anodic and separation peak potentials are illustrated in **Table 1**. The more excellent ΔE_p value with more significant redox peak currents at the GCE/Bi–AgNPs nanosensor showcases the superior electron transfer kinetics and sizeable active area of the Bi–AgNPs nanosensor surface.

Table 1. Illustration of the E_{pa}, E_{pc} and ΔE_p for clean GCE and GCE/Bi–AgNPs.

Electrode	E_{pa} (mV)	E_{pc} (mV)	ΔE_p
Clean GCE	368	226	142
GCE/Bi–AgNPs	318	111	207

The scan rate studies (**Fig. 2a**) were employed to study the electron transfer kinetics of the modified GCE/Bi–AgNPs electrode and the clean GCE (Makombe *et al.*, 2016). It is observed that with an increase in scan rate, the peak currents also increase along with the shifting of peak potential to greater values which is a result of the transfer of electrons between $[Fe(CN)_6]^{3-/4-}$ and the GCE/Bi–AgNPs nanosensor surface. This phenomenon results in better sensing behavior for the GCE/Bi–AgNPs nanosensor. In the calculation of the active surface area of the fabricated nanosensor, we used the Randles–Sevcik equation (**Eq. 1**),

$$I_{pa} = (2.69 \, x \, 10^5) n^{3/2} D^{1/2} C A v^{1/2} \quad (1)$$

where n stands for the number of electrons ($n = 1$), A represents the surface area of the GCE/Bi–AgNPs nanosensor, and C is the concentration of the redox probe (1 mmol/L), D stands for the diffusion coefficient, I_{pa} stands for oxidation peak current, and v is the scan rate (V s^{-1}). We construct a profile of I_{pa} versus the square root of the scan rate ($v^{1/2}$) in **Fig. 2b**, the determined active surface area of the fabricated nanosensor was 0.150 cm^2. This active surface area of the fabricated nanosensor is much greater than the surface area of the clean GCE (0.070 cm^2). The calculated result showcase that the nanoparticles of Bi–Ag result in a vast surface area of the working electrode.

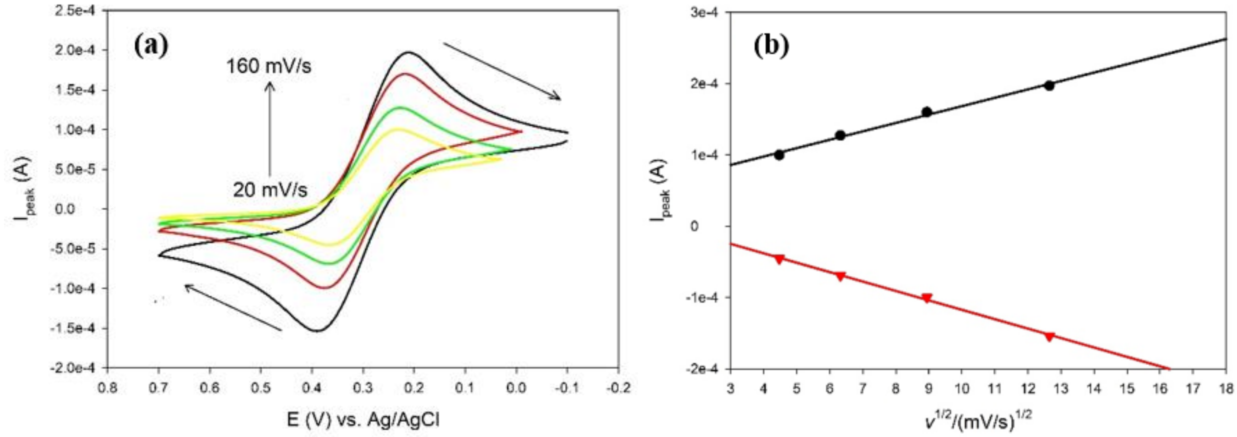

Figure 2. The study of scan rates of GCE/Bi–AgNPs in 0.1 M KCl containing 5.0 mmol/L $[Fe(CN)_6]^{3-/4-}$ in **(a)** The profile of I_{pa} vs. square root of scan rates in **(b)**.

3.2. Effect of various pHs on UA detection

The pH value is significant in detecting UA and was optimized by measuring the DPV responses of the constructed nanosensor in 80 µmol/L UA concentration. This study exploited different pH ranges of PBS to investigate the influences of the oxidation of UA peak currents. We studied the effect of pH (0.1 mol/L PB) on the DPV determination of UA in the range of pH 4.0 to pH 8.0 (N = 3). **Figure 3a** illustrates that the pH increases linearly between pH 4.0 and 5.0 and sharply declines from 5.0 to 8.0. The pH 5.0 has the highest anodic peak current responses, according to **Fig. 3a**. In this study, pH 5.0 was chosen as the optimum pH and was exploited as the supporting electrolyte in all DPV measurements. **Figure 4** illustrates the solution dependence on UA electrooxidation on the Bi–Ag/GCE nanosensor. The electrons and protons in this mechanism equally play their part in the oxidation of UA.

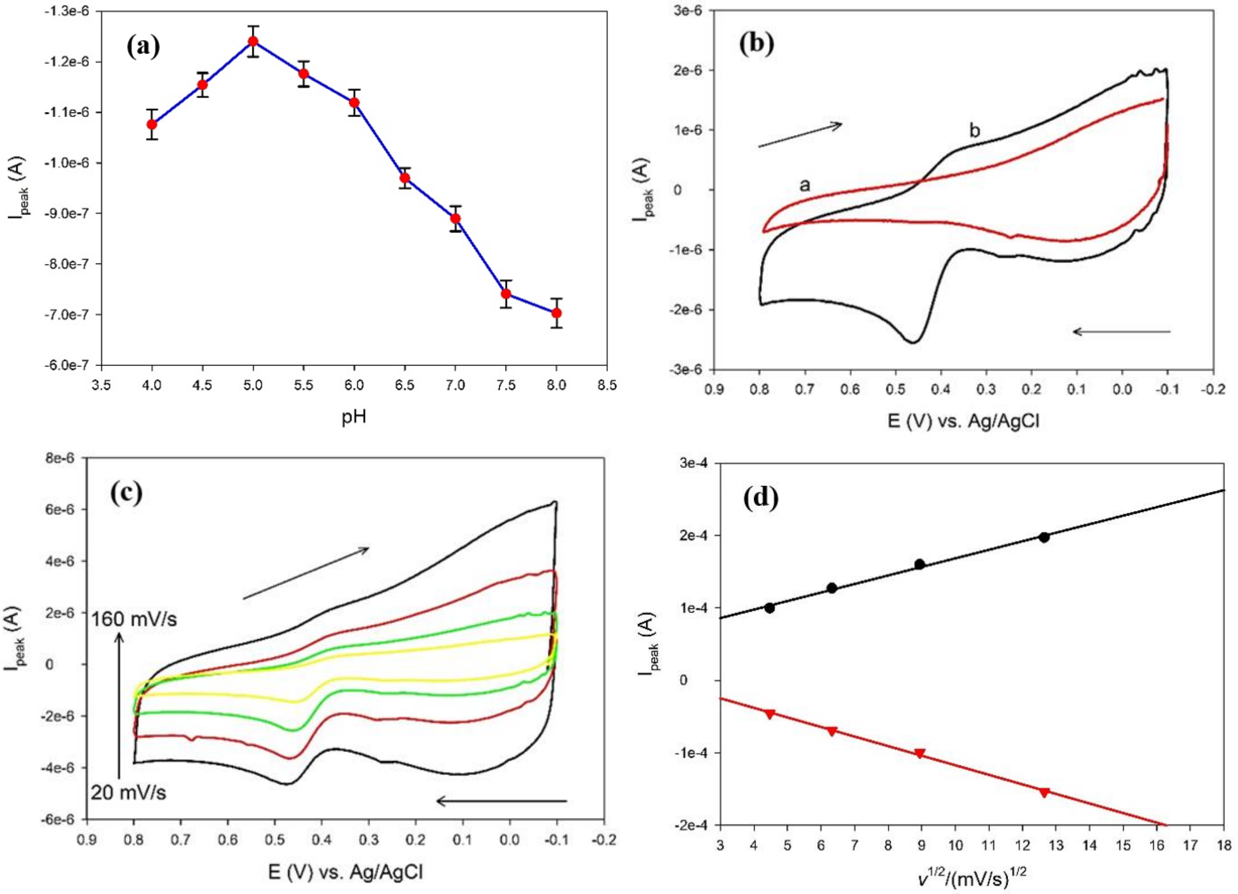

Figure 3. **(a)** pH optimization of 0.1 mol/L PBS; **(b)** curve a: CV curves for 80 µmol/L UA at clean GCE; curve b: constructed nanosensor; **(c)** Cyclic voltammograms for 80 µmol/L UA at GCE/Bi–AgNPs nanosensor in a 0.1 mol/L PBS (pH = 5.0) at scan rates of 20 to 160 mV s^{-1}; **(d)** Profile for peak current versus square root of scan rates.

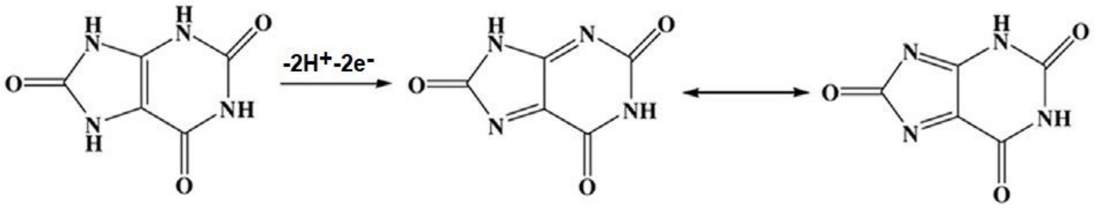

Figure 4. A Mechanism for the electrochemical oxidation of UA.

Figure 3b, we compared the CV of the constructed nanosensor with the CV of clean GCE using an 80 µmol/L UA solution. The constructed GCE/Bi–AgNPs nanosensor had a higher current response, showing that the electrochemical performance is excellent for UA sensing. The values of the anodic peak potential of UA at the GCE/Bi–AgNPs nanosensor are at about 440 mV. The chemically modified electrodes used to determine UA concentration also showed similar oxidation peak values (Liu *et al.*, 2019; Makombe *et al.*, 2016).

3.3 Effect of scan rates on UA detection

Cyclic voltammetry was used for scan rate studies of 80 µmol/L UA at the fabricated nanosensor in a 0.1 mol/L PBS (pH = 5.0) using increasing scan rates. As showcased in **Fig. 3c**, the anodic peak currents increase and shift to positive peak potentials with increasing scans of 20 to 160 mV s^{-1}. The oxidation and reduction peak currents for UA at GCE/Bi–AgNPs nanosensor generated linear profiles with linear equations are shown in **Fig. 3d**. We found that the oxidation peak currents versus the square root of the scan rate ($\sqrt{v}$) obey linearity. The profile equation was expressed as $I_{pa} = 2.01 \times 10^{-8}\ v^{1/2}$ (mV s^{-1}) – 7.0×10^{-7} ($R^2 = 0.994$) and $I_{pc} = 7.1 \times 10^{-9}\ v^{1/2}$ (mV s^{-1}) -3.62×10^{-8} ($R^2 = 0.998$). These equations suggest a diffusion–controlled process at the surface of the GCE/Bi–AgNPs sensor (Sangamithirai *et al.*, 2018). The profile of E_{pa} and E_{pc} versus ln v also showcase linearity with profile equations as $E_{pa} = -5.09 \times 10^{-5}$ ln v $+1.14 \times 10^{-4}$ ($R^2 = 0.993$) and $E_{pc} = 4.63 \times 10^{-5}$ ln v -4.13×10^{-5} ($R^2 = 0.996$). We used Laviron's Equations to calculate the electrochemical parameters such as n, α, and k_s, which refer to the number of electrons transferred, the electron transfer coefficient, and the standard electron transfer rate constant (Laviron, 1979).

$$E_{pa} = \frac{E^{0\prime}+2.3RT}{(1-\alpha)nF\ logv} \tag{2}$$

$$E_{pc} = \frac{E^{0\prime}-2.3RT}{\alpha nF\ logv} \tag{3}$$

$$logk_s = \alpha\log(1-\alpha) + (1-\alpha)\log\alpha - log(\frac{RT}{nFv}) - \frac{(1-\alpha)\alpha nF\Delta E_p}{2.3RT} \tag{4}$$

we were applying **Eqs. 2** and **3**, and the calculated values of n and α were reported as 2.1 and 0.87. Then, from **Eq. 4**, we calculated the value for k_s to be 0.61 s^{-1}.

3.4. DPV analysis of UA

Electrochemical measurements were recorded for UA in 80 µmol/L of UA model solutions at a GCE/Bi–AgNPs nanosensor, and clean GCE using DPV are demonstrated in **Fig. 5a**. Oxidation peak currents that are well–defined were recorded for UA in both cases. For the GCE/Bi–AgNPs electrode higher peak current value was produced and observed in the voltammogram. As followed at the clean GCE, the anodic peak potential of UA is recorded at +0.35 V (vs. Ag/AgCl), and at the fabricated nanosensor, the oxidation peak potential shifted to +0.39 V (vs. Ag/AgCl). The individual determination of UA at the fabricated nanosensor surface was investigated in a 0.1 mol/L PBS (pH 5.0) using DPV as the analytical mode. The UA oxidation peak currents in **Fig. 5b** increase linearly with increasing concentrations of UA under optimal experimental conditions. The constructed profile showcases that UA's linear detection range is 5 to 80 µmol/L. The profile equation is illustrated by $I_{pa\ (\mu A)} = -2.63 \times 10^{-8}\ C_{UA}$ (µmol/L) -1.59×10^{-6} with R^2 of 0.9964 and showcases the linear relationship. The detection limit measured for UA using the GCE/Bi–AgNPs nanosensor is down to 0.6 µmol/L at S/N = 3 (LOD = 3Sb/q; where Sb refers to the standard deviation of the blank and q is the slope of the linear plot). Additionally, **Table 1** compares the linear range and the detection limit for the GCE/Bi–AgNPs nanosensor with other similar electrode materials. In **Table 2**, we concluded that the GCE/Bi–AgNPs nanosensor performance is comparable to sensors modified by other electrode materials, including linear ranges and the detection limits (LODs).

3.5 Interference studies

Possible substances in samples of natural juices that might interfere in the determination of UA at the fabricated nanosensor surface were studied by adding different ions to a 0.1 mol/L PBS (pH = 5.0). For this study, ions that might interfere, such as AA, K^+, Na^+, SO_4^{2-}, and CAF, were added to an equal amount of 40 µmol/L UA, and the sensor was immersed in the mixed solution. According to the results in **Fig. 6a**, AA and CAF did not show interference in the determination of UA in the presence of these interfering ions. In contrast, K^+ and Na^+ showed interference in the determination of UA in the presence of these two positive interfering ions. The anodic peak current for K^+ and Na^+ was significantly lower than that of AA and CAF. The same trend was observed for SO_4^{2-} anodic peak currents, showing that these ions interfere in UA's determination, indicating that this electrochemical sensor has reasonable specificity towards UA.

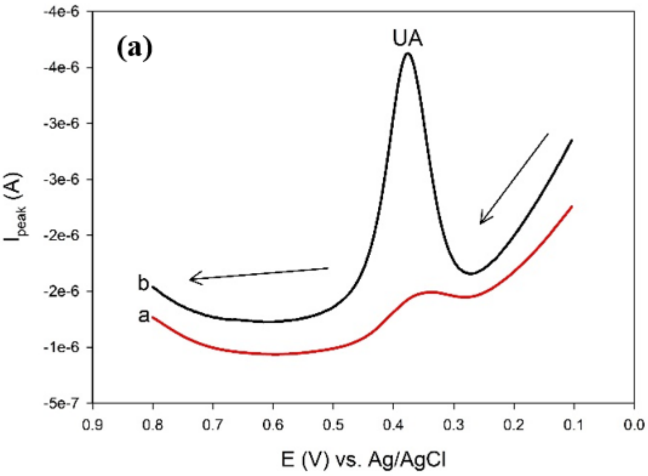

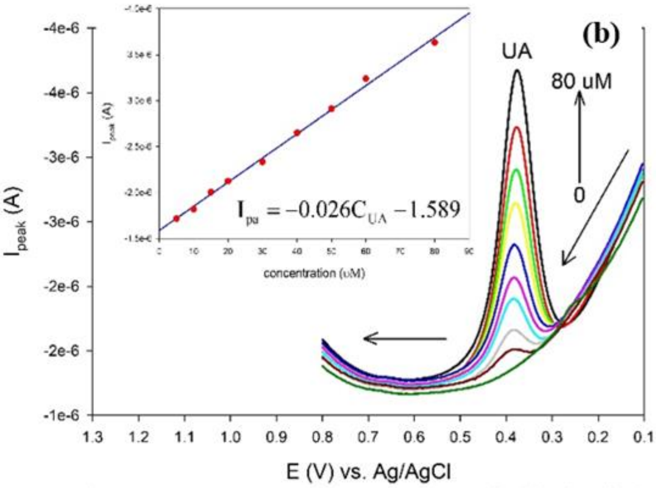

Figure 5. (a) curve a: DPV results of the clean GCE; curve b: versus the fabricated nanosensor, both in 80 μmol/L UA solution were illustrated; **(b)** the DPV results of 0.1 mol/L PBS (pH = 5.0) containing increasing concentrations of UA and (inset) the corresponding profile for UA analysis.

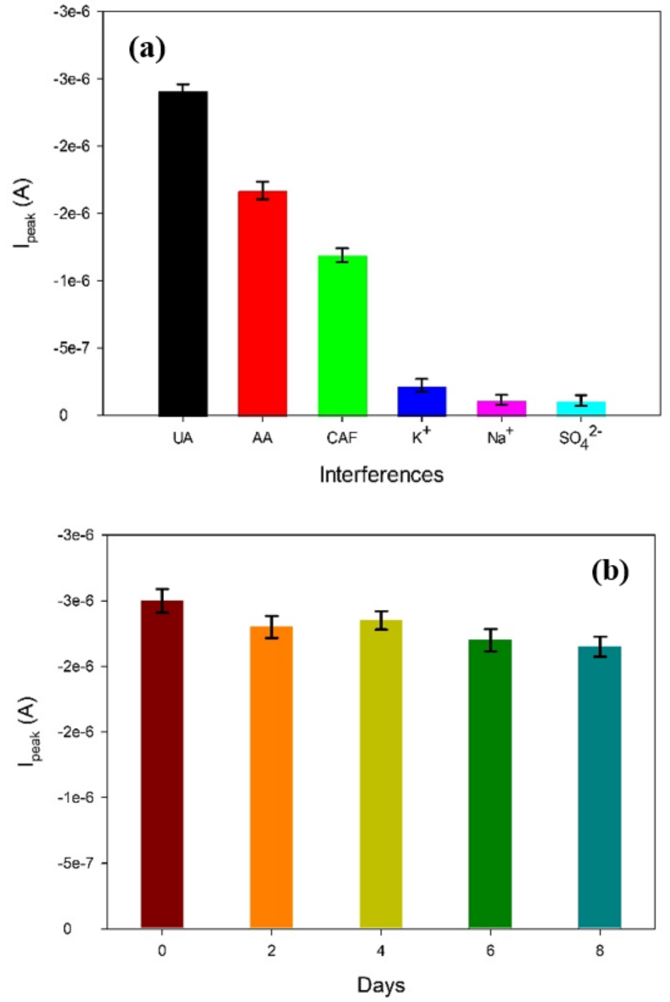

Figure 6. (a) Interference test of UA in the presence of AA, CAF, K^+, Na^+, and SO_4^{2-} that might interfere at a GCE/Bi–AgNPs nanosensor surface; **(b)** Stability tests of GCE/Bi–AgNPs nanosensor.

3.6. Effect of repeatability and stability

The repeatability, storage stability, and reproducibility of the GCE/Bi–AgNPs nanosensor were studied using the DPV measurements in 0.1 mol/L PB (pH = 5.0) containing 40 μmol/L of UA. For the storage stability study (**Fig. 6b**), the sensitivity of the fabricated sensor was measured over eight days under ambient temperature. After eight days, the nanosensor produced an anodic peak current with a slight decrease in the current response. A response current of 80% was observed after eight days. Therefore, the stability results in **Fig. 6b** of the fabricated nanosensor were good enough and resulted in continual operation.

In the case of repeatability in **Fig. 7a**, ten repetitive measurements were recorded using the same electrode with a relative standard deviation (RSD) of 3.22%. The reproducibility was also studied using six independent measurements with six different sensors constructed under similar conditions. The results obtained for the reproducibility test display a good RSD of 3.80% and are shown in **Fig. 7b**. The results (**Fig. 6b** and **7**) indicate that the fabricated nanosensor has excellent reproducibility, repeatability, and storage stability for UA detection.

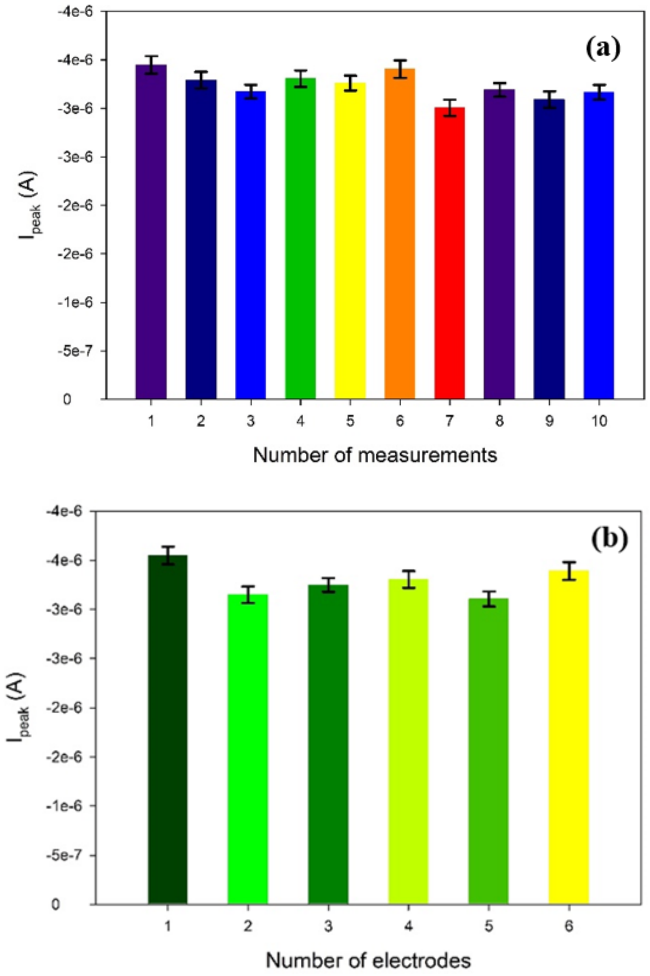

Figure 7. (a) illustrates the repeatability analysis of GCE/Bi–AgNPs nanosensor for ten repeated measurements; **(b)** the reproducibility analysis of GCE/Bi–AgNPs nanosensor for six separate electrodes.

Table 2. Illustration of the various sensors used that contain different nanomaterials in the determination of UA.

Materials	Linear ranges (µmol/L)	LOD (µmol/L)	References
PEDOT/Au NPs	1.5–150	0.08	Ali *et al.*, 2017
CNCo	2.0–110	0.83	Liu *et al.*, 2019
PtNi@MoS$_2$	0.5–600	0.1	Ma *et al.*, 2019
Ta/Ni	1.0–1400	0.1	Zhao *et al.*, 2019
a–Fe$_2$O$_3$/PAn (NTs)	0.01–5.0	0.038	Mahmoudian *et al.*, 2019
Au1Pt$_2$NPs/S–NS–GR	1–1000	0.038	Zhang *et al.*, 2018
HNP–AuAg	5–425	1.0	Hou *et al.*, 2016
ErGO/PEDOT:PSS	10–100	1.08	Wang *et al.*, 2022
2D g–C$_3$N$_4$/WO$_3$	0.01–900	0.0022	Rajesh *et al.*, 2022
Bi–AgNPs	5–80 µM	0.6	This study

3.7. Actual samples analysis

The developed GCE/Bi–Ag nanosensor was practically exploited for the electrochemical analysis of UA in some natural fruit juice samples by using a standard addition method. Firstly, the actual samples of fruit juices were diluted ten times with 0.1 mol/L PBS (pH 5.0). This procedure was applied before the detection of UA to decrease the matrix effect without any other treatment. After diluting, we added known quantities of standard UA to the natural fruit juice samples, and recoveries were determined. We also used Eq. 5 for the estimated recovery values of the spiked UA samples.

$$\% \text{ recoveries} = C_i \times C_o / C_x \times 100 \qquad (5)$$

where C_i refers to the UA concentration experimentally obtained, C_o stands for the unspoked fruit juice samples, and C_x refers to the spiked concentration of UA in the fruit juice samples.

In Table 3, the DPV results are illustrated, showing good recoveries ranging from 98.9% to 105.1% (n = 3) and the RSDs ranging from 2.1% to 3.2% for apple juice. In the case of orange juice, the spiked UA sample recoveries ranged from 102% to 109%, with RSDs of 1.89% to 2.76%. The good recoveries for UA indicated the potential usefulness of the GCE/Bi–Ag nanosensor for the practical determination of UA in actual samples. These recovery results suggest that the electrochemical procedure has great potential for accurate, sensitive, easy, and fast detection of UA in natural fruit juice samples.

Table 3. Analysis of UA in actual fruit juice samples (n = 3) using GCE/Bi–Ag nanosensor.

Sample	Added (µmol/L)	Found (µmol/L)	Recovery (%)	RSD (%)
Apple Juice	10	10.4	104	2.1
	20	19.78	98.9	2.5
	30	31.53	105.1	3.2
Orange Juice	10	10.9	109	1.89
	20	20.7	103.5	2.76
	30	30.6	102	2.03

4. Conclusions

In summary, we have constructed an electrochemical procedure using for the first time a GCE/Bi–Ag nanosensor for the individual detection of UA in actual samples of fruit juices. The results obtained in this investigation conclude that the Bi–AgNPs have highly dispersed active sites with high surface area. These properties displayed higher peak currents for the fabricated nanosensor in contrast with the clean GCE. This phenomenon is due to enhanced electrocatalytic activity toward the oxidation of UA in model standard solutions. At the surface of the fabricated nanosensor well, distinct peaks for UA analysis were recorded with good linear regression responses of the currents for the oxidation peak. The nanosensor obtained a detection limit of 0.6 µmol/L with an $R^2 = 0.999$ for UA detection. Moreover, the GCE/Bi–Ag nanosensor brought good reproducibility, repeatability and stability, excellent anti–interference ability, and satisfied recoveries for the UA detection in actual samples.

Authors' contributions

Conceptualization: Charlton Van der Horst; Vernon Somerset; **Data curation:** Charlton Van der Horst; Vernon Somerset; **Formal Analysis:** Charlton Van der Horst; Vernon Somerset; **Funding acquisition:** Vernon Somerset; **Investigation:** Charlton Van der Horst; Vernon Somerset; **Methodology:** Charlton Van der Horst; Vernon Somerset; Eric de Souza Gil; **Project administration:** Vernon Somerset; **Resources:** Vernon Somerset; **Software:** Not applicable; **Supervision:** Vernon Somerset; **Validation:** Eric de Souza Gil; **Visualization:** Charlton Van der Horst; Vernon Somerset; Eric de Souza Gil; **Writing – original draft:** Charlton Van der Horst; Vernon Somerset; **Writing – review & editing:** Charlton Van der Horst; Vernon Somerset; Eric de Souza Gil.

Data availability statement

All data sets were generated or analyzed in the current study.

Funding

Not applicable.

Acknowledgments

The authors acknowledge the laboratory infrastructure and administrative support provided by the Cape Peninsula University of Technology (CPUT). The collaboration with the Universidade Federal de Goiás, Brazil research laboratories is greatly acknowledged.

Conflict of interest

The authors declare that there is no conflict of interest.

References

Abbas, M. W.; Soomro, R. A.; Kalwar, N. H.; Zahoor, M.; Avci, A.; Pehlivan, E.; Hallam, K. R.; Willander, M. Carbon quantum dot coated Fe_3O_4 hybrid composites for sensitive electrochemical detection of uric acid. *Microchem. J.* **2019**, *146*, 517. https://doi.org/10.1016/j.microc.2019.01.034

Ali, A.; Jamal, R.; Abdiryim, T.; Huang, X. Synthesis of monodispersed PEDOT/Au hollow nanospheres and its application for electrochemical determination of dopamine and uric acid. *J. Electroanal. Chem.* **2017**, *787*, 110. https://doi.org/10.1016/j.jelechem.2017.01.051

Bai, Z.; Zhou, C.; Xu, H.; Wang, G.; Pang, H.; Ma, H. Polyoxometalates-doped Au nanoparticles and reduced grapheneoxide: A new material for the detection of uric acid in urine. *Sens. Actuators B*. **2017**, *243*, 361. https://doi.org/10.1016/j.snb.2016.11.159

Beitollahi, H.; Sheikhshoaie, I. Electrocatalytic and simultaneous determination of isoproterenol, uric acid and folic acid at molybdenum (VI) complex-carbon nanotube paste electrode. *Electrochim. Acta*. **2011**, *56*, 10259. https://doi.org/10.1016/j.electacta.2011.09.017

Benjamin, S. R.; de Oliveira Neto, J. R.; de Macedo, I. Y. L.; Bara, M. T. F.; da Cunha, L. C.; Carvalho, L. A. F.; Gil, E. S. Electroanalysis for quality control of acerola (Malpighiaemarginata) fruits and their commercial products. *Food Anal. Methods*. **2015**, *8*, 86–92. https://doi.org/10.1007/s12161-014-9872-0

Boroumand, S.; Chamjangali, M. A.; Bagherian, G. Double injection/single detection asymmetric flow injection manifold for spectrophotometric determination of ascorbic acid and uric acid: Selection the optimal conditions by MCDM approach based on different criteria weighting methods. *Spectrochim. Acta Part A*. **2017**, *174*, 203–213. https://doi.org/10.1016/j.saa.2016.11.031

Brainina, K. Z.; Bukharinova, M. A.; Stozhko, N. Y.; Sokolkov, S. V.; Tarasov, A. V. M.; Vidrevich, M. B. Electrochemical Sensor Based on a Carbon Veil Modified by Phytosynthesized Gold Nanoparticles for Determination of Ascorbic Acid. *Sensors*. **2020**, *20*, 1800. https://doi.org/10.3390/s20061800

Choi, H. K.; Mount, D. B.; Reginato, A. M. Pathogenesis of gout. *Ann. Intern. Med*. **2005**, *143* (7), 499–516. https://doi.org/10.7326/0003-4819-143-7-200510040-00009

Das, T. R.; Sharma, P. K. Hydrothermal-assisted green synthesis of Ni/Ag@rGO nanocomposite using Punica granatum juice and electrochemical detection of ascorbic acid. *Microchem. J.* **2020**, *156*, 104850. https://doi.org/10.1016/j.microc.2020.104850

Erden, P. E.; Kilic, E. A review of enzymatic uric acid biosensors based on amperometric detection. *Talanta*. **2013**, *107*, 312–323. https://doi.org/10.1016/j.talanta.2013.01.043

Fukuda, T.; Muguruma, H.; Iwasa, H.; Tanaka, T.; Hiratsuka, A.; Shimizu, T.; Tsuji, K.; Kishimoto, T. Electrochemical determination of uric acid in urine and serum with uricase/carbon nanotube /carboxymethylcellulose electrode. *Anal. Biochem*. **2020**, *590*, 113533. https://doi.org/10.1016/j.ab.2019.113533

Ganesh, P. S.; Kumara Swamy, B. E. Simultaneous electroanalysis of norepinephrine, ascorbic acid and uric acid using poly(glutamic acid) modified carbon paste electrode. *J. Electroanal. Chem*. **2015**, *752*, 17–24. https://doi.org/10.1016/j.jelechem.2015.06.002

Hou, J.; Xu, C.; Zhao, D.; Zhou, J. Facile fabrication of hierarchical nanoporous AuAg alloy and its highly sensitive detection towards dopamine and uric acid. *Sens Actuators B*. **2016**, *225*, 241–248. https://doi.org/10.1016/j.snb.2015.11.035

Huang, S. H.; Shih, Y. C.; Wu, C. Y.; Yuan, C. J.; Yang, Y. S.; Li, Y. K.; Wu, T. K. Detection of serum uric acid using the optical polymeric enzyme biochip system. *Biosens Bioelectron*. **2004**, *19*, 1627–1633. https://doi.org/10.1016/j.bios.2003.12.026

Kanbay, M.; Jensen, T.; Solak, Y.; Le, M.; Roncal-Jimenez, C.; Rivard, C.; Lanaspa, M. A.; Nakagawa, T.; Johnson, R. J. Uric acid in metabolic syndrome: from an innocent bystander to a central player. *Eur. J. Intern. Med*. **2016**. *29*, 3–8. https://doi.org/10.1016/j.ejim.2015.11.026

Lakshmi, D.; Whitcombe, M. J.; Davis, F.; Sharma, P. S.; Prasad, B. B. Electrochemical detection of uric acid in mixed and clinical samples: a review. Electroanalysis. **2011**, *23*, 305–320. https://doi.org/10.1002/elan.201000525

Laviron, E. General expression of the linear potential sweep voltammogram in the case of diffusionless electrochemical systems. *J. Electroanal. Chem. Interfacial Electrochem*. **1979**, *101*, 19–28. https://doi.org/10.1016/S0022-0728(79)80075-3

Li, X. L.; Li, G.; Jiang, Y. Z.; Kang, D.; Jin, H.; Shi, Q.; Jin, T.; Inoue, K.; Todoroki, K.; Toyo'Oka, T. Human nails metabolite analysis: A rapid and simple method for quantification of uric acid in human fingernail by high-performance liquid chromatography with UV-detection. *J. Chromatogr. B*. **2015**, *1002*, 394–398. https://doi.org/10.1016/j.jchromb.2015.08.044

Liu, L.; Liu, L.; Wang, Y.; Ye, B-C. A novel electrochemical sensor based on bimetallic metal–organic framework-derived porous carbon for detection of uric acid. *Talanta*. **2019**, *199*, 478–484. https://doi.org/10.1016/j.talanta.2019.03.008

Luo, X.; Cai, N.; Cheng, Z. Determination of Uric Acid in Plasma by LC–MS/MS and Its Application to an Efficacy Evaluation of Recombinant Urate Oxidase. *Anal. Sci*. **2013**, *29*, 709–713. https://doi.org/10.2116/analsci.29.709

Ma, L.; Zhang, Q.; Wu, C.; Zhang, Y.; Zeng, L. PtNi bimetallic nanoparticles loaded MoS_2 nanosheets: Preparation and electrochemical sensing application for the detection of dopamine and uric acid. *Anal. Chim. Acta*. **2019**, *1055*, 17–25. https://doi.org/10.1016/j.aca.2018.12.025

Mahmoudian, M. R.; Basirun, W. J.; Sookhakian, M.; Woi, P. M.; Zalnezhad, E.; Hazarkhani, H.; Alias, Y. Synthesis and characterization of a-Fe_2O_3/polyaniline nanotube composite as electrochemical sensor for uric acid detection. *Adv. Powder Technol*. **2019**, *30*, 384–392. https://doi.org/10.1016/j.apt.2018.11.015

Makombe, M.; Van der Horst, C.; Silwana, B.; Iwuoha, E.; Somerset, V. Antimony film sensor for sensitive rare earth metal analysis in environmental samples. *J. Environ. Sci. Health Part A*. **2016**, *8*, 597–606. https://doi.org/10.1080/10934529.2016.1159857

Misra, N.; Kumar, V.; Borde, L.; Varshney, L. Localized surface plasmon resonance-optical sensors based on radiolytically synthesized silver nanoparticles for estimation of uric acid. *Sens. Actuators B*. **2013**, *178*, 371–378. https://doi.org/10.1016/j.snb.2012.12.110

Papavasileiou, M. V.; Karamanou, A. G.; Kalogeropoulos, P.; Moustakas, G.; Patsianis, S.; Pittaras, A. Uric acid blood levels and relationship with the components of metabolic syndrome in hypertensive patients. *J. Hum. Hypertens*. **2016**, *30*, 414–417. https://doi.org/10.1038/jhh.2015.53

Raj, C. R.; Ohsaka, T. Electroanalysis of ascorbate and dopamine at a gold electrode modified with a positively charged self-assembled monolayer. *J. Electroanal. Chem*. **2001**, *496 (1–2)*, 44–49. https://doi.org/10.1016/S0022-0728(00)00335-1

Rajesh, M.; Yan, W-M.; Yen, Y-K. Solvothermal synthesis of two-dimensional graphitic carbon nitride/tungsten oxide nanocomposite: a robust electrochemical scaffold for selective determination of dopamine and uric acid. *J. Appl. Electrochem*. **2022**, *52*, 1231–1248. https://doi.org/10.1007/s10800-022-01699-6

Riches, P. L.; Wright, A. F.; Ralston, S. H. Recent insights into the pathogenesis of hyperuricaemia and gout. *Hum. Mol. Genet*. **2009**, *18*, R177–R184. https://doi.org/10.1093/hmg/ddp369

Sadikoglu, M.; Taskin, G.; Demirtas, F. G.; Selvi, B.; Barut, M. Voltammetric Determination of Uric Acid on Poly(*p*-Aminobenzene Sulfonic Acid)-Modified Glassy Carbon Electrode. *Int. J. Electrochem. Sci*. **2012**, *7*(11), 11550–11557.

Sangamithirai, D.; Munusamy, S.; Narayanan, V.; Stephen, A. A voltammetric biosensor based on poly(o-methoxyaniline)-gold nanocomposite modified electrode for the simultaneous determination of dopamine and folic acid. *Mater Sci. Eng. C*. **2018**, *91*, 512–523. https://doi.org/10.1016/j.msec.2018.05.070

Silwana, B.; Van der Horst, C.; Iwuoha, E.; Somerset, V. Reduced Graphene Oxide Impregnated Antimony Nanoparticle Sensor for Electroanalysis of Platinum Group Metals. *Electroanalysis*. **2016**, *28* (7), 1597–1607. https://doi.org/10.1002/elan.201501071

Tadesse, Y.; Tadese, A.; Saini, R. C.; Pal, R. Cyclic Voltammetric Investigation of Caffeine at Anthraquinone Modified Carbon Paste Electrode. *Int J. Electrochem*. **2013**, *2013*, 1–7. https://doi.org/10.1155/2013/849327

Van der Horst, C. Development of a Bismuth-Silver Nanofilm Sensor for the Determination of Platinum Group Metals in Environmental Samples. PhD's Thesis, University of the Western Cape: Bellville, South Africa, 2015.

Van der Horst, C.; Silwana, B.; Iwuoha, E.; Somerset, V. Synthesis and characterisation of bismuth-silver bimetallic nanoparticles for electrochemical sensor applications. *Anal. Lett*. **2015a**, *48*, 1311–1332. https://doi.org/10.1080/00032719.2014.979357

Van der Horst, C.; Silwana, B.; Iwuoha, E.; Somerset, V. Bismuth-silver bimetallic nanosensor application for the voltammetric analysis of dust and soil samples. *J. Electroanal. Chem*. **2015b**, *752*, 1–11. https://doi.org/10.1016/j.jelechem.2015.06.001

Van der Horst, C.; Silwana, B.; Iwuoha, E.; Somerset, V. Application of a bismuth-silver nanosensor for the simultaneous determination of Pt-Rh and Pd-Rh complexes. *J. Nano Res*. **2016a**, *44*, 126–133. https://doi.org/10.4028/www.scientific.net/JNanoR.44.126

Van der Horst, C.; Silwana, B.; Iwuoha, E.; Gil, E.; Somerset, V. Improved detection of ascorbic acid with a bismuth-silver nanosensor. *Food Anal. Method*. **2016b**, *9*, 2560–2566. https://doi.org/10.1007/s12161-016-0444-3

Van der Horst, C. Silwana, B. Iwuoha, E. Somerset, V. Voltammetric analysis of platinum group metals using a bismuth-silver bimetallic nanoparticles sensor. In. *Recent Progress in Organometallic Chemistry*, Chapter 6; Rahman, M. M., Asiri, A. M.; Eds.; INTECH, Croatia, 2017a; pp 123. https://doi.org/10.5772/68132

Van der Horst, C.; Silwana, B.; Iwuoha, E.; Somerset, V. Electrocatalytic evaluation of a horseradish peroxidase biosensor based on a novel Bi-Ag bimetallic nanocomposite. Proc. Technol. **2017b**, *27*, 179–182. https://doi.org/10.1016/j.protcy.2017.04.077

Van der Horst, C.; Silwana, B.; Iwuoha, E.; Somerset, V. Spectroscopic and voltammetric analysis of platinum group metals in road dust and roadside soil. *Environments*. **2018**, *5* (11), 120. https://doi.org/10.3390/environments5110120

Van der Horst, C.; Silwana, B.; Gil, E.; Iwuoha, E.; Somerset, V. Simultaneous Detection of Paracetamol, Ascorbic Acid, and Caffeine Using a Bismuth-Silver Nanosensor. *Electroanalysis*. **2020**, *32*, 3098–3107. https://doi.org/10.1002/elan.202060389

Van der Horst, C.; Somerset, V. Nanoparticles Application in the Determination of Uric Acid, Ascorbic Acid, and Dopamine. *Russian J. Electrochem*. **2022**, *58*, 341–359. https://doi.org/10.1134/S102319352205010X

Wan, W.; Xu, X.; Zhao, D. B.; Pang, Y. F.; Wang, Y. X. Polymorphisms of uric transporter proteins in the pathogenesis of gout in a Chinese Han population. *Genet. Mol. Res*. **2015**, *14* (1), 2546–2550. https://doi.org/10.4238/2015.March.30.13

Wang, H.; Cao, T.; Zhou, Y.; Liu, L.; Zhang, X.; Tong, Z. A facile approach to synthesis methylene blue/reduced graphene oxide nanocomposite and simultaneous determination of dopamine and uric acid. *J. Appl. Electrochem*. **2022**, *52*, 1067–1080. https://doi.org/10.1007/s10800-022-01695-w

Wayu, M. B.; Di Pasquale, L. T.; Schwarzmann, M. A.; Gillespie, S. D.; Leopold, M. C. Electropolymerization of β-cyclodextrin onto multi-walled carbon nanotube composite films for enhanced selective detection of uric acid. *J. Electroanal. Chem*. **2016**, *783*, 192–200. https://doi.org/10.1016/j.jelechem.2016.11.021

Yue, H. Y.; Zhang, H.; Chang, J.; Gao, X.; Huang, S.; Yao, L. H.; Lin, X. Y.; Guo, E. J. Highly sensitive and selective uric acid biosensor based on a three-dimensional graphene foam/indium tin oxide glass electrode. *Anal. Biochem*. **2015**, *488*, 22–27. https://doi.org/10.1016/j.ab.2015.07.007

Zhang, K.; Chena, X.; Lia, Z.; Wang, Y.; Sun, S.; Wang, L.; Guo, T.; Zhang, D.; Xue, Z.; Zhou, Lu, X. Au-Pt bimetallic nanoparticles decorated on sulfonated nitrogen sulfur co-doped graphene for simultaneous determination of dopamine and uric acid. *Talanta*. **2018**, *178*, 315–323. https://doi.org/10.1016/j.talanta.2017.09.047

Zhang, X.; Zhang, Y-C.; Ma, L-X. One-pot facile fabrication of graphene-zinc oxide composite and its enhanced sensitivity for simultaneous electrochemical detection of ascorbic acid, dopamine and uric acid. *Sens. Actuators B*. **2016**, *227*, 488–496. https://doi.org/10.1016/j.snb.2015.12.073

Zhao, M.; Zhao, J.; Qin, L.; Jia, H.; Liu, S. Synthesis of Ta/Ni microcavity array film for highly sensitive uric acid detection. *J. Electroanal. Chem*. **2019**, *834*, 86–93. https://doi.org/10.1016/j.jelechem.2018.12.053

ECLÉTICA QUÍMICA

Eclet. Quim. 49 | e-1479, 2024

Original Article

https://doi.org/10.26850/1678-4618.eq.v49.2024.e1479

Identification and theoretical study of the regioselectivity of the synthesis reaction of an α-heterocyclic α-amino ester

Mohammed El **Mesky**[1], Hicham **Zgueni**[1], Mohamed **Jabha**[1], Youssef **Youssefi**[1], Nabil **Amri**[2], M'barek **Azdouz**[1], Ahmad **Oubair**[1], Driss **Chebabe**[1], Mohamed **Azrour**[1], El Houssine **Mabrouk**[1+]

Abstract

The interest of amino acids no longer needs to be demonstrated, given the involvement of these compounds in various fields, both as basic elements of peptide and protein structures and as independent entities. We report the regioselective synthesis of an N-protected α,α-diamino carboxylic ester derived from glycine. Our synthetic strategy is based first on the preparation of methyl 2-azido-2-benzamidoacetate and then on the N-alkylation reaction between the latter and the 1H-1,2,4-triazole-3-amine with three methods. The theoretical study by the DFT method and Marvinsketch software explains well the reaction's regioselectivity and good compatibility between the experimental and computational results. The products synthesized during this strategy are identified and characterized by spectral analysis: mass spectrometry, ^{1}H NMR and ^{13}C NMR.

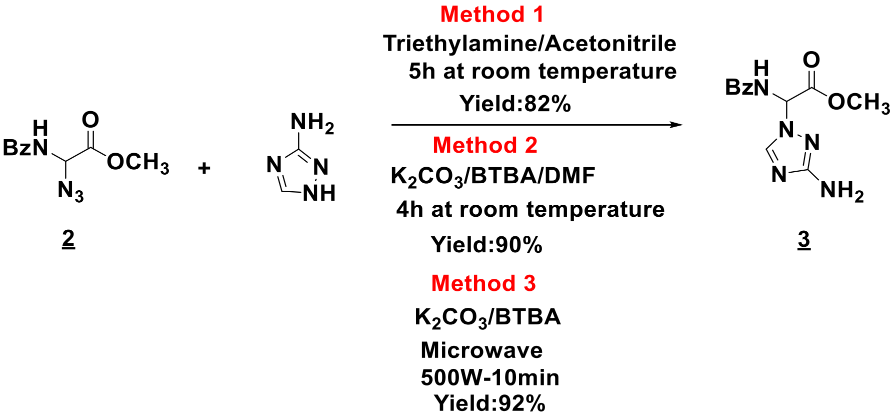

Article History

Received February 28, 2023
Accepted August 27, 2024
Published December 26, 2024

Keywords

1. 1H-1,2,4-triazole-3-amine;
2. heterocyclic compounds;
3. carboxylic amino esters.

Section Editors

Michelle Jakeline Cunha Rezende

Highlights

- α-Heterocyclic α-amino esters were synthesized by three methods and characterized.
- The synthesis of N-protected α,α-diamino carboxylic ester derived was reported.
- The regioselective synthesized compound was obtained from glycine.
- The theoretical study was done by the DFT method and Marvinsketch software.
- This method and the software were explored to explain the reaction regioselectivity.

[1]University of Moulay Ismail, Faculty of Sciences and Technics, Errachidia, Morocco. [2]Sidi Mohamed Ben Abdellah University, Faculty of Sciences, Fez, Morocco.
+Corresponding author: El Houssine Mabrouk, **Phone:** +212618788704, **Email address:** mabrouk.elhoussine@gmail.com

1. Introduction

Heterocyclic compounds represent most molecules used in industry and are the subject of very active research worldwide. They have an important role in biological, pharmacological, and agrochemical industrial processes (vitamins, hormones, antibiotics, dyes, etc.) (Azimi *et al.*, 2021; Rhazi *et al.*, 2022), and they also constitute the basic structures of many alkaloids, at the origin of a large variety of drugs. From a chemical point of view, most heterocyclic compounds' stability is due to a conjugated or aromatic system. Nitrogenous heterocyclic compounds are important because they often constitute the active principle of various substances used in the pharmacological, biological, and industrial fields (Faisal *et al.*, 2019).

Five-membered heterocyclic systems are very active, triazoles constitute a class among them that have found, since their discovery, diversified applications in the fields of medicine, agrochemical, industrial and catalysis (Khilkovets *et al.*, 2022; Ramesh *et al.*, 2011). Triazole molecules do not exist in nature; various methods synthesize them. Triazoles have a pseudo-aromatic structure, which results in an interaction between π bonds, a large dipole moment, and a great capacity to form hydrogen bonds (Abboud *et al.*, 2001). They are very stable compounds concerning other chemical reagents, oxidation, and reduction. Triazole derivatives have been reported to have various biological activities such as antidiabetic (Ouyang *et al.*, 2008), antitubercular (Cetin *et al.*, 2018; Radi *et al.*, 2017), anti-inflammatory, antifungal (Kumar *et al.*, 2013; Ramirez-Prada *et al.*, 2017), and antibacterial (Diculescu *et al.*, 2016; Graillot *et al.*, 2012) properties. Today, various triazole drugs have been widely used in medicine, such as antifungals (Fluconazole, Voriconazole, and Itraconazole) (El-Sabbagh *et al.*, 2009), anticancer drugs (Letrozole and Anastrozole) (Perez-Fernandez *et al.*, 2014) as well as antivirals (Ribavirin) (Bandgar *et al.*, 2009). Recently, 1,2,4-triazole derivatives have benefited from several agricultural and medical studies due to their interesting structural features and biological activities. These derivatives have various biological properties, in particular antimicrobial activity, antimalarial activity, anticonvulsive activity, anti-leishmanial activity, anti-Alzheimer activity, and antidiabetic activity (Abdu *et al.*, 2017; Abu-Hashem *et al.*, 2016; Ansari *et al.*, 2017; Insuasty *et al.*, 2010; Karrouchi *et al.*, 2018; Knorr *et al.*, 1883; Ozdemir *et al.*, 2015; Shilpy *et al.*, 2018; Zarrouk *et al.*, 2012).

Non-proteinogenic amino acids are becoming of greater industrial importance with the development of new methods of synthesis leading to a wide range of substances present, including alkaloids, antibiotics, and proteins (Ngo *et al.*, 2011). Most heterocyclic amino acids (Banno *et al.*, 2017; Christian *et al.*, 2005) of plant origin exhibiting various biological properties (Schenk *et al.*, 1991) are fundamental in biological processes (Costantino *et al.*, 2004; Jorgensen *et al.*, 2007).

Triazolic amino acids are bioactive heterocycles (Boibessot *et al.*, 2016; Stanley *et al.*, 2010; Thirumurugan *et al.*, 2013) representing an interesting class of amino acids that have few physiological activities (Albada *et al.*, 2017; Cativiela *et al.*, 2007; Dondoni *et al.*, 2006; Hughes *et al.*, 2007a; b; Nájera and Sansano 2007; Risseeuw *et al.*, 2013; Vogt *et al.*, 2007).

The work presented in this article first aims to identify a triazole α-aminoester synthesized by three methods and then to study the regioselectivity of this reaction. The valorization of this product by the evaluation of its activities and its applications will be the subject of subsequent work.

2. Experimental

2.1. General

All the chemicals used are commercial and analytical grade, and do not require further purification. The TLC is used to monitor the progress of the reactions (Merck, silica gel 60 F254), while UV light is utilized to see the spots (VILBER LOURMAT, VL-215.LC). Nuclear Magnetic Resonance (NMR) spectra (^{1}H, ^{13}C) were recorded employing a Bruker AM 300 spectrometer operating at frequencies of 300.13 MHz (for ^{1}H) and 75.47 MHz (for ^{13}C). NMR data is reported in parts per million (ppm) and is referenced to tetramethylsilane (for ^{13}C). Mass spectra were recorded using a PolarisQ Ion Trap GC/MSn mass spectrometer.

2.2. Typical procedure for nucleophilic substitution

2.2.1. Method 1

2.73 mmol of methyl 2-azido-2-benzamidoacetate were added to a mixture of 3.0 mmol of 1H-1,2,4-triazole-3-amine, 3.3 mmol of triethylamine, and 8 mL of dry acetonitrile stirred for 45 min. The reaction was carried out at room temperature for five hours. After removal of the solvent under reduced pressure, the residue was quenched with a saturated aqueous solution of ammonium chloride or sodium hydrogenocarbonate (15 mL) and extracted with dichloromethane (15 mLx 3). The organic phase was dried in sodium sulfate (Na_2SO_4) and the solvent was evaporated under reduced pressure. The product was purified by column chromatography on silica gel using hexane/ether (2:1) as eluent. Yield: 82%.

2.2.2. Method 2

To 10 mmol of 1H-1,2,4-triazole-3-amine in 30 mL of dimethyl-formamide or acetone, 15 mmol (2.10 g) of potassium carbonate are added in small portions and a catalytic amount of tetra-n-butylammonium bromide (1 mmol, 0.34 g BTBA). The mixture was stirred for 15 min and then 9.09 mmol of the methyl 2-azido-2-benzamidoacetate were added. The reaction was left for four hours at room temperature. At the end of the reaction and after evaporation of the solvent, the residue obtained was washed with hexane. The organic phase was then dried and purified by column chromatography on silica gel using an ether/hexane mixture (1:2) as eluent. Yield: 90%.

2.2.3. Method 3

A mixture of 1H-1,2,4-triazol-3-amine (5.0 mmol), methyl 2-azido-2-benzamidoacetate (4.55 mmol), tetrabutylammonium bromide (0.17 g, 0.50 mmol, and potassium carbonate (2.8 g, 20 mmol) on silica (or clay) as support was heated in a domestic microwave oven in an employing Meyer flask with a power of 500 W for 10 min. After cooling down, the reaction mixture was extracted with dichloromethane (3 x 15 mL). Then the organic layer was dried with Na_2SO_4, filtered, and the solvent was evaporated to dryness. The solid material was purified by using flash chromatography or recrystallization from hexane or ethanol to afford the desired product:2-(3-amino-1H-1,2,4-triazol-1-yl)-2-benzamidoacetate. Yield: 92%.

2.3. Product characterization data

2.3.1. Methyl 2-azido-2-benzamidoacetate 2

White solid; M.p.: 81 °C; Yield 92%; M.S-E.I: m/z ($C_{10}H_{10}N_4O_3$)=234 [M]; **^{13}C NMR** ($CDCl_3$, δ(ppm)): 167.73, 167.21 ($\underline{C}O$, 2C); 132.90, 132.84, 129.02, 128.03 ($\underline{C}_{arom}$, 6C); 65.64 ($\underline{C}α$, 1C); 53.41 ($\underline{C}H_3$). **^{1}H NMR** ($CDCl_3$, δ(ppm)): 9.8(1H, d, NH, *J*=7.8 Hz); 7.5-7.9 (5H, 3m, $5H_{arom}$); 5.8 (1H, d, Hα, *J*=7.8 Hz); 3.7 (3H, s, CH_3).

2.3.2. Methyl 2-(3-amino-1H-1,2,4-triazol-1-yl)-2-benzamidoacetate 3

White solid;M.p.: 215 °C; M.S-E.I: m/z ($C_{12}H_{13}N_5O_3$)= 275.1013 [M]; **^{13}C NMR** ($CDCl_3$, δ(ppm)):168.15, 165.62, ($\underline{C}O$, 2C); 155.73, 149.86, 133.00, 128.92, 127.36, 106.40 (C_6H_5 aromatic carbons); 60.72 ($\underline{C}α$, 1C); 54.01 ($\underline{C}H_3$). **^{1}H NMR** ($CDCl_3$, δ(ppm)): 7.5–8.1 (7H, 3 m, $1NH_{amid}$ +$1H_{triazol}$+$5H_{arom}$); 6.5 (1H, d, Hα, *J*=7.2 Hz); 5.6 (2H, br s, NH_2); 3.9 (3H, s, CH_3).

2.3.3. Methyl 2-((1H-1,2,4-triazol-3-yl)amino)-2-benzamidoacetate 4

White solid;M.p.: 208 °C; **^{13}C NMR** ($CDCl_3$, δ(ppm)): 171.21, 168.91, ($\underline{C}O$, 2C); 149.79, 146.00, 134.79, 131.90, 128.94, 127.63 (C_6H_5 aromatic carbons); 71.92 ($\underline{C}α$, 1C); 50.90 ($\underline{C}H_3$). **^{1}H NMR** ($CDCl_3$, δ(ppm)): 7.5–8.1 (7H, 3 m, $1NH_{amid}$ +$1H_{triazol}$+$5H_{arom}$); 5.8 (1H, d, Hα, *J*=7.2 Hz); 4.7 (1H, s, NH); 3.9 (3H, s, CH_3).

The signal from the NH proton of the triazole ring is not observed on the spectrum, its value is greater than the 8.3 maximum value on our spectrum.

3. Results and discussion

By continuing our research work on the synthesis of heterocycles (Mabrouk *et al.*, 2010; 2013; 2020); we present in this manuscript our strategy for the preparation of a heterocyclic α-aminoester with three methods.

After the preparation and protection of the methyl ester of glycine according to the reaction (**Fig. 1**), the brominationof the latter is carried out following a radical reaction by N-bromosuccinimide or by dibromine in the presence of α,α'-azo-bis-isobutyronitrile (AIBN) in catalytic quantity, under the irradiating action of a 300 W lamp. The methyl 2-azido-2-benzamidoacetate 2 is obtained by substitution of the bromide nucleofuge by the azide group (**Fig. 1**). Methyl 2-azido-2-benzamidoacetate 2 contains a nucleofuge (azido) which is a good leaving group. The use of 1H-1,2,4-triazole-3-amine which contains two active sites leads to nucleophilic substitution (Achamlal *et al.*, 1997; Steglich *et al.*, 1983). The last step in this synthetic strategy is the nucleophilic substitution of methyl 2-azido-2-benzamidoacetate 2 by 1H-1,2,4-triazole-3-amine according to three modes of activation (**Fig. 1**).

Our estimate was to have two products with the predominance of one over another, but the spectroscopic data (MS, ^{13}C NMR, and ^{1}H NMR) obtained showed the existence of only a single product: 2-(3-amino-1H-1,2,4-triazol-1-yl)-2-benzamidoacetate 3 (**Fig. 2**). In what follows, we will discuss the modes of activation of the synthesis of this product and present our point of view on the regioselectivity of this reaction.

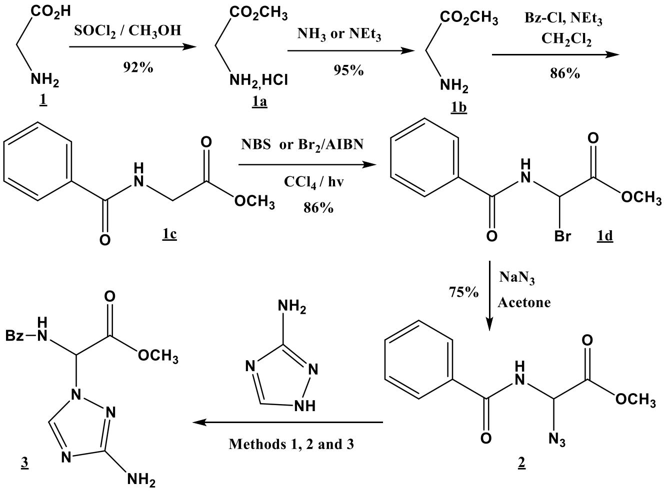

Figure 1. Different steps in the synthesis strategy of 2-(3-amino-1H-1,2,4-triazol-1-yl)-2-benzamidoacetate 3.

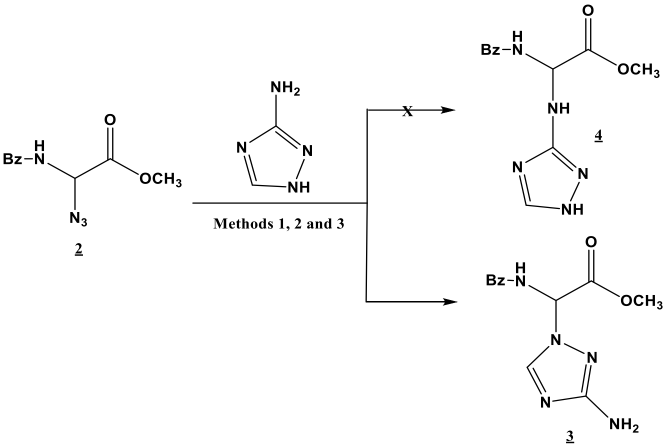

Figure 2. Regioselectivity of the synthesis reaction.

The substitution reaction of methyl 2-azido-2-benzamidoacetate 2 by 1H-1,2,4-triazole-3-amine using the mode of activation in the presence of triethylamine as a base in acetonitrile, leads to 2-(3-amino-1H-1,2,4-triazol-1-yl)-2-benzamidoacetate 3 after five hours at room temperature, with 82% yield (**Fig. 3**). Phase transfer catalysis is another method of activating the synthesis of 2-(3-amino-1H-1,2,4-triazol-1-yl)-2-benzamidoacetate 3 which consists of carrying out the reaction in the DMF, potassium carbonate, and BTBA catalyst for four hours at room temperature. The N-alkylated product 3 is obtained in this case with a yield of 90% (**Fig. 3**).

The procedure by microwave irradiation is selected to compare its effectiveness as the best mode of activation of this reaction to optimize the result of synthesis and the experimental conditions. Indeed, the N-alkylation product 3 is prepared by irradiating a mixture of 1H-1,2,4-triazole-3-amine, methyl 2-azido-2-benzamidoacetate 2, K_2CO_3, and BTBA on silica as support under a power of 500 W for 10 min with 92% (**Fig. 3**).

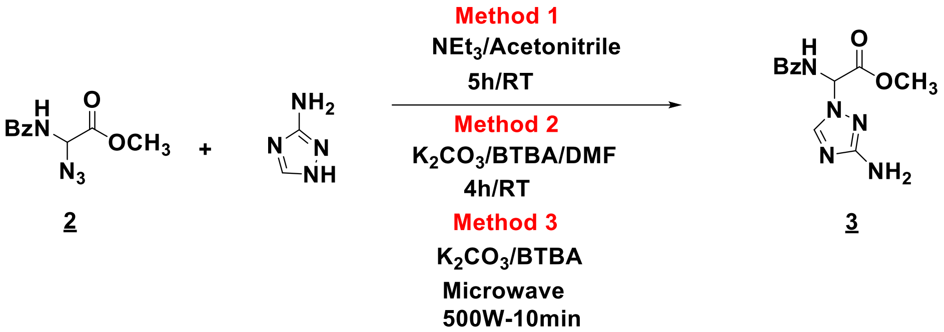

Figure 3. Different methods for activating the 2-(3-amino-1H-1,2,4-triazol-1-yl)-2-benzamidoacetate 3 synthesis reaction.

Based on the different mesomeric forms (**Fig. 4**) and under the mild conditions of this reaction, we see that the NH_2 group is not active and therefore, there will be no N-alkylation through this site. This result is proven experimentally. Under the reaction conditions (use of a base, room temperature), isomer (e) is more stable than isomer (a) (**Fig. 4**).

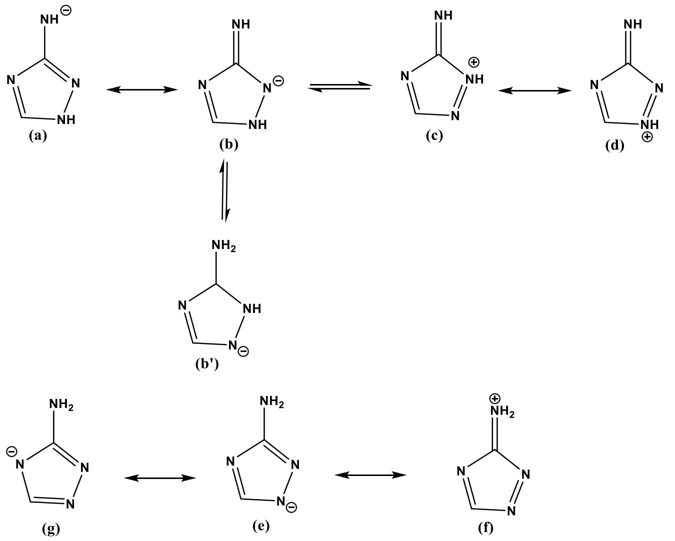

Figure 4. Different mesomeric forms of isomers (a) and (e).

From these observations, it can be concluded that the basicity and nucleophilicity of isomer (e) are greater than that of isomer (a). These results are confirmed by the theoretical study (**Table 1**) and by the Marvinsketch software (**Table 2**). Therefore, the results obtained experimentally coincide well with those obtained theoretically.

We gather the variations of free reaction enthalpy **ΔG_r** characterizing the reactions taking place between methyl 2-azido-2-benzamidoacetate 2 and the isomers (a) and (e) (**Table 1**).

The free enthalpy variations **ΔG_r** of reactions (1) and (2) are negative, therefore these two reactions are possible and favored thermodynamically. The free enthalpy value ΔGr corresponding to reaction (1) is lower than that corresponding to reaction (2). But the reaction with isomer (e) is preferentially favored over the reaction with isomer (a).

According to the optimized structure of the amine used (**Fig. 5**), it can be seen that the proton bound to the N(1) atom is more acidic than that bound to NH_2, which justifies the formation of the anionic form (e) instead of obtaining the form (a).

Table 1. Thermodynamic quantities characterizing the possible reactions between methyl 2-azido-2-benzamidoacetate 2 and isomers (a) and (e) calculated by DFT/B3LYP 6-31G (d, p).

Reactions	ΔGr (Kcal/mol)
(1) from isomer (a)	−30.66
(2) from isomer (e)	−9.72

Table 2. Percentage of the basic form (e) in the range of pH 11-13.5.

Atoms	11	12	12.5	13	13.5
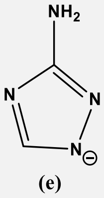 (e)	55.93%	88.53%	95.10%	99.72%	99.99%

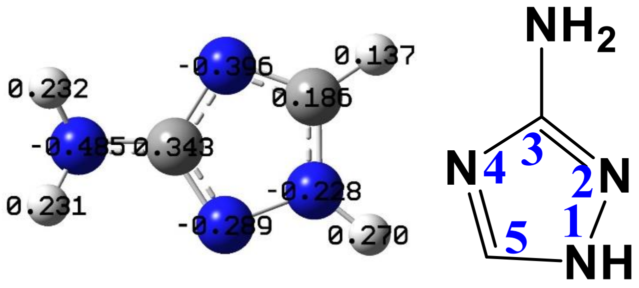

Figure 5. Structure of 1H-1,2,4-triazole-3-amine optimized by DFT/B3LYP/6-31G (d, p).

The Marvinsketch software gives the distribution (%) and the domain of predominance of the acid/base forms of a molecule or an ion according to the pH. The simulation made by the Marvinsketch software shows the existence of a single basic form of 1H-1,2,4-triazole-3-amine in the range of pH 11-13.5 (**Table 2**), which explains the unexpected regioselectivity of the reactivity of the secondary amine relative to the primary amine. The product formed is the result of nucleophilic substitution of the secondary amine.

The selective addition of 1H-1,2,4-triazole-3-amine to azide 2 was difficult due to the presence of several competing nucleophilic centers on 1H-1,2,4-triazole-3-amine. Regioselective addition was found to occur only at the endocyclic **N-1** atom of

1H-1,2,4-triazole-3-amine when the reaction was carried out under kinetic control at room temperature. The increase in temperature can lead to the formation of a thermodynamically more stable compound (Junaid *et al*., 2019). Indeed, the reaction was carried out at reflux by methods 1 and 2 under the same experimental conditions (**Fig. 6**) led to the desired product 4 which is thermodynamically more stable and whose spectroscopic and physicochemical characteristics (melting point, frontal ratio) are different from those of product 3. The yields of these reactions are successively 84.5% and 91.5%.

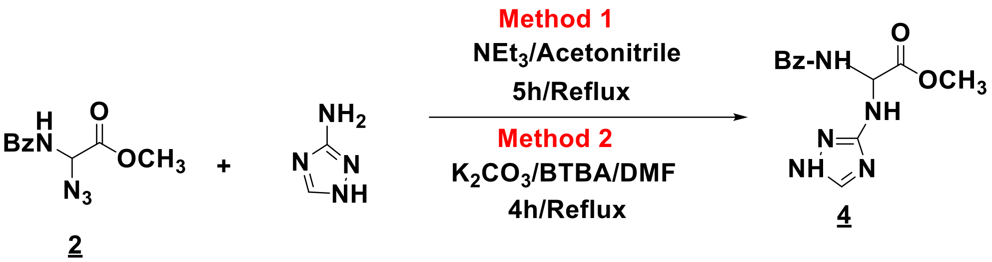

Figure 6. Synthesis of methyl 2-((1H-1,2,4-triazol-3-yl)amino)-2-benzamidoacetate 4 by thermodynamic control.

4. Conclusions

The synthesis of heterocyclic systems is currently an important research axis, not only from the point of view of the fundamental research of heterocycles but also because of the broadening of the practical applications of these compounds. It is necessary to develop new methods and procedures to easily and quickly construct complex heterocyclic molecules from simple precursors.

Triazole and its derivatives represent an important class in the family of heterocycles since these molecules of particular structures are found in important biological building blocks.

The three modes of activation of the synthesis reaction of 2-(3-amino-1H-1,2,4-triazol-1-yl)-2-benzamidoacetate 3 are effective. Microwave irradiation has increasingly become a preferable, economical, and environmental method. The use of computational studies is a new approach to fully understanding the regioselectivity of the reaction and its reaction mechanism. Methyl 2-(3-amino-1H-1,2,4-triazol-1-yl)-2-benzamidoacetate 3 is the product obtained regioselectively by kinetic control. On the other hand, methyl 2-((1H-1,2, 4-triazol-3-yl)amino)-2-benzamidoacetate 4 is the product synthesized by thermodynamic control.

Authors' contributions

Conceptualization: El Houssine Mabrouk; **Data curation**: Mohammed El Mesky; Hicham Zgueni; **Formal Analysis**: El Houssine Mabrouk; Nabil Amri; **Funding acquisition**: Not applicable; **Investigation**: El Houssine Mabrouk; Nabil Amri; Driss Chebabe; **Methodology**: El Houssine Mabrouk; Mohamed Jabha; **Project administration**: El Houssine Mabrouk; Mohamed Azrour; **Resources**: El Houssine Mabrouk; Mohammed El Mesky; Youssef Youssefi; **Software**: Not applicable; **Supervision**: El Houssine Mabrouk; Mohamed Jabha; **Validation**: El Houssine Mabrouk; Nabil Amri; **Visualization**: El Houssine Mabrouk; M'barek Azdouz; Ahmad Oubair; **Writing – original draft**: El Houssine Mabrouk; M'barek Azdouz; **Writing – review & editing**: El Houssine Mabrouk.

Data availability statement

All data sets were generated or analyzed in the current study.

Funding

Not applicable.

Acknowledgments

The authors are grateful to the "Moroccan Association of Theoretical Chemists" (AMCT) for its pertinent help concerning the programs.

Conflict of interest

The authors declare that there is no conflict of interest.

References

Abboud, J.-L. M.; Foces-Foces, C.; Notario, R.; Trifonov, R. E.; Volovodenko, A. P.; Ostrovskii, V. A.; Alkorta, I.; Elguero, J. Basicity of N-H- and N-Methyl-1,2,3-Triazoles in the Gas Phase, in Solution, and in the Solid State – An Experimental and Theoretical Study. *Eur. J. Org. Chem.* **2001**, *2001* (16), 3013–3024. https://doi.org/10.1002/1099-0690(200108)2001:16<3013::AID-EJOC3013>3.0.CO;2-Y

Abdu, T.; Adnan, A. B.; Yimer, S. Screening of some pyrazole derivatives as promising antileishmanial agent. *African Journal of Pharmacy and Pharmacology*. **2017**, *11* (2), 32–37. https://doi.org/10.5897/AJPP2016.4401

Abu-Hashem, A. A.; Gouda, M. A. Synthesis and Antimicrobial Activity of Some Novel Quinoline, Chromene, Pyrazole Derivatives Bearing Triazolopyrimidine Moiety. *Journal of Heterocyclic Chemistry*. **2016**, *54* (2), 850–858. https://doi.org/10.1002/jhet.2645

Achamlal, S.; Elachgar, A.; El Hallaoui, A.; El Hajji, S.; Roumestant, M. L.; Viallefont, Ph. Synthesis of α-Triazolyl α -Amino Acid Derivatives. *Amino Acids.* **1997**, *12* (3–4), 257–263. https://doi.org/10.1007/BF01373006

Albada, B.; Metzler-Nolte, N. Highly Potent Antibacterial Organometallic Peptide Conjugates. *Acc. Chem. Res.* **2017**, *50* (10), 2510–2518. https://doi.org/10.1021/acs.accounts.7b00282

Ansari, A.; Ali, A.; Asif, M.; Shamsuzzaman, S. Review: biologically active pyrazole derivatives. *New Journal of Chemistry*. **2017**, *41* (1), 16–41. https://doi.org/10.1039/C6NJ03181A

Azimi, F.; Azizian, H.; Najafi, M.; Hassanzadeh, F.; Sadeghi-aliabadi, H.; Ghasemi, J. B.; Ali Faramarzi, M.; Mojtabavi, S.; Larijani, B.; Saghaei, L.; Mahdavi, M. Design and Synthesis of Novel Quinazolinone-Pyrazole Derivatives as Potential α-Glucosidase Inhibitors: Structure-Activity Relationship, Molecular Modeling and Kinetic Study. *Bioorganic Chem.* **2021**, *114*, 105127. https://doi.org/10.1016/j.bioorg.2021.105127

Bandgar, B. P.; Gawande, S. S.; Bodade, R. G.; Gawande, N. M.; Khobragade, C. N. Synthesis and biological evaluation of a novel series of pyrazole chalcones as anti-inflammatory, antioxidant and antimicrobial agents. *Bioorg. Med. Chem.* **2009**, *17* (24), 8168–8173. https://doi.org/10.1016/j.bmc.2009.10.035

Banno, Y.; Sasaki, S.; Kamata, M.; Kunitomo, J.; Miyamoto, Y.; Abe, H.; Taya, N.; Oi, S.; Watanabe, M.; Urushibara, T.; Hazama, M.; Niwa, S.; Miyamoto, S.; Horinouchi, A.; Kuroshima, K.; Amano, N.; Matsumoto, S.; S.; Matsunaga, S. Design and synthesis of a novel series of orally active, selective somatostatin receptor 2 agonists for the treatment of type 2 diabetes. *Bioorg. Med. Chem.* **2017**, *25*, 5995–6006. https://doi.org/10.1016/j.bmc.2017.09.031

Boibessot, T.; Bnimlis, D.; Jean, M.; Benfodda, Z.; Meffre, P. Synthesis of a Novel Rhizobitoxine-Like Triazole-Containing Amino Acid. *Synlett.* **2016**, *27*, 2685–2688. https://doi.org/10.1055/s-0036-1588300

Cativiela, C.; Díaz-de-Villegas, M. D. Recent Progress on the Stereoselective Synthesis of Acyclic Quaternary α-Amino Acids. *Tetrahedron Asymmetry.* **2007**, *18* (5), 569–623. https://doi.org/10.1016/j.tetasy.2007.02.003.

Cetin, A.; Bildirici, I. A study on the synthesis and antimicrobial activity of 4-acyl-pyrazoles. *J. Saudi Chem. Soc.* **2018**, *22* (3) 279–296. https://doi.org/10.1016/j.jscs.2016.05.008

Christian, O. E.; Compton, J.; Christian, K. R.; Mooberry, S. L.; Valeriote, F. A.; Crews, P. Using Jasplakinolide to Turn on Pathways That Enable the Isolation of New Chaetoglobosins from Phomospis Asparagi. *J. Nat. Prod.* **2005**, *68* (11), 1592–1597. https://doi.org/10.1021/np050293f

Pelliciari, R.; Raimondo, M.; Marinozzi, M.; Natalini, B.; Costantino, G.; Thomsen, C. *(S)-(+)-2-(3‘*-Carboxybicyclo[1.1.1]pentyl)-glycine, a Structurally New Group I Metabotropic Glutamate Receptor Antagonist. *Journal of Medicinal Chemistry*. **1996**, *39*, 2874-2876. https://doi.org/10.1021/jm960254o

Diculescu, V. C.; Chiorcea-Paquim, A.-M.; Oliveira-Brett, A. M. Applications of a DNA-Electrochemical Biosensor. *Trends Anal. Chem.* **2016**, *79*, 23–36. https://doi.org/10.1016/j.trac.2016.01.019

Dondoni, A.; Massi, A. Design and Synthesis of New Classes of Heterocyclic *C*-Glycoconjugates*and* Carbon-Linked Sugar and Heterocyclic Amino Acids by Asymmetric Multicomponent Reactions (AMCRs). *Acc. Chem. Res.* **2006**, *39*, 451–463. https://doi.org/10.1021/ar068023r

El-Sabbagh, O. I.; Baraka, M. M.; Ibrahim, S. M.; Pannecouque, C.; Andrei, G.; Snoeck, R.; Rashad, A. A. Synthesis and antiviral activity of new pyrazole and thiazole derivatives. *Eur. J. Med. Chem.* **2009**, *44* (9), 3746–3753. https://doi.org/10.1016/j.ejmech.2009.03.038

Faisal, M.; Saeed, A.; Hussain, S.; Dar, P.; Larik, F. A. Recent Developments in Synthetic Chemistry and Biological Activities of Pyrazole Derivatives. *J. Chem. Sci*. **2019**, *131*, 70. https://doi.org/10.1007/s12039-019-1646-1

Graillot, V.; Tomasetig, F.; Cravedi, J.-P.; Audebert, M. Evidence of the in Vitro Genotoxicity of Methyl-Pyrazole Pesticides in Human Cells. *Mutat. Res.* **2012**, *748* (1–2), 8–16. https://doi.org/10.1016/j.mrgentox.2012.05.014

Hughes, R. A.; Moody, C. J. From Amino Acids to Heteroaromatics—Thiopeptide Antibiotics, Nature's Heterocyclic Peptides. *Angew. Chem. Int. Ed.* **2007a**, *46* (42), 7930–7954. https://doi.org/10.1002/anie.200700728

Hughes, R. A.; Moody, C. J. Von Aminosäuren zu Heteroarenen – Thiopeptid-Antibiotika als heterocyclische Peptide aus der Natur. *Angew. Chem*. **2007b**, *119* (42), 8076–8101. https://doi.org/10.1002/ange.200700728

Insuasty, B.; Tigreros, A.; Orozco, F.; Quiroga, J.; Abonia, R.; Nogueras, M.; Sanches, A.; Cobo, J. Synthesis of novel pyrazolic analogs of chalcones and their 3-aryl-4-(3-aryl-4, 5- dihydro-1H-pyrazol-5-yl)-1-phenyl-1H-pyrazole derivatives as potential antitumor agents. *Bioorg. Med. Chem.* **2010**, *18* (14), 4965–4974. https://doi.org/10.1016/j.bmc.2010.06.013

Jorgensen, C. G.; Bräuner-Osborne, H.; Nielsen, B.; Kehler, J.; Clausen, R. P.; Krogsgaard-Larsena, P.; Madsena, U. Novel 5-substituted 1-pyrazolol analogues of ibotenic acid: Synthesis and pharmacology at glutamate receptors.*Bioorg. Med. Chem*. **2007**, *15 (10)*, 3524-3538. https://doi.org/10.1016/j.bmc.2007.02.047

Junaid, A.; Lim, P. L. F.; Zhou, Y. P.; Chui, W. K.; Dolzhenko. A. V. Fused Heterocyclic Systems with an s-Triazine Ring. 34. Development of a Practical Approach for the Synthesis of 5-Aza-iso guanines. *Molecules.* **2019**, *24*, 1453. https://doi.org/10.3390/molecules24081453

Karrouchi, K.; Radi, S.; Ramli, Y.; Taoufik, J.; Mabkhot, Y.; Al-aizari F.; Ansar, M. Synthesis and Pharmacological Activities of Pyrazole Derivatives: A Review. *Molecules.* **2018**, *23* (1), 134. https://doi.org/10.3390/molecules23010134

Khilkovets, A.; Karpenko, Y.; Bigdan, O.; Parchenko, M.; Parchenko, V. Synthetic and biological aspects of studying the properties of 1,2,4-triazole derivatives. *Scientific Journal of Polonia University.* **2022**, *51* (2), 324–331. https://doi.org/10.23856/5138

Knorr, L. Einwirkung von Acetessigester Auf Phenylhydrazin. *Berichte Dtsch. Chem. Ges*. **1883**, *16* (2), 2597–2599. https://doi.org/10.1002/cber.188301602194

Kumar, V.; Kaur, K.; Gupta, G. K.; Sharma, A. K. Pyrazole Containing Natural Products: Synthetic Preview and Biological Significance. *Eur. J. Med. Chem*. **2013**, *69*, 735–753. https://doi.org/10.1016/j.ejmech.2013.08.053

Mabrouk, E. H.; Elachqar, A.; El Hallaoui, A.; Alami, A. Synthesis of New Racemic α,α-Diaminocarboxylic Ester Derivatives. *Molecules.* **2010**, *13*, 9354-9363. https://doi.org/10.3390/molecules15129354

Mabrouk, E. H.; Elachqar, A.; El Hallaoui, A.; Alami, A.; El Hajji, S.; Martinez, J.; Rolland, V. Synthesis of new racemic α-heterocyclic α, α-diamino esters and α-aminoester carboxylic. *Arabian Journal of Chemistry.* **2013**, *6*, 93–96. https://doi.org/10.1016/j.arabjc.2010.09.023

Mabrouk, E. H.; Arrousse, N.; Korchi, A.; Lachgar, M.; Oubair, A.; Elachqar, A.; Jabha, M.; Lachkar, M.; El hajjaji, F.; Rais, Z.; Taleb, M. Intelligence Way from Eco-friendly Synthesis Strategy of New Heterocyclic Pyrazolic Carboxylic α-Amino Esters. *Chem. Res. Chinese Universities.* **2020**, *6*, 1–7. https://doi.org/10.1007/s40242-020-0173-4

Nájera, C.; Sansano, J. M. Catalytic Asymmetric Synthesis of Alpha-Amino Acids. *Chem. Rev.* **2007**, *107* (11), 4584–4671. https://doi.org/10.1021/cr050580o

Ngo, J. T.; Tirrell, D. A. Noncanonical Amino Acids in the Interrogation of Cellular Protein Synthesis. *Acc. Chem. Res*. **2011**, *44* (9), 677–685. https://doi.org/10.1021/ar200144y

Ouyang, G.; Cai, X.J.; Chen, Z.; Song, B.A.; Bhadury, P.S.; Yang, S.; Zeng, S. Synthesis and antiviral activities of pyrazole derivatives containing an oxime moiety. *J. Agric. Food. Chem.* **2008**, *56* (21) 10160–10167. https://doi.org/10.1016/j.bmc.2008.09.070

Ozdemir, A.; Altıntop, M.D.; Kaplancıklı, Z.A.; Can, O.D.; Demir Ozkay, U.; Turan- Zitouni, G. Synthesis and evaluation of new 1, 5-diaryl-3-[4-(methyl-sulfonyl) phenyl]- 4, 5-dihydro-1h-pyrazole derivatives as potential antidepressant agents. *Molecules.* **2015**, *20* (2), 2668–2684. https://doi.org/10.1002/ardp.201200479

Perez-Fernandez, R.; Goya, P.; Elguero, J. A review of recent progress (2002–2012) on the biological activities of pyrazoles, Arkivoc: Onl. *J. Org. Chem.* **2014,** *2013*, 233–293. https://doi.org/10.3998/ark.5550190.p008.131

Radi, S.; El Massaoudi, M.; Bacquet, M.; Degoutin, S.; Adarsh, N.N.; Robeyns, K.; Garcia, Y. A novel environment-friendly hybrid material based on a modified silica gel with a bis pyrazole derivative for the removal of Zn II, Pb II, Cd II, and Cu II traces from aqueous solutions. *Inorg. Chem. Front*. **2017**, *4* (11) 1821–1831. https://doi.org/10.1039/C7QI00322F

Ramesh, B.; Bhalgat, C. M. Novel dihydropyrimidines, and its pyrazole derivatives: synthesis and pharmacological screening. *Eur. J. Med. Chem*. **2011**, *46* (5), 1882–1891. https://doi.org/10.1016/j.ejmech.2011.02.052

Ramirez-Prada, J.; Robledo, S. M.; Velez, I. D.; del Pilar Crespo, M.; Quiroga, J.; Abonia, R.; Insuasty, B. Synthesis of novel quinoline-based 4,5-dihydro-1H-pyrazoles as potential anticancer, antifungal, antibacterial and antiprotozoal agents. *Eur. J. Med. Chem*. **2017**, *131,* 237–254. https://doi.org/10.1016/j.ejmech.2017.03.016

Rhazi, Y.; Chalkha, M.; Nakkabi, A.; Hammoudan, I.; Akhzazane, M.; Bakhouch, M.; Chtita, S.; El Yazidi, M. Novel Quinazolinone–Isoxazoline Hybrids: Synthesis, Spectroscopic Characterization, and DFT Mechanistic Study. *Chemistry*. **2022**, *4*, 969–982. https://doi.org/10.3390/chemistry4030066

Risseeuw, M.; Overhand, M.; Fleet, G. W. J.; Simone, M. I. A Compendium of Cyclic Sugar Amino Acids and Their Carbocyclic and Heterocyclic Nitrogen Analogues. *Amino Acids.* **2013**, *45* (4), 613–689. https://doi.org/10.1007/s00726-013-1521-1

Schenk, S. U.; Werner, D. β-(3-isoxazolin-5-on-2-yl)-alanine from Pisum: Allelopathic properties and antimycotic bioassay - ScienceDirect. *Photochemistry*. **1991**, *30*, 467–470. https://doi.org/10.1016/0031-9422(91)83706-Q

Shilpy, A.; Deepika, P.; Dhirender, K.; Girish, K. G.; Ajay, K. Combinatorial Chemistry & HighThroughput Screening. **2018**, *21*,194–203.

Stanley, N. J.; Hutchinson, M. R.; Kvist, T.; Nielsen, B.; Mathiesen, J. M.; Bräuner-Osborne, H.; Avery, T. D.; Tiekink, E. R. T.; Pedersen, D. S.; Irvine, R. J.; Abell, A. D.; Taylor, D. K. A New Metabotropic Glutamate Receptor Agonist with in Vivo Anti-Allodynic Activity. *Bioorg. Med. Chem*. **2010**, *18* (16), 6089–6098. https://doi.org/10.1016/j.bmc.2010.06.051

Steglich, W.; Kober, R. Untersuchungen zur Reaktion von Acylaminobrommalonestern und Acylaminobromessigestern mit Trialkylphosphiten-eine einfache Synthese von 2-Amino-2-(diethoxyphosphoryl)Essigsäure Ethylester. *Liebigs Ann Chem*. **1983**, *4*, 599–609. https://doi.org/10.1002/jlac.198319830409

Thirumurugan, P.; Matosiuk, D.; Jozwiak, K. Click Chemistry for Drug Development and Diverse Chemical-Biology Applications. *Chem. Rev*. **2013**, *113* (7), 4905–4979. https://doi.org/10.1021/cr200409f

Vogt, H.; Brse, S. Recent approaches towards the asymmetric synthesis of α,α-disubstituted α-amino acids. *Org. Biomol. Chem*. **2007**, *5*, 406–430. https://doi.org/10.1039/B611091F

Zarrouk, A.; Zarrok, H.; Salghi, R.; Bouroumane, N.; Hammouti, B.; Al-Deyab, S. S.; Ebn Touhami, M.; Bouachrine, M.; Oudda, H.; Boukhris, S. The Adsorption and Corrosion Inhibition of 2-[Bis-(3,5-dimethyl-pyrazol-1-ylmethyl)- amino]-pentanedioic Acid on Carbon Steel Corrosion in 1.0 m HCl. *Int J Electrochem. Sci.* **2012**, *8* (9), 10215–10232. https://doi.org/10.1016/S1452-3981(23)13198-1

ECLÉTICA QUÍMICA

Eclet. Quim. 49 | e-1504, 2024

Original Article, Education in Chemistry and Correlated Areas

https://doi.org/10.26850/1678-4618.eq.v49.2024.e1504

The concept of chemistry laboratory in high school

Fatma **Alkan**[1+]

Abstract

This research aims to determine the cognitive structures of high school students in the "chemistry laboratory" and to reveal their alternative concepts using the independent word association test and the drawing-writing technique. The sample of the study consists of 60 high school students. Content analysis was used to evaluate the data obtained from the sample group. The codes from the data were brought together and categories were created. In the analysis of the data, sentences and drawings obtained from the writing and drawing techniques were also evaluated separately. When students' answer words are analyzed, it is seen that the concepts related to chemistry laboratory are Laboratory equipment (f:99), Chemical agent (f:41), Protective materials (f:29), Jobs (f:15), Operations in the laboratory (f:49) and Chemistry concepts (f:53). It was determined that the cognitive structures of high school students towards the concept of chemistry laboratory were related to laboratory equipment, chemical agent, protective materials, jobs, operations in the laboratory, chemistry concepts named six categories.

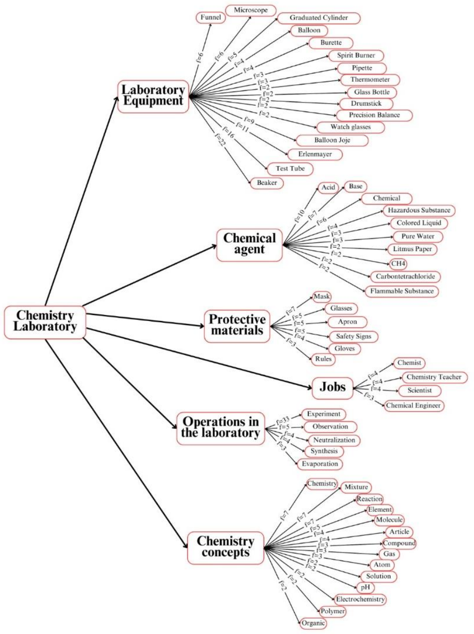

Article History

Received July 17, 2023
Accepted September 03, 2024
Published December 29, 2024

Keywords

1. chemistry laboratory;
2. high school students;
3. word association test;
4. cognitive structures;
5. chemistry.

Section Editors

Natany Dayani de Souza Assai

Highlights

- Definition of the chemistry laboratory as an area of discovery.
- The laboratory is important for chemistry.
- Chemistry laboratories foster safety awareness.

[1]Hacettepe University, Faculty of Education, Ankara, Turkey. **+Corresponding author:** Fatma Alkan, **Phone:** +903122976787, **Email address:** alkanf@hacettepe.edu.tr

1. Introduction

Experimental applications in science are closely related to practical studies, namely laboratories (Gray, 2014). It is known by everyone that laboratories are a natural feature of school science (Wei and Liu 2018; Wellington and Ireson 2012). It would be more effective to describe the relationship of laboratories with science at school as follows, just as cooking belongs to the kitchen or gardening belongs to the garden, science learning manifests itself with metaphors that it belongs to the science laboratory (Hofstein *et al.*, 2013).

It is also accepted by many authors in the literature that laboratory teaching, in which students experiment in the laboratory, is the most basic and essential component of science courses (Hofstein and Lunetta, 1982; Hofstein and Lunetta, 2004; Johnstone and Al-Shuaili, 2001; Reid and Shah, 2007; White, 1996). Improving students' understanding of science, understanding the nature of science, creating scientific events in the mind, practical skills, problem solving, interest and motivation are reported as the goals of laboratory teaching (Hofstein and Lunetta, 2004).

In the studies aimed at the objectives of the chemistry laboratory, for example, the objectives of the general chemistry laboratory such as being interested in science, having laboratory techniques and skills, developing critical thinking skills, establishing a connection between the course content and the laboratory, and creating collaborative group work skills are revealed (Bruck *et al.*, 2010). The goals of the chemistry laboratory are seen as the realization of meaningful learning by focusing on cognitive, affective and psychomotor areas. Bretz *et al.* (2013) examined cognitive, affective and psychomotor goals in detail in their study. Cognitive goals are thought to be establishing a connection between the course and laboratory work, establishing a connection between the laboratory and daily life, emphasizing the laboratory and providing conceptual understanding, linking the laboratory content between mathematics and other sciences, and adapting critical analysis. Affective goals included establishing relationships between the real world and the laboratory, developing the ability to work independently and collaborating. Among the psychomotor goals are learning to use laboratory equipment and laboratory techniques.

Experimenting in the laboratory is related to the goals set in the affective field. For example, finishing the experiment quickly and late, or getting good grades from the test result or making a mistake and sharing it with the lecturer (DeKorver and Towns, 2015). It has been determined that students follow some steps without thinking or understanding while doing experiments in the laboratory. It has been revealed that students have difficulties in self-control in laboratory lessons. As a result, it is not possible to establish a connection between the operations performed in the experiment and theoretical knowledge. Students only focus on experimental procedures and aim to finish the experiment without understanding it (Galloway and Bretz, 2016). In developing students' reasoning and argumentation levels, it is very important to think deeply about the evidence obtained from experiments and to realize how to use the experimental results. For this reason, it is of great importance to conduct experiments in chemistry lessons at all levels of education (Uzuntiryaki-Kondakci *et al.*, 2021). Laboratory applications and task-based activities enable students to develop different skills such as self-assessment (Wu *et al.*, 2023). Starting from teacher candidates, teachers should focus on the importance of chemistry and teaching intellectual processes to ensure sustainability. Teachers trained in this subject can ensure that their students in their classes go through the same process (Delaney *et al.*, 2021). Focusing on student-centered practices in chemistry teaching not only increases students' academic success, but also increases their belief that they can manage their own learning process and improves their motivation (Cascolan, 2023). The knowledge that students have about the laboratory also sheds light on how laboratory teaching should be planned. The selection of materials used in daily life is very important in experiments to be carried out in the laboratory (Hakim *et al.*, 2022). Reconciling chemistry with daily life positively affects students' participation and motivation in class (Mustafaoğlu and Yücel, 2022a). Determining students' concepts about the laboratory actually reveals what they know and do not know about chemistry subjects. In this way, it is clarified what to do when planning the lecture, what difficulties to choose when choosing experiments on the subject, and what to pay attention to regarding safety when conducting experiments (Triayuni *et al.*, 2023). The knowledge level of high school students about chemistry and chemicals is revealed very effectively with the word association test. Students have a lot of fun while using this application, and it also enables them to write realistic expressions (Alkan *et al.*, 2021). Based on these laboratory data, it is necessary to determine the cognitive structures of the students for the chemistry laboratory. This research was carried out to determine the cognitive structures of high school students about "chemistry laboratory" and to reveal their alternative concepts by using the independent word association test and the drawing-writing technique. In this way, the cognitive structures of the students for the chemistry laboratory will be determined and the points to be considered in laboratory teaching will be emphasized.

2. Experimental

2.1. Research design

Phenomenological methods explain the phenomena that are known but do not have a detailed understanding. In this study, the phenomenography method, one of the qualitative research methods, was used. We cannot think that we fully comprehend the phenomena such as events, experiences, perceptions and concepts that we encounter in various forms in our lives. The phenomenology method is used to investigate the phenomena whose meaning we cannot fully comprehend (Yıldırım and Şimşek, 2006). In this study, the cognitive structures of high school students regarding the concept of chemistry laboratory was examined with the independent word association test.

2.2. Participants

The sample of the study consists of 60 high school students studying in Turkey. The sample of the study was determined by a purposive sampling method. Purposive sampling is a widely used technique in qualitative research. This technique is preferred in identifying and selecting rich situations to use limited resources effectively (Patton, 2002). Purposeful sampling is a sample selection method used to select samples depending on the purposes of the research to be conducted (Fraenkel *et al.*, 2012). High school students who took chemistry courses in high school were included in the sample group. Students were informed about the study. Participant consent was obtained from the students who wanted to participate in the study. Initially, the study started with 72 high school students. Twelve students (n=12) were excluded from the study because they did not continue later. High school students filled out a voluntary participation form before participating in the research. Table 1 shows the demographic information of the research sample group.

Table 1. Demographic details and characteristics of sampling.

Categories		f	%
Gender	Female	26	43.3
	Male	34	56.7
Grade	9th class	5	8.33
	10th class	6	10
	11th class	6	10
	12th class	43	71.7
Total		**60**	**100**

The sample of the study consists of 60 high school students. 26 females (43.3%), 34 males (56.7%). The distribution of students by grades is 5 students in 9th grade, 6 students in 10th grade, 6 students in 11th grade and 43 students in 12th grade.

2.3. Instrumentation

The word association test (WAT) was used as a data collection tool in the research. It was aimed to collect detailed data in order to reveal the cognitive structure of the sample group regarding the concept of "chemistry laboratory". While applying for the word association test, the points that the students would probably have difficulty were explained. In addition, sufficient time was given to the students. The word association test was administered to 72 high school students. Of these, 60 were evaluated. While evaluating the obtained data; first the concepts that come to mind of the students about the concept of "chemistry laboratory" were categorized and the counting method was used. Figure 1 shows the word association test.

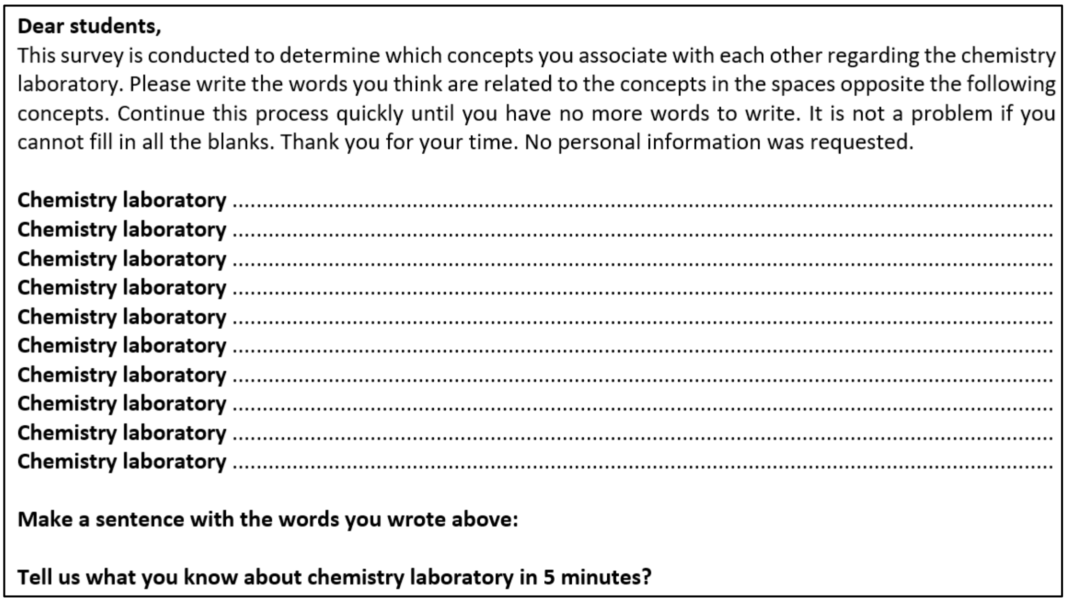

Dear students,
This survey is conducted to determine which concepts you associate with each other regarding the chemistry laboratory. Please write the words you think are related to the concepts in the spaces opposite the following concepts. Continue this process quickly until you have no more words to write. It is not a problem if you cannot fill in all the blanks. Thank you for your time. No personal information was requested.

Chemistry laboratory ....
Chemistry laboratory ....
Chemistry laboratory ....
Chemistry laboratory ....
Chemistry laboratory ....
Chemistry laboratory ....
Chemistry laboratory ....
Chemistry laboratory ....
Chemistry laboratory ....
Chemistry laboratory ....

Make a sentence with the words you wrote above:

Tell us what you know about chemistry laboratory in 5 minutes?

Figure 1. Word association test for chemistry laboratory keyword.

2.4. Data analysis

As a result of the word association test, the evaluation of the data obtained from the sample group for the key concept of "chemistry laboratory" was carried out with the content analysis method. Categories were created by establishing a relationship between the answer words for the chemistry laboratory, which is the key concept. Words that are repeated only once and that are not relevant were not taken into consideration. The answer words of the students were first examined by the researchers within the framework of relevance to the subject, and some of them were excluded. In the content analysis, the frequencies of the words in the categories were also calculated. Sentences and drawings obtained from the writing and drawing techniques of the word association test were also analyzed. Answer words, writing and drawing technique data analysis and students' views on the key concept were examined in depth (Rennie and Jarvis, 1995). The results were analyzed by considering the categories created according to the key concept. Content analysis is done to reach the concepts that will explain the data and to reveal the relationships between these concepts (Yıldırım and Şimşek, 2006). First of all, the data should be divided into categories, upper and lower classifications should be made and supported with numerical data (Sönmez and Alacapınar, 2011). Then, the codes emerging from the data are brought together and categories are created (Cresswell, 2018). In the analysis of the data obtained from WAT, the number of repeated words is examined in the first place, then the connection between the words is created. For this, the semantic relationship technique is used (Atasoy, 2004).

3. Results and discussion

3.1. Findings obtained from the Word Association test

In the study, high school students' perceptions of the chemistry laboratory were examined with the word association test. According to WAT, 302 answer words were collected from 60 students. In the data analysis, 16 words (5.30%) were excluded due to reasons such as not being relevant or being repeated once (Kostova and Radoynovska, 2010; Kurt, 2013). 286 answer words were examined, it was determined that they consisted of 55 repetitive words and were grouped under 6 categories. Table 2 provides details.

Table 2. Distribution of cognitive structure obtained by the word association test related to the concept of "chemistry laboratory" by categories.

Categories	Concepts and frequencies		f
Laboratory equipment	Beaker (22)	Burette (4)	99
	Test Tube (16)	Spirit burner (3)	
	Erlenmayer (11)	Pipette (3)	
	Balloon Joje (9)	Thermometer (2)	
	Funnel (6)	Glass Bottle (2)	
	Microscope (6)	Drumstick (2)	
	Graduated Cylinder (5)	Precision Balance (2)	
	Balloon (4)	Watch glasses (2)	
Chemical agent	Acid (10)	pure water (3)	41
	Base (7)	litmus paper (2)	
	Chemical (6)	CH4 (2)	
	Hazardous substance (4)	Carbontetrachloride (2)	
	Colored liquid (3)	flammable substance (2)	
Protective materials	Mask (7)	Safety signs (5)	29
	Glasses (5)	Gloves (4)	
	Apron (5)	Rules (3)	
Jobs	Chemist (4)	scientist (4)	15
	Chemistry teacher (4)	chemical engineer (3)	
Operations in the laboratory	Experiment (33)	Synthesis (4)	49
	Observation (5)	Evaporation (3)	
	Neutralization (4)		
Chemistry concepts	Chemistry (7)	Gas (3)	53
	Mixture (7)	Atom (3)	
	Reaction (7)	Solution (2)	
	Element (5)	pH (2)	
	molecule (4)	Electrochemistry (2)	
	Article (4)	Polymer (2)	
	Compound (3)	Organic (2)	
Total	**55 words**		**286**

The first category is the "Laboratory equipment" category. The frequency of this category, which consists of 16 answer words, is 99. In the category of laboratory equipment, students are Beaker (22), test tube (16), Erlenmayer (11), balloon Joje (9), funnel (6), microscope (6), graduated cylinder (5), glass balloon (4), burette (4), spirit cooker (3), pipette (3), thermometer (2), glass bottle (2), baguette (2), precision balance (2), and watch glass (2).

The second category is "Chemical agent" and the frequency of 10 answer words is 41. In the chemical agent category, acid (10), base (7), chemical (6), hazardous substance (4), colored liquid (3), pure water (3), Litmus paper (2), CH_4 (2), carbon tetrachloride (2), flammable substance (2).

The third category "Protective materials" is represented by 6 answer words and its frequency is 29. Answer words; mask (7), goggles (5), apron (5), safety signs (5), gloves (4), rules (3).

The fourth category "Jobs" is 15 in frequency with 4 answer words. In this category chemist (4), chemistry teacher (4), scientist (4), chemical engineer (3)

The fifth category, "Operations in the laboratory", consists of 5 answer words, while the frequency is 49. In this category, experiment (33), observation (5), neutralization (4), synthesis (4), evaporation (3) are seen as the answer words.

The sixth and final category is "Chemistry concepts" The frequency of 14 response words is 53. Sixth category chemistry (7), mixture (7), reaction (7), element (5), molecule (4), substance (4), compound (3), gas (3), atom (3), solution (2), pH (2), electrochemistry (2), polymer (2), organic (2).

In order to better understand the cognitive structure model that emerged based on the findings obtained as a result of the word correlation test related to the chemistry laboratory concept of the students, the categories and the words representing the category were created by creating a figure. Cognitive structure model was shown in **Fig. 2**.

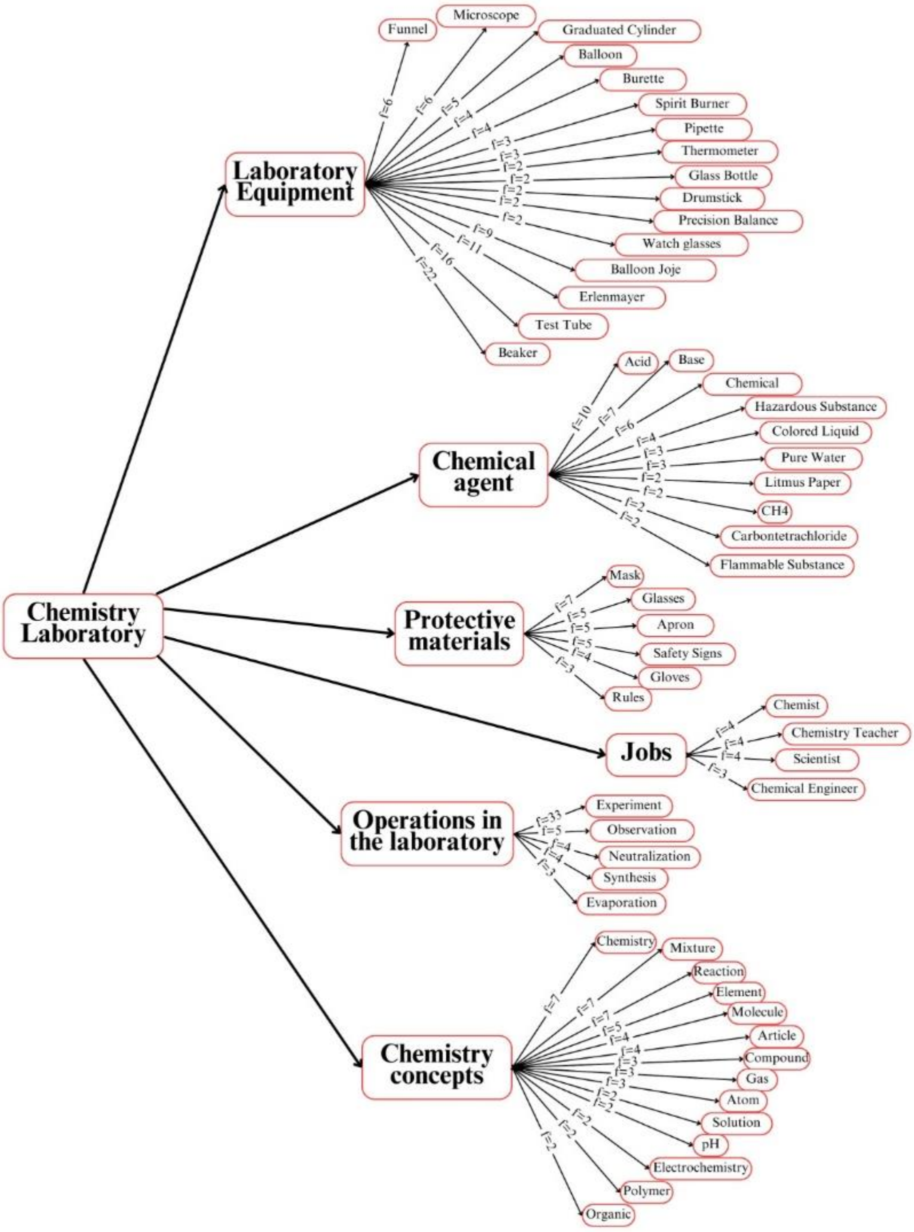

Figure 2. Cognitive structure for the concept of chemistry laboratory.

3.2. Findings from the writing-drawing technique

Students were asked to form sentences at the end of the word association test for the concept of chemistry laboratory. In WAT, students' writing technique sentences were also evaluated. The frequencies of the sentences written by the students were analyzed in the determined categories. In **Table 3**, the frequencies of the sentences written by the students for the concept of chemistry laboratory are given.

Table 3. WAT writing technique distribution of sentences by categories and frequencies.

Categories	f
Laboratory equipment	16
Chemical agent	2
Protective materials	10
Jobs	3
Operations in the laboratory	19
Chemistry concepts	10
Total	**60**

When the table is examined, it is seen that the highest frequency value is in the category of "operations performed in the laboratory" (f: 19). Examples of sentences belonging to this category are given below. Next to the sentence examples, the numbers represent the codes given to the students.

S29: Acid, the amounts of which we determined with the help of graduated cylinder, and with the help of some of our chemistry teachers, we reacted in a glass container so that salt and water were released. This reaction is called the neutralization process.

S23: New substances are synthesized as a result of the reaction that takes place in the beaker with acid and base.

S24: Acids and bases react chemically to form salt and water.

S17: In the neutralization reaction, acid and base react to form water and salt water, which is an ionic compound.

The second-high frequency value is in the category of "Laboratory materials" (f: 16). Examples of sentences for this category are as follows.

S5: Materials such as beaker, flask, test tube, separating funnel, graduated cylinder are indispensable materials for experimentation in the chemistry laboratory.
S9: These instruments, which are sensitive glasses, are used for experimentation. For example, a straw is used to transfer a substance from one container to another container.
S25: We used a separating funnel to separate the liquids that we mixed accidentally.
S56: Beaker is used in some evaporation reactions.

It is seen that the frequency value of the "Protective materials" category is (f: 10). Below are examples of sentences that describe this category.

S47: We conducted experiments on acids and bases in the chemistry laboratory and learned information about flammable and combustible materials.
S45: We should be careful while doing experiments.
S28: When we are going to do an experiment in the laboratory; we must obey the laboratory rules by wearing glasses, gloves and aprons.
S7: Protective materials such as goggles, masks, etc.

While the frequency value of the category "Chemistry concepts" is (f: 6), examples of sentences explaining this category are below.

S34: Chemistry from alchemy; examines the structure and properties of atoms, elements or compounds.
S46: Organic is a difficult subject.
S57: I wrote the first words that came to my mind and these words explain chemistry to me. In chemistry, if there is no matter or element, there can be no combination, and without it, experiments cannot be done, and new information cannot be reached.

While the frequency value of the "Occupations" category is (f: 3), examples of sentences explaining this category are below.

S55: When I say a science laboratory, I think of it as being free. People working in the laboratory need to be passionate and passionate about their work. After all, you may fail because of an experiment you've been working on for years, and you have to be excited for science to continue.
S33: The chemist did an experiment using gloves, beakers and microscope.

While the frequency value of the "Chemicals" category is (f: 2), examples of sentences explaining this category are below.

S13: There may be abrasive substances in homogeneous mixtures placed in capsules in chemistry experiments.
S41: The list of words that come to mind when I think of the laboratory are chemicals.

3.3. Findings obtained by drawing-writing technique

Students made 57 drawings in the word association test. Eight of them were not included in the study due to reasons such as not being related to the subject, and the drawings made by 49 students were examined according to categories. The findings obtained are summarized in Table 4.

Table 4. Distribution of results obtained by drawing technique related to the concept of chemistry laboratory according to categories frequencies and drawing examples.

Categories	Drawing (f)	Drawing examples
Equipment and materials	22	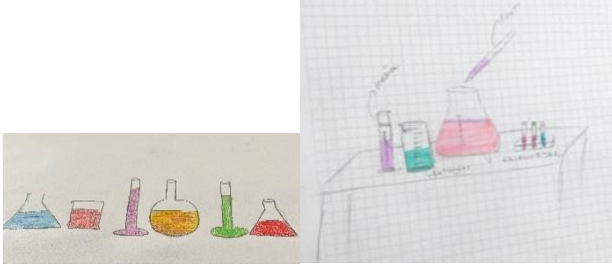
The experimental setup	27	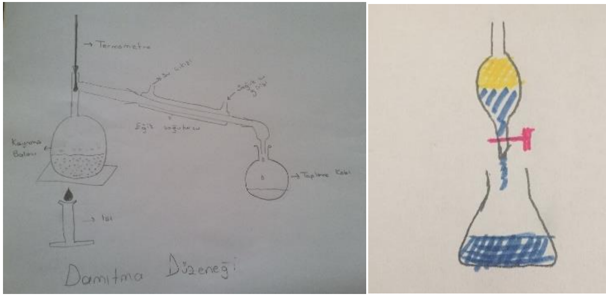

When Table 4 is examined, it is noted that the category with the highest frequency in student drawings is the experimental setup category (f:27), while the second place is the category of tools-equipment and materials (f:22). Categories and drawing examples are also included in the table.

This research was conducted to reveal the cognitive structures of high school students regarding the concept of "chemistry laboratory" through the independent word association test. When WAT answer words are examined, it is noticed that the variety of concepts is high (f:286). When the answer words of the students were analyzed, it was determined that the concepts related to the chemistry laboratory were gathered in 6 categories: Laboratory equipment, chemical agent, protective materials, jobs, operations in the laboratory, and chemistry concepts. It is the category of "laboratory equipment" with the highest frequency (f: 99). The frequency of the chemical agent category is 41. The protective materials category is 29, the Jobs category is 15, the operations in the laboratory category is 49, and the chemistry concepts category is 53.

Chemistry is an experimental science. Experimentation is the most important requirement to become an expert in this field. It is unacceptable that traditional laboratory programs have too little content to provide training for the development of this skill (Pickering, 1984). In chemistry, experiments carried out in the laboratory and the results obtained should be an important component of course evaluation, otherwise failure will occur (Wilson, 1987). Traditional teaching produces learning characterized by superficial and superficial memorization. Students do not forget very little of what they have learned, and they have difficulty in applying this information they have not forgotten (Saint-Jean, 1994).

Chemistry, which is described as a difficult science among young people, is also seen as challenging, difficult and boring. The reason for this belief, which is accepted by the students, may be abstract topics such as the structure of the atom or chemical bonds in chemistry. It is difficult to visualize how these issues came to be. Elimination of this prejudice of students about chemistry will be possible with laboratory practices and activities (Mujtaba *et al*., 2020; Rüschenpöhler and Markic, 2020). Chemistry laboratory practices should be used to emphasize the experimental nature of chemistry (Wilson, 1987). For this reason, the concept of chemistry laboratory has great importance at every level of education.

Teaching multiple representations can be used to develop the cognitive structure of chemistry (Derman and Ebenezer, 2020). Molecular geometry, chemical calculation and reaction balancing are seen as the most difficult topics (Fitriyana *et al*., 2023). Revealing the relationship between chemistry and daily life in the high school chemistry curriculum will make it easier for teachers to teach the lesson (Mustafaoğlu and Yücel, 2022b) and will support students in reducing their prejudices and concerns about chemistry (Altundağ and Yücel, 2022). Before starting a chemistry course in high school, students' perceptions of chemistry should be determined and course contents should be arranged according to these perceptions (Altundağ *et al*., 2022). With appropriate teaching methods, it was determined that there was an increase in the number of response words and the connections between them in the word association test on a specific subject such as saponification (Baptista, 2019). In terms of chemistry laboratory concepts, the most repeated category by students is the materials used in the laboratory. Next come the concepts of chemistry and operations in the laboratory. From this point of view, it is revealed that laboratory-related applications should be given more space while planning the chemistry curriculum.

4. Conclusions

The research shows that 286 meaningful words obtained from sixty students are interested in the chemistry laboratory of high school students. By benefiting from this interest, chemistry laboratory applications should be given more place for students to love and understand chemistry. Especially high school level is an education level where prejudices can be eliminated before starting university education. In high school, students should do more experiments in the lessons and enter the chemistry laboratory. In this way, meaningful learning will be realized by realizing the concrete applications of the abstract concepts of chemistry.

Data availability statement

The data will be available upon request.

Funding

Not applicable.

Acknowledgments

I would like to thank all the students who volunteered to contribute to the data collection process for the research.

Conflict of interest

The authors declare that there is no conflict of interest.

References

Alkan, F.; Dinçdemir, D.; Yücel, A. S. Examining high school students' cognitive structures on the concept of cleaning agent through word association test. *J. Penelitian dan Pembelajaran IPA*. **2021**, *7* (2), 134–151. https://doi.org/10.30870/jppi.v7i2.12058

Altundağ, C. K.; Mustafaoğlu, F. T.; Yücel, A. S. Developing a scale: Perceptions of high school students about the relationship between chemistry and daily life. *J. Ilmiah Peuradeun*. **2022**, *10* (3), 721–746. https://doi.org/10.26811/peuradeun.v10i3.718

Altundağ, C.; Yücel, A. S. Development of an anxiety scale for chemistry. *J. Educ. Teach. Train.* **2022**, *13* (1), 1–8. https://doi.org/10.47750/jett.2022.13.01.001

Atasoy, B. *Science Learning and Teaching*. Ankara: Asil Publishing, 2004.

Baptista, M.; Martins, I.; Conceição, T.; Reis, P. Multiple representations in the development of students' cognitive structures about the saponification reaction. *Chem. Educ. Res. Pract.* **2019**, *20*, 760–771. https://doi.org/10.1039/C9RP00018F

Bretz, S.; Fay, M.; Bruck, L. B.; Towns M. H. What faculty interviews reveal about meaningful learning in the undergraduate laboratory. *J. Chem. Educ.* **2013**, *90* (3), 5–7. https://doi.org/10.1021/ed300384r

Bruck, L. B.; Bretz, S. L.; Towns, M. Faculty perspectives of undergraduate chemistry laboratory: goals and obstacles to success. *J. Chem. Educ.* **2010**, *87* (12), 1416–1424. https://doi.org/10.1021/ed900002d

Cascolan, H. M. S. Exploring students' academic performance, motivational orientation and self-regulated learning strategies towards chemistry. *Int. J. STEM Educ. Sustain.* **2023**, *3* (2), 225–239. https://doi.org/10.53889/ijses.v3i2.215

Cresswell, J. W. *Qualitative Research Methods*. Ankara: Siyasal Publishing, 2018.

DeKorver, B. K.; Towns, M. H. General chemistry students' goals for chemistry laboratory coursework. *J. Chem. Educ.* **2015**, *92* (12), 2031–2037. https://doi.org/10.1021/acs.jchemed.5b00463

Delaney, S.; Ferguson, J. P.; Schultz, M. Exploring opportunities to incorporate systems thinking into secondary and tertiary chemistry education through practitioner perspectives. *Int. J. Sci. Educ.* **2021**, *43* (16), 2618–2639. https://doi.org/10.1080/09500693.2021.1980631

Derman, A.; Ebenezer, J. The effect of multiple representations of physical and chemical changes on the development of primary pre-service teachers' cognitive structures. *Res. Sci. Educ.* **2020**, *50*, 1575–1601. https://doi.org/10.1007/s11165-018-9744-5

Fitriyana, N.; Pratomo, H.; Wiyarsi, A.; Marfuatun. In-service high school chemistry teachers' view towards chemistry: Is it a difficult subject? *AIP Conf. Proc.* **2023**, *2556* (1) 040016. https://doi.org/10.1063/5.0109916

Fraenkel, J. R.; Wallen, N. E.; Hyun, H. H. *How to design and evaluate research in education*. New York: McGraw Hill, 2012.

Galloway, K. R.; Bretz, S. L. Video episodes and action cameras in the undergraduate chemistry laboratory: Eliciting student perceptions of meaningful learning. *Chem. Educ. Res. Pract.* **2016**, *17* (1), 139–155. https://doi.org/10.1039/c5rp00196j

Gray, R. The distinction between experimental and historical sciences as a framework for improving classroom inquiry. *Sci. Educ.* **2014**, *98* (2), 327–341. https://doi.org/10.1080/02635143.2019.1667321

Hakim, A.; Jufri, A. W.; Jamaluddin, J.; Ramandha, M. E. P. Natural Product Chemistry (NPC) Laboratory Activity in Indonesia. *Int. J. STEM Educ. Sustain.* **2022**, *2* (1), 94–104. https://doi.org/10.53889/ijses.v2i1.53

Hofstein, A.; Kipnis, M.; Abrahams, I. Z. *How to learn in and from the chemistry laboratory*. In *Teaching Chemistry: A Studybook*, edited by A. Hofstein and I. Eilks. Netherlands: Sense, 2013; pp. 153–182. https://doi.org/10.1007/978-94-6209-140-5_6

Hofstein, A.; Lunetta, V. N. The role of the laboratory in science teaching: Neglected aspects of research. *Review of Educ. Res.,* **1982**, *52* (2), 201–217. https://doi.org/10.2307/1170311

Hofstein, A.; Lunetta V. N. The laboratory in science education: Foundations for the twenty-first century. *Sci. Educ.* **2004**, *88* (1), 28–54. https://doi.org/10.1002/sce.10106

Johnstone, A. H.; Al-Shuaili, A. Learning in the laboratory; some thoughts from the literature. *Univ. Chem. Educ.* **2001**, *5* (2), 42–51.

Kostova, Z.; Radoynovska, B. Motivating students' learning using word association test & concept maps. *Bulgar. J. Sci. Educ. Policy* **2010**, *4* (1), 62–98.

Kurt, H. Biology student teachers' cognitive structure about "Living Thing". *Educ. Res. Rev.* **2013**, *8* (12), 871–880. https://doi.org/10.5897/ERR2013.1408

Mujtaba, T.; Sheldrake, R.; Reiss, M. J. Chemistry for All. Reducing inequalities in chemistry aspirations and attitudes. Royal Society of Chemistry, **2020**.

Mustafaoğlu, F. M., Yücel, A. S. Context-based teaching experiences of chemistry teachers: expectations, gains and applicability conditions. *J. Turk. Sci. Educ.* **2022a**, *19* (3), 958–978. https://doi.org/10.36681/tused.2022.158

Mustafaoğlu, F. T.; Yücel, A. S. Developing context-based teaching competencies of chemistry teachers: designing and implementing context-based activities. *J. Penelitian dan Pembelajaran IPA*. **2022b**, *8* (2), 126–152. https://doi.org/10.30870/jppi.v8i2.16491

Patton, M. Q. *Qualitative research & evaluation methods.* London: Sage Publications, Inc., 2002.

Pickering, M. The state of the art of teaching labs: What hath OSHA wrought? *J. Chem. Educ.* **1984**, *61* (10), 861–863. https://doi.org/10.1021/ed061p861

Reid, N.; Shah I. The role of laboratory work in university chemistry. *Chem. Educ. Res. Pract.* **2007**, *8* (2), 172–185. https://doi.org/10.1039/B5RP90026C

Rennie, L. J.; Jarvis, T. Children's choice of drawings to communicate their ideas about technology. *Res. Sci. Educ.* **1995**, *25*, 239–252. https://doi.org/10.1007/BF0235739

Rüschenpöhler, L.; Markic, S. Secondary school students' acquisition of science capital in the field of chemistry. *Chem. Educ. Res. Pract.* **2020**, *21* (1), 220–236. https://doi.org/10.1039/c9rp00127a

Saint-Jean, M. *L'apprentissage par problèmes dans l'enseignement supérieur.* Service d'aide à l'enseignement, Université de Montréal, Québec, 1994.

Sönmez, V.; Alacapınar, F. G. *Illustrated Scientific Research Methods*. Ankara: Anı Publishing, 2011.

Triayuni, T.; Irwandi, D.; Muslim, B. Development of STEM Based-Integrated Electrochemistry Enrichment Book: An Analysis Review. *Int. J. STEM Educ. Sustain.* **2023**, *3* (1), 125–138. https://doi.org/10.52889/ijses.v3i1.110

Uzuntiryaki-Kondakci, E.; Tuysuz, M.; Sarici, E.; Soysal, C.; Kilinc, S. The role of the argumentation-based laboratory on the development of pre-service chemistry teachers' argumentation skills. *Int. J. Sci. Educ.* **2021**, *43* (1), 30–55. https://doi.org/10.1080/09500693.2020.1846226

Wei, B.; Liu. H. An experienced chemistry teacher's practical knowledge of teaching with practical work: The PCK perspective. *Chem. Educ. Res. Pract.* **2018**, *19*, 452–462. https://doi.org/10.1039/c7rp00254h

Wellington, J.; Ireson, G. *Science Learning, Science Teaching*. London: Routledge, 2012. https://doi.org/10.4324/9780203134962

Wilson, H. Problem-solving laboratory exercises. *J. Chem. Educ.* **1987**, *64* (10), 895–896. https://doi.org/10.1021/ed064p895

Wu, M.; Sun, D.; Yang, Y.; Li, M.; Sun, J. Investigating students' performance at self-regulated learning and its effects on learning outcomes in chemistry class at the senior secondary school. *Int. J. Sci. Educ.* **2023**, *45* (16), 1395–1418. https://doi.org/10.1080/09500693.2023.2209693

Yıldırım, A.; Şimsek, H. *Qualitative research methods in the social sciences*. Ankara: Seçkin Publishing, 2006.